BOREAL FOREST ECOSYSTEM CHARACTERIZATION AT SITE AND LANDSCAPE SCALES USING MULTISPATIAL RESOLUTION REMOTE SENSING DATA

by

Paul Michael Treitz

A thesis
presented to the University of Waterloo
in fulfillment of the
thesis requirement for the degree of
Doctor of Philosophy
in
Geography

Waterloo, Ontario, Canada, 1997

© Paul Michael Treitz 1997

National Library of Canada
Acquisitions and Bibliographic Services
395 Wellington Street
Ottawa ON K1A 0N4
Canada

Bibliothèque nationale du Canada
Acquisitions et services bibliographiques
395, rue Wellington
Ottawa ON K1A 0N4
Canada

Your file Votre référence

Our file Notre référence

The author has granted a non-exclusive licence allowing the National Library of Canada to reproduce, loan, distribute or sell copies of his/her thesis by any means and in any form or format, making this thesis available to interested persons.

The author retains ownership of the copyright in his/her thesis. Neither the thesis nor substantial extracts from it may be printed or otherwise reproduced with the author's permission.

L'auteur a accordé une licence non exclusive permettant à la Bibliothèque nationale du Canada de reproduire, prêter, distribuer ou vendre des copies de sa thèse de quelque manière et sous quelque forme que ce soit pour mettre des exemplaires de cette thèse à la disposition des personnes intéressées.

L'auteur conserve la propriété du droit d'auteur qui protège sa thèse. Ni la thèse ni des extraits substantiels de celle-ci ne doivent être imprimés ou autrement reproduits sans son autorisation.

0-612-21392-7

Canada

The University of Waterloo requires the signatures of all persons using or photocopying this thesis. Please sign below, and give address and date.

ACKNOWLEDGMENTS

I would first like to thank Dr. Philip Howarth, my advisor and mentor. His support, encouragement and counsel is greatly appreciated. Also, I would like to thank the committee members, Dr. Ellsworth LeDrew, Dr. Barry Boots and Dr. Ric Soulis. Their insight and thoughtfulness provided important contributions to the process and product. My appreciation is also extended to the external examiner, Dr. Cheryl Pearce, for a close scrutiny of the thesis and helpful comments. I am indebted to the Rinker Lake field teams which included Dennis Paradine, Valdis Kalnins, Brenda Fooks and Paul Shepherd. I would also like to thank the following for support of the Rinker Lake field program: Ken Baldwin, John Ford, Lawrence Gray, Larry Hill, Andrew Jano, John Miller, Gerry Racey, Benoit Rivard, Ted Senese, Richard Sims and Sheila Walsh. I want to give special thanks to Ken Baldwin, Paul Shepherd and Dennis Paradine for thoughtful discussions in the field and helping me rationalize my approach to ecosystem classification and mapping. Also, for technical assistance with a smile, I want to thank Doug Dunlop, Joe Piwowar and Marko Dumancic. Finally, I want to acknowledge friends which became integral to my daily life in Waterloo: Lynn, Mary, Jean, Caron, Yifang, Doug, Roger, Marko, Tim, Joe, Derek, Greg, Mike and John. Thank you.

Funding for this research has been provided through the Northern Ontario Development Agreement, Northern Forestry Program. Several agencies contributed to the success of the field program, including: Canadian Forest Service - Natural Resources Canada; Northwest Region Science and Technology Unit - Ontario Ministry of Natural Resources; Earth-Observations Laboratory - Institute for Space and Terrestrial Science; and the Provincial Remote Sensing Office - Ontario Ministry of Natural Resources. Additional financial support for field work was provided through the University of Waterloo (scholarships and teaching assistantships), the Natural Sciences and Engineering Research Council of Canada (NSERC) - Research Grant awarded to Philip Howarth and the Undergraduate Student Research Awards program, and the Environmental Youth Corps program funded by the Ontario Ministry of Natural Resources.

Lastly, I would like to thank my immediate and extended families. They have always been supportive, patient and understanding. In particular, I want to thank my wife Barb, our son Joshua, my mother Gladys and Shirley and Les.

DEDICATION

To Barb.....for never doubting me, even when I doubted myself.....

and to Joshua.....daddy's home.....

ABSTRACT

Detailed forest ecosystem classifications have been developed for large regions of northern Ontario. These ecosystem classifications provide tools for ecosystem management that constitute part of a larger goal of integrated management of forest ecosystems for long-term sustainability. These classification systems provide detailed stand-level characterization of forest ecosystems at a local level. However, for ecological approaches to forest management to become widely accepted by forest managers, and these tools to be widely used, methods must be developed to characterize and map or model ecosystem classes at landscape scales for large regions.

In this study, the site-specific Northwestern Ontario Forest Ecosystem Classification (NWO FEC) was adapted to provide a landscape-scale (1:20000) forest ecosystem classification for the Rinker Lake Study Area located in the Boreal Forest north of Thunder Bay, Ontario. Multispatial resolution remote sensing data were collected using the Compact Airborne Spectrographic Imager (CASI) and analysed using geostatistical techniques to obtain an understanding of the nature of the spatial dependence of spectral reflectance for selected forest ecosystems at high spatial resolutions. Based on these analyses it was determined that an optimal size of support for characterizing forest ecosystems (i.e., optimal spatial resolution), as estimated by the mean ranges of a series of experimental semivariograms, differed based on (i) wavelength; (ii) forest ecosystem class (and at low altitude as a function of mean maximum canopy diameter (MMCD)); and (iii) altitude of the remote sensing system. In addition, maximum semivariance as estimated from the sills of the experimental semivariograms increased with density of understory.

Based on the estimates for optimal spatial resolutions for six landscape-scale forest ecosystem classes, a series of spectral-spatial features were derived from the high-altitude CASI data (4 metre spatial resolution) using spatial averaging. Linear discriminant analysis for various spectral-spatial and texture feature combinations indicated that a spatial resolution of approximately 6 m was optimal for discriminating the six-landscape scale ecosystem classes. Texture features, using second-order spatial statistics that were derived from the 4 m remote sensing data, also significantly improved discrimination of the classes over the original 4 m data. Finally, addition of terrain descriptors, particularly elevation within a local region, improved discrimination of the six landscape scale ecosystem classes. It has been demonstrated that in a low-relief boreal environment, addition of textural and geomorphometric variables to high-resolution CASI reflectance data provides improved discrimination of forest ecosystem classes. Although these improvements are statistically significant, the absolute classification accuracies are not at levels suitable for operational classification and mapping.

The analysis presented here represents the initiation of a complex modelling approach that is necessary for improving forest ecosystem characterization and prediction using additional primary datasets and derived datasets that possess various levels of measurement. Not only are optimal or multispatial resolution remote sensing data required, but also appropriately scaled terrain and landscape features depicting soil texture, nutrient and moisture regimes. Incorporation of these types of terrain-specific variables with reflectance data should provide further improvement in forest ecosystem classification and modelling at landscape scales.

TABLE OF CONTENTS

ABSTRACT vi

LIST OF TABLES x

LIST OF FIGURES xii

CHAPTER 1 INTRODUCTION 1
1.1 Background 1
1.2 Research Issues 3
1.2.1 Research Issue 1 - Spatial Resolution 3
1.2.2 Research Issue 2 - Data Integration 3
1.2.3 Research Issue 3 - Remote Sensing Forest Ecosystem Classification 3
1.3 Forest Ecosystem Classification 4
1.4 Scaling Issues in Geographical Research 5
1.5 Forest Ecosystems at Stand and Landscape Scales 6
1.6 Organization of the Thesis 9

CHAPTER 2 FOREST RESOURCE MANAGEMENT AND ECOLOGICAL LAND CLASSIFICATION WITH EMPHASIS ON ONTARIO 11
2.1 Introduction 11
2.2 Forest Resource Management 11
2.3 Vegetation Ecology 12
2.3.1 Forest Site Characteristics 14
2.3.2 Forest Stand Characteristics 17
2.4 Forest Ecological Classification - Regional and Local Scales 19
2.4.1 Ecological Land (Forest) Classification 19
2.4.2 Forest Ecosystem Classification (FEC) 25
2.4.3 Northwestern Ontario Forest Ecosystem Classification (NWO FEC) 28
2.5 Natural Forest Landscape Management 39
2.6 Summary 40

CHAPTER 3 REMOTE SENSING FOR FOREST ECOSYSTEM CHARACTERIZATION 43
3.1 Remote Sensing of Forests 43
3.1.1 Satellite Remote Sensing 44
3.1.2 Airborne Remote Sensing 45
3.2 Forest Information Extraction 49
3.2.1 Change Analysis 49
3.2.2 Biophysical Remote Sensing 51
3.2.3 Forest Classification 60
3.3 Remote Sensing Spatial Resolution (Scale) 73
3.3.1 Spatial Resolution (Scale) and Multispectral Classification 73
3.3.2 The Modifiable Areal Unit Problem (MAUP) 74
3.3.3 Selecting an Appropriate Spatial Resolution 75
3.3.4 Remote Sensing at Multiple Spatial Resolutions (Scales) 77
3.4 Remote Sensing and Data Integration for Forest Ecosystem Characterization 79
3.4.1 Describing Forest Ecosystems at Regional, Landscape and Local Scales 79
3.4.2 The Relationship between Remote Sensing Spatial Resolution and Forest Ecosystem Scales 85

3.4.3 A Remote Sensing and Data Integration Strategy for Forest Ecosystem Characterization 86
3.5 Summary 87

CHAPTER 4 STUDY AREA AND DATA DESCRIPTION 90
4.1 Study Area Description 90
4.1.1 Physiography and Bedrock Geology 93
4.1.2 Quaternary Geology 93
4.1.3 Forest Ecosystems 93
4.2. Ground Reference Data Collection From FEC Plots 96
4.2.1 Vegetation Data 100
4.2.2 Mensuration Data 100
4.2.3 V-Type Transects 104
4.3 Remote Sensing Data 108
4.3.1 Landsat Data 108
4.3.2 Compact Airborne Spectrographic Imager Data 109
4.3.4 Ancillary Remote Sensing Data 114
4.4 Digital Elevation Data 114
4.4.1 Gradient Model 115
4.4.2 Local Relief 117
4.5 Summary 118

CHAPTER 5 SPATIAL ANALYSIS OF REMOTE SENSING DATA 120
5.1 Introduction 120
5.2 Spatial Structure of Remote Sensing Data 121
5.3 Variogram Analysis of CASI Reflectance Data 125
5.4 Results 130
5.5 Discussion 144
5.5.1 Forest Ecosystem Class 145
5.5.2 Spectral Wavelength 147
5.5.3 Altitude/Spatial Resolution/Scale 149
5.6 Conclusions 150

CHAPTER 6 SPECTRAL, SPATIAL AND TERRAIN VARIABLES FOR DISCRIMINATING LANDSCAPE-SCALE FOREST ECOSYSTEM CLASSES 153
6.1 Introduction 153
6.2 Methods 154
6.2.1 Remote Sensing (Reflectance) Variables 154
6.2.2 Forest Ecosystem Reflectance Data Collection 156
6.2.3 CASI Spectral Feature Selection 159
6.2.4 Spectral-Spatial Features 160
6.2.5 Texture Features 164
6.2.6 Terrain Features 169
6.2.7 Linear Discriminant Analysis (LDA) 170
6.2.8 Maximum-Likelihood Classification (MLC) and Neural-Network Classification (NNC) 171
6.3 Results 172
6.3.1 Linear Discriminant Analysis 172
6.3.2 Maximum-Likelihood and Neural-Network Classification 176
6.4 Discussion 177
6.5 Conclusions 181

CHAPTER 7 SUMMARY, CONCLUSIONS AND RECOMMENDATIONS 184
7.1 Summary 184
7.2 Conclusions 187
7.2.1 Research Issue 1 - Spatial Resolution 187
7.2.2 Research Issue 2 - Data Integration 189
7.2.3 Research Issue 3 - Remote Sensing Forest Ecosystem Classification 190
7.3 Recommendations 190

REFERENCES 193

APPENDIX A Sustainable Forests: A Canadian Commitment 234

APPENDIX B Low-Altitude Semivariogram Analysis 237

APPENDIX C Medium-Altitude Semivariogram Analysis 248

APPENDIX D Mensuration Data for FEC Plots 254

APPENDIX E Geometric Correction of CASI Flight Lines 256

APPENDIX F Field Sample Locations 269

APPENDIX G Average Jeffries-Matusita Distance Measures 272

APPENDIX H Generation of CASI Spatial Features 275

APPENDIX I Classification Accuracy (Discriminant Function) - Contingency Tables for Validation Data 279

APPENDIX J Maximum Likelihood Classification Accuracy - Contingency Tables for Validation Data 292

APPENDIX K Neural Network Classification Accuracy - Contingency Tables for Validation Data 295

LIST OF TABLES

TABLE 2.1 FACTORS AFFECTING FOREST GROWTH. 17
TABLE 2.2 LEVELS OF GENERALIZATION FOR ECOLOGICAL LAND SURVEY 23
TABLE 2.3 THE EVOLUTION OF FOREST AND ECOLOGICAL LAND CLASSIFICATION IN CANADA AND ONTARIO 24
TABLE 2.4 LIST OF NWO FEC V-TYPES. 30
TABLE 2.5 LIST OF NWO FEC SOIL TYPES. 32
TABLE 2.6 AN ESTIMATE OF THE ABILITIES OF EXISTING RESOURCE INVENTORIES IN ONTARIO TO MEET INFORMATION REQUIREMENTS FOR INTEGRATED RESOURCE MANAGEMENT 41

TABLE 3.1 EARTH RESOURCES SATELLITE SYSTEMS 44
TABLE 3.2 EXAMPLES OF DAMAGE ASSESSMENT OF FORESTS USING REMOTE SENSING 52
TABLE 3.3 FACTORS AFFECTING SPECTRAL RESPONSE OF FOREST CANOPIES 54
TABLE 3.4 EXAMPLES OF BIOPHYSICAL REMOTE SENSING OF FORESTS 55
TABLE 3.5 EXAMPLES OF RATIO-BASED INDICES FOR BIOPHYSICAL STUDIES 58
TABLE 3.6 FOREST CLASSIFICATION WITH LANDSAT MSS 61
TABLE 3.7 FOREST CLASSIFICATION WITH LANDSAT TM 63
TABLE 3.8 SOME APPLICATIONS OF TEXTURE ANALYSIS FOR LAND-COVER CLASSIFICATION 70
TABLE 3.9 STAND AND LANDSCAPE LEVEL APPLICATIONS OF THE NWO FEC 81
TABLE 3.10 ECOLOGICALLY SIGNIFICANT FOREST CLASSES AT THE SITE AND LANDSCAPE LEVELS 83
TABLE 3.11 LANDSCAPE LEVEL FOREST ECOSYSTEM GROUPINGS FOR THE RINKER LAKE STUDY AREA 85
TABLE 3.12 RELATIONSHIP BETWEEN REMOTE SENSING SYSTEMS AND ECOLOGICAL LAND SURVEY MAPPING SCALES AND LEVELS 86

TABLE 4.1 FEC V-TYPE SAMPLES 103
TABLE 4.2 CORRECTION FACTORS FOR TREE SPECIES AGE CALCULATIONS. 104
TABLE 4.3 SENSOR CHARACTERISTICS FOR LANDSAT-5. 108
TABLE 4.4 DESCRIPTION OF THE COMPACT AIRBORNE SPECTROGRAPHIC IMAGER (CASI) 110
TABLE 4.5 CASI IMAGING MODE WAVELENGTHS. 111
TABLE 4.6 MULTIPLE SPATIAL RESOLUTION CASI DATA COLLECTED FOR THIS STUDY 111

TABLE 5.1 TERMS AND SYMBOLS USED IN THE DESCRIPTION OF THE VARIOGRAM....123
TABLE 5.2 REFLECTANCE VALUES (DN) FROM A SAMPLE TRANSECT (580-601NM)....128
TABLE 5.3 GEOSTATISTICAL ANALYSIS OF A SINGLE TRANSECT (580-601NM)....129
TABLE 5.4 SAMPLE OF GEOSTATISTICAL ANALYSIS BY STAND....129
TABLE 5.5 SUMMARY OF GEOSTATISTICAL ANALYSIS OF FOREST ECOSYSTEMS (ALTITUDE=600M)..132
TABLE 5.6 SUMMARY OF GEOSTATISTICAL ANALYSIS OF FOREST ECOSYSTEMS (ALTITUDE=1150M) 139
TABLE 5.7 SUMMARY OF OPTIMAL TEXTURAL WINDOW OPERATORS FOR LOW- AND MEDIUM-ALTITUDE CASI DATA....143
TABLE 5.8 SUMMARY OF FOREST MENSURATIONAL PARAMETERS....143

TABLE 6.1 SUMMARY OF GEOMETRIC CORRECTION OF CASI FLIGHT LINES....155
TABLE 6.2 FEC V-TYPE SAMPLES FOR THE RINKER LAKE STUDY AREA....158
TABLE 6.3 FEATURE SELECTION BASED ON JEFFRIES-MATUSITA (J-M) DISTANCE....160
TABLE 6.4 "OPTIMAL" SPATIAL RESOLUTION CASI DATASET BASED ON SEMIVARIOGRAM ANALYSIS....161
TABLE 6.5 FEATURE DATASETS FOR LINEAR DISCRIMINANT ANALYSIS....174
TABLE 6.6 CLASSIFICATION ACCURACY (LINEAR DISCRIMINANT FUNCTION) BY CLASS....174
TABLE 6.7 CORRELATION MATRIX FOR Z-SCORES - DIFFERENCES OF PROPORTIONS FOR VALIDATION DATA....175
TABLE 6.8 CLASSIFICATION ACCURACY BY CLASS FOR LDA, MLC AND NNC....177

LIST OF FIGURES

FIGURE 2.1 THE FOUR MAJOR DESCRIPTORS AFFECTING A SITE REGION. 15
FIGURE 2.2 ECOLOGICAL FRAMEWORK FOR FOREST ECOSYSTEM CLASSIFICATIONS (FEC). 26
FIGURE 2.3 ORGANIZATION OF FEC SOIL AND VEGETATION TYPES 27
FIGURE 2.4 NWO FEC VEGETATION KEY USED TO DETERMINE V-TYPE. 29
FIGURE 2.5 NWO FEC SOILS KEY USED TO DETERMINE SOIL TYPE. 31
FIGURE 2.6 SAMPLE OF NWO FEC V-TYPE DESCRIPTION. 33
FIGURE 2.7 SAMPLE OF NWO FEC SOIL-TYPE DESCRIPTION. 34
FIGURE 2.8 NWO FEC V-TYPE ORDINATION. 35
FIGURE 2.9 APPLICATION OF THE NWO FEC V-TYPE ORDINATION. 36
FIGURE 2.10 TREATMENT UNITS SUPERIMPOSED ON THE NWO FEC V-TYPE ORDINATION. 37
FIGURE 2.11 SAMPLE OF NWO FEC TREATMENT UNIT DESCRIPTION. 37

FIGURE 4.1 LOCATION OF THE RINKER LAKE RESEARCH AREA IN NORTHWESTERN ONTARIO. 91
FIGURE 4.2 LOCATION OF THE STUDY SITE WITHIN THE RINKER LAKE RESEARCH AREA. 92
FIGURE 4.3 TREMBLING ASPEN (WHITE BIRCH) / MOUNTAIN MAPLE (V8). 95
FIGURE 4.4 BLACK SPRUCE MIXEDWOOD / FEATHERMOSS (V20). 95
FIGURE 4.5 MAP OF THE RINKER LAKE STUDY SITE SHOWING 1993 PLOT LOCATIONS. 98
FIGURE 4.6 MAP OF THE RINKER LAKE STUDY SITE SHOWING 1994 PLOT LOCATIONS. 99
FIGURE 4.7 NWO FEC VEGETATION CARD. 101
FIGURE 4.8 SAMPLE NWO FEC VEGETATION DATA COMPILATION. 102
FIGURE 4.9 NWO FEC FORESTRY DATA CARD. 105
FIGURE 4.10 SAMPLE NWO FEC FORESTRY DATA COMPILATION. 106
FIGURE 4.11 MAP SHOWING TRANSECTS SAMPLED FOR V-TYPE IN 1994 AND 1995. 107
FIGURE 4.12 LANDSAT TM IMAGE OF THE STUDY SITE - JUNE 20, 1992. 109
FIGURE 4.13 MAP OF RINKER LAKE STUDY SITE SHOWING FLIGHT LINES AND PIF LOCATIONS. 112
FIGURE 4.14 HIGH ALTITUDE CASI DATA FOR PART OF THE RINKER LAKE STUDY SITE. 113
FIGURE 4.15 MID ALTITUDE CASI DATA FOR PART OF THE RINKER LAKE STUDY SITE. 113
FIGURE 4.16 LOW ALTITUDE CASI DATA FOR PART OF THE RINKER LAKE STUDY SITE. 114
FIGURE 4.17 DIGITAL ELEVATION MODEL FOR THE RINKER LAKE STUDY SITE. 116
FIGURE 4.18 WINDOW FOR COMPUTING DERIVATIVES OF ELEVATION MATRICES. 116
FIGURE 4.19 SLOPE IMAGE OF THE RINKER LAKE STUDY SITE. 117
FIGURE 4.20 LOCAL RELIEF IMAGE OF THE RINKER LAKE STUDY SITE. 118

FIGURE 5.1 THE SHAPE AND DESCRIPTION OF A "CLASSIC" VARIOGRAM. 123
FIGURE 5.2 VARIOGRAMS DERIVED FROM SELECTED FOREST STANDS / ECOSYSTEMS (ALTITUDE=600M). 133
FIGURE 5.3 LOW-ALTITUDE RANGE VALUES (580 - 601 NM) FOR FOREST ECOSYSTEM COMPLEXES IN THE RINKER LAKE STUDY AREA. 134
FIGURE 5.4 LOW-ALTITUDE RANGE VALUES (744 - 750 NM) FOR FOREST ECOSYSTEM COMPLEXES IN THE RINKER LAKE STUDY AREA. 134
FIGURE 5.5 COMPARISON OF VARIOGRAM CURVES FOR A LOWLAND BLACK SPRUCE STAND (V37)... 135
FIGURE 5.6 LOW-ALTITUDE SEMIVARIANCE (580NM - 601 NM) FOR FOREST ECOSYSTEM COMPLEXES IN THE RINKER LAKE STUDY AREA. 136
FIGURE 5.7 LOW-ALTITUDE SEMIVARIANCE (744NM - 750 NM) FOR FOREST ECOSYSTEM COMPLEXES IN THE RINKER LAKE STUDY AREA. 136
FIGURE 5.8 VARIOGRAMS DERIVED FROM SELECTED FOREST STANDS / ECOSYSTEMS (ALTITUDE=1150M). 140
FIGURE 5.9 MEDIUM-ALTITUDE RANGE VALUES (580 - 601 NM) FOR FOREST ECOSYSTEM COMPLEXES IN THE RINKER LAKE STUDY AREA. 141
FIGURE 5.10 MEDIUM-ALTITUDE RANGE VALUES (744 - 750 NM) FOR FOREST ECOSYSTEM COMPLEXES IN THE RINKER LAKE STUDY AREA. 141
FIGURE 5.11 MEDIUM-ALTITUDE SEMIVARIANCE (580 - 601 NM) FOR FOREST ECOSYSTEM COMPLEXES IN THE RINKER LAKE STUDY AREA. 142
FIGURE 5.12 MEDIUM-ALTITUDE SEMIVARIANCE (744 - 750 NM) FOR FOREST ECOSYSTEM COMPLEXES IN THE RINKER LAKE STUDY AREA. 142

FIGURE 6.1 HIGH-ALTITUDE CASI AND LANDSAT TM MOSAIC FOR THE RINKER LAKE STUDY AREA. 157
FIGURE 6.2 SPECTRAL-SPATIAL FEATURES FOR CASI BAND 3 REFLECTANCE 162
FIGURE 6.3 SPECTRAL-SPATIAL FEATURES FOR CASI BAND 7 REFLECTANCE 163
FIGURE 6.4 LANDSAT TM FEATURES. 164
FIGURE 6.5 MEAN TEXTURE FEATURES FOR CASI BANDS 3 AND 7. 168
FIGURE 6.6 CONTRAST TEXTURE FEATURES FOR CASI BANDS 3 AND 7. 168
FIGURE 6.7 CORRELATION TEXTURE FEATURES FOR CASI BANDS 3 AND 7 169
FIGURE 6.8 TERRAIN VARIABLES: ELEVATION, GRADIENT AND LOCAL RELIEF 170

CHAPTER 1

INTRODUCTION

1.1 Background

Although commercial timber production remains the major resource use of Canada's forests, additional demands on forested land now include non-timber values such as recreation, wilderness, fish and wildlife, water, and aesthetics. Forests are also becoming valued for education, the maintenance of biodiversity and regulation of the global ecosystem. To manage these values in an integrated manner, an improved understanding of forest resources and the interactions among them is required. To achieve this understanding and include these disparate demands within a truly integrated management system will require further development of forest resource databases (Forestry Canada, 1990). Fortunately, there is a commitment by the Government of Canada to address these challenges for managing Canada's forested lands. Specifically, the Canadian Council of Forest Ministers (CCFM), trustee of the National Forest Strategy, has outlined a series of strategic directions and commitments that pertain to maintaining sustainability of Canada's forests through management for long-term health of forest ecosystems (Canada Council of Forest Ministers, 1992; National Forest Strategy Coalition, 1994). Strategies that are directly related to the research presented in this thesis are summarized in Appendix A. Similarly, the Ontario Ministry of Natural Resources (OMNR) has adopted new policies and implemented new legislation to explicitly require ecological approaches to resource utilization and protection (Anonymous, 1994a; 1995).

To achieve an integrated management system for long-term sustainability, detailed knowledge of the forest is required, complemented by an understanding of the relationships between those structural characteristics and the environment. The objective of sustainability is the maintenance of ecosystem integrity and protecting natural diversity and vital processes (Salwasser 1990; Jensen and Everett, 1994). Ecologically-sustainable development of forest ecosystems therefore requires spatial information about the ecological components as well as the timber resources in a region (Mackey *et al.*, 1994a). Hence, there is a requirement to define the forest both from an ecosystem (unit) and an ecological (process) perspective. A

wide variety of information can be accumulated from studying these characteristics and the relationships between them. This information needs to be organized and simplified in a manner which facilitates enhanced decision-making at a variety of levels. From an ecological perspective, this organization has traditionally been done using quantitative analyses for classification (Hill, 1979; Gauch, 1982).

In response to concerns regarding ecological issues such as ecologically sustainable development and conservation of biodiversity, researchers are attempting to identify, characterize and understand meaningful ecological units that constitute the landscape and signify the core of these issues (Sims and Mackey, 1994). The land 'unit,' a fundamental concept in landscape ecology, is described as an expression of landscape as a system, defining an ecologically homogeneous tract of land at a particular scale of study (Zonneveld, 1989). The land unit provides the basis for studying topologic (vertical heterogeneity) as well as chorologic (horizontal heterogeneity) landscape ecologic relationships and can best be examined spatially by viewing them synoptically from above. Land units are generally mapped using characteristics of the most obvious (mappable) land attributes: landform, soil and vegetation (Zonneveld, 1989).

Knowledge of the biological and physical environments is required to define units that have ecological meaning. However, few studies on the definition and examination of spatially distributed ecological units have been undertaken in Canada's boreal forest (Sims and Mackey, 1994). Forest ecosystem units that are defined according to some combination of vegetation, soils, site and local climate, or some spatially contiguous aggregation of such forest sites, can be recognized at a range of scales (Sims *et al.*, 1994) and are typically nested within other ecosystems in a hierarchy of scales (Bailey, 1987). To operationally manage ecosystems at any scale, it is necessary to understand the aggregations upward and the subdivision downward in the hierarchy. Attached to the concept of scale is a certain level of perceived detail with respect to structure and process (Hills and Pierpoint, 1960; Rowe and Sheard, 1981) which will vary with scale as one structure or process is supplanted with another (Sims *et al.*, 1994). The appropriate scale of analysis for various processes has been under serious debate (Nir, 1987). There is agreement, however, that changes in scale change the important relevant variables (Meentemeyer, 1989). The emphasis in this thesis is on the characterization of forest ecosystem units at the microscale level; corresponding to stand (< 1:10 000) and landscape (1:10 000 to 1:50 000) scales. Here, classification units are segregated based on specific soil, topographic and vegetational characteristics. At the community or stand level, more specific consideration is made of quantitative soil and vegetational parameters (Uhlig and Jordan, 1996).

1.2 Research Issues

The goal of this research is to determine the extent to which forest ecosystems, related to the Northwestern Ontario Forest Ecosystem Classification (FEC), can be discriminated using remote sensing data collected at various spatial resolutions. In order to achieve this goal, several research issues need to be examined. These are:

1.2.1 Research Issue 1 - Spatial Resolution

Remote sensing data may provide important forest structural and ecosystem information. As part of the research into the effects of spatial resolution on the spectral expression of forest ecosystems, the spatial aspects of remote sensing reflectance data for forest ecosystems at high spatial resolutions are examined. The objective of this analysis is to determine the optimal spatial resolutions for discriminating particular forest ecosystems. These analyses include the following:

- semivariogram analyses of remote sensing reflectance data for forest stands at different spatial resolutions to gain an understanding as to how spectral reflectance within forest stands is affected by spatial aggregation and to determine the optimal scales at which forest ecosystems may be discriminated by remote sensing
- generation of spatially averaged and texture features that represent the optimal scales of information identified in the high resolution data.

1.2.2 Research Issue 2 - Data Integration

A second objective of this study is to determine the extent to which terrain variables can improve forest ecosystem mapping within the boreal forest of northwestern Ontario. In order to model forest ecosystems, an integrated dataset is developed that incorporates multi-spatial resolution remote sensing data and landscape variables. Remote sensing data acquired for the study area and data derived from elevation data are integrated into a common database. Although the spatial resolutions will differ between the remote sensing data and the terrain variables, it is anticipated that the information content will represent a similar scale (i.e., a landscape scale of approximately 1:20 000). This stage of the research involves discriminant analysis of multi-spatial resolution remote sensing data, textural features and terrain data to determine optimal data sets for discriminating forest ecosystems.

1.2.3 Research Issue 3 - Remote Sensing Forest Ecosystem Classification

In an ecological approach to land classification, coherent terrain units are interpreted based on a complex of factors including vegetation, landforms and drainage. Based on the results of the discriminant analysis, classification of the optimal dataset will be performed. A number

of classification algorithms (e.g., maximum likelihood, neural networks) are tested for this purpose.

In summary, this research aims to model the effect of remote sensing spatial resolution on spatial aggregation of forest spectra in order to discriminate and classify forest ecosystems at appropriate scales. Traditional methods of extraction have proven inadequate due to a poor understanding of how canopy (and understory) spectra are sampled and/or integrated at a range of spatial scales. Also, since detailed ecosystem classes within the FEC can be grouped into similar ecological units for representation at coarser scales, it seems reasonable that multi-spatial resolution remote sensing data will be useful for separating various levels of FEC information. Finally, this research aims to improve classification and mapping of forest ecosystems by integrating remote sensing data with other spatial data, primarily derived from terrain variables.

1.3 Forest Ecosystem Classification

Rowe (1961) defines an ecosystem as a topographical unit of the landscape displaying a relative homogeneity with respect to the form and structure of the land and the vegetation communities supported. Ecosystems are structural features within the landscape, with both their structure and function closely tied to the reciprocal interactions of the physical environment and the biotic components (Barnes, 1986). Forest ecosystem classifications are based on ecological principles and are used by resource managers for planning and management, as well as frameworks to address issues of biodiversity and sustainable development (Sims and Mackey, 1994; Sims *et al.*, 1994). For easy application of the classification, it needs to be based on readily identifiable (or inferred) features of the land for easy identification in the field. In addition, use of a hierarchical classification system can support decision-making at several administrative or geographic levels through the aggregation or division of the elements of the classification (Driscoll *et al.*, 1984). Hills (1952) stressed the physiographic characteristics of ecosystems since these are generally stable and largely in control of vegetation development (Burger and Pierpoint, 1990). Hills' "total site type" incorporated both the physiographic and biotic elements of ecosystems which provided the foundation upon which subsequent forest ecosystem classifications for Ontario are based. These ecologically based classifications provide a spatio-temporal framework for ecosystem identification and inventory (Uhlig and Jordan, 1995).

Detailed forest ecosystem classifications have now been developed and implemented for large portions of northern Ontario (e.g., Jones *et al.*, 1983; Sims *et al.*, 1989; McCarthy *et al.*, 1994). These field classifications are intended for application at the "stand level",

normally within relatively small (i.e., 10 ha) forested areas, and are consequently difficult to implement for large tracts of forested land which are characteristic of northern Ontario. They are also designed for mature forest stands (> 50 years) and do not apply to recently disturbed or regenerating sites, or to other land-cover types within the boreal forest. Hierarchical frameworks which guide the development and applications of these classifications have evolved in parallel to these classification systems (e.g., Racey *et al.*, 1989). Application of multiple classification and inventory templates in developing solutions for ecosystem management objectives remains problematic for large jurisdictions. However, hierarchical applications can define units and express ecosystem complexity in terms of key functional and structural components (Uhlig and Jordan, 1995).

1.4 Scaling Issues in Geographical Research

Scale has been defined as "the spatial or temporal dimension of an object or process, characterized by both grain and extent" (Turner *et al.*, 1989a, p. 246). Although scale is central to geographic thought and study, geographers have been criticized for seldom stating their scales of analysis anymore explicitly than scientists in other disciplines (Meentemeyer, 1989). This is not to say that much philosophical discussion on spatial scales and methodologies for dealing with scale have not been presented. Abler *et al.*, (1971) include scale as one of the primary spatial variables in geography, along with area, range, distance, direction, spatial geometries and patterns, spatial connectivity, isolation, diffusion and spatial associations.

When initiating a study involved in describing forest ecosystems, it is important to recognize whether one is working with absolute or relative space. Absolute space, which involves a Euclidean perspective, is the most common type of space encountered in studies involving inventory, planning and mapping. In this regard, absolute space is closely associated with the 'unit' component of an ecosystem. It is the easiest type of space to deal with in regards to hierarchical classification, since classes can be nested within others at different levels (Meentemeyer, 1989). In relative space, not only is space defined by the spatial elements within an ecosystem, but also by the spatial processes (e.g., migration, diffusion) occurring within and between ecosystems and their environment. When studying the relationships between (among) spatial patterns/forms and functions, processes and rates often define the scales and regions of analysis (Meentemeyer, 1989). When spatial processes are examined within an ecosystem framework, space may no longer be Euclidean, and therefore difficult to map in absolute space. Selecting the appropriate scale of analysis to study processes is very difficult. However, it is generally accepted that changes in scale will

change or shift in importance the relevant variables affecting processes (Meentemeyer, 1989; Turner *et al.*, 1989b). In addition, information is often lost as spatial data are considered at coarser scales of resolution (Henderson-Sellers *et al.*, 1985; Meentemeyer and Box, 1987).

Spatial autocorrelation is one of the most significant methodological problems associated with spatial analyses. Spatial autocorrelation has been stated very simply by Tobler (1969) in his first law of geography: near things are more related than distant things. Without spatial autocorrelation, however, the surface of the earth would be entirely stochastic and therefore there would be no recognition of spatial pattern at any scale of observation. Spatial autocorrelation for phenomena and processes are likely to vary with scale as a function of the degree of spatial heterogeneity (Meentemeyer, 1989). In this sense, the scale (spatial resolution) needs to correspond to the spatial heterogeneity (White, 1987). Therefore, with respect to forest ecosystems, stands which exhibit different spatial heterogeneities require examination at different scales. Since scales vary as a function of within-site and across-site variability, it is important in selecting an appropriate scale of observation to minimize within-site variability and maximize across-site variability. These scales will differ for forest ecosystems exhibiting different levels of complexity.

Meentemeyer (1989) suggests that if results of analyses are to be transferable to other settings, particularly in the exercise of modeling, nearly every geographic primitive (e.g., area, shape, distance, scale) needs to be controlled in the experimental design. If the results are dependent on the size of the spatial unit in an analysis, there is a danger for unjustifiable inferences. Specifically, empirical results correlating spatial processes from spatial form are generally scale-specific and patterns which appear ordered at one scale may appear random at another scale. It has therefore been suggested that there is a requirement for multi-scale research (e.g., Abler, 1987; Turner *et al.*, 1989a; 1989b; Meentemeyer, 1989). This is a result of (i) the notion that there are no simple rules for selecting the "proper" scale for analysis (Clark, 1985) and (ii) information content varies between scales.

1.5 Forest Ecosystems at Stand and Landscape Scales

Forest managers require process and structural information on ecosystems at both stand and landscape levels. Processes that generate heterogeneity within a forest stand are dependent upon the scale of analysis. At the stand level (i.e., 10 ha; < 1:10 000), detailed site-based information can be collected to describe and classify forest ecosystems in considerable detail. At this level, variations due to slope, vegetational effects, site nutrient status and soil features can have significant impact on pattern and distribution of ecosystem units (Sims *et al.*, 1994). With knowledge of the biological and physical components of the landscape, managers will

have the capability of identifying ecological characteristics and be able to predict the impacts of responses of the landscape to management (Sims and Mackey 1994). It has been emphasized by Rowe (1984) that landscape ecosystems should be the focus of study as opposed to plant communities or populations which are taxonomic concepts. In this way, the functional aspects of the ecosystem will be emphasized.

Landscape or *landschaft* has traditionally been a technical term basic to geographic thought, but has been defined in many ways. For instance, Hellpach (1935; p. 348) defined *landschaft* as "the total impression aroused in us by a piece of the earth's surface and the corresponding section of sky." Here, Hellpach refers to the sensation that a surface elicits from an observer, generally perceived as viewing the scene vertically from above (Hartshorne, 1939). Granö (1929) describes the sensation as being a function of the objects within an area that are responsible for the observer's concept of landscape. In expressing his perspective on landscape or *landschaft*, Hartshorne (1939; p. 164) presents the following:

> The reality that we are defining as "landscape" is essentially only a surface. The form of the surface is determined primarily by the relief of the land, but is also affected in minor degree by the height of forests and, in urban areas particularly, of man's buildings. The material character of the landscape is expressed by colour and texture and may be observed by sight and feeling. To designate the material character of the landscape apart from its surface configuration, we may use the term "landscape cover." Over most of the world this consists of the uppermost surface of vegetation - whether natural, wild, or cultivate - and of the surface of water.

This description of landscape incorporates two elements important in discriminating ecosystem units within the landscape from a synoptic perspective, "colour" and "texture." Although these descriptors refer largely to the aesthetic nature of the landscape, the spatial arrangements of these coloured and textured objects portray the complex of related processes in an area that give rise to the overall landscape. At the landscape level, ecological units are primarily a function of landform features. Sims *et al.* (1994) state that most landform and surficial patterns within a regional landscape, either individually or in complexes, have a standard set of vegetation communities that can be described along toposequences across them. Regardless of the definition, landscapes consist of very complex ecological systems that function at broad spatio-temporal scales. Within the framework of hierarchy theory, such systems are composed of relatively isolated levels, each of which operates at a distinct time and space scale (O'Neill *et al.*, 1989).

The forest ecosystem classifications developed for Ontario's forests are designed for stand level (i.e., 10 ha) analysis, but are adaptable for applications at landscape scales (e.g., 1:20 000). Site classifications at the landscape level can provide the basis for detailed

application and planning. However, detailed ground level classifications, used in conjunction with spatial modelling techniques that take advantage of remote sensing and geographic information system (GIS) technologies, will provide more effective adaptation of management and planning applications to detailed forest ecosystem classification. These technologies provide the opportunity to perform advanced spatial analyses through the application of spatially explicit statistical techniques which can be critical for mapping ecosystems, although confined primarily to analysis in absolute space (Meentemeyer, 1989; Turner *et al.*, 1989a). However, Zonneveld (1989) cautions that a GIS cannot be considered a basic tool for land unit assessment by itself since the land unit is not a mere compilation of independent building blocks, nor are the boundaries of separately surveyed land attribute mapping units guaranteed to coincide.

Remote sensing and digital image analysis techniques offer potential for assisting in the analysis of large forest tracts for identification of appropriate ecosystem classes or aggregations of ecologically similar classes. However, satellite remote sensing data are acquired at predetermined spatial resolutions, designed primarily for general land-cover and land-use analysis and mapping. Although airborne systems are capable of acquiring data in a variety of resolutions (i.e., spatial, spectral and temporal), optimal resolutions for specific terrain analyses are generally not known. This problem has been presented by Woodcock and Strahler (1987) in their paper discussing the scale dependence of prediction in remote sensing. Remote sensing data are generally collected at a single spatial resolution in comparison to the many scales at which nature's "units" and "processes" exist. It is therefore difficult to identify a single spatial resolution (scale) of remote sensing data that will provide the most suitable level of information for extracting forest ecosystem characteristics. It is anticipated that multi-scale remote sensing data will provide suitable information at a variety of levels for forest ecosystem classification.

Spectral data alone are not likely to sufficiently dissect the landscape into ecologically meaningful units. Other descriptors of the landscape are required to incorporate ecological characteristics of the landscape. These descriptors include geomorphometric variables (e.g., elevation, aspect and slope) and soils information. The natural distributions of plant species and vegetation associations are the result of complex interrelations between the genetically-controlled response of plants to both landscape and disturbance processes (Mackey *et al.*, 1994b). Landscape processes are responsible for determining the availability of energy (i.e., radiative, thermal), moisture and mineral nutrients, referred to by Mackey *et al.* (1994a) as the primary environmental regimes (PERS). For example, Sims *et al.* (1989) linked the PERS of soils moisture and mineral nutrients to the distribution of mature forest

ecosystem classes within northwestern Ontario. Disturbance processes (e.g., fire, insect infestations, disease) on the other hand are linked closely with successional changes in vegetation (Mackey *et al.*, 1994b). Again, these processes operate at a range of scales.

For ecological forest management, more complex and detailed information on forest ecosystems is required than has traditionally been supplied by the forest timber cruise. Hence, more ambitious ground data collection techniques are employed for ecosystem characterization (McLean and Uhlig, 1987). However, for forest landscape management and planning, this highly intensive form of data collection is not practical and therefore attempts to map the forest in this manner have met with resistance from forest practitioners. For forest ecosystem classification to be adopted in some form (i.e., at one or many scales) by the forest industry, methods that incorporate remote sensing and GIS, and which are supported by intensive field surveys, require development. There have been few attempts to systematically delineate spatially distributed and ecologically significant forest units within the Boreal Forest of Canada (Sims and Mackey, 1994).

The research outlined in this thesis is one of a series of projects with a primary focus on improving forest ecosystem discrimination and mapping for the purpose of resource management and the estimation of biodiversity characteristics at intermediate spatial scales. This series of research projects being conducted at Rinker Lake and other sites should improve the understanding of spatially distributed ecological interaction and relationships in boreal forest areas (Sims and Mackey, 1994). Specifically, this thesis examines the structural characteristics of forest ecosystems using high-resolution airborne remote sensing data. This spatial analysis is a precursor to deriving spectral-spatial and textural features from the remote sensing data for combination with terrain variables to determine the discriminability of forest ecosystems at landscape scales.

1.6 Organization of the Thesis

In Chapter 1, the background and rationale for pursuing a method for discriminating forest ecosystems (based on the NWO FEC) using remote sensing data are described. The research issue that is in the forefront of this study is that of the effect of spatial resolution and scale of observations on forest ecosystem discrimination. The relationship between spatial resolution and scale has been described as they relate to discriminating forest ecosystems. Chapter 2 contains a description of the evolution of forest management from timber management to integrated forest ecosystem management. Related to this shift in paradigm is an emphasis on forest ecosystem classification as opposed to a strict forest inventory based on mensurational parameters. A review of remote sensing studies related to forestry and the evolution of

ecological land classification is presented in Chapter 3. In Chapter 4, the study area and data collection methods are described. The research methods and results of the spatial analysis of the multi-spatial resolution remote sensing data are presented and discussed in Chapter 5. Likewise, Chapter 6 contains the research methods, results and discussion of the discriminant analysis and classification of the remote sensing data in combination with terrain variables. Conclusions based on the research conducted as part of this thesis and recommendations for future work are put forward in Chapter 7.

CHAPTER 2

FOREST RESOURCE MANAGEMENT AND ECOLOGICAL LAND CLASSIFICATION WITH EMPHASIS ON ONTARIO

2.1 Introduction

In this chapter, the evolution of forest information requirements for forest management in Ontario is described. The focus of forest management, both theoretically and to a lesser extent operationally, has evolved as a result of societal demands towards managing forests within an ecosystem framework. This ecosystem framework reflects the objectives and needs of forest management, which then in turn define the requirements for the forest survey. This framework provides for management of ecosystems for multiple uses at multiple scales. Since forest ecosystems are functional units, approaches to forest management which emphasize the interrelationships of ecosystem components will be most useful for integrated resource management (Barnes, 1986).

The ecosystem approach to the survey and mapping of forested lands was pioneered in Ontario by G.A. Hills and was paralleled nationally with the development of ecological land classifications (ELC) (Wiken and Ironside, 1977). These integrated regional classifications have been refined for application at local levels with classifications such as the Northwestern Ontario Forest Ecosystem Classification (NWO FEC). It is the description of these applications of forest management that provides the background for devising methodologies for classifying and mapping ecosystems, at both local and landscape scales, from remote sensing data.

2.2 Forest Resource Management

Historically, forest management concepts in Canada have evolved through various phases, chronologically identified as resources exploitation, timber management, multiple use and integrated resource management (Booth *et al.*, 1993). Forest resource management can no longer emphasize the narrow perspectives of sectoral resource values and traditional land-use patterns that are based on short-term objectives (Uhlig and Jordan, 1995). Societal demands

on forest managers now include conservation and sustainable development as critical components of any forest management plan. Sustainable development promotes the continuing use of natural resources while maintaining their long-term renewability (Brundtland, 1987). Sustainable development, as opposed to sustainable yield, is required to maintain Canada's biodiversity as well as to keep Canada's forest industry competitive in a global market (Booth *et al.*, 1993). Integral to sustainable development is the maintenance of forest structure and function in order to provide long-term productivity and conservation of Canada's forests. These objectives are akin to paradigms of conservation biology (e.g., Soulé, 1986; Ginsberg, 1987) and landscape ecology (e.g., Forman and Godron, 1986) which are trying to develop guidelines for preserving biological diversity at different geographical and temporal scales (Hansson, 1992). In particular, landscape ecology is primarily concerned with maintaining biodiversity in the overall landscape through the examination of flows and processes (Forman and Godron, 1986; Hansson and Angelstam, 1991).

Forests develop through the dynamic relationships between the physical and biological site characteristics and their history of natural and human impacts. Forest management has recognized the need to understand and describe these ecological relations of forests. Deterioration of the forest results when they are managed without attention to ecosystem dynamics and processes. Treatment of Canada's forests in this manner provides additional information about the relationships between forests and their environment, information necessary for successful natural forest landscape management. This emphasis on ecosystems also provides a better understanding of forest contributions and/or responses to global environmental change. It is important that resource managers examine closely the factors that dictate how forests develop. These factors will vary across Canada, particularly with respect to climate, physiography and soils. In addition, management practices will vary between provinces according to utilization pressures, data collection and standards for forest management practices. The ecosystem approach is being adopted across Canada, as forest managers begin to examine forested lands from an ecosystem perspective (e.g., Klinka *et al.*, 1979; Corns and Annas, 1986; Stanek and Orloci, 1987; Meidinger and Pojar, 1991; Banner *et al.*, 1993). The following sections briefly describe the ecosystem concept and the evolution of ecosystem information requirements for forest management with an emphasis towards Ontario.

2.3 Vegetation Ecology

In order to manage forests effectively, the forest manager must have a thorough understanding of forest ecology and forest ecosystems. In response to this requirement, forest

site information is becoming more vital for detailed management of forest tracts at both the regional and local levels (Bonnor and Morrier, 1981). Indeed, a comprehensive knowledge of the structure and functions at the stand level will provide a clearer understanding of the structure and functions that exist and operate at the landscape scale (Sims and Uhlig, 1992). This section presents a general outline of forest ecology, followed by a brief description of forest ecology research in site classification for the boreal forest of northern Ontario.

Mueller-Dombois and Ellenberg (1974, p.9) describe vegetation ecology as:

> the study of both the structure of vegetation and vegetation systematics. This includes the investigation of species composition and the sociological interaction of species in communities. It further includes the study of community variation in the spatial or geographic sense, and the study of community development, change, and stability in the time sense. Vegetation ecology is concerned with all geographic levels of plant communities, from broad physiognomic formations in the sense of biomes .. to the very fine floristic patterns occurring on an area less than a square meter in size. Vegetation ecology is very much concerned with correlations between environment and vegetation, and with the causes of community formation.

As defined above, the ecosystem approach to forest management deals with the composition, development, geographic distribution and environmental relationships of plant communities. The emphasis in this thesis focuses on vegetation systematics; that is, the classification of typical vegetation communities. However, vegetation systematics is no longer considered an end in itself, as environmental effects on vegetation development must also be considered. An ecosystem concept emphasizes this point in that an organism and its environment form a functional system in nature (Tansley, 1935).

Ecosystems are defined based upon both structural and functional aspects. Thus a forest ecosystem can be described, in part, according to the vegetation of its component strata: e.g., tree layer, shrub layer, herb layer and ground layer, as defined by environmental factors such as climate, physiography and soils. Also, ecosystems are open systems which have inputs and outputs, and experience a specific set of responses and processes (Ovington, 1962). The ecosystem concept cannot replace established vegetation and plant community concepts as these are still necessary to characterize particular ecosystems in space (i.e., geographically) and over time (Mueller-Dombois and Ellenberg, 1974). The ecosystem concept, however, emphasizes the need to consider all of those components which serve to define and functionally regulate ecosystems.

In classifying ecosystems, the vegetation ecologist aims to integrate vegetation and environment. Depending on the emphasis of the particular study, ecosystem boundaries can

result from plant community boundaries (Sukachev, 1945), soil or landform boundaries (Hills, 1960), or from a combination of vegetation and environmental characteristics, as preferred by Rowe *et al.* (1961). The combined approach has been successful in providing ecological data for applied research in forest and site evaluation studies, where the ecosystem components can be employed as indicators of the more transparent site factors, particularly for growth and yield studies (Mueller-Dombois and Ellenberg, 1974). Ecosystem classification organizes the knowledge of particular environments, providing a common scientific basis for the management of renewable resources (Klinka *et al.*, 1980). This process must be initiated by a detailed examination of ecosystem site parameters.

Since forests are a complex of surface attributes (i.e., an ecosystem), classification of forest ecosystems should not only take into consideration forest properties, but should also reflect spatial patterns (Bailey, 1976). Since the development of ecosystems is influenced to some degree by adjacent ecosystems, regardless of scale, there is an intrinsic advantage of assessing land in terms of interacting units at various scales of grouping. Grouping objects based on their spatial relationships rather than solely their taxonomic properties is called regionalization (Bailey, 1976).

This aspect brings into play an entire body of literature devoted to the concept of landscape ecology. Scientists with backgrounds in geography and biology have provided much insight into understanding the landscape and therefore contributing to the development of landscape ecology. Troll (1971) defined landscape ecology as the physical and biological relationships that govern the different spatial units of a region. These relationships can be defined as vertical (i.e., within a spatial unit) or horizontal (i.e., between adjacent or neighbouring spatial units). However, the emphasis in landscape ecology is generally placed on the horizontal, with landscape being defined as heterogeneous land areas composed of a cluster of interacting ecosystems which are repeated in similar form throughout (Forman and Godron, 1986). Scale is an integral aspect of landscape, although the principles of landscape ecology apply to ecological mosaics at any scale. In studying the structure, function and change of landscapes and associated landscape elements, managers can apply these principles in natural forest landscape management. By considering landscape structure, function and development, this approach fits well with the application of the ecosystem concept at multiple scales.

2.3.1 Forest Site Characteristics

The Society of American Foresters has generally defined site as an area considered as to its ecological factors and with reference to its capacity to produce forests or other vegetation; it

is the ultimate expression of the combination of biotic, climatic, and soil conditions of a (usually) very localized geographic area (Society of American Foresters, 1950). In Ontario, G. Angus Hills and his colleagues developed an hierarchical classification, referred to as the "Ontario Site Classification System" (Hills 1952; 1953; 1958; 1960; 1961; 1976; Hills and Pierpoint, 1960; Hills *et al.*, 1970). This ecological classification system emphasizes the physiographic characteristics of sites and is organized into a multi-level framework for forest management information (Sims and Uhlig, 1992).

A Site Region has been characterized by Hills (1960) as a very broad geographic area in which the same vegetation succession will occur on the same physiographic site, provided the type and degree of disturbance are the same. This provides a management framework for the forester whereby silvicultural treatments will be relatively consistent. Conceptually similar terms to "site region" include "ecoregion" (Crowley, 1967), "physiographic region," "biophysical unit," "landscape," "natural region" (Lacate, 1969), and "biogeoclimatic zone" (Krajina, 1965). The four major descriptors of a Site Region are climate, physiography, vegetation (e.g., forest), and soil. Each are closely interrelated, insomuch as change in one will impact the others (Figure 2.1). Hills developed a series of Site Region maps for Ontario, initially defining seven regions based on temperature regime (Hills, 1952), and later incorporating effective humidity to identify additional site regions (Hills, 1958; Hills, 1960). Forest species may occur in several ecoregions, but may occur in association with different physiographic conditions within different regions.

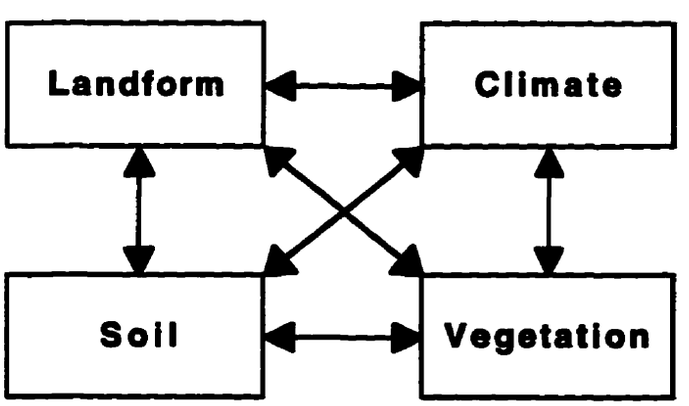


Figure 2.1 The four major descriptors affecting a Site Region (Hills, 1952).

In a regional context, climate is one of the major factors affecting forest development, both directly and in relation to its influence on soil features and development, and topographic variables (e.g., insolation resulting from slope and aspect). The importance of climate is emphasized by the identification of ecoclimatic regions of Canada (Ecoregions

Working Group, 1989). Ecoclimatic regions are defined as "broad areas on the earth's surface characterized by distinctive ecological responses to climate, as expressed by vegetation and reflected in soils, water and wildlife" (Ecoregions Working Group, 1989, p.1). Vegetation succession will be similar for sites within an ecoclimatic region if these sites possess similar environment and terrain conditions (e.g., soils, parent material and terrain position). Ecoclimatic regions adapt themselves nicely into the concept of natural forest landscape management in that vegetation responses and yields are expected to be similar on comparable sites within the same ecoclimatic region. At the Site Region scale, macroclimate is considered to be relatively uniform, since these regions are established by comparing natural successions of vegetation on similar landforms, rather than using meteorological data (Hills, 1960). The Site Region thereby is instrumental in forest management, since it represents an area that will respond similarly to natural disturbances and forestry practices within similar combinations of landforms and forest types (Hills, 1960).

For the many interests incorporated into integrated resource management, a concept of site is required which can be tied to a common frame of reference. To achieve this, it is necessary to look upon site as a total environment; an integrated complex of all the features within a defined area (Hills, 1952). However, Hills (1952) stressed that a site can be characterized by a select number of site components. Due to their stability, he selected physiographic features as the primary basis for representing site.

The management of forest resources is also dependent upon a knowledge of the biological productivity of the land (Hills, 1961). Ecological principles are used to rate physiographic sites for potential biologic productivity. Factors which affect forest growth are identified in Table 2.1. It must be remembered, however, that direct correlations between absolute levels of these factors and forest growth cannot be established since they are all interrelated, and the effect of each will vary according to changes in the other factors (Hills, 1960). This knowledge of site provided the basis for determining the capability of areas for forest production (e.g., timber-use capability (Hills, 1961). This theme extended to the Canada Land Inventory and Ontario Land Inventory of the 1960s and 1970s (Department of Forestry and Rural Development, 1965; 1966; Anonymous, 1977). The purpose of these inventories was to collect a mass of information on the land's characteristics and to classify the land according to its capabilities in each of four sectors: agriculture, forestry, recreation, and wildlife. The limitations prescribed to assess forestry capability were climate, soil moisture, permeability and depth of rooting zone, soil fertility, toxicity, stoniness, and inundation (Department of Forestry and Rural Development, 1966).

Ecological parameters that are important for silviculture include soil fertility, slope,

soil texture, parent material, drainage (moisture regime) and aspect. With these parameters, it is possible to predict the type of regeneration and its potential growth (Levac, 1991). These parameters can only be obtained through detailed examination of site type, a small homogeneous area of land which is homogeneous with respect to the features that dictate the development of natural vegetation on a local area (Hills, 1976). Examination of the forest environment from this perspective provides a basis for the initiation of forest classification.

Table 2.1 Factors Affecting Forest Growth (adapted from Whittaker, 1957; Hills, 1960).

Soil	Nutrient Elements Toxic Elements	includes elements that are not nutritive or toxic, but control the degree of availability of nutrients to the plant
	Soil Moisture Soil Aeration Soil Structure Soil Reaction (pH)	many of these are directly related to the soil profile, while others are more closely related to broader land features (e.g., topography, geologic materials and ground water)
Climate	Atmospheric Features	includes atmospheric features such as sunlight, heat, water and carbon dioxide supplied to the above-ground portion of the forest vegetation; provides mixing of oxygen, carbon dioxide and heat to the organisms both above and below the soil surface
Vegetation	Forest	includes all the higher plants which synthesize material from sunlight
Fauna		includes all the animals which consume, either directly or indirectly, the products synthesized by plants
Saprobes		the group of non-green organisms which reduce organic matter (e.g., micro-organisms, fungi)
Human		human disturbance may be either (1) occasional and/or irregular (e.g., forest fire) or (2) sustained or regular (e.g., planned logging operations, silvicultural treatments)

2.3.2 Forest Stand Characteristics

In the past, emphasis has been placed on managing Ontario's forest resources for timber and fibre production. In response to managers' requirements regarding timber volume and yield estimates, a small-scale, province-wide inventory of forest stands was implemented by the Ontario Ministry of Natural Resources. This group established the Forest Resources Inventory (FRI) section within the Timber Management Division in 1946. The FRI provides a small-scale characterization of the forest and is a starting point for forest management planning at the management unit level. However, it is often relied on for planning at the stand level and when used in this context is incorrectly applied (Baskerville, 1986). One of the

primary objectives of this inventory was to determine the total quantities and the locations of merchantable timber in the province by species and products. From a management perspective, the main concern when the FRI was designed was that of sustainable yield. This survey provides information on stand types, timber volume, stand age, stocking and tree age, but provides limited ecological information. Also, the type maps of the FRI capture only the stand variability for the variables assessed that are observable at a single scale. The confidence in the FRI representation of the forest decreases as forest complexity increases (Baskerville, 1986).

Aerial photographs, combined with ground sampling, became the basis for the FRI program. The first document outlining the forest resources inventory procedure for Ontario was published in 1960, with subsequent editions in 1965 and 1978 (Anonymous, 1978). Of primary importance in the inventory is the measurement of parameters that are related directly to timber harvesting (e.g., volume estimates). To obtain general statistical data on forest stands, the forest is stratified using airphoto analysis techniques. Then, sufficient ground samples are located in each stratum to meet a predetermined level of accuracy within the stratum, and for the forested area as a whole (Anonymous, 1978; Schreuder and Bonner, 1987). Field-based and airphoto interpretation data are correlated to extrapolate statistics for similar stands not sampled in the field. Parameters measured in the field include species composition, stand type, basal area, stand age, tree height, site class and stocking. Forest stands are classified for yield forecasting based on a "site class" parameter (Plonski, 1974), an expression of site quality determined by the height of dominant or co-dominant trees at a specified age (Bonnor and Morrier, 1981). This represents a phytosociological approach to classifying forested lands by indicating the land's productive capacity (Gimbarzevsky, 1978). The FRI has been the dominant information source for determining annual allowable cuts (AACs) (Baskerville, 1986), but often these are grossly overestimated leading to unsustainable harvest levels and public criticism of forest management in Ontario (Paradine, 1994a). Also, the FRI has been demonstrated to be only marginally adequate for prescribing silvicultural treatments (Baskerville, 1986).

The FRI is not designed for implementation of forest management, but is designed as a reconnaissance-level management tool. Specifically, the FRI was designed to estimate volume and forecast yield, and is not suited for prescribing harvesting or silvicultural activities (Pierpoint, 1986). The accuracy of the forest-type maps produced through interpretation of 1:15 840 and 1:20 000 scale airphotos is limited by the intensity of the field sampling and the skill and time devoted to the interpretation. As a result, the FRI only provides an indication of resource composition or form and provides no insight into how

resources are integrated or interrelated (Kleckner, 1981). In this context, there is no consideration of land potential for integrated resource management or sensitivity to management practices. As a result, ecological classifications of forested lands in Ontario have been developed to complement and improve site-specific data for the FRI.

2.4 Forest Ecological Classification - Regional and Local Scales

Classification is the process of ordering or arranging objects into groups or sets based on their interrelationships, whether observed or inferred. Regardless of the approach used (e.g., inductive, deductive, integrated or component), the objective of resource classification should be to simplify the management of land and resources. Classification has taken on a broader meaning to include identification (i.e., the process of assigning unidentified objects to a known class) and regionalization (i.e., the process of identifying and mapping objects over space)(Kleckner, 1981).

Scale becomes a significant issue when classifying ecosystems, and subsequently when attempting to identify and map ecosystems. Hence, ecological classifications are generally built upon an hierarchical framework with an associated hierarchy of mapping scales ranging from regional to local scales. Hierarchical structuring indicates that at any given level within the hierarchy, there are various biological processes interacting within the system (O'Neill *et al.*, 1989). For example, there are processes interacting at lower levels and the particular level of interest is contributing to processes at higher levels. Therefore, processes at any given level are limited by (i) the potential behaviour of its component entities and (ii) by environmental constraints dictated by higher levels (O'Neill *et al.*, 1989). These hierarchies provide a framework for a variety of applications within the context of integrated resource management. Here, the frameworks for surveying and classifying ecosystems are presented. Scale issues, as they pertain to ecosystem mapping and potential for remote sensing, are discussed in detail in Chapter 3.

2.4.1 Ecological Land (Forest) Classification

Forests have been classified from two major perspectives: the geographic and the ecologic. An example of the former includes Rowe (1972) based on Halliday's (1937) forest classification for Canada. The forest regions defined by this work are based on forest characteristics only, and even though climate and physiography may be described, strong ecological links between the forest and these factors are not implicit. The ecological approach to defining the spatial distribution of forests is based on ecosystem structure and function, incorporating vegetation and site characteristics in a climatic and physiographic

zonal system. These define the forest-environment relationships to provide a sound basis for forest management (Hills, 1960), which can be applied at a variety of scales for multiple purposes. In essence, the landscape is perceived as a series of ecosystems, variable in size and nested within one another in a spatial hierarchy (Rowe *et al.*, 1961).

Rowe (1979, p.23) defines ecological land classification as:

> an integrated approach to land survey in which areas of land are classified and mapped according to their ecological unity. The classification process includes the description, the comparison and the synthesis of data related to the biological and physical characteristics of the land.

Driscoll *et al.* (1984) identified two general kinds of ecological classifications for natural resources: integrated and ecosystem element or component. Ecosystem-element classification describes a single component of the landscape (e.g., soil, vegetation, landform, water and climate) to form a hierarchy for each element individually. The Ecoclimatic Regions of Canada represents such a classification, although relationships of climate to vegetation development are emphasized.

The integrated classification incorporates various aspects of the landscape (e.g., vegetation, soil, climate, landforms and water) into a coordinated unit. Systems developed by Bailey (1980) and Wiken and Ironside (1977) reflect this approach. The premise here is to develop a system that expresses the interactive nature of these components to form a unit in relation to adjacent units in a spatial hierarchy (Rowe, 1972). In this sense, ecosystem classification provides a spatio-temporal framework for ecosystem identification, surveying and mapping (Uhlig and Jordan, 1995).

The classification techniques developed through the work of Hills and his colleagues had a major influence on the development of the Canada Land Inventory (CLI) (Department of Forestry and Rural Development, 1965; 1966; McCormack, 1966; 1970) and the Ontario Land Inventory (Anonymous, 1977) in the 1960s and 70s. The physiographic approach was applied to the systematic mapping of the physical characteristics of a landscape to provide a firm base for determining biological productivity and capability to support various uses (Gimbarzevsky, 1978). The CLI was a cooperative federal-provincial program that was administered under the Agricultural Rehabilitation and Development Act (ARDA) of June 1961. The CLI represents a reconnaissance survey (1:250 000 and smaller) of land capabilities and uses (for forestry, agriculture, recreation and wildlife) designed to provide necessary information for resource and land-use planning at the municipal, provincial and federal levels. It was not designed as a management tool since it does not provide the detailed information required for management of individual parcels (Environment Canada, 1978).

Also, since it did not treat the various components within an integrated framework, it was not a true ecological classification. For forestry, the objectives were directed towards providing a classification system rating the potential (productive) capability of the land under indigenous tree species growing at full stocking and under good management (Rees, 1977). In Ontario, Site Regions (Hills, 1960) may be used as a basis for the description of forest capability classes (Boissonneau *et al.*, 1972).

The development of an Ecological (Biophysical) Land Classification in Canada was based on a need for baseline data for the interpretation of the Canada Land Inventory (Wiken and Ironside, 1977; Wiken *et al.*, 1981; Wickware and Rubec, 1989). It was initiated in 1964 by the National Committee on Forest Land (NCFL) which established the Subcommittee on Biophysical Land Classification to study alternatives for a rapid inexpensive approach to land survey. This subcommittee published guidelines outlining a methodology to classify and map ecologically significant units of land, as depicted by their inherent biological and physical characteristics (Wiken and Ironside, 1977) with the purpose of defining units of land significant for resource use and conservation (Rowe, 1979). These physical and biological characteristics include parent material, landform, hydrology, vegetation, climate and fauna (Wickware and Rubec, 1989). These units, or terrestrially based ecosystems, vary with respect to (i) the components that are represented; (ii) spatial size or extent; and (iii) the number and kind of characteristics shared (Wiken *et al.*, 1981). As a result, in the variations in size and commonalities between units, the ELC possesses a hierarchy that is tied closely to scale.

The objective of this interdisciplinary survey was to map and describe ecologically distinct areas of the earth's surface at a variety of spatial scales. The resulting interpretive maps were based on biophysical and physical characteristics defining criteria at each level of generalization (Wickware and Rubec, 1989). The hierarchical nature of ELC, provides for the transfer of information between scales and allows for the aggregation or division of ecological relationships between scales. Although data can be collected and mapped at the site level, data may be scaled upward and be presented at a variety of smaller scales. This provides decision-making information at several administrative or geographic levels (Wiken and Ironside, 1977; Damman, 1979).

Initially, a four-level Biophysical Land Classification system was proposed to divide the natural environment into land units that were a combination of landforms and landform patterns, soils and vegetation (Lacate, 1969) (Table 2.2). Each land unit within a particular level is a more detailed sub-division of the previous level. Since this system was based on classification of vegetated environments, it was well-suited to inventories of forest and

forest-tundra regions. These four levels of generalization were applied in a number of ecological land surveys (Gimbarzevsky, 1978). The basic mapping unit was that of "land type" delineated as a topographic unit occurring on a particular type of parent material. Forests were then mapped within each land type.

Over the last two decades, numerous ecological land surveys have been performed in a variety of environments within Canada. It was observed that Lacate's original four levels of generalization often proved inadequate and, as a result, were modified to suit specific environmental conditions. For instance, Thie (1974) observed that Lacate's system was more land oriented than an integrated land and water system. Although Wiken *et al.* (1981) recognized that the Biophysical Land Classification described an integrated approach to differentiating ecological units within an hierarchical framework, they recognized that the classification was negligent in characterizing land as a terrestrial ecosystem at all levels. This is because it emphasized different environmental factors at different levels and therefore lacked a unifying ecological thread between levels. For example, the land region focused on the effect of ecoclimate on vegetation development, whereas the land district is defined primarily by physiography and geology. As a result, the levels of generalization have evolved over the past 20 years. This evolution is not only in response to a range of different environmental conditions, but also to new mapping technologies, including remote sensing. These levels of generalization are presented in Table 2.2. A summary of the major developments in forest classification in Canada and Ontario is outlined in Table 2.3.

Table 2.2 Levels of Generalization for Ecological Land Survey (adapted from Hills, 1958; Lacate, 1969; Environmental Conservation Task Force, 1981; Wiken, 1986; Wickware and Rubec, 1989; Sims *et al.*, 1994; Uhlig and Jordan, 1995)

Ecological Unit Common Scales of Mapping	Primary Controlling Factors	Definitions
Macroscale	zonal climate, broad geology, and physiography	
Ecoregion‡ Land Region* Site Region** 1:3 000 000 to 1:1 000 000		a part of an ecoprovince characterized by a distinctive ecological response to regional climate, as expressed by vegetation, soils, water and fauna; characterized by regional climate reflected in the vegetation, but is heterogeneous in terms of other ecological phenomena
Mesoscale	landform patterns, physiography, etc.	
Land District* Site District** 1:1 000 000 to 1:500 000		characterized by a distinct relief pattern, geology, geomorphology and associated regional vegetation; range of parent materials
Ecodistrict‡ 1:500 000 to 1:125 000		a part of an ecoregion characterized by a distinctive pattern of relief, geology, geomorphology, vegetation, soils, water and fauna
Ecosection‡ Land System* Land Type** 1:250 000 to 1:50 000		a part of an ecodistrict throughout which there is a recurring pattern of terrain, soils, vegetation, water bodies and fauna
Microscale	local relief, soil type, vegetation, elevation, etc.	
Ecosite‡ (Landscape Level) Land Type* Site Type** 1:50 000 to 1:10 000		a part of an ecosection having a relatively uniform parent material, soil and hydrology, and a chronosequence of vegetation
Ecoelement‡ (Stand Level) <1:10 000 Landtypes Phase 1:2 500		a part of an ecosite displaying uniform soil, topographical, vegetative and hydrological characteristics (e.g., plant community)

* represent levels of generalization defined by Lacate (1969)
** represent levels of generalization defined by Hills (1958)
‡ Canada Committee on Ecological Land Classification (CCELC) Units (1976)

Table 2.3 The Evolution of Forest and Ecological Land Classification in Canada and Ontario (adapted from Hills, 1960; Rowe, 1972; Sims and Uhlig, 1992)

Reference(s)	Synopsis
Regional Level	
Halliday, 1937	produced the original work 'Forest Regions of Canada'; a comprehensive description of the areal distribution of Canada's forests
Rowe, 1972	revised the work of Halliday 'Forest Regions of Canada'; a comprehensive description of the areal distribution of Canada's forests
Hills, 1952; Hills, 1958; Hills, 1960; Hills and Pierpoint, 1960	development of the 'Ontario Site Classification System'; an hierarchical classification that emphasizes physiographic characteristics of sites and is organized as a multilevel framework for forest management
Department of Forestry and Rural Development, 1965; 1966	stemming from the mapping techniques developed by Hills, the 'Canada Land Inventory' (CLI) was developed, evaluating land capability across Canada at scales of 1:250 000 and smaller
Anonymous, 1977	similar to the CLI, the Ontario Land Inventory (OLI) was developed as a land-capability evaluation program for extensive portions of the province
Lacate, 1969; CCELC, 1976	also based on Hills' work, techniques were adapted for an extensive set of land-classification surveys conducted in northern Canada during the 1960s and 1970s ('Ecological Land Classifications'); these programs were intended to provided multiple-resource inventories of northern terrain or broad-area treatments at a regional or provincial level;
Wickware and Rubec, 1989	'Ecoregions of Ontario' is a synthesis and integration of a wide range of environmental information for Ontario within the national ecological database framework developed by the CCELC since 1976
National Vegetation Working Group, 1990	the proposed 'Canadian Vegetation Classification System' uses a combination of physiognomic, structural dominance, and floristics criteria in a seven-level hierarchy
State of Environment Reporting (SOER) Group of Environment Canada, Ottawa, 1994	ongoing activities of the SOER Group to develop a nationally acceptable set of Ecozones and Ecoregions based upon climate, physiography, vegetation and broad soil/landform patterns; in Ontario, Hills' Site Regions are prominent in the definitions of the main terrain units
Local Level	
Hills *et al.*, 1960 (from Sims and Uhlig, 1992)	examined forest succession patterns as they relate to physiography in the Northern Clay Belt (soil moisture regime, depth to bedrock, landform and humus types were recorded for each vegetation type)
Zoltai, 1965; Zoltai, 1974	Hills' approach was applied to an area in NW Ontario where 24 land types were identified based on geologic material, soil texture, soil depth, stoniness and common overstories
Jones *et al.*, 1983 Merchant *et al.*, 1989; Sims *et al.*, 1989	a series of Forest Ecosystem Classifications (FEC) developed for the Northern Clay Belt, Algonquin Region and Northwestern Ontario
McCarthy *et al.*, 1994	FEC completed for Northeastern Ontario

2.4.2 Forest Ecosystem Classification (FEC)

Recently, forest management has emphasized the need to understand and describe the ecological relations of forests. The ecosystem approach is being adopted across Canada as forest managers begin to examine forested lands from an ecosystem perspective. For example, the British Columbia Biogeographic Ecosystem Classification (BC BEC) (Krajina, 1969; Klinka et al., 1979; Meidinger and Pojar, 1991; Banner *et al.*, 1993) has provided detailed ecological survey data since 1987 and has raised the awareness of forest managers to ecological relationships and processes (Pojar *et al.*, 1987). Other forest ecosystem classifications have been developed for Alberta (Alberta Biophysical Ecosystem Classification (A BEC) (Corns and Annas, 1986)), New Brunswick (Zelazny *et al.*, 1989) and Newfoundland (Damman Forest Site Classification) (Meades and Moores, 1989)).

In Ontario, the pioneering work of G.A. Hills and his colleagues in developing an ecological framework for recognizing and describing forest sites in Ontario, along with other regional-level and local-level studies, spawned the development of a series of Forest Ecosystem Classifications (FECs) for northern Ontario. The goal of these FECs is to permit the "accurate, consistent and practical description of forest ecosystems so that existing and new management knowledge can be organized, communicated and used more effectively" (Sims and Uhlig, 1992, p. 68). FECs aim to contribute to the organization of silvicultural practices, and to the knowledge and application of integrated forest management. The framework upon which FEC systems are based incorporates those components of forest stand and site which contribute to local forest characteristics (i.e., canopy and understory vegetation, soils, landform, general climatic regime, and regional physiography (Figure 2.2)). Studies that demonstrate the applicability of FECs to forest management include those by Stanclik (1986), Towill *et al.* (1988), Racey *et al.* (1989) and Wickware (1989).

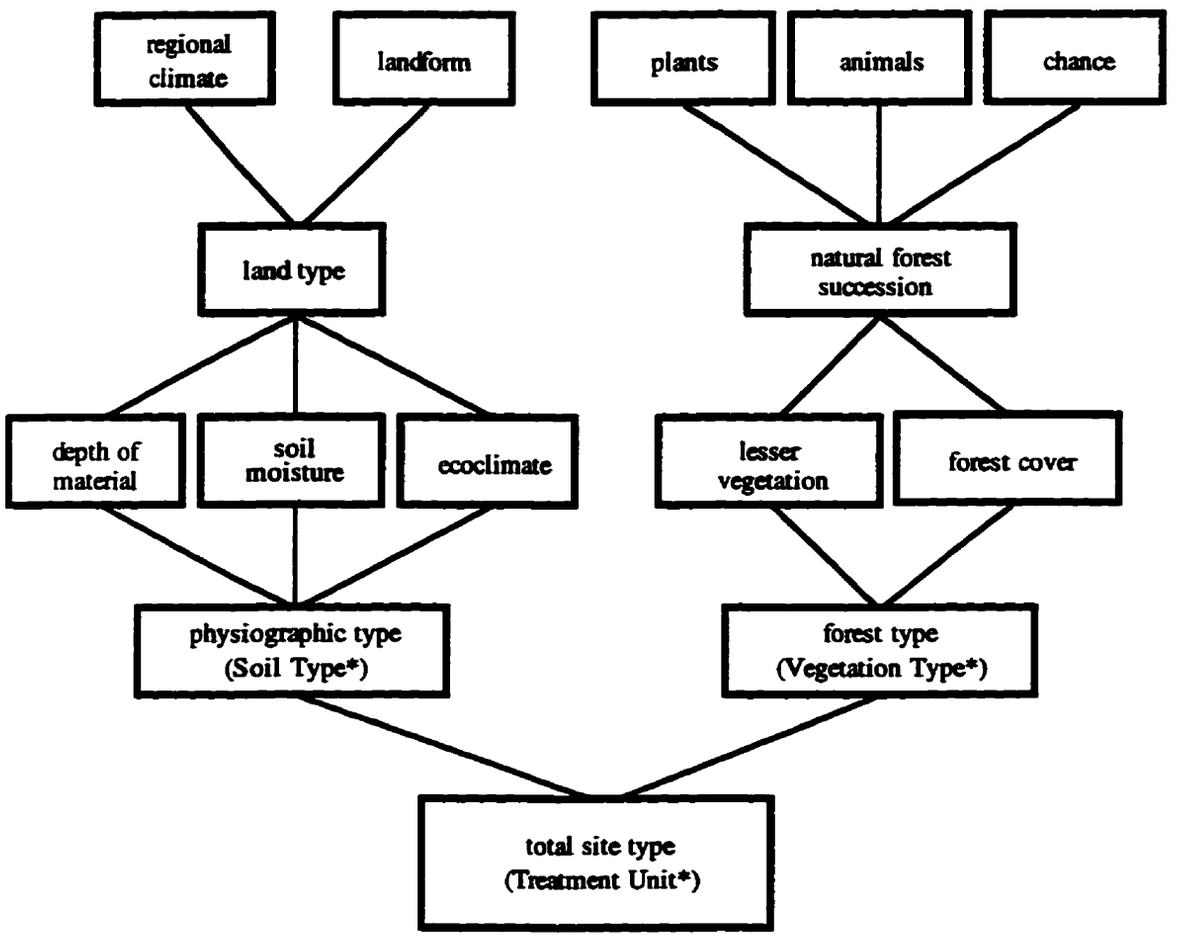


Figure 2.2 Ecological framework for Forest Ecosystem Classifications (FEC) *analogous terms for the NWO FEC (from Sims and Uhlig, 1992) (adapted from Hills and Pierpoint, 1960; Racey *et al.*, 1989).

Forest ecosystem vegetational parameters are summarized through computer-assisted ordination techniques, e.g., detrended reciprocal averaging analysis (Hill, 1979; Gauch, 1982). For Ontario FECs, ordinations are based on relative abundance information for a large number of vegetation species sampled within 10 m x 10 m sample plots. Forest Ecosystem Classifications are primarily intended to be applied at the stand level, and to provide information about those local forest stands, vegetation, soil and site conditions that the forest manager requires for management plans and strategies. The basic units of FECs are "Vegetation Units" and "Soil Units" that are determined through a "key" system (Sims *et al.*, 1989). FEC units (i.e., vegetation and soil units) do not aggregate into truly integrated units as such (Baldwin, 1996) and hence do not represent true hierarchical integration as described by Bailey (1996) and Rowe (1980). However, ecologically similar vegetation units can be

grouped to form lower-resolution units on the basis of general vegetation and soil/site conditions (Sims *et al.*, 1989; Racey *et al.*, 1989). This also provides potential for integration with other forestry data collected and mapped at various scales.

To adapt to a broader landscape level for a variety of management purposes, field-level units can be integrated to create "ecological units" (Hills and Pierpoint, 1960), which have been referred to as Operational Groups (OGs) (Jones *et al.*, 1983), Treatment Units (TUs) (Racey *et al.*, 1989), or Site Types (STs) (Merchant *et al.*, 1989) (Figures 2.2 and 2.3). These aggregations of FEC Soil and Vegetation Types possess similar species composition, productivity, and macroclimatic or ecological properties (Racey *et al.*, 1989), and can be combined with existing forest management knowledge to improve management interpretations and decisions (Sims and Uhlig, 1992) (Figure 2.3).

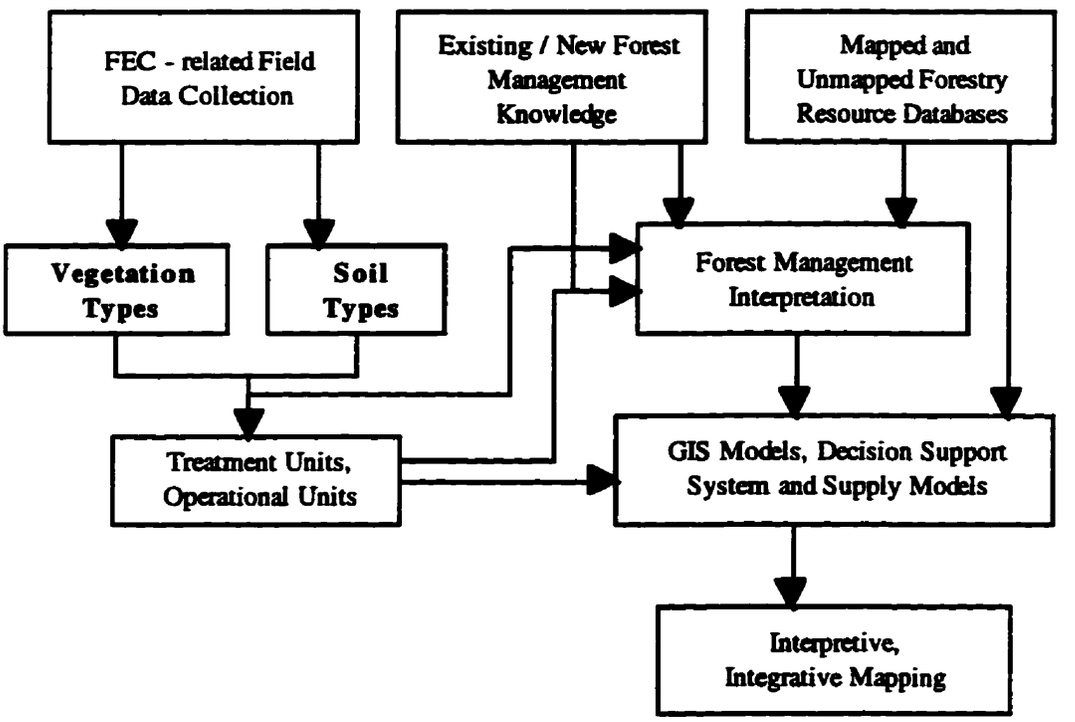


Figure 2.3 Organization of FEC Soil and Vegetation Types (with the input of management information and knowledge, management interpretation may be developed iteratively) (from Sims and Uhlig, 1992).

Forest Ecosystem Classifications have been completed for the Clay Belt (Jones *et al.*, 1983), Northwestern and North Central Ontario (Sims *et al.*, 1989), Northeastern Ontario (McCarthy *et al.*, 1994), and for sites supporting red and white pine stands (*Pinus resinosa* and *P. strobus*) in the Algonquin Region of Central Ontario (Merchant *et al.*, 1989). FECs are currently under development for the Central Region. An extensive FEC computerized

database has been developed that incorporates detailed soil, site and vegetation information from mature or harvestable forest stands (McLean and Uhlig, 1994). This database has been used to acquire a better understanding of the nature, distribution and relationships of soil/site and vegetation in northern Ontario (e.g., Baldwin *et al.*, 1990; Sims *et al.*, 1990; Sims and Baldwin, 1991; Walsh and Wickware, 1991). These classification systems provide ecological information on the structural and functional aspects of a forest ecosystem, information that can be incorporated into forest management practices (Sims *et al.*, 1989; Baldwin *et al.*, 1990).

2.4.3 Northwestern Ontario Forest Ecosystem Classification (NWO FEC)

The Northwestern Ontario Forest Ecosystem Classification (NWO FEC) (Sims *et al.*, 1989) is based on data collected from relatively mature natural forests (> 50 years) occurring over a range of landform and soil/site conditions throughout northwestern Ontario. Landform features with a wide range of slope positions, soil textures and moisture conditions are represented in the NWO FEC. Classification of forest ecosystems is based on a composite of Vegetation (V) and Soil (S) Types. The NWO FEC consists of 38 Vegetation Types and 22 Soil Types.

V-Types are identified through a "keying" process (Figure 2.4). Initially, tree species are used to move within the key, whereas understory and ground-cover conditions are used to move to finer divisions within the key . Vegetation Types are initially divided in three broad categories; mainly hardwood (11 V-Types); conifer mixedwood (9 V-Types) and conifer (18 V-Types)(Table 2.4). Soil Types are initially classified by depth to bedrock, deep soils being greater than 100 cm to bedrock (Figure 2.5). There are thirteen S-Types representing deep soil conditions and nine representing shallow to moderately deep (20 to 100 cm) soil conditions (Table 2.5). Subsequent classification of deep soils is based on field assessments of soil moisture, soil texture and organic-layer characteristics, while shallow soils are differentiated by depth to bedrock, thickness of organic layer and soil texture. Detailed descriptions of all V-Types and S-Types are presented in the NWO FEC field guide (Sims *et al.*, 1989)(e.g., Figures 2.6 and 2.7).

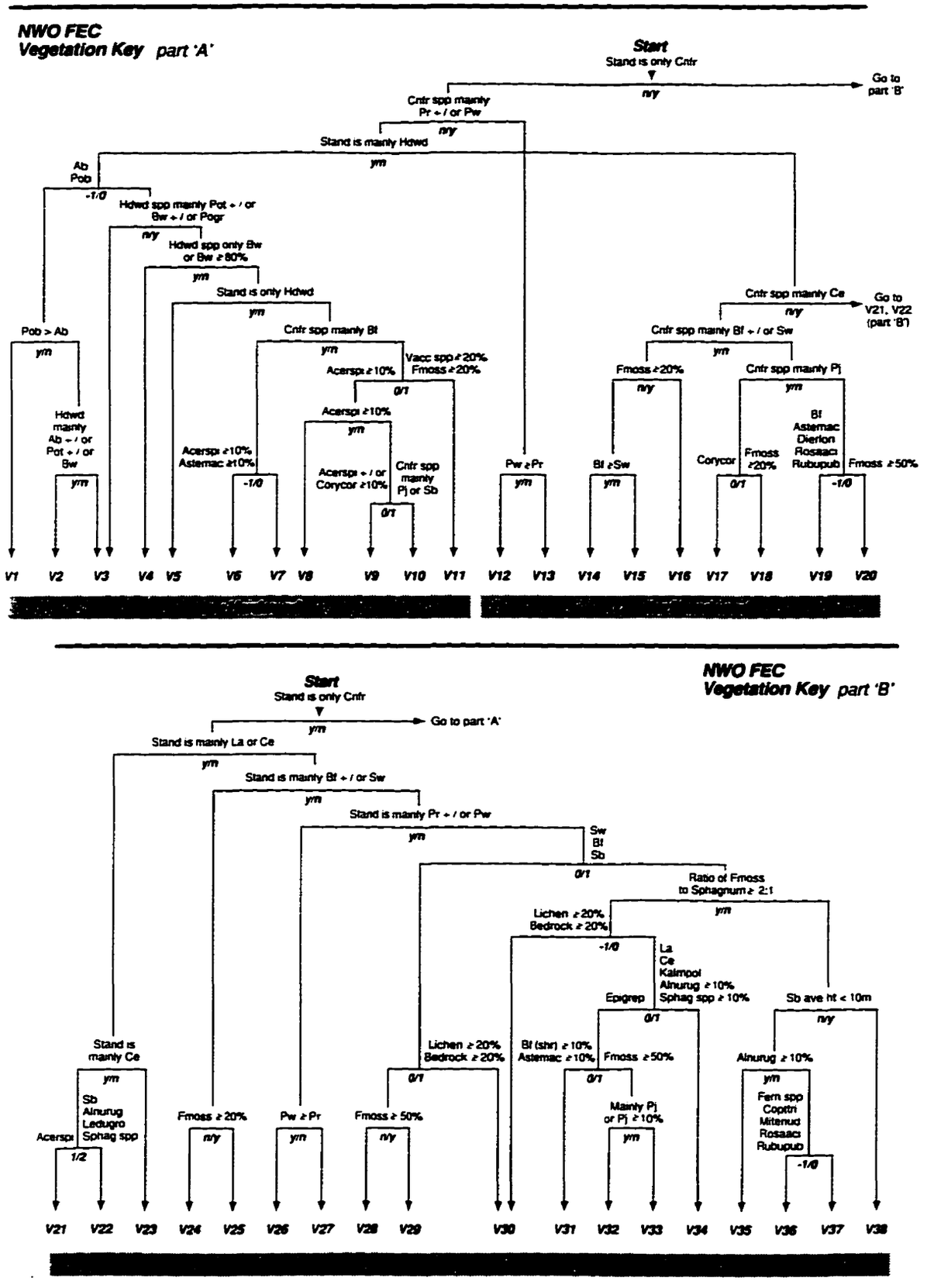


Figure 2.4 NWO FEC vegetation key used to determine V-Type (Sims *et al.*, 1989).

Table 2.4 List of NWO FEC V-Types (Sims *et al.*, 1989).

Mainly Hardwood Vegetation Types

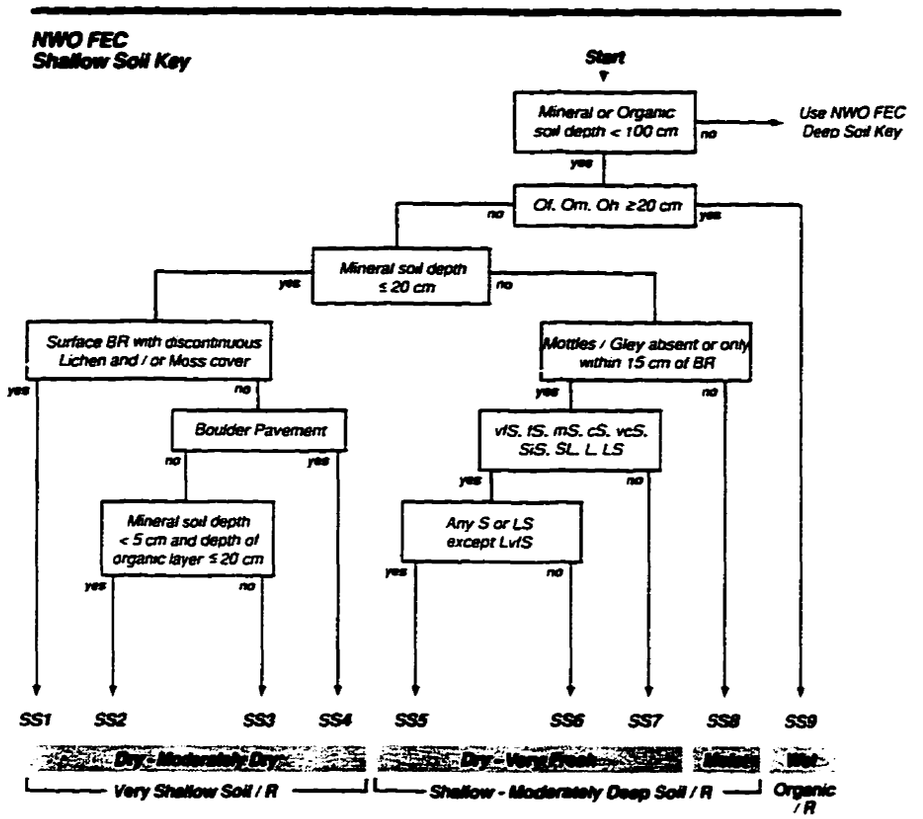
V1	Balsam Poplar Hardwood and Mixedwood
V2	Black Ash Hardwood and Mixedwood
V3	Other Hardwoods and Mixedwoods
V4	White Birch Hardwood and Mixedwood
V5	Aspen Hardwood
V6	Trembling Aspen (White Birch) - Balsam Fir / Mountain Maple
V7	Trembling Aspen - Balsam Fir / Balsam Fir Shrub
V8	Trembling Aspen (White Birch) / Mountain Maple
V9	Trembling Aspen Mixedwood
V10	Trembling Aspen - Black Spruce - Jack Pine / Low Shrub
V11	Trembling Aspen - Conifer / Blueberry / Feathermoss

Conifer Mixedwood Vegetation Types

V12	White Pine Mixedwood
V13	Red Pine Mixedwood
V14	Balsam Fir Mixedwood
V15	White Spruce Mixedwood
V16	Balsam Fir - White Spruce Mixedwood / Feathermoss
V17	Jack Pine Mixedwood / Shrub Rich
V18	Jack Pine Mixedwood / Feathermoss
V19	Black Spruce Mixedwood / Herb Rich
V20	Black Spruce Mixedwood / Feathermoss

Conifer Vegetation Types

V21	Cedar (inc. Mixedwood) / Mountain Maple
V22	Cedar (inc. Mixedwood) / Speckled Alder / Labrador Tea
V23	Tamarack (Black Spruce) / Speckled Alder / Labrador Tea
V24	White Spruce - Balsam Fir / Shrub Rich
V25	White Spruce - Balsam Fir / Feathermoss
V26	White Pine Conifer
V27	Red Pine Conifer
V28	Jack Pine / Low Shrub
V29	Jack Pine / Ericaceous Shrub / Feathermoss
V30	Jack Pine - Black Spruce / Blueberry / Lichen
V31	Black Spruce - Jack Pine / Tall Shrub / Feathermoss
V32	Jack Pine - Black Spruce / Ericaceous Shrub / Feathermoss
V33	Black Spruce / Feathermoss
V34	Black Spruce / Labrador Tea / Feathermoss (Sphagnum)
V35	Black Spruce / Speckled Alder / Sphagnum
V36	Black Spruce / Bunchberry / Sphagnum (Feathermoss)
V37	Black Spruce / Ericaceous Shrub / Sphagnum
V38	Black Spruce / Leatherleaf / Sphagnum



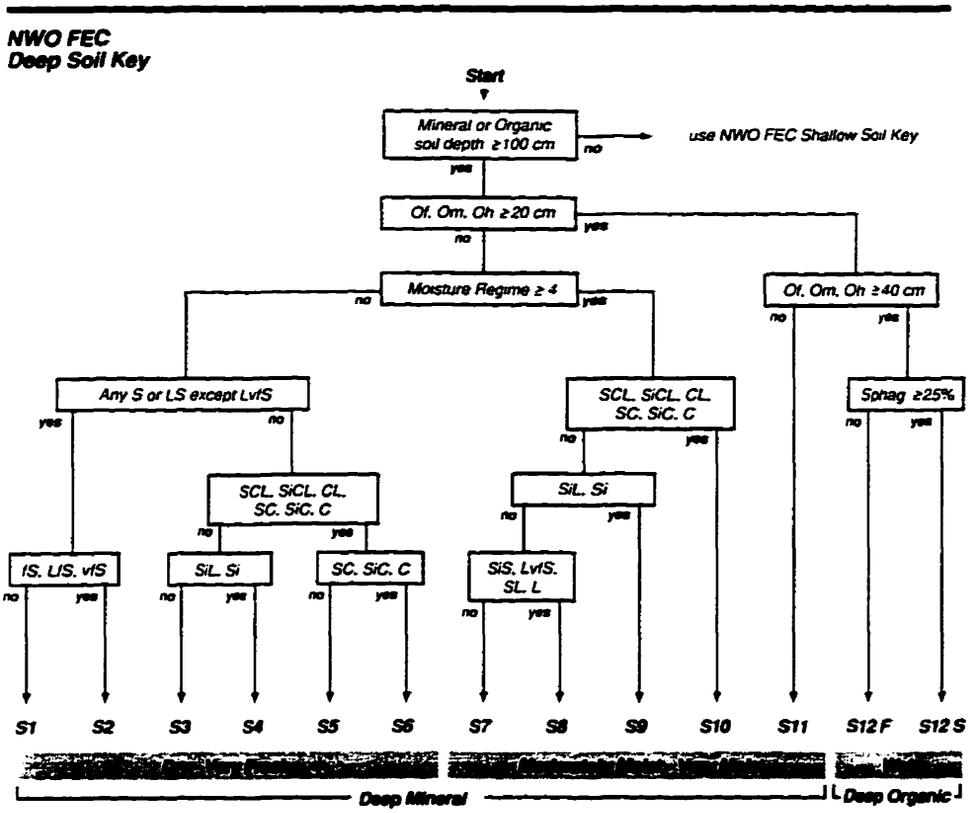


Figure 2.5 NWO FEC Soils key used to determine Soil Type (Sims *et al.*, 1989).

Table 2.5 List of NWO FEC Soil Types (Sims *et al.*, 1989).

Deep Mineral Soil Types

S1	Dry / Coarse Sandy
S2	Fresh / Fine Sandy
S3	Fresh / Coarse Loamy
S4	Fresh / Silty - Silt Loamy
S5	Fresh / Fine Loamy
S6	Fresh / Clayey
S7	Moist / Sandy
S8	Moist / Coarse Loamy
S9	Moist / Silty - Silt Loamy
S10	Moist / Fine Loamy - Clayey
S11	Moist / Peaty Phase

Deep Organic Soil Types

S12F	Wet / Organic [Feathermoss]
S12S	Wet / Organic [Sphagnum]

Very Shallow Soil Types

SS1	Discontinuous Organic Mat on Bedrock
SS2	Extremely Shallow Soil on Bedrock
SS3	Very Shallow Soil on Bedrock
SS4	Very Shallow Soil on Boulder Pavement

Shallow to Moderately Deep Soil Types

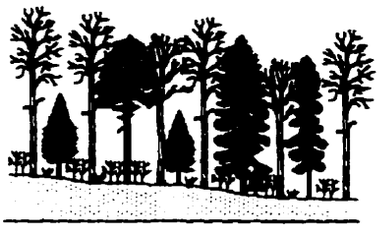
SS5	Shallow - Moderately Deep / Sandy
SS6	Shallow - Moderately Deep / Coarse Loamy
SS7	Shallow - Moderately Deep / Silty - Fine Loamy - Clayey
SS8	Shallow - Moderately Deep / Mottles - Gley
SS9	Shallow - Moderately Deep / Organic - Peaty Phase

V8

Trembling Aspen (White Birch) / Mountain Maple

General Description (n=49): Hardwood mixedwood stands with an abundance of broadleaved herbs and shrubs in the understory. Dense thickets of *Acer spicatum* are characteristic. Occurring mainly on deep, fresh to dry, well to rapidly drained mineral soils.





Overstory Species

trembling aspen [10]
white birch [6]
white spruce [5]
black spruce [5]
jack pine [4]
balsam fir [3]

Common Understory Species

Shrubs: **Acer spicatum**, Rubus pubescens, balsam fir, Corylus cornuta, Diervilla lonicera, trembling aspen, Rosa acicularis, Amelanchier spp., Linnaea borealis, Sorbus decora, Lonicera canadensis

Herbs: Aralia nudicaulis, Streptopus roseus, Clintonia borealis, Maianthemum canadense, Aster macrophyllus, Trientalis borealis, Cornus canadensis, Viola renifolia, Galium triflorum, Lycopodium clavatum, Mitella nuda, Coptis trifolia

Mosses: Pleurozium schreberi, Ptilium crista-castrensis, Rhytidiadelphus triquetrus, Plagiomnium cuspidatum

Forest Floor Cover

Broadleaf litter: 84 Moss: 7 Wood: 5

Soil / Site Characteristics

Soil Groups:	(dp d-f) [7], (mod dp) [1], (dp m) [1]
Thickness of Organic Layer:	[LFH] - (6-15) [8], (1-5) [2]
Surface Texture:	c. loamy [5], silty [2], f. sandy [1], c. sandy [1], clayey [1]
C Texture (when present):	c. loamy [3], c. sandy [2], f. sandy [2], silty [2], clayey [1], f. loamy [1]
Moisture Regime / Drainage:	fresh [7], dry [2], moist [2] / well [5], rapid [4], poor [1]
Mode of Deposition:	morainal [5], glaciofluvial [3], lacustrine [2]

Comments: Within NW Ontario, **V8** is most common in the Central Plateau section of the NC Region; it is found infrequently in the NW Region. Stands of this Type are ecologically similar to those of **V5**, **V6** and **V9**. **V8** stands are distinguished from those of **V5** and **V6** on the basis of overstory composition; higher abundance of *Acer spicatum* separates them from stands of **V9**. Stands of **V8** are often found on calcareous soils.

Figure 2.6 Sample of NWO FEC V-Type description (Sims *et al.*, 1989).

S4

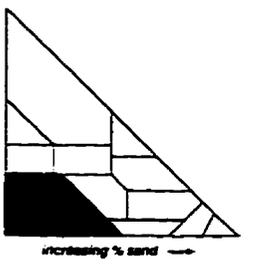
Fresh / Silty - Silt Loamy

General Description (n=98)

Fresh, silty or silt loamy soils. Primarily developed in lacustrine and glaciofluvial parent materials.

Soil / Site Characteristics

Thickness of Organic Layer:	[LFH] - (6-15)[7], (1-5)[2], (16-25)[1]
Forest Humus Form:	fibrimor[5], humifibrimor[2], raw moder[1], medium mull[1]
Surface Texture:	silt loam[5], silty sand[1], sandy loam[1], silt[1], other[3]
C Texture:	silt loam[8], silt[2]
Depth to Mottles / Gley:	none[7], (51-75)[2], (76-100)[1]
Depth to Carbonates:	none[5], (≤ 50)[3], (> 50)[2]
Moisture Regime / Drainage:	fresh[7], v. fresh[3] / well[5], mod. well[3], imperfect[1], rapid[1]
Mode of Deposition:	lacustrine[5], glaciofluvial[3], morainal[1], fluvial[1]



Typical Horizons

L, F, Ae, Bm, Ck

Forest Floor Cover and Associated Vegetation

Upland, black spruce stands are often associated with **S4** soils, especially in the NW Region. In addition, a variety of mixedwood stand conditions is encountered. Forest floor cover is usually dominated by a mixture of broadleaf litter and feathermoss.

Comments

S4 is most common in deep lacustrine and glaciofluvial deposits in the eastern Central Plateau section (NC Region) and in the Dryden and Lac Seul areas (NW Region). Silt loamy soils represent the dominant condition within the Type; silty soils are rare, occurring mainly to the northeast of L. Superior. Coarse fragment content is characteristically low (< 20%). The forest humus condition is typically a thin fibrimor. *Bf* horizons are occasionally present. **S4** soils are generally classed as Brunisols; Podzols and Luvisols are less common. Carbonates are often present in **S4** soils of the NC Region, where they tend to occur within 50 cm of the soil surface; calcareousness is less common in the NW Region. On bedrock controlled topography, soils of **S4** may intergrade with those of **SS7**.

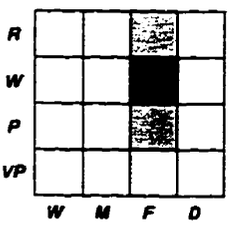


Figure 2.7 Sample of NWO FEC Soil-Type description (Sims *et al.*, 1989).

Ecosystem structure and function are largely regulated along energy, moisture, nutrient and disturbance gradients which are controlled by climate, physiography, soils, hydrology, and flora and fauna (Barnes *et al.*, 1982). However, the influence of each of these factors varies with spatial and temporal scales. For example, at regional scales abiotic factors tend to dominate ecosystem structure and function, while at finer scales both abiotic and biotic factors are important (Damman, 1979)

When displayed graphically, the NWO FEC V-Type ordination can be represented by a two-dimensional diagram (Figure 2.8). This ordination represents a summary of all of the abundance information for all vegetation species recorded in over 2100 NWO FEC field plots. When the average vegetational composition for each V-type is plotted in the ordination, the similarities between V-Types are illustrated graphically (and represented mathematically) by the corresponding distances between them in the diagram. V-Types that are situated close together are more similar than those situated far apart.

Although the axes are not calibrated to an absolute scale, two environmental gradients can be inferred: soil moisture and soil nutrient regime. Therefore, the ordination provides an effective method of relating soil moisture and nutrient conditions to average vegetational composition (Sims *et al.*, 1989). Soil moisture regime and nutrient regime are considered major environmental determinants for the vegetation gradient (Sims *et al.*, 1989; Mackey *et al.*, 1994a). It is also possible to overlay information about other soil/site or vegetation parameters on the ordination and to group V-Types which share similar conditions (e.g., based on major tree species; forest-floor cover, dominant soil-texture classes and moisture regime) (Figures 2.8 and 2.9) (Sims *et al.*, 1989).

These ecological interpretations (termed "Treatment Units") prove useful for a variety of forest management applications, particularly as soil, vegetation, site and climatic factors determine opportunities or limitations to forest management and planning (Racey *et al.*, 1989) (Figures 2.10 and 2.11). These groupings provide a framework upon which a forest manager can adapt integrated management strategies and objectives particularly for silvicultural and wildlife habitat interpretations and management applications.

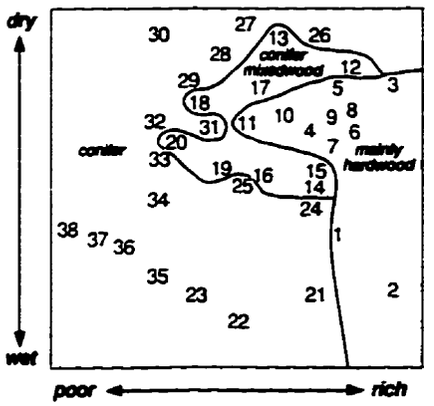


Figure 2.8 NWO FEC V-Type ordination (Sims *et al.*, 1989).

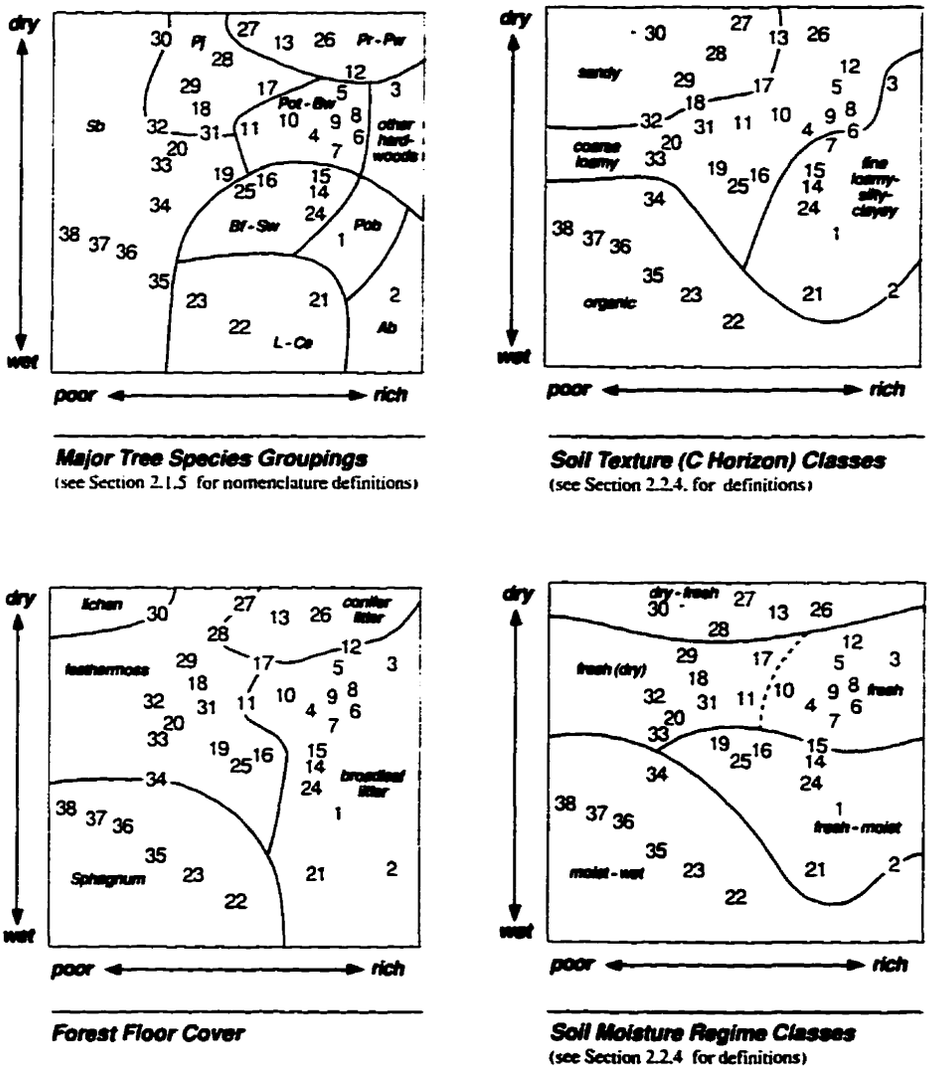


Figure 2.9 Application of the NWO FEC V-Type ordination (Sims *et al.*, 1989).

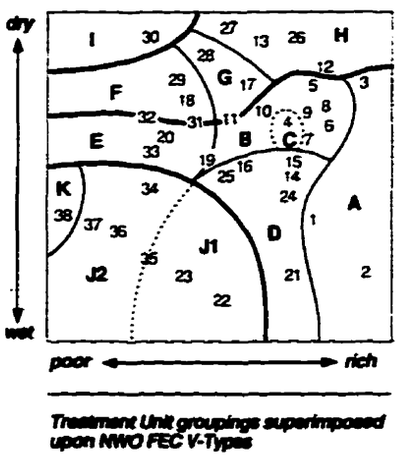


Figure 2.10 Treatment Units superimposed on the NWO FEC V-Type ordination (Racey *et al.*, 1989).

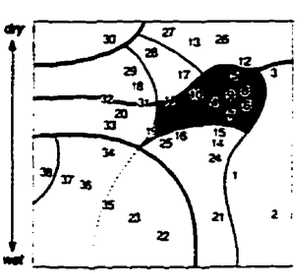
Treatment Unit B

Aspen Hardwood and Mixedwood

Phase B1: Dry - Fresh Soils
Phase B2: Moist Soils

Vegetation Types

V5, V6, V7, V8, V9, V10, V11, V19. Stands range from pure aspen to aspen mixed with white birch, balsam fir, jack pine, black spruce or white spruce. The understory is usually productive with a dense, tall and low shrub layer.

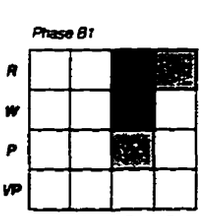


Soil / Site Characteristics

Common NWO FEC Soil Types:

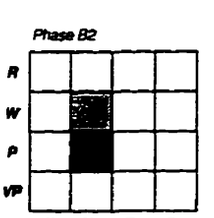
Phase B1: ***S3, S6, S2, S1, S4.*** Deep, moderately dry to very fresh, sandy and coarse loamy, with some clayey, soils.

Phase B2: ***S8, S7, S10, S9.*** Deep, moist to very moist, fine loamy and clayey soils (a wide range of textures).



Mode of Deposition:

Phase B1: morainal, glaciofluvial, lacustrine
Phase B2: lacustrine, morainal, glaciofluvial



Drainage:

Phase B1: rapid to moderately well
Phase B2: imperfect to poor

Figure 2.11 Sample of NWO FEC Treatment Unit description (Racey *et al.*, 1989).



Management Considerations

Harvesting Constraints:

Phase B1: No constraints due to season of harvest. Budworm mortality of balsam fir component could reduce harvest efficiency.

Phase B2: Clayey and fine loamy soils are susceptible to compaction and erosion; winter or dry season harvest may mitigate these risks. Occasional large quantities of rapidly degrading trembling aspen may reduce harvest efficiency.

Competition:

Phase B1: Woody shrub and tree competition from trembling aspen. *Acer spicatum*, *Alnus crispa*, *Corylus cornuta* and balsam fir can be expected. Herbaceous competitors include *Aster macrophyllus* and *Calamagrostis canadensis*. Chemical tending may be necessary. Hexazinone cannot be used on these sandy and coarse loamy soils.

Phase B2: Expect "very heavy" competition from those species mentioned for ***Phase B1***. Chemical tending will be necessary if converting the stand to conifers.

Diseases: Highly susceptible to *Armillaria* spp. in ***Phase B1*** and to a lesser degree in ***Phase B2***. Balsam fir, white spruce and black spruce may also be susceptible to *Inonotus tomentosus* on the same sites where *Armillaria* spp. occurs.

Insects: Stands are vulnerable to spruce budworm if the proportion of balsam fir and white spruce in the stand exceeds 20% of total crown volume.

Regeneration: Regenerates to trembling aspen naturally after summer or winter harvest. Winter harvest of these sites will result in a greater density of suckering. Stand conversion to jack pine, white spruce or black spruce is an option on these sites. A mixedwood condition may be established by planting spruce in a patch-shelterwood situation. Large planting stock may be required for stand conversion.

Limitations to Equipment: Excessive slash from limbs or unmerchantable trees may hinder efforts to expose mineral soil through mechanical site preparation.

Wildlife: Value as moose cover is low in the pure hardwood stands but can increase with higher conifer composition in the understory. Browse production capacity is high, both before and after harvest. Important food source for beavers, other rodents and hare. Value for marten and fisher will increase with age, conifer composition, number of snags and structural diversity.

Comments

Excessive residual hardwood material (limbs, stumps and unmerchantable timber) may contribute to *Armillaria* spp. inoculum leading to infection of subsequent stand. Clonal variation among aspen stands makes soil productivity relationships very difficult to establish, and clonal quality must be considered in any decision on stand conversion. ***Phase B2*** can present serious competition levels and will require more effort to establish crop trees in a stand conversion program; productivity for black spruce, jack pine and trembling aspen will be fairly high.

Figure 2.11 Cont'd

2.5 Natural Forest Landscape Management

Booth *et al.* (1993) propose a new phase or philosophy to forest management that extends integrated resource management to a natural forest landscape approach that is based on the principle of ecological sustainability. This is concerned with maintaining forest ecological integrity and capability to serve all the functions and values dependent upon it. In this sense, the forest landscape is considered an ecosystem unto itself, rather than simply a sum of parts (Barnes, 1986) and implies a coarser scale of observation. Hills (1976, p. 73) defines a natural landscape as "any part of the ecosphere in which the relationship between plant and animal communities and their physical environment is the focus of enquiry." Natural landscape units vary in size and are formed by patterns of natural ecosystems. Rowe (1979) discussed the concept of "environmental management" as a process whereby managers are responsible for safeguarding the components and relationships of the landscape environment that are critical to continued functioning and renewal of the biosphere. However, as custodians, managers are often restricted by the nature of their own background and specialty, e.g., forestry, geology, wildlife, soils, recreation, hydrology, ecology, climate.

Natural forest landscape management differs from integrated forest resource management in that its roots are ecological as opposed to economic, although the goals of integrated resource management include the conservation of biodiversity while maintaining sustainable production of commercial forest products (Thompson and Welsh, 1993). This approach manages the forest at a larger regional or landscape scale, as opposed to the local or stand level, and aims to maintain a continuing supply of all natural forest ecosystem types. Within the scope of integrated resource management, Thompson and Welsh (1993) argue that maintenance of ecosystem types at the landscape scale can maintain commercial forest production as well as conserve biodiversity. Until recently, emphasis on forest management was at the stand level, which was appropriate while it met the benefits that society espoused. Now, however, society demands a wider range of benefits that correspond to new values placed on the forest resource. At the landscape scale, management is more amenable to a range of forest structures, values and uses. Within this framework, landscapes are viewed, classified and managed in ecological terms for sustainable development (Booth *et al.*, 1993).

Rowe (1979) presents a number of arguments regarding an integrated approach to ecological studies and data collection for environmental management, not the least of which is that environment be viewed as an hierarchy of geographic functional wholes or systems ranging from the biosphere to the region and so on, down to the smallest area of significance. Therefore, it is important that environmental management and, in turn, natural forest landscape management be undertaken at more than one scale, with the management of the

landscapes as important as the individual ecosystem. However, the tools (e.g., political, ecologic and technical) for such an holistic approach to forest management are not yet established.

2.6 Summary

Forest information requirements in Ontario have evolved from primarily inventory data to an integration of soil/site and vegetation conditions for a more comprehensive approach to forest ecosystem characterization. The importance of describing a forest from a more holistic viewpoint has been recognized by resource managers as a requirement for integrated resource management and, potentially, natural forest landscape management. Although forest ecosystem classification cannot solve land-use problems, it provides a basis for improved forest productivity and integrated management (Klinka *et al.*, 1980) at a time when forest resources are under increasing pressure.

There are a limited number of resource survey databases available in Ontario, each providing only a part of the information required for silviculture or integrated resource management (Sims and Uhlig, 1992). A comprehensive summary of resource inventories for Ontario has been published by Pierpoint and Uhlig (1985). Some of these are outlined in Table 2.6 along with an interpretation of their overall ability to provide information for integrated resource management. Note that the FEC provides more information related to the forest stand and soil/site, information that can be used effectively for integrated resource management.

Ecological land classification is a basic tool of landscape management that provides an integrated description of the landscape. To properly implement landscape management of forest ecosystems, basic information regarding the structure, function and spatial distribution of the matrix of ecosystems is required. This landscape matrix represents the most extensive and connected landscape element type and plays a predominant role in landscape dynamics (Forman and Godron, 1986). In Ontario, there has been much work on defining ecosystems at various scales and developing inventories of the components that comprise those ecosystems. For example, the NWO FEC provides for functional and structural ecological information that can be incorporated into forest management. These inventories need to be utilized at both the stand and landscape scale. Forest landscape managers require descriptions of patterns, size and thematic character of landscape features. For mapping at landscape scales, natural ecosystems can be synthesized or grouped into patterned units of convenience, for evaluation of areas for specific land uses (Hills, 1976). To ensure the adoption of these types of intensive inventories, technologies and methods must be developed that can reduce

the amount of intensive ground survey. Remote sensing, digital image analysis techniques and data integration within geographic information systems (GIS) offer potential for assisting in the characterization of forest ecosystems at various scales. To support the implementation of forest ecosystem classifications, research into the utilization of remote sensing and GIS technologies for grouping information on vegetation, soils, climate and topography for ecosystems is required. Since ecological land classification attempts to integrate vegetation and physiography, it is important to evaluate how remote sensing and GIS can be utilized within an integrated mapping framework using data collected and mapped at various resolutions and scales.

Table 2.6 An Estimate of the Abilities of Existing Resource Inventories in Ontario to meet Information Requirements for Integrated Resource Management *
(O=not useful, X=useful, XX=very useful) (from Sims and Uhlig, 1992)

	FRI	FEC	Agriculture Soil Survey	OLI	SO/NO EGTS
Planning Horizon					
Short-med. term (1-5 yr.)	XX	XX	X	X	X
Long-term (5-20 yr.)	XX	XX	XX	XX	XX
Normal scale/resolution	1:20 000	Ground-based	1:10 000 (variable)	1:250 000	1:100 000
Extent of coverage in Ontario	widespread	local surveys	scattered (small areas)	widespread	widespread
Species composition	XX	XX	O	O	O
Working group	XX	X	O	O	O
Stand density and spacing	XX	X	O	O	O
Present productivity	XX	XX	O	O	O
Potential site quality	O	XX	XX	X	X
Product type/product amount	X	X	O	O	O
Non-commercial forest types	X	X	X	O	O
Depth of mineral soil	O	XX	XX	X	X
Depth / type of organic matter	O	X	XX	X	X
Soil moisture regime	O	XX	XX	XX	X
Soil texture	O	XX	XX	XX	XX
Macro/microtopography	O	X	XX	X	X
Surficial geology/landforms	O	X	X	X	XX
Wildlife browse prediction	O	XX	X	O	O
Fisheries concerns	X	X	XX	X	XX
Competition prediction	O	XX	X	O	O
Windfirmness	X	X	X	O	O

* FRI = Provincial Forest Resources Inventory (Osborn, 1989); FEC = Forest Ecosystem Classification; OLI = Ontario Land Inventory (Anonymous, 1977); SO/NO EGTS = Southern Ontario-Northern Ontario Engineering and Terrain Survey Maps (e.g., Mollard and Mollard, 1981)

Forests of the future will be more planned, managed and regulated in a conscious effort to maintain biological diversity and support a range of forest values, not just timber

resources. At the same time, some areas will be more intensely managed for timber and fibre production (Forestry Canada, 1990). It is proposed that these objectives can be achieved through the maintenance of ecosystems at the landscape and stand levels. However, this can only be successful when forest resource managers have the necessary resource information with which to effectively evaluate multiple uses. The FEC must now be extended to become more of a mapping tool as opposed to simply a classification tool. For this to become practical, methods of extending the FEC from the site-specific scale to a landscape scale for mapping (e.g., 1:20 000) need to be pursued. Remote sensing and GIS technology offer potential to extend the FEC for northwestern Ontario to a landscape scale in order to better understand the spatial patterns and processes of ecosystems in an integrated approach to forest landscape management. These technologies, along with a comprehensive discussion of spatial resolution and scale, are discussed in Chapter 3 within the context of mapping forest ecosystems.

CHAPTER 3

REMOTE SENSING FOR FOREST ECOSYSTEM CHARACTERIZATION

Remote sensing is the science of deriving information about an object from measurements made at a distance from the object. The quantity most frequently measured in present-day remote sensing systems is the electromagnetic energy emanating from objects of interest as opposed to other possibilities (e.g., seismic waves, sonic waves, and gravitational force) (D.A. Landgrebe, in Swain and Davis, 1978). Remote sensing of electromagnetic energy in the visible and near-infrared portions of the spectrum at high and medium spatial resolutions (i.e., 1 m to 80 m) will be the primary focus of attention in the following sections. These are the primary data used for analysing vegetation at site and landscape scales.

Remote sensing in forestry can be divided into two major components: data acquisition (using sensors to record variations in the way earth-surface features reflect or emit electromagnetic energy) and information extraction (data analysis using visual or digital techniques). Both these components are closely related in that the method by which remote sensing data are collected has a direct impact on the type of information that can be extracted from the data. As a result, most remote sensing data are collected in a specific manner to optimize information extraction.

3.1 Remote Sensing of Forests

Remote sensing data used in forestry studies range from coarse-resolution weather satellite data (>1 km) to high spatial and spectral resolution data acquired with airborne sensors (≤10 m). Medium-resolution earth-resources satellite data with spatial resolutions ranging from 10 m to 80 m provide large-area coverage and are suitable for measuring coarse biophysical parameters or for segmenting the forest into general forest types. Meanwhile, high-resolution airborne and satellite remote sensing data (i.e., spatial resolutions ≤10 m) are primarily used in specific case studies or for research where detailed information on forest stand and structural characteristics is examined.

3.1.1 Satellite Remote Sensing

With the launch of the first Earth Resources Technology Satellite (ERTS-1) in 1972 (later renamed Landsat-1), a new era began with respect to land-resource mapping. Never before was systematic, repetitive, medium-resolution (i.e., 80 m) multispectral data available for the earth's surface. The Multispectral Scanner (MSS) has been carried by each of the five satellites launched in the Landsat series to date. Landsat-4, launched in 1982, carried a second scanner, the Thematic Mapper (TM). Currently Landsat-5 carries both of these multispectral scanners. The Landsat program has provided data for over two decades with Landsat-5 currently in operation. The spectral, spatial and temporal characteristics of Landsat sensors are outlined in Table 3.1. In 1986, the French launched the first of a series of earth-observation SPOT ("Système Pour l'Observation de la Terre" ("Earth-Observation System")) satellites. These satellites incorporate linear array detectors[1] to acquire data at higher spatial resolutions than Landsat (Table 3.1).

Table 3.1 Earth Resources Satellite Systems

Sensor	Spectral Range (μm)	Number of Spectral Bands	Spatial Resolution (m)	Temporal Resolution (days)
Landsat				
Multispectral Scanner (MSS)	0.5-0.6	4	80	16
	0.6-0.7		80	
	0.7-0.8		80	
	0.8-1.1		80	
Thematic Mapper (TM)	0.45-0.52	7	30	16
	0.52-0.60		30	
	0.63-0.69		30	
	0.76-0.90		30	
	1.55-1.75		30	
	2.08-2.35		30	
	10.4-12.5		120	
SPOT*				
HRV (XS)	0.50-0.59	3	20	26
	0.61-0.68		20	
	0.79-0.89		20	
HRV (P)	0.51-0.73	1	10	26

* SPOT consists of two identical High Resolution Visible imaging systems, each of which can operate in either three-band multispectral mode (XS) or single-band panchromatic mode (P). Pointable optics (through a range of +/- 27° off-nadir) provide potential for increased temporal coverage.

[1] Linear arrays normally consist of a series of charge-coupled devices (CCDs) positioned end-to-end. Each detector element is dedicated to sensing a defined range of electromagnetic energy for a single ground resolution cell along any given scan line. The data for each scan line are electronically compiled by sampling each element along the array (Lillesand and Kiefer, 1994). This technology eliminates the need for a rotating mirror to scan across the ground surface, thereby increasing the amount of time that electromagnetic energy can be collected by a detector element.

A number of studies have been carried out comparing data acquired from different satellite sensors when used in forest studies. Lulla (1983) provides a useful summary of studies where Landsat MSS data were used for vegetation analysis and mapping. In comparing Landsat MSS and TM data for forest species identification, Evans and Hill (1990) found that TM performed slightly better than MSS for discriminating between pine species, but was not significantly better for separating pine and hardwood stands. However, Williams and Nelson (1986) achieved a 20 percent improvement in the mapping of detailed Level III (most detailed level of the Anderson *et al.* land cover / land use classification system for use with remote sensor data (1:20 000 - 1:80 000 scale) (Anderson *et al.*, 1976)) forest cover with TM data as opposed to MSS. Bradbury *et al.* (1985) compared Landsat MSS and TM data for classifying woodland and other land-cover types for an area in South Wales. It was found that TM data achieved 90 percent classification accuracy for woodland and provided suitable accuracy levels for identification of some tree species.

In comparisons of Landsat TM and SPOT XS data for biophysical analysis, Ripple *et al.* (1991) determined that the near-infrared bands of both sensors had strong negative correlations to the logarithm of softwood volume (XS 3, $r = -0.89$; TM 4, $r = -0.83$). In addition, Ripple *et al.* (1991) determined that XS and TM data sets exhibited high band-to-band correlations. In a similar study of forest inventory parameters, Brockhaus and Khorram (1992) found that TM data were more likely to be significantly correlated with stand parameters, such as basal area and age class, than SPOT data. When equivalent bands of the two sensors were used to classify six forest classes and one water class in scenes from North Carolina, SPOT achieved slightly better accuracy (74.4 percent versus 70.8 percent). However, when all TM spectral features were included in the classification process, overall accuracy increased to 88.5 percent. Horler and Ahern (1986) found the middle-infrared bands of Landsat TM to be particularly useful for analyzing stem density of coniferous forests, especially for forest regeneration sites in western Ontario, Canada. This would indicate that the spectral resolution of TM is more important than the improvement in spatial resolution that SPOT XS provides. The importance of the additional spectral bands of TM (e.g., mid-infrared) for discriminating ground features has been confirmed for other sites with different environmental conditions (Williams and Nelson, 1986; DeGloria and Benson, 1987; Chavez and Bowell, 1988; Franklin and Wilson, 1991; Joria *et al.*, 1991).

3.1.2 Airborne Remote Sensing

Airborne remote sensing systems present a versatile alternative to spaceborne satellite systems. Airborne systems are flexible with respect to data acquisition parameters (e.g., time of acquisition, frequency of coverage and spatial resolution). As a result, airborne systems provide the best opportunity to collect data that are optimal for extracting specific forest parameters of interest to the user (e.g., damage assessment during insect infestations, monitoring regeneration and analysing forest structural parameters). However, the optimal conditions for data collection are not readily known. In addition, certain characteristics of high spatial resolution data (e.g., spectral variability, bidirectional reflectance) have confounded efforts to extract forest information digitally from remote sensing data. Details of forest stand structure (e.g., density, crown closure, understory) create a very complex mosaic of spectral reflectance values at high spatial resolutions. A review of remote sensing studies using airborne multispectral scanners and imaging spectrometers is presented below. An emphasis is placed on Canadian sensors and studies.

Multispectral scanner (MSS) data acquired from aircraft can be used as a primary source of information, as supplemental data to support more extensive satellite surveys or to provide a testing ground for proposed satellite sensors. Numerous forestry applications for airborne multispectral scanners can be found in the literature. For example, airborne MSS have been used for forest studies on a stand (Irons *et al.*, 1991; Franklin *et al.*, 1991; Miller *et al.*, 1991) and single-tree basis (Hughes *et al.*, 1986; Yuan *et al.*, 1991: Gougeon, 1995), and for estimating biophysical parameters such as biomass (Jensen and Hodgson, 1985), green leaf area index (Curran and Williamson, 1987), and forest-stand parameters (e.g., tree height, crown closure, tree and stand vigour, stand age) (Butera, 1986; Danson, 1987). Measurements of these parameters may then be used to model additional stand characteristics such as basal area and volume (Smith, 1986; Hall *et al.*, 1989).

Airborne multispectral scanners have been used successfully in discriminating tree species using principal components analysis (Leckie and Dombrowski, 1984), evaluating forest regeneration (Brand *et al.*, 1991), and assessing spruce budworm damage on a stand (Ahern *et al.*, 1991a) and single-tree basis (Kneppeck and Ahern, 1989; Leckie *et al.*, 1992). Treitz *et al.* (1992a) reported variable results for identifying detailed ecological classes using 5 m resolution MEIS data in conjunction with a parametric classifier. These variable classification accuracies were attributed to the large spectral variance of forest stands caused by heterogeneous canopies at 5 m spatial resolution.

To date, satellite data have provided relatively poor spatial, spectral and temporal

resolutions for detailed study of forest-stand dynamics. Even with airborne multispectral scanners, remote sensing data collection is limited to a specified and finite number of spectral bands. However, in the past decade, imaging spectrometers have been developed to acquire continuous spectra over land and water surfaces. These include the Advanced Solid-State Array Spectroradiometer (ASAS) (Irons *et al.*, 1991), Airborne Visible-Infrared Imaging Spectrometer (AVIRIS) (Vane *et al.*, 1987; 1993), Compact Airborne Spectrographic Imager (CASI) (Babey and Anger, 1989; Borstad *et al.*, 1989) and the Shortwave Infrared Full Spectrum Imager (SFSI) (Neville *et al.*, 1995). Research into the development of these airborne sensors and analysis of high spectral resolution data (Gaö, 1993; Kruse *et al.*, 1993) will provide a background for development of spaceborne imaging spectrometers for the Earth Observing System (EOS)[2]. Some potential sensors are the Moderate Resolution Imaging Spectrometer (MODIS) (Ardanuy *et al.*, 1991) and High-Resolution Imaging Spectrometer (HIRIS) (National Aeronautics and Space Administration, 1987; Goetz and Herring, 1989) and the European Space Agency's proposed Medium Resolution Imaging Spectrometer (MERIS) (Iantosca *et al.*, 1992). The development of high spectral resolution imaging spectrometers will permit improved study of those narrow-band spectral reflectance features which are characteristic of specific vegetation canopies.

Through field and laboratory studies, a variety of these narrow spectral band features have been shown to be related to changes in vegetation condition and amount. These include physiological characteristics such as chlorophyll amount and/or type (Horler *et al.*, 1983; Rock *et al.*, 1988; 1994; Vogelmann *et al.*, 1993) and canopy chemical characteristics and their relation to carbon cycling (Peterson *et al.*, 1988; Wessman *et al.*, 1988; 1989). High spectral resolution sensors can also be used in the study of bidirectional reflectance characteristics of forest canopies (e.g., Ranson *et al.*, 1994; Abuelgasim and Strahler, 1994). An understanding of these characteristics is essential for the correlation of remote sensing measurements with biomass, species composition, stand structure and reflectance, particularly for wide-view-angle sensors.

Imaging spectrometry data, in conjunction with suitable analysis techniques, may provide a basis for quantitatively measuring phenological change in vegetated terrain which

---

[2]"The Earth Observing System (EOS) is one of the primary components of the NASA-initiated concept Mission to Planet Earth (MTPE). The MTPE is an international earth science program aimed at providing the observations, understanding, and modelling capabilities needed to assess the impacts of natural events and human-induced activities on the earth's environment. EOS is the centrepiece of NASA's contribution to the program. It includes a series of polar-orbiting platforms for long-term global observations, operated in concert with polar-orbiting and mid-inclination platforms developed by Europe and Japan. EOS is envisioned to begin in 1998 and continue for at least 15 years" (Lillesand and Kiefer, 1994; p. 513-514).

results from changes in primary productivity and vegetation vigour. The phenological changes may be in response to regional- and/or global-scale environmental or climatic changes (Miller *et al.*, 1990a). Two assumptions must be satisfied if imaging spectrometry is to be useful in the biophysical analysis of terrestrial ecosystems (National Aeronautics and Space Administration, 1987). First, there must be a strong correlation between canopy characteristics and the rates at which processes important to the biosphere occur. Second, these canopy characteristics must be successfully measured using high spectral resolution remote sensing data. Miller *et al.* (1990a) identified the most significant biogeophysical parameters that can affect plant vigour and primary productivity in terrestrial ecosystems as (i) leaf chlorophyll content, (ii) photosynthetically absorbed radiation (PAR), (iii) canopy water content, and (iv) soil nitrogen content. The authors proposed that it is possible to derive chemical and morphological characteristics from a variety of spectral reflectance parameters that can be measured using various remote sensing tools. These include the measurement of red-edge[3] spectral position (Horler *et al.*, 1983; Rock *et al.*, 1988; Boochs *et al.*, 1990; Miller *et al.*, 1990b; 1991; Vogelmann *et al.*, 1993; Elvidge *et al.*, 1993), normalized difference vegetation index (Tucker *et al.*, 1986), moisture stress index (Cohen, 1991) and shortwave infrared reflectance parameters related to canopy chemistry parameters (Peterson *et al.*, 1988; Wessman *et al.*, 1988; 1989). Further examples of the use of remote sensing data in biophysical studies are discussed in Section 3.2.2.

The CASI has been involved in a number of forestry studies with encouraging results. Representative studies include measuring vegetation red-edge parameters (Miller *et al.*, 1991), deriving spectral signatures for tree species (Gong *et al.*, 1992a), determining surface reflectance anisotropy (Franklin *et al.*, 1991), and identifying forest species and stand parameters (Franklin *et al.*, 1991; Gillespie *et al.*, 1992; Franklin, 1994). Palmier and Ansseau (1992) used laboratory studies of spectra, specifically the red edge, to define spectral bands for CASI data collection to assess chlorosis and stress in sugar maple (*Acer saccharum* Marsh.). For forest-cover mapping, it has been demonstrated that high-resolution CASI data (2.5m) were highly successful in discriminating lodgepole pine (*Pinus contorta* Dougl.), balsam poplar (*Populus balsamifera* L.), trembling aspen (*Populus tremuloides* Michx.) and cottonwood (*Populus trichocarpa* Torr. & Gray), without the addition of ancillary variables (Franklin *et al.*, 1991). The authors also confirmed the variability of

[3]The red edge is the slope of a reflectance spectrum over the range 0.68 to 0.76 μm. Shifts to longer or shorter wavelengths are used to document changes in the chemical or morphological status or health of plants. For example, trees stressed by high concentrations of heavy metals in the soils often display a characteristic shift of the red edge towards shorter wavelengths, often referred to as the blue shift (Lillesand and Kiefer, 1994).

remote measurements of radiance as a consequence of topography and viewing-angle changes. This is a significant observation, and underlies the importance of atmospheric corrections for application of remote sensing data in biophysical analysis and classification.

3.2 Forest Information Extraction

Remote sensing data can be used for a variety of different applications in forestry. The following discussion examines uses of remote sensing for monitoring forest change and biophysical parameters, and for mapping and classifying forest stands.

3.2.1 Change Analysis

The repetitive, synoptic coverage of satellite, and to a lesser extent, airborne remote sensing systems provides for the monitoring of dynamic change in forest environments. This ranges from dramatic short-term changes (e.g., forest harvesting, fire, insect damage) to more subtle long-term changes in forest ecosystems (e.g., succession, growth/regeneration, primary productivity). In the latter sense, satellite data should prove useful for monitoring ecosystem responses caused by environmental change. For monitoring change caused by harvesting or insect activity, temporal satellite data can be used to identify significant levels of forest canopy alteration. Initially, only changed versus unchanged canopies require identification. Once areas of change have been identified, more detailed sampling can be undertaken in order to define the nature of such changes. Landsat TM has become an operational tool for the identification of areas of dramatic change, usually caused by harvesting or fire. As a result, Landsat TM has been used to update large forest databases (Maclean *et al.*, 1992; Maus *et al.*, 1992).

Insect, disease and environmental damage to forest tree species has long been of primary interest to forest managers. Mapping and quantification of forests damaged by biotic and abiotic factors is crucial to managing forest operations, in particular for the planning of control or remedial programs. For instance, in 1985, the spruce budworm (*Choristoneura fumiferana* Clem.) inflicted moderate and severe defoliation on 25.2 million hectares in eastern Canada, the Great Lakes States, and northeastern United States (Leckie *et al.*, 1988a). Early identification of areas affected by insect damage, and timely information on rates of spread/movement, in particular, are required as one component of a program to ensure the long-term viability of the forest industry in Canada. Satellite sensing of insect damage is somewhat limited due to low spatial resolution, poor spectral characteristics and restricted acquisition times of existing platforms (Nelson, 1983; Rencz and Nemeth, 1985), although

more recent high spatial resolution satellites with pointable optics[4] (i.e., SPOT) have demonstrated some success (Franklin and Raske, 1994). Muchoney and Haack (1994) tested four change-detection techniques (principal components analysis, image differencing, spectral-temporal change classification, and post-classification change differencing) to detect gypsy moth defoliation using SPOT multispectral data. Although accuracies for all methods were low, potential for defoliation assessment was demonstrated using principal components analysis and image differencing techniques.

Efforts towards classifying levels of damage caused by spruce budworm have been mainly limited to airborne systems (Ahern *et al.*, 1986; Leckie and Ostaff, 1988; Ahern *et al.*, 1991a). Leckie (1987) has provided a useful review of the factors affecting defoliation assessment using airborne MSS data and the problems encountered. Research examining the spectral characteristics of cumulative damage caused by spruce budworm, leading to selection of optimal sensor spectral bands, has been carried out by Leckie *et al.* (1988a; 1988b; 1989). The spectral differences observed as a result of defoliation were wide-spectral-band features, with the blue, red, near-infrared and middle-infrared showing the greatest sensitivity for discrimination. Although current airborne and satellite sensors operate in these bands, there remains potential for optimizing sensor spectral bands (Leckie *et al.*, 1988a). Examples of remote sensing studies dealing with forest damage assessment are presented in Table 3.2. From examination of these studies, it is evident that (i) the ability to remotely detect forest damage is related to the actual extent of damage; (ii) high spatial resolution data are generally required to quantify the changes that can be detected; and (iii) in general, visual assessment in combination with expert knowledge may be more successful than digital analysis of high-resolution data for monitoring change.

Ahern *et al.* (1991a) identified three areas of research required for spruce budworm damage assessment. These were (i) identification of optimal cost-effective spatial resolutions; (ii) radiometric corrections for large off-nadir viewing angles; and (iii) development of reliable methods for correcting for variable atmospheric path radiance and transmission. As these current limitations are overcome, operational aerial defoliation survey methods using multispectral scanner data should become feasible. For operational forest inventory mapping, including change analysis, Leckie *et al.*, (1995) identify visual discrimination of forest species and parameters as providing the greatest potential. This process requires high-resolution digital multispectral data; radiometric calibration and

[4]Pointable optics provide the opportunity for side-to-side off-nadir viewing, allowing for more frequent coverage of a specific area, as well as full-scene stereoscopic imaging from two different satellite tracks.

atmospheric correction; correction for bidirectional reflectance distribution function (BRDF), geometric correction; and image enhancement (Leckie *et al.*, 1995).

3.2.2 Biophysical Remote Sensing

In addition to identifying short-term change, remote sensing data can also be used to collect biophysical information that can be useful for monitoring and predicting long-term changes of ecosystems. In his review article on biophysical remote sensing, Jensen (1983) stated that data collected by remote sensing (ratio-scaled data) for biophysical variables may be more suitable for modelling and simulation than land-use and land-cover information (nominal-scaled data), which are often used in modelling physical processes. Recent studies using remote sensing methods have focused on the study of biogeochemical processes, including biogeochemical cycles. For these studies, inventories of vegetation characteristics (e.g., biomass, primary productivity, photosynthetic activity) and physiologic processes (transpiration flux, leaf moisture content) are essential.

Characteristics of a plant canopy (e.g., composition, height, density, sociability) are, collectively, strong indicators as to the state of an ecosystem as a whole and represent the physical interface for which optical remote sensing is able to provide quantitative measures. For example, changes in water and nutrient availability are reflected in the amount and seasonal duration of leaf area, in addition to changes in reflectance (National Aeronautics and Space Administration, 1987). Conventional forest inventories acquired through the analysis of aerial photographs provide a starting point for predicting forest growth by characterizing forest stands with respect to species, age, stocking and site quality. However, these standard forest inventories fail to describe stands adequately in terms of the key determinants to stand growth - the structure and quantity of the foliage present in the stand canopy.

Satellite data provide an attractive potential solution to this problem since these data are able to quantitatively characterize stand canopies via spectral reflectance at frequent intervals (Ahern *et al.*, 1991b). Some fundamental biophysical variables that can be measured directly include colour and spectral signature, vegetation chlorophyll absorption characteristics, vegetation biomass, vegetation moisture content, soil moisture content, temperature and texture/surface roughness (Jensen, 1983). As an example, all other conditions being equal, a decrease in vegetation moisture content will be accompanied by an increase in reflectance in the middle-infrared spectral wavelengths. Hybrid variables can be derived from fundamental variables (e.g., vegetation stress can be derived from vegetation chlorophyll absorption characteristics and moisture content) (Jensen, 1983). In addition to forest cover type, the most common forest characteristics that have been studied with remote

sensing data involve stand structure, in particular, crown closure, basal area, leaf-area index (LAI) and tree size (Spanner *et al.*, 1984a; Franklin *et al.*, 1986; Peterson *et al.*, 1986).

Table 3.2 Examples of Damage Assessment of Forests using Remote Sensing

Condition	Synopsis	Reference
Spruce Budworm	evaluates the factors affecting defoliation assessment (radiometric, topographic, scene related, etc.) and emphasizes that the magnitude of these factors can be larger than the range of differences between healthy and severely defoliated trees	Leckie, 1987
Spruce Budworm	from *in situ* spectrometer measurements, determined that the most effective bands for discriminating levels of defoliation were: 2030-2210, 660-670, 1560-1620, and 770-790 nm	Leckie *et al.*, 1988a
Mountain Pine Beetle	tested SPOT-enhanced visual products to determine effectiveness in detecting insect mortality; areas 1-2 ha in size with 80-100% red crowns could be detected; not suitable for control program	Sirois and Ahern, 1988
Eastern Hemlock Looper	SPOT HRV multispectral data were classified to successfully discriminate two classes of hemlock looper damage, moderate/severe and light	Franklin, 1989
Mountain Pine Beetle	MEIS 1.2m data were superior to MEIS 3.4m and conventional aerial photography for detection of red crowns through visual interpretation in British Columbia; natural colour composites were optimal for visual assessment	Kneppeck and Ahern, 1989
Sugar Maple Decline	found a close relationship between sugar maple decline and spectral (principal component 2) and texture (contrast) features in aerial multispectral video imagery; based on examination of single-tree canopies	Yuan *et al.*, 1991
Spruce Budworm	7m resolution MEIS data was acquired to classify cumulative defoliation and three levels of current defoliation (light, moderate, severe); a per-pixel MLC based on 8 spectral bands achieved 72% accuracy for six classes relevant to defoliation survey; the majority of misclassifications were between adjacent healthy and current defoliation classes	Ahern *et al.*, 1991a
Norway Spruce *(Picea abies (L.) Karst.)* Defoliation	found that the decrease in TM band 4 reflectance was the single consistent spectral effect of moderate defoliation on Norway Spruce (ratio methods seemed inappropriate when defoliation was the sole symptom of decline as opposed to defoliation and chlorosis) (stand parameters requiring control included age, density and proportion of hardwood and conifer components)	Ekstrand, 1994
Spruce Budworm	SPOT multispectral data along with NDVI and chromaticity measures were used to discriminate four damage classes; discrimination of damage classes was improved when the sample sites were stratified by species composition, density, age and height	Franklin and Raske, 1994
Spruce Budworm	with a limited number of sample plots, spectral discrimination of four levels of defoliation using high altitude videographic data ($2m^2$) was 68% accurate, which increased to 78% when a texture image was included	Franklin *et al.*, 1995

Jensen (1983) warns, however, that in order to extract meaningful information on biophysical properties, the nature of spatial, spectral, temporal and radiometric resolutions must be understood. These properties are loosely coupled with a number of factors which influence the optical properties of forest canopies. It is particularly important to understand the effects of these parameters on forest canopy spectral response in order to quantitatively interpret biophysical variables. These factors are summarized in Table 3.3. For example, correcting for atmospheric effects increases the slope of the regression line for TM spectral radiance and LAI, thereby producing greater sensor sensitivity to LAI (Running *et al.*, 1986).

Estimates of ground biophysical variables from spectral reflectance measurements can be derived using two types of analysis techniques: (i) deterministic or stochastic canopy radiation models; or (ii) empirical spectral indices. Analytical techniques model the radiative transfer process between the land surface and the sensor to invert reflectance measurements to a particular physical parameter (Otterman *et al.*, 1987; Goel, 1988). Goel (1988) presents a useful overview of the factors affecting canopy reflectance (e.g., incoming solar flux, spectral properties of vegetation elements, canopy architecture and scattering from the soil or ground-surface features) and how these factors can be used to model canopy reflectance. Nemani *et al.* (1993) describe radiation models as rigorous in their treatment of radiative transfer in vegetation canopies, but are difficult to parameterize and are often developed for relatively homogeneous vegetation covers. Consequently, these are more suited to agricultural canopies as opposed to heterogeneous forest canopies consisting of species mixtures with variations in leaf optical and structural properties. Radiative transfer models rarely simulate forest heterogeneity or generally require input data for parameterization at resolutions that are difficult to obtain. Research on invertible canopy models has made significant progress (e.g., Li and Strahler, 1985; 1986; Goel and Grier, 1986a; 1986b; 1988; Franklin and Strahler, 1988), but for forest conditions, such models are not yet operational (McGwire *et al.*, 1993).

The majority of studies which estimate biophysical variables from remotely sensed data (Table 3.4) have used empirical techniques to relate spectral data and various derivatives to biophysical parameters. If biophysical parameters are strongly correlated with remotely sensed radiance data, then these data can be used to predict those biophysical characteristics for variable scene and sensor characteristics over large areas. For example, index-based techniques have been used to estimate vegetation parameters (e.g., LAI, biomass, IPAR) or soil attributes (e.g., composition, brightness, moisture) (McGwire *et al.*, 1993). If strong correlations could be obtained consistently with these biophysical parameters, they would prove useful for monitoring long-term environmental changes of such critical characteristics as primary productivity.

Table 3.3 Factors Affecting Spectral Response of Forest Canopies

Factors	Description	Reference
External		
Size of Viewed Area	variability of the spectral response of a forest canopy will depend on the size of the instantaneous field of view	Guyot *et al.*, 1989
Sun Elevation	solar radiation penetrates more deeply into a canopy at steep angles; bidirectional reflectance increases in the visible and decreases in the near-infrared with increasing sun elevation, particularly with dense forest canopies; leaf transmittance is low in the visible, but up to 50% in the near-infrared	Kimes *et al.*, 1986; Guyot *et al.*, 1989
Zenith View Angle	natural surfaces do not perform as Lambertian reflectors; spectral radiance of surfaces varies as a function of view, zenith and orientation angles; bidirectional reflectance for continuous canopies is wavelength dependent	Stohr and West, 1985; Guyot *et al.*, 1989; Curran, 1980
Cloud Cover	clouds modify the irradiance level for a given sun elevation and significantly change the proportion of direct and diffuse radiation reaching the earth's surface	Guyot *et al.*, 1989
Atmospheric Aerosols	modify the optical path between the satellite and earth surface; wavelength dependent; more pronounced at shorter wavelengths	Guyot *et al.*, 1989
Wind Speed	affects the geometry of the forest canopy	Guyot *et al.*, 1989
Internal		
Orientation of Tree Rows (plantations)	light penetration varies as a function of row direction (a function of plantation); these structural aspects of plantations are thought to be more directly correlated with spectral response than canopy cover	Guyot *et al.*, 1989; Danson and Curran, 1993
Soil Optical Properties	background spectra may confound changes in the spectral response of the overstory vegetation; optical properties of soil show an increase in reflectance from the visible to middle-infrared	Ranson *et al.*, 1986; Guyot *et al.*, 1989
Canopy Geometry (closure, density)	the most significant factor acting on the optical properties of forest canopies (controls the fractions of overstory and understory visible to the sensor)	Guyot *et al.*, 1989
Terrain (slope angle and aspect)	terrain elements account for appreciable variations in response in all wavelength bands; slope and aspect can produce a wide range of pixel values within one cover class; this effect is linked to solar elevation and azimuth	Stohr and West, 1985
Height, Vigor and Composition of Species	density, height and vigor of vegetation and percent composition of species affect the spectral response of forest canopies; these affects directly impact forest change assessment and classification	Price, 1986; Riordan, 1982; Wickware and Howarth, 1981

Table 3.4 Examples of Biophysical Remote Sensing of Forests

Variable(s)	Synopsis	Reference
LAI	strong correlations between LAI and Landsat TM reflectance of aspen early in the growing season disappeared as the understory developed	Badhwar *et al.*, 1986a
Spectral Shift (*blue shift*)	detected a 5nm shift away from the normal inflection point of the red edge reflectance feature towards shorter wavelengths; a result of stress	Rock *et al.*, 1988
Forest Damage (foliar loss (%))	TM shortwave-IR to near-IR band ratios were found to correlate well with ground-based measurements of forest defoliation	Vogelmann and Rock, 1988
Forest Productivity	TM data, in conjunction with biogeographical and ground plot data, were used to successfully model forest productivity at the landscape level, but the reliability of single pixel estimates was poor	Cook *et al.*, 1989
LAI	the relationship between LAI of coniferous forests and TM data corrected for atmospheric effects and sun-surface-sensor geometry was affected by canopy closure, understory vegetation and background reflectance	Spanner *et al.*, 1990a
Timber Volume	vegetation-condition indices generated from shortwave-IR and near-IR TM bands showed strong correlations with net annual spruce-fir volume change; useful for stand development forecasting	Ahern *et al.*, 1991b
Timber Volume	found good correlations between stand volume and normalized difference of TM bands 4 and 5 for homogeneous stands (this capability was reduced at low volumes due to spatial heterogeneity and at high volumes due to complete canopy closure)	Gemmel and Goodenough 1992
Single-Tree Defoliation	a linear relationship existed between visually estimated tree defoliation for trees with >20% defoliation and spectral features of 40cm MEIS data; NDVI provided the best correlations with defoliation	Leckie *et al.*, 1992
LAI	demonstrated the potential use of Landsat TM data for studying seasonal dynamics in forest canopies by obtaining strong correlations between LAI and NDVI for Sept'88 and Mar'89	Curran *et al.*, 1992
Canopy Density	Landsat TM4 was shown to be the primary element for developing vegetation indices for correlation with canopy density; canopy density showed stronger correlations for coniferous stands as opposed to deciduous; and low canopy density and rugged terrain were the major error sources for canopy density estimation	Chiao, 1992
Foliar Biochemical Content	AVIRIS data were shown to have strong correlations with chlorophyll and cellulose and to a lesser extent nitrogen and lignin; maps of chlorophyll were obtained after temporally averaging 4 dates of imagery; while maps of cellulose; lignin and nitrogen were obtained after temporal and spatial averaging	Smith and Curran, 1995

Curran (1980) observed that as biomass increases and the canopy becomes more complete (i.e., LAI increases), the relationship between multispectral reflectance and vegetation amount can be considered linear for the majority of cases. Numerous studies have since shown the correlation between remotely sensed red and near-infrared reflectance of coniferous forest stands to plant biomass (LAI) (Tucker *et al.*, 1981; Spanner *et al.*, 1984a; Badhwar *et al.*, 1986a; 1986b; Franklin, 1986; Running *et al.*, 1986; Peterson *et al.*, 1987; Spanner *et al.*, 1990b). There is a consistent negative relationship between red radiance and LAI, and a weak or slightly positive relationship between near-infrared radiance and LAI. As a result of increased green vegetation and shadow within the canopy, there is a decrease in visible reflectance. An increase in near-infrared reflectance should also occur; however, increased shadow in a complex canopy acts to suppress near-infrared reflectance. This influence of canopy is significant, and even in stands with variable understory, canopy cover is considered the most important variable in determining canopy reflectance (Spanner *et al.*, 1990a; Stenback and Congalton, 1990). Conversely, in a coniferous forest plantation which is managed to maintain a large amount of green vegetation with little spatial variation, this relation may be weaker, as stand structural characteristics (tree density, mean tree height, mean tree diameter) become more closely correlated with stand spectral response (Herwitz *et al.*, 1989; Danson and Curran, 1993). For open canopies, near-infrared reflectance from understory, particularly broadleaved species, dominates the overall reflectance (Badhwar *et al.*, 1986a).

Many of these investigations have suggested that simple transformations of band reflectances are more closely correlated with plant biophysical qualities (Wiegand *et al.*, 1991) and are generally less sensitive to external variables such as the solar zenith angle. An example of one of these transformations is the "normalized difference vegetation index" (NDVI) (Badhwar *et al.*, 1986b), although there are also various derivatives of NDVI (White 1991; Kogan 1990). Along with NDVI, the most common vegetation indices utilize the information content of the red and near-infrared canopy reflectance or radiances. This transformation is highly correlated with green-leaf biomass (Jensen, 1983). Chlorophyll absorption in the visible portion (0.5-0.7 μm) of the spectrum is high (reflectance <20%), whereas reflectance and transmittance are about equal in the near-infrared portion (40-50%) (Smith, 1983). This physiological relationship has been used to estimate the intercepted, photosynthetically-active radiation (IPAR) of plant canopies (Asrar *et al.*, 1984; Sellers, 1985; Baret and Guyot, 1991; Sellers *et al.*, 1992) percent canopy cover (Richardson and Wiegand 1977), chlorophyll content (Tucker 1977) and LAI (Asrar *et al.*, 1984; Baret and Guyot, 1991) through the use of various ratios (Sellers, 1985). Nemani *et al.*, (1993) used the

middle-infrared band of Landsat TM to correct for understory and background effects on NDVI for estimating LAI. Some of these ratios and their applications are described in Table 3.5. It must be remembered that these indices are also sensitive to the internal and external factors that affect spectral reflectance of vegetation (i.e., those described in Table 3.4). However, Goward *et al.* (1994) found that variations in vegetation indices for western Oregon originate from changes in both canopy spectral characteristics and background spectral reflectance, rather than simple variations in LAI or percent canopy closure. Caution must therefore be taken when relating changes in vegetation indices to vegetation physiognomic properties at regional and global scales.

The use of vegetation indices with wide spectral-band remote sensing data is not appropriate for areas of low green-canopy cover since background rock, soil, ground surface and litter materials produce a range of vegetation index values (Huete *et al.*, 1985; Elvidge and Lyon, 1985; Huete and Tucker, 1991). The development of high spectral resolution imaging sensors (e.g., AVIRIS, CASI) has led to the study of terrestrial materials using new analysis techniques. Once the physical nature of the materials within the sensor field of view are determined, quantitative estimates of their abundance can be made using spectral mixture analysis methods (Roberts *et al.*, 1993; Foody and Cox, 1994). For example, spectral mixing methods have been used to model the relative contributions of green vegetation and soils to image spectra (Huete, 1986; Smith *et al.*, 1990a; 1990b; Gong *et al.*, 1992a; Roberts *et al.*, 1993). Such methods provide derived quantitative estimates of vegetation and soil abundance (e.g., Smith *et al.*, 1990a; 1990b), as well as non-photosynthetic vegetation and shade (Roberts *et al.*, 1993).

Leaf area of closed canopy forests is an important ecological parameter used in numerous studies. Leaf-area index (LAI) is a standard expression for the leaf area of a plant community and is defined as the total leaf area per unit ground cover (Herwitz *et al.*, 1989). Light interception, gas exchange, photosynthesis and biomass production are all closely related to LAI (Nemani *et al.*, 1993; Peterson *et al.*, 1987; Herwitz *et al.*, 1989; Bonan, 1993). Regional variations in LAI have been found to be linearly related to site water balance (Nemani and Running, 1989) and above-ground net primary production and stand volume (Gholz, 1982; McLeod and Running, 1988). For global change studies, satellite-derived measures of vegetation cover type and LAI may be used to provide more accurate estimates of the carbon content and exchange rates of global vegetation than are possible with current data (Running *et al.*, 1986). For instance, Mack *et al.* (1990) used vegetation indices derived from Landsat MSS data to examine the relationship between vegetation cover and CO_2 flux density for an agricultural and forested area.

Table 3.5 Examples of Ratio-based Indices for Biophysical Studies (adapted from Cohen, 1991; Major *et al.*, 1990)

Index	Landsat TM Equivalent	Description	Origin
Near-IR / Red Reflectance Ratio (Ratio Vegetation Index))	TM4/TM3	responds to changes in amount of green biomass, chlorophyll content and leaf-water stress	Birth and McVey, 1968; Tucker, 1979
Normalized Difference Vegetation Index (NDVI)	(TM4-TM3)/(TM4+TM3)	responds to changes in amount of green biomass, chlorophyll content and leaf-water stress	Rouse *et al.*, 1974; Tucker 1979; Cihlar *et al*, 1991; Sellers *et al.*, 1992; Goward *et al.*, 1994; Yoder and Waring, 1994
Infrared Index	(TM4-TM5)/(TM4+TM5)	infrared index more closely tracks changes in plant biomass and water stress than NDVI	Hardisky *et al.*, 1983
Moisture Stress Index	TM5/TM4	tracks changes in plant water stress	Rock *et al.*, 1985
Leaf Water Content Index	$\frac{-\log[1-(TM4-TM5)]}{-\log[1-(TM4_{ft}-TM5_{ft})]}$ ft represents reflectance in the specified bands when leaves are at their max. relative water content	responds to changes in water stress	Hunt *et al.*, 1987
Mid-IR Index	TM5/TM7	shows a strong correlation with soil moisture	Musick and Pelletier, 1988
Vegetation Condition Index (VCI)	$\frac{100(NDVI_{ij}-NDVImin_j)}{NDVImax_j-NDVImin_j}$	portrays weather dynamics more effectively than NDVI for non-homogeneous areas by removing the influences of geographic resources such as climate, soil, vegetation type and topography	Kogan, 1990
Perpendicular Vegetation Index (PVI)	$\frac{[s(TM4)-TM3+a]}{[1+(s)^2]^{1/2}}$ a = soil line intercept s = slope of the soil line	attempts to eliminate differences in soil background and is most effective under conditions of low LAI (arid and semi-arid environments)	Richardson and Wiegand, 1977; Wiegand *et al.*, 1991
Weighted Difference Vegetation Index (WDVI)	TM4-s*TM3 s = slope of the soil line	WDVI is a mathematically simpler version of PVI, but it has an unrestricted range	Clevers, 1988

Table 3.5 continued

Index	Landsat TM Equivalent	Description	Origin
Soil Adjusted Vegetation Index (SAVI)	$\frac{(TM4-TM3)(1+L)}{(TM4+TM3+L)}$	L is a correction factor which ranges from 0 for very high vegetation cover to 1 for very low vegetation cover; minimizes soil-brightness induced variations	Huete, 1988; Huete and Tucker, 1991; Qi *et al.*, 1993
Transformed Soil Adjusted Vegetation Index (TSAVI)	$\frac{s[TM4-s(TM3)-a]}{[aTM4+TM3-a*s+X*(1+s*s)]}$ a = soil line intercept s = slope of the soil line X = adjustment factor to minimize soil noise	modifications of Huete (1988) SAVI to compensate for soil variability due to changes in solar elevation, leaf-angle distribution and LAI	Baret *et al.*, 1989; Major *et al.*, 1990 Richardson and Wiegand, 1990; Baret and Guyot, 1991; Wiegand *et al.*, 1991
Modified SAVI (MSAVI)	$\frac{(TM4-TM3)(1+L)}{(TM4+TM3+L)}$ L = 1 - 2*s*NDVI*WDVI s = slope of the soil line	this index provides a variable correction factor L which is the product of NDVI and WDVI; the level of vegetation cover does not have to be known *a priori* to calculate L	Qi *et al.*, 1994
Vegetation Indices and surface temperature	T_s/NDVI T_s = land surface temperature	the slope of T_s/NDVI can be interpreted biophysically as regional surface evapotranspiration	Lambin and Ehrlich, 1995
Atmospherically Resistant Vegetation Index (ARVI)	$\frac{TM4-TM_{rb}}{TM4+TM_{rb}}$ TM_{rb} = TM3-γ(TM1-TM3)	minimizes atmospheric-induced variations; utilizes the difference in radiance between the blue and red channels, via a γ function to correct the radiance in the red channel and stabilize the index to variations in aerosol content	Kaufman and Tanré, 1992
Soil and Atmospherically Resistant Vegetation Index (SARVI)	$\frac{TM4-TM_{rb}(1+L)}{TM4+TM_{rb}+L}$ TM_{rb} = TM3-γ(TM1-TM3)	both atmospheric and canopy background corrections can be combined; minimizes soil and atmospheric noise; results in a more stable NDVI	Kaufman and Tanré, 1992
Modified Normalized Difference Vegetation Index (MNDVI)	$\frac{NDVI(1+C_2H_2)}{1+C_1H_1}$ H_1, H_2 are functions of blue, red and NIR reflectances and atmospheric-, canopy background-, and vegetation-feedback coefficients; C_1, C_2 are weighted constants	further reduces atmospheric and soil contamination by incorporating both soil adjustment and atmospheric resistance concepts into a feedback-based equation	Liu and Huete, 1995
Soil and Atmospheric resistant vegetation Index (SARVI2)	$\frac{2.5(TM4-TM3)}{(1+TM4+6TM3-7.5TM1)}$	simplification of MNDVI by removing NDVI component	Huete *et al.*, 1997

From the above discussion, it is evident that remote sensing has the potential to provide information for the definition and mapping of spatial patterns in ecosystems, as well as their change in time. This includes not only the monitoring of biophysical variables related to forest ecosystem structure and processes, but also the definition of forest ecosystem units as presented in the following discussion.

3.2.3 Forest Classification

Landsat MSS has been used primarily for generalized forest-type mapping (Bryant *et al.*, 1980; Kalensky *et al.*, 1981; Pettinger, 1982). Success has also been achieved for forest site-type mapping (Tom and Miller 1980; Hame, 1984) and for species and structural mapping, but only in association with the careful treatment of training statistics (Walsh, 1980) or the addition of ancillary variables (Strahler *et al.*, 1980) (Table 3.6). Classifications have been improved by integrating MSS spectral data with digital elevation data and associated geomorphometric variables (Strahler *et al.*, 1980; Franklin *et al.*, 1986; Franklin, 1987), as well as texture measures (Franklin and Peddle, 1989) (Table 3.6). Landsat MSS has proven successful for generalized forest mapping due primarily to the large spatial resolution (80m) which averages the spectral characteristics of forest structure, thereby reducing variance and spectral overlap between broad cover classes. This produces spectral characteristics for general cover types which often fit the normal distribution of parametric classifiers, particularly for areas of low relief. The addition of ancillary data (e.g., geomorphometric variables) or additional feature processing (e.g., texture) provides enhanced classification results.

Improved spatial, spectral and radiometric characteristics of Landsat TM have led to numerous forest studies for the purpose of classifying forest types and structural characteristics. Congalton *et al.* (1993) stated that the spatial resolution of SPOT and Landsat TM are a major improvement over Landsat MSS. A survey of the literature indicates that more detailed information is available from Landsat TM data (Table 3.7). However, due to the increased heterogeneity of the spectral data representing cover classes, the extraction of information requires more sophisticated analysis and classification techniques. The increase in spectral 'noise' that accompanies higher spatial resolution data indicates that such 'noise' is usually related to variations in structural properties of forest communities (Peterson *et al.*, 1986). Hence, TM may provide researchers with a greater ability to extract stand structural characteristics.

Table 3.6 Forest Classification with Landsat MSS

Variable(s)	Technique*	Description	Reference
Spatially Complex Vegetation	UC (MLC)	difficult correlating spectral classes and ground classes; small land-cover units and rugged terrain complicated interpretation; UC not demonstrated to be superior to SC	Townshend and Justice, 1980
Coniferous Species (including stand and site characteristics)	controlled clustering (MLC)	12 surface-cover types (merged from 59 spectral clusters) were mapped to an average accuracy of 88.8%; slope angle, aspect and surface cover affected spectral variability	Walsh, 1980
Timber Height and Density (to estimate timber volume for homogeneous strata)	(i) UC; (ii) model 'region type' with DTM	the authors developed a stratification procedure for a high-relief forest environment incorporating tone (MSS), texture and geomorphometric variables	Strahler *et al.*, 1980; Franklin *et al.*, 1986
Forest Site Index (9)	LDA spectral and ancillary variables	achieved 97% training accuracy when combining 19 image and map variables; MSS alone achieved 43%	Tom and Miller, 1980
Conifer Species Canopy Density Crown Diameter	UC (guided clustering)	guided clustering defined a maximum number of low-variance spectral classes; by matching spectral curves of known and unknown spectral classes, it was possible to assign spectral classes to categories	Mayer and Fox, 1981
Softwood, Hardwood, Regeneration	SC, UC (MLC)	performed generalized forest-type mapping (reconnaissance stage) and emphasized a multistage approach	Kalensky *et al.*, 1981
Anderson's Classification (Levels I, II, III)	modified clustering (MLC)	successful for mapping at Anderson's Level I (83.0%); detailed mapping at Levels II and III achieved 52.2% accuracy	Pettinger, 1982
Forest Site Types	MLC	used a multi-stage process to improve the efficiency of mapping site types	Hame, 1984
Forest Cover Types (species level for conifers)	SC, UC (MLC)	results indicated that classification accuracy is more dependent on forest composition and distribution than on a particular classification scheme	Hudson, 1987
Mountainous Landscape Classes	LDA	geomorphometric and MSS data (75%); MSS data alone (46%)	Franklin, 1987
Forest Types (within a moderate relief boreal environment)	LDA	texture algorithm improved classification; geomorphometric variables provided the greatest improvement to classification	Franklin and Peddle, 1989

* SC=supervised classification; UC=unsupervised classification; MLC=maximum likelihood classification; LDA=linear discriminant analysis

SPOT data have now come into wide use for land-cover and land-use mapping. For forest mapping, concern has been raised recently regarding the low dynamic range of data acquired over forested regions which may prevent satisfactory classification results (De Wulf *et al.*, 1990; Borry *et al.*, 1990). It has also been noted that there is high correlation between SPOT XS Bands 1 and 2. De Wulf *et al.* (1990) had limited success extracting forest-stand parameters (e.g., stand density, stand age, average tree diameter, stand basal area, average canopy height and stand volume) from both multispectral and panchromatic data and as a result considered SPOT data as L-resolution[5] (Strahler *et al.*, 1986) with respect to forest canopy structure. For visual and digital analysis of SPOT multispectral data, the date of acquisition is a key element to successful forest mapping and analysis; data acquired in the early part of the growing season provide superior results (Borry *et al.*, 1990). Upon achieving unimpressive classification accuracies for vegetation classes using SPOT data (corrected for terrain), Baker *et al.* (1991) noted that spectral classification alone may not be sufficient. The inclusion of certain geomorphometric variables (Franklin and Wilson, 1991; Franklin *et al.*, 1994) in a high-relief environment as well as texture features (Franklin and Peddle, 1990) generally improved the classification accuracies achieved with SPOT multispectral data.

Information content in an image is expressed by the 'intensity' of each pixel (i.e., tone or colour) and by the spatial arrangement of pixels (i.e., texture, shape and context) in the image (Lee and Philpot, 1991). Campbell (1987) defines image texture as the apparent roughness or smoothness of an image region, usually the result of an irregular surface being illuminated from an oblique angle causing a pattern of highlighted and shadowed areas. Texture contains important information about the structural arrangements of surfaces and their relationships to the surrounding environments (Haralick *et al.*, 1973). Coarse textures are those for which the distribution of pixel values changes only slightly with distance and fine textures are those for which the distribution changes rapidly with distance (Haralick 1979). Texture is an important functional attribute of a remotely sensed image and is therefore an important contributor to scene information extraction. Although texture has long been recognized as an important clue in the visual recognition of objects in aerial photographs, conventional automated processing traditionally has not exploited this component of remote sensing data.

---

[5]L-resolution is a term defined by Strahler *et al.*, (1986) and indicates that the spatial resolution cells within the remote sensing image are larger than the elements within the ground scene. These elements on the ground are therefore not resolvable. H-resolution, on the other hand, indicates that the spatial resolution cells are smaller than the elements within the scene, and therefore the individual elements may be resolved.

Table 3.7 Forest Classification with Landsat TM

Variable(s)	Technique*	Description	Reference
Nine Forest Classes (species, terrain derived)	SC, MLC	TM provided superior forest-type mapping and condition assessment information than MSS; average accuracy for nine forest classes was 69%; improved when forest categories were merged	Hopkins *et al.*, 1988
Nine Natural Resource Categories	SC, MLC	tested a variety of TM band combinations and found that six TM bands provided the highest overall classification accuracy (92.4%)	Karteris, 1990
Species and Age Groups (pine plantations)		TM imagery was inadequate for separating species; age classes were separable	Coleman *et al.*, 1990
Landscape Classes, High Relief	LDA	classification accuracy increased from 55.8% to 77.6% when geomorphometric variables were included with TM data	Franklin and Moulton, 1990
Canopy Closure and Forest Understory	UC	the data were stratified into three categories of canopy closure; presence or absence of understory in each category was then evaluated using spectral response pattern analysis; understory presence or absence (55 - 69% accurate)	Stenback and Congalton, 1990
Three Forest Types and Eight Land-Cover Classes	PCA, LDA, MLC	TM data were transformed using PCA and combined with geomorphometric variables to provide mapping accuracies of 76%	Franklin, 1992
Successional Stages	UC, MLC	a wetness index and a TM 4/5 ratio and TM 4 were the best features for distinguishing between old growth and mature forests; accuracy (71.7%)	Fiorella and Ripple, 1993
Species, Size Class (structure, crown closure)	SC, UC ancillary variables	in-depth spectral analysis was performed to determine the strength of the correlation between the spectral data and vegetation; SC and UC were performed and similarities between the spectral statistics for each classification were compared using a clustering algorithm (accuracies > 80%)	Congalton *et al.*, 1993
Six Forest and Five Nonforest Classes (canopy change)	vegetation indices "guided" clustering	"guided" clustering of Landsat TM bands and various vegetation indices provided classification accuracies of 75% for six forest classes and five nonforest classes; misclassification resulted from stands being a mix of two or more species which also differ in size, density, crown closure and age	Bauer *et al.*, 1994

* SC=supervised classification; UC=unsupervised classification; MLC=maximum likelihood classification; LDA=linear discriminant analysis; PCA=principal component analysis

It is well known that actual landscapes consist of a spectrally diverse assemblage of features, which become increasingly complex as spatial resolution increases. Indeed, the use of texture explicitly implies that the resolution cells are smaller than the elements in the scene model, because numerous measurements are required for each element or class in order to allow the characteristic spatial texture to occur (Woodcock and Strahler, 1987). Since the finer details of an image that contribute to spatial variability are lost as spatial resolution decreases, multi-resolution analyses produce more detailed textural signatures that can be used for classification (Van Gool *et al.*, 1985). In order to extract more information from digital remote sensing data, image classification should include information regarding the overall pattern of variation that characterizes each category. However, the majority of image classification procedures, particularly in operational use, rely on spectral 'intensity' characteristics alone, and thus are oblivious to the spatial information content of the image. These types of per-point classifiers do not perform well in environments where there is an excess of boundary pixels or where there is substantial spectral overlap between the chosen informational classes (Martin *et al.*, 1988).

Textural algorithms, on the other hand, attempt to measure image texture by quantifying the distinctive spatial and spectral relationships which occur among neighbouring pixels. For a forested environment, where local variance is high, texture measures should be more valid than contextual methods because they rely on spatial variation to differentiate classes (Woodcock and Strahler, 1987). In response to the need to extract information based upon the spatial arrangement of digital image data, numerous texture algorithms have been developed. These include methodologies based upon: (i) structural approaches (Carlucci, 1972; Haralick, 1979; Conners and Harlow, 1980a; Vilnrotter *et al.*, 1986; Hay, 1994); (ii) spatial frequency patterns (Bajcsy and Liebermann, 1976); (iii) first-order statistics (Hsu, 1978; Irons and Petersen, 1981; Laur *et al.*, 1987; Arai, 1993); (iv) second-order statistics (Haralick *et al.*, 1973; Galloway, 1975; Haralick, 1979; Sun and Wee, 1982); (v) texture spectrum (Wang and He, 1990; Gong *et al.*, 1992b); and (vi) spectral texture pattern matching (Lee and Philpot, 1991). Useful summaries of methodological approaches to measuring texture are provided by Haralick (1979) and Marceau (1989).

Statistical measures of image texture have generally been considered superior to structural methods and are more generally used in remote sensing image analysis. Originating from the psychophysical vision texture research of Bella Julesz, (e.g., Julesz 1975) second-order statistics were identified as playing a significant role in human visualization of texture. This work provided the framework upon which Haralick *et al.*, (1973) developed the Grey-Level Co-occurence Matrix (GLCM) method of texture analysis.

Current psychophysical research indicates that it may be only density changes (a first-order statistic) of a primitive called *textons*, that explain pre-attentive (or instantaneous) texture discrimination (Julesz, 1981). Based on these modified psychophysical texture theories, Hay and Niemann (1994) reject the application of second-order statistical texture methods for structural analysis of forests stands. The structural methodology subsequently proposed incorporates high spatial resolution remote sensing data and the key characteristics (i.e., physical size, shape and spatial arrangement of objects) of human texture perception to discriminate texture within stands. In this approach, the objects must be discernible, thereby requiring each object of interest in the scene to be represented by a number of picture elements. Also, the height of each object is required, a parameter that currently can only be obtained by ground surveys. This approach, however, is not suitable for L-resolution image data where object-specific information (i.e., individual trees) is not available. However, texture remains a key characteristic and identifier of the nature of the scene, either based on spatial arrangements of a series of objects, or on the physical processes occurring at the surface.

Statistical texture measures are also more appropriate than structural measures in traditional land-cover and land-use classification. Since classification procedures are already based on a stochastic assumption (i.e., pixels are considered discrete samples of the scene they represent, and are randomly clustered in feature space according to their spectral characteristics at a specific moment in time and at a specific geographic location), it follows that statistical texture measures are best suited to probabilistic multispectral classification. The challenge has traditionally been in identifying appropriate descriptive statistics that have some relationship with human visual perception, such as fineness and coarseness, contrast, directionality, roughness and regularity (Haralick, 1986). Today, there are a wide range of statistical measures of texture available which include methods based on the statistical distribution of local properties in the spatial domain (e.g., edge detection (Rosenfeld *et al.*, 1970; Thompson 1977; Davis *et al.*, 1979; Shanmugan *et al.*, 1979); grey-level difference method (Weszka *et al.*, 1976; Mason 1979; Rosenfeld *et al.*, 1982); grey-level run-lengths method (Galloway, 1975); local extrema measures (Mitchell *et al.*, 1977; Mitchell and Carlton, 1978; Crombie *et al.*, 1982); transformations based on first- and second-order statistics (Hsu, 1978; Laur *et al.*, 1987; Irons and Peterson 1981; Haralick *et al.*, 1973; Sun and Wee, 1983)). Other texture methods operate on the spatial frequency domain (e.g., autocorrelation function, optical and digital transforms (Bajcsy and Lieberman, 1976; Conners and Harlow, 1980a; Roan and Aggarwal, 1987; Matsuyama *et al.*, 1983)).

In studies comparing statistical texture measures, second-order grey-level co-occurrence statistical techniques tended to be superior to other statistical methods (e.g., power spectra (Lendaris and Stanley, 1970), grey-level run lengths (Galloway, 1975), grey-level difference method (Weszka *et al.*, 1976; Mason 1979)) for capturing the textural content of an image (Weszka *et al.*, 1976; Haralick, 1979; Conners and Harlow, 1980b; Marceau, 1989; Gong *et al.*, 1992b; Barber *et al.*, 1993). Second-order statistical approaches, such as those developed by Haralick *et al.* (1973) and Sun and Wee (1983), make use of grey-level probability density functions, which are generally computed as the conditional joint probability of pairs of pixel grey levels in a local area of the image. The grey tone spatial dependence approach characterizes texture by the co-occurrence of its grey tones. Texture information is assessed by computing for various values of distance and angle, several measures representing the way the matrix elements are distributed about the main diagonal e.g. fine texture indicates that pixels at distance d to each other are quite different, so the entries in the matrix will be quite distributed over the matrix; in the case of a coarse texture pairs of pixels separated by distance d would be quite similar. Statistical measures computed from the GLCM that are sensitive to the distribution of the entries about the diagonal should be sensitive to these textures.

Conners and Harlow (1980b) demonstrated the superiority of the grey-level spatial dependence method over the first-order statistic method to capture the texture content of an image. The superiority of second-order statistics over first-order statistics comes from the fact that lower-order statistics are included into higher-order ones resulting in increase potential for discrimination (Julesz 1975). For example, different texture patterns may share common first-order statistics and, therefore not be discriminated by them, but their second order statistics can be different, thereby permitting their differentiation. For this reason, second order statistical techniques offer potential for land cover and land use mapping by capturing a significant level of spatial information required to discriminate land features, of being compatible with probabilistic models already used for multispectral classification and being relatively simple to apply using existing computer systems and classification algorithms (Marceau 1989).

A number of studies incorporating texture analysis into classification of land cover and land use are outlined in Table 3.8. It is evident that texture data provide additional information that can be used for the classification of certain forest structural attributes. For instance, stand structural characteristics (e.g., diameter at breast height (dbh), crown diameter, density, basal area, and age) have been found to be highly correlated with texture images generated from SPOT panchromatic data (Cohen and Spies, 1992). Texture also

appears to be more evident at higher spatial resolutions (e.g., ≤10m) as stand structural characteristics tend to, at these levels, dominate the scene (Yuan *et al.*, 1991; Franklin and McDermid, 1993). Ecologists are also examining these texture measures for development as "pattern indices" for ecological data sets (Musick and Grover, 1990).

Fractals, first described by Mandelbrot (1977), have been used for examining spatial phenomena encompassing various scales (Lam and Quatrochi, 1992). It has been proposed that multifractal analysis be used to describe how spatial patterns and processes vary in space and time and between scales (De Cola 1993). Specific to remote sensing, researchers have examined the fractal dimension of remote sensing images to determine the applicability of fractal analysis to feature extraction from remote sensing data (e.g., De Cola, 1989; Lam, 1990; de Jong and Burrough, 1995). De Cola (1989) examined the complexity of generalized land cover types by applying fractal analysis to thematic data derived from Landsat TM data. It was shown that urban land cover possessed more complex spatial patterns than intensive agriculture. Similarly, Lam (1990) analysed Landsat TM data and ranked urban land cover, coastal and rural land cover as having the highest to lowest fractal dimensions. It was also observed that Landsat TM data, in general, possessed higher fractal dimensions than DTM surfaces at approximately the same scale range. This may indicate that Landsat TM data possesses information on terrain characteristics in addition to land cover.

Analysis of spatial forms and process using fractals is limited for both practical and theoretical reasons (Lam, 1990). First, remote sensing data represent empirical fractal data, which require that we abandon the concept of self-similarity except within a range of scales (De Cola, 1993). Since real spatial phenomena result from scale specific processes, their descriptions vary depending on how, where and when they are measured, thereby being a function of local variables (De Cola, 1993). This phenomenon can prove useful, however, in that the fractal dimension can be used to summarize the scale changes of spatial phenomenon (Lam and Quatrochi, 1992). Secondly, since self-similarity only exists over a certain range of scales, it is difficult to know the point at which self similarity ends for a curve or surface. Third, the calculated fractal dimension appears to be dependent on the particular method used (e.g., variogram, line-divider method, triangular prism) (Jaggi *et al.*, 1993).

Although, suited to various types of data and analysis, fractals have not proven significantly useful in analysis of remote sensing data. For instance, Roach and Fung (1994) found that fractal geometry is not useful as a primary classification tool in a forestry context. Similarly, de Jong and Burrough (1995) found that the reflectance properties of land cover units on Landsat TM data did not behave like real fractals. This was attributed to the scale of the data. Also, results were not repeatable when determining fractal dimensional using

contrasting techniques. It appears that the strength of fractals likely lies with simulation and modelling, since, based on the concept of self-similarity, realistic curves and surfaces can be generated.

Research into the classification of remotely sensed data has been pursued for approximately three decades and has involved many different strategies (e.g., supervised/unsupervised, per-pixel/per-field, textural, contextual). Pixels are grouped into various classes using a suitable classifier (e.g., minimum distance, maximum likelihood algorithms) or multivariate analysis (e.g., discriminant, principal components) or both. No single strategy has proven best for all situations; the most suitable approach is dependent upon the nature of the data collected, the availability of additional or collaborative terrain data, the characteristics of the surface being 'sensed' and the ultimate objectives and/or products desired from the classifier. The analyst is responsible for devising suitable strategies for collecting remote sensing and ground information, and for applying suitable analysis techniques to the data for a particular environment. To analyse the data correctly, the analyst requires a good understanding of the physical nature of the remote sensing data as well as the statistical tools used to group such data into relevant classes.

The analyst frequently does not have a large choice of classification algorithms in which pixels or comparable spatial neighbourhoods are assigned to a particular class. Traditionally, classification algorithms have relied on spectral data alone for pixel assignment. As discussed by Robinove (1981), the philosophical basis for multispectral classification implies that the multispectral data represent an acceptable surrogate for the attributes of the ground features that are of interest and that spectral classes separated within the data correspond to a distribution of ground-cover classes. In fact, information classes are generally subsets of a continuum of reflectances and in classification are applied against the geometric character of the classifier (Richards and Kelly, 1984).

Given the relatively small range of classification algorithms available, analysts may be forced to select classifiers which may not be appropriate for the data they are analyzing. This situation is becoming more problematic, particularly as new data types with increased spatial, spectral and radiometric resolutions become available. Some of the classifiers commonly used are statistical in nature and include non-parametric classifiers such as minimum-distance-to-means, parallelepiped, and linear discriminant analysis (LDA) (Duda and Hart, 1973; Tom and Miller, 1984a; Kershaw, 1987; Campbell, 1987). Parametric classifiers are also used, such as the maximum-likelihood classifier (MLC) and its sophisticated extension, the Bayesian classifier (Campbell, 1987).

Parametric classifiers such as the MLC have become widely used in operational

remote sensing. These classifiers calculate the statistical probability of each pixel value belonging to each class or category, as defined by the analyst; they are then assigned to the class with the highest probability. This sequence of events is performed by first taking into account the mean vector and covariance matrix of the spectral categories and then calculating probability density functions (PDF). However, the MLC model assumes normality, whereby the pixels sampled to define the decision rules of the classifier possess a normal or Gaussian distribution. This assumption has been reasonable for common spectral response patterns, which are encountered when using medium to low spatial resolution data (e.g., Landsat MSS - 80m) (Lillesand and Kiefer, 1994). The Bayesian classifier is similar to the MLC, but allows for the input of *a priori* probabilities for each class, which are then multiplied by the PDF determined from training data in order to quantify the *a posteriori* probability (Campbell, 1987). The use of *a priori* probabilities in MLC has been shown to improve classification accuracies (Strahler, 1980), but the approach is often not implemented since appropriate information is rarely known.

When using the MLC, certain preprocessing procedures can be applied to the data to render them more amenable to the statistical assumptions of the classifier. These procedures are intended to reduce variance within the spectral classes which can be considered either as noise or inherent heterogeneities within the land-cover class. These procedures include multivariate transformations of feature space, such as principal components analysis (PCA) which is used to examine the interrelationships between a large number of spectral vectors. PCA is also used to reduce the dimensionality of the original data with minimal information loss.

Table 3.8 Some Applications of Texture Analysis for Land-Cover Classification

Texture Method(s)	Synopsis	Reference
GLCM	incorporating texture features into a linear discriminant analysis of Landsat MSS data improved accuracies up to 7.1%; using four orientations of the co-occurrence provided higher accuracies than using average textures; this could be related to topographic orientation (e.g., slope/aspect)	Franklin and Peddle, 1989
GLCM	classes containing either mixed vegetation patterns or possessing a strong relationship to structural features (e.g., topography) showed improved classification accuracy using tone and texture information	Franklin and Peddle, 1990
GLCM	the authors found significant improvement in classification accuracy for some land-cover classes when incorporating texture measures; window size is a dominant factor affecting accuracies	Marceau *et al.*, 1990
First-order statistics: Standard deviation	texture processing was compared to per-field sampling and low-pass filtering to improve land-cover classification accuracy; texture improved accuracy 2.4% for single-date and 3.9% for a two-date analysis	Curran and Pedley, 1990
GLCM	texture measures for TM data were greater than for MSS data; by adding texture features to a multitemporal data set, classification improved 1.6% to 4.7%	Arai, 1991
GLCM	when texture features were incorporated into classifications of land cover in a moderate/high relief environment using synthetic aperture radar and SPOT multispectral data, accuracies increased 11% and 15% respectively	Peddle and Franklin, 1991
First-order statistics: Standard deviation, Absolute difference	texture of the SPOT 10m data was strongly correlated with stand structural characteristics, whereas TM texture was weakly correlated; the spatial resolution of TM data is too coarse to detect the spatial variability within the forest stands studied	Cohen and Spies, 1992
First-order statistics: Variance	the range of variability derived from image semivariograms, calculated over lodgepole pine stands, were used to identify optimal window sizes and were most useful for estimating canopy coverage	Franklin and McDermid, 1993
Neighbouring Grey-Level Dependence Matrix (NGLDM)	texture features derived from the NGLDM for airborne synthetic aperture radar (SAR) imagery improved discrimination of agricultural crops over tone alone	Rotunno *et al.*, 1996
GLCM, NGLDM, Grey-Level Difference Vector (GLDV)	in a comparison of GLCM, NGLDM and GLDV texture features derived from multi-polarimetric SAR data, the GLCM texture feature provided the highest classification accuracies	Treitz *et al.*, 1996

Spatial filtering[6] has been used as a preprocessing and/or postprocessing technique in order to improve classification accuracy (Cushnie and Atkinson, 1985; Toll, 1985). These context-dependent operators come in a variety of forms (e.g., mean, median) and are used to alter a pixel value according to its relationship with pixel values within a specified neighbourhood or window. For example, a mean filter will smooth an image to greater degrees as the "window size" or array of pixels upon which the filter is applied, is made progressively larger. A median filter, on the other hand, will smooth noise and also retain edges or boundaries. Both approaches effectively reduce the spatial resolution of the data and, logically, one must question the degree of information 'lost' in such a process. Similar techniques can be applied after the data have been classified. To improve the accuracy of per-point classifications, a post-classification smoothing filter can be applied to the classified data, whereby an isolated class (noise) is assigned to the class category representative of the majority of pixels surrounding it (Thomas, 1980). This technique, however, does not incorporate the true spatial characteristics of the class; it is only concerned with context as it relates to classified data and will only be effective for isolated pixels or groups of pixels (Lee and Philpot, 1991).

Improvements in per-pixel classification have been observed with the use of linear discriminant analysis (LDA) (Tom and Miller, 1984a). This method relaxes the restriction of the data meeting a specified distribution (i.e., normal); and results in decision rules for assigning pixels to a particular class which are more flexible, though perhaps less certain. As a result, the data play a much more prominent role in the creation of decision rules. LDA uses the pooled covariance matrix and reduces a multivariate problem to a univariate one by defining the weighted combination of input variables that best describe the separation among the groups (Tom and Miller, 1984a; Franklin, 1992). As a result, LDA is less sensitive to the number of input variables as compared to MLC (Peddle, 1993).

Efforts are currently being placed on the use of contextual classifiers to extract spatial information (Wharton, 1982; Gurney and Townshend, 1983; Gong and Howarth, 1992; Gong, 1994). Whereas texture refers to the spatial variation within a contiguous group of pixels that contribute to the overall appearance of the image, context refers to the spatial relationship of a pixel (or group of pixels) to pixels in the remainder of the image (Gurney

[6]Spatial filtering is a localized enhancement process by which pixel values from an original image are modified on the basis of the grey-levels of neighbouring pixels. Spatial filtering is performed on image data to emphasize or de-emphasize image data of certain spatial frequencies (i.e., the roughness of the tonal variations occurring in an image). Low pass filters are used to emphasize low frequency features (e.g., agricultural crops) whereas high pass filters are used to emphasize high frequency features (e.g., road networks, geologic lineaments).

and Townshend, 1983; Campbell, 1987). The basis of contextual classification lies with the premise that pixels of a given class are likely to be surrounded by pixels of the same class. This premise is likely to hold true for classes that are larger than the pixel size. However, at high spatial resolutions, individual spectral components of land-cover classes become distinguishable. This spatial/spectral variability may compromise contextual classification in certain environments. Treitz *et al.* (1992b) used SPOT data and a contextual classifier to improve land-use classification accuracy in a rural-urban fringe environment, which contained numerous land-use classes (discrete variables). In a forest and certain other environments, continuous variables may dominate, and, under such circumstances, the premise for contextual classification may not be valid.

New developments in image classification include non-parametric classifiers (Skidmore and Turner, 1988), advanced iterative clustering techniques (Guo and Haigh, 1994), the use of fuzzy sets for information representation (Wang, 1990a; 1990b; Foody and Cox, 1994), evidential approaches for multisource data analysis (Lee *et al.*, 1987; Wilkinson and Megier, 1990; Veronese and Mather, 1992; Peddle, 1993) and neural networks (Ersoy and Hong, 1990; Benediktsson *et al.*, 1990; Bischof *et al.*, 1992; Fernandez, 1992; Foody *et al.*, 1992; Benediktsson *et al.*, 1993; Foody, 1995). Evidential and neural network classifiers have a number of advantages when compared to many statistical classifiers: (i) they are not restricted by underlying statistical models (e.g., normal distribution); (ii) they are not sensitive to variance thresholds; (iii) they are able to adequately handle increased numbers of input variables; and (iv) they are capable of processing data of different variable types (e.g., nominal, ordinal, interval and ratio) (Peddle, 1993; Benediktsson, 1993).

Neural network and evidential reasoning classifiers have demonstrated superior classification capabilities when compared to traditional statistical classifiers (e.g., LDA, MLC) (e.g., Downey *et al.*, 1992; Foody *et al.*, 1992; Peddle, 1993; Foody, 1995), particularly for non-normally distributed training data (Benediktsson *et al.*, 1993). The neural network classifier performs a segmentation of the original data to different spatial resolutions (scales). Spectral signatures and spatial frequency textural information are used to guide an anisotropic diffusion process which smooths within-cover-class segments at different scales (Fernandez, 1992). Although these classifiers show promising classification results, they are generally slower to "train" than traditional statistical techniques. For most neural network classifiers, the training process is computationally very complex and requires a large number of training samples, and such requirements may translate into a long implementation phase.

Franklin and Wilson (1992) used a three-stage approach to classification; it was initiated with a quadtree-based segmentation operator, followed by a Gaussian minimum-

distance-to-means test, and then a test incorporating ancillary geomorphometric data and a spectral curve measure. Knowledge-based and expert systems promise to improve remote sensing image classification through the integration of knowledge and reasoning (Schowengerdt and Wang, 1989; Srinivasan and Richards, 1990; Ton *et al.*, 1991). However, these attributes are often site and application specific (Wang and Newkirk, 1988; Skidmore, 1989), a situation which renders difficult the widespread use of such techniques.

3.3 Remote Sensing Spatial Resolution (Scale)

Spatial resolution is a fundamental concept in remote sensing and plays a significant role in the planning of any remote sensing investigation. Townshend (1981) and Forshaw *et al.* (1983) provide insightful background on the concept of spatial resolution and its various meanings. Here, we consider spatial resolution as the instantaneous field of view (IFOV) of the sensing system, which is the area on the ground viewed at any particular instant in time. With this definition, spatial resolution is analogous to the scale of the observations (Woodcock and Strahler, 1987). For the purpose of this discussion, the term spatial resolution will be used not only in the traditional sense, but also as a surrogate for scale (Csillag, 1991; Lam and Quattrachi, 1992).

3.3.1 Spatial Resolution (Scale) and Multispectral Classification

One of the major considerations in any remote sensing forestry application is to determine the spatial resolution of the data that best meets the objectives of the project. For example, to study within-stand forest patterns, the optimal resolution may depend on detailed characteristics such as crown diameter, species, size (age) or spatial pattern. The optimal spatial resolution will, however, vary as the specific within-stand characteristics change. Thus it is important to understand how spatial resolution affects the spectral and spatial expression of forest attributes.

Researchers investigating the effects of spatial resolution on classification accuracy have generally found that classification performance improves at lower spatial resolutions for various classification hierarchies (Latty and Hoffer, 1981; Markham and Townshend, 1981; Brass *et al.*, 1983; Townshend, 1983; Irons *et al.*, 1985; Cushnie, 1987). Wiersma and Landgrebe (1979) identified two counteracting forces that affect classification accuracy as a function of spatial resolution. These are: (i) heterogeneous targets and (ii) the percentage of boundary pixels within a scene. As spatial resolution increases, the proportion of pixels falling on, or near, boundaries of objects in the scene decreases, thereby reducing the number of mixed pixels and hence improving classification accuracy. However, there is a

corresponding increase in spectral variability of surface features with an increase in sensor spatial resolution. This results in poor statistical separability between features, giving rise to poor classification accuracies using traditional classifiers. Changes in classification accuracy which accompany changes in spatial resolution are thus a function of the relative importance of 'scene noise' and boundary pixels (Markham and Townshend, 1981). It is also notable that scene noise may vary considerably among land-cover categories and across spectral bands for the same cover class. In addition, spectral variability for landscape (forest) features varies non-linearly across different spatial scales of observation in conjunction with complex spatial heterogeneity and non-linearities in dynamics of landscape features across spatial scales (Turner *et al.*, 1989).

Closely associated with the high spectral variability of high resolution imagery is the large amount of spatial information inherent in the data. Over the past ten years, as higher spatial resolution satellite and airborne remote sensing data became available, it was discovered that conventional analysis techniques did not provide satisfactory results (Townshend, 1983; Hodgson and Jensen, 1987; Jensen and Hodgson, 1987). As a result, the research focus has shifted towards developing new techniques for exploiting spatial information (e.g., Sun and Wee, 1983; Woodcock *et al.*, 1988a; 1988b; Lee and Philpot, 1991; Yuan *et al.*, 1991; Franklin and McDermid, 1993; Hay and Niemann, 1994). Woodcock and Strahler (1987) examined various cover types at SPOT and Landsat TM resolutions and found the local image variance to be high for forested and urban/suburban cover types. They suggested that texture, context and mixture modeling be incorporated into information extraction techniques for these data. Of particular focus has been the development of new classification algorithms that incorporate textural and contextual measures. However, to date, the development of more sophisticated sensors and more complex classification techniques, be they supervised or unsupervised, parametric or non-parametric, spectral, textural, contextual or knowledge-based, has not led to satisfactory results on a repetitive basis (Marceau, 1992). Terrestrial and photogrammetric measurements remain the standard for the majority of scientific and operational mapping projects. For this reason, a more detailed examination of surface features and their relationship to remote sensing spatial resolution is required.

3.3.2 The Modifiable Areal Unit Problem (MAUP)

Remote sensing images represent comprehensive spatial samples of terrain or other surfaces, and each pixel contains the integrated radiant flux for the surface features (e.g., trees, shrubs, ground cover, soil and shadows in a forested environment) over an area corresponding to the

spatial resolution of the sensor. Based on traditional remote sensing methods, it is implied that there is a strong and predictable correlation between the measured radiance and the surface features of interest. However, surface features possess different sizes, shapes, and spatial distribution, as well as spectral characteristics, which would indicate that for an arbitrary sampling grid such as that imposed by remote sensing systems, there is really no intrinsic geographic meaning to the spectral measurements recorded (Marceau, 1994a). Arbitrary sampling does not necessarily provide a suitable model for nature. In nature, scales of phenomena are dictated by the physical laws that dominate at each level and, rather than being arbitrary, tend to concentrate around discrete levels that may be far apart (Klemes, 1983). It has also proven difficult to apply statistical image analysis techniques to spectral data acquired in this manner (i.e., using an arbitrary sampling grid) in order to extract meaningful information with a high degree of accuracy and repeatability. This observation is embodied in the modifiable areal unit problem (MAUP), as described by Openshaw (1984).

The MAUP is actually comprised of two sets of interacting problems, the first associated with spatial scale and the other with spatial aggregation (Openshaw, 1984). For example, a variety of different analysis results may be obtained as the same areal data are iteratively grouped into larger areal units for analysis. Hence, analysis results are dependent on scale. Second, at any given spatial scale, data may be aggregated in a variety of ways. In essence, the scale problem indicates a failure to understand the processes or phenomena that occur at different scales and the aggregation problem indicates a failure to discriminate the objects of geographical enquiry (Dudley, 1992). In studies of spatial data, including remote sensing studies, interpretation of those data is a scale- and aggregation-dependent phenomenon. Upon examination of the scale and spatial aggregation problems in remote sensing, Marceau (1992) found that there is a scale and aggregation level that is specific to the discrimination and analysis of each ground feature of interest in the scene. It is therefore necessary to identify an optimal spatial resolution for analysis. As defined by Marceau *et al.*, (1994b, p. 106) optimal resolution is the "spatial sampling grid corresponding to the scale and aggregation level characteristic of the geographical entity of interest." This approach will require a multi-scale sampling design for data acquisition, analysis and interpretation.

3.3.3 Selecting an Appropriate Spatial Resolution

Two assumptions identified by Duggin and Robinove (1990) as being implicit in passive remote sensing data acquisition and analysis are that data be (i) collected and (ii) analysed at an appropriate scale to detect and quantify the features of interest in the image. These are requirements for an adequate exploration of the spatial character of the surface features and

are intended to ensure that spectral characteristics or classes in the image correspond to information classes required by the user. To select an appropriate scale for data acquisition and analysis, the spatial structures of the ground surface features and of the images must be understood. Specifically, it is important to understand the manner in which images of a scene change as a function of spatial resolution. A suitable scale for observations is a function of (i) the type of environment being studied and (ii) the type of information required (Woodcock and Strahler, 1987), although suitable consideration must also be given to the techniques used to extract information from the remotely sensed data.

Spatial structure of an image is determined by the relationship between the size of the objects in the scene and spatial resolution. There are two approaches that can be taken to examine the spatial structure of a scene (Marceau, 1992). First, detailed field information characterizing the spatial structure of the surface features can be collected and compared to the information content of remote sensing data collected at a variety of spatial resolutions in order to determine the influence of surface features on information extraction. It has been shown that when spatial resolution is considerably smaller or larger than the surface feature of interest, it is likely that sample pixels for these features will exhibit high spectral variance, whereas if the spatial resolution samples the appropriate mixture of feature attributes, spectral variance will be at a minimum (Woodcock and Strahler, 1987; Marceau *et al.*, 1994b). A reciprocal approach consists of modelling scenes of a known structure (discrete elements distributed over a continuous surface) to derive the spatial structure they portray in digital images acquired from them (Jupp *et al.*, 1988). Models have been used to simulate a forest scene in order to determine optimal resolution (Li and Strahler, 1985; Woodcock and Strahler, 1987); however, these are generally over-simplified, as they usually assume that scenes are composed of objects arranged in a mosaic that completely covers the area or objects that are distributed on a continuous background.

Various tools have been developed to measure the spatial structure of digital images. For example, the spatial structure of images has been investigated using spatial autocorrelation (Craig and Labovitz, 1980; Campbell, 1981; Labovitz and Masuoka, 1984), one- and two-dimensional variograms (Woodcock and Strahler, 1985), fractals (De Cola, 1989; Lam, 1990); plotting local variance as a function of spatial resolution (Woodcock and Strahler, 1987), determining the minimal spectral variance of a class (Marceau *et al.* 1994b), and by overlaying grids on aerial photographs and counting the number of land-use categories that occur in each grid cell (Simonett and Coiner, 1971). Using grids of different sizes, Simonett and Coiner (1971) demonstrated that the complexity of the scene and spatial resolution determines the number of pixels that contain multiple land-cover types. Woodcock

and Strahler (1987) assessed spatial structure by graphing the local variance in images as a function of spatial resolution. The peak of the variance generally occurs at a slightly smaller spatial resolution than the size of the element in the scene. It was noted by Woodcock and Strahler (1987) that local variance for a forest stand decreased below spatial resolutions of 3-4m. This indicated that assumptions of spectral per-pixel classifiers were once again valid, but only on a per-tree basis rather than on a stand basis. Marceau *et al.* (1994b) used minimum spectral variance to define the optimal spatial resolution for each class and found that stand spatial and structural characteristics were the dominant features contributing to the optimal spatial resolution.

An alternate approach utilizes the semivariogram, which originates from the theory of regionalized variables developed by Matheron (1963). The semivariogram is used to measure the spatial dependence of neighbouring observations for any continuously varying phenomenon. Hence, it is a technique that can be applied to spectral data (radiance/reflectance), a phenomenon for which position in time and space is known. In this manner, spatial variation in images can be examined in relation to ground scene and sensor parameters (Woodcock *et al.*, 1988a).

3.3.4 Remote Sensing at Multiple Spatial Resolutions (Scales)

An important question surrounding the selection of an appropriate spatial resolution was suitably phrased by Openshaw and Taylor (1979, p.143): "what objects at what scales do we want to investigate?" Information is a scale-dependent phenomenon. Often it is assumed that just one scale will provide the desired results for a complex problem. This assumption requires examination and must be used with caution since the data in a remote sensing image are non-hierarchical in a classification sense (Everett and Simonett, 1976). For example, Marceau *et al.* (1994a) examined a natural forest environment at a variety of scales and concluded that there is no unique spatial resolution at which all geographic entities could be discriminated. Everett and Simonett (1976) described the environmental modulation transfer function to formalize the notion that applying a single resolution to many environments will not produce a uniform class of information for all environments. Environments are too complex over space and time to be reduced to a single spatial resolution (scale). In remote sensing studies, spatial resolutions (scales) are generally imposed on nature, often without necessarily knowing if those scales reflect natural patterns/forms/functions. However, as researchers into the character of nature, we must search for those scales of nature which exist and try to understand their interrelationships and patterns (Klemes, 1983).

In many remote sensing studies, it has been observed that there are dramatic

inconsistencies in the classification results between one class and another, leading to poor overall accuracies. Intuitively, classes that demonstrate poor accuracies have not been sampled at an appropriate resolution or they are not separable at any particular resolution (i.e., the class label does not represent the spatial structure of the class). It has been observed that the utilization of a single scale of remotely sensed data tends to cause the image to operate as a spatial frequency filter (Clark, 1990). Patterns higher in frequency than the spatial resolution of the data and lower in frequency than the size of the scene are inherently filtered out. In this case, only a subset of the natural variation of the surface is captured. Remote sensing spatial resolutions (scales) must be matched to the frequency of variation in nature, variations which do not occur at a single spatial resolution. Clark (1990) used multiple scales to map ice-flow landform features which resulted in radically new interpretations of the dynamics and behaviour of the Laurentide Ice Sheet. Analysis of multiple scales (a geographer's strength, see Stone (1972)) may be a more appropriate approach for identifying forest classes from remote sensing data.

From the preceding discussion on spatial resolution (scale), it is evident that more attention must be paid to the attributes of surface features and how these attributes are characterized in image data. Duggin and Robinove (1990) expressed concern that although remote sensing analysts are generally very analytical with regard to the interpretation procedures applied to quantitative analysis of digital image data, there is less attention paid to image data selection, sensor design and calibration, and optimal environmental conditions for data acquisition. In fact, there is generally a poor understanding of the assumptions involved in linking ground-level attributes with the spatial and spectral measurements recorded by the sensor. This must be done at a detailed level in order to isolate and understand the major components contributing to spectral reflectance at smaller scales. With this knowledge, sampling systems can be designed to optimize the segregation of various levels of features in a scene. This approach identifies a requirement for characterization of surface features at various spatial resolutions (scales), in order to determine the effect of spectral and spatial aggregation on surface feature extraction. Analysis of high spatial and spectral resolution data will improve our understanding of the spatial and spectral components of a forest canopy and their relative effects.

3.4 Remote Sensing and Data Integration for Forest Ecosystem Characterization

In this section, the rationale for developing an ecosystem classification scheme at a landscape scale for application to remote sensing and data integration for spatial analysis and mapping is described. Initially, ecosystems at regional, landscape and local scales are described. This is followed by a rationale for aggregating V-Types of the NWO FEC for landscape scale analysis. This landscape level classification scheme is then analysed with regards to remote sensing and terrain information that is either collected or optimized to a nominal scale of 1:20 000.

3.4.1 Describing Forest Ecosystems at Regional, Landscape and Local Scales

Ecosystem classifications capture and organize existing knowledge about ecosystems and facilitate the consistent identification of definable landscape units that can be mapped and used for planning purposes (Brenner and Jordan, 1991; Uhlig and Jordan, 1995). Typically, one set of ecosystems is nested within another in a hierarchy of spatial extents. Hierarchical classifications also provide a stable conceptual framework for modelling, analysing, interpreting and applying ecological knowledge at different scales (Uhlig and Jordan, 1995). These multi-scale classification schemes provide a framework around which data and knowledge can be accumulated and are necessary for ecosystem management (Bailey, 1987; ECOMAP, 1993). In effect, ecological land classification is an essential tool for landscape management in that it provides a description of landscape variables. To properly manage ecosystems, knowledge of the relationships of ecosystems within and between levels is necessary for aggregation upward or division downward (Sims and Mackey, 1994).

Ecological units within a classification hierarchy are discriminated on the basis of their physical, process and biological characteristics. At all levels the primary factor is climate, and how energy and materials are exchanged. Mapping coherent ecosystem units involves the detection of boundaries between distinctive groupings of physical and biological variables where one unit differs from the next based on a single variable or collective sets of characteristics (Wiken *et al.*, 1981). However, ecosystem units, irrespective of scale, are hypothetical constructs that facilitate stratification and testing of actions and responses (Bailey *et al.*, 1985; Barnes, 1984).

Ecological land classification refers to an integrated approach to land survey whereby land areas are classified and mapped as ecosystems according to some predefined ecological unity. Ecological land classification aims to segment the land surface into areal units of

various scales, each assumed to have a certain internal homogeneity and functional integrity (Rowe, 1979). The framework upon which ecological land classification is built implies some logical patterning of vegetation and soil to landform. Rowe (1980) defines classification as the subdivision of the landscape into ecosystem units at various scales. This process involves two stages: (1) the identification, description and logical grouping of landscape units (classification); and (2) the spatial division of the landscape (mapping) (Barnes, 1986).

Rowe (1979) stresses the importance of the mapping unit in ecological land classification. The primary methodology for stratifying the landscape into ecological units at various scales involves the examination of various thematic maps and remote sensing images, combined with preconceived notions of logical groupings that will give rise to ecological units that will be shuffled, grouped and regrouped based on perceived relationships, at the same scale level as well as between scales or levels in the hierarchy. A clear distinction must be drawn between 'map units,' which may be heterogeneous as a result of scale, and logical 'taxonomic units,' which are homogeneous by definition. The extent to which map units correspond to taxonomic units depends on the scale at which the landscape is examined (Rowe, 1979). Taxonomic units are developed from plot samples, and then the typology is applied to other sites. The NWO FEC represents a multi-factor taxonomic scheme since ordination of vegetation and soils are used to determine vegetative types and at a smaller scale, treatment units.

At regional scales (i.e., macroscale) climate variables, large physiographic units or general vegetation patterns are used to stratify geographic areas. Processes at these scales include primary productivity and biogeochemical cycles (Hills, 1960; Bailey, 1980). At the mesoscale level (i.e., ecodistrict), variables that give rise to different ecological units include recurring topographic, geologic, landform and broad soil patterns. At both the macroscale and mesoscale levels, landforms strongly influence climatic patterns, local energy environments related to slope and aspect, the flow of nutrients and moisture and disturbance regimes such as fire levels (Uhlig and Jordan, 1995; Bailey 1987; Hills 1960; 1961). Land type associations and land types are also at the mesoscale level. These units can be defined as mosaics of ecosystems as seen synoptically from above (Uhlig and Jordan, 1995). At these scales, classification, modelling and mapping are useful for studying landscape patterns, setting broad management targets and facilitating some aspects of field management such as forest growth and yield prediction (Uhlig and Jordan, 1995).

At landscape (1:20 000) and local scales (< 1:10 000) (i.e., microscale), the partitioning of ecosystems is based on more specific criteria with respect to edaphic,

topographic and vegetational features. At these scales quantitative information on soil and vegetation parameters at the community or stand level are used to classify and characterize forest ecosystems in considerable detail (e.g., Sims *et al.*, 1989). The NWO FEC has been applied at both the landscape level (e.g. 1:20 000 mapping scale) and stand level (e.g., 10 ha) for ecological description. Some of these are outlined in Table 3.9.

Table 3.9 Stand and Landscape Level Applications of the NWO FEC (adapted from Sims *et al.*, 1994)

Stand Level	Landscape Level
species autecology	construct landform toposequences
soil moisture requirements	correlate interpreted climatic features with forest humus forms
wildlife habitat preferences	develop spatial models of forest ecosystem processes

At the microscale level, variations in slope (gradient/aspect), site nutrient status, vegetational effect and soil features (e.g., surficial landform patterns, bedrock controls, soil texture, drainage or moisture regime) impact ecosystem distribution and pattern. The combination of these factors will affect local climate regimes and thereby affect vegetation growing patterns (Sims *et al.*, 1994). Vegetation is used in most multiple-component methods of ecosystem classification and most often used in single-component methods (Barnes, 1986). The primary reason for this is that vegetation can be viewed as a photometer, integrating the effect of the other factors affecting ecosystem definition (i.e., climate, soil and physiography). However, care must be exercised when using vegetation as the primary indicator for defining ecosystems, at all scales of analysis. For example, Barnes (1986, p. 12) lists the following points as requiring consideration:

- vegetation is complex and may require the identification and use of the entire complement of trees, shrubs, herbs, vines and often mosses and lichens;
- vegetation is highly sensitive to disturbance, and the ecologist must understand forest history and the disturbance response of the species;
- vegetation varies greatly in occurrence, coverage, and phytomass; species may be absent by chance;
- vegetation varies in vertical structure; its structure and the architecture of the crowns of the tree and shrub layers may be as important to consider as species composition
- vegetation is dynamic, and the patterns of biological succession for different sites and the array of natural and human disturbances should be understood.

Key functional processes which can be limiting and thereby affect ecosystem development include energy, moisture, nutrient and disturbance gradients (Urban *et al.*,

1987; ECOMAP, 1993). These processes contribute to ecological heterogeneity as depicted by ecosystem structure, pattern of occurrence and function (Uhlig and Jordan, 1995). As stated earlier, these processes are affected by climate, landform, topography, geology, soils and hydrology and vary along both spatial and temporal scales. Determining the ecosystem units to study is problematic since spatial boundaries are often difficult to define. It is likely, regardless of the selection, that the ecosystem units will be a product of human perception (Allen and Hoekstra, 1991).

At landscape scales, aggregation of detailed ecosystem units is necessary for mapping, particularly in complex environments (Wiken *et al.*, 1981). In order to derive forest ecosystem classes at landscape scales from the NWO FEC, detailed V-Types were grouped according to their tendency to occur together, as observed under field conditions. In many instances, the classes corresponded to the Treatment Units as described by Racey *et al.*, (1989). These associations are outlined in Table 3.10. Treatment units represent broader landscape units than do individual V-Types and Soil Types and respond similarly to certain management activities (Sims *et al.*, 1989). It must be noted that these are synthetic arrangements of vegetation-soil combinations that are perceived to require similar harvesting and silvicultural treatments. Aggregation of detailed ecosystem units provides information at operational scales, i.e., scales at which spatial information is generated that can be incorporated into harvest schedule plans where mapped information is presented at a scale of 1:20 000 (Mackey *et al.*, 1994a). Reference to Figures 2.8 and 2.9 will also provide insight into the manner in which V-Types are grouped. The similarity between V-Types is portrayed by the location and proximity at which V-Types occur within the two dimensional ordination portraying soil moisture and nutrient regimes as the axes.

There are a number of V-Types which aggregate together based on their similarity with respect to their occurrence under similar soil moisture and nutrient regimes. For example, black spruce mixedwood classes (V19, V20) are often found in association with pure conifer (black spruce and jack pine) classes (V31, V32, V33). These classes are very similar, particularly with respect to canopy characteristics and feathermoss ground cover. Soil moisture and nutrient regimes vary along a continuum and do not portray distinct breaks or boundaries. For this reason, black spruce, which occurs under a range of soil moisture and nutrient conditions has a number of V-Types which grow in upland and lowland site conditions. At the landscape scale, black spruce is classed as either upland, lowland, or wetland black spruce. As a result, V34 (Black Spruce / Labrador Tea/ Feathermoss (Sphagnum)) which represents a variable transition zone between the Upland Black Spruce / Jack Pine and Lowland Black Spruce has been grouped with the Lowland Black Spruce at

the Landscape Level. In addition, V23 (Tamarack (Black Spruce) / Speckled Alder / Labrador Tea) will often complex with V35 and V34 (particularly when Speckled Alder is prevalent in V34). Trembling aspen (white birch) / mountain maple (V8) were often observed in close proximity to Jack Pine Mixedwood / shrub rich (V17). The landscape level ecosystem units derived for the Rinker Lake study area are summarized in Table 3.11.

Table 3.10 Ecologically Significant Forest Classes at the Site and Landscape Levels (adapted from Sims *et al.*, 1989; Racey *et al.*, 1989; Baldwin 1995)

	Site Level Mapping Scale 1:10 000	Landscape Level * Mapping Scale 1:20 000	
V-Type	**Description**	**V-Type Associations†**	**Treatment Units and Description††**
	Mainly Hardwood		
V1	Balsam Poplar Hardwood and Mixedwood	V1, V2, V3	**A** Miscellaneous Hardwoods and Mixedwoods
V2	Black Ash Hardwood and Mixedwood		
V3	Other Hardwoods and Mixedwoods		
V4	White Birch Hardwood and Mixedwood	V4	**C** White Birch Hardwood and Mixedwood
V5	Aspen Hardwood	V5, V6, V7, V8, V9, V10, V11, (V19)	**B** Aspen Hardwood and Mixedwood
V6	Trembling Aspen (White Birch) - Balsam Fir / Mountain Maple		
V7	Trembling Aspen - Balsam Fir / Balsam Fir Shrub		
V8	Trembling Aspen (White Birch) / Mountain Maple		
V9	Trembling Aspen Mixedwood		
V10	Trembling Aspen - Black Spruce - Jack Pine / Low Shrub		
V11	Trembling Aspen - conifer / blueberry / Feathermoss		
	Conifer Mixedwood		
V12	White Pine Mixedwood	V12, (V26), V13, (V27)	**H** Red or White Pine Conifer and Mixedwood
V13	Red Pine Mixedwood		
V14	Balsam Fir Mixedwood	V14, V15, (V24), V16, (V25), (V19, V21)	**D** Balsam Fir - White Spruce Conifer and Mixedwood
V15	White Spruce Mixedwood		
V16	Balsam Fir - White Spruce Mixedwood / Feathermoss		
V17	Jack Pine Mixedwood / Shrub Rich	V17, (V28), (V11)	**G** Jack Pine / Shrub Rich
V18	Jack Pine Mixedwood / Feathermoss	V18, (V29) (V31, V32)	**F** Jack Pine / Feathermoss
V19	Black Spruce Mixedwood / Herb Rich	V19, V20 (V31, V32, V33) (V11)	**E** Black Spruce - Jack Pine / Feathermoss
V20	Black Spruce Mixedwood / Feathermoss		

Table 3.10 continued

		Conifer	
V21	Cedar (inc. Mixedwood) / Mountain Maple	V21	**D** Balsam Fir - White Spruce Conifer and Mixedwood
V22	Cedar (inc. Mixedwood) / Speckled Alder / Sphagnum	V22	**J** Black Spruce / Wet Organic
V23	Tamarack (Black Spruce) / Speckled Alder / Sphagnum	V23 (V35)	**J** Black Spruce / Wet Organic
V24	White Spruce - Balsam Fir / Shrub Rich	V24, (V14, V15), V25 (V16, V19)	**D** Balsam Fir - White Spruce Conifer and Mixedwood
V25	White Spruce - Balsam Fir / Feathermoss		
V26	White Pine Conifer	V26 (V12) V27 (V13)	**H** Red or White Pine Conifer and Mixedwood
V27	Red Pine Conifer		
V28	Jack Pine / Low shrub	V28 (V17) (V11)	**G** Jack Pine / Shrub Rich
V29	Jack Pine / Ericaceous Shrub / Feathermoss	V29 (V18)	**F** Jack Pine / Feathermoss
V30	Jack Pine - Black Spruce / Blueberry / Lichen	V30	**I** Jack Pine - Black Spruce / Blueberry / Lichen
V31	Black spruce - Jack Pine / Tall Shrub / Feathermoss	V31, V32, V33, (V19, V20)	**E** Black Spruce - Jack Pine / Feathermoss
V32	Jack Pine - Black Spruce / Ericaceous Shrub / Feathermoss		
V33	Black Spruce / Feathermoss		
V34	Black Spruce / Labrador Tea / Feathermoss (Sphagnum)	V34, V35, (V23), V36, V37 (V22)	**J** Black Spruce / Wet Organic
V35	Black Spruce / Speckled Alder / Sphagnum		
V36	Black Spruce / Bunchberry / Sphagnum (Feathermoss)		
V37	Black Spruce / Ericaceous Shrub / Sphagnum		
V38	Black Spruce / Leatherleaf / Sphagnum	V38	**K** Black Spruce / Leatherleaf / Sphagnum

* based on vegetation and soil/site conditions

† V-Types in brackets () indicate an observed potential for aggregating with this group of V-Types

†† Treatment Units as defined by Racey *et al.*, 1989

Table 3.11 Landscape Level Forest Ecosystem Groupings for the Rinker Lake Study Area

Landscape Level Forest Ecosystem Groupings Mapping Scale 1:20 000		
Description	**V-Type Complexes†**	**Treatment Unit††**
	Mainly Hardwoods	
White Birch Hardwood and Mixedwood	V4	C White Birch Hardwood and Mixedwood
Aspen Dominated Hardwood and Mixedwood	V5, V6, V7, V8, V9, V10, V11 (V19)	B Aspen Hardwood and Mixedwood
	Conifer Mixedwoods	
White Spruce / Balsam Fir Conifer and Mixedwood	V14, V15, V16, V21, V24, V25, (V19)	D Balsam Fir - White Spruce Conifer and Mixedwood
Jack Pine Mixedwood / Shrub Rich	V17, V28, (V11)	G Jack Pine / Shrub Rich
Jack Pine Mixedwood / Feathermoss	V18, V29, (V11)	F Jack Pine Feather Moss
	Conifer	
Cedar Mixedwood	V22	J Black Spruce / Wet Organic
Upland Black Spruce / Jack Pine	V19, V20, V31, V32, V33	E Black Spruce - Jack Pine / Feathermoss
Lowland Black Spruce	V23, V34, V35, V36, V37 (V22)	J Black spruce / Wet Organic
Wetland Black Spruce	V38	K Black Spruce / Leatherleaf / Sphagnum

† V-Types in brackets () indicate a strong potential for aggregating with this group of V-Types
†† Treatment Units as defined by Racey *et al.*, 1989

3.4.2 The Relationship between Remote Sensing Spatial Resolution and Forest Ecosystem Scales

In Canada, the use of remote sensing has historically been integrated into ecological land survey approaches, in the form of multistage sampling procedures for various scales of survey (Rubec, 1983) (Table 3.12). However, emphasis has been placed on small scale interpretation. Landsat MSS has been instrumental in many ecological surveys, providing information at the ecoregion and ecodistrict levels (Wickware and Rubec, 1989).

Table 3.12 Relationship between Remote Sensing Systems and Ecological Land Survey Mapping Scales and Levels (Wickware and Rubec, 1989)

Remote Sensing Source	Ecological Land Survey Mapping Level	Mapping Scales
Satellite imagery	Ecoregion	1:3 000 000 - 1:1 000 000
High altitude photography	Ecodistrict	1:500 000 - 1:125 000
Moderately high altitude photography	Ecosection	1:250 000 - 1:50 000
Low altitude photography	Ecosite	1:50 000 - 1:10 000
Low altitude or ground photography	Ecoelement	1:10 000 - 1:2 500

In the above hierarchy, the prime factors at each scale vary differently between climate, biota, soil and relief. Even though specific biotic indicators and physiographic controls can be useful for determining ecological units at specific scales, they are also useful when suitably generalized at other scales (Rowe, 1979). For example, the broad physiognomic character of vegetation that reflects regional climate (i.e., ecoregion) is vastly different from the species composition and abundance that reflects local climate (i.e., ecosite). Care must be taken when mapping levels based on one or two significant physiographic or biologic features, that the boundaries defined have ecological meaning. It is more likely, that integration of as many of these factors as possible will produce boundaries of ecological significance.

3.4.3 A Remote Sensing and Data Integration Strategy for Forest Ecosystem Characterization

To classify forest ecosystems at landscape scales using remote sensing data, it seems logical to attempt to maximize between-class (i.e., forest ecosystem) spectral characteristics by minimizing the within-class spectral variability. However, one also desires to maximize forest ecosystem definition by retaining detail (e.g., boundaries or transitional areas). Since forest ecosystems differ based on their structural components and ecological processes, multi-spatial resolution remote sensing data are necessary to provide optimal descriptors while maintaining precise boundaries and scene detail. However, there is a poor understanding of what spatial resolutions are appropriate given the different characteristics of forest ecosystems. In this study, multi-spatial resolution CASI data are analyzed using semivariogram analysis to determine the spatial and spectral characteristics of landscape-scale forest ecosystems. It is hypothesized that these analyses will identify appropriate spatial resolutions for optimally characterizing different landscape scale forest ecosystems as applied to the NWO FEC. Semivariogram analysis facilitates the selection of appropriate window operators for texture processing. Texture features provide appropriate scaling for discrimination of specific landscape scale forest ecosystems. This analysis and subsequent

processing provides for the integration and combination of ecosystem class-specific regularized images.

The majority of studies that examine spatial resolution and the effects on forest spectral expression generally degrade fine resolution data to mimic coarser resolutions/scales (e.g., Markham and Townshend, 1981; Woodcock and Strahler, 1987; Cohen *et al.*, 1990; Marceau, 1992). Here, CASI data are collected at three altitudes to provide spectral data at three different spatial resolutions, thereby eliminating the need to apply interpolation algorithms to simulate data of contrasting spatial resolutions. Also, remote sensing data have rarely been calibrated to reflectance, a process that allows for the comparison of data at different altitudes. In this study, CASI data have been calibrated to reflectance.

In digital image classification of remote sensing data, quantitative statistical decision rules based on spectral reflectance of vegetative elements are imposed on image data to define ecological units. This approach is that of a systematic scientist. To attempt to incorporate a more holistic approach to classification of ecological units using remote sensing data, it seems appropriate to incorporate terrain attributes (e.g., elevation, gradient, aspect, surficial geology) into the statistical decision rules. At landscape scales, the primary causes which determine the differences between ecosystem units are topographic position, parent material, and slope, aspect and inclination with controlling factors being moisture regime, soil fertility, microclimate and snow depth. At the stand level, these causes and controlling factors are important along with disturbance history (Damman, 1979). It therefore seems reasonable to expect digital terrain descriptors (e.g., elevation, gradient, aspect, geomorphology) in combination with spectral data to assist in the discrimination of landscape scale forest ecosystem classes.

3.5 Summary

In Chapter 3, the current role of remote sensing for forestry and ecological land classification has been described. An examination of the relevant literature has revealed that the results of digital image classification for forestry studies using remote sensing data are, at best, varied. This can be largely attributed to an incorrect matching of remote sensing data to the variables (i.e., information classes) being sought and/or use of inappropriate processing and classification algorithms. However, when suitable information requirements are applied to the appropriate remote sensing data set, along with the appropriate analysis techniques, results can be positive (e.g., Pettinger, 1982; Hame 1984; Franklin, 1987; Franklin and Peddle, 1989; Congalton *et al.*, 1993). In such studies, the value of satellite data for forest classification has been clearly demonstrated.

Airborne sensors that generate high spatial and spectral resolution data are now available for remote sensing applications. However, due to high spectral variability within information classes, these data are not suited to traditional image analysis techniques developed for use with satellite data. This is largely due to inappropriate sampling or regularization of classes based on a single arbitrary sampling grid (i.e., spatial resolution imposed by the sensor/acquisition parameters). Research is currently underway on image analysis techniques which attempt to incorporate textural and contextual information into statistical decision rules. However, the nature of the spectral variability within forest ecosystem classes must be understood to optimize data acquisition and processing strategies. For instance, due to variable structure and processes occurring in different forest ecosystems, multi-spatial resolution data are likely required for optimal discrimination and classification. Also, classifiers that are not limited by data distribution rules (i.e., Gaussian) are being developed to operate with a variety of data types, including nominal data sets. Such classifiers should prove useful for the analysis of high spatial resolution remote sensing data in conjunction with other types of spatial data.

It has been proposed that landscape scale site classification can provide the basis for detailed applications and planning, especially when spatial analysis and modelling techniques are applied using remote sensing and other spatial data in conjunction with field-oriented classifications (Sims *et al.*, 1994). It is recognized that many ecological and timber resources cannot be directly sensed using remotely sensed data, but must be modelled or derived from other sources of primary data. This is a natural conclusion based on an holistic ecosystem concept. That is why the basis for this study is to develop a methodology that integrates appropriately scaled remote sensing data with terrain descriptors for large area classification and mapping of landscape scale forest ecosystems (areas with similar soils, vegetation and topography). Many early authors envisioned the appropriate application of ecosystem classification in a multi-thematic planning framework (e.g., Hills, 1960; 1961; Rowe, 1979). This approach is becoming more feasible for large area analysis with the development of technology (e.g., GIS, remote sensing, relational database management systems (RDMS) and Global Positioning Systems (GPS)). However, the method for accurate and consistent application have not as yet been developed nor rigorously tested. The approach taken in this study, is to collect high resolution remote sensing data, derive appropriately scaled images for different forest ecosystems (through semivariogram analysis and texture processing) and integrate these features representing optimal scales of reflectance with terrain descriptors, derived for landscape scale analysis. It is hypothesized that by deriving optimal spectral,

textural and terrain descriptors of the vegetation and landscape, discrimination of forest ecosystems can be optimized.

CHAPTER 4

STUDY AREA AND DATA DESCRIPTION

4.1 Study Area Description

The study site is located approximately 100 km north of Thunder Bay, Ontario within the Central Plateau section of the Boreal Forest Region (Rowe, 1972) (Figure 4.1). The study site is part of the Rinker Lake Research Area (RLRA) established by the Department of Natural Resources - Forestry Canada. The RLRA is approximately 900 km^2 and was established in 1983 to serve as an area of intensive boreal forest research, whereby a common database could be developed and shared amongst scientists involved in studying forests and forest dynamics. An ambitious multidisciplinary and multiagency research project was initiated in the RLRA in 1992. The principal goal of this project is to "assimilate and integrate findings of various researchers into a predictive, over-time ecological model (or set of models) that can be applied to resource management planning, and the elucidation of ecosystem processes at an operational forest scale" (Sims and Mackey, 1994 p. 666). This study represents a small component of the larger research project being conducted in the RLRA. The study site used in this research, approximately 6 km by 14 km, is located centrally within the RLRA (Figure 4.2). The study site is bisected by Hwy #527, with various logging roads providing access to additional forested areas.

The area consists of a diverse mosaic of forest stand-types with various soil and landform conditions, primarily of glacial origin. The topography is generally rolling and the terrain is bedrock-controlled. The terrain consists of a parallel series of gently undulating hills with scattered rocky outcrops. The soils and parent material of the area, along with previous cultural activities, play a significant role in forest ecosystem development in the area.

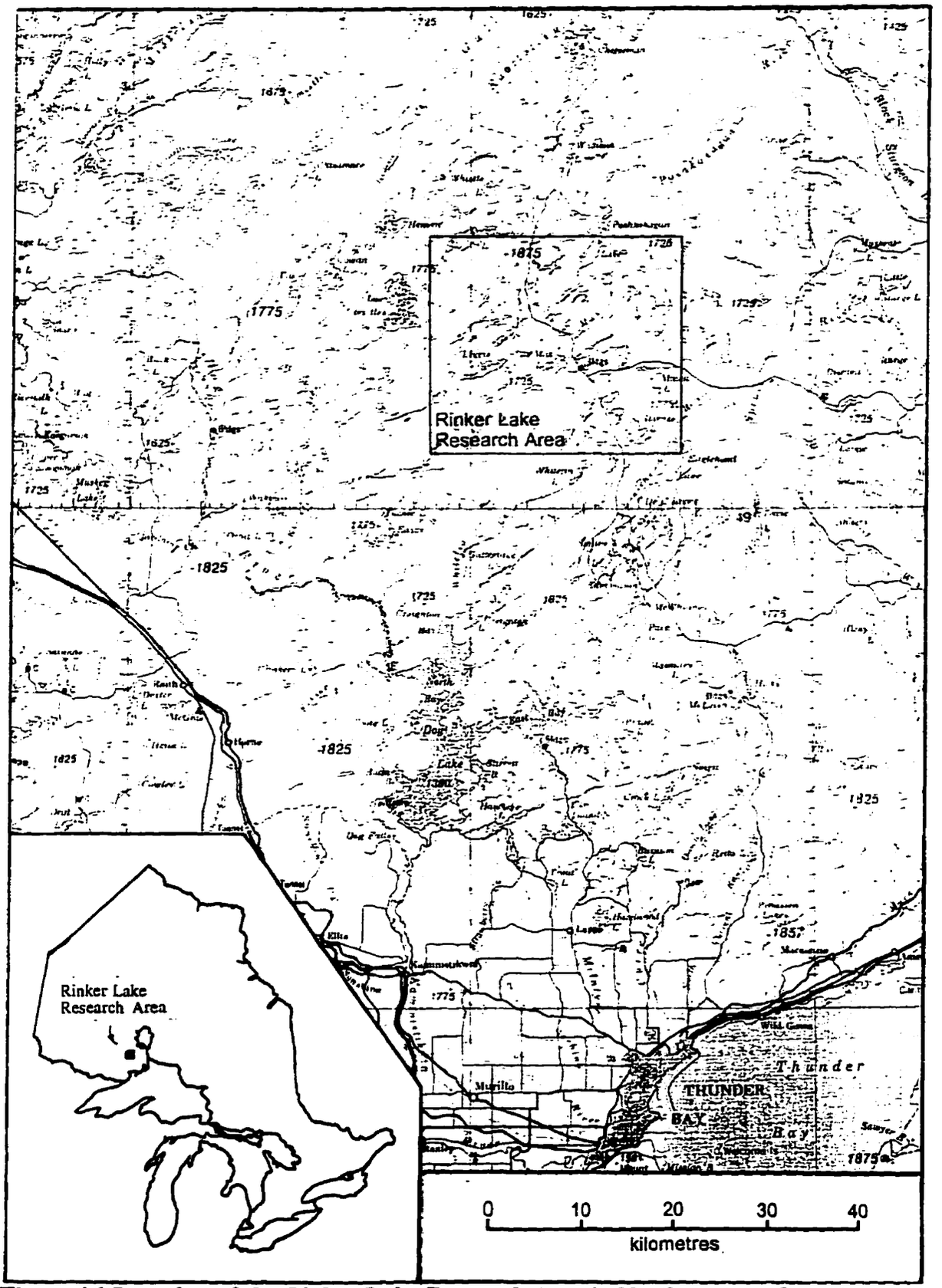


Figure 4.1 Location of the Rinker Lake Research Area in Northwestern Ontario (NTS 1:500 000; Thunder Bay, 53 SE, 4th ed., 1974).

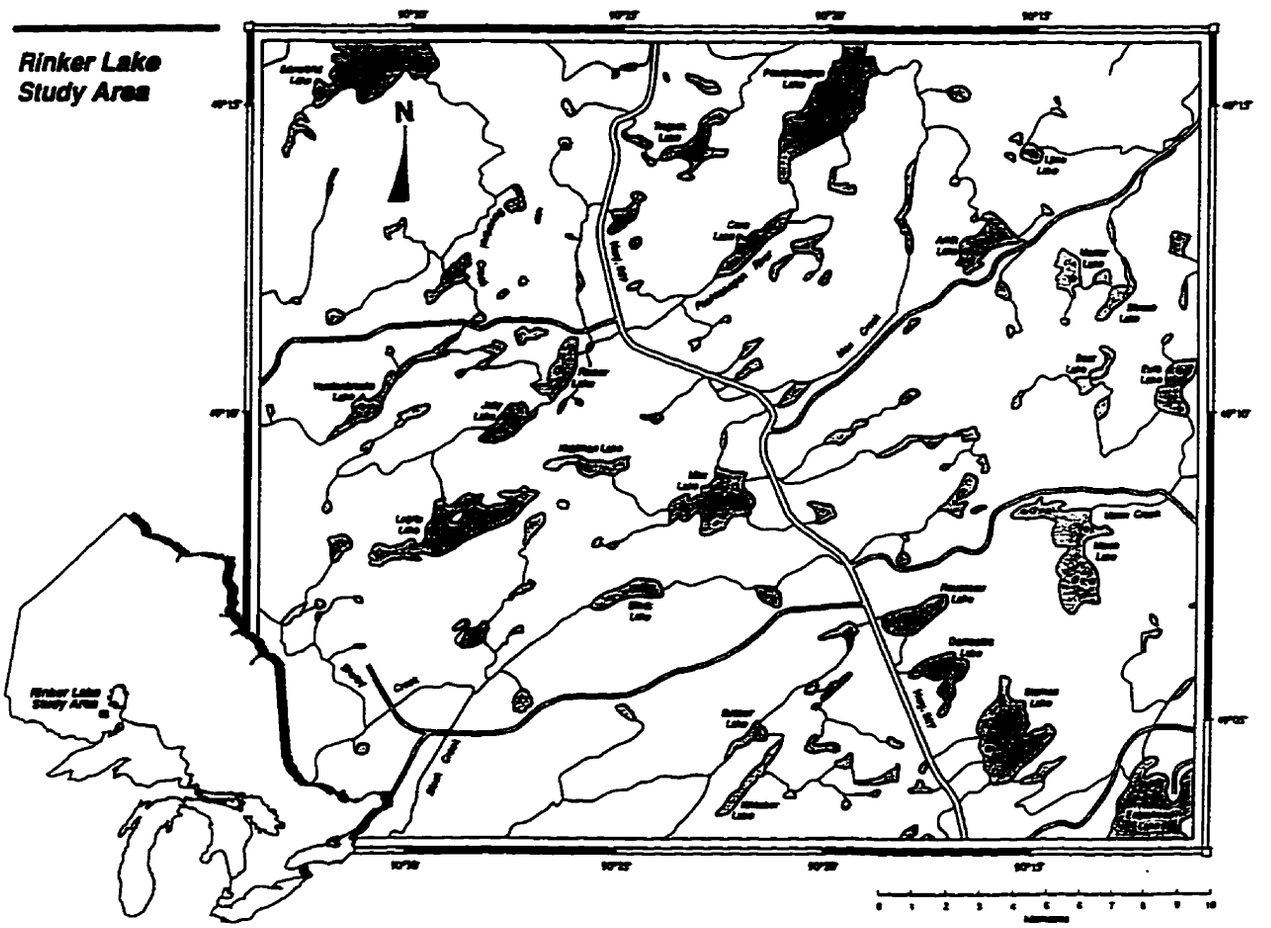


Figure 4.2 Location of the study site within the Rinker Lake Research Area.

The study area falls within the Moist Mid-Boreal Ecoclimatic Region (Ecoregions Working Group, 1989). Ecoclimatic regions define areas that are characterized by distinctive ecological responses to climate, as expressed by vegetation and reflected in soils, wildlife and water (Ecoregions Working Group, 1989). In this region, summers are warm and rainy (60-90 mm/month) while winters are cold and snowy with somewhat less precipitation than during the summer months. Total annual average precipitation is about 735 mm (Anonymous, 1982). Seven months of the year have mean daily temperatures above 0°C (Ecoregions Working Group, 1989). The growing season is estimated to extend from May 1 to August 31 with an average total of 300 to 375 mm of rain during that period (Walsh *et al.*, 1994).

4.1.1 Physiography and Bedrock Geology

The physiography of the study site is bedrock-controlled with elevations ranging from 430 m to 530 m. The study site lies within the Severn Upland physiographic unit, in the James Bay Region of the Precambrian Shield (Mollard and Mollard, 1981). Rocks underlying the area include Archean "greenstone" belt assemblages of metavolcanic and metasedimentary rocks, granites, unmetamorphosed shales and limestones of the Proterozoic Sibly Group, and diabase (Ford, 1994). These formations display a distinct northeast to southwest orientation (Pye, 1968; Shilts *et al.*, 1987). Nipigon diabase constitutes the youngest formations in the area, forming prominent ridges and knobs. The most common glaciogenic landforms in the area are eskers and esker-kame complexes, predominantly in low-lying terrain (Walsh *et al.*, 1994). Several small creeks drain the area to the northeast into Lake Nipigon. Areas of poor drainage are dominated by bogs and fens.

4.1.2 Quaternary Geology

The glacial deposits in the area originate from the Wisconsinan glaciation. The predominant ice flow was from the northeast to southwest. Glacial drift is generally less than 3 m with till being the oldest and most widespread sediment in the area (Walsh *et al.*, 1994). This till consists of a predominantly sand to silty-sand matrix with a coarse fragment content ranging from < 5% to > 30% (Walsh *et al.*, 1994). Amongst the glaciofluvial deposits (i.e., eskers, crevasse fills, kames and kame terraces) sediment texture and level of sorting vary, although moderately well- to well-sorted sand and gravelly sand are predominant. Mineral soils in the area are moderately deep to deep, with significant amounts of coarse fragments, while very thin soils, exposed bedrock and organic soils occur to a lesser extent throughout the study area (Walsh *et al.*, 1994). Bunisolic and Podsolic soil types (fine sandy and coarse loamy soils) are most common in the study area (Anonymous, 1993).

4.1.3 Forest Ecosystems

Trembling aspen (*Populus tremuloides*) and black spruce (*Picea mariana*) are dominant with jack pine (*Pinus banksiana*), white spruce (*Picea glauca*), balsam fir (*Abies balsamea*), white birch (*Betula papyrifera*), white cedar (*Thuja occidentalis*) and tamarack (*Larix laricina*) occurring in various mixtures. Forest-stand overstories are monospecific or mixed, and understories range from shrub- and/or herb-rich to poor (Walsh *et al.*, 1994). The FEC applicable to the study area is the Northwestern Ontario FEC (Sims *et al.*, 1989). Within the study site, species mixes occur on a variety of soil/site conditions. While even-aged jack pine stands are generally found on well-drained, coarse-textured soils, black spruce stands occur on sites ranging from shallow mineral soils overlying bedrock to deep, poorly drained

organic wetlands (Anonymous, 1994). Many of the major tree species, such as balsam fir, white spruce, trembling aspen and white birch, tend to occur in stands of a mixed nature on soils ranging from dry to moist and coarse-textured to fine (Anonymous, 1994). As a result, forest ecosystems cannot be modelled easily based simply on resident surficial / soil conditions.

Mature forests within the study site are mainly mixed, two-storied stands consisting of trembling aspen, jack pine, black spruce, balsam fir and white spruce on hilltops and slopes, with black spruce stands dominating lower positions (Anonymous, 1994). Pure and mixed aspen stands tend to possess abundant shrub and herb components (e.g., *Acer spicatum* and *Corylus cornuta*); they have average ages in the range of 80-100 years. Black spruce occurs on a range of upland and lowland site conditions and generally in association with jack pine, balsam fir and/or white spruce, and to a lesser extent with aspen and/or white birch, tamarack or cedar (Walsh *et al.*, 1994). Wetland organic sites, dominated by cedar, spruce and tamarack, are scattered throughout the study area.

Second-growth forests (i.e., 30-40 years old) are prevalent on the eastern side of Hwy #527 and along the Camp 45 Road, whereas recent cutover (i.e., <10 years) can be found on both sides of the highway. Second-growth forest canopies are dominated by balsam fir and black spruce, with various mixtures of these species occurring with white birch, white spruce, and/or trembling aspen (Walsh *et al.*, 1994). Based on field observations, forest age ranges from new growth in recently cut areas to over 200 years in lowland *Picea mariana* and *Thuja occidentalis* stands. The median age of the forest within the study site is approximately 80 years (Paradine, 1994b).

Shrub species within the study site are characteristic of the Boreal Forest. Shrub vegetation in forest ecosystems ranges from tall shrub-rich sites (e.g., *Abies balsamea, Acer spicatum, Alnus rugosa, Alnus crispa, Corylus cornuta*) (Figure 4.3) to low shrub-poor sites (e.g., *Vaccinium myrtelloides, Diervilla lonicera, Ledum groenlandicum, Linnaea borealis or Gaultheria hispidula*) (Paradine, 1994b) (Figure 4.4). Herb species are also characteristic of the boreal environment and common species include *Cornus canadensis, Aster macrophyllus, Aralia nudicalis* and *Frageria virginiana.* Herb species presence and abundance are sensitive to overstory and shrub conditions, as well as soil characteristics. *Sphagnum spp.* and feathermoss (e.g., *Pleurozium schreberi*) dominate the ground cover in the lowland sites, with feathermoss also occurring frequently in upland areas.



Figure 4.3 Trembling Aspen (White Birch) / Mountain Maple (V8).



Figure 4.4 Black Spruce Mixedwood / Feathermoss (V20).

The landscape pattern and the stand-level ecology have been affected by a variety of factors including extensive and repetitive forest fires, pathogens, insect infestations and various human activities such as timber harvesting, fire management, mining and recreation (Anonymous, 1994). Forest harvesting, in particular, has been considerable in the study area at various intervals within the last 35 years. Currently, a range of second-growth forests of varying ages is developing within the study site (Sims and Mackey, 1994). The landscape in the area has been affected by the removal of the most merchantable forest stands, with only less-merchantable stands and poorer-quality sites remaining. Currently, forest harvesting is intensive, particularly with regards to the harvesting of stands dominated by mature *Populus tremuloides*. The study site falls within the Spruce River Forest Management Agreement with Abitibi-Price Inc.

4.2. Ground Reference Data Collection From FEC Plots

Forest ecosystem data used in this study were collected by two primary groups. Forestry Canada, which has had ongoing studies in the Rinker Lake Research Area since 1983, provided a significant portion of the forest ecosystem data from field seasons in 1983, 1984 and 1993. Field teams from the University of Waterloo and ISTS at York University collected ground data over three field seasons: 1993, 1994 and 1995. This section outlines the data-collection methods for determining V-Types for the purposes of this study. All data collected in 1993 and 1994, along with selected data sets from Forestry Canada, are presented in the Rinker Lake Data Report (Kalnins *et al.*, 1994).

Detailed ground data were collected using a methodology devised by Forestry Canada for characterizing V-Types within a forest stand (McLean and Uhlig, 1987). These data were to serve a variety of purposes, but here, V-Type was the primary data used for the analysis. These ground samples, referred to as FEC plots, are 10 m x 10 m quadrats where V-Types are determined based on the presence and abundance of canopy and secondary trees; high, low and dwarf shrubs, broadleaf herbs; mosses and lichens.

Detailed FEC plot data were collected by the University of Waterloo and ISTS teams for 71 forested sites (Series 2601 to 2671) within the study area during the periods June 21-July 15, 1993 and July 4-15, 1994 (Figures 4.5 and 4.6). Plot locations were determined by the following guidelines:

1. Plots were located within relatively large forest stands whose species composition was either homogeneous (e.g., a pure stand of black spruce) or homogeneous in its heterogeneity (e.g., a mixed stand of black spruce, aspen and jack pine in uniform proportions throughout the stand). This was to assist in plot location on

the remotely sensed imagery as well as to expand plot boundaries on the remote sensing imagery to facilitate pixel sampling for classification.

2. Forest stands selected for sampling were large enough so that plots would be a minimum of 50 m from the edge of the stand. This was to minimize edge effects, both ecological and spectral, of adjacent forest stands.
3. Attempts were made to acquire data for as many V-Types as possible, given the restrictions of access and presence within the study area.
4. Sample sites had to be located within the ground coverage of the CASI data.
5. Sample sites had to be reasonably accessible from a road to allow more time for field sampling.

With these guidelines in mind, sample plot locations were identified using black-and-white aerial photographs (1:15 840) or colour-infrared photographs (1:10 000). The Forest Resources Inventory (FRI) was also used to assist in evaluating stands based on stand composition. Once candidate stands were identified, azimuth directions and distances to potential samples from the nearest access point were plotted on the appropriate airphoto. Plot locations were then located on the ground using a compass and 50 m chain. After travelling the appropriate distance on a given bearing, the nearest tree was selected as the centre tree for the plot. However, this point was sometimes rejected if it did not appear to represent the stand as a whole. This modification was generally a result of (i) the plot location falling within a clearing caused by a blowdown; (ii) an uncharacteristic species-mix in relation to the stand (noise); or (iii) was in close proximity to the edge of the stand. In the case of rejection, the plot was moved 20 - 50 m perpendicular to or along the original bearing. The boundaries of the plot would then be measured and marked around the centre tree.

These data were supplemented with an additional 32 FEC plots sampled by Forestry Canada (Series 001 to 200) (Figure 4.5). Since these plots were selected primarily to study the relationships between vegetation, soils and different landforms, they were not selected using the guidelines discussed above. These plots generally occur along a toposequence, proceeding from the top of the landform to the valley bottom. Since forest composition changes rapidly along such sequences, these plots often do not represent large areas of forest with uniform composition. Hence, it is often difficult to correlate these plots spatially with remote sensing data.

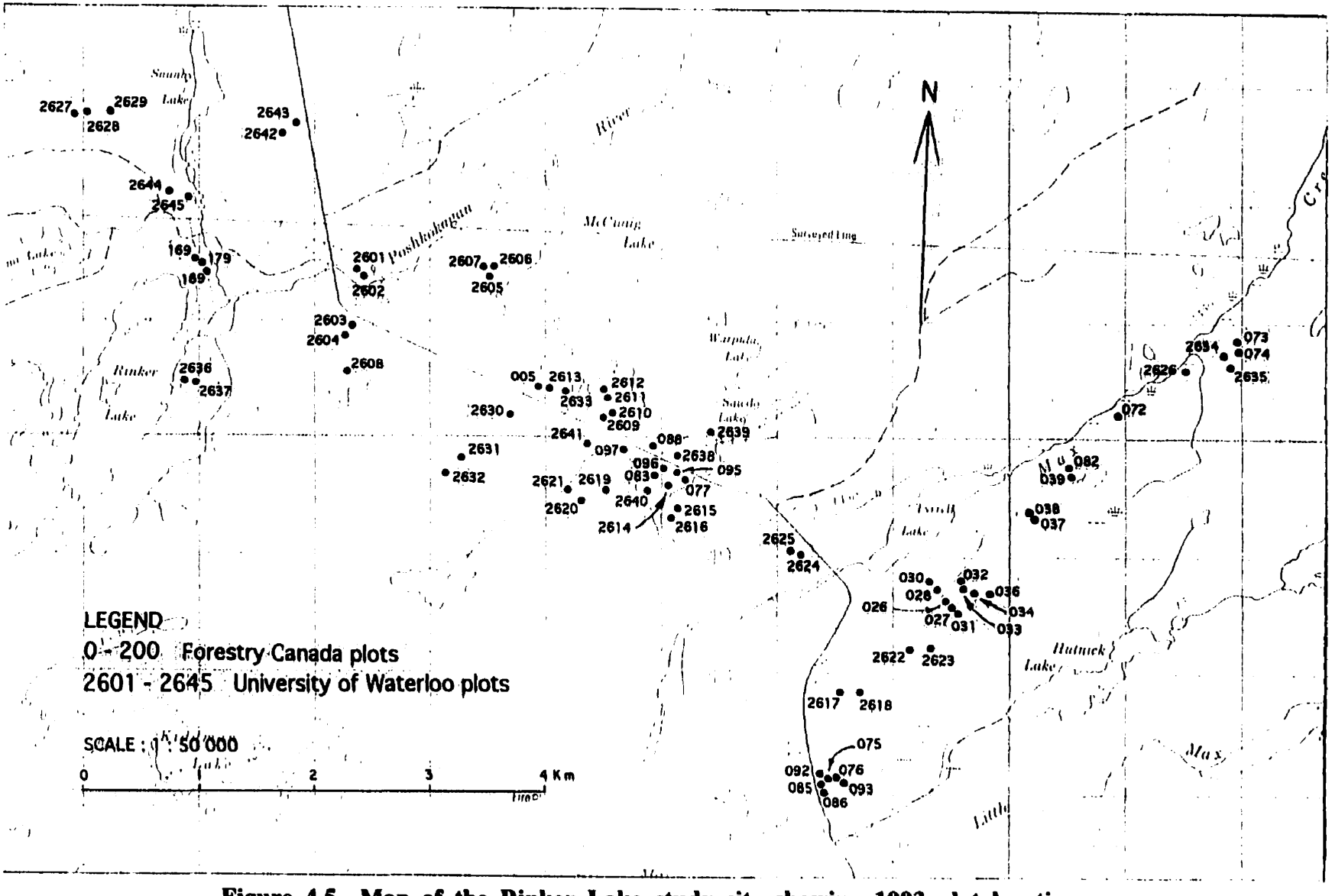


Figure 4.5 Map of the Rinker Lake study site showing 1993 plot locations. (NTS 1:50 000, Eaglehead Lake, 52 H/3, 3rd ed., 1979).

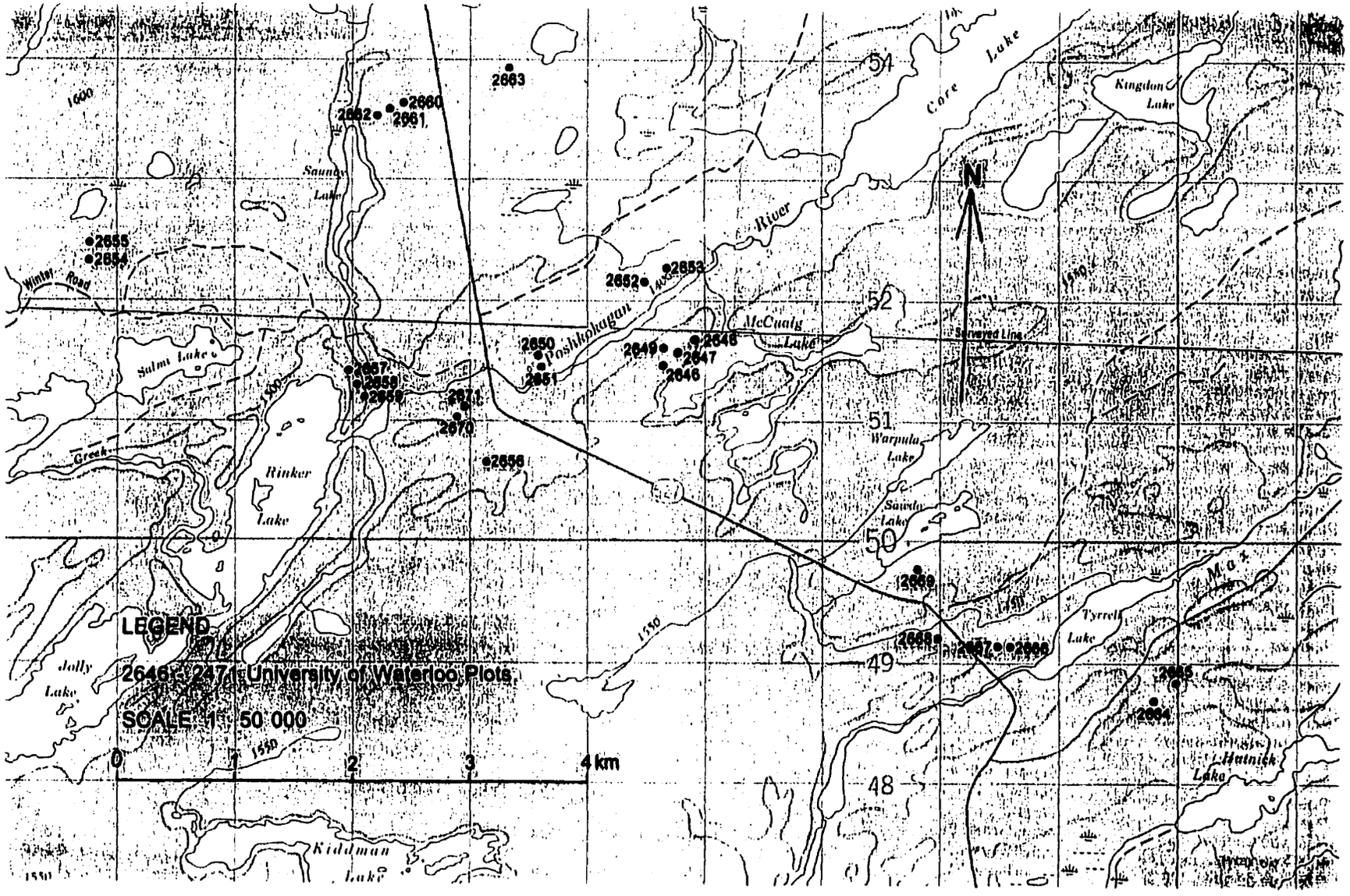


Figure 4.6 Map of the Rinker Lake study site showing 1994 plot locations. (NTS 1:50 000, Eaglehead Lake, 52 H/3, 3rd ed., 1979).

Data collected for each 10 m x 10 m sample plot included: differential Global Positioning System (GPS) data; (ii) vegetation data (e.g., species and percent cover for tree, shrub and herb layers); (iii) mensuration data (e.g., age, height, density, diameter breast height (dbh)); and (iv) canopy data (e.g., crown diameter). In total, plot data were collected for 25 of the 38 V-Types within the NWO FEC. Of the 13 V-Types not sampled, six of these were characteristic of the Great-Lakes St. Lawrence forests to the south of the study site, whereas the rest were either too small in size to sample effectively, were inaccessible, or did not occur within the study site (Kalnins *et al.*, 1994).

4.2.1 Vegetation Data

Vegetation within a sample plot was divided into the following layers:

1. trees - dominant, co-dominant, understory (i.e., > 10 m tall or > 10 cm dbh);
2. shrubs - all plant species which have some woody portion above ground throughout the whole year (tall > 2 m; low 0.5 - 2 m; dwarf < 0.5 m);
3. herbs - plants without woody portions above ground throughout the year, but not mosses or lichens;
4. mosses (Feathermoss, *Sphagnum* spp.) and lichens.

Plant species were identified and their total cover (percent canopy cover) estimated within the appropriate vegetation layer. These data were recorded on NWO FEC Vegetation Data Cards (Figure 4.7) and compiled in a spreadsheet of digital form (Figure 4.8). The compilation of these data for each FEC plot is presented in the Rinker Lake Data Report 1993-1994 (Kalnins *et al.*, 1994). FEC plot samples are summarized by V-Type in Table 4.1. To provide a visual record of the plot, four ground, two eye-level and two oblique canopy photographs were taken.

4.2.2 Mensuration Data

Mensuration data collected for each of the FEC sample plots included:

- species of each tree;
- diameter breast height (dbh) of each tree;
- tree heights (for average trees of each dominant species); and
- tree ages (taken at breast height for average trees of each dominant species) (correction factors were added to the number of rings in order to compensate for the number of years it takes for each tree species to grow to breast height under the general conditions in northwestern Ontario).

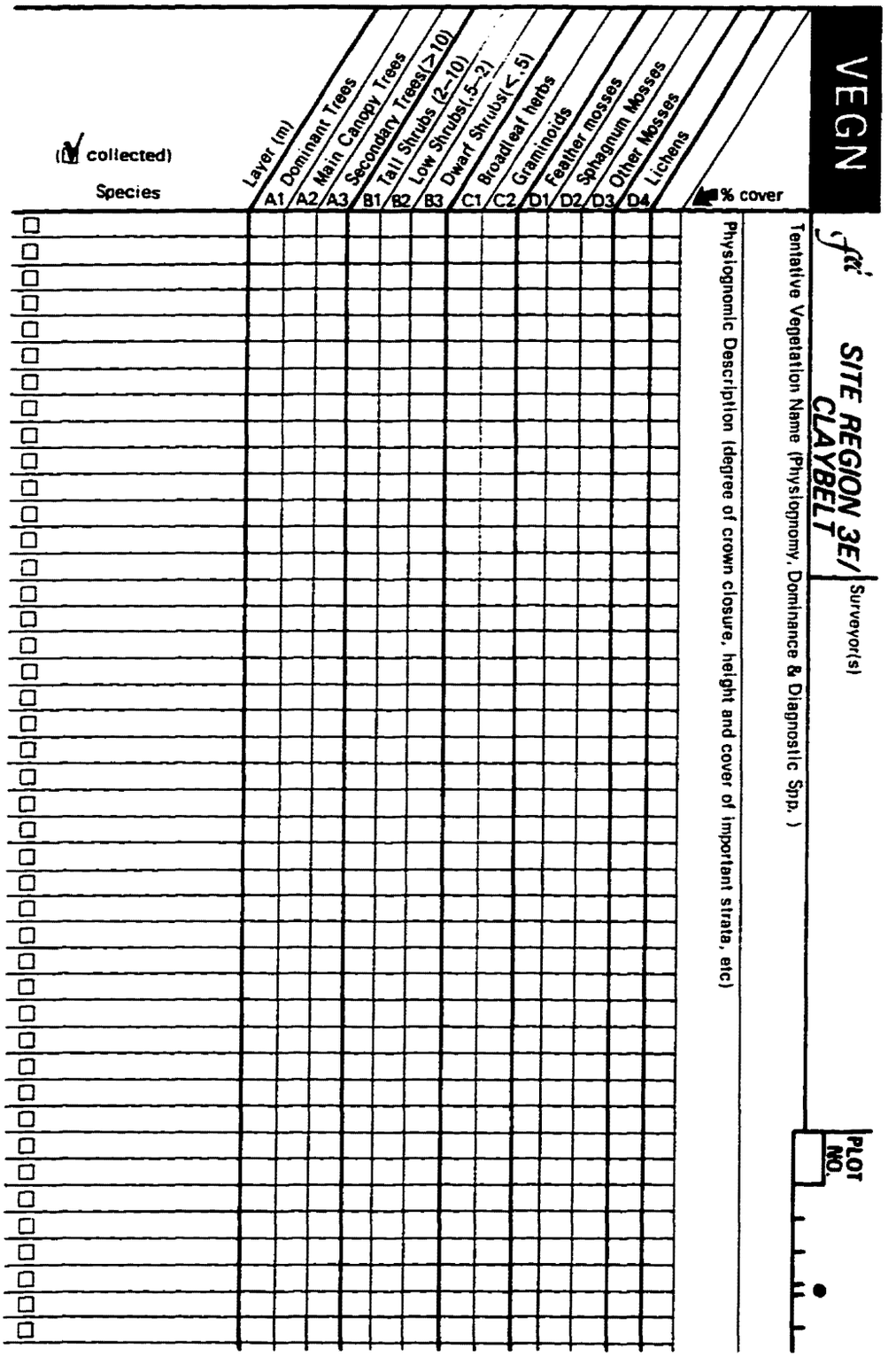


Figure 4.7 NWO FEC Vegetation Card (Forestry Canada, 1990).

1993 Rinker Lake Study Vegetation Card

DATE 93/06/28
PLOT # 2609
LOCATION 95 m. @ 70° (3.1 km S. of RL Rd. on Hwy. 527, on left)
V-TYPE V10 high shrub, feathermoss

	Species	Dominant Trees	Main Canopy Trees	Secondary Trees (>10)	Tall Shrubs (2-10)	Low Shrubs (0.5-2)	Dwarf Shrubs (>0.5)	Broadleaf Herbs	Graminoids	Feather Mosses	Sphagnum Mosses	Other Mosses	Lichens	Total Cover
1	Picemar		7	3	1									
2	Poputre	40			1									41
3	Abiebal				5	0								5
4	Acerspi					3								3
5	Amelhum					2								2
6	Sorbdec					1								1
7	Lonihir					1								1
8	Dierlon					15								15
9	Ribetri					1								1
10	Aralnud					10								10
11	Comcan							1						1
12	Rosaaci						2							2
13	Clinbor							0						0
14	Linnbor						15							15
15	Pleusch									30				30
16	Rubupub							2						2
17	Triebor							0						0
18	Vaccmyr						1							1
19	Maiacan							0						0
20	graminoid								0					0
21	Streros							0						0
22	Astemac							0						0
23	old man's bd												0	0
24	fungus												0	0
25	Lycoann											0		0
26	Hylospl									0				0
27	Ryhtacq												0	0
28	Peltaph												0	0
29	Pyrocor							0						0
Total % cover by layer		40	0	0	6	33	18	3	0	30	0	0	0	

# dead snags	2
# fallen dead trees	9

NOTES (including physiognomic description)
- Some brown litter, some moss cover- 50%/50%
- Some Po canopy thin with dead branches. Mossy spruce
- Most herbs blooming

Figure 4.8 Sample NWO FEC Vegetation Data Compilation.

Table 4.1 FEC V-Type Samples

V-Type	FEC Description	Identification of Complete FEC Plots 1993/1994	Transect and Sample No. for Supplementary V-Types 1994/1995	Transect and Sample No. for V-Type / Mensuration Plots 1995
	Mainly Hardwood			
V1	Balsam Poplar Hardwood and Mixedwood			
V2	Black Ash Hardwood and Mixedwood			
V3	Other Hardwoods and Mixedwoods			
V4	White Birch Hardwood and Mixedwood	2631, 2636	S4, T7, T16	A14
V5	Aspen Hardwood	2605, 2606, 2607, 2644, 2645, 2647	PP2, PP27, PP28, S12, S28, T1, T4, T5,	A12, A15
V6	Trembling Aspen (White Birch) - Balsam Fir / Mountain Maple	2617, 2620, 2632, 2648, 2654, 2655	A37, D1, I3, G5, S1, T11, T19	A16
V7	Trembling Aspen - Balsam Fir / Balsam Fir Shrub	077, 189, 2610, 2614, 2638, 2639	A38, I5, PP26	A17
V8	Trembling Aspen (White Birch) / Mountain Maple	2619, 2630, 2646	A33, A34, A35, A36, D3, G3, S2, S8, S10, S11, S14, S17, S24, S25, S26, S27, S29, S30, S31, T2, T10, T12, T23, T24, T25, T26, T29	A1, A2, A9, A11, A26, A27, A28
V9	Trembling Aspen Mixedwood	2649, 2658	A29, I1, P2, P7, R46	A13
V10	Trembling Aspen - Black Spruce - Jack Pine / Low Shrub	179, 2603, 2604, 2609, 2615, 2670, 2671	I4, P1, P3, P5, P6, P9, PP1, PP11, S9	R15
V11	Trembling Aspen - Conifer / Blueberry / Feathermoss		P8, R40, R44, S7, S20, S23	A24, R8, R14, R21, R22
	Conifer Mixedwood			
V12	White Pine Mixedwood			
V13	Red Pine Mixedwood			
V14	Balsam Fir Mixedwood	095	G1, T13, T17	
V15	White Spruce Mixedwood	038, 2637, 2657	T21, T22	
V16	Balsam Fir - White Spruce Mixedwood / Feathermoss	2624, 2625, 2628, 2659, 2669	01, T14, T15, T20,	
V17	Jack Pine Mixedwood / Shrub Rich	(169, 2627, 2662	A30, H6,	A3, A10
V18	Jack Pine Mixedwood / Feathermoss	(2660, 2661	A31, H1, H3, H4	R2, R5
V19	Black Spruce Mixedwood / Herb Rich	(027, 073, 075, 085, 096, 2616, 2626, 2634	A4, A5, A6, A8, I2, L2, PP4, PP5, PP14, PP15, PP17, R41, R45, R47, S3, S6, S13, S16, S19, S22, T8, T19, T27, T28	A25, R1, R3, R4, R10, R12, R17, R18
V20	Black Spruce Mixedwood / Feathermoss	082	R27	R7, R13, R20, R23
	Conifer			
V21	Cedar (inc. Mixedwood) / Mountain Maple	097	T18	
V22	Cedar (inc. Mixedwood) / Speckled Alder / Sphagnum	088, 2621, 2641		
V23	Tamarack (Black Spruce) / Speckled Alder / Sphagnum		PP24, R32, R33, R43, S18,	R11
V24	White Spruce - Balsam Fir / Shrub Rich		I6	
V25	White Spruce - Balsam Fir / Feathermoss	026, 032, 033, 037		
V26	White Pine Conifer			
V27	Red Pine Conifer			
V28	Jack Pine / Low shrub			
V29	Jack Pine / Ericaceous Shrub / Feathermoss			
V30	Jack Pine - Black Spruce / Blueberry / Lichen		R28, R35	
V31	Black spruce - Jack Pine / Tall Shrub / Feathermoss	028, 034, 2629	PP12, PP16, S15	
V32	Jack Pine - Black Spruce / Ericaceous Shrub / Feathermoss	074, 076, 086, 2635, 2640	L3, L4, L6, L7	
V33	Black Spruce / Feathermoss	005, 031, 039, 072, 2664, 2665, 2666	A7, K1, K3, K4, K5, K6, R25, R38, S5	
V34	Black Spruce / Labrador Tea / Feathermoss (Sphagnum)	030, 083, 093, 2633	A22, A34, J2, M1, PP3, PP25, PP29, R37, S33, S34	R9
V35	Black Spruce / Speckled Alder / Sphagnum	036, 2608, 2643, 2656, 2667, 2668	A19, A20, A21, A23, A39, E2, E3, N2, N4, PP6, R29, R30, R34, R36, R39, R42, T3	A18, R24
V36	Black Spruce / Bunchberry / Sphagnum (Feathermoss)	2611, 2612, 2613, 2651	E1, M2, M4, R26	
V37	Black Spruce / Ericaceous Shrub / Sphagnum	092, 2601, 2602, 2618, 2623, 2650, 2653	B1, B3, C6, F3, F4, J1, J3, J4, N1, Q4, Q5	
V38	Black Spruce / Leatherleaf / Sphagnum	2622, 2642, 2652, 2663	C1, C2, C4, C5, J6, Q2, R31	

The heights of three representative trees were measured using Suunto clinometers. The ages of these three trees were determined from ring counts of cores extracted with an increment bore with the appropriate correction factor applied by species (Table 4.2).

Table 4.2 Correction Factors for Tree Species Age Calculations (Paradine, 1994b).

Species	Correction Factor (years)
Abies balsamea	10
Betula papyrifera	7
Larix larcina	10
Picea glauca	10
Picea mariana	8
Pinus banksiana	5
Populus tremuloides	5
Thuja occidentalis	8

Variable-area subplots were established at each FEC plot. These plots were located 17 m from opposite corners of the FEC plot where the species composition was similar to that in the FEC plot. At these subplots, a 2-Basal Area Factor (BAF) prism measurement was taken to determine basal area by species. In addition, mean spacing interval (MSI) measurements (i.e., distance from a centre tree to the five nearest trees) were taken at these plots, as well as from the centre tree of the FEC plot. MSI is calculated as follows (Day, 1992):

$$MSI = \frac{\frac{\Sigma \text{ distance of five nearest trees to a centre tree}}{5} + \frac{\Sigma \text{ distance of four nearest trees to a centre tree}}{4}}{2}$$

Mensuration data were tabulated on FEC Forestry Data Cards (Figure 4.9) and compiled in spreadsheet files (Figure 4.10). A complete complement of mensuration data is presented in the Rinker Lake Data Report: 1993-1994 (Kalnins *et al.*, 1994). These data are used qualitatively for comparison to the results of the semivariogram analysis to determine which mensuration parameters may be related to optimal spatial resolutions for remote sensing data.

4.2.3 V-Type Transects

In 1994 and 1995, a series of transects was traversed through selected forest stands in order to collect additional V-Type data (Figure 4.11). These samples of V-Type characterization only, occurred at fixed intervals of 50 m along predetermined transects. These samples are identified by V-Type and transect in Table 4.1.

FOR *ftd* **SITE REGION 3E/ CLAY BELT**

Stand Sample Plot Size ☐ 10m x 10m ☐ Other (____m x ____m)

PLOT NO.

TREES (10cm + dbh)

	Species/Diameter (cm)						
1							
2							
3							
4							
5							
6							
7							
8							
9							
10							
11							
12							
13							
14							
15							
16							
17							
18							
19							
20							
21							
22							
23							
24							
25							
Total							

Species	Ht.	Age @dbh	BA	Notes

Stand Condition (e.g. overmature, insect damage, rot, fire)

Stand Origin

Stand Future Development

Figure 4.9 NWO FEC Forestry Data Card (Forestry Canada, 1990).

1993 Rinker Lake Study Mensuration Card

DATE 93/06/28 GPS N: 49° 10' 54.127"
PLOT # 2609 W: 89° 22' 50.647"

Species											
Tree No.	Picemar	Picegla	Abiebal	Pinubas	Larilar	Thujocc	Betupap	Poptre	Popbal	Fraxnig	Sorbdec
Prism 1	3		2					12			
Prism 2	6							13			
Height 1	14.25										
Height 2	15.5										
Height 3								21.5			
Age 1	68										
Age 2	82										
Age 3											
Diameter (cm)											C.H.
1	14.4							25.1			4.4
2	13.1							22.6			3.4
3	16.8							21			3.4
4	15.3							26.5			3.2
5	17.7							23.6			4.4
6								17			4
7								20.3			4
8								21.4			4
9								17.1			4
10								14.3			2
11								21.4			4
12								23.5			3
13								26.3			4
14								23.1			4
15								21			2
Crown Health	3.4							3.5			
MMCD	2.5							4			

Mean Spacing Index

Tree No.	P0	P1	P2	Average
1	0.98	3.12	1.78	
2	2.43	4.51	2.69	
3	2.96	4.83	2.79	
4	3.2	4.92	3.11	
5	3.22	5.63	3.35	
MSI	2.48	4.47	2.67	3.21

Canopy Closure (%)
50

Stand condition
- Po is rotting
- may have had a fire history. Sb attacked by budworm, young

Stand origin

Stand future development
- Spruce coming in, poplar. Sb on top of a rich, heavy herb and shrub rich understorey
- Po will be gone in 15 years, GPS 3m in front of center tree
- A bit less spruce in other parts of stand

Figure 4.10 Sample NWO FEC Forestry Data Compilation.

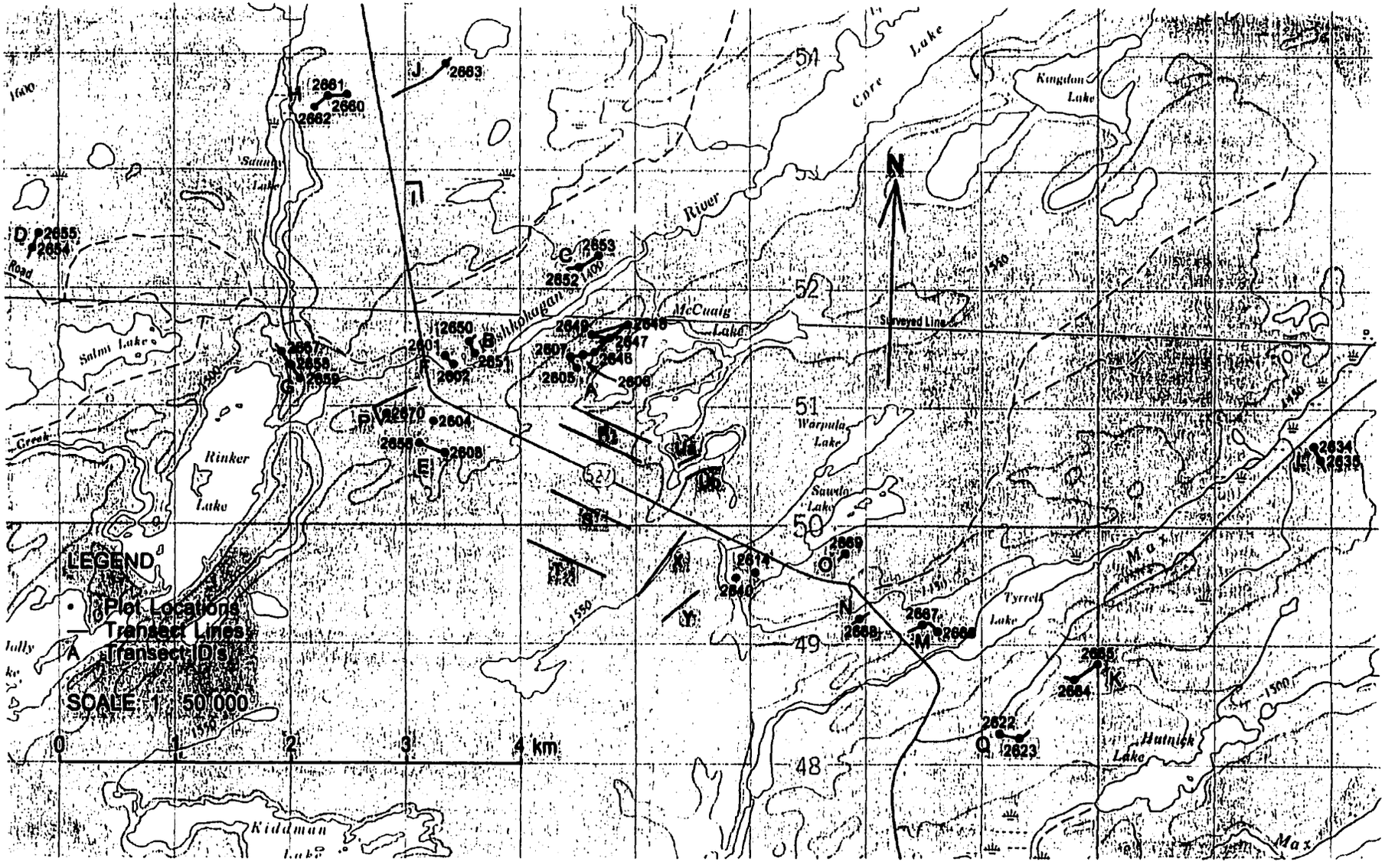


Figure 4.11 Map showing transects sampled for V-Type in 1994 and 1995. (NTS 1:50 000, Eaglehead Lake, 52 H/3, 3rd ed., 1979).

4.3 Remote Sensing Data

The acquisition of remotely sensed data at a variety of spatial resolutions was central to the objectives of this study. These data were acquired from satellite (i.e., Landsat) and the Compact Airborne Spectrographic Imager (CASI). These data are described below.

4.3.1 Landsat Data

The Landsat Thematic Mapper (TM) sensor collects data in six spectral bands at 30 m resolution and in a seventh thermal-infrared band at 120 m resolution. The spectral, spatial and temporal characteristics of Landsat TM data are summarized in Table 4.3. Landsat-5 has a 705 km high, sun-synchronous, near-polar orbit with a repeat cycle of 16 days. Due to the poor temporal frequency associated with the Landsat TM and the poor weather conditions experienced at Rinker Lake during the summers of 1993 and 1994, few satisfactory Landsat TM scenes were collected for the study area (Track 25, Frame 26; 48° 53' N 88° 55' W) during the peak growing season. Cloud-free Landsat TM data were acquired for June 20, 1992 (Figure 4.12).

Table 4.3 Sensor Characteristics for Landsat-5.

Spectral Bands (μm)	Spatial Resolution (metres)	Radiometric Resolution (digital numbers)
1) 0.45 - 0.52	30	256
2) 0.52 - 0.60	30	256
3) 0.63 - 0.69	30	256
4) 0.76 - 0.90	30	256
5) 1.55 - 1.75	30	256
6) 10.5 - 12.5	120	256
7) 2.08 - 2.35	30	256

With respect to the phenological development of vegetation in the area, the June 1992 data closely coincide with the start of field work on June 21, 1993. For the objectives of the study, it was felt that ground-cover conditions for the summer of 1992 would be similar to those observed during the summer field program of 1993. However, an infestation of forest tent caterpillars occurred in the summer of 1992 which may have affected the foliage conditions of *Populus tremuloides*.



Figure 4.12 Landsat TM image of the study site - June 20, 1992.

4.3.2 Compact Airborne Spectrographic Imager Data

The CASI is a visible/near-infrared pushbroom imaging spectrograph with a reflection grating and a two-dimensional CCD solid-state array measuring 512 x 288 pixels (Shepherd, 1994). This instrument is portable, in that it can be mounted in various lightweight aircraft and helicopters or on a ground-based platform. The CASI looks vertically downward imaging successive lines over the terrain, building up a two-dimensional image based on the forward movement of the aircraft. This imaging system is able to collect data in two modes: spectral mode, where continuous spectra for ground-resolution elements are collected for up to 288 spectral bands for a selected subset of the 512 CCD elements in the cross-track direction; and spatial mode, where a more limited number of spectral bands is recorded, but complete spatial coverage for the swath is provided. The CCD sensor is read out and digitized to 12-bits and recorded on 8 mm video cassette by an Exabyte recorder. The

specifications of the CASI are outlined in Table 4.4.

The cross-track resolution across the 35° field of view (FOV) is a function of the height above ground level (AGL) and equates to 1.23 m ground resolution per 1 km AGL (Shepherd, 1994). The along-track ground resolution is approximately equal to the product of the integration time and the aircraft speed, and is directly proportional to the number of bands being recorded in spatial mode or the number of look directions in spectral mode (Shepherd, 1994). The spatial resolution characteristics of CASI data therefore do not resemble those of traditional remote sensing systems. That is, image pixels collected by the CASI are not necessarily square, but are often rectangular, with different dimensions in the cross- and along-track directions.

Table 4.4 Description of the Compact Airborne Spectrographic Imager (CASI) (adapted from Gower *et al.*, 1992).

Parameter	Description
Spectral Coverage	418 nm to 926 nm using 288 detectors; sampling interval 1.8 nm; spectral resolution 2.9 nm
Spectral Mode	39 spectra of the full 418 nm to 926 nm range are recorded, with 2.9 nm resolution, from 39 different directions across the swath; a full-resolution image at a predetermined wavelength is also recorded to assist in track recovery
Spatial Coverage	35.5° swath, with standard lens; single camera gives 612 pixels; sampling interval 1.2 mrad; spatial resolution 1.6 mrad
Spatial Mode	spectral pixels are grouped to form up to 15 bands (512 pixels wide); band width and spectral position are under software control; the number of bands governs the integration time

Compact Airborne Spectrographic Imager (CASI) data were acquired by the Provincial Remote Sensing Office (PRSO) from a Piper Navajo Chieftan aircraft on July 30, 1993. In order to minimize bidirectional reflectance (BDRF) and effectively cover the study area, flight lines were oriented parallel to the solar azimuth (i.e., away from the sun), restricting data collection to a two-hour time window (10:30 a.m. to 12:30 p.m. local time) (Figure 4.13).

Thirteen flight lines were flown over the study site at a ground speed of 149 knots, heading 300 degrees true, parallel to the longest straight portion of Hwy #527 (Figure 4.13) with the sensor pointing at nadir. Although CASI data were collected over the test site in both spectral and spatial mode, only spatial-mode data are analysed in this research. Spatial-mode data were collected in nine spectral bands (Table 4.5) and at three different altitudes to produce images at three different spatial resolutions. The spatial-mode data were collected with an integration time of 70 milliseconds. The spatial resolutions of the remote sensing data are 0.73 m x 5.36 m (Figure 4.14); 1.39 m x 5.36 m (Figure 4.15); and 3.18 m x 5.36 m (Figure 4.16).

Table 4.5 CASI Imaging Mode Wavelengths.

Channel Number	Centre Wavelength	Bandwidth (nm)	Band Range (nm)
1	450.31	31.18	434.72 - 465.90
2	549.47	20.80	539.07 - 559.87
3	590.50	20.88	580.06 - 600.94
4	633.48	20.94	623.01 - 643.95
5	670.30	15.60	662.50 - 678.10
6	739.72	10.22	734.61 - 744.83
7	746.95	6.62	743.64 - 750.26
8	790.38	10.24	785.26 - 795.50
9	873.85	28.44	859.63 - 888.07

Two additional flight lines were flown over pseudoinvariant features (PIFs) (gravel, pavement and clover) to assist in image calibration. These flight lines were flown at 170 m AGL and possessed a spatial resolution of 0.21 m x 5.36 m. The CASI data were converted to radiance using software developed at the Institute for Space and Terrestrial Science (ISTS), with input from Itres Research (the manufacturer of the CASI), using algorithms found in Baby and Soffer (1992). This conversion was applied in order to eliminate artifacts present in the imagery and to convert digital numbers from arbitrary values to physical units of radiance (Shepherd, 1994). The data were then converted to reflectance to eliminate atmospheric effect and compensate for changes in solar illumination during image acquisition (Shepherd, 1994). Calibration to reflectance provides a basis for comparison of reflectance values between adjacent flight lines and between different altitudes. A hybrid model was used to perform this calibration using PIFs and an on-board downwelling irradiance sensor (Incident Light Probe (ILP)) (Shepherd, 1994; Shepherd *et al.*, 1995). These data were also corrected for aircraft roll and are described in Table 4.6.

Table 4.6 Multiple Spatial Resolution CASI Data Collected for this Study (Shepherd 1994).

Altitude (m AGL)	File Name	Flight Line	Across-Track Resolution (m)	Along-Track Resolution (m)	Swath Width (m)
2630	T059F04	2	3.18	5.36	1630
2630	T059F05	1	3.18	5.36	1630
2630	T059F06	3	3.18	5.36	1630
2630	T061F02	4	3.18	5.36	1630
2630	T061F03	5	3.18	5.36	1630
1150	T059F09	2	1.39	5.36	815
1150	T059F10	9	1.39	5.36	815
1150	T059F11	10	1.39	5.36	815
600	T060F02	2	0.73	5.36	410
600	T060F03	11	0.73	5.36	410
600	T060F04	12	0.73	5.36	410
600	T060F05	10	0.73	5.36	410
600	T060F06	9	0.73	5.36	410

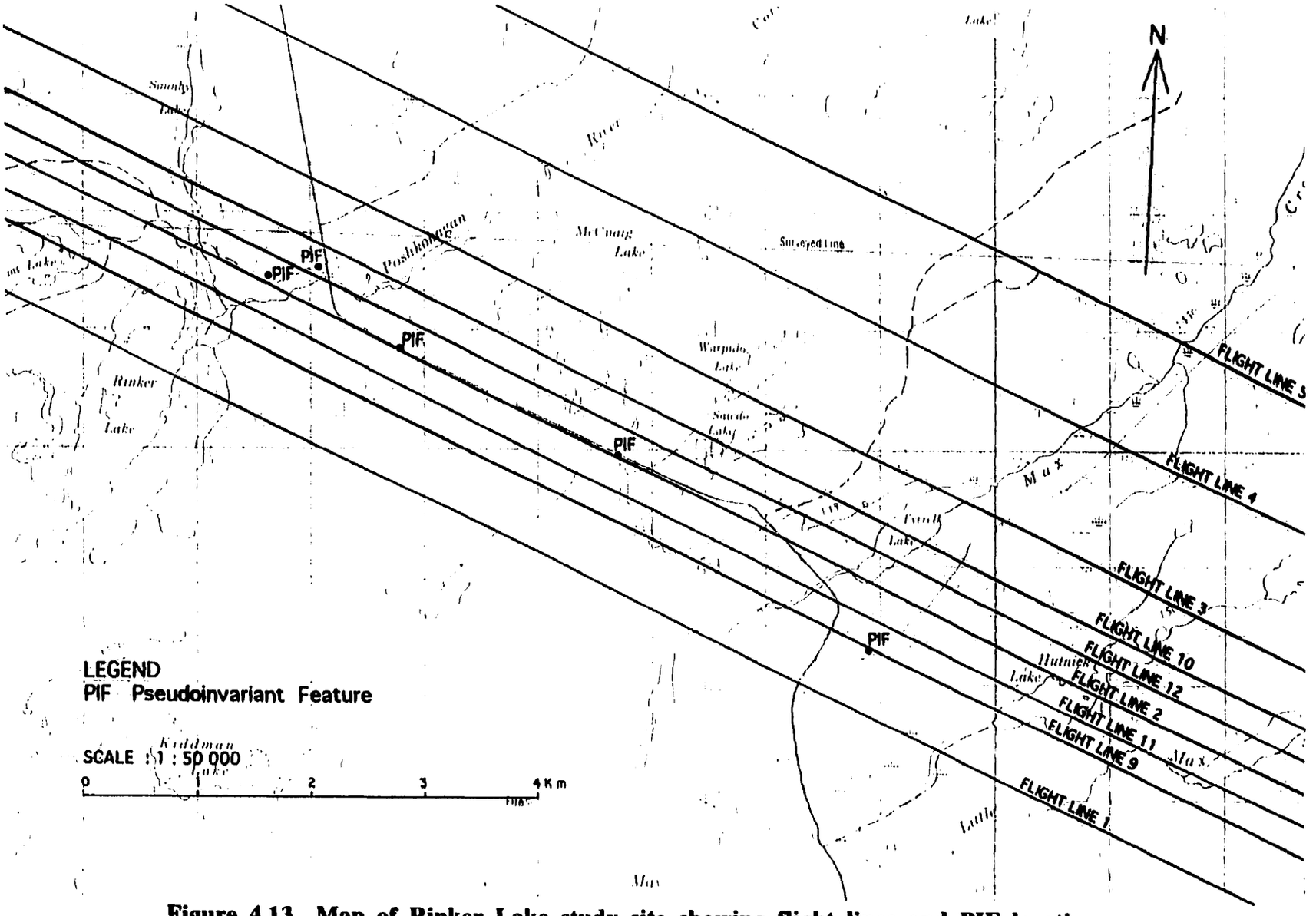


Figure 4.13 Map of Rinker Lake study site showing flight lines and PIF locations. (NTS 1:50 000, Eaglehead Lake, 52 H/3, 3rd ed., 1979).



Figure 4.14 High altitude CASI data for part of the Rinker Lake study site.

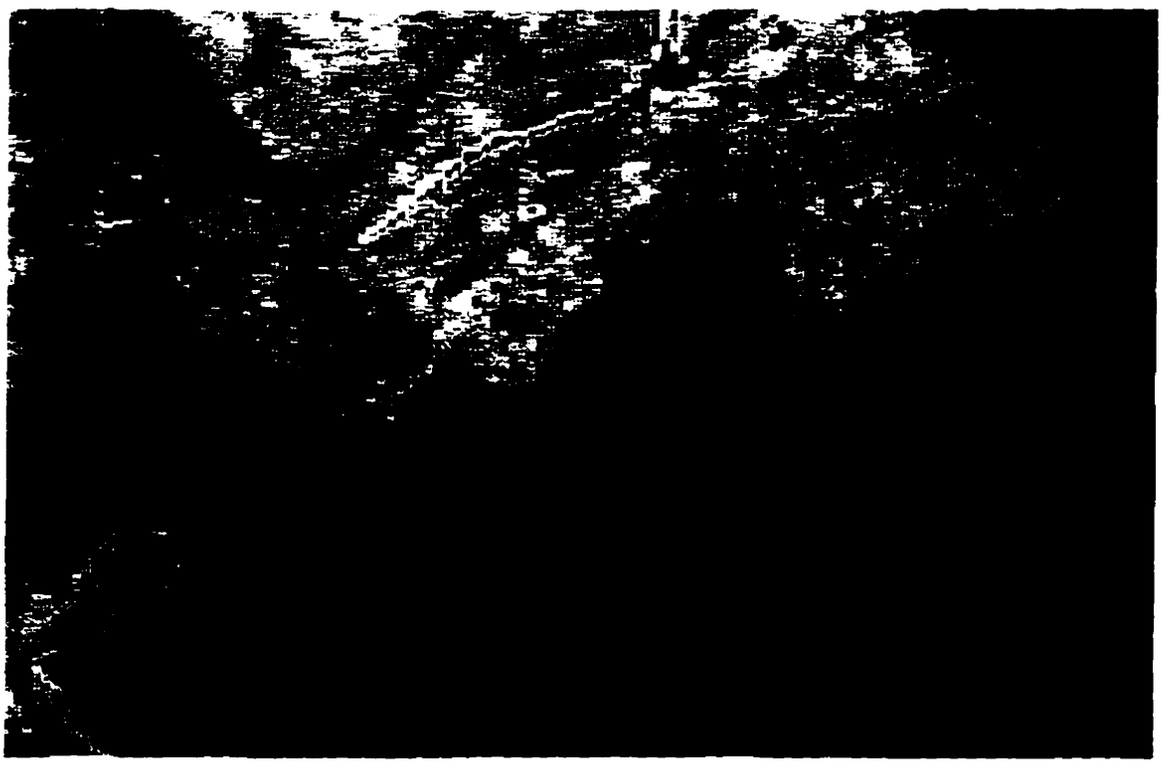


Figure 4.15 Mid altitude CASI data for part of the Rinker Lake study site.



Figure 4.16 Low altitude CASI data for part of the Rinker Lake study site.

4.3.4 Ancillary Remote Sensing Data

Aerial photographs were used in the field to select forest stands for which detailed calibration and validation data could be collected (i.e., FEC plot locations and V-type transects). Colour-infrared aerial photographs (1:10 000) acquired in September, 1992 were used in conjunction with 1988 summer black-and-white aerial photographs (1:15 840). These data were also used for reference during data analysis.

4.4 Digital Elevation Data

A digital elevation model (DEM) can be defined as a georeferenced, ordered array of numbers that represents the spatial distribution of elevations above some arbitrary datum, generally metres above sea level (Moore *et al.*, 1991). A DEM can take three different forms: (i) triangulated network; (ii) contour-based network; and (iii) regular grid network (Moore *et al.*, 1991). Of the three, regular grid networks are computationally more efficient and more compatible with other types of gridded data, such as remote sensing data.

The DEM for the entire Rinker Lake Research Area was produced by the Department of Natural Resources - Forestry Canada. This DEM was generated at a 20 m grid using the

data (contours and streamline data) from the 1:20 000 scale OBM Series (Hutchinson, 1989). The ability of ANUDEM to produce reliable DEMs stems from a variety of features (Hutchinson, 1989; Hutchinson and Dowling, 1991; Mackey *et al.*, 1994b). These include:

1. computational efficiency;
2. interpolation provides flexibility to follow sharp changes in terrain associated with ridges and sometimes streams and other landscape features;
3. a drainage-enforcement algorithm attempts to remove all sinks from the fitted DEM which are not specified by the user, thereby maintaining a connected surface drainage pattern; and
4. incorporating streamline data in the interpolation to assist in drainage enforcement, thereby improving streamline placement and removal of additional sinks (streamlines will lie at the bottom of associated valleys).

A subset of the DEM representing the study site is presented in Figure 4.17.

Two first-order derivatives of altitude (gradient and aspect) are easily calculated from an elevation model. These measures characterize the slope of a surface, defined by a plane tangent to the surface as modelled by the DEM at any given point. In this case, each point is represented by a 20 m cell and the plane is defined by a 3 x 3 pixel window about that cell. Aspect was not included in this study since it represents a directional variable. Directional variables do not satisfy the assumptions of a normal distribution for parametric statistical analysis. Another first-order derivative of elevation, local relief, was derived from the elevation data.

4.4.1 Gradient Model

A gradient image portrays the rate of maximum change in elevation between neighbouring cells (0 to 90°). Degree gradient for any given cell in the matrix is calculated as the gradient of a plane formed by the vectors connecting the neighbouring cells in a 3 x 3 cell window, where each cell contains an elevation (Figure 4.18).

Gradient is calculated as follows (Burrough, 1986; ESRI, 1994):

$$\tan G = [(\delta Z/\delta X)^2 + (\delta Z/\delta Y)^2]^{1/2}$$

$$\text{Gradient (degrees)} = \text{atan}(\tan G) * 57.29578$$

where Z is altitude and X and Y are the coordinate axes.

The east-west and north-south gradients are estimated by the following (Horn, 1981):

$$[\delta Z/\delta X]_{i,j} = [(Z_{i+1,j+1} + 2Z_{i+1,j} + Z_{i+1,j-1}) - (Z_{i-1,j+1} + 2Z_{i-1,j} + Z_{i-1,j-1})]/8\delta X$$

$$[\delta Z/\delta Y]_{i,j} = [(Z_{i+1,j+1} + 2Z_{i,j+1} + Z_{i-1,j+1}) - (Z_{i+1,j-1} + 2Z_{i,j-1} + Z_{i-1,j-1})]/8\delta Y$$

where δX and δY are the distances between cell centres in the east-west and north-south directions, respectively. The slope image was derived using the above algorithms as implemented in ARC/INFO (ESRI, 1994) (Figure 4.19).

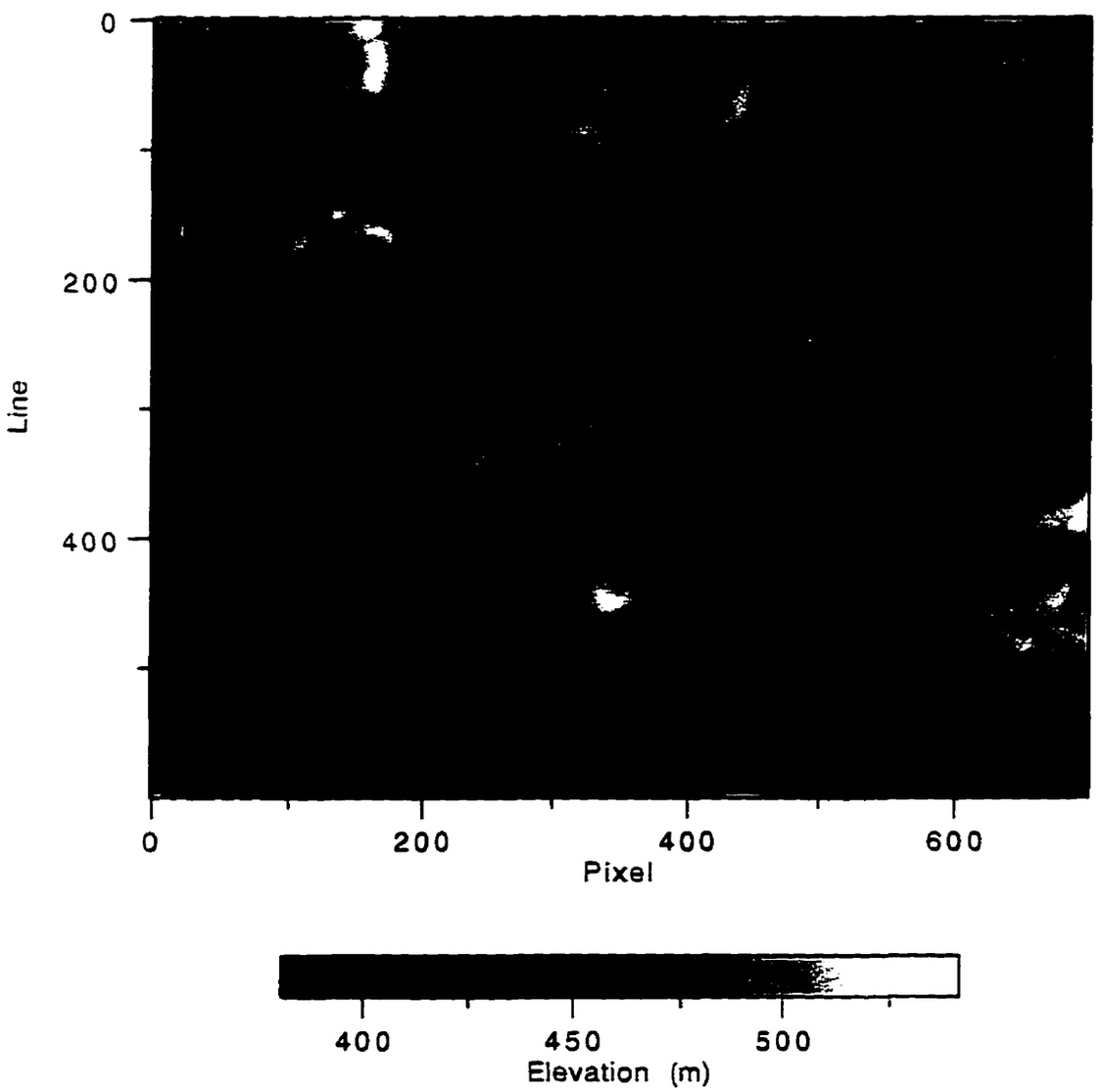


Figure 4.17 Digital elevation model for the Rinker Lake study site.

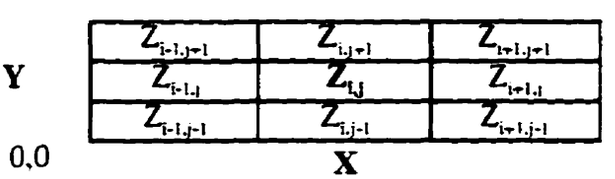


Figure 4.18 Window for computing derivatives of elevation matrices.

4.4.2 Local Relief

In order to quantify the local variability in elevation and gradient, a map of local relief was generated by calculating the range of altitude within a 5 x 5 pixel moving window. This image effectively portrays the maximum change in altitude within a 100 m x 100 m (1 ha) area and represents a first-order statistical derivative of elevation (Figure 4.20).

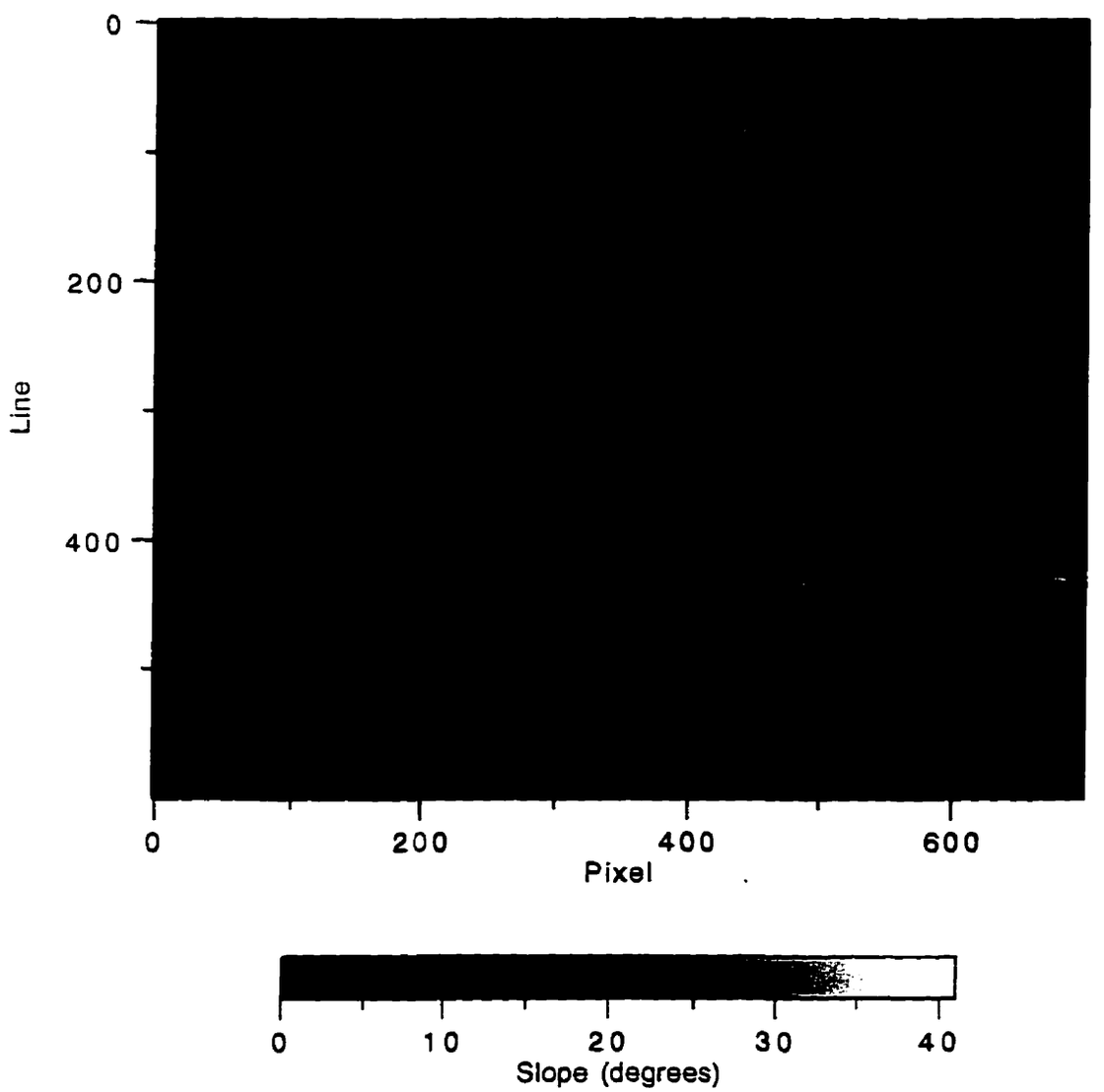


Figure 4.19 Slope image of the Rinker Lake study site.

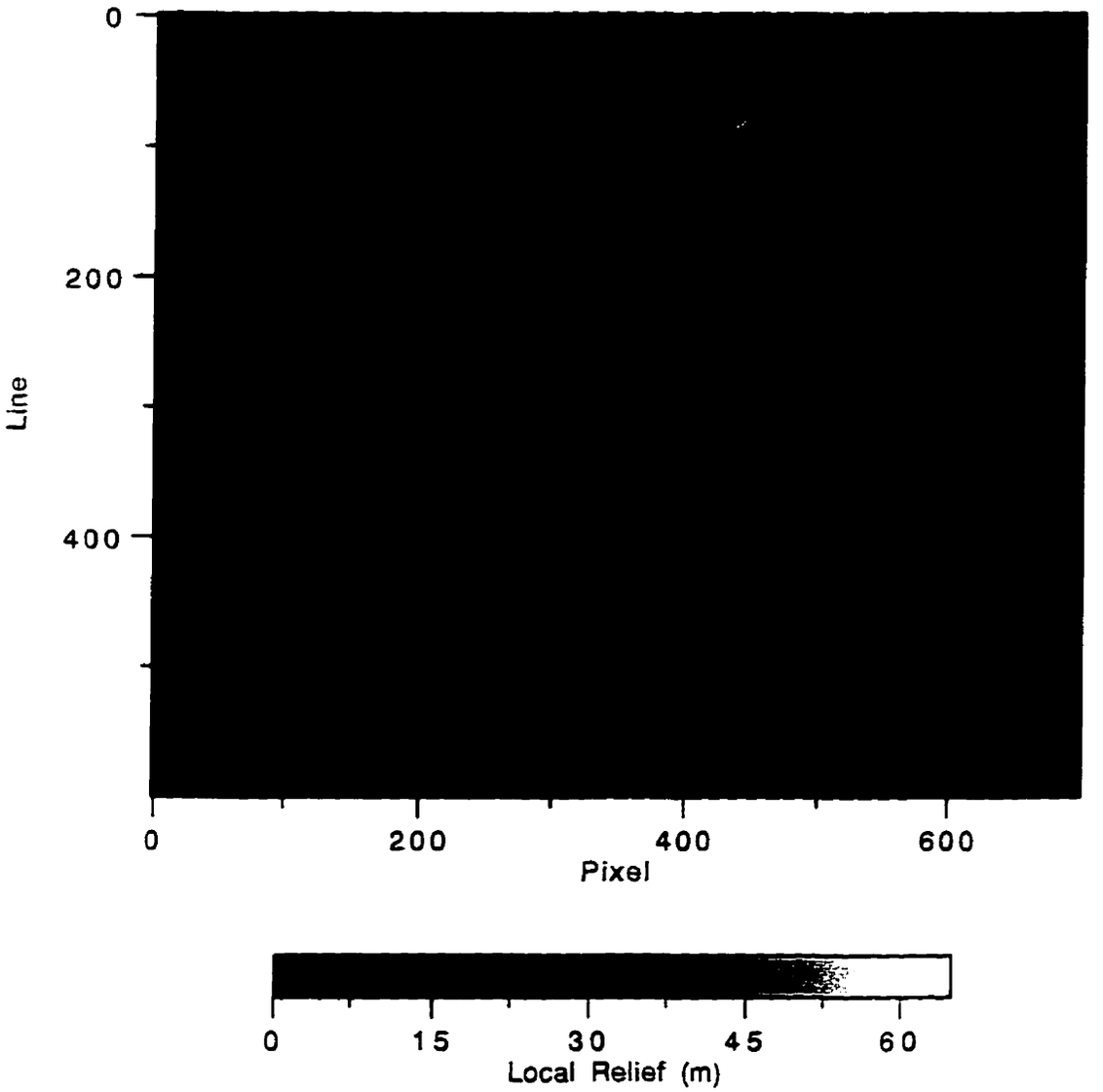


Figure 4.20 Local Relief image of the Rinker Lake study site.

4.5 Summary

In this chapter, the study area and the data collected for this research are described. The study site, situated within the larger Rinker Lake Research Area established by the Department of Natural Resources - Forestry Canada, possesses a complex mosaic for forest stand types with various soil and landform conditions, characteristic of a glaciated landscape. Detailed forest ecological data were collected on the ground during three field seasons (1993-1995) in order to characterize the sample sites within the Forest Ecological Classification (FEC) for northwestern Ontario. These data ranged from a very detailed collection of ecological

parameters to a simple characterization of the sample site to V-Type. Multiple scales of remote sensing data were acquired and collected for the study site. These included Landsat TM and three altitudes of CASI data. The airborne data were calibrated to reflectance. This allowed for comparison of the spectral characteristics of FEC V-Types, not only between adjacent flight lines at the same altitude, but also between different altitudes. Finally, a DEM and digital data on the geomorphology of the study area were acquired. Geomorphometric variables (i.e., gradient and local relief) were derived from the DEM.

CHAPTER 5
SPATIAL ANALYSIS OF REMOTE SENSING DATA

5.1 Introduction

In order for remote sensing of forest ecosystems over large areas to become operational, spatial resolutions of remote sensing data must be appropriate for the specific application. It is spatial resolution that determines the information content and measurement error of an image (Atkinson, 1993). For instance, to discriminate forest ecosystems at a landscape scale, a spatial resolution that best characterizes the spectral reflectance for a particular forest ecosystem should be optimized. However, detailed information on stand and canopy structure and dynamics, as detected through remote sensing, is required to improve our understanding of forest stands in order to develop methods for classifying and mapping forests at landscape scales. In order to select a proper or optimal spatial resolution, information is required on the spatial characteristics of the surface under investigation. In this study, it is expected that this spatial resolution will vary for different forest ecosystem classes or aggregations of classes.

Atkinson (1993) defines information in relation to remote sensing data and spatial variability as the true or underlying value of the property of interest over a given support at a given time and place. Support refers to the size, geometry and orientation of the space over which a measurement is made. Spatial resolution of remotely sensed data corresponds to the size of support of the remotely sensed data. Traditionally, spatial data proximity relationships have not been used in remote sensing data analyses. This is due to a poor understanding of the nature and causes of spatial variation in remote sensing data, a complex interaction between scene and sensor parameters. The value of spatial information, however, is not in dispute. It has been the lack of understanding of its nature that have limited the exploitation of spatial information in remote sensing data analyses. In this chapter, variogram analysis of forest ecosystems is applied to low- altitude (600m AGL) and medium-altitude (1150m AGL) CASI data in order to explore the spatial information content of remote sensing reflectance data at these two spatial resolutions/scales. This analysis, whereby range and sill values of experimental variograms for different ecosystem classes are derived, is expected to

reveal variations based on stand structure and processes occurring in these ecosystems. It is anticipated that this detailed analysis will provide ecosystem-specific information whereby optimal spatial resolutions (i.e., size of support) for acquiring remotely sensed reflectance data can be identified.

5.2 Spatial Structure of Remote Sensing Data

Jupp *et al.* (1988) describe many remote sensing scenes as spatial arrangements of two- or three-dimensional objects superimposed on a uniform background. In this scenario, they consider a discrete object scene model as an appropriate abstraction of the scene. In this model, one or more classes of objects can be described by a unique set of properties or parameters. This abstraction is appropriate for certain applications of remote sensing and digital image analysis. However, within a forest ecosystem context, not only does the canopy structure vary with ecosystem type, but the background can also vary significantly with respect to composition and structure. The manner in which ecosystems vary will also be a function of spectral wavelength sensed, since canopy penetration and the nature of energy interaction with surface structures differs between spectral bands.

In the above model, the resolution cells of the remote sensing data are small relative to the objects in the scene. In this case, it is possible to identify the size and shape of the objects based on the spectral properties of the object. This has been described as the High-resolution case (H-resolution) (Strahler *et al.*, 1986). The spatial structure of these images can therefore be measured based on unique spectral properties of the objects in the scene. When the objects in the scene are much larger than the spatial resolution of the sensor, it follows that adjacent pixels in the scene are going to be spectrally similar (i.e., spatially autocorrelated). The mean distance at which this spatial autocorrelation breaks down is related to the size, spacing and shape of the objects in the scene, as well as the spatial resolution of the sensor in relation to the size of the objects in the scene (Jupp *et al.*, 1988).

On the other hand, when the objects in the scene are smaller than the resolution cell size recorded by the sensor, the radiance recorded for that resolution cell represents a combination of radiances for the objects and background (e.g., tree canopies and understory). This scenario has been described as the Low-resolution case (L-resolution) (Strahler *et al.*, 1986). For a forested environment, a dense canopy will likely continue to exhibit high spatial autocorrelation since the number of objects integrated over the spatial resolution of the sensor will remain relatively uniform. However, if the forest canopy is sparse, there may be significant spectral variation over short distances. Again, this is dependent on the size, shape and density of the objects in the scene (e.g., canopy and understory) and the relationships

between the sizes of the objects in the scene and the sizes of the resolution cells of the digital image data.

Jupp *et al.* (1988) describe two methods of approaching the analysis of spatial structure in digital remotely sensed images. The first of these involves the definition of various parameters that measure spatial structures which are then applied to real images (Woodcock, 1985). A second approach involves the definition of a scene model, whereby the spatial structure of discrete objects on a background are examined with respect to their effect on the spatial structure of an image taken of them. In this thesis, the first approach is used to examine the spatial structure of high-resolution CASI reflectance data of natural forest ecosystems, characteristic of northwestern Ontario. Using these types of measurements on various forest ecosystems at different spatial resolutions, it is possible to gain insight into the impact of spatial structure on information extraction from these data.

The reflectance values of a remotely sensed image are a function of spatial position during image acquisition. In the realm of geostatistics, these reflectance values are a function of spatial position and can therefore be considered as values of a "regionalized variable." The theory of regionalized variables (Matheron, 1963) assumes that the spatial variation of any continuous variable is the sum of three major components (Burrough, 1987). These components are:

1. structural (associated with a constant mean value or a constant trend);
2. random and spatially correlated; and
3. random and not spatially correlated (i.e., noise / residual error).

To apply regionalized variable theory to the analysis of remotely sensed data, adoption of a stochastic view of the landscape and its spatial structure is required (Jupp *et al.*, 1988). A stochastic surface provides a better model of the irregularities of spatial variability as opposed to a smooth mathematical function. This is a logical assumption since underlying processes and properties of the landscape will produce many similar scenes scattered across the landscape. In fact, this is intrinsic to the classification of ecosystems in the NWO FEC. It is assumed that similar ecosystems will arise from similar environmental conditions and processes linked closely to landscape.

The key to the theory of regionalized variables is the variogram, a second-order spatial statistic (Olea, 1977). Remote sensing reflectance measurements may be thought of as comprising the true or underlying value of a property (i.e., information) and a component of measurement error (Atkinson, 1993). These components of variation are embedded in the experimental or measured variogram (Figure 5.1, Table 5.1). The variogram is used to describe the spatial correlation between samples in close proximity. In variogram analysis

and basic to regionalized variable theory, two additional assumptions are required: (i) spatial stationarity, which assumes that the parameters of the underlying function (i.e., regionalized variable) do not vary with spatial position; and (ii) ergodicity which assumes that spatial statistics taken over the area of the image as a whole are unbiased estimates of those parameters (Jupp *et al.*, 1988). The assumption of stationarity is generally appropriate in digital image processing, at least locally or in increments (i.e., within the range of the variogram), where scan angle and terrain effects are minimal. The assumption of ergodicity is generally valid for remote sensing data since the reflectance surface is considered stochastic (Jupp *et al.*, 1988).

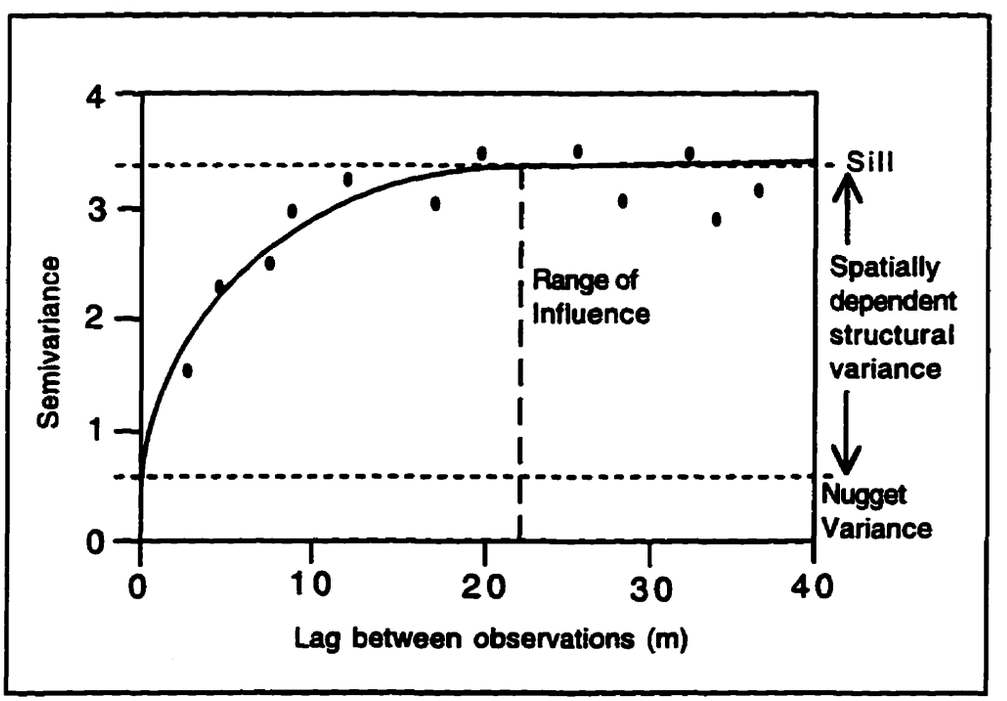


Figure 5.1 The shape and description of a "classic" variogram.

Table 5.1 Terms and Symbols used in the Description of the Variogram (Curran, 1988)

Term	Definition
Lag	distance (and direction in two or more directions) between sampling pairs
Sill	maximum level of semivariance
Range	point on lag axis where semivariance reaches a maximum; places closer than the range are related; places further apart are not
Nugget variance	point where the extrapolated relationship between the two variables intercepts the semivariance axis; represents spatially independent variance
Spatially dependent structural variance	sill minus nugget variance

The variogram has proven useful in remote sensing because it enables researchers to relate some of the descriptors of the variogram to the spatial characteristics of the scene. The internal spatial variability of information classes of interest determines how small a ground-resolution element can be before it detects unnecessary within-class variability. In this scenario, the variogram is ideal, since it defines the distance above which the ground-resolution elements are not related. Therefore, a ground-resolution element larger than the range will likely average the within-class spatial variability and provide a suitable descriptor for that class (Woodcock and Strahler, 1987; Curran, 1988). The range therefore provides a measure of the size of the elements in the scene and has been suggested as a useful indicator in selecting the optimal spatial resolution, or support, for discriminating the features embedded in the image variogram (Curran, 1988; Woodcock *et al.*, 1988a; 1988b).

Variogram analysis has been applied to examine spatial variability as a function of waveband (Curran, 1988); image resampling problems (Ramstein and Raffy, 1989); the signal-to-noise ratio in hyperspectral imagery (Curran and Dungan, 1989); sampling schemes in support of remote sensing data acquisition (Webster *et al.*, 1989; Atkinson, 1991); scale differences for simulated disc models (Woodcock *et al.*, 1988a) and agricultural fields (Atkinson, 1993); optimal spatial resolution for remote sensing of conifer canopy structure in plantations (Atkinson and Danson, 1988); and efficient sampling of remote sensing data for storage and retrieval (Atkinson *et al.*, 1990). Woodcock *et al.* (1988b) calculated variograms from real digital images and found: (i) the density of coverage of objects in the scene affects the height of the variogram; (ii) object size affects the range of influence of the variogram; and (iii) the variance in the distribution of the sizes of objects affects the shape of the variogram (i.e., as variance increases the shape of the variogram curve becomes more rounded). Lathrop and Pierce (1991) used variogram analysis of forest canopy transmittance measurements and Landsat TM near-infrared/red ratio data to examine the scale of variation in canopy structure and determine the most appropriate scale at which to sample transmittance. This analysis depicted the similarity between the two sets of data with respect to spatial autocorrelation structure. The range of the variogram was used to aggregate the Landsat TM and transmittance data sets for regression analysis by averaging segments of the transect (where segment length equals variogram range). It was discovered, that by averaging within an appropriate landscape unit (e.g., hillslopes), large-scale variability of measurements, due to small forest gaps, was reduced. In the analysis presented in this chapter, the within-parcel scale of study (within-stand variability) is examined in order to determine optimal descriptors to improve separability of forest ecosystems at a between-parcel scale.

5.3 Variogram Analysis of CASI Reflectance Data

In this study, experimental variograms derived from CASI reflectance data are used to estimate the underlying variogram for selected forest ecosystems. In order to properly construct a variogram, high spatial resolution remotely sensed data (i.e., closely spaced sample points) are required to characterize the fine detail of spatial dependence. It has been shown that at the Landsat TM spatial resolution, the sills of variograms are very flat and ranges very short, providing little spatial structure information at this resolution (Woodcock *et al.*, 1988b; Cohen *et al.*, 1990).

Variograms are generated from visible and near-infrared data and are fitted using a spherical model in order to estimate the range and sill of the variogram. This analysis is a required prerequisite to estimating optimal sizes of support for remote sensing data acquisition or textural processing. The variogram is used to measure the spatial dependence of neighbouring observations for any continuously varying phenomenon. Hence, it is a technique that can be applied to spectral data, a variable for which position in time and space is known. In this manner, spatial variation in images can be examined in relation to ground scene and sensor parameters (Woodcock *et al.*, 1988a). The variogram plots semivariance (γ) against spatial separation along a given relative orientation and provides a concise and unbiased depiction of the scale and pattern of spatial variability (Curran, 1988). The semivariance (γ) is half the expected squared difference between values of reflectance at a distance of separation or lag, h, a vector in both distance and direction. Similar to the manner in which sample variance estimates true variance of a variable's population, the sill represents the semivariance estimate of the true variance of a regionalized variable. The variogram or $\gamma(h)$ is calculated as:

$$\gamma(h) = \frac{1}{2(n-h)} \sum_{i=1}^{n-h} [Z(x_i) - Z(x_i + h)]^2$$

where h is the lag (or distance in pixels) over which γ (semivariance) is measured, n is the number of observations used in the estimate of $\gamma(h)$, and Z is the value of the variable of interest at spatial position x_i. The value $Z(x_i + h)$ is the variable value at distance h from x. In this study, $\gamma(h)$ estimates the variability of reflectance, Z, as a function of spatial separation. In essence, the variogram measures the correlation between pixels at successively greater distances and will demonstrate a peak in variance when pixels become independent of one another. This lag interval to the peak in variance is known as the 'range of influence' of the variogram (Figure 5.1, Table 5.1). A phenomenon, know as the nugget effect, is often observed when modelling the semivariogram. This phenomenon has the physical

interpretation of a distinct jump in variance at an initial short lag. The nugget effect was originally observed when core samples were analysed and minerals, that tend to occur in nuggets, gave rise to this effect. This feature of the semivariogram represents spatially independent variance.

The most acceptable models used in variogram analysis are the spherical, exponential, linear or a combination of two or three of these; however, the linear and spherical seem to be the most appropriate for determining the shortest lags from sample data (Curran, 1988). Although there is no "correct" model to use to fit the variogram in any given situation, a spherical model (the most frequently used model) was used here (Brooker, 1991). This model is often referred to as the optimal model for a variogram since it possesses a well-defined sill and the meaning of the range of influence can easily be interpreted (Clark, 1979). Not all models for the shape of a variogram share these characteristics. Clark (1979) identifies three criteria for selecting a model, dictated by the specific interests of an application. These are: (i) behaviour near the origin; (ii) the fit near the sill; and (iii) the determination of the range of influence. This isotropic model is appropriate under the assumption that reflectance does not have any preferred direction, i.e., anisotropy. The accuracy of the modelling process is dependent on (i) the number of pairs of points used in the calculation of the variogram; and (ii) the lag distance between data pairs. To estimate the appropriate parameters for a spherical model, the points of the experimental variogram are first plotted along with the variance of the data, the variance usually being about equal to the sill (Brooker, 1991). Nugget, range and sill estimates are then input to the spherical model and interactively modified to achieve a "best fit" to the measured values (Figure 5.1, Table 5.1).

It should be noted that the spherical models are designed for punctual variograms, or variograms which are derived from point measurements. However, remotely sensed image data are area measurements. In this case, the variogram is referred to as regularized, an averaging of the regionalized variable over a given length or area. Here the regularizing area equates to the instantaneous field of view (IFOV) of the sensor, defined by the point spread function and the integration period over which reflectance is recorded by the CASI sensor. Simply, the pixel dimensions define the extent of regularization. Hence, the equation defined above is used to model the regularized variogram in order to estimate the range and sill values. Therefore, variation at a scale finer than the regularization cannot be detected and variations less than 2-3 times the scale of regularization cannot be defined with confidence (Woodcock *et al.*, 1988a). In fact, the geometry of the support may be complex due to the point spread function (PSF) of the sensor. This may be particularly significant here due to the

integration period and resulting elongated nature of the CASI reflectance pixel. In addition, the true support is likely greater than the spatial resolution of the sensor (Atkinson and Curran, 1995) and likely varies across the image due to the scan angle of the sensor.

For the purpose of this study, a single visible band (580-601nm) and a near-infrared band (744-750nm) were used for calculating semivariance and deriving variograms from low- and medium-altitude CASI data. Homogeneous stands (landscape units) of sufficient size were identified on aerial photographs and located on the low- and medium-altitude CASI images. To examine the spatial variability of forest ecosystems at high spatial resolutions, transects of 100 pixels in the cross-track direction were extracted from the CASI data for selected forest stands representing individual V-Types or complexes of V-Types (Table 5.1). The distance, or lag (h), over which the variogram is to be measured needs to be larger than the range of influence and large enough for any periodicities in the data to become apparent (Woodcock *et al.*, 1988a). The length of the lag (h) determines the number of potential lags in any particular transect. The confidence associated with the semivariance calculation decreases with increasing lag (i.e., the number of calculations decreases with increasing lag length). Webster (1985) recommends that lags should not exceed a fifth to a third of the transect length. Here a lag equal to 20 pixels was selected for analysis of transects of 100 pixels for most stands.

Orientation of the sampling transect is important on anisotropic surfaces that have a repetitive pattern. Anisotropy can be associated with patterns in the orientation of objects in the scene or to the direction of illumination. The forested environment/terrain analysed in this study consist of naturally developed ecosystems with no modification by man. The terrain was influenced by glaciation and the surficial geology displays a distinct north-east to south-west orientation (i.e., the direction of movement of a series of ice sheets). Due to the rectangular nature of the pixels in the CASI data, cross-track pixels were analysed since, in most cases, this was the only direction a sufficient number of pixels could be obtained. In a few stands, along-track transects were analysed. However, the variograms were poorly defined and the ranges observed were only 2-3 pixels in length.

CASI images are calibrated to reflectance but are stored as 16-bit integers for more efficient storage and data processing (Table 5.2). The relationship between CASI digital number (DN) and reflectance is:

$$\text{Reflectance } (R) = (\text{CASI DN})10^{-6}$$

CASI data were subjected to variogram analysis[1] to estimate range and sill values for each transect. An example of the output of the geostatistical analysis for a single transect is presented in Table 5.3. A series of transects was analysed for each forest stand, from which the mean ranges and sills were calculated to characterize the stand / landscape unit at the two altitudes (Table 5.4, Appendix B, Appendix C). The shapes of the variograms were also examined and classified as either classic, periodic, aspatial, periodic-classic, unbounded, or multifrequency. The "classic" variogram (Figure 5.1) is bounded by a sill and is most often encountered in environments where repetitive patterns are absent. The "periodic" variogram occurs across a repetitive pattern, while the "aspatial" variogram occurs along a repetitive pattern or on a homogeneous surface. A "periodic-classic" variogram represents a repetitive pattern on a spatially variable surface; "unbounded," along a surface with a definite trend which is not reached within the transect length; and "multifrequency," over an area in which there are two or more repetitive patterns (Curran, 1988).

Table 5.2 Reflectance Values (CASI DN and *R*) from a Sample Transect (580-601nm)

Aspen Dominated Hardwood - V5/V8

X	Y	CASI DN	*R*	X	Y	CASI DN	*R*	X	Y	CASI DN	*R*	X	Y	CASI DN	*R*
1	1	1463	.01463	26	1	1677	.01677	51	1	2087	.02087	76	1	2027	.02027
2	1	1696	.01696	27	1	1614	.01614	52	1	2372	.02372	77	1	2372	.02372
3	1	1709	.01709	28	1	1582	.01582	53	1	2437	.02437	78	1	2537	.02537
4	1	1636	.01636	29	1	1510	.01510	54	1	2705	.02705	79	1	2704	.02704
5	1	1611	.01611	30	1	1687	.01687	55	1	2670	.02670	80	1	2605	.02605
6	1	1521	.01521	31	1	1597	.01597	56	1	2411	.02411	81	1	2182	.02182
7	1	1509	.01509	32	1	1813	.01813	57	1	2184	.02184	82	1	2155	.02155
8	1	1483	.01483	33	1	1660	.01660	58	1	1866	.01866	83	1	1905	.01905
9	1	1604	.01604	34	1	1699	.01699	59	1	1830	.01830	84	1	1393	.01393
10	1	1772	.01772	35	1	1813	.01813	60	1	2201	.02201	85	1	1402	.01402
11	1	1859	.01859	36	1	1748	.01748	61	1	2262	.02262	86	1	1810	.01810
12	1	1641	.01641	37	1	1441	.01441	62	1	1808	.01808	87	1	2061	.02061
13	1	1201	.01201	38	1	1794	.01794	63	1	1493	.01493	88	1	2478	.02478
14	1	1245	.01245	39	1	1777	.01777	64	1	1359	.01359	89	1	2728	.02728
15	1	1468	.01468	40	1	1456	.01456	65	1	1393	.01393	90	1	2739	.02739
16	1	1648	.01648	41	1	1567	.01567	66	1	1585	.01585	91	1	2513	.02513
17	1	1808	.01808	42	1	1641	.01641	67	1	1935	.01935	92	1	2318	.02318
18	1	1760	.01760	43	1	1563	.01563	68	1	2369	.02369	93	1	2078	.02078
19	1	1631	.01631	44	1	1567	.01567	69	1	2561	.02561	94	1	1896	.01896
20	1	1507	.01507	45	1	1738	.01738	70	1	2163	.02163	95	1	1930	.01930
21	1	1524	.01524	46	1	2031	.02031	71	1	1833	.01833	96	1	1964	.01964
22	1	1643	.01643	47	1	2440	.02440	72	1	1640	.01640	97	1	2170	.02170
23	1	1786	.01786	48	1	2481	.02481	73	1	1553	.01553	98	1	2365	.02365
24	1	1830	.01830	49	1	2309	.02309	74	1	1550	.01550	99	1	2702	.02702
25	1	1709	.01709	50	1	2020	.02020	75	1	1788	.01788	100	1	2697	.02697

[1] Geostatistical software: VARIOWIN (V.2.1) developed by Y.Pannatier at the Institute of Mineralogy of the University of Lausanne Switzerland (Pannatier, Y.,1994. MS-Windows for Exploratory Variography and Variogram Modeling in 2D. In Proceedings, Statistics of Spatial Processes: Theory and Applications. Capasso, V., Girone G. and Posa, D. Eds., Bari, Italy, Sep. 27-30, 1993 pp. 165-170).

Table 5.3 Geostatistical Analysis of a Single Transect (580-601nm)

Aspen Dominated Hardwood - V5/V8

Variable: Reflectance Direction: 0 Angular Tolerance: 90 Data Variance: 1.56827e+05

Lag	Npairs	Mean |h|	Semivariance	Standardized Semivariance*
1	198	1	23,383	0.15
2	196	2	67,031	0.44
3	194	3	108,210	0.71
4	192	4	137,675	0.90
5	190	5	146,198	0.95
6	188	6	134,144	0.86
7	186	7	115,484	0.74
8	184	8	100,325	0.64
9	182	9	94,849	0.60
10	180	10	98,606	0.63
11	178	11	104,342	0.68
12	176	12	112,367	0.74
13	174	13	124,933	0.84
14	172	14	144,514	0.98
15	170	15	163,873	1.10
16	168	16	169,579	1.14
17	166	17	161,178	1.08
18	164	18	145,894	0.97
19	162	19	123,240	0.81
20	160	20	101,921	0.67

* Standardized Semivariance is obtained by dividing the Semivariance by the Data Variance

Table 5.4 Sample of Geostatistical Analysis by Stand

Transect A (#Lags = 20)
Aspen Dominated Hardwood (V5/V8)

Transect	Range (pixels)	Range (m)	Range (m^2)	Sill (10^6)	Cov/Cor (10^6)	IGF (10^{-5})	Type	Comments
(580.6-600.9 nm)								
a13	4.80	3.36	18.01	126.40	156.83	4.72	Periodic	difficult to fit model (10 pixel cycle)
a23	13.00	9.10	48.78	289.00	232.04	0.82	Classic	slight dip @ 4-5 pixels
a33	10.20	7.14	38.27	395.00	305.72	5.33	Periodic-Classic	smooth curve
a43	10.00	7.00	37.52	390.00	310.01	6.46	Periodic-Classic	very similar to periodic-classic curve in Curran for deciduous
a53	5.00	3.50	18.76	180.00	162.06	9.50	Periodic-Classic	poor fit due to periodicity
a63	6.00	4.20	22.51	440.00	392.41	2.77	Classic	
Mean	8.17	5.72	30.64	303.40	259.85			
Median	8.00	5.60	30.02	339.50	268.88			
Std. Dev.	3.37	2.36	12.66	127.53	92.89			
Minimum	4.80	3.36	18.01	126.40	156.83			
Maximum	13.00	9.10	48.78	440.00	392.41			
Near-Infrared (743.8-758.3 nm)								
a17	5.80	4.06	21.76	13020.00	20932.70	2.56	Periodic-Classic	smooth curve
a27	9.20	6.44	34.52	14600.00	13249.00	2.96	Periodic-Classic	
a37	10.20	7.14	38.27	21000.00	18811.50	1.74	Classic	difficult to identify sill and range
a47	10.80	7.56	40.52	24000.00	18640.00	2.95	Classic	variable sill
a57	7.00	4.90	26.26	10600.00	11828.40	7.09	Multi-frequency	first sill used in range determination
a67	9.20	6.44	34.52	24200.00	30073.20	1.58	Periodic-Classic	10 pixel cycle
Mean	8.70	6.09	32.64	17903.33	18922.47			
Median	9.20	6.44	34.52	17800.00	18725.75			
Std. Dev.	1.92	1.35	7.21	5807.70	6495.94			
Minimum	5.80	4.06	21.76	10600.00	11828.40			
Maximum	10.80	7.56	40.52	24200.00	30073.20			

5.4 Results

A summary of critical variogram parameters for the low-altitude data is presented in Table 5.5. Here, the mean ranges observed for each stand are presented, along with the mean sill (semivariance) values. It must be emphasized that these values represent the mean ranges and sills determined by sampling a stand-specific number (n) of transects of 100 pixels each, within the CASI imagery, for selected forest stands (Table 5.5; Figure 5.3; Appendix B).

At the low altitude, and for the stands sampled, the mean ranges derived from the variograms for the visible band (580-601nm) indicate that trembling aspen-dominated hardwood and mixedwood (ASP/M) and conifer mixedwood (CONM) stands have greater ranges (≅ 8 pixels / 5.8 m) than upland black spruce (UBS) stands (≅ 6.5 pixels / 4.7 m) and lowland black spruce (LBS) stands (≅ 4.5 pixels / 3.5 m) (Table 5.5; Figure 5.3). Range values vary significantly for transects within similar forest ecosystems. For example, ranges in the visible band for ASP/M stands vary from 4 to 16 pixels. Whereas the minimum ranges do not vary greatly between stands of similar ecosystem class (e.g., ASP/M; 4-5.6 pixels), the maximum ranges vary significantly (e.g., ASP/M; 10-16 pixels)), particularly between stands of differing ecosystem classification (e.g., LBS (3 pixels) to ASP/M (16 pixels). In general, the range values for the visible band increase with stand complexity, which corresponds loosely with the continuum from pure hardwood to pure conifer. Hardwood stands, generally occur on richer sites and represent a more complex stand structure, whereas pure conifers generally occur on sites of lower productivity and possess a simpler structure.

A similar trend is observed with respect to the range values for the near-infrared data whereby ASP/M and CONM stands have greater ranges than LBS. For example, range values are approximately 10 pixels / 7.3m for ASP/M and CONM; 9 pixels / 6.6m for UBS; and 7 pixels / 5.9m for LBS (Table 5.5; Figure 5.4). Again, there is a diversity in range values within and between stands. For example, the ASP/M stands possess range values between a minimum of 5 pixels and a maximum of 20 pixels. The minimum range values for ASP/M vary between 5 and 8 pixels whereas the maximum ranges vary from 9 to 20 pixels. As with the visible data, the minimum range values do not vary greatly for stands of similar class; however, the maximum values display a wide range between stands of similar class and, in particular, between stands of different classes.

The ranges derived for the near-infrared data are greater than those derived for the visible data for each ecosystem class (e.g., 6 pixels / 4.4m (near-infrared) versus 4 pixels / 2.9m (visible) for LBS (Stand B - V36/37/38)) (Figure 5.5). In fact, in all the stands studied, the mean ranges derived for the near-infrared data are greater than the corresponding ranges for the visible data (Table 5.5; Figures 5.3 and 5.4). It is important to remember that the

visible and near-infrared data were sampled from the same transects, thereby sampling the same reflectance surface. The ranges are also much more variable for the near-infrared data in contrast with the visible data (Figure 5.5).

The sills for the ASP/M and CONM stands are much greater than those of the LBS stands, particularly for the near-infrared data (Table 5.5; Figures 5.6 and 5.7). For example, the mean near-infrared semivariance (sill) for Stand A (ASP/M - V5/V8) is approximately $1.79e+10^7$; for Stand T (CONM - V8/V14/V15/V16/V19) it is $2.23e+10^7$ but for Stand F (LBS- V37) the value is $1.60e+10^6$ (Table 5.5; Figure 5.7). Although the trend is similar in the visible band, the differences are not as extreme. The variability between minimum and maximum sill values within stands of similar class is also high for ASP/M and CONM for both the visible and near-infrared data (Table 5.5; Figures 5.6 and 5.7).

Cedar mixedwood (CM) (Stand X - V22) and Lowland Black Spruce (Stand M - V34/V35/V36) display high semivariance in the visible band, relative to the other stands, a characteristic that is not evident in the near-infrared data (Figures 5.6 and 5.7). Also, LBS (Stand Q - V37/38) exhibits higher semivariance than the other lowland black spruce, particularly in the near-infrared. This stand, is predominantly V38, black spruce / leatherleaf / sphagnum, and possesses a very open canopy.

The shape of the variograms generally resembled the "classic" form with various permutations, including the classic-periodic and classic-multifrequency. In some cases, the variogram shape appears to be more complex in the visible than in the near-infrared. For instance, the shapes for the variograms for the UBS (Stand K) are of the classic variety for the near-infrared data, but are classed as classic-multifrequency for the visible data. The variograms for the near-infrared data appear to have a "smoother" shape as opposed to those derived for the visible data. The northwest slope of Stand P (Pnw) possesses a more variable variogram in the visible band; however, this variability is not evident in the near-infrared band. Also, the variability is not evident in either waveband for the south-eastern slope of Stand P (Pse). In Stand P, some of the transects in the near-infrared are unbounded, indicating that a range value was not reached within the lag period used for calculating the variogram. This was not the case for the visible reflectance data.

Table 5.5 Summary of Geostatistical Analysis of Forest Ecosystems (Altitude=600m)

Altitude = 600 m AGL Spatial Resolution = 0.73m x 5.36m (3.9 m²)

Forest Stand	Vegetation Type/Complex	Transects (@100 pixels)	Minimum Range (h)	Maximum Range (h)	Mean Range (h)	Mean Range (m)	Mean Range (m²)	Minimum Sill ('000)	Maximum Sill ('000)	Mean Sill ('000)	Mean Cov/Cor ('000)	Primary Variogram Shape
Visible (556nm - 661nm)												
A	Aspen-Dominated Hardwood - V5/V6/V8/V9	6	4.80	13.00	8.17	5.96	31.97	126.40	440.00	303.40	259.65	Classic-Periodic
Sw	Aspen-Dominated Hardwood - V5/V8	5	4.00	8.20	6.16	4.50	24.10	65.80	280.00	149.54	145.10	Classic-Multifrequency
D	Aspen-Dominated Hardwood - V6/V8	7	5.00	13.60	7.37	5.38	28.84	82.00	240.00	139.82	125.06	Classic-Periodic
Y	Aspen-Dominated Hardwood - V6/V8	10	4.80	16.00	8.52	6.22	33.34	110.00	680.00	273.16	245.47	Classic-Periodic
P	Aspen Complex - V9/V10/V11	11	5.00	15.00	8.45	6.17	33.06	205.00	680.00	344.64	335.16	Classic-Periodic
Pse	Aspen Complex - V9/V10/V11	6	5.60	15.00	8.90	6.50	34.82	185.00	610.00	363.53	344.59	Classic
Pnw	Aspen Complex - V9/V10/V11	6	4.00	12.00	6.73	4.91	26.33	161.04	340.00	259.99	249.56	Classic-Periodic
Se	Aspen Mixedwood - V8/V11/V19	5	5.40	10.20	7.56	5.52	29.58	171.00	313.12	216.03	227.25	Classic-Periodic
T	Aspen / Conifer Mix - V8/V14/V15/V16/V19	10	5.20	13.60	7.44	5.43	29.11	175.00	320.00	249.08	231.68	Classic-Multifrequency
X	Cedar Mixedwood - V22	8	4.00	9.00	5.40	4.67	25.04	170.00	720.00	365.50	304.19	Classic-Periodic
K	Upland Black Spruce - V33	10	3.80	11.60	6.62	4.83	25.90	84.37	230.00	167.37	168.10	Classic-Multifrequency
M	Lowland Black Spruce - V34/V35/V36	5	4.00	6.80	5.55	4.05	21.72	225.40	540.00	401.35	350.86	Classic-Periodic
N	Lowland Black Spruce - V35	4	2.80	4.50	3.68	2.69	14.40	150.00	315.00	221.25	249.50	Multifrequency
E	Lowland Black Spruce - V35/V36	10	3.80	8.60	5.62	4.10	21.99	110.00	420.00	234.60	206.84	Classic
Ua	Lowland Black Spruce - V35/V36/V37	5	2.80	5.00	3.86	2.89	15.49	190.00	230.00	214.00	197.59	Classic
Ub	Lowland Black Spruce - V35/V36/V37	5	3.20	6.40	4.84	3.53	18.94	82.00	240.00	200.40	177.35	Classic-Periodic
F	Lowland Black Spruce - V37	4	2.80	5.40	4.00	2.92	15.65	82.00	180.00	116.25	107.18	Classic
B	Lowland Black Spruce - V36/V37/V38	5	2.20	2.80	2.52	1.84	9.86	97.50	194.00	127.66	132.71	Classic
Q	Lowland / Wetland Black Spruce - V37/V38	9	2.60	5.60	3.93	2.87	15.38	152.78	285.20	228.15	247.66	Classic
Near Infrared (744nm - 750nm)												
A	Aspen-Dominated Hardwood - V5/V6/V8/V9	6	5.80	10.80	8.70	6.35	34.04	10600.00	24200.00	17903.33	18922.47	Classic-Periodic
Sw	Aspen-Dominated Hardwood - V5/V8	5	5.00	9.40	7.84	5.72	30.68	6232.00	20000.00	10926.40	9859.78	Classic-Multifrequency
D	Aspen-Dominated Hardwood - V6/V8	7	6.20	18.00	10.69	7.80	41.83	7900.00	21000.00	13242.86	10732.96	Classic
Y	Aspen-Dominated Hardwood - V6/V8	10	6.00	19.40	11.68	8.53	45.70	13500.00	31000.00	25580.00	19937.50	Classic-Periodic
P	Aspen Complex - V9/V10/V11	11	6.00	17.00	9.76	7.12	38.19	7088.00	25800.00	18976.00	17554.51	Classic-Periodic
Pse	Aspen Complex - V9/V10/V11	6	6.00	19.00	11.43	8.34	44.72	10500.00	33300.00	24652.00	21776.46	Classic
Pnw	Aspen Complex - V9/V10/V11	6	7.00	16.00	10.50	7.67	41.08	7900.00	20000.00	14927.50	14491.99	Classic
Se	Aspen Mixedwood - V8/V11/V19	5	7.80	9.20	8.28	6.04	32.40	9940.00	17600.00	13848.00	16929.64	Classic-Multifrequency
T	Aspen / Conifer Mix - V8/V14/V15/V16/V19	10	7.00	17.00	11.36	8.29	44.45	9790.00	33000.00	22266.67	19603.80	Classic-Periodic
X	Cedar Mixedwood - V22	8	6.00	9.80	7.68	5.61	30.05	4951.00	14000.00	9368.88	8778.18	Classic-Periodic
K	Upland Black Spruce - V33	10	5.80	14.00	8.89	6.49	34.78	1745.00	3900.00	2853.00	2780.74	Classic
M	Lowland Black Spruce - V34/V35/V36	5	6.00	13.60	8.65	6.31	33.85	4411.50	9000.00	6075.63	6103.95	Classic
N	Lowland Black Spruce - V35	4	6.00	12.20	9.60	7.01	37.56	4000.00	6900.00	4868.50	4565.10	Classic-Periodic
E	Lowland Black Spruce - V35/V36	10	4.60	9.80	6.64	4.85	25.98	1985.00	9700.00	5407.00	5098.45	Classic
Ua	Lowland Black Spruce - V35/V36/V37	5	4.80	7.80	6.12	4.47	23.95	2050.00	4200.00	3217.20	2854.20	Classic-Periodic
Ub	Lowland Black Spruce - V35/V36/V37	5	4.20	7.60	5.68	4.15	22.22	1400.00	5400.00	4130.00	4033.80	Classic-Periodic
F	Lowland Black Spruce - V37	4	3.80	5.80	4.60	3.36	18.00	1200.00	2100.00	1633.50	1613.56	Classic
B	Lowland Black Spruce - V36/V37/V38	5	4.00	11.40	7.00	5.11	27.39	1400.00	3192.00	2038.40	2044.90	Classic-Periodic
Q	Lowland / Wetland Black Spruce - V37/V38	9	5.00	14.60	7.27	5.31	28.45	5200.00	12740.00	8363.92	8135.67	Classic-Periodic

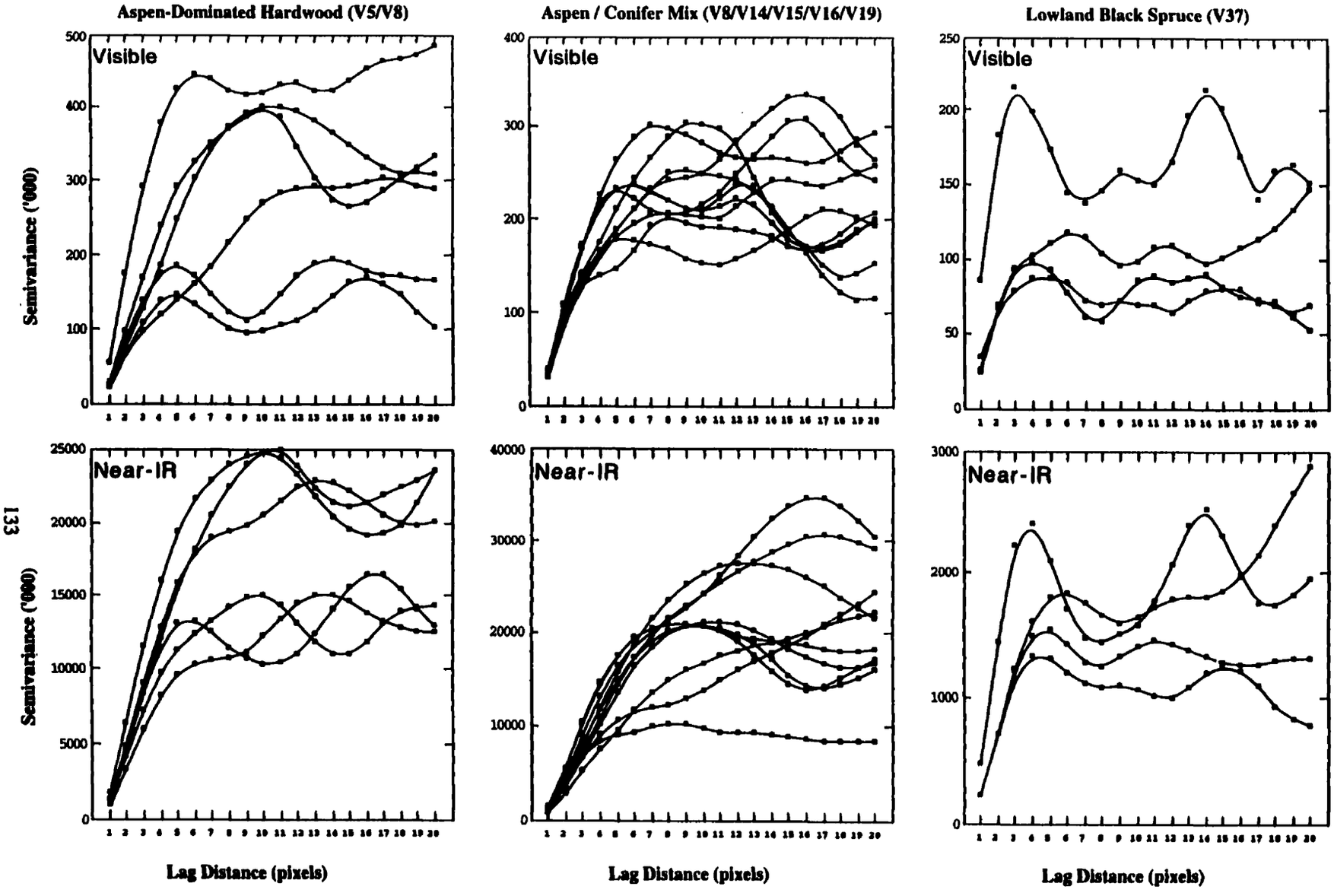


Figure 5.2 Variograms derived from selected forest stands / ecosystems (altitude=600m).

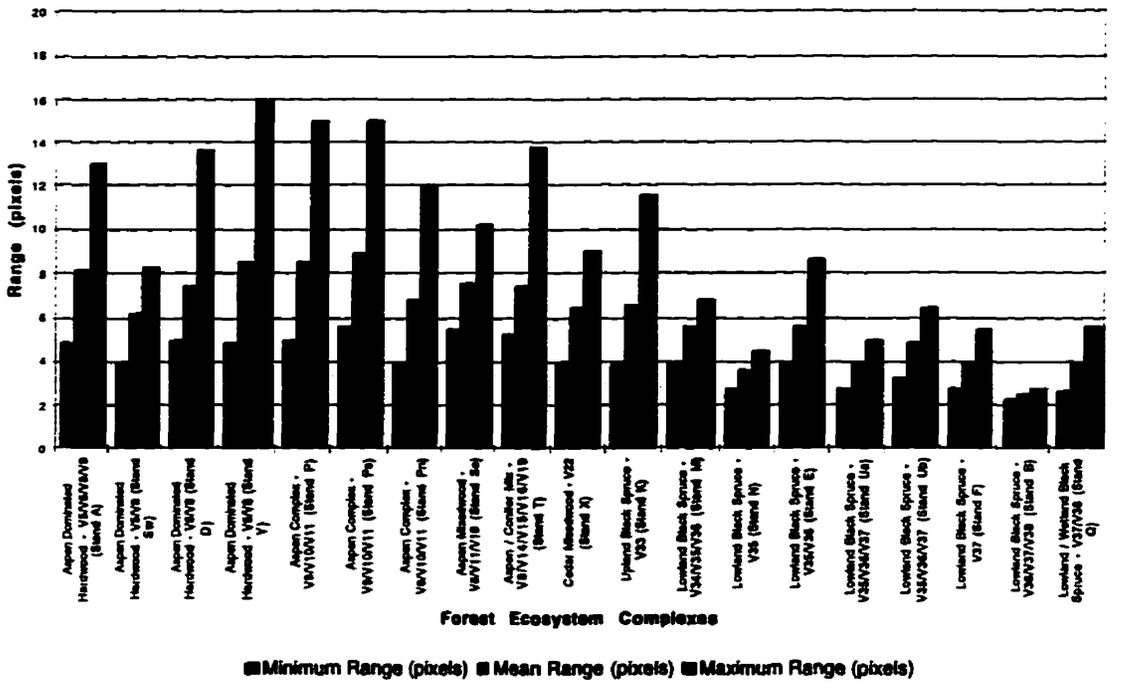


Figure 5.3 Low-altitude range values (580 - 601 nm) for forest ecosystem complexes in the Rinker Lake Study Area.

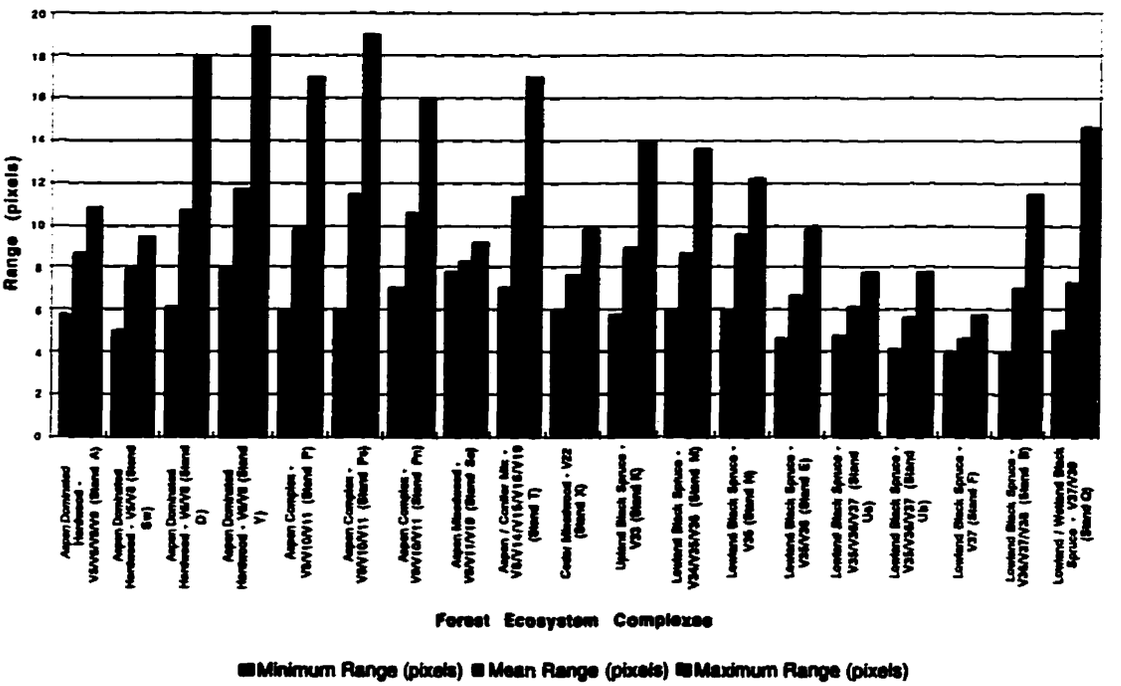


Figure 5.4 Low-altitude range values (744 - 750 nm) for forest ecosystem complexes in the Rinker Lake Study Area.

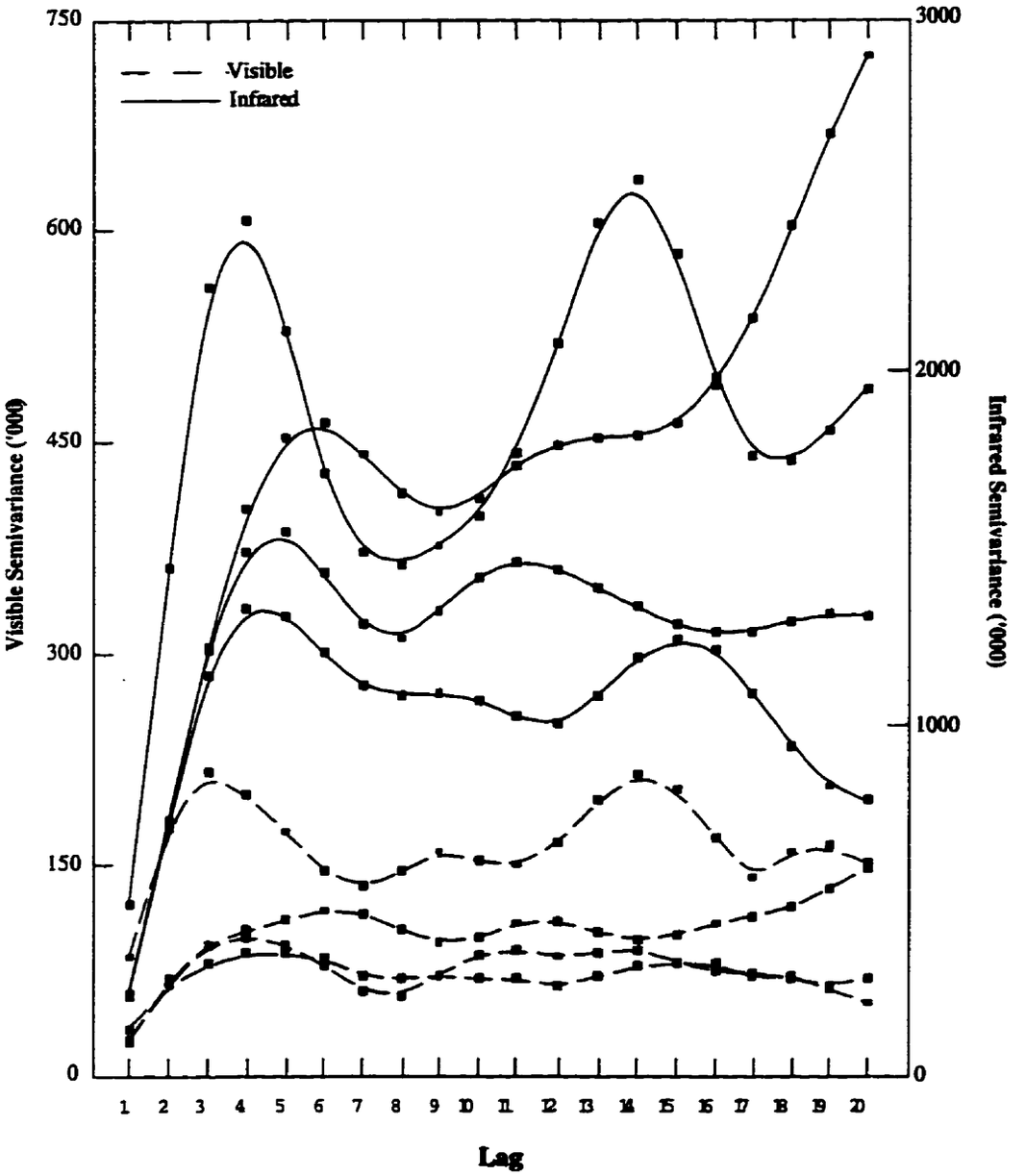


Figure 5.5 Comparison of variogram curves for a Lowland Black Spruce stand (V37).

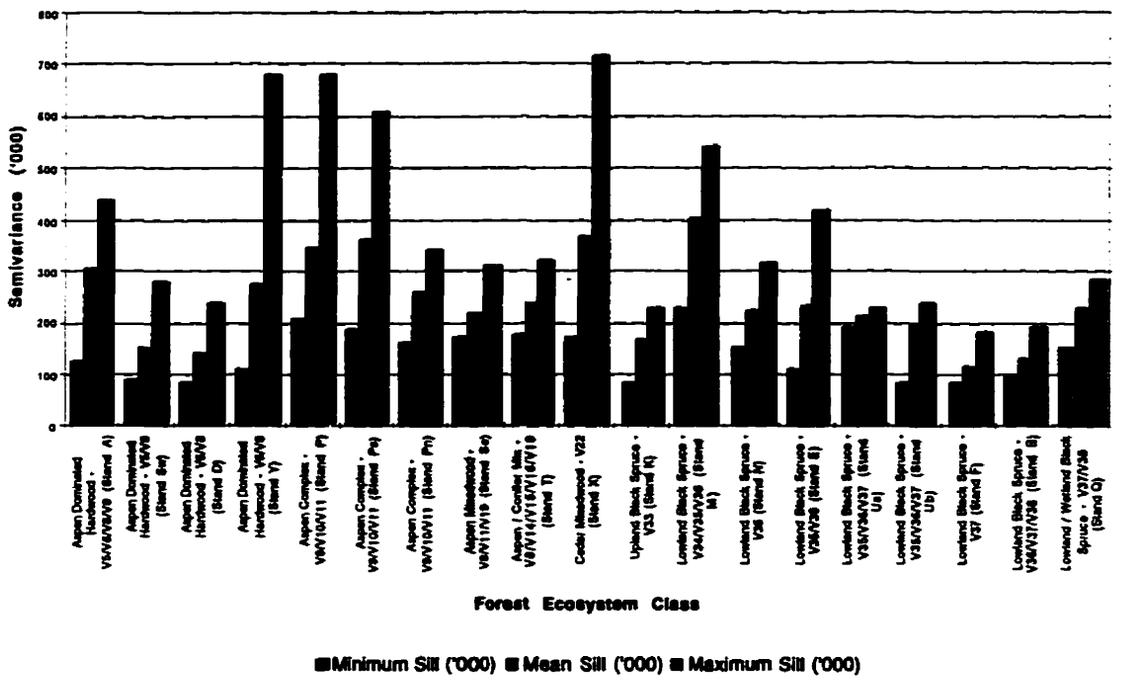


Figure 5.6 Low-altitude semivariance (580nm - 601 nm) for forest ecosystem complexes in the Rinker Lake Study Area.

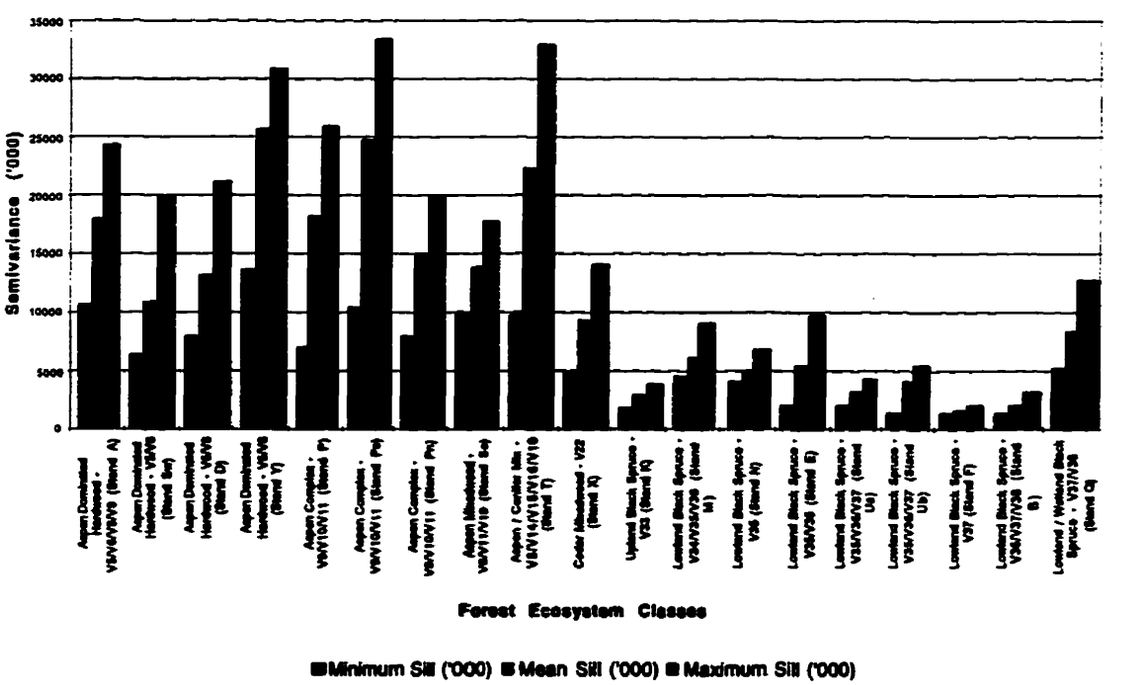


Figure 5.7 Low-altitude semivariance (744nm - 750 nm) for forest ecosystem complexes in the Rinker Lake Study Area.

For the medium-altitude imagery, the ranges for the visible data are greater for ASP/M and CONM than for LBS (≅6.5 pixels / 9.0 m versus 3.5 pixels / 4.9m) (Table 5.6; Figures 5.8 and 5.9). Lowland / Wetland Black Spruce (L/WBS), however, demonstrate range values greater than the typical LBS stand (≅5 pixels / 7.0 m) (Figure 5.9). Similarly, the range values for ASP/M stands are greater than LBS for the near-infrared data and demonstrate more variability than in the visible band (9 pixels / 12.5 m versus 7 pixels / 9.7 m) (Figures 5.9 and 5.10). The differences in mean ranges between the ASP/M stands and the LBS stands for the near-infrared data are not as pronounced as in the low-altitude data (Figures 5.4 and 5.10). However, the ranges for the near-infrared data are greater than those for the visible data for all stands, particularly LBS (e.g., 7 pixels / 9.7 m versus 3.5 pixels / 4.9 m) (Table 5.6; Figures 5.9 and 5.10).

Ranges derived from the medium-altitude data are greater for all stands, in both the visible and near-infrared bands, than for those measured in the low-altitude data (Table 5.5; Table 5.6). For example, the approximate ranges for the ASP/M stands in the visible band are 8 pixels / 5.8 m for the low-altitude data and 6.5 pixels / 8.9 m for the 1150 m data (Table 5.7). The absolute difference is less for LBS which has approximate ranges of 4.5 pixels / 3.3 m for the 600 m data and 3.5 pixels / 4.9 m for the medium-altitude data (Table 5.7). The range differences observed between the 1150 m and 600 m data are greatest for the near-infrared. For example, the mean ranges for ASP/M from the 600 m and 1150 m data are 10 pixels / 7.3 m and 9 pixels / 12.5 m respectively, and for LBS, 7 pixels / 5.1 m and 7 pixels / 9.7 m respectively.

As with the 600m data, the sills for the ASP/M and CONM stands are much greater than those of the Lowland Black Spruce stands, particularly in the near-infrared data (Table 5.6; Figures 5.11 and 5.12). For example, the mean near-infrared semivariance (sill) for Stand A (ASP/M - V5/V8) is approximately $9.06e+10^6$; for Stand T (CONM - V8/V14/V15/V16/V19) it is $1.54e+10^7$ and for Stand F (LBS - V37) it is $1.14e+10^6$ (Table 5.6; Figure 5.12). However, these levels are lower than for the corresponding stands in the low-altitude data. The contrast between ASP/M and LBS is greatest in the near-infrared, but it is still significant in the visible. Again, the variability between minimum and maximum sill values within stands of similar class is highest for ASP/M and CONM for both the visible and near-infrared. Stand N, a LBS stand, demonstrates the highest range values in the visible band while at the same time demonstrating one of the lowest range values in the near-infrared, consistent with other LBS stands (Table 5.6; Figures 5.11 and 5.12). A similar observation is made for Stand Q (L/WBS - V37/V38).

Variograms derived from the visible data generally resemble the "classic" form and in the near-infrared the "classic-periodic" form (Table 5.6). The curves appear to have a "smoother" character in the near-infrared than in the visible, albeit with a higher incidence of periodicity (Figure 5.8).

A summary of optimal spatial resolutions for the landscape-scale ecosystem classes is presented in Table 5.7 as estimated from both low- and medium-altitude reflectance data. In addition, a summary of key forest mensurational parameters for sample plots collected for the stands used in the variogram analysis is presented in Table 5.8. In comparing Tables 5.7 and 5.8, a number of observations can be made:

- stem density varies greatly between ecosystem classes, particularly between ASP/M and LBS, which corresponds to large differences in optimal support sizes between these ecosystem classes;
- the heights of the tree between different ecosystem classes correspond not only to differences in range values for corresponding classes, but also to the levels of semivariance exhibited by different ecosystem classes;
- mean maximum canopy diameter (MMCD) of 5m for ASP/M and CONM stands corresponds closely to visible range values at 600m (5.8m and 5.5m respectively);
- MMCD estimates are less for CM, LBS, UBS and L/WBS than the ranges derived from low-altitude visible and near-infrared data;
- the percent of high shrub is large for ASP/M and CONM; and
- low shrub is greatest for L/WBS, LBS and ASP/M.

Although entirely qualitative, there are a number of observations relating the range and semivariance estimates derived from the remotely sensed reflectance data to forest mensuration parameters that can be made. For instance, ecosystems such as ASP/M and CONM which have low stem density also have larger range values, whereas LBS has a high density of stems associated with small range values (Table 5.7 and 5.8). Also, ASP/M and CONM stands contain trees of greater heights than UBS, LBS, CM or L/WBS (Table 5.8), a characteristic that may contribute to higher estimates of semivariance for ASP/M and CONM. Crown diameter, as expressed by MMCD, seems to be the parameter most closely associated with range values, particularly for the visible data. High percentages of high shrub are associated with ecosystems exhibiting high range and semivariance estimates (i.e., ASP/M and CONM) (Table 5.7).

Table 5.6 Summary of Geostatistical Analysis of Forest Ecosystems (Altitude=1150m)

Altitude = 1150m AGL Spatial Resolution = 1.39m x 5.36m (7.5 m²)

Forest Stand	Vegetation Type/Complex	Transects (n) (@100 pixels)	Minimum Range (h)	Maximum Range (h)	Mean Range (h)	Mean Range (m)	Mean Range (m²)	Minimum Sill ('000)	Maximum Sill ('000)	Mean Sill ('000)	Mean Cov/Cor ('000)	Primary Variogram Shape
Visible (580nm - 601nm)												
A	Aspen-Dominated Hardwood - V5/V6/V8/V9	7	4.60	12.20	7.20	10.01	53.64	35.40	183.00	117.49	110.91	Classic
Y	Aspen-Dominated Hardwood - V6/V8	7	4.20	9.60	6.28	8.74	46.83	150.00	390.00	226.13	202.01	Classic
P	Trembling Aspen Complex - V9/V10/V11	9	3.60	9.40	5.64	7.85	42.05	124.20	330.00	194.62	205.99	Classic-Periodic
T	Aspen / Conifer Mix - V8/V14/V15/V16/V19	10	4.60	10.60	6.18	8.59	46.04	120.00	300.00	197.99	185.76	Classic-Periodic
X	Cedar Mixedwood - V22	8	3.00	8.80	5.53	7.68	41.16	96.00	318.00	217.50	214.59	Classic
K	Upland Black Spruce - V33	5	3.00	5.00	3.52	4.89	26.23	115.00	195.99	153.69	157.33	Classic
N	Lowland Black Spruce - V35	3	4.50	5.25	4.75	6.60	35.39	270.00	295.00	279.27	260.67	Classic-Periodic
U	Lowland Black Spruce - V35/V36/V37	5	2.40	6.40	3.28	4.56	24.44	92.00	113.40	107.48	109.20	Classic
F	Lowland Black Spruce - V37	6	2.10	4.50	2.95	4.10	21.98	42.20	107.00	72.94	78.50	Classic
B	Lowland Black Spruce - V36/V37/V38	6	2.25	4.00	3.04	4.23	22.66	42.76	116.00	75.66	75.06	Classic
Q	Lowland / Wetland Black Spruce - V37/V38	7	3.60	6.40	5.17	7.19	53.56	131.00	200.00	176.89	173.60	Classic
Near Infrared (744nm - 758nm)												
A	Aspen-Dominated Hardwood - V5/V6/V8/V9	7	6.40	14.00	9.20	12.79	68.54	6000.00	12000.00	9057.14	8051.43	Classic
Y	Aspen-Dominated Hardwood - V6/V8	7	5.80	13.40	9.17	12.75	68.33	6545.00	31000.00	16746.14	13949.71	Classic-Periodic
P	Trembling Aspen Complex - V9/V10/V11	9	5.40	13.60	8.69	11.95	64.07	5400.00	32500.00	12958.89	13696.56	Classic-Periodic
T	Aspen / Conifer Mix - V8/V14/V15/V16/V19	10	5.20	19.00	10.04	13.96	74.80	11000.00	23500.00	15387.00	14056.00	Classic-Periodic
X	Cedar Mixedwood - V22	8	6.00	17.20	10.18	14.14	75.81	2440.00	10100.00	5230.00	4610.50	Classic-Periodic
K	Upland Black Spruce - V33	5	5.00	6.40	5.60	7.78	41.72	1080.00	2170.00	1460.00	1317.22	Classic-Periodic
N	Lowland Black Spruce - V35	3	5.25	7.00	5.98	8.32	44.58	3100.00	5500.00	4533.33	4016.67	Classic-Periodic
U	Lowland Black Spruce - V35/V36/V37	5	5.00	12.40	7.72	10.73	57.52	809.10	1650.00	1284.22	1442.69	Classic-Periodic
F	Lowland Black Spruce - V37	6	4.65	14.00	7.63	10.89	58.36	522.00	2200.00	1143.75	1056.67	Classic-Periodic
B	Lowland Black Spruce - V36/V37/V38	6	5.40	7.50	6.51	9.05	48.52	643.00	1490.00	1122.75	1162.50	Classic-Periodic
Q	Lowland / Wetland Black Spruce - V37/V38	7	5.20	11.60	7.17	9.97	74.27	2900.00	5800.00	4180.60	4362.54	Classic-Periodic

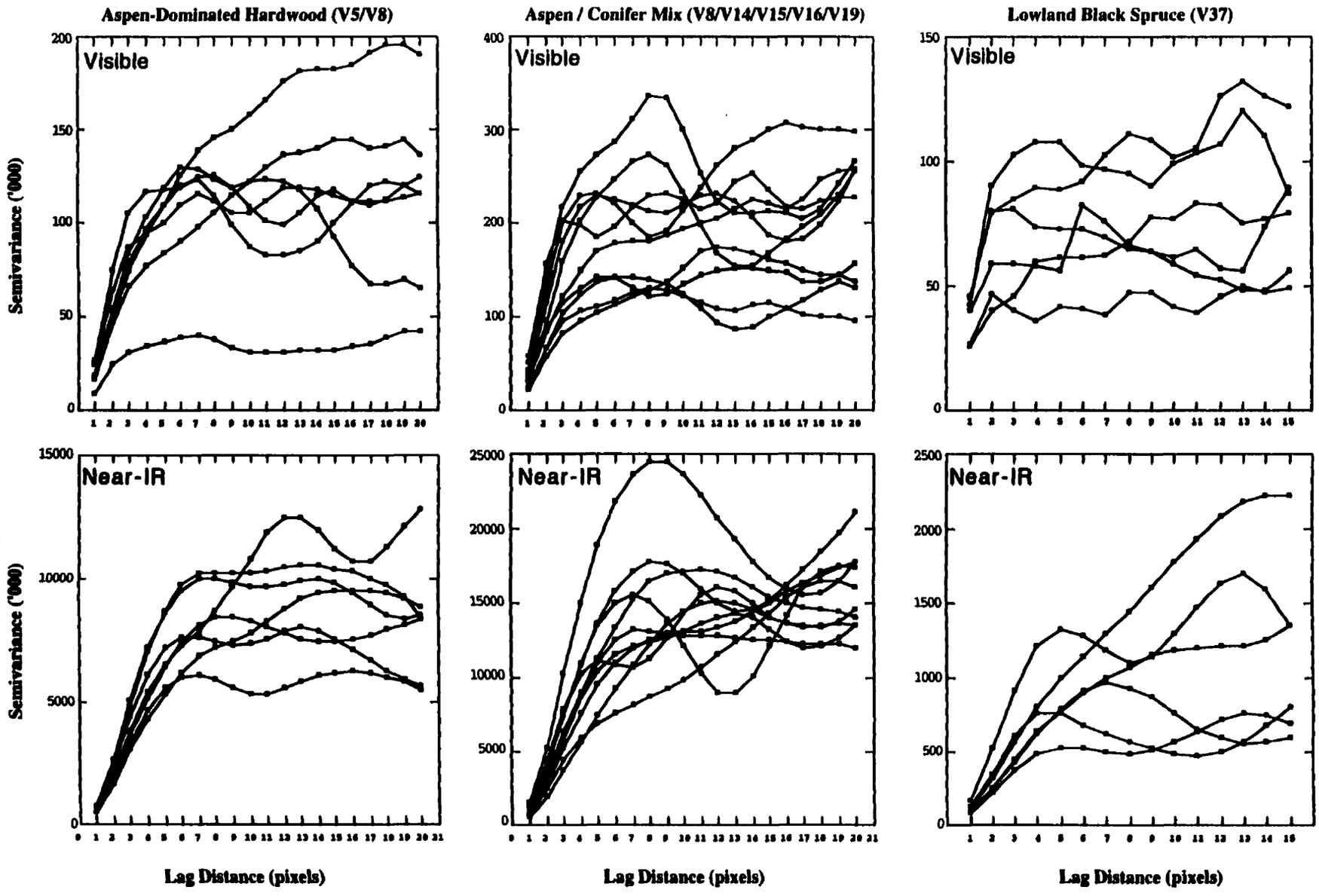


Figure 5.8 Variograms derived from selected forest stands / ecosystems (altitude=1150m).

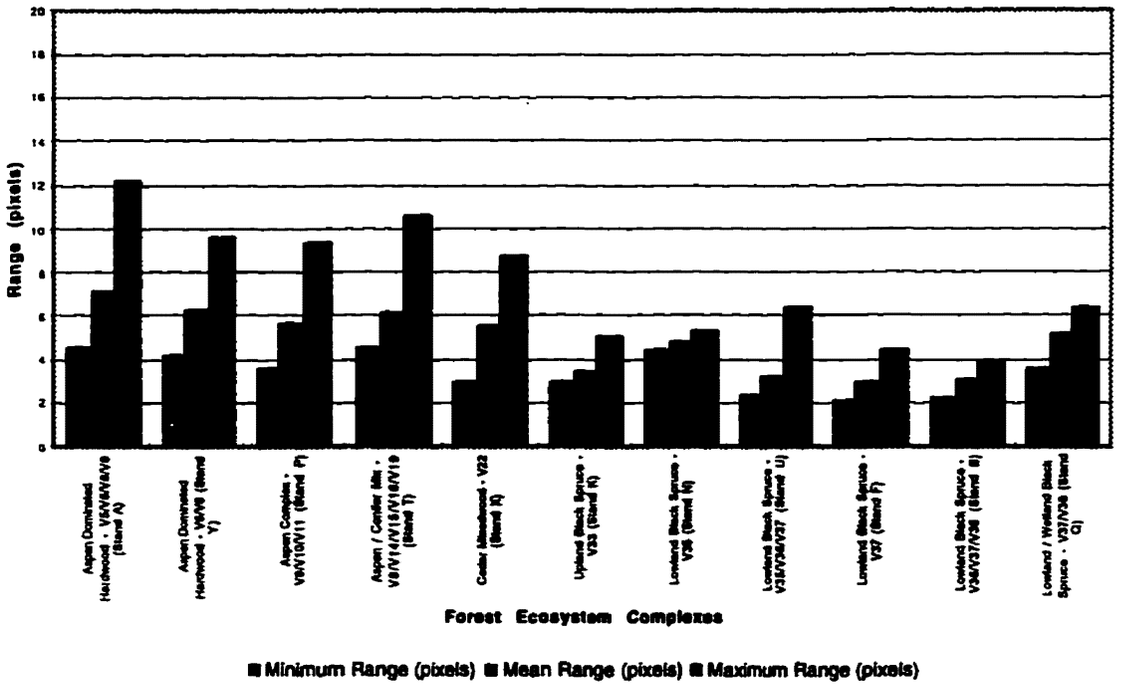


Figure 5.9 Medium-altitude range values (580 - 601 nm) for forest ecosystem complexes in the Rinker Lake Study Area.

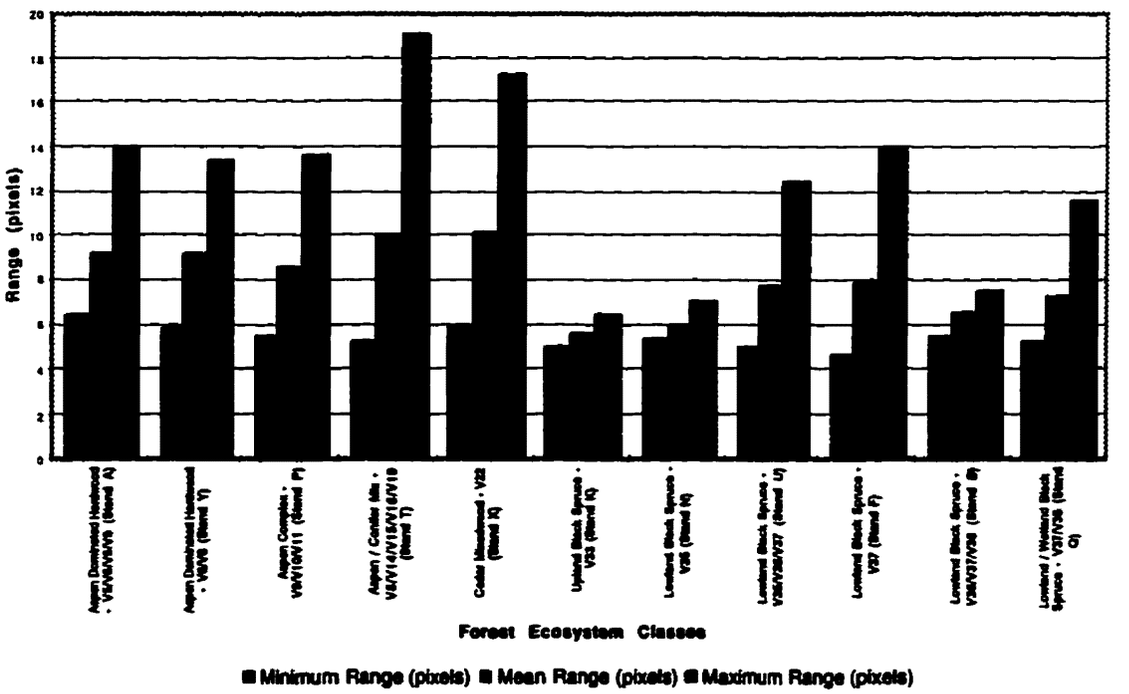


Figure 5.10 Medium-altitude range values (744 - 750 nm) for forest ecosystem complexes in the Rinker Lake Study Area.

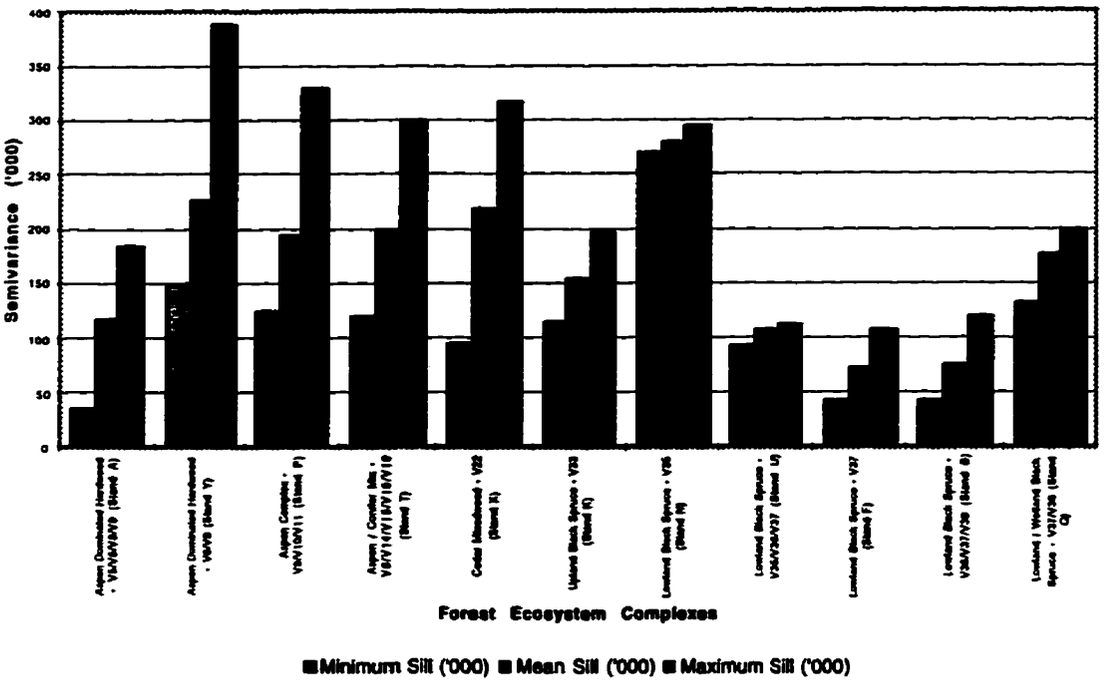


Figure 5.11 Medium-altitude semivariance (580 - 601 nm) for forest ecosystem complexes in the Rinker Lake Study Area.

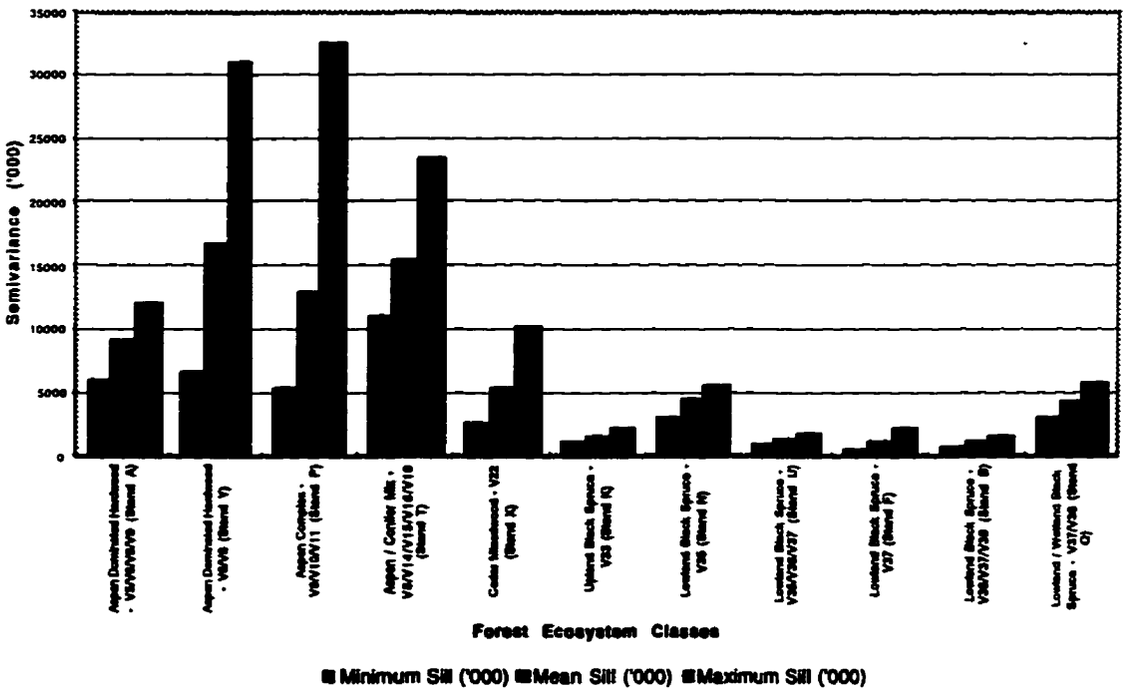


Figure 5.12 Medium-altitude semivariance (744 - 750 nm) for forest ecosystem complexes in the Rinker Lake Study Area.

Table 5.7 Summary of Optimal Textural Window Operators for Low- and Medium-Altitude CASI Data

Landscape Scale	Low Altitude (600m)		Medium Altitude (1150m)	
Forest Ecosystem Classes	Visible	Near Infrared	Visible	Near Infrared
Aspen-Dominated Hardwood and Mixedwood	8 pixels 5.8m / 31m^2	10 pixels 7.3m / 38m^2	6.5 pixels 9.0m / 48m^2	9.0 pixels 12.5m / 67m^2
White Spruce / Balsam Fir Conifer and Mixedwood	7.5 pixels 5.5m / 30m^2	10 pixels 7.3m / 39m^2	6 pixels 8.3m / 45m^2	10 pixels 13.9m / 75m^2
Cedar Mixedwood	6.5 pixels 4.7m / 25m^2	7.5 pixels 5.5m / 30m^2	5.5 pixels 7.6m / 41m^2	10 pixels 13.9m / 75m^2
Upland Black Spruce / Jack Pine	6.5 pixels 4.7m / 25m^2	9 pixels 6.6m / 35m^2	3.5 pixels 4.9m / 26m^2	5.5 pixels 7.6m / 41m^2
Lowland Black Spruce	4.5 pixels 3.3m / 18m^2	7 pixels 5.1m / 27m^2	3.5 pixels 4.9m / 26m^2	7.0 pixels 9.7m / 52m^2
Lowland / Wetland Black Spruce	4 pixels 2.9m / 16m^2	7 pixels 5.1m / 27m^2	5 pixels 7.0m / 38m^2	7.0 pixels 9.7m / 52m^2

Table 5.8 Summary of Forest Mensurational Parameters

Forest Ecosystem Classes	Dominant Species	Density (#/ha)	MMCD (m)	Height (m)	Tree Cover (%)	High Shrub (%)	Low Shrub (%)
Aspen-Dominated Hardwood and Mixedwood	**Populus tremuloides** Picea mariana Abies balsamea Pinus banksiana Betula papyrifera	663	5	22	54	60	35
White Spruce / Balsam Fir Conifer and Mixedwood	**Populus tremuloides** Picea glauca Abies balsamea Picea mariana Betula papyrifera	1050	5	19	66	63	18
Cedar Mixedwood	**Thuja occidentalis** Picea mariana	1500	2	12	54	15	25
Upland Black Spruce / Jack Pine	**Picea mariana** Pinus banksiana	1350	1	10	60	13	14
Lowland Black Spruce	**Picea mariana** Abies balsamea Larix larcina	1700	2	15	33	12	40
Lowland / Wetland Black Spruce	**Picea mariana**	900	2	10	10	0	67

5.5 Discussion

Atkinson and Curran (1995) identify two criteria by which the optimal size of support or spatial resolution can be chosen. First, the spatial variation or information of interest is important when selecting the optimal spatial resolution. Second, to estimate the mean of some property over a region, the size of support determines the precision of the estimation. When the objective is to map some property by local estimation (i.e., reflectance), the spatial variation in the sample determines the precision of the estimates of the spatial variation amongst them, which in turn determines the information displayed (Dungan *et al.*, 1993). However, when the objective is to estimate the mean of some property over the region of interest, the spatial variation in the sample determines the precision of the estimate only and information is no longer a valid criterion (Atkinson and Curran, 1995).

Range and sill values are of particular interest in analysing the different forest ecosystem complexes since the range indicates the distance at which pixels are no longer correlated and the sill is a measure of the variability of the reflectance values for the transect across the stand. The range value can be described as the point or distance at which the variogram reaches the sill. Within the range, the differences between reflectance values are spatially dependent. The importance here is that the range is often related to the size or scale of the largest elements in the scene that produce the correlation structure (Jupp *et al.*, 1989) and thereby represents the optimal distance at which samples should be collected. It provides a measure of the distance around a point at which spatial interpolation or processing is valid. The sill, or the point at which the variogram levels off (usually at a value equal to the general data variance), indicates the level of variability in the surface and implies that at these values of the lag, there is no spatial dependence between the reflectance values. This is because all estimates of variances of differences are invariant with distance. If a sill is not reached within a given distance or range, a trend may be present in the data (e.g., a scan-angle brightness effect across the image). Alternatively, the domain of definition of the data is too small for the scales of pattern in the regionalized variable (Jupp *et al.*, 1989).

In this variogram analysis, there appeared to be no nugget effect, representing spatially independent variance, which generally arises from measurement error (Huijbregts, 1975). Here, measurement error would arise from errors in the sensor, from the analog-to-digital conversion or from preprocessing. In the absence of spatially independent variance, the variogram would normally pass through the origin. In fact, many of the variograms observed in this analysis appeared to have a negative intercept, rather than a positive one. This has been noted previously and is attributed to the fact that remote sensing data are

regularized, and therefore appear below or inside the punctual variogram (Woodcock *et al.*, 1988b). Since the area which is sensed by the IFOV of a remote sensing instrument is often larger than the spatial resolution of the sensor (based on analog-to-digital conversion/sampling) the condition of a negative intercept should be more common. The effect that this process has is that adjacent measurements (pixels) should be more strongly related to an associated lower value for semivariance than expected. However, Atkinson (1993) observed a nugget effect, albeit small compared to the underlying variation of the variogram. The effect was particularly evident at the highest spatial resolution (1.5 m x 1.5 m pixel) and was attributed to high signal-to-noise ratios. However, the nugget variance decreased with increasing spatial resolution for both spectral bands, implying an inverse relationship with spatial resolution. Here, measurement errors should be minimal since the CASI data were calibrated to reflectance and corrected for atmospheric variations between altitudes.

Based on the results observed from the variogram analysis, there are three primary trends or characteristics that require discussion. These are:

1. range and semivariance estimates vary as a function of forest ecosystem class;
2. range and semivariance estimates vary as a function of spectral wavelength; and
3. range and semivariance estimates vary as a function of altitude/spatial resolution/scale.

These trends are related to the interactions between ground scene and sensor parameters. Forest ecosystems represent ground-scene parameters and vary as a function of stand/site characteristics and disturbance history. The structures and processes of these ecosystems differ and as a result produce variable reflectance patterns. Reflectance also varies as a function of wavelength, not only the intensity at that wavelength, but the spatial patterns that arise from contrasting interactions at canopy and subcanopy levels. As the support changes with altitude, the manner in which energy is recorded by the sensor varies, in all likelihood, non-linearly.

5.5.1 Forest Ecosystem Class

At low altitude, the ASP/M and CONM stands have greater range values than pure conifer, particularly lowland conifer where canopy and understory are generally simple and homogeneous. At this resolution, individual trees may be the dominant feature affecting the variogram, particularly for the ASP/M stands since the mean crown diameters of aspen trees (MMCD = 5 m) (Table 5.8) are approximately equal to the ranges of influence (visible = 5.8 m; near-infrared = 7.3 m) (Table 5.7). This finding would be consistent with results reported by Cohen *et al.* (1990) where the ranges for 1m spatial resolution data were related to the

mean tree canopy sizes of the stands. In contrast, variograms based on 10 m and 30 m pixels contained significantly less useful information. However, since, in this study, pixels are not square and individual trees are not observable, it is more likely that the range and semivariance result from the integration of a uniform number of tree crowns with understory and ground-cover components. The ASP/M and CONM stands also exhibit the lowest stem density, a parameter that is correlated with MMCD and may contribute to the greater ranges observed for these ecosystems (Table 5.8). Atkinson and Danson (1988) used variograms to measure spatial dependence in coniferous and oak plantations. They found the range of the variogram was related to stand age and species, and were able to determine the optimal spatial resolutions for even-aged stands. Curran (1988) analysed 2 m x 2 m spatial resolution data and found minimum range values for coniferous plantations to be 12m and deciduous woodland 26 m. This illustrates the contrast between (i) coniferous and deciduous forest; and (ii) artificial and regularly spaced trees versus natural and variably spaced trees. Bowers *et al.* (1994) were able to measure differences in variogram characteristics for thinned, unthinned, damaged and undamaged balsam fir stands using SPOT panchromatic data. These spatial characteristics were superior to spectral measures for examining damage incidence and forest structure (stems/hectare).

The relationship between stand density and semivariance is also evident in this study. For example, Stand Q (L/WBS - V37/38) has higher semivariance measures and greater range estimates than other LBS stands due to a lower density (900 stems/ha versus 1700 stems/ha) and tree cover (10% versus 33%) (Table 5.8). Stand X (CM - V22) and Stand M (LBS - V34/V35/V36) exhibit unusually high semivariance in the visible, relative to other conifer stands, approaching levels similar to ASP/M and CONM. These two stands display unique stand parameters. For instance, CM is not only dense, but it has an unusual stand structure in that the stems are not necessarily vertical, but grow in various orientations, some being almost horizontal to the ground. This stand also exhibits various degrees of openness in certain areas, but it was exceedingly difficult to traverse due to the dense nature of the canopy and understory. Also, scattered black spruce protrude through the cedar canopy, creating a complex canopy surface. Stand M (LBS) on the other hand is a very open stand (density = 300 stems/ha; mean spacing index (MSI) = 5.3m, tree cover = 8%) (Appendix D). This sparse stand possesses higher semivariance values than stands of higher density. This indicates that stand density has a direct impact on the nature of the variogram, since the character of the trees (e.g., height, MMCD) is similar to other LBS stands (Appendix D). This is particularly true for visible reflectance data, since in an open canopy there is more potential for interaction with understory shrub components, creating greater semivariance as

observed for Stands N (LBS) and Q (L/WBS). The majority of LBS stands possess a large number of stems/ha of uniform height and crown diameter, thereby exhibiting a relatively smooth surface at these scales. Cohen *et al.* (1990) also observed that stands with simple canopy structures had lower sill values than stands with complex canopies or gaps in the canopy.

The LBS stands exhibit a higher degree of regularization (i.e., lower semivariance) than do the ASP/M and CONM stands. The variability between variograms also indicates the complex nature of the ASP/M and CONM stands, a result of contributions from a variable canopy as well as sparse to dense understory. In a lowland environment, the drainage and nutrients are more uniform, thereby giving rise to a more uniform environment. In the case of LBS, this environment is one with a poorer nutrient regime, deriving a more simple ecological structure with lower diversity. The variability in range and semivariance estimates may also be related to location within the scan swath, since spatial resolution varies slightly from nadir to the edge of the scan. However, this is not expected to be a major factor, since the CASI is a narrow-swath sensor (i.e., 512 detector elements). This analysis suggests that to optimally characterize forest ecosystems, in the L-resolution case, that coarser resolutions would best be used to characterize complex ecosystems and finer resolutions would provide optimal discrimination of boundaries for simpler ecosystems. Historically, variable classification accuracies by class have resulted from this characteristic of single spatial resolution remote sensing data. Therefore, multiple spatial resolutions should be applied for discriminating forest ecosystems exhibiting differing stand structures and processes.

5.5.2 Spectral Wavelength

Similar to the visible reflectance data analysis, ASP/M and CONM stands have greater ranges than LBS within the near-infrared band. This would indicate that similar features/phenomena (e.g., tree crowns and associated understory) are influencing the spectral reflectance in the near-infrared data for these ecosystems. The sills for the ASP/M and CONM stands are much greater than those of the LBS stands, particularly in the near-infrared data. This indicates that the trembling aspen stands have increased layering with a higher percentage of cover than the black spruce stand. It appears that the complexity of the stand is more prevalent with the near-infrared data, likely due to the greater penetration of near-infrared energy through the canopy. Not only should spatial resolutions be optimized for specific forest ecosystem classes, but also for the spectral wavelengths being collected. At least, the contrasting interaction of visible and near-infrared energy should be thought of as distinct, and data acquired appropriately. Here, it has been demonstrated that visible and near-infrared energy are measuring slightly different structures/processes, and to optimize

discrimination of those structures/processes, visible and near-infrared data should be collected at different resolutions or at least be processed differently. Curran (1988) suggested that after analysis of variograms from different wavelengths, a minimum range should be identified to define a minimum spatial resolution for remote sensing data acquisition. However, this ignores the potential for multispatial resolution data for different wavebands to assist in the discrimination of features that have defined different ranges in different spectral bands.

The mean ranges derived for the near-infrared data are, in all cases, greater than the corresponding ranges for the visible data. This would indicate that different features/phenomena are being measured in the near-infrared as opposed to the visible, or the proportional contributions of dominant features/phenomena (e.g., tree crowns) to reflectance differ between bands. It is likely that the near-infrared band contains more ground-cover information since near-infrared energy has greater potential for penetration through a forest canopy. Therefore, ground cover such as sphagnum moss may have an important effect on near-infrared reflectance from black spruce stands with little or no shrub layer. This supports observations by Paradine (1994a) who used multivariate analysis of CASI radiance data to explain variability of forest ecosystem parameters. In a comparison of the visible and near-infrared spectral bands of Landsat TM and SPOT, Chavez (1992) found that the near-infrared band contains more spatial information than the visible band.

In general, the shapes of the variograms are smoother and more rounded for the near-infrared data as opposed to the visible. The near-infrared and visible data may be sampling different scales of information, particularly since the visible data have a higher frequency of variable sills and periodicity, with shapes more often resembling the classic-periodic and classic-multifrequency. The near-infrared may be sampling a coarser scale of structures/processes, since some of these minor perturbations are smoothed out in the near-infrared variograms. Unbounded variograms are more common for complex stands in the near-infrared than in the visible. This would indicate that the scale of structures/processes in the near-infrared is larger than the lag (i.e., 20 pixels). Periodicity and variability of sills may indicate the complexity of the canopy and correspond to clumpiness of canopy and understory trees. However, no consistent patterns were observed within individual stands.

Remotely sensed data for vegetated areas possess a lower dynamic range and amplitude of reflectance in the visible portion of the spectrum as opposed to the near-infrared. This results in a lower spatial variability for the visible reflectance data. In the near-infrared, the higher dynamic range for vegetation provides for the characterization of more subtle/local spatial variations. This characterization, as evidenced by the variogram analysis,

suggests that for optimal discrimination of forest ecosystem classes at a landscape scale, rather than at a local scale, more regularization in the near-infrared than in the visible portion of the spectrum is required. Alternatively, larger window sizes for textural operators should be applied to the near-infrared data to compensate for the increased spatial information and variability in this waveband.

5.5.3 Altitude/Spatial Resolution/Scale

Ranges derived from the medium-altitude data are greater than those measured from the low-altitude data (Tables 5.5 and 5.6). For example, the mean range for Stand A (ASP/M - V5/V6/V8/V9) is approximately 6m at the low altitude while at the medium altitude it is approximately 10m (Tables 5.5 and 5.6). This observation would indicate that different features/phenomena or aggregations of features/phenomena (e.g., possibly 2-3 tree canopies and associated understories) are being measured at the medium resolution. Thus, spatial pattern for these stands is scale-dependent. This illustrates the effect of increasing the size of support as measured by the IFOV of the sensor. In essence, the zone of influence or the zone where pixels remain spatially autocorrelated increases with a larger support.

The sills are typically lower for the medium-altitude data, indicating increased regularization as a result of decreased variability or complexity of forest-stand reflectance at this resolution (Table 5.5 and 5.6). In essence, scene components become finer portions of the next level of larger landscape objects (Hay *et al.*, 1996). The observed differences in the magnitude of semivariance of forest ecosystems at both resolutions indicates that ASP/M and CONM stands have increased layering with a greater volume of total cover than the LBS stands. The complexity of the stand is more prevalent with the near-infrared data, since near-infrared energy has a greater capability of interacting with understory components. Similar results were reported by Atkinson (1993) for visible and near-infrared data at 1.5m x 1.5m and 2m x 2m spatial resolutions over a single agricultural field. In addition, these findings also correspond to those of Woodcock *et al.*, (1988a) who applied variogram analysis to a discrete disc model where the number of objects, density of coverage, size and shape of objects (i.e., discs) was altered. It was observed that when there was a change in scale, or increase in regularization, the following occurred: (i) the height of the sill (or the variance of the variable) decreased; (ii) the range of influence, or the distance to the sill increased; and (iii) the height of the variogram at the first measured interval of h increased relative to the sill.

Based on the analysis of reflectance data for forest ecosystems in northwestern Ontario, it has been demonstrated that the shape of the variogram depends on (i) the variable being measured in the ground data (e.g., reflectance from the tree canopy and understory);

(ii) the spectral wavelengths interacting with the ground features and recorded by the remote sensing instrument; and (iii) the size and spacing of the sample points or ground-resolution elements (the support/spatial resolution). This was supported by Woodcock *et al.* (1988a) who attributed the shape of the variogram to the variance of the sizes of the objects in the image (i.e., the more rounded the variogram, the greater the variance in the size of objects). Breaks in the slope of the variogram were associated with the size of objects in the scene. It is important to recognize that the relationship between the size of the object in the scene and the size of the resolution cell (regularizing unit or support) has a marked effect on the shape of the variogram in both the H-resolution and L-resolution cases.

5.6 Conclusions

The approach taken in this chapter has been to attempt to understand the nature and causes of spatial variation in remotely sensed data of forest ecosystems as they relate to ground scene and sensor parameters. This analysis is a precursor to the application of spatial processing techniques for extracting scene-specific information.

As a result of the construction and analysis of variograms for forest ecosystems from low- and medium-altitude CASI reflectance data, the following conclusions with respect to range estimates for forest ecosystems can be drawn:

1. **Range estimates within the low- and medium-altitude reflectance data differ between various forest ecosystem classes, and at low-altitude appear to be related to canopy diameter (i.e., MMCD).** Similar correlations have been observed by Woodcock *et al.* (1988b) and Cohen *et al.* (1990). It is likely that there is not a clear relationship of range to MMCD due to the severely elongated nature of the pixel at this altitude. The range may more effectively represent the proportion of the area covered by the dominant object in the pixel or support (e.g., tree crown).
2. **Range estimates vary as a function of wavelength (i.e., there were contrasting estimates derived for the visible and near-infrared wavebands).** This would indicate that different spatial processes are being measured at these two wavelengths, or at the very least, different proportions of structures/processes are being measured. Since a greater percentage of near-infrared energy is likely to penetrate the canopy, the understory has a greater impact on the return signal, thereby modifying the impact of tree crown on the nature of the variogram. In the near-infrared there may be lower correlation with upper-canopy components than in the visible.

3. **Range estimates vary as a function of altitude/spatial resolution/scale.** The range estimates derived for each of the forest ecosystems were greater for the medium-altitude data than for the low-altitude data. At medium-altitude, it is likely that the proportion of the area covered by a uniform mix of tree canopy, understory and shrub is controlling the point at which the variogram reaches the sill.

In addition, conclusions concerning semivariance estimates (i.e., sills) include the following:

1. **Although it is a qualitative assessment, there appears to be a direct relationship between percent cover of understory and semivariance (i.e., height of the variogram).** Woodcock *et al.* (1988a; 1988b) attributed the increase in height of the variogram to the density of objects (e.g., trees) within the scene over a uniform background. It is suggested here that, although semivariance is related to density of trees in natural ecosystems, it is more closely related to multiple layers of vegetation (i.e., tree canopy density/variability and understory density/variability). In this regard, the height of the variogram can provide useful information on the type of forest ecosystem present. This supports findings by Cohen *et al.* (1990) who attributed the height of the sill to vertical layering and percent canopy cover.
2. **Again, albeit qualitative, an inverse relationship appears to exist between tree density (number of stems/ha) and semivariance for wetland coniferous forest ecosystems (V38).** Coniferous forest ecosystems with low tree density tend to have higher estimates of semivariance, particularly in the visible band, and in some cases are associated with larger range estimates. Canopies with large open gaps allow significant reflectance contributions from the low-shrub layer.
3. **Increased regularization (i.e., lower semivariance) of reflectance data for all forest ecosystems is characteristic of the medium-altitude data.** This increased regularization does not translate into smaller range estimates.

Remotely sensed data often exhibit several scales of variation or information at a single spatial resolution. This has been exhibited in this analysis of reflectance for forest ecosystems in northwestern Ontario. Contrasting ecosystems possess different scales of variation, variation which is reflected in the contrasting range and semivariance estimates from the experimental variograms. Indeed, it has been stated that the ability to derive information about multiple scales of variation in images from variograms may prove to be one of the attractive features of variograms (Woodcock *et al.*, 1988b). Although the detection

of multiple scales of variation has been demonstrated, interpretation of their characteristic differences remains difficult.

Based on these observations, it is anticipated that the potential for identifying forest ecosystems at a variety of levels will be improved by applying spatial analysis techniques (e.g., texture processing, spatial interpolation) to multispatial resolution remote sensing data. The identification of a single optimal spatial resolution for forest ecosystem discrimination may not be appropriate. Instead, it may be more suitable to analyze multispatial resolution data with appropriate processing techniques to classify forest ecosystems for various scales of information.

The spatial structures of the scene and of the images must be understood in order to select appropriate spatial resolutions for data acquisition and analysis. Specifically, it is important to understand the manner in which images of a scene change as a function of spatial resolution. It has been shown that when spatial resolution is considerably smaller or larger than the surface feature of interest, it is likely that sample pixels for these features will exhibit high spectral variance, whereas if the spatial resolution samples the appropriate mixture of feature attributes, spectral variance will be at a minimum (Woodcock and Strahler, 1987). Variogram analysis is a technique to determine the information content embedded in remote sensing reflectance data at different scales. Here it has been demonstrated that information content not only differs between forest ecosystems at different spatial resolutions, but also between visible and near-infrared bands at the same spatial resolution.

For mapping by remote sensing it is important that the spatial variation or information of interest be resolved (Gu *et al.*, 1992). In mapping forest ecosystems by remote sensing, it is the objective to estimate the mean reflectance of different forested surfaces, under the assumption that the mean reflectances for different forest ecosystems represent discriminable objects. This estimation requires the appropriate regularization of reflectance arising from stand structural characteristics. However, it is not expected that optimal spatial processing of reflectance data or collection of reflectance data at what are deemed optimal and multiple scales will, by themselves, provide sufficient discrimination of forest ecosystems, even at landscape scales. The reason for this is that optimally regularized reflectance is not likely to represent a highly efficient surrogate for a forest ecosystem class. Therefore, suitable discrimination and classification of forest ecosystems will require remote sensing at optimal and multiple scales in combination with additional terrain descriptors related to ecosystem class. Based on this premise, the concept of developing an integrated methodology for forest ecosystem discrimination and classification at landscape scales is pursued in Chapter 6.

CHAPTER 6

SPECTRAL, SPATIAL AND TERRAIN VARIABLES FOR DISCRIMINATING LANDSCAPE-SCALE FOREST ECOSYSTEM CLASSES

6.1 Introduction

In an ecological approach to land classification, coherent terrain units are interpreted based on a complex of factors including vegetation, landforms and drainage. Since forest ecosystems in northwestern Ontario are defined, in part, by physiography, incorporation of terrain variables with remote sensing data is essential for successful mapping of forest ecosystems over large tracts of land. It has been demonstrated that geomorphometric variables (e.g., elevation, gradient) provide additional information for discriminating land-cover classes in combination with satellite remote sensing data in high-relief environments (e.g., Peddle and Franklin, 1991; Franklin *et al.*, 1994). However, it is not clear whether these terrain variables contribute additional information for discriminating forest ecosystem classes when combined with high-resolution remote sensing data within localized regions in low- to moderate-relief boreal environments.

The Forest Ecosystem Classification (FEC) for northwestern Ontario represents an ecologically based classification which incorporates physiographic and biotic elements of the forest ecosystem. The framework upon which FECs are based incorporates those components of forest site that contribute to forest development (i.e., canopy and understory vegetation, soils, landform, general climatic regime, and regional physiography) (Sims and Uhlig, 1992). FECs were developed for stand-level (i.e., <1:10,000) application to provide information regarding vegetation, soil and site conditions. However, this high-resolution ecosystem classification is difficult to implement for large tracts of boreal forest that are characteristic of much of northwestern Ontario. Since FECs are somewhat hierarchical, field-level units can be aggregated to create lower-resolution ecosystem units (Racey *et al.*, 1989). Thus, integration of appropriately "scaled" and spatially processed georeferenced remote sensing data and spatially geocoded terrain information offers potential for assisting in the analysis of

large tracts of forest for identification of relevant landscape-scale ecosystem classes, particularly in the context of an hierarchical classification scheme.

High-resolution Compact Airborne Spectrographic Imager (CASI) data are spatially averaged to generate "optimally" and variously-scaled remote sensing data, as derived through the semivariogram analysis of Chapter 5. Also, texture measures, a function of within-stand variability and spatial scale, are derived from the high-altitude remote sensing data, again, in the context of the spatial analysis outlined in Chapter 5. Finally, CASI spectral and spatial variables are used in combination with texture variables and geomorphometric variables (i.e., elevation, local relief, gradient) to test the discriminability of forest ecosystems at a landscape scale (i.e., 1:20,000). High-resolution CASI data are analysed in combination with terrain variables derived from a 1:20,000-scale elevation model, all of which are registered within an integrated dataset. These data are evaluated to determine their ability to discriminate and classify forested ecosystems in northwestern Ontario at a landscape level.

6.2 Methods

6.2.1 Remote Sensing (Reflectance) Variables

As described in Chapter 4, CASI data were acquired over the study site on July 30, 1993. Here, the high-altitude CASI reflectance data (2630 m AGL - 3.18 m x 5.36 m) are analysed. These data approximate the lower limits of "optimal" spatial resolutions identified for certain forest ecosystem classes, as reported in Chapter 5 (Table 5.7). For example, the spatial resolution of the high-altitude data, i.e., 17 m^2, approximates the optimal spatial resolution identified for Lowland/Wetland Black Spruce with the low-altitude data (i.e., 16 m^2).

In order to integrate CASI data, acquired or processed to "optimal" spatial resolutions, with other terrain data, a georeferenced database for the Rinker Lake Study Area was developed incorporating remote sensing and terrain variables. A common spatial resolution of 4 m x 4 m was selected for this database, representing the "highest common factor" for the high-altitude CASI data as well as the 20 m digital elevation model and georeferenced Landsat TM variables (see Chapter 4 for a description of these variables). Due to the lack of cultural features in the study area, the high-altitude CASI reflectance data were registered to a Landsat TM scene that was georeferenced to the Universal Transverse Mercator (UTM) projection at a 4 m pixel spacing. For CASI flight line 2, a fourth-order polynomial and a nearest-neighbour resampling algorithm were applied to register the CASI data to a 4 m pixel within the georeferenced dataset. Although the CASI data had been

corrected for aircraft roll, registration errors persisted (e.g., mean residuals in the x and y direction are 3 and 7 pixels, respectively) (Table 6.1; Appendix E). Based on this methodology, the remaining four CASI flight lines were georeferenced to the same database using fourth- or fifth-order polynomials. This work was done by Geomatics International as part of their contribution to NODA Contract 4002, the project from which the collection of the CASI data was funded (Table 6.1; Appendix E). As a result, the five CASI flight lines were combined with Landsat TM data to form a mosaic covering the entire study area (Figure 6.1).

The two northernmost flight lines (flight lines 4 and 5) exhibited higher overall reflectance characteristics than flight lines 1, 2 and 3. Flight lines 4 and 5 were acquired later in the day, and as a result the bidirectional reflectance factor (BDRF) effects are apparent since the flight path is no longer parallel to the sun's azimuth. Collection of reflectance data for analysis of forest ecosystem classes from flight lines 4 and 5 was avoided where possible.

Table 6.1 Summary of Geometric Correction of CASI Flight Lines

Flight Line	GCPs	Order	Residuals (pixels)			Residuals (metres)		
			Easting	Northing	Vector	Easting	Northing	Mean
Flight Line 1	153	Fifth	10.71	5.44	12.01	42.8	21.8	48.0
Flight Line 2	58	Fourth	3.27	7.03	7.76	13.1	28.1	52.4
Flight Line 3	134	Fifth	11.33	3.94	11.99	45.3	15.8	48.0
Flight Line 4	80	Fourth	7.38	4.19	8.48	29.5	16.8	33.9
Flight Line 5	98	Fourth	5.98	4.49	7.48	23.9	18.0	29.9
Overall Mean Residuals			**7.73**	**5.02**	**9.54**	**30.8**	**20.1**	**38.2**
Mean Residuals (Lines 1-3)			**8.44**	**5.47**	**10.59**	**33.8**	**21.9**	**42.4**

A summary of the residuals for each flight line is reported in Table 6.1. It is evident that large registration errors exist for each of the flight lines fitted to the georeferenced database (i.e., approximately 10 pixels / 40 m). This has significant implications on collection of reflectance data for analysis with terrain variables. As a result, reflectance data representing ground sample sites were limited to areas where stands of landscape-level forest ecosystems were large to avoid overlap with terrain variables that are, in fact, associated with different landscape variables. For instance, sample locations that were within 10 pixels / 40 m of a perceived edge between landscape-level classes were avoided where possible. Georeferencing of airborne remote sensing data is an area where improvement is required if these high-resolution data are to be integrated with other spatial data within a spatially referenced information system.

6.2.2 Forest Ecosystem Reflectance Data Collection

For this study, detailed V-Types were aggregated to six landscape-scale ecosystem classes that were present in the Rinker Lake Study Area (Table 6.2). Forest ecosystem ground data were then aggregated into the six landscape-scale forest ecosystem classes. Based on this grouping, sites were located in the CASI image data. Only sites that could be accurately located and fell within a relatively large homogeneous area were selected for analysis. The accuracy and precision of the registration of the CASI flight lines to a georeferenced database had a direct impact on the location of ground-plot locations. Sample sites used for characterizing each landscape-scale class are reported in Table 6.2 by V-Type. A sample consisting of 1500 calibration pixels and 1500 validation pixels (250 calibration and validation pixels per sample for each of the six classes) was collected.

Forest ecosystem sites were located on the georeferenced, high-altitude imagery using GPS coordinates. However, due to the error observed in the registration process, these positions were checked against the 1:8000 colour-infrared photographs and distance and direction measurements used in the field. For each landscape-scale forest ecosystem class, 20 sites were located for a total of 120 sites. For each site, a 20m x 20m area, corresponding to 25 pixels, was extracted from the CASI high-altitude (4 m) image dataset and used in the calculation of mean and covariance for each class. The sample locations are listed in Appendix F.

In cases where there were only a few forest stands of a particular landscape-scale forest ecosystem class (i.e., cedar mixedwood and wetland black spruce), attempts were made to collect calibration and validation data from separate stands or from the same stand on different flight lines. When this was not possible, samples were taken from different locations within the stand.

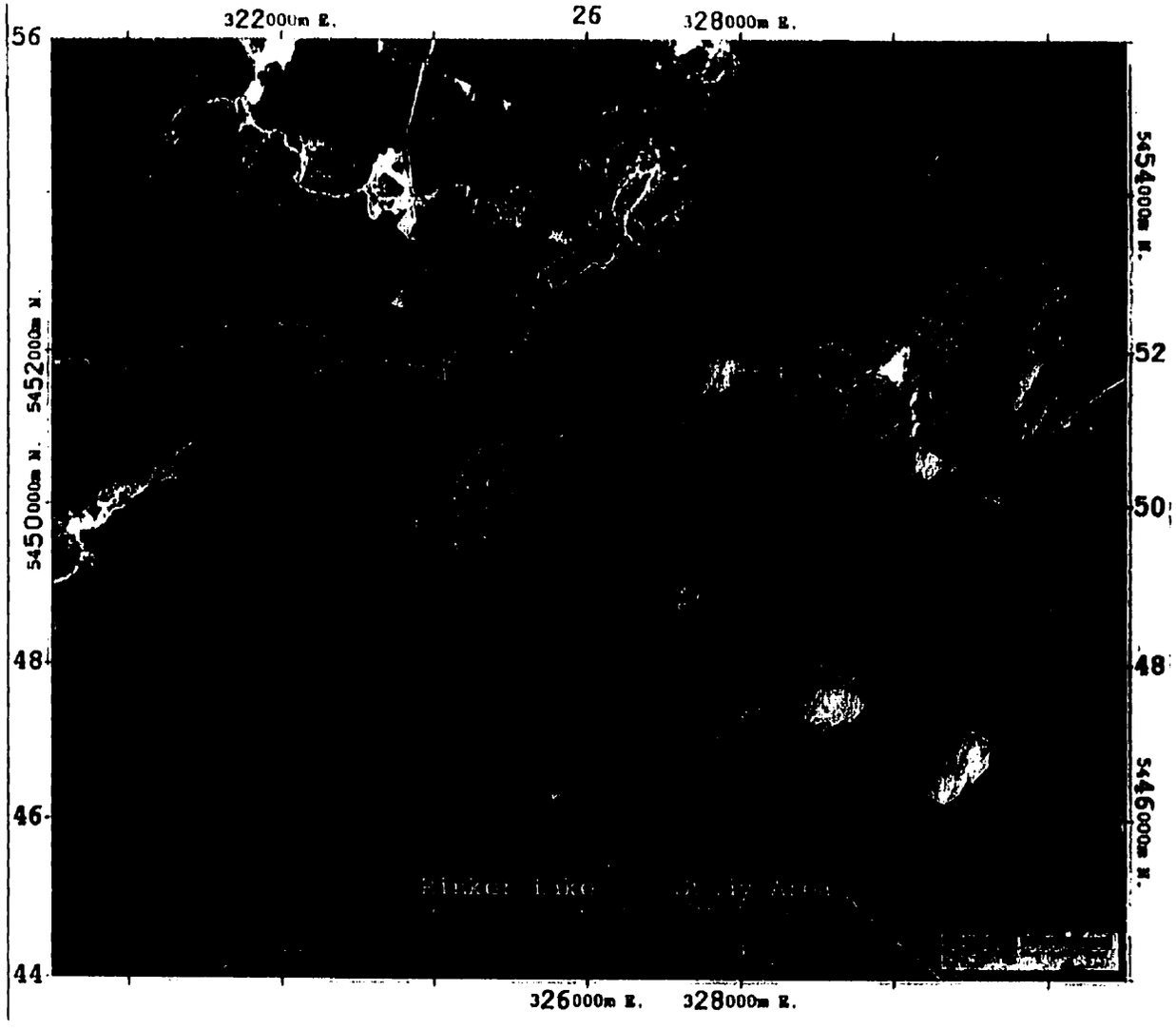


Figure 6.1 High-altitude CASI and Landsat TM mosaic for the Rinker Lake study area.

Table 6.2 FEC V-Type Samples For the Rinker Lake Study Area

V-Type	FEC Description	FEC Samples (Plots / Transects)	
		Calibration	Validation
	Aspen-Dominated Hardwood and Mixedwood		
V5	Aspen Hardwood	2606, T1	2645, S28
V6	Trembling Aspen (White Birch) - Balsam Fir / Mountain Maple	2655, A37	2620, 2648
V7	Trembling Aspen - Balsam Fir / Balsam Fir Shrub	2610, A17	2639, PP26
V8	Trembling Aspen (White Birch) / Mountain Maple	A27, T25	2619, S10
V9	Trembling Aspen Mixedwood	2649	2658
V10	Trembling Aspen - Black Spruce - Jack Pine / Low Shrub	2671	2609
	White Spruce / Balsam Fir Conifer and Mixedwood		
V14	Balsam Fir Mixedwood	G1, T17	095, T13
V15	White Spruce Mixedwood	2637, 2657, T22	038, T21
V16	Balsam Fir - White Spruce Mixedwood / Feathermoss	2624, 2628A, T14, T20	2625, 2659, 2628B, T15
V24	White Spruce - Balsam Fir / Shrub Rich		I6
V25	White Spruce - Balsam Fir / Feathermoss	032, 037	026, 033
	Cedar Mixedwood		
V22	Cedar (inc. Mixedwood) / Speckled Alder / Sphagnum	2621, X1, X2, X6, X7, X8, X12, W1, W2, W3	2641, X3, X4, X5, X9, X10, X11, W4, W5, W6
	Upland Black Spruce / Jack Pine		
V31	Black spruce - Jack Pine / Tall Shrub / Feathermoss	034, PP12, PP16A, S15	2629, PP16B
V32	Jack Pine - Black Spruce / Ericaceous Shrub / Feathermoss	2640A	2640B
V33	Black Spruce / Feathermoss	031, 2664, A31, K8, S5	2665, 2666, A7, A30, K2, K7, R25
	Lowland Black Spruce		
V34	Black Spruce / Labrador Tea / Feathermoss (Sphagnum)	PP25	2633
V35	Black Spruce / Speckled Alder / Sphagnum	2656, 2668, A19, R29	2608, A23
V36	Black Spruce / Bunchberry / Sphagnum (Feathermoss)	2611, 2612	2613, 2651
V37	Black Spruce / Ericaceous Shrub / Sphagnum	2601, 2602, 2623	2650, 2653, N1, U1, U2
	Wetland Black Spruce		
V38	Black Spruce / Leatherleaf / Sphagnum	2622, 2652, 2663, C1, J6, Q8, Q9, Q10, R31A, R31B	2642, C6, J7, J8, Q2, Q6, Q7, V1, V2, V3

6.2.3 CASI Spectral Feature Selection

Band 1(435-466 nm) was eliminated from analysis due to noise and poor dynamic range. Also, it was observed that Bands 8 (785-795 nm) and 9 (860-888 nm) suffered from poor focus and therefore were omitted from this analysis. To reduce the data dimensionality of the remaining six bands of CASI data, the Jeffries-Matusita (J-M) distance, a statistical separability measure (often referred to as Bhattacharrya distance), was used to evaluate candidate feature subsets. J-M distance is a measure of the average difference between the two-class density functions (Swain and Davis, 1978). It is defined as:

$$J_{ij} = \int_{\chi} \left[\sqrt{p(x \mid w_i)} - \sqrt{p(x \mid w_{jl})} \right]^2 dx$$

where J_{ij} is the J-M distance between class i and class j, χ is the entire feature space, and $p(x \mid w_i)$ is the probability density that a member of class i is found at x (Richards, 1993). This definition has obvious physical meaning; it is a measure of the amount of overlap between the probability density functions of two classes. If one assumes that the class probability density functions are normal, then the above equations can be shown to reduce to:

$$J_{ij} = 2\left(1 - e^{-\alpha}\right)$$

where

$$\alpha = \frac{1}{8}\left(U_i - U_j\right)^T \left(\frac{\Sigma_i + \Sigma_j}{2}\right)^{-1} \left(U_i - U_j\right) + \frac{1}{2} \ln \left(\frac{\left|\left(\Sigma_i + \Sigma_j\right)\right|}{2\left(\left|\Sigma_i\right| \cdot \left|\Sigma_j\right|\right)^{-1/2}} \right)$$

where U_i and Σ_i are the mean vector, and covariance matrix, respectively, for class i (Richards, 1993). As can be seen, α is constrained to be non-negative, and J_{ij} ranges between 0 and 2.

In this study, CASI feature selection was achieved using the following procedure to collect reflectance data for the six landscape-scale ecosystem classes:

1. As described above, forest ecosystem sites were located on the georeferenced, high-altitude imagery using GPS coordinates. For each landscape-scale forest ecosystem class, 10 calibration sites were used to calculate the mean and covariance for each class (Table 6.2; Appendix F).
2. The number of CASI features was determined (i.e., 1, 2, 3, 4, 5, or 6)
3. Feature subsets of the specified number of features were determined. For each candidate feature set, the average J-M distance was calculated for each landscape-scale class pair.

4. This process was repeated for each possible combination of the specified number of CASI features identified in Step 2, and the average J-M distance for each feature subset was tracked.
5. The maximum of the average J-M distance was used to select the best feature subset for the given number of features desired.
6. Steps 2 to 5 were repeated for different numbers of CASI features. These results are reported in Table 6.3 and Appendix G.

Based on this analysis, CASI spectral channels (variables) 3, 5 and 7 were selected for spatial averaging to "optimal" spatial resolutions/scales, texture analysis and integration with terrain variables.

Table 6.3 Feature Selection Based on Jeffries-Matusita (J-M) Distance

Number of Features	Channel						Maximum J-M Distance Average
	2	3	4	5	6	7	
1						y	0.591
2	y					y	0.877
3		y		y		y	0.987
4		y		y	y	y	1.081
5	y		y	y	y	y	1.136
6	y	y	y	y	y	y	1.165

6.2.4 Spectral-Spatial Features

Specific spatial resolutions for visible and near-infrared reflectance data were identified for the six landscape-scale ecosystem classes based on the semivariogram analysis presented in Chapter 5 (Table 6.4). Based on these findings, a series of spectral-spatial features were derived for CASI bands 3, 5 and 7 using the technique of non-overlapping spatial averaging (Shepherd, 1996). With this technique, the mean reflectance within a non-overlapping square window is calculated and assigned to an output image. The input window is then moved a distance equivalent to the window size and a new mean reflectance value is calculated. This process is repeated over the entire image. Here a one metre database was developed from the high-altitude data, meaning that the original database of 4m (3500 pixels by 3000 lines) was written to a database of 14000 pixels by 12000 lines. CASI Bands 3, 5, and 7 were then spatially averaged to 5 m and 6 m while CASI Band 7 was averaged to 6 m and 7 m spatial resolutions. These spatial resolutions reflect the results of the semivariogram analysis with the optimal resolutions being larger for the near-infrared data than for the visible. Although it is unclear how closely spatial averaging simulates multiscale remote sensing data, it has been demonstrated to be superior to algorithms such as cubic convolution and bilinear interpolation for upscaling spectral signals (Hay and Niemann, 1996). Non-overlapping

spatial averaging assumes that smaller-scale systems behave similarly to the average of larger-scale systems. However, differing structural processes occur within the landscape at various scales and do not necessarily interact in a linear fashion (Hay and Niemann, 1996).

The 5m, 6m and 7m CASI datasets were georeferenced to the 4m dataset using a first-order polynomial and nearest-neighbour resampling algorithm. The results of the geocoding of these data are presented in Appendix H. Sub-areas representing these spatially averaged features are presented in Figures 6.2 and 6.3. These can be compared to Landsat TM data with similar spectral characteristics in Figure 6.4.

Table 6.4 "Optimal" Spatial Resolution CASI Dataset based on Semivariogram Analysis

CASI Spectral Variable	Spatial Resolution	Landscape Level Ecosystem Classes*					
		1	2	3	4	5	6
CASI (580 - 601 nm)	4 metres					■	■
	5 metres			■	■		
	6 metres	■	■				
CASI (663 - 678 nm)	4 metres					■	■
	5 metres			■	■		
	6 metres	■	■				
CASI (744 - 750 nm)	5 metres					■	■
	6 metres			■	■		
	7 metres	■	■				

* 1. Aspen-Dominated Hardwood and Mixedwood; 2. White Spruce / Balsam Fir Conifer and Mixedwood; 3. Cedar Mixedwood; 4. Upland Black Spruce / Jack Pine; 5. Lowland Black Spruce; and 6. Wetland Black Spruce

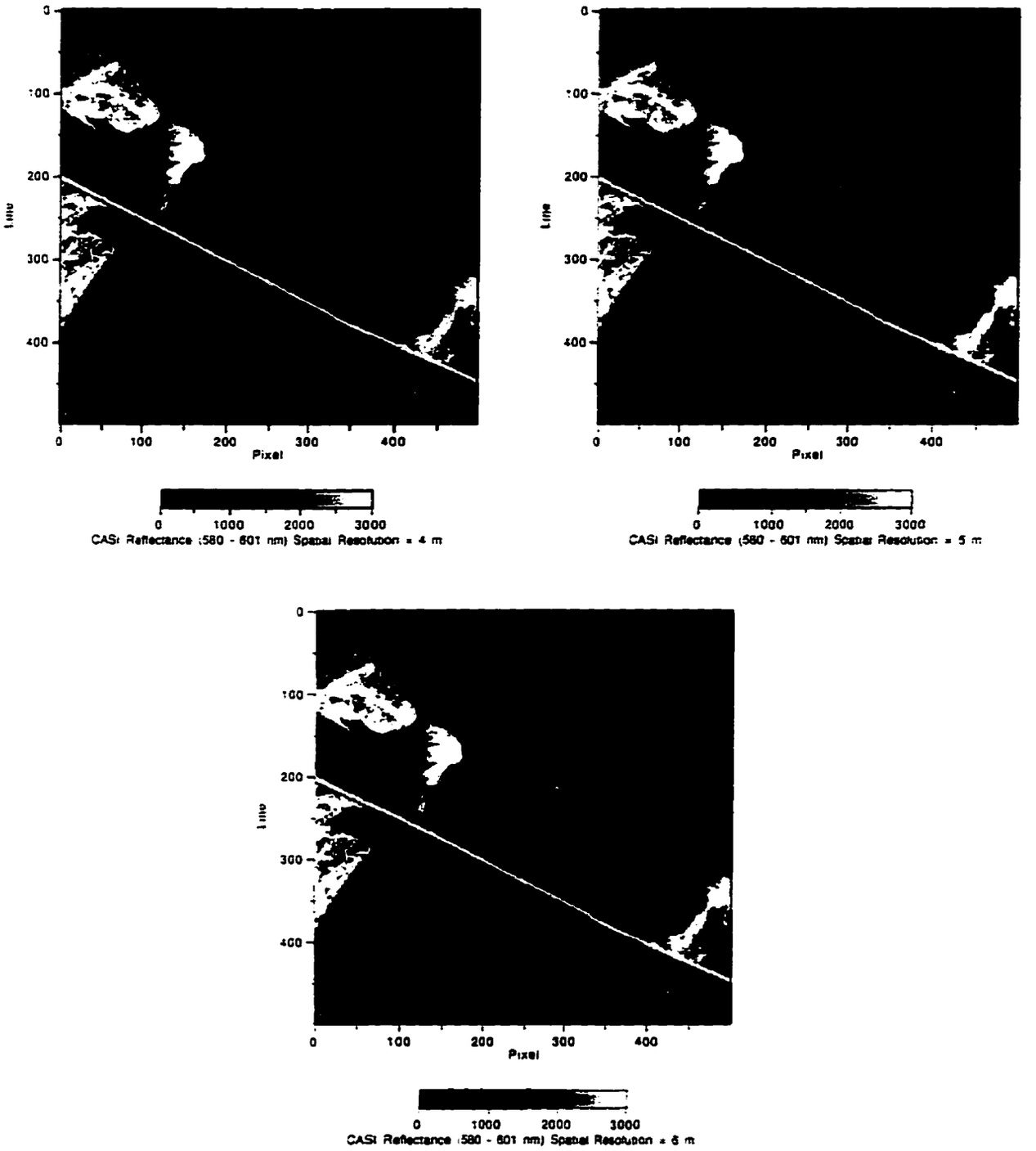


Figure 6.2 Spectral-spatial features for CASI Band 3 reflectance.

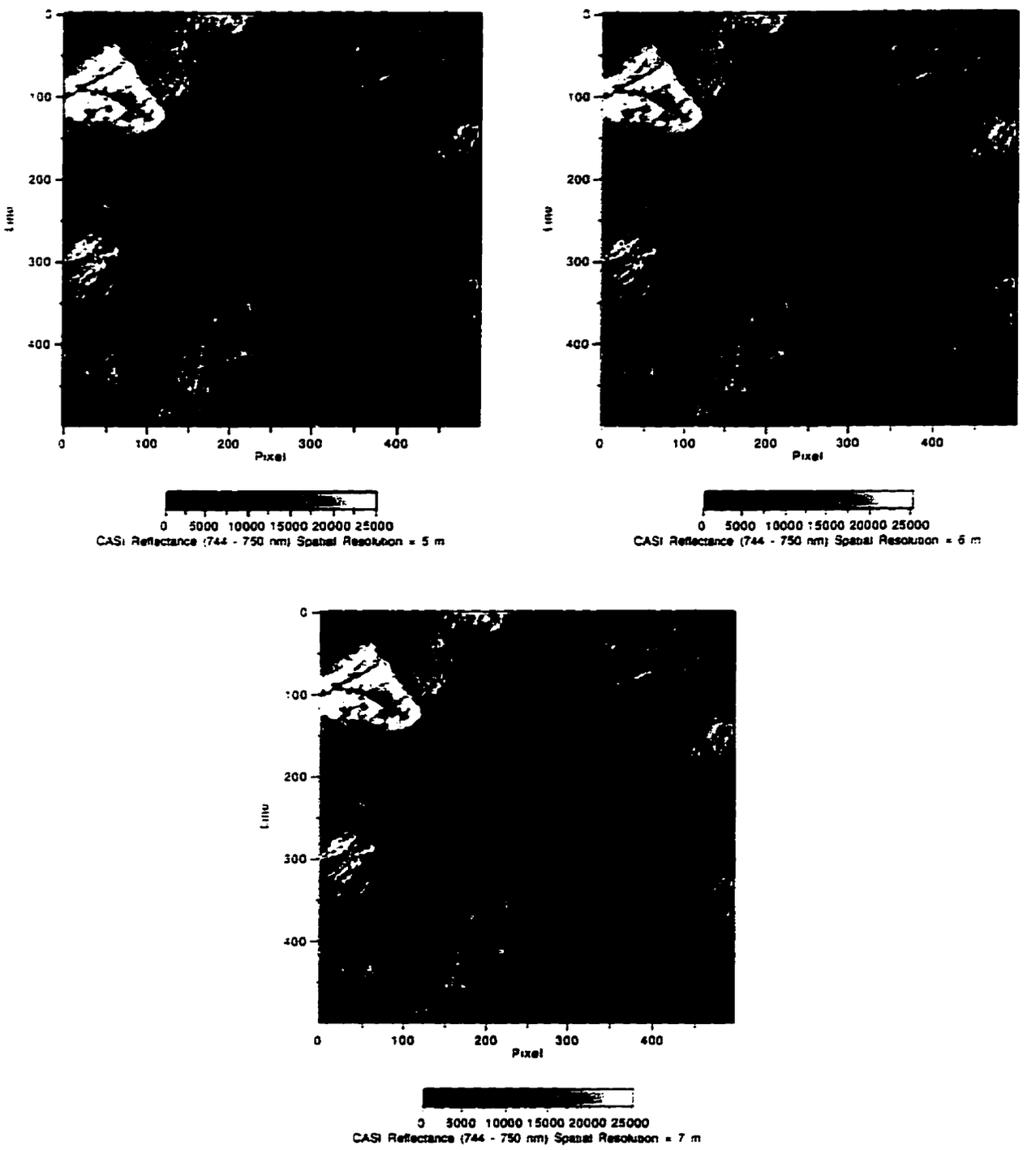


Figure 6.3 Spectral-spatial features for CASI Band 7 reflectance.

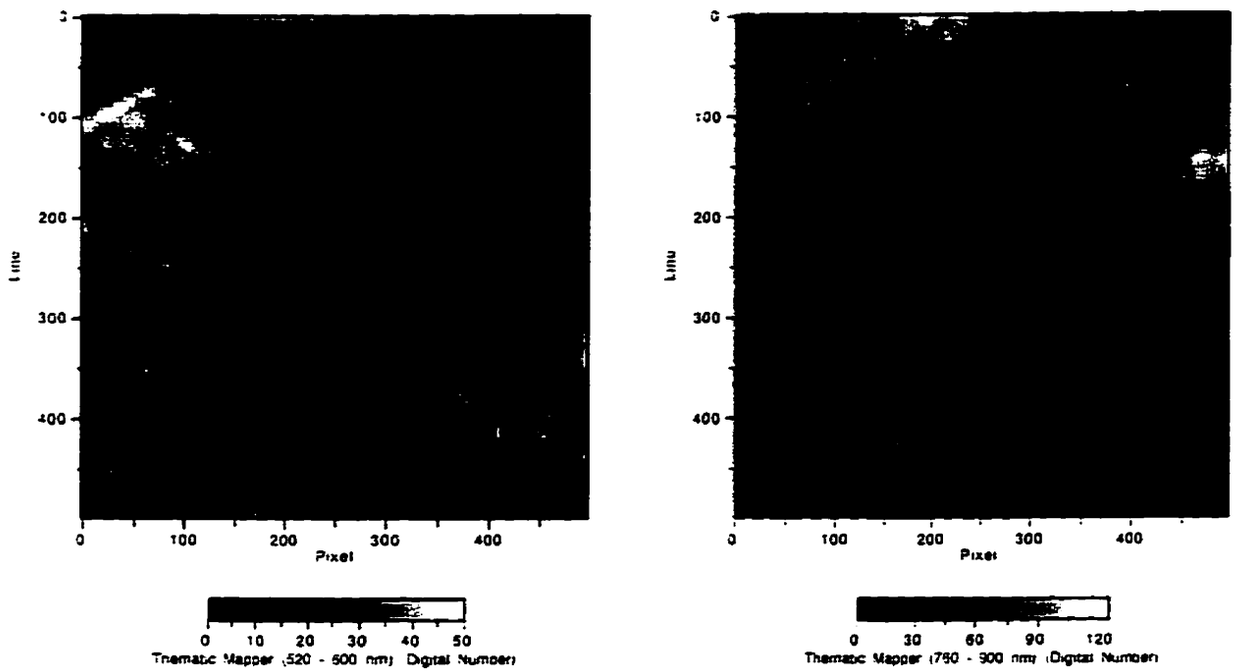


Figure 6.4 Landsat TM features.

6.2.5 Texture Features

Traditionally, tone (i.e., spectral intensity / reflectance) has been the primary focus for most image analysis and hence information extraction in remote sensing studies. Here, texture analysis is examined as an important contributor to scene information extraction. Texture contains important information about the structural arrangement of surfaces and their relationships to the surrounding environment (Haralick *et al.*, 1973). Although texture has long been recognized as an important clue in the visual recognition of objects in imagery, conventional automated processing, traditionally, has not exploited this component of remote sensing data. In this study, the Grey-Level Co-occurrence Matrix (GLCM) statistical method is used to generate texture features from high-altitude CASI data. Since the objective was to combine texture features with spectral-spatial and terrain features, texture processing was applied to the high-altitude data since it was of sufficient spatial coverage and geometric accuracy to combine with the other spatial features and relate to the ground plot data.

The GLCM method can be defined as a matrix of relative frequencies in which two neighbouring pixels, separated by distance δ and having an angular relationship α, occur on the image, one with grey tone i, and the other with grey tone j (Haralick *et al.*, 1973). The power of the GLCM approach is that it characterizes the spatial interrelationships of the grey tones in a textural pattern and can do so in a way that is invariant under monotonic grey-tone transformations. On the other hand, it does not capture the shape aspects of the tonal

primitives and therefore is not well-suited for textures composed of large-area primitives (Haralick 1979). Hence, this technique is suited to the CASI data analyzed in this study (i.e., L-resolution data). The objective of these statistical approaches is to translate visual texture properties into quantitative descriptors in a manner that they can be used to discriminate relevant land features using additional image processing techniques. It has been shown that classification accuracies are improved when texture features are incorporated into image classification (Peddle and Franklin, 1991; Barber and LeDrew, 1991; Rotunno *et al.*, 1996).

The GLCM is a two-dimensional array that provides the conditional joint probabilities of all pairwise combinations of pixels within a defined computation window (W_{nm}) (Haralick *et al.*, 1973). The co-occurrence of grey values represents the probability of any two pairs of grey values occurring at a user-defined interpixel sampling distance (δ) and orientation (α):

$$\Pr(x) = \{Cij|\delta,\alpha\}$$

The co-occurrence matrix (C_{ij}) is then defined as (Haralick *et al.*, 1973):

$$C_{ij} = \frac{P_{ij}}{\sum_{ij=1}^{n} P_{ij}}$$

where P is the frequency of occurrence of grey levels i and j, and n is the total number of pixel pairs based on the window W_{nm} and interpixel sampling distance (δ).

The texture statistics generated from the GLCM represent a single spatial measure of the image texture (Barber and LeDrew, 1991). These statistics are characterized as point estimates since each statistic provides a single measure of the distribution of grey-level pairs within the GLCM. The characteristic texture of an image is related to the distances of the co-occurrence matrix entries from the main diagonal. Features with characteristic coarse textures containing large areas of relative homogeneity will tend to cluster close to the diagonal of the matrix since reference and neighbouring pixels will have similar grey values. Features with characteristic fine textures will produce higher frequencies of co-occurrences further from the diagonal. Texture statistics are therefore used to measure the distribution of co-occurrences about the main diagonal. Of the 13 texture features that Haralick *et al.*, (1973) describes that can be derived from the GLCM, Ulaby *et al.*, (1986) tested and defined four that were independent texture features (i.e., not correlated). These were contrast, inverse moment, sum of squares and correlation. Of these four, Ulaby *et al.*, (1986) found contrast and inverse moment were the best features for separating five land-use categories.

GLCM analysis was performed on a 6-bit linear transformation of the original 16-bit high-altitude CASI data using measures of contrast, mean and correlation. Quantization-level

scaling is performed to reduce data storage and increase computational efficiency during matrix calculations (PCI Inc., 1996). These analyses were performed on CASI visible (580 - 601 nm) and near-infrared data (744 - 750 nm). Texture features (contrast, mean and correlation) (Figures 6.5, 6.6 and 6.7) based on GLCMs were generated using PCI EASI/PACE software (PCI, 1996):

Contrast

$$\sum_{i=1}^{n}\sum_{j=1}^{n} C_{ij}(i-j)^2$$

Mean

$$\sum_{i=1}^{n}\sum_{j=1}^{n}\left(C_{ij}\right)\bullet i$$

Correlation

$$\sum_{i=1}^{n}\sum_{j=1}^{n}\frac{(i-\mu_x)(j-\mu_y)C_{ij}}{\sigma_x\sigma_y}$$

where: *Cij*- the *ijth* entry of the co-occurrence matrix
n- the number of pixel pairs in the image at (δ,α)
i- grey-level intensity value of the ith reference row
j- grey-level intensity value of the jth neighbour column
μ_x- the mean of row i
μ_y- the mean of column j
σ_x- the standard deviation of row i
σ_y- the standard deviation of column j

Although these features measure the same characteristics of the data (i.e., texture), they are interpreted differently. The contrast statistic is a measure of the amount of local variation present in an image (Haralick *et al.*, 1973; Ulaby *et al.*, 1986; Pultz and Brown, 1987; Barber, 1989). Contrast is a measure that is associated with the average grey-level difference between neighbouring pixels and is sensitive to standard deviation but not mean (Barber, 1989). A low-contrast image results in a concentration of entries around the diagonal of the GLCM and, consequently, a low value for the computed contrast statistic (Baraldi and Parmiggiani, 1995). The mean texture statistic incorporates both tone and texture information. This is achieved by incorporating the grey level of the *ith* line of the matrix in the texture calculation. The correlation statistic is analogous to Pearson's product moment correlation and is sensitive to the correlation between grey values and the probability density functions at each of the grey-level pairs. The correlation texture statistic is sensitive to both mean and standard deviation (Barber, 1989).

In generating each of these texture features, three parameters must be selected. These include: (i) window size for which the co-occurrence matrix will be generated; (ii) interpixel

sampling distance; and (iii) direction for pixel co-occurrence within the sampling window. For feature generation, an appropriate window size is one that is large enough so that a meaningful joint distribution of grey tones can be computed to characterize specific land covers, yet is small enough to minimize the transitional effects of the texture calculation at boundaries between adjacent classes. Based on results observed in Chapter 5, where the variability and optimal spatial resolutions determined for the visible and near-infrared data were different, a 5 x 5 pixel window was used for generating the GLCM for the visible data and a 7 x 7 pixel window for the near-infrared data. These window sizes were selected for application to the high-altitude CASI data to account for the differences between the visible and near infrared data and to generate a meaningful joint distribution of grey tones. However, it must be noted that optimal textural window operators were defined in Chapter 5 based on low- and medium-altitude CASI data (Table 5.7). These estimates portray smaller spatial dimensions than are used here for the high-altitude CASI data. It is assumed that the relationship between reflectances of the low-, medium- and high-altitude CASI data is not linear. In this respect, based on semivariogram analysis of low- and medium-altitude data, the texture processing of the high-altitude data addresses texture at a smaller scale than was observed in the low- and medium-altitude data.

The interpixel sampling distance is selected based on the coarseness or fineness of the textures present in the image. For example, for fine-texture features, a short inter-pixel sampling distance would be suitable whereas a greater distance would be appropriate for coarse-textured images. However, since there are generally a variety of degrees of fineness and coarseness within an image, an interpixel sampling distance of one is valid to characterize different degrees of texture.

Haralick *et al.*, (1973) proposed calculating second-order statistics for the co-occurrence matrix in four directions (0° , 45°, 90°, 135°). If the objective is to create invariant features after rotation, this method is appropriate (Vickers and Modestino, 1982). However, in a study by Franklin and Peddle (1989) it was observed that individual texture orientations produced higher class accuracies than average texture measures using the four orientations. This is significant, in that computation time can be dramatically reduced without losing textural information. In this study, only one directional measure was used, since it was assumed that no particular forest ecosystem exhibited a preferential directionality. Here, the evaluation of the GLCM technique is based on the discrimination of the six landscape-scale forest ecosystem classes from these texture features. Texture features generated from the GLCM are classified individually and in combination using a linear discriminant function.

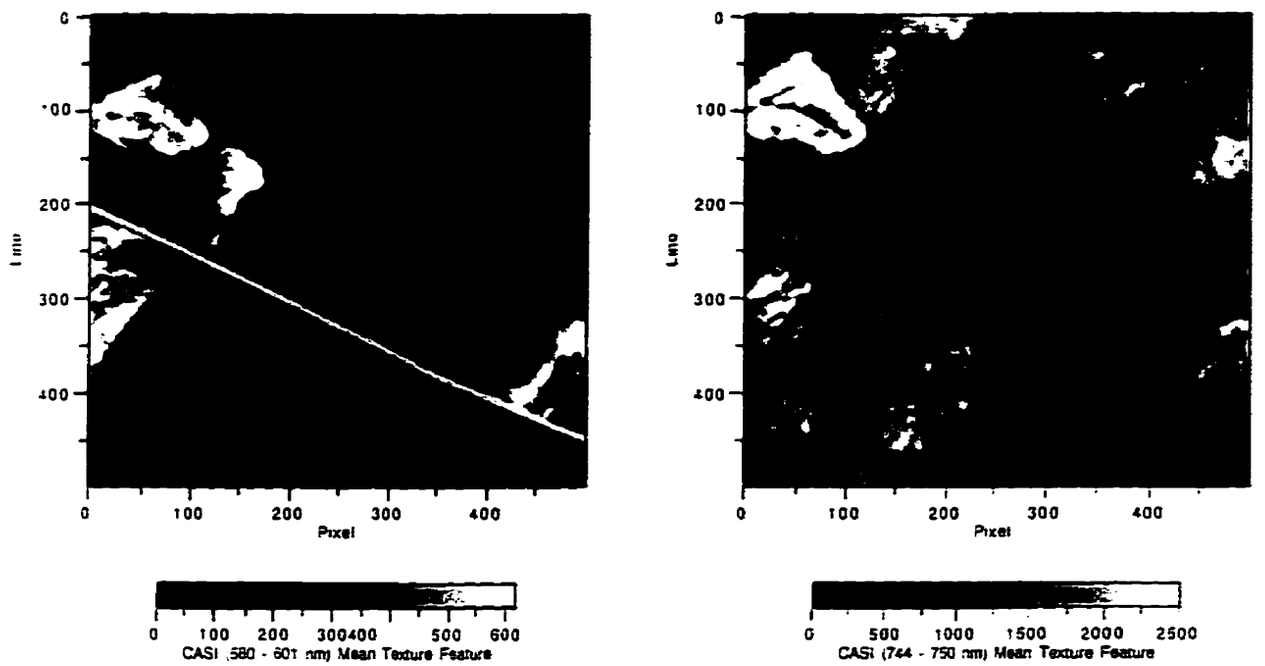


Figure 6.5 Mean texture features for CASI Bands 3 and 7.

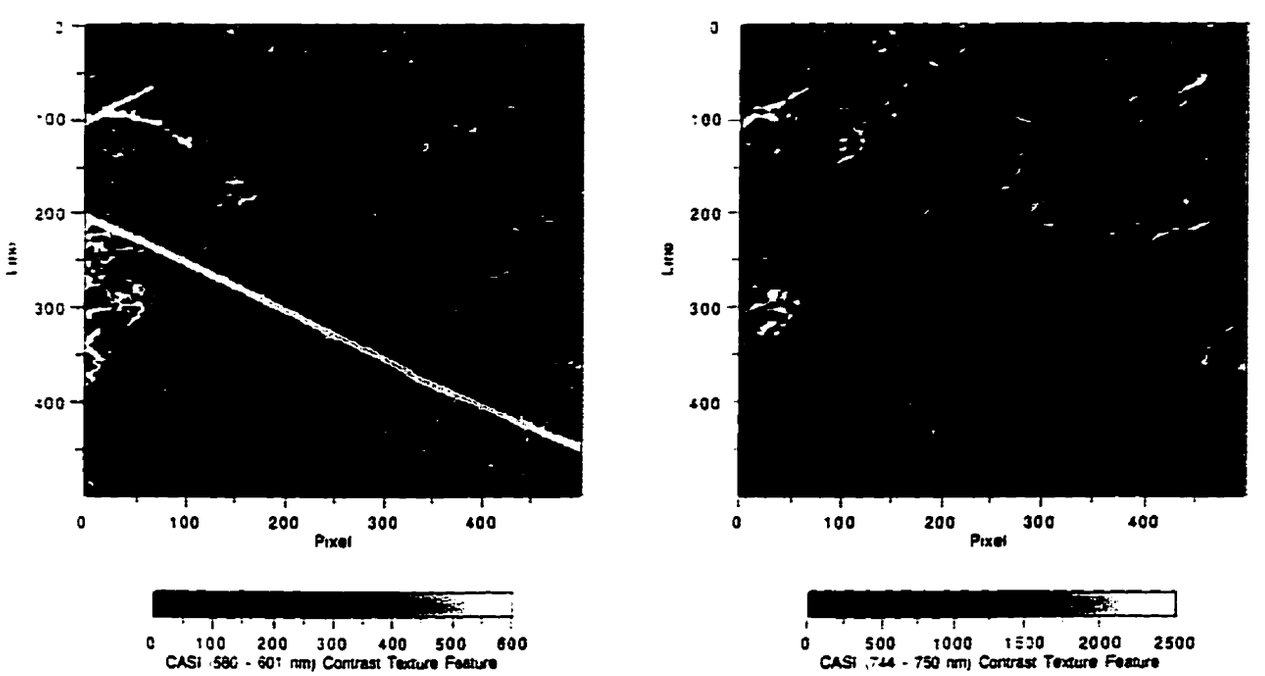


Figure 6.6 Contrast texture features for CASI Bands 3 and 7.

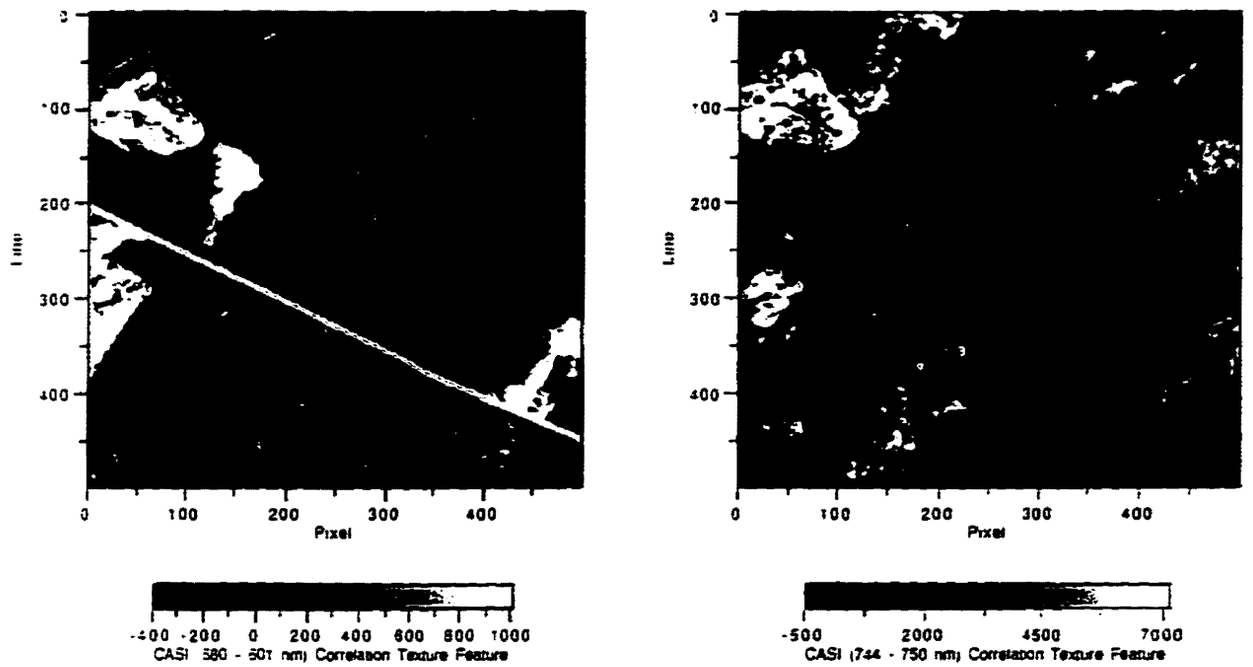


Figure 6.7 Correlation texture features for CASI Bands 3 and 7.

6.2.6 Terrain Features

The digital elevation model (DEM) for the entire Rinker Lake Research Area is described in Section 4.4 along with first-order derivatives of elevation: gradient and local relief. These data are at a nominal spatial resolution of 20 m. As noted previously, the DEM was derived from the digital topographic data (contours and streamline data) from the 1:20 000-scale OBM Series. These features are reproduced in Figure 6.8 for a smaller portion of the study area.

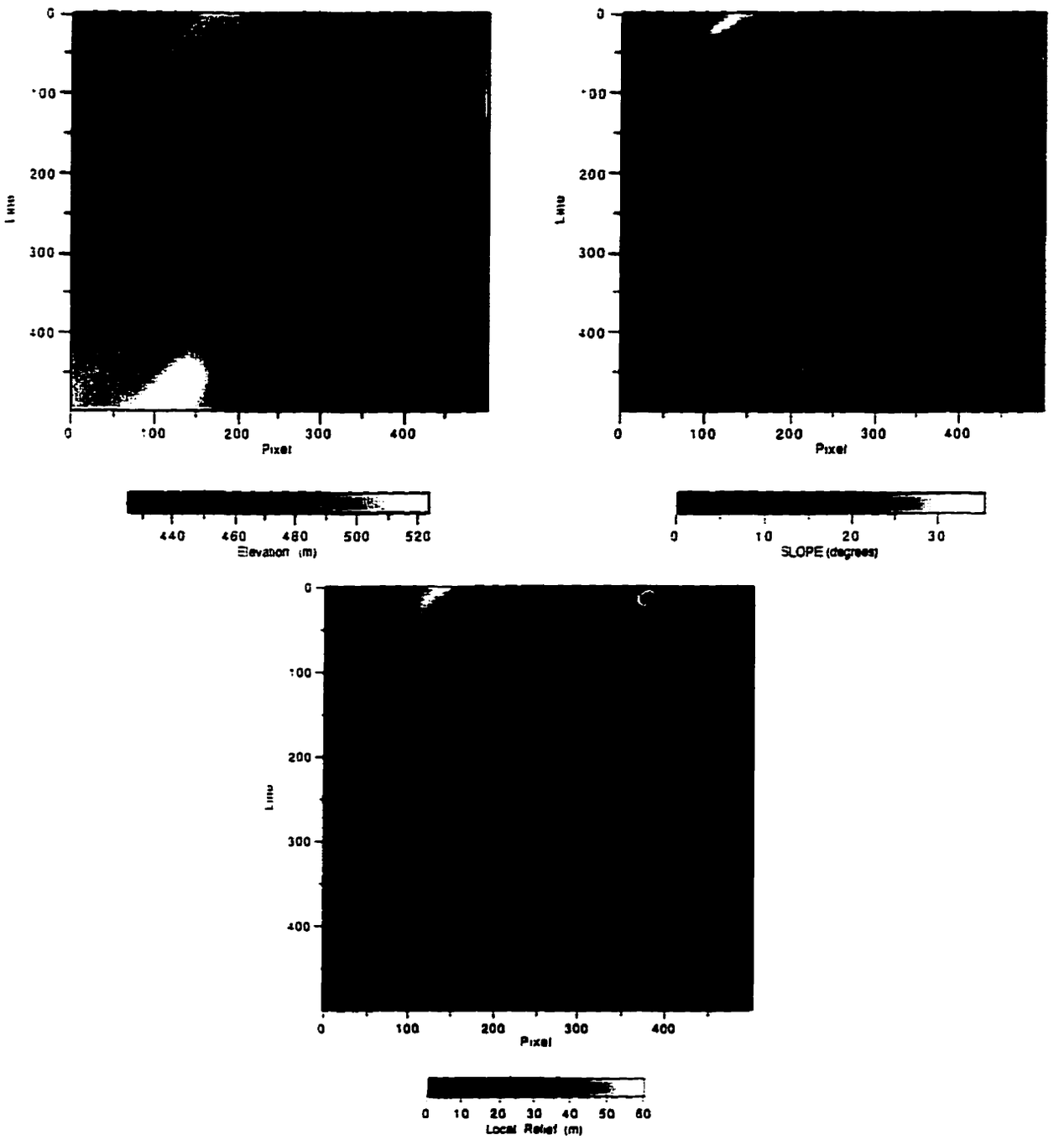


Figure 6.8 Terrain variables: elevation, gradient and local relief.

6.2.7 Linear Discriminant Analysis (LDA)

Linear discriminant analysis (LDA) procedures were applied within SYSTAT™ (SYSTAT Inc., 1992) to explore the relative discriminatory power of the (i) spectral-spatial, (ii) texture,

(iii) terrain and (iv) combinations of spectral-spatial, texture and terrain variables. According to Duda and Hart (1973), LDA does not have a rigorous requirement for an underlying statistical model. In this sense, LDA is not seriously affected by limited deviations from normality or limited inequality of variances (Davis, 1986). In this analysis, Fisher's method, which is based on a single with-groups covariance matrix derived from calibration data is applied (SYSTAT, 1992). This method first derives a transform that minimizes the ratio of the difference between group multivariate means and their within-group multivariate variance. This transform is used to find a discriminant function as the orientation that optimizes the separability of classes while at the same time minimizing the internal spread of each individual class distribution (Tom and Miller, 1984). An input pixel is then assigned to a particular class based on its location along the discriminant function axis. Discriminant analysis as a classification technique has been shown to be less sensitive to the number of variables and deviations from the normal (Gaussian) distribution as opposed to other methods such as maximum likelihood (Tom and Miller, 1984). Linear discriminant analysis / classification was applied to determine the features / variables that may be most appropriate for classification using maximum-likelihood and neural-network (NNC) classifiers.

6.2.8 Maximum-Likelihood Classification (MLC) and Neural-Network Classification (NNC)

Based on the results of the linear discriminant analysis, multisource classification using maximum-likelihood classification decision rules and neural-network classification based on the Generalized Delta Rule for learning (Pao, 1989) was performed on the datasets identified as providing optimal discrimination of the six landscape-scale ecosystem classes. MLC is the standard classification algorithm used in remote sensing and is included here, largely for comparison to the linear discriminant function and neural network classification results. MLC uses the mean vector, variance-covariance and correlation statistics derived from a set of calibration data to estimate a set of probability functions for each class. Based on the probability density function, each pixel is assigned to the class that its feature vector most closely resembles. MLC is a parametric classifier which possesses inherent assumptions such as the input data are multivariate normal, independent and have approximately equal variances (Tom and Miller, 1984). Under these conditions, and for a limited number of variables, MLC has proven to be a powerful technique in remote sensing data analysis and has been widely implemented. However, when these assumptions are violated, MLC is subject to poor performance (Peddle, 1993). This is becoming more evident with the adoption of high-resolution sensors and ancillary data types that do not necessarily meet

these assumptions.

NNCs are computational systems which emulate the computational abilities of biological systems using simple, interconnected "nodes" or artificial "neurons." These nodes emulate biological neurons by accepting input data from other nodes, performing simple operations on the data and selectively passing the results on to other artificial neurons. The nodes of one layer are connected to nodes of the layer immediately below. NNCs consist of interconnected processing units that are organized into two or more layers: an input layer, "hidden" layers and an output layer. The input layer is activated by the input image or terrain variables whereas the output layer depicts the output classes that are to be trained. Here, the six landscape-scale classes were used in the classification procedures. The input images and terrain data varied according to the spectral, spatial and integrated datasets used in the analysis.

The most commonly used and reported paradigm in neural-network applications is that of the back-propagation artificial neural network (Gallant, 1993). This stems from the ability of the back-propagation algorithm to learn complicated multidimensional mapping (Hecht-Nielsen, 1990). The training and operation of a neural network is based upon training-derived weight values associated with one-way vectors joining nodes within a network. The back-propagation refers to the training method by which the connection weights of the network are adjusted. The NNC performs a segmentation of the original data to different spatial resolutions (scales). Although these classifiers show promising classification results, they are generally slower to "train" than traditional statistical techniques. For most neural-network classifiers, the training process is computationally very complex and requires a large number of training samples, and such requirements may translate into a long implementation phase. In this study, EASI/PACE software NNCREAT, NNTRAIN and NNCLASS (PCI, 1996) were applied using a single hidden layer with eight units.

6.3 Results

6.3.1 Linear Discriminant Analysis

The variable sets used in this analysis are defined in Table 6.5. The minimum number of variables for any trial was one, the maximum, nine. For each set of variables, calibration data were used to generate a discriminant function, which was then applied to the validation data to obtain individual and mean class accuracies (Table 6.6). The Kappa coefficient ($\hat{K}$) was calculated for the validation accuracies of each classification. The Kappa coefficient is a

measure of agreement between the ground sample classes and those derived through classification of remote sensing data. This measure accounts for all elements of the confusion matrix and excludes the agreements that occur by chance (Rosenfield and Fitzpatrick-Lins, 1986). These are also summarized in Table 6.6. The accuracy results (i.e., contingency tables) for each variable-set classification are presented in full in Appendix I. Difference of proportions tests were performed to determine the significance of the differences between classification accuracies for the various combinations of input variables. The z-scores derived for these tests are reported in Table 6.7.

Based on the results presented in Table 6.6, it is important to note that the CASI 4 m data (SPEB) provide greater discrimination of the six landscape-scale classes than comparable spectral bands of Landsat TM (SPEA)(Kappa Coefficient ($\hat{K}$)=0.403 versus $\hat{K}$=0.289)(Table 6.6). The CASI 6m dataset (SPAC) provided the highest accuracies among the spectral-spatial variables ($\hat{K}$=0.488) (Table 6.6) and were significantly greater than the 4 m data (SPEB) (z-score = 3.88) (Table 6.7). The 6 m data (SPAC) also provided greater discrimination of the six landscape-scale classes than the "optimal" spatial resolution dataset (SPAA)($\hat{K}$=0.430); the 5 m dataset (SPAB)($\hat{K}$=0.470) and the 6m and 7m dataset (SPAD)($\hat{K}$ =0.469)(Table 6.6; Table 6.7).

Among the texture datasets, TEXF provides the highest classification accuracy ($\hat{K}$ =0.560)(Table 6.6), significantly greater than TEXA (z-score = 3.47) and TEXC (z-score = 2.84), as well as all spectral-spatial and terrain feature datasets (Tables 6.6 and 6.7). The texture dataset, TEXF, which incorporates six texture features (Table 6.5), does not provide significant improvement in classification accuracy over TEXB, a three texture-feature dataset ($\hat{K}$=0.560 versus $\hat{K}$=0.542; z-score = 0.87). Of the three texture features tested, the mean texture feature provides the greatest discrimination, followed by contrast and correlation.

Table 6.5 Feature Datasets for Linear Discriminant Analysis

Variable Set	Description
SPEA	Landsat Thematic Mapper - Bands 2, 3 and 4
SPEB	CASI Bands 3, 5, 7
SPAA	Optimal Spatial Resolutions by class (4m, 5m, 6m and 7m) for CASI Bands 3, 5 and 7
SPAB	CASI Bands 3, 5, and 7 at 5 metre spatial resolution
SPAC	CASI Bands 3, 5, and 7 at 6 metre spatial resolution
SPAD	CASI Bands 3, 5 (6m) and Band 7 (7m)
TEXA	Texture Statistics: Mean - Bands 3 and 7
TEXB	Texture Statistics: Mean - Bands 3 and 7; Contrast - Band 7
TEXC	Texture Statistics: Mean - Bands 3 and 7; Correlation - Band 7
TEXD	Texture Statistics: Mean - Bands 3 and 7; Contrast and Correlation - Band 7
TEXE	Texture Statistics: Mean, Contrast, - Bands 3 and 7; Correlation - Band 7
TEXF	Texture Statistics: Mean, Contrast, Correlation - Bands 3 and 7
DEM	Digital Elevation Model (DEM)
REL	Local Relief Elevation (range within 100m x 100m window)
GRAD	Gradient
TERA	Local Relief and DEM
TERB	Local Relief, DEM and Gradient
INTA	SPAC and TEXB
INTB	SPAC and TERB
INTC	SPAC, TERB and TEXB

Table 6.6 Classification Accuracy (Linear Discriminant Function) by Class

	Percent Classification Accuracy by Class*							
Variable Set	1	2	3	4	5	6	Mean Accuracy (%)	Kappa Coefficient ($\hat{K}$)
SPEA	45.6	18.0	58.4	28.8	62.8	30.8	40.7	0.289
SPEB	78.4	33.2	41.2	14.0	63.2	71.6	50.3	0.403
SPAA	72.4	32.4	62.8	15.2	63.6	68.4	52.5	0.430
SPAB	78.0	38.4	58.4	14.0	66.4	80.0	55.9	0.470
SPAC	72.4	36.8	63.6	17.2	75.6	78.4	57.3	0.488
SPAD	72.0	36.8	57.2	15.6	76.4	76.4	55.7	0.469
TEXA	70.8	25.6	54.0	29.6	73.6	89.2	57.1	0.486
TEXB	70.8	31.6	56.0	36.4	86.8	89.2	61.8	0.542
TEXC	78.4	19.2	66.0	25.2	80.4	80.4	58.3	0.499
TEXD	**81.2**	18.4	67.6	30.4	88.0	80.0	60.9	0.531
TEXE	80.8	18.0	64.8	31.6	86.8	93.2	62.5	0.550
TEXF	78.0	18.4	64.8	**40.0**	84.4	94.4	63.3	0.560
DEM	10.0	40.0	70.0	20.0	60.0	67.2	44.5	0.334
REL	24.0	21.6	54.0	15.6	32.4	76.4	37.3	0.248
GRAD	30.0	10.0	56.0	2.0	26.8	89.2	35.7	0.228
TERA	20.0	40.0	70.0	0.0	60.0	70.0	43.3	0.320
TERB	28.0	40.0	70.0	0.0	60.0	70.0	44.7	0.336
INTA	70.4	44.8	76.4	21.6	85.2	78.8	62.9	0.554
INTB	77.6	43.2	78.8	14.0	81.6	80.0	62.5	0.550
INTC	77.2	**46.4**	**85.2**	23.6	**93.2**	80.0	67.6	0.611

* Values in bold represent the highest classification accuracies for each class.

Table 6.7 Correlation Matrix for Z-Scores - Differences of Proportions for Validation Data*

Variable Set	SPEA	SPEB	SPAA	SPAB	SPAC	SPAD	TEXA	TEXB	TEXC	TEXD	TEXE	TEXF	DEM	REL	GRAD	TERA	TERB	INTA	INTB
SPEB	**5.24**																		
SPAA	**6.44**	1.21																	
SPAB	**8.29**	**3.07**	1.87																
SPAC	**9.09**	**3.88**	**2.68**	0.81															
SPAD	**8.22**	**3.00**	1.80	-0.07	-0.88														
TEXA	**8.98**	**3.77**	2.57	0.70	-0.11	0.77													
TEXB	**11.54**	**6.36**	**5.16**	**3.30**	2.49	**3.35**	**2.60**												
TEXC	**9.60**	**6.60**	**3.20**	1.33	0.52	1.40	0.63	-1.98											
TEXD	**11.07**	**5.80**	**4.60**	**2.82**	2.01	**2.89**	2.12	-0.49	1.49										
TEXE	**11.95**	**6.77**	**5.58**	**3.71**	**2.91**	**3.79**	**3.02**	0.41	2.39	0.90									
TEXF	**12.39**	**7.22**	**6.03**	**4.17**	**3.36**	**4.24**	**3.47**	0.87	**2.84**	1.36	0.45								
DEM	2.10	**-3.14**	**-4.35**	**-6.21**	**-7.01**	**-6.13**	**-6.99**	**-9.08**	**-7.53**	**-9.08**	**-9.98**	**-10.33**							
REL	-1.91	**-7.14**	**-8.33**	**-10.17**	**-10.97**	**-10.10**	**-10.96**	**-13.09**	**-11.48**	**-12.93**	**-13.89**	**-14.24**	**-4.01**						
GRAD	**-2.86**	**-8.08**	**-9.27**	**-11.10**	**-11.90**	**-11.03**	**-11.79**	**-14.32**	**-12.60**	**-13.85**	**-14.72**	**-15.15**	**-4.95**	-0.95					
TERA	1.44	**-3.81**	**-5.01**	**-6.87**	**-7.67**	**-6.79**	**-7.56**	**-10.13**	**-8.18**	**-9.65**	**-10.53**	**-10.98**	-0.66	**3.35**	**4.29**				
TERB	2.18	**-3.07**	**-4.27**	**-6.13**	**-6.94**	**-6.06**	**-6.83**	**-9.40**	**-7.45**	**-8.93**	**-9.81**	**-10.26**	0.07	**4.08**	**5.03**	0.74			
INTA	**12.13**	**6.96**	**5.76**	**3.90**	**3.09**	**3.98**	**3.21**	0.60	**2.58**	1.09	0.19	-0.26	**10.07**	**13.99**	**14.98**	**10.72**	**10.00**		
INTB	**11.95**	**6.77**	**5.58**	**3.71**	**2.91**	**3.79**	**3.02**	0.41	2.39	0.90	0.00	-0.45	**9.88**	**13.80**	**14.72**	**10.53**	**9.81**	0.19	
INTC	**14.77**	**9.65**	**8.46**	**6.61**	**5.81**	**6.68**	**5.92**	**3.32**	**5.29**	**3.81**	**2.91**	2.46	**12.73**	**16.60**	**17.50**	**13.37**	**12.66**	**2.72**	**2.91**

Values reported in bold are significant for $\alpha = 0.05$.
Values reported in bold and underlined are significant for $\alpha = 0.01$.

Terrain variables by themselves do not provide significant discrimination of any of the six landscape-scale classes. However, of the four terrain variables tested, elevation (DEM) provides the best discrimination ($\hat{K}$=0.334), significantly greater discrimination than other single terrain variables (Table 6.7). It is interesting to note that the DEM provides significantly greater discrimination of the six landscape-scale classes than the three TM bands (SPEA)(z-score = 2.10). In combination, elevation, gradient and local relief (TERB)($\hat{K}$=0.336) provide a slight improvement over DEM alone; however, it is not significant ($z = 0.07$).

Finally, integrating spectral-spatial, texture and terrain variables (INTC) provides the greatest discrimination of the six landscape-scale ecosystem classes, significantly greater than all other datasets ($\hat{K} = 0.611$)(Tables 6.6 and 6.7). When spectral-spatial variables are combined with either texture variables (INTA - $\hat{K} = 0.554$) or terrain variables (INTB - $\hat{K}$=0.550) alone, the results are not significantly different from using texture features alone (e.g., TEXB - $\hat{K}$=0.542)(z-scores = 0.60 and 0.41 respectively)(Tables 6.6 and 6.7).

When examining the individual class accuracies, it is evident that upland black spruce / jack pine is consistently poorly classified (Table 6.6). Of the variables tested, there is no variable that provides suitable discrimination of upland black spruce / jack pine. Similarly, the white spruce / balsam fir landscape-scale class is poorly discriminated. The accuracies for the remaining four landscape-scale classes range from 77.2% to 93.2% (Table 6.6).

6.3.2 Maximum-Likelihood and Neural-Network Classification

The results of the MLC and NNC are presented in Table 6.8 (Appendices J and K respectively). The classification accuracies for the LDA are also reported in Table 6.8 for comparison. While the LDA and MLC results are similar, the NNC results are disappointing. In all cases examined, the NNC results are lower than the LDA or MLC accuracies (Table 6.8). Also, it should be noted that as the number of feature variables increases, there is a corresponding increase in unclassified pixels with the MLC, and since these pixels are not included in the contingency table accuracy analysis, the Kappa values are artificially high for datasets with high dimensionality (e.g., INTA, INTB, INTC) (Table 6.8).

Table 6.8 Classification Accuracy by Class for LDA, MLC and NNC*

Variable Set		Percent Classification Accuracy by Class** 1	2	3	4	5	6	UC	Mean	Kappa
SPEB	LDA	78.4	33.2	41.2	14.0	63.2	71.6	0.0	50.3	0.403
	MLC	61.6	26.0	44.8	14.8	76.8	73.6	3.2	49.6	0.415
	NNC	86.0	34.4	60.4	19.2	14.0	66.0	0.0	46.7	0.360
SPAC	LDA	72.4	36.8	63.6	17.2	75.6	78.4	0.0	57.3	0.488
	MLC	53.6	36.0	67.6	19.2	79.6	73.6	4.1	45.9	0.487
	NNC	83.2	37.6	79.6	18.4	40.0	66.8	0.0	54.3	0.451
TEXB	LDA	70.8	31.6	56.0	36.4	86.8	89.2	0.0	61.8	0.542
	MLC	54.0	36.4	60.4	33.2	74.8	81.2	5.0	56.7	0.515
	NNC	95.2	9.6	66.4	46.4	35.2	72.0	0.0	54.1	0.450
TERB	LDA	28.0	40.0	70.0	0.0	60.0	70.0	0.0	44.7	0.336
	MLC	33.2	51.6	77.6	2.0	49.6	54.4	0.3	50.4	0.418
	NNC	70.0	4.0	91.6	0.0	60.0	0.0	0.0	37.6	0.251
INTA	LDA	70.4	44.8	76.4	21.6	85.2	78.8	0.0	62.9	0.554
	MLC	50.9	44.0	75.6	32.8	67.2	75.6	10.6	57.5	0.572
	NNC	97.2	28.4	56.8	42.4	44.0	56.8	0.0	54.3	0.451
INTB	LDA	77.6	43.2	78.8	14.0	81.6	80.0	0.0	62.5	0.550
	MLC	60.8	57.6	76.0	13.2	68.4	76.0	17.7	58.7	0.654
	NNC	88.4	24.4	56.4	22.4	92.4	62.4	0.2	57.7	0.494
INTC	LDA	77.2	46.4	85.2	23.6	93.2	80.0	0.0	67.6	0.611
	MLC†	66.4	59.2	72.8	24.0	56.8	72.4	21.3	58.6	0.694
	NNC†	98.8	24.8	62.4	20.0	62.4	69.2	1.1	56.3	0.482

* LDA - Linear Discriminant Analysis; MLC - Maximum-Likelihood Classification; NNC - Neural-Network Classification

** Values in bold represent the highest classification accuracies for each class.

† UC - Unclassified (percent of total)

†† In these classifications, a total of 6 feature variables was used (2 spectral-spatial; 2 texture; 2 terrain).

6.4 Discussion

Although the mean classification accuracies and Kappa coefficients depict poor discrimination of the six landscape-scale ecosystem classes, there are important aspects of the results that merit discussion. First, Aspen-Dominated Hardwood and Mixedwood, Cedar Mixedwood, Lowland Black Spruce and Wetland Black Spruce are the classes most easily discriminated whereas Upland Black Spruce and White Spruce / Balsam Fir are more difficult. If the discrimination of the latter two landscape-scale classes could be improved, the overall results would improve significantly. It is not by chance that these two classes represent the most variable of conditions, both spectrally, spatially and in reference to the terrain. Here, it should be noted that classification accuracy is a function not only of technique, but also of the class structure used with respect to the spatial and radiometric precision of the data (Hutchinson, 1982). These two classes in particular, require close examination, as to the conditions under which they may be uniquely characterized, either spectrally, spatially, or with reference to more specific terrain characteristics. It is likely that examination of these two classes from a class perspective is required, in that they may require further segregation or aggregation in order to consider them as mappable units or

classes. The remaining four classes appear to be discriminable at appropriate levels, although these may also require reorganization to improve discriminability while maintaining ecological significance.

In terms of the spectral-spatial variables used to map the six landscape-scale classes, the dataset consisting of three CASI spectral bands at a spatial resolution of 6m (SPAC) provided the best discrimination, albeit low ($\hat{K}$= 0.488) when compared to other spectral-spatial variables (Table 6.6). The differences were not great, but were statistically significant. In particular, it was demonstrated that Landsat TM data provided poor discrimination ($\hat{K}$=0.289) of the six landscape-scale classes. This would suggest that the regularization over a 30m pixel exceeded the spatial variability for the landscape-scale ecosystem classes embedded within the landscape. It is anticipated that the six landscape-scale classes analysed here would have to be collapsed even further to be applicable to the scale of Landsat TM data collection. Also, the dataset combining 6m and 7m data had a slightly lower LDA classification accuracy than the 6m dataset, suggesting that the optimal resolution was exceeded. Although not conclusive, this observation would support the semivariogram analysis and spatial resolution estimates presented in Chapter 5.

On the other hand, the dataset that combined 4m, 5m, 6m, and 7m data, based on suggested spatial resolutions by class from Chapter 5, did not produce the best results among the spectral-spatial variables. This may be linked to the fact that the estimates derived from the semivariogram analysis represent the mean sizes of support for a number of transects taken from each of the six landscape-scale classes. Possibly it would be more prudent to over-estimate the size of support based on the experimental variograms in order to optimally regularize the variability within the six landscape-scale classes. There may be some relationship between the mean size of support and maximum size of support observed from a sample of experimental variograms to optimally determine the spatial resolution per class. This estimate then may best account for the spatial variability within the class. The estimate may not necessarily have the same relationship to the mean for each class, but may vary based on the level of variability of each class. Regardless, it seems apparent that selecting an optimal spatial resolution for spectral data collection alone does not provide sufficient discriminatory power for classifying and mapping the six landscape-scale classes studied here. With the spatial resolutions examined, there is still significant within-class variability to contribute to poor between-class separability.

Texture, or the intrinsic spatial variability of a remote sensing image, is recognized as an important interpretive tool for discriminating different land-use types. Texture, as portrayed in an image, is a function of scale. As spatial resolution increases, land-cover

elements tend to be characterized by groups of pixels whose spatial arrangement tends to possess characteristic patterns or textures. A texture field within a remote sensing image is described as homogeneous if the spatial arrangement of pixel values are more homogeneous (as a unit) within than between texture fields (Barber and LeDrew, 1991). In order to characterize texture, the tonal primitive properties of the image must be characterized as well as the spatial interrelationships between them (Haralick, 1979).

Texture transformation is a method by which original reflectance information is transformed into a new feature that contains only texture information or a combination of tone and texture information. It has been demonstrated that texture transforms have a role in remote sensing data analysis of land cover and land use (Hsu, 1978; Jensen and Toll, 1982; Agbu and Nizeyimana, 1991); agricultural crop separability (Rotunno *et al.*, 1996; Treitz *et al.*, 1996) and in forested environments (Franklin and Peddle, 1990; Cohen and Spies, 1992; Hay and Niemann, 1994). Peddle and Franklin (1991) determined that spatial co-occurrence matrices contain important textural information that assists with the discrimination of classes demonstrating high within-class variability and structural / geomorphometric patterns. However, tone and texture are not independent concepts but bear an inextricable relationship to one another. Combinations of tone and texture statistics often provide optimal results in land-cover and land-use classification (Ulaby *et al.*, 1986; Franklin and Peddle, 1990). Indeed, various "texture transforms" include information on both tone and texture.

In this study, texture variables provide accuracies equal to, or greater than, any of the spectral-spatial variables. This supports the assertion that texture information is present within these L-resolution reflectance data and is characterized to some degree by the texture transforms to assist in the discrimination of these landscape-scale classes. In addition, the mean texture feature provided the greatest discrimination among the classes since it not only characterizes texture, but contains tonal information as well. Mean texture features combined with the contrast texture feature for CASI band 7 (744 nm - 750 nm) contributes additional textural information to provide additional discrimination for the forest ecosystem classes using three texture variables. Addition of other textural features (e.g., correlation) does not significantly improve class discrimination (Table 6.7).

It is evident that the terrain features tested here (i.e., elevation, local relief, and gradient) do not provide great discriminatory power for the six landscape-scale classes examined. However, it does appear that within a small region, local elevation and gradient can be used to assist in the discrimination of forest ecosystem classes when combined with other descriptors. It must be emphasized that for a low- to moderate-relief boreal environment, these variables, particularly elevation, would have to be used within a relatively

small local area, emphasizing the local variation between ecosystem types. Slope, on the other hand, may have potential for use at more regional scales. Although elevation, local relief and gradient provided the greatest discriminatory power (LDA $\hat{K}$= 0.336; MLC $\hat{K}$= 0.418)(Table 6.8), they did not in combination provide significantly greater discrimination than elevation alone (LDA - $\hat{K}$= 0.334)(Tables 6.6 and 6.7).

Based on the analyses presented, the integration of spectral data collected at appropriate resolutions with terrain information and texturally processed features offers promise for discriminating and classifying forest ecosystem classes. When the three types of variables were combined (INTC), a mean classification accuracy of 67.6% ($\hat{K}$ = 0.611 was achieved using LDA. Although this does not approach operational levels, it indicates that spectral, spatial and terrain variables, in combination, offer potential for discriminating forest ecosystems classes in low- to moderate-relief boreal environments. Further refinements on these three constituents may provide the necessary discrimination required for operational classification and mapping of large areas of northern boreal forest. Specifically, improvement in discriminating certain ecosystem types such as upland black spruce / jack pine and white spruce / balsam fir conifer and mixedwood would increase significantly the potential for classification and mapping.

Improvements in per-pixel classification have been observed with the use of linear discriminant analysis (LDA) (Tom and Miller, 1984). This method relaxes the restriction of the data meeting a specified distribution (i.e., normal). It results in decision rules for assigning pixels to a particular class which are more flexible, though perhaps less certain. As a result, the data play a much more prominent role in the creation of decision rules. LDA uses the pooled covariance matrix and reduces a multivariate problem to a univariate one by defining the weighted combination of input variables that best describe the separation among the groups (Tom and Miller, 1984; Franklin, 1992). As a result, LDA is less sensitive to the number of input variables as compared to MLC (Peddle, 1993). This is demonstrated with a corresponding increase in unclassified pixels using MLC as the number of input variables increased (Table 6.8). In general, the LDA and MLC classification accuracies were similar (Table 6.8). This is not surprising given that they are expected to perform similarly when using datasets that are independent, normally distributed, and have equal variances (Tom and Miller, 1984).

NNCs have a number of advantages when compared to many statistical classifiers: (i) they are not restricted by underlying statistical models (e.g., normal distribution); (ii) they are not sensitive to variance thresholds; (iii) they are able to adequately handle increased numbers of input variables; and (iv) they are capable of processing data of different variable

types (e.g., nominal, ordinal, interval and ratio) (Benediktsson *et al.*, 1993). In remote sensing applications, neural-network classifiers have demonstrated mixed classification capabilities when compared to traditional statistical classifiers such as LDA and MLC (e.g., Foody, 1995; Leverington and Duguay, 1996). Based on variable results, the use of neural-network classifiers is still experimental.

Here, the NNC did not provide improved classifcation results over either the LDA or MLC. The results observed are similar to those reported by Leverington and Duguay (1996) who found classification accuracies to be similar using maximum-likelihood and neural-network classifiers for two case studies involving unisource and multisource data sets. Although using neural-network classifiers with multisource data can improve classification accuracy, the contribution of each data layer is neither observed nor fully discovered (Wang and Civco, 1996). As a result, the behaviour of the neural network is not as intuitive as that of other classification algorithms which can be visualized both mathematically and geometrically (Leverington and Duguay, 1996). While more data layers can provide additional information, they may also provide redundant information or noise. Here, variables identified in the discriminant analysis were used to provide the optimal input to the MLC and NNC algorithms.

6.5 Conclusions

In Chapter 6, the results of the semivariogram analysis of Chapter 5 were applied to define and derive reflectance data at spatial scales (i.e., spectral-spatial features) appropriate for discriminating six landscape-scale forest ecosystem classes. Second, given the relationship between forest and site, it was hypothesized that combining appropriately scaled remote sensing data with terrain descriptors/variables should improve the discriminability of landscape-scale forest ecosystem classes for the boreal forest of northwestern Ontairo. Although not completely encouraging in terms of absolute classification accuracies, various conclusions can be made regarding optimal scales of remote sensing data and the integration of terrain variables with reflectance data for discriminating forest ecosystem classes in a low- to moderate-relief boreal environment. These include:

1. **Careful consideration must be given to the relationships between the forest classes of interest and the appropriate remote sensing spatial resolutions to sample those classes.** To maximize discriminability of these classes a spatial resolution that minimizes (regularizes) within-class variability, but maximizes between-class discrimination is required. Here it was demonstrated that 6 m reflectance data provided the best discrimination of the landscape-scale forest

ecosystem classes studied. This spatial resolution or scale provided greater discrimination than the following spectral-spatial datasets: (i) a 5 m dataset; (ii) a combined dataset of 6 m and 7 m data; (iii) an "optimal" dataset (by class) of 4 m, 5 m, 6 m and 7 m data; and (iv) a Landsat TM dataset (30 m). However, multiple spatial resolutions / scales of remote sensing reflectance data may be required, depending on the nature of the classes to be discriminated and their structure, as well as their characteristic visible and near-infrared reflectance.

2. **Texture features derived from L-resolution CASI reflectance data provide significant information for discrimination of landscape-scale forest ecosystem classes.** Here, texture variables provide accuracies equal to or greater than any of the spectral-spatial variables. It is clear that texture information is present within these L-resolution reflectance data and is characterized to some degree by GLCM texture transforms to assist in the discrimination of these landscape-scale forest ecosystem classes. However, closer examination of this issue with respect to the low- and medium-altitude CASI data is required for texture characterization at larger scales.
3. **Terrain variables alone provide weak discrimination of forest ecosystem classes. However, when used in combination with spectral-spatial variables, they improve the discrimination of landscape-scale forest ecosystem classes.** It must be emphasized that for a low- to moderate-relief boreal environment, these variables, particularly elevation, would have to be used within a relatively small local area, emphasizing the local variation between ecosystem types. Slope, on the other hand, may have potential for use at more regional scales. It is postulated that more precise descriptors or models of terrain are required for integration with appropriate spectral-spatial reflectance features in a low- to moderate-relief boreal environment. These features must be derived from geomorphometric and soils data to model soil texture classes and moisture and nutrient regimes.
4. **The integration of spectral data collected at appropriate resolutions with terrain information and texturally-processed features offers promise for discriminating and classifying forest ecosystem classes.** A mean classification accuracy of 67.6% ($\hat{K} = 0.611$) was achieved when combining spectral-spatial, textural and terrain variables. This represents a significant improvement over using spectral-spatial, texture or terrain variables alone or in combinations of two variable types. This level of accuracy is not sufficient for operational classification and mapping, but it does indicate that appropriately-scaled spectral,

textural and terrain variables provide a basis for classification and mapping of large forest regions based on ecological criteria. Further refinements of these three constituents may provide the necessary discrimination required for operational classification and mapping of large areas of northern boreal forest.

5. **The NNC did not provide improved results over traditional statistical classification techniques (i.e., LDA and MLC).** Further testing of NNC is required prior to adoption of NNC as an operational classification algorithm in forest classification and mapping with variables that meet the assumptions of existing statistical classifiers. The real advantage of NNC will not likely be realized until variables, that do not necessarily satisfy the assumptions of traditional parametric classifiers, are included in the classification.

It has been demonstrated that in a low-relief boreal environment, addition of textural and geomorphometric variables to high-resolution airborne remote sensing reflectance data provides improved discrimination of forest ecosystem classes. Although these improvements are statistically significant, the absolute classification accuracies are not yet at levels suitable for operational classification and mapping. Further refinements, particularly of forest ecosystem class structure and terrain descriptors, are required for operational mapping of forest ecosystem classes.

CHAPTER 7
SUMMARY, CONCLUSIONS AND RECOMMENDATIONS

7.1 Summary

In the field of forest ecosystem classification, it is recognized that forests develop through the inter-relationships among climate, at both micro and macro scales, physiography, soils and vegetation. Forest ecosystems in northern Ontario, and elsewhere, are now being defined using these characteristics or inputs at local/stand levels. These efforts have culminated in a series of forest ecosystem classifications that characterize forests using forest canopy, understory and ground-cover species as well as soil/site characteristics. These local/stand classifications require significant data-collection efforts which are impractical for large regions of Ontario's forested lands. As Ontario adopts a more ecological approach to forest-land management and planning, spatial analysis and modelling techniques that incorporate field, remote sensing and other primary data are required to characterize and model forest ecosystems for large areas at landscape scales.

In this study, the vegetation types (V-Types) of the forest ecosystem classification for northwestern Ontario (NWO FEC) were examined to devise a logical, landscape-scale forest ecosystem class structure that would give rise to land units that would be both meaningful to ecologists and forest managers (Table 3.11). Intuitively, this scheme seemed appropriate not only for remote sensing data analysis, but also for discrimination based on terrain descriptors. It was therefore the goal of this research to develop a methodology for discriminating and classifying landscape-scale forest ecosystems using remote sensing and terrain data in conjunction with appropriate spatial processing and classification decision rules. A spatial analysis approach was applied to provide insight into the interaction of reflectance for various forest ecosystems with the intention of defining appropriate spatial resolutions/scales for discriminating forest ecosystems at landscape scales. The results of these analyses are intended to provide forest managers and planners with information regarding appropriate remote sensing and data-integration methodologies for application to the NWO FEC for forest ecosystem analysis and mapping for large areas of northwestern Ontario.

In this thesis, it was hypothesized that a multiscale approach would provide more

appropriate analysis results than a single-scale approach to remote sensing data analysis. The realization of space in data acquisition and classification is fundamental to forest ecosystem characterization and analysis using remote sensing and other primary data types. In particular, remote sensing reflectance data are a function of the space on which they are sampled as a result of the interactions within and between objects/variables and processes occurring on the landscape. Hence, there is an intuitive relationship between data-acquisition scale and information. Information has been described by Openshaw (1978) as a scale- and aggregation-dependent phenomenon. Specific to this study, it has been observed that different forest ecosystems exhibit different scales and aggregation levels, thereby suggesting that a multiple-scale or hierarchical approach be implemented for statistical analysis of remote sensing data acquired over these surfaces. In this study, a multiscale approach was adopted to attempt to best characterize, and hence discriminate, landscape-scale forest ecosystem classes.

To date, selection of remote sensing spatial resolutions has been arbitrary, whether the data be acquired from a satellite platform or an airborne system. There has generally not been close scrutiny as to the optimal dataset for a given land-cover / land-use class structure. The advent of higher-resolution sensors has led to the collection of higher spatial resolution data, without necessarily improving classification accuracy for a developed class structure. Spatial analysis studies of the interaction between landscape and sensor parameters are required in various disciplines to ensure progress in the adoption of appropriate remote sensing methodologies. In this thesis, a solid spatial theory concerning the reflectance of forest ecosystems was implemented, whereby a logic was devised to relate ground features (ecosystem structures and processes) with appropriate spatial processing and analysis models to best discriminate forest ecosystem classes at landscape scales.

The initial approach taken in this thesis was to attempt to understand the nature and causes of spatial variation of remotely sensed data for forest ecosystems as they relate to ground scene and sensor parameters. This analysis was a precursor to application of spatial processing techniques for extracting scene-specific information. A geostatistical examination of low-altitude airborne remote sensing reflectance data was performed to determine the predictive distances at which reflectances from various forest ecosystems were no longer correlated, representing the distance of an optimal size of support (pixel). It is important that the spatial structures of the scene and of the images be understood in order to select appropriate spatial resolutions for data acquisition and analysis. Specifically, it is important to understand the manner in which images of a scene change as a function of spatial resolution. It has been shown that when spatial resolution is considerably smaller or larger

than the surface feature of interest, it is likely that sample pixels for these features will exhibit high spectral variance, whereas if the spatial resolution samples the appropriate mixture of feature attributes, spectral variance will be at a minimum (Woodcock and Strahler, 1987). Variogram analysis is a technique to determine the information content embedded in remote sensing reflectance data at different scales. The range value, estimated from the semivariogram (in pixels or absolute distance measurements), represents the distance over which reflectance values become independent of one another along a transect of image data. Here, mean range values were estimated from a set of experimental variograms for each of the six landscape-scale forest ecosystem classes.

These estimates are used in this analysis to derive spectral-spatial features that are meant to regularize, and hence reduce, the within-class variability while attempting to maintain maximum between-class discrimination, requirements for obtaining accurate classification accuracies using statistical classifiers. Regularization is simply the process of increasing the size of support over which a spatial process (e.g., reflectance) is averaged. Here it is equated to increasing the remote sensing pixel size and thereby coarsening spatial resolution. It has been stated that regularization is a key to understanding the relations between spatial dependence and size of support (Atkinson and Curran, 1995). The effects of regularization are similar to the effect imposed by the IFOV of a sensor capturing the reflectance of a scene (Woodcock *et al.*, 1988a). It was determined that different "optimal" spatial resolutions exist for different ecosystems, reinforcing the concept of a multiscale approach for detection and analysis. Here it has been demonstrated that information content differs, not only between forest ecosystems at different spatial resolutions, but also between visible and near-infrared bands at the same spatial resolution.

For mapping by remote sensing it is important that the spatial variation or information of interest be resolved (Gu *et al.*, 1992). In mapping forest ecosystems by remote sensing, it is the objective to estimate the mean reflectance of different forested surfaces, under the assumption that the mean reflectances for different forest ecosystems represent discriminable objects/forest stands. This estimation requires the appropriate regularization of reflectance arising from stand structural characteristics. However, it is not expected that optimal spatial processing of reflectance data or collection of reflectance data at what are deemed optimal and multiple scales will, by themselves, provide sufficient discrimination of forest ecosystems, even at landscape scales. The reason for this is that optimally regularized reflectance is not likely to represent a highly efficient surrogate for forest ecosystem class. Therefore, suitable discrimination and classification of forest ecosystems will require remote

sensing at optimal and multiple scales in combination with appropriate terrain descriptors related to ecosystem class.

7.2 Conclusions

7.2.1 Research Issue 1 - Spatial Resolution

The effects of spatial resolution on the spectral expression of forest ecosystems at high spatial resolutions were examined using semivariogram analysis of reflectance data for landscape-scale forest ecosystem stands. As a result of the construction and analysis of experimental variograms for forest ecosystems from low- (600m AGL) and medium-altitude (1150m AGL) CASI reflectance data, the following conclusions are drawn based on the interpretation of the range and sill values:

1. **Range estimates within the low- and medium-altitude reflectance data differ between various forest ecosystem classes; and at low-altitude appear to be related to canopy diameter (i.e., MMCD).** A direct relationship of range to MMCD is complicated by the severely elongated nature of the pixels at low altitude. The range may more effectively represent the proportion of the area covered by the dominant object in the pixel or support (e.g., tree crown) in conjunction with the related mix of understory and ground cover.
2. **Range estimates vary as a function of wavelength (i.e., there were contrasting estimates derived for the visible and near-infrared wavebands).** A greater percentage of near-infrared energy is likely to penetrate the canopy and interact with the understory. The understory therefore has a greater impact on the near-infrared signal, thereby modifying the impact of tree crown on the nature of the variogram.
3. **Range estimates vary as a function of altitude/spatial resolution/scale.** The range estimates derived for each of the forest ecosystems were greater for the medium-altitude data than for the low-altitude data. In essence, the resolvable objects become a multiple of individual elements. This characteristic may also be linked to the elongated nature of the CASI pixel, due to a sub-optimal method of sampling regular-shaped objects within the canopy.
4. **Although it is a qualitative assessment, there appears to be a direct relationship between percent cover of understory and semivariance (i.e., height of the variogram).** Although semivariance is related to density of trees (Woodcock *et al.*, 1988a; 1988b) in natural ecosystems, it may be more closely related to multiple layers of vegetation (i.e., tree canopy density/variability and understory density/variability).

In this regard, the height of the variogram can provide useful information on the type of forest ecosystem present.

5. **For wetland coniferous forest ecosystems (V38), there is an inverse relationship between tree density (number of stems/ha) and semivariance.** Coniferous forest ecosystems with low tree density tend to have higher estimates of semivariance, particularly in the visible band, and in some cases are associated with larger range estimates. Stands of very low tree density exhibit high spectral variability, particularly for the visible bands. Under these conditions, the low-shrub and ground layers contribute significantly to spectral reflectance.
6. **Increased regularization (i.e., lower semivariance) of reflectance data for all forest ecosystems is characteristic of the medium-altitude data.** However, this increased regularization does not correspond to shorter range estimates.

Based on the estimates for optimal spatial resolutions for the six landscape-scale classes, a series of reflectance features were derived from the high-altitude data (4m spatial resolution) using spatial averaging. Spectral-spatial features were derived from the 4m data to represent spatial resolutions of 5m and 6m for the visible and near-infrared channels (CASI3, CASI5) in addition to a 7m feature for the near-infrared channel (CASI7). The following conclusions were made based on the discriminant analysis of six landscape-scale forest ecosystem classes using various spectral-spatial features:

7. **Careful consideration must be given to the relationships between the forest ecosystem classes of interest and the appropriate remote sensing spatial resolutions to sample reflectance from those classes.** To maximize discriminability of these classes a spatial resolution that minimizes (regularizes) within-class variability, but maximizes between-class discrimination is required. Here it was demonstrated that 6m reflectance data provided the best discrimination of the landscape-scale forest ecosystem classes studied. However, it is still argued that multiple spatial resolutions/scales of remote sensing reflectance data may be required, depending on the nature of the classes to be discriminated and their structure, as well as their characteristic visible and near-infrared reflectance.
8. **Texture features derived from L-resolution CASI reflectance data provide significant information for discrimination of landscape-scale forest ecosystem classes.** Texture variables derived from the 4 m reflectance data provided accuracies equal to, or greater than, any of the spectral-spatial variables. Texture information is embedded within the 4 m data and is characterized to some degree by GLCM texture statistics.

Remotely sensed data often exhibit several scales of variation or information at a single spatial resolution. This has been exhibited in this analysis of reflectance for forest ecosystems in northwestern Ontario. Contrasting ecosystems possess different scales of variation, variation which is reflected in the contrasting range and semivariance estimates from the experimental variograms.

7.2.2 Research Issue 2 - Data Integration

Given the relationship between forest and site, it was hypothesized that combining appropriately scaled remote sensing data with terrain descriptors/variables should improve the discriminability of landscape-scale forest ecosystem classes for the boreal forest of northwestern Ontario. Various conclusions can be made regarding the integration of terrain variables with spectral-spatial and texture features for discriminating forest ecosystem classes in a low- to moderate-relief boreal environment. These include:

1. **Terrain variables alone provide weak discrimination of forest ecosystem classes in a low- to moderate-relief boreal environment. However, when used in combination with spectral-spatial and texture variables, they improve the discrimination of landscape-scale forest ecosystem classes.** For a low- to moderate-relief boreal environment, these variables, particularly elevation, must be used within a relatively small local area, emphasizing the local variation between ecosystem types. This is due to the fact that the drainage, which largely affects forest ecosystem development, is bedrock controlled in these areas, thereby giving rise to similar ecosystem types at a range of elevations.
2. **The integration of spectral data collected at appropriate resolutions with terrain information and texturally processed features offers promise for discriminating and classifying forest ecosystem classes.** A mean classification accuracy of 67.6% ($\hat{K} = 0.611$) was achieved when combining spectral-spatial, textural and terrain variables. This represents statistically significant improvements over using spectral-spatial, texture or terrain variables alone or in combinations of two variable types. These results indicate that appropriately scaled spectral, textural and terrain variables may provide a basis for classification and mapping of large forest regions based on ecological criteria.

It has been demonstrated that in a low-relief boreal environment, addition of textural and geomorphometric variables to high-resolution airborne remote sensing reflectance data provides improved discrimination of forest ecosystem classes. Although these improvements are statistically significant, the absolute classification accuracies are not at levels suitable for operational classification and mapping. There were considerable inconsistencies in the per-

class accuracies affecting the overall reliability of the classification produced. This remains a function of within-class variability and between-class similarity. The two landscape-scale classes that contributed to poor overall results were the Upland Black Spruce class and the White Spruce / Balsam Fir Conifer and Mixedwood class. The upland conifer was similar spectrally to the lowland black spruce, whereas the white spruce / balsam fir conifer and mixedwood represented a varied group of V-types.

7.2.3 Research Issue 3 - Remote Sensing Forest Ecosystem Classification

1. **The NNC did not provide improved results over traditional statistical classification techniques (i.e., LDA and MLC).** Further testing of NNC is required prior to adoption of NNC as an operational classification algorithm in forest classification and mapping with variables that meet the assumptions of existing statistical classifiers. The real advantage of NNC will not likely be realized until variables that do not meet the assumptions of traditional statistical classifiers are derived and implemented within a classification or modelling approach to ecosystem mapping.

The data analysed in this study (i.e., spectral-spatial, texture and terrain variables) all represent continuous variables suited to analysis using parametric classifiers. The potential of non-traditional classifiers is not likely to be observed until variables representing discrete or ordinal variables are incorporated into the classification or modelling of forest ecosystem classes.

7.3 Recommendations

The landscape-scale classification scheme presented in this thesis was derived from close examination of the NWO FEC and is closely linked to the treatment units derived from stands of similar vegetation type based on similar nutrient and moisture regimes. The final classification scheme was also derived in close consultation with ecologists and observations on the manner in which individual V-types cluster in the field into communities. Based on the poor discrimination observed, particularly for two of these classes Upland Black Spruce and White Spruce / Balsam Fir Conifer and Mixedwood, this scheme should be scrutinized. There may be a more appropriate selection of landscape-scale classes, or combination of landscape and stand-level classes, that would provide more suitable classification results using reflectance and terrain descriptors. It must be remembered that the six landscape-scale classes used are abstractly defined (i.e., theoretically differentiated) when, in reality, there is a continuum of variation between these classes, sometime as subtle as varying proportions of elements within the class. In fact, this is the basis for ecological classification. There is no

doubt that classification and mapping cannot be carried out in the absence of a forest ecosystem classification scheme. This classification scheme must provide ecologically meaningful units characterizing specified conditions that are homogeneous, or at least homogeneous in their heterogeneity, at landscape scales. Since the boundaries are difficult to define ecologically, it follows that any surrogate of these ecosystems will also vary along a gradient or continuum.

Damman (1979) stated that if vegetation is to play a role in discriminating and mapping meaningful ecological units, it is important that the vegetation criteria selected are suitable indicators of the factors controlling the differences between units recognized at various mapping scales. On the other hand, the remote sensing data (i.e., reflectance values) used in this study are surrogates for the vegetation cover. Unfortunately, reflectance alone does not provide a comprehensive surrogate for vegetation, and, it appears, does not provide a strong criterion for ecosystem discrimination. Many ecological (and timber) resources cannot be sensed directly through remote sensing reflectance data, but must be modelled from other primary data sources. Spectral-spatial features do provide a significant amount of information that can be utilized for discrimination; however, additional spatial variables are required to more precisely describe forest ecosystems. More precise descriptors or models of terrain that incorporate soil texture, nutrient and moisture regimes are likely necessary for integration with appropriate spectral-spatial reflectance features to adequately model forest ecosystem classes in a low- to moderate-relief boreal environment. This, however, is problematic since these variables are not readily available for incorporation into such models. Methods must be developed whereby these variables can be modelled or derived for incorporation into a forest ecosystem classification model using remote sensing reflectance data. These features must be derived from geomorphometric and soils data to model soil texture classes and moisture and nutrient regimes. Mackey *et al.* (1994) emphasized the need for spatially reliable estimates of the landscape processes that control the availability and distribution of energy, moisture and mineral nutrients for modelling ecosystems. These, therefore, can provide the basis for developing spatially referenced predictive models of plant/vegetation-environment response (Mackey *et al.*, 1994a). Within this framework, information regarding causal processes is as important as data about the extant landscape patterns. These processes dominate local scales and will be difficult to derive from landscape-scale variables (e.g., elevation and surficial geology).

There remains a need to better understand the relationships between stand reflectance and sensor parameters to define optimal, possibly multiple spatial resolutions/scales for characterizing forest ecosystems. Although these aspects were examined in this research, the

form of the remote sensing data acquisition (i.e., rectangular pixels arising through a long integration period characteristic of the CASI sensor at low altitudes) complicated these analyses. It is unclear as to what artifacts occurred as a result of geostatistical analysis of these data. Further examination is required under conditions where square pixels can be acquired in order to more confidently relate individual elements on the surface (e.g., tree crowns) to reflectance.

In addition, there must be a corresponding analysis of reflectance characteristics arising from selection of appropriate class structure in conjunction with the spatial and radiometric precision of the data. This aspect of remote sensing data analysis requires geographic reasoning, defined by Merchant (1984) as the systematic application of geographic knowledge and understanding. Finally, the methods for optimizing classification of appropriate forest ecosystem classes resides with the selection of suitable ecosystem descriptors of various data types and application of decision rules that satisfy the nature of those variables. This requires attention to spatial logic, the formal expression and systematic application of decision rules based upon the characteristics and relationships of a specific landscape as depicted in remote sensing data (Merchant, 1984).

In this respect, the remote sensing data analysis presented here, and incorporation of additional primary variables, represents the beginning of a complex modelling approach that is necessary for improving forest ecosystem characterization and prediction using additional primary datasets and derived datasets that possess a range of levels of measurement. Not only are appropriate or multispatial resolution remote sensing data required, but also appropriately scaled terrain and landscape features. For instance, variables depicting soil moisture regime and mineral nutrient regimes are closely associated with ecosystem development. Incorporation of these types of terrain-specific variables with reflectance data should provide further improvement in forest ecosystem classification and modelling at landscape scales.

REFERENCES

Abler, R.F. 1987. What Shall we say? To whom shall we speak? **Annals of the American Association of Geographers**, Vol. 77. pp. 511-524.

Abler, R.F., Adams, J. & Gould, P. 1971. **Spatial Organization: the Geographer's View of the World**, Prentice-Hall Inc., Englewood Cliffs, New Jersey, 587 pp.

Abuelgasim, H.H. & Strahler, A.H. 1994. Modeling bidirectional radiance measurements collected by the Advanced Solid-State Array Spectroradiometer (ASAS) over Oregon transect forests. **Remote Sensing of Environment**, Vol. 47. pp. 261-275.

Agbu, P.A. & Nizeyimana, E. 1991. Comparisons between spectral mapping units derived from SPOT image texture and field soil map units. **Photogrammetric Engineering and Remote Sensing**, Vol. 57(4). pp. 397-405.

Ahern, F.J., Bennett, W.J. & Kettela, E.G. 1986. An initial evaluation of two digital airborne imagers for surveying spruce budworm defoliation. **Photogrammetric Engineering and Remote Sensing**, Vol. 52(10). pp. 1647-1654.

Ahern, F.J., Sirois, J., McColl, W.D., Gauthier, R.P., Alfoldi, T.T., Patterson W.H. & Erdle, T.A. 1991a. Progress toward improving aerial defoliation survey methods by using electronic imagers. **Photogrammetric Engineering and Remote Sensing**, Vol. 57(2). pp. 187-193.

Ahern, F. J., Erdle, T., Maclean, D. A. & Kneppeck, I. D. 1991b. A quantitative relationship between forest growth rates and Thematic Mapper reflectance measurements. **International Journal of Remote Sensing**, Vol. 12(3). pp. 387-400.

Allen, T.F.H. & Hoekstra, T.W. 1991. Role of Heterogeneity in Scaling of Ecological Systems. pp. 24-46, In J. Kolasa & S.T.A. Pickett (Eds.), **Ecological Heterogeneity**, Ecological Studies: Analysis and Synthesis Series. Vol. 86. Springer-Verlag, New York, 326 pp.

Anderson, J.R., Hardy, E., Roach J. & Witmer, R. 1976. **A Land Use and Land Cover Classification Scheme for Use with Remote Sensor Data**. USGS Professional Paper 964, United States Geological Survey, Washington, D.C., 28 pp.

Anonymous, 1977. **A Ready Reference to the Ontario Land Inventory**, Ontario Ministry of Natural Resources, Toronto, Ontario, Canada, 75 pp.

Anonymous, 1978. **Forest Inventory Procedure for Ontario**, Third Edition, Ontario Ministry of Natural Resources, Toronto, Ontario, Canada, 31 pp.

Anonymous, 1982. **Canadian Climate Normals: Volume 3; Precipitation**, Environment Canada, Atmospheric Environment Service, 602 pp.

Anonymous, 1993. **Ecosystem Mapping: the Leading Edge**. Rinker Lake Study Area Field Tour, July 8, 1993.

Anonymous, 1994a. **Bill 171: An Act to Revise the Crown Timber Act to Provide for the Sustainability of Crown Forests in Ontario**. Government of Ontario, Printed by the Legislative Assembly of Ontario, Toronto, Ontario, 37 pp.

Anonymous, 1994b. **The Physical Environment of the Rinker Lake Research Area**. pp. 8-9, In Rinker Lake Ecological Study Tour - Field Tour Book. A workshop presented at the Global to Local: Ecological Land Classification Conference, Thunder Bay, Ontario Canada, August 14-18, 66 pp.

Anonymous, 1995. **Direction 90's - Moving Ahead 1995**. Government of Ontario Press, Ontario Ministry of Natural Resources, Toronto, Ontario, 18 pp.

Ardanuy, P.E., Han D. & Salomonson, V.V. 1991. The Moderate Resolution Imaging Spectrometer (MODIS) science and data system requirements. **IEEE Transactions on Geoscience and Remote Sensing**, Vol. 29(1). pp. 75-88.

Arai, K. 1991. Multi-temporal texture analysis in TM classification. **Canadian Journal of Remote Sensing**, Vol. 17(3). pp. 263-270.

Arai, K. 1993. A classification method with a spatial-spectral variability. **International Journal of Remote Sensing**, Vol. 14(4). pp. 699-709.

Asrar, G., Fuchs, M., Kanemasu, E.T. and Hatfield, J.L. 1984. Estimating absorbed photosynthetic radiation and leaf area index from spectral reflectance in wheat. **Agronomy Journal**, Vol. 76. pp. 300-306.

Atkinson, P.M. 1991. Optimal ground-based sampling for remote sensing investigations: estimating the regional mean. **International Journal of Remote Sensing**, Vol. 12. pp. 559-567.

Atkinson, P.M. 1993. The effect of spatial resolution on the experimental variogram of airborne MSS imagery. **International Journal of Remote Sensing**, Vol. 14. pp. 1005-1011.

Atkinson P.M. & Curran, P.J. 1995. Defining an optimal size of support for remote sensing investigations. **IEEE Transactions on Geoscience and Remote Sensing**, Vol. 33(3). pp. 768-776.

Atkinson, P. & Danson, F. 1988. Spatial resolution for remote sensing of forest plantations. pp. 221-223, In **International Geoscience and Remote Sensing Symposium (IGARSS'88): Remote Sensing, Moving Toward the 21st Century**, September 12-16, 1988, Edinburgh, Scotland, European Space Agency, Paris, France, 3 Volumes, 1858 pp.

Atkinson, P.M., Curran, P.J. & Webster, R. 1990. Sampling remotely sensed imagery for storage, retrieval, and reconstruction. **Professional Geographer**, Vol. 42(3). pp. 345-353.

Babey, S. K. & Anger, C. D. 1989. A Compact Airborne Spectrographic Imager (CASI). pp. 1028-1031, In Proceedings, **International Geoscience and Remote Sensing Symposium (IGARSS'89) / 12th Canadian Symposium on Remote Sensing,** July 10-14, 1989, Vancouver, B.C. Published by IGARSS'89, 5 Volumes, 3001 pp.

Babey, S. & Soffer, R. 1992. Radiometric Calibration of the Compact Airborne Spectrographic Imager (CASI). **Canadian Journal of Remote Sensing**, Vol. 18(4). pp. 233-242.

Badhwar, G.D., MacDonald, R.B., Hall, F.G. & Carnes, J.G. 1986a. Spectral characterization of biophysical characteristics in a boreal forest: relationship between Thematic Mapper Band reflectance and leaf area index for aspen. **IEEE Transactions on Geoscience and Remote Sensing**, Vol. 24(5). pp. 322-326.

Badhwar, G.D., MacDonald, R.B. & Mehta, N.C. 1986b. Satellite-derived leaf-area-index and vegetation maps as input to global carbon cycle models - a hierarchical approach. **International Journal of Remote Sensing**, Vol. 7(2). pp. 265-281.

Baker, J.R., Briggs, S.A., Gordon, V., Jones, A.R., Settle, J.J., Townshend, J.R.G. & Wyatt, B.K. 1991. Advances in classification for land cover mapping using SPOT HRV imagery. **International Journal of Remote Sensing**, Vol. 12(5). pp. 1071-1085.

Bailey, R.G. 1976. **Ecoregions of the United States**. U.S. Department of Agriculture, Forest Service, Inter-mountain Region, Ogden, UT, (map).

Bailey, R.G. 1980. **Description of the Ecoregions of the United States**. U.S. Department of Agriculture, Forest Service, Miscellaneous Publication 1391, Washington, D.C. 77 pp.

Bailey, R.G. 1987. Suggested Hierarchy of Criteria for Multiscale Ecosystem Mapping. **Landscape and Urban Planning**, Vol. 14. pp. 313-319.

Bailey, R.G., Zoltai, S.C. & Wiken, E.B. 1985. Ecological regionalization in Canada and the United States. **Geoforum**, Vol. 16. pp. 265-275.

Bajcsy, R. and Liebermann, L. 1976. Texture gradient as a depth cue. **Computer Graphics and Image Processing**, Vol. 5. pp. 52-67.

Baldwin, K. 1995. **Personal Communication**. June 1995.

Baldwin, K. A., Johnson, J. A., Sims, R. A. & Wickware, G. M. 1990. **Common Landform Toposequences of Northwestern Ontario**. Forestry Canada., Ontario Region, Sault Ste. Marie, Ontario COFRDA Rep. 3303, Ontario Ministry of Natural Resources., Thunder Bay, Ontario, NWOFTDU Technical Report 49, pp. 26.

Banner, A., MacKenzie, W., Haeussler, S., Thomson, S., Pojar, J. & Trowbridge, R., 1993. **A Field Guide to Site Identification and Interpretation for the Prince Rupert Forest Region**. Land Management Handbook 26, British Columbia Ministry of Forests, Crown Publications Inc., Victoria, B.C.

Baraldi, A. & Parmiggiani, F. 1995. An investigation of the textural characteristics associated with grey level cooccurrence matrix statistical parameters. **IEEE Transactions on Geoscience and Remote Sensing**, Vol. 33(2). pp. 293-304.

Barber, D. 1989. **Texture measures for SAR sea ice discrimination: an evaluation of univariate statisical distributions**. Earth-Observations Laboratory, Institute for Space and Terrestrial Science Technical Report, ISTS-EOL-TR89-005, Department of Geography, University of Waterloo, Ontario, Canada, 56 pp.

Barber, D.G., & LeDrew, E.F. 1991. SAR sea ice discrimination using texture statistics: a multivariate approach. **Photogrammetric Engineering and Remote Sensing**, Vol. 57(4). pp. 385-395.

Barber, D.G., Shokr, M.E., Fernandes, R.A., Soulis, E.D., Flett, D.G. & LeDrew, E.F. 1993. Comparison of second-order classifiers for SAR sea ice discrimination. **Photogrammetric Engineering and Remote Sensing**, Vol. 59(9). pp. 1397-1408.

Baret, F., Guyot, G., & Major, D. 1989. TSAVI: A vegetation index which minimizes soil brightness effects on LAI or APAR estimation, pp. 1355-1358, In Proceedings, **International Geoscience and Remote Sensing Symposium (IGARSS'89) / 12th Canadian Symposium on Remote Sensing**, July 10-14, 1989, Vancouver, B.C. Published by IGARSS'89, 5 Volumes, 3001 pp.

Baret, F. & Guyot, G. 1991. Potentials and limits of vegetation indices for LAI and APAR assessment. **Remote Sensing of Environment**, Vol. 35. pp. 161-173.

Barnes, B.V. 1984. Forest ecosystem classification and mapping in Baden-Wurttenberg, West Germany. In Proceedings, J.G. Bockhiem (Ed.), **Forest Land Classification: Experiences, Problems, Perspectives**, March 18-20, 1984, University of Wisconsin Press, Madison, Wisconsin, pp. 49-65.

Barnes, B.V. 1986. Varieties of experience in classifying and mapping forestland ecosystems. In Proceedings, G.M. Wickware & W.C. Stevens, (Eds). **Site Classification in Relation to Forest Management**, Great Lakes Forestry Centre, Canadian Forest Service, Sault Ste. Marie, Ontario, August 27-29, 1985, Canada-Ontario Joint Forestry Research Committee Symposium Proceedings 0-P-14, pp. 5-23.

Barnes B.V., Pregitzer, K.S., Spies, T.A. & Spooner, V.H. 1982. Ecological Forest Site Classification. **Journal of Forestry**, Vol. 80. pp. 493-498.

Baskerville, G.L. 1986. **An Audit of Management of the Crown Forests of Ontario.** Government of Ontario, Ontario. 97 pp.

Bauer, M.E., Burk, T.E., Ek, A.R., Coppin, P.R., Lime, S.D., Walsh, T.A., Walters, D.K., Befort, W. & Heinzen, D.F. 1994. Satellite inventory of Minnesota forest resources. **Photogrammetric Engineering and Remote Sensing**, Vol. 60(3). pp. 287-298.

Benediktsson, J.A., Swain, P.H. & Ersoy, O.K. 1990. Neural network approaches versus statistical methods in classification of multisource remote sensing data. **IEEE Transactions on Geoscience and Remote Sensing**, Vol. 28. pp. 540-552.

Benediktsson, J.A., Swain P.H. & Ersoy, O.K. 1993. Conjugate-gradient neural networks in classification of multisource and very-high-dimensional remote sensing data. **International Journal of Remote Sensing**, Vol. 14(15). pp. 2883-2903.

Birth, G.S. & McVey, G. 1968. Measuring the color of growing turf with a reflectance spectrophotometer. **Agronomy Journal**, Vol. 60. pp. 640-643.

Bischof, H., Schneider, W. & Pinz, A.J. 1992. Multispectral classification of Landsat-images using neural networks. **IEEE Transactions on Geoscience and Remote Sensing**, Vol. 30(3). pp. 482-490.

Boissonneau, A.N., Williams, J.R.M., Zoltai, S.C., Crombie, G.N., McNeely, H.A. & Bates, D. 1972. **The Canada Land Inventory: Land Capability Classification for Forestry**, Report No. 4, Environment Canada, Ottawa, Ontario, pp. 31-43.

Bonan, G.B. 1993. Importance of leaf area index and forest type when estimating photosynthesis in boreal forests. **Remote Sensing of Environment**, Vol. 43. pp. 303-314.

Bonnor, G.M. & Morrier, K.C. 1981. Site classification from air photos in a forest inventory. **The Forestry Chronicle**, Vol. 57(12). pp. 26-27.

Boochs, F., Kupfer, G., Dockter, K. & Kuhbauch, W. 1990. Shape of the red edge as vitality indicator for plants. **International Journal of Remote Sensing**, Vol. 11(10). pp. 1741-1753.

Booth, D.L., Boulter, D.W.K., Neave, D.J., Rotherhams, A.A. & Welsh, D.A. 1993. Natural forest landscape management: A strategy for Canada. **Forestry Chronicle**, Vol. 69(2). pp. 141-145.

Borry, F.C., De Roover, B.P., De Wulf, R.R. & Goossens, R.E. 1990. Assessing the value of monotemporal SPOT-1 imagery for forestry applications under flemish conditions. **Photogrammetric Engineering and Remote Sensing**, Vol. 56(8). pp. 1147-1153.

Borstad, G.A., Hill, D.A. & Kerr, R.C. 1989. The Compact Airborne Spectrographic Imager (CASI). pp. flight and laboratory examples. pp. 2081-2084, In Proceedings, **International Geoscience and Remote Sensing Symposium (IGARSS'89) / 12th Canadian Symposium on Remote Sensing**, July 10-14, 1989, Vancouver, B.C. Published by IGARSS'89, 5 Volumes, 3001 pp.

Bowers, W.W., Franklin, S.E., Huddak, J. & McDermid, G.J. 1994. Forest structural damage analysis using image semivariance. **Canadian Journal of Remote Sensing**, Vol. 20(1). pp. 28-36.

Bradbury, P.A., Haines-Young, R.H., Mather, P.M. & MacDonald, A. 1985. The use of remotely sensed data for landscape classification in Wales: the status of woodlands in the landscape. pp. 401-410, In **Advanced Technology for Monitoring and Processing Global Environment Data**, Proceedings of the International Conference of the Remote Sensing Society and the Center for Earth Resources Management, September 9-12, 1985, University of London, England, Remote Sensing Society, Reading, England.

Brand, D.G., Leckie, D.G. & Cloney, E.E. 1991. Forest regeneration surveys: design, data collection and analysis. **The Forestry Chronicle**, Vol. 67(6). pp. 649-657.

Brenner, R.N., & Jordan, J.K. 1991. The role of an ecological classification system in forest plan development and implementation. In **Proceedings of the 1991 Symposium on Systems Analysis in Forest Resources**, March 3-6, 1991, Charleston, South Carolina, 189 pp.

Brass, J.A., Spanner, M.A., Ulliman, M.A., Peterson, D.L., Ambrosia, V.G. & Brockhaus, J. 1983. Thematic Mapper Simulator research for forest resource mapping in the Clearwater National Forest, Idaho. pp. 1323-1332, In Proceedings, **Seventeenth International Symposium on Remote Sensing of Environment**, May 9-13, 1983, Ann Arbor, Michigan, Environmental Research Institute of Michigan, Ann Arbor, Michigan, 3 Volumes, 1446 pp.

Brockhaus, J.A. & Khorram, S. 1992. A comparison of SPOT and Landsat-TM data for use in conducting inventories of forest resources. **International Journal of Remote Sensing**, Vol. 13(16). pp. 3035-3043.

Brooker, P.I., 1991. **A Geostatistical Primer**, World Scientific, London, 95 pp.

Brundtland, G.H., 1987. **Our Common Future**, World Commission on Environment and Development, Oxford University Press, Oxford, 400 pp.

Bryant, E., Dodge, A.G.J. & Warren, S.D. 1980. Landsat for practical forest type mapping: a test case. **Photogrammetric Engineering and Remote Sensing**, Vol. 46(12). pp. 1575-1584.

Buis, J.S., Acevedo, W., Wrigley, R.C., & Alexander, D.A. 1983. The role of spatial, spectral and radiometric resolution on information content. pp. 330-338, In D.C. MacDonald and D.B. Morrison (Eds.), **Machine Processing of Remotely Sensed Data: 9th International Symposium**, June 21-23, 1983, Purdue University, West Lafayette, Indiana, Purdue Research Foundation West Lafayette, Indiana, 430 pp.

Burger, D. & Pierpoint, G. 1990. Trends in forest site and land classification in Canada. **The Forestry Chronicle**, Vol. 66(4). pp. 91-96.

Burrough, P.A., 1987. **Principles of Geographic Information Systems for Land Resources Assessment**, Monographs on Soil and Resources Survey No. 12, Clarendon Press, Oxford, 194 pp.

Butera, M.K. 1986. A correlation and regression analysis of percent canopy closure versus TMS spectral response for selected forest sites in the San Juan National Forest, Colorado. **IEEE Transactions on Geoscience and Remote Sensing**, Vol. 24. pp. 122-128.

Campbell, J.B. 1981. Spatial correlation effects upon accuracy of supervised classification of land cover. **Photogrammetric Engineering and Remote Sensing**, 47. pp. 355-357.

Campbell, J. B. 1987. **Introduction to Remote Sensing.** The Guilford Press, New York, U.S. pp. 557

Canada Committee on Ecological Land Classification, 1976. In J. Thie & G. Ironside (Eds.), **Ecological (Biophysical) Land Classification in Canada**, May 25-28, 1976, Petawawa, Ontario, Environment Canada, Lands Directorate, Ottawa, Ecological Land Classification Series No. 1, 269 pp.

Canadian Council of Forest Ministers, 1992. **Sustainable Forests: A Canadian Commitment**, National Forest Strategy, Canadian Council of Forest Ministers, March 1992, 351 St. Joseph Boulevard, Hull Quebec, K1A 1G5, 51 pp.

Carlucci, L. 1972. A formal system for texture language. **Pattern Recognition**, Vol. 4. pp. 53-69.

Chavez, P.S. Jr. 1992. Comparison of spatial variability in visible and near-infrared spectral images. **Photogrammetric Engineering and Remote Sensing**, Vol. 58(7). pp. 957-964.

Chavez, P.S. Jr. & Bowell, J.A. 1988. Comparison of the spectral information content of Landsat Thematic Mapper and SPOT for three different sites in the Phoenix, Arizona region. **Photogrammetric Engineering and Remote Sensing**, Vol. 54(12). pp. 1699-1708.

Cihlar, J., St.-Laurent, L., & Dyer, J.A. 1991. Relation between the Normalized Difference Vegetation Index and Ecological Variables, **Remote Sensing of Environment**, Vol. 35. pp. 279-298.

Clark, C.D. 1990. Remote sensing scales related to the frequency of natural variation: an example from paleo-ice-flow in Canada. **IEEE Transactions on Geoscience and Remote Sensing**, Vol. 28(4). pp. 503-508.

Clark, I. 1979. **Practical Geostatistics**, Applied Science Publishers LTD, London, 129 pp.

Clark, W.C. 1985. Scales of climatic impacts. **Climate Change**, Vol. 7. pp. 5-27.

Clevers, J.G.P.W. 1988. The derivation of a simplified reflectance model for the estimation of leaf area index. **Remote Sensing of Environment**, Vol 35. pp. 53-70.

Cohen, W.B. 1991. Response of vegetation indices to changes in three measures of leaf water stress. **Photogrammetric Engineering and Remote Sensing**, Vol. 57(2). pp. 195-202.

Cohen, W., Spies, T. & Bradshaw, G. 1990. Semivariograms of digital imagery for analysis of conifer canopy structure. **Remote Sensing of Environment**, Vol. 34. pp. 167-178.

Cohen, W. B. & Spies, T. A. 1992. Estimating structural attributes of Douglas-Fir / Western Hemlock forest stands from Landsat and SPOT imagery. **Remote Sensing of the Environment**, Vol. 41. pp. 1-17

Coleman, T.L., Gudapati, L. & Derrington, J. 1990. Monitoring forest plantations using Landsat Thematic Mapper data. **Remote Sensing of Environment**, Vol. 33. pp. 211-221.

Congalton, R.G., Green, K. & Teply, J. 1993. Mapping old growth forest on national forest and park lands in the Pacific Northwest from remotely sensed data. **Photogrammetric Engineering and Remote Sensing**, Vol. 59(4). pp. 529-535.

Conners, R.W., & Harlow, C.A., 1980a, Toward a structural textural analyzer based on statistical methods. **Computer Graphics and Image Processing**, Vol. 12(3). pp. 224-256.

Conners, R.W., & Harlow, C.A., 1980b, A theoretical comparison of texture algorithms. **IEEE Transactions on Pattern Analysis and Machine Intelligence**, Vol. 2(3). pp. 204-222.

Cook, E.A., Iverson, L.R. & Graham, R.L. 1989. Estimating forest productivity with Thematic Mapper and biogeographical data. **Remote Sensing of Environment**, Vol. 28. pp. 131-141.

Corns, I. G. W. & Annas, R. M. 1986. **Field Guide to Forest Ecosystems of West-Central Alberta.** Canadian Forest Service, Edmonton, Alberta, 251 pp.

Craig, R.G. & Labovitz, M.L. 1980. Sources of variation in Landsat autocorrelation. pp. 1755-1767, In **14th International Symposium on Remote Sensing of Environment**, April 23-30, 1980, San Jose, Costa Rica, Environmental Research Institute of Michigan, Ann Arbor, Michigan, 3 Volumes, 1923 pp.

Crombie, M.A., Rand R.S. & Friend, N. 1982. **An Analysis of the Max-Min Texture Measure.** U.S. Army Corps of Engineers, Engineer Topographic Laboratories, 42 pp.

Crowley, J.M., 1967. Biogeography in Canada. **Canadian Geographer**, Vol. 11, pp. 312-326.

Csillag, F. 1991. Resolution Revisited. pp. 15-28, In Proceedings, **AutoCarto 10**, 10th International Symposium on Computer-Assisted Cartography, March 25-28, 1991, Baltimore Maryland, American Society for Photogrammetry and Remote Sensing and the American Congress on Surveying and Mapping, Bethesda, Maryland, 444 pp.

Curran, P.J. 1980. Multispectral remote sensing of vegetation amount. **Progress in Physical Geography**, Vol. 4. pp. 315-341.

Curran, P. J. 1988. The semivariogram in remote sensing: an introduction. **Remote Sensing of the Environment**, Vol. 24. pp. 493-507

Curran, P.J. & Dungan, J.L. 1989. Estimation of signal-to-noise: a new procedure applied to AVIRIS data. **IEEE Transactions on Geoscience and Remote Sensing**, Vol. 14. pp. 620-628.

Curran, P.J. & Williamson, H.D. 1987. Airborne MSS data to estimate GLAI. **International Journal of Remote Sensing**, Vol. 8(1). pp. 57-74.

Curran, P.J. & Pedley, M.I. 1990. Airborne MSS for land cover classification II. **Geocarto International**, Vol. 5(2). pp. 15-26.

Curran, P. J., Dungan, J. L. & Gholz, H. L. 1992. Seasonal LAI in slash pine estimated with Landsat TM. **Remote Sensing of the Environment**, Vol. 39(1). pp. 3-13.

Cushnie, J.L. 1987. The interactive effect of spatial resolution and degree of internal variability within land cover types and classification accuracies. **International Journal of Remote Sensing**, Vol. 8(1). pp. 15-29.

Cushnie, J.L. & Atkinson, P. 1985. Effect of spatial filtering on scene noise and boundary detail in TM imagery. **Photogrammetric Engineering and Remote Sensing**, Vol. 51(9). pp. 1183-1193.

Damman, A. W. H. 1979. The role of vegetation analysis in land classification. **Forestry Chronicle**, Vol. 55(5). pp. 175-182.

Danson, F.M. 1987. Estimating forest stand parameters using airborne MSS data. pp. 46-54, In **Advances in Digital Image Processing**, Proceedings of the Thirteenth Annual Conference of the Remote Sensing Society, September 7-11, 1987, Department of Geography, University of Nottingham, Nottingham, England, Remote Sensing Society, Nottingham, England, 675 pp.

Danson, F.M. & Curran, P.J. 1993. Factors affecting the remotely sensed response of coniferous forest plantations. **Remote Sensing of Environment**, Vol. 43. pp. 55-65.

Davis, J.C. 1986. **Statistics and Data Analysis in Geology** (2nd edition), New York, John Wiley and Sons, 646 pp.

Davis, L.S., S.A. Johns, & J.K. Aggarwal, 1979. Texture analysis using generalized co-occurrence matrices. **IEEE Transaction on Pattern Analysis and Machine Intelligence**, Vol. PAMI-1, pp.

Day, R. J. 1992. **A Manual of Silviculture.** School of Forestry, Lakehead University. Laboratory Manual No. 1 (14th edition).

De Cola, L., 1993. Multifractals in image processing and process imaging, pp. 282-304, In N.S.-N Lam & L. De Cola (Eds.), **Fractals in Geography**, Prentice Hall, Englewood Cliffs, New Jersey, 308 pp.

Department of Forestry and Rural Development, 1965. **The Canada Land Inventory: Objectives, Scope and Organization.** Department of Forestry and Rural Development, Report No. 1, Ottawa, Ontario, Canada, 12 pp.

Department of Forestry and Rural Development, 1966. **The Canada Land Inventory.** The Information and Technical Services Division, Department of Forestry and Rural Development, Ottawa, Ontario, 6 pp.

DeGloria, S.D. & Benson, A.S. 1987. Interpretability of advanced SPOT film products for forest and agricultural survey. **Photogrammetric Engineering and Remote Sensing**, Vol. 53(1). pp. 37-44.

DeWulf, R.R., Goosens, R.E., Roover, B.D. & Borry, F.C. 1990. Extraction of forest stand parameters from panchromatic and multispectral SPOT-1 data. **International Journal of Remote Sensing**, Vol. 11(9). pp. 1571-1588.

Downey, I.D., Power, C.H., Kanellopoulos, I., & Wilkinson, G. 1992. A performance comparison of Landsat TM land cover classification based on neural network techniques and traditional maximum likelihood and minimum distance algorithms. pp. 518-528 In A.P. Cracknell & R.A. Vaughan (Eds.), **Remote Sensing from Research to Operation**, Proceedings of the 18th Annual Conference of the Remote Sensing Society, September 15-17, 1992, University of Dundee, Dundee, Scotland, Remote Sensing Society, Nottingham, England, 620 pp.

Driscoll, R. S., Merkel, D. L., Radloff, D. L., Synder, D. E. & Hagihara, J. S. 1984. **An Ecological Land Classification Framework for the United States**. United States Department of Agriculture, Forest Service, Washington, D.C. Miscellaneous. Publication. No. 1439, 56 pp.

Duda, R.O. & Hart, P.E. 1973. **Pattern Classification and Scene Analysis**, John Wiley and Sons, New York, 482 pp.

Dudley, G. 1992. Scale, aggregation, and the modifiable areal unit problem. **Operational Geographer**, Vol. 9(3). pp. 28-33.

Dungan, J.L. Peterson, D.L., & Curran, J.L. 1993. Alternative approaches for mapping vegetation quantities using ground and image data. pp. 237-261, In W. Michener, J. Brunt & S. Stafford (Eds.), **Environmental Information Management and Analysis: Ecosystem to Global Scales**, Taylor and Francis, London, 555 pp.

Duggin, M.J. & Robinove, C.J. 1990. Assumptions implicit in remote sensing data acquisition and analysis. **International Journal of Remote Sensing**, 11(10). pp. 1669-1694.

ECOMAP, 1993. **National Hierarchical Framework for Ecological Units.** USDA Forest Service, Washington, DC. 20 pp.

Ecoregions Working Group, 1989. **Ecoclimatic Regions of Canada, First Approximation.** Ecoregions Working Group of the Canada Committee on Ecological Land Classification, Ecological Land Classification Series, No. 23, Sustainable Development Branch, Canadian Wildlife Service, Conservation and Protection, Environment Canada, Ottawa, Ontario. 119 pp. and map at 1:7,500,000 scale.

Ekstrand, S. 1994. Assessment of forest damage with Landsat TM: correction for varying forest stand characteristics. **Remote Sensing of Environment**, Vol. 47. pp. 291-302.

Elvidge, C.D. & Lyon, R.J.P. 1985. Influence of rock-soil spectral variation on the assessment of green biomass. **Remote Sensing of Environment**, Vol. 17. pp. 265-279.

Elvidge, C.D., Chen, Z. & Groenveld, D.P. 1993. Detection of trace quantities of green vegetation in 1990 AVIRIS data. **Remote Sensing of Environment**, Vol. 44. pp. 271-279.

Environment Canada, 1978. **The Canada Land Inventory: Objectives, Scope and Organization,** Report No. 1, Lands Directorate, Environment Canada, Ottawa, Ontario, 61 pp.

Environmental Conservation Task Force, 1981. **Ecological Land Survey Guidelines for Environmental Impact Analysis.** Ecological Land Classification Series No. 13, Lands Directorate, Environment Canada, Ottawa, Ontario, 44 pp.

Ersoy, O.K. & Hong, D. 1990. Parallel, self-organizing, hierarchical neural networks. **IEEE Transactions of Neural Networks**, Vol. 1. pp. 167-178.

ESRI Inc., 1994. **ArcInfo Users Manual**, Environmental Systems Research Institute Inc., 380 New York Street, Redlands, California, variously paged.

Evans, D. L. & Hill, J. 1990. Landsat TM versus MSS data for forest type identification. **Geocarto International**, Vol. 3. pp. 13-20

Everett, J. & Simonett, D.S. 1976. Principles, concepts and philosophical problems in remote sensing. pp. 85-127, In J. Lintz & D.S. Simonett (Eds.), **Remote Sensing of Environment**, Addison-Wesley, London, 694 pp.

Fernandez, R.A. 1992. **A Multilevel Multispectral Aggregation Network.** Unpublished Master of Applied Science Thesis, University of Waterloo, Waterloo, Ontario, Canada. 120 pp.

Fiorella, M. & Ripple, W.J. 1993. Determining successional stage of temperate coniferous forests with Landsat satellite data. **Photogrammetric Engineering and Remote Sensing**, Vol. 59(2). pp. 239-246.

Foody, G.M., 1995. Land cover classification by an artificial neural network with ancillary information. **International Journal of Geographical Information Systems**, Vol. 9(5), pp. 527-542.

Foody, G.M., McCulloch, M.B., & Yates, W.B. 1992. An assessment of an artificial neural network for image classification. pp. 498-507 in A.P. Cracknell & R.A. Vaughan (Eds.), **Remote Sensing from Research to Operation**, Proceedings of the 18th Annual Conference of the Remote Sensing Society, September 15-17, 1992, University of Dundee, Dundee, Scotland, Remote Sensing Society, Nottingham, England, 620 pp.

Foody, G.M. & Cox, D.P. 1994. Sub-pixel land cover composition estimation using a linear mixture model and fuzzy membership functions. **International Journal of Remote Sensing**, Vol. 15(5). pp. 619-631.

Ford, J., 1994. Surficial Geology of the Rinker Lake Research Area, pp. 30-32 in **Rinker Lake Ecological Study Tour - Field Tour Book**, A workshop presented at the Global to Local: Ecological Land Classification Conference, August 14-18, 1994, Thunder Bay, Ontario, Canada, 66 pp.

Forestry Canada, 1990. **The State of Forestry in Canada: 1990 Report to Parliament.** Forestry Canada, Ottawa, Ontario, Canada, 80 pp.

Forman, R. T. & Godron, M. 1986. **Landscape Ecology.** John Wiley and Sons, Toronto, 619 pp.

Forshaw, M.R.B., Haskell, A., Miller, P.F., Stanley, D.J. & Townshend, J.R.G. 1983. Spatial resolution of remote sensing imagery. **International Journal of Remote Sensing**, Vol. 4(3). pp. 497-520.

Frank, T.D. 1988. Mapping dominant vegetation communities in the Colorado Rocky Mountain Front Range with Landsat Thematic and digital terrain data. **Photogrammetric Engineering and Remote Sensing**, Vol. 54(12). pp. 1727-1734.

Franklin, J.F. 1986. Thematic Mapper analysis of coniferous forest structure and composition. **International Journal of Remote Sensing**, Vol. 7(10). pp. 1287-1301.

Franklin, J., Logan, T.L., Woodcock, C.E. & Strahler, A.H., 1986. Coniferous forest classification and inventory using Landsat and digital terrain data. **IEEE Transactions on Geoscience and Remote Sensing**, Vol. 24(1). pp. 139-149.

Franklin, J. & Strahler, A. 1988. Invertible canopy reflectance modeling of vegetation structure in semiarid savanna. **IEEE Transactions on Geoscience and Remote Sensing**, Vol. 26. pp. 809-825.

Franklin, S.E. 1987. Terrain analysis from digital patterns in geomorphometry and Landsat MSS spectral response. **Photogrammetric Engineering and Remote Sensing**, Vol. 53(1). pp. 59-65.

Franklin, S.E. 1989. Classification of hemlock looper defoliation using SPOT HRV imagery. **Canadian Journal of Remote Sensing**, Vol. 15(3). pp. 178-182.

Franklin, S.E. 1992. Satellite remote sensing of forest type and landcover in subalpine forest region, Kananaskis Valley, Alberta. **Geocarto International**, Vol. 4. pp. 25-35.

Franklin, S.E. 1994. Discrimination of subalpine forest species and canopy density using digital CASI, SPOT PLA and Landsat TM data. **Photogrammetric Engineering and Remote Sensing**, Vol. 60(10). pp. 1233-1241.

Franklin, S.E. & Peddle, D.R. 1989. Spectral texture for improved class discrimination in complex terrain. **International Journal of Remote Sensing**, Vol. 10(8). pp. 1437-1443.

Franklin, S.E. & Peddle, D.R. 1990. Classification of SPOT HRV imagery and texture features. **International Journal of Remote Sensing**, Vol. 11(3). pp. 551-556.

Franklin, S.E. & Moulton, J.E. 1990. Variability and classification of Landsat Thematic Mapper imagery in Kluane National Park. **Canadian Journal of Remote Sensing**, Vol. 16(2). pp. 2-13.

Franklin, S.E. & Wilson, B.A. 1991. Vegetation mapping and change detection using SPOT HRV and Landsat Thematic Mapper imagery in Kluane National Park. **Canadian Journal of Remote Sensing**, Vol. 17(1). pp. 2-17.

Franklin, S.E. & Wilson, B.A. 1992. A three-stage classifier for remote sensing of mountain environments. **Photogrammetric Engineering and Remote Sensing**, Vol. 58(4). pp. 449-454.

Franklin, S.E., Blodgett, C.F., Mah, S. & Wrightson, C. 1991. Sensitivity of CASI data to anisotropic reflectance, terrain aspect, and deciduous forest species. **Canadian Journal of Remote Sensing**, Vol. 17(4). pp. 314-321.

Franklin, S. E. & McDermid, G. J. 1993. Empirical relations between digital SPOT HRV and CASI spectral response and lodgepole pine (Pinus contorta) forest stand parameters. **International Journal of Remote Sensing**, Vol. 14(12). pp. 2331-2348.

Franklin, S.E. & Raske, A.G. 1994. Satellite remote sensing of spruce budworm forest defoliation in western Newfoundland. **Canadian Journal of Remote Sensing**, Vol. 20(1). pp. 37-48.

Franklin, S.E., Connery, D.R. & Williams, J.A. 1994. Classification of alpine vegetation using Landsat Thematic Mapper, SPOT HRV and DEM data. **Canadian Journal of Remote Sensing**, Vol. 20(1). pp. 49-56.

Franklin, S.E., Waring, R.H., McCreight, R.W., Cohen, W.B., & Fiorella, M., 1995. Aerial and satellite sensor detection and classification of Western Spruce Budworm defoliation in a subalpine forest. **Canadian Journal of Remote Sensing**, Vol. 21(3). pp. 299-308.

Gallant, S.I. 1993. **Neural Network Learning and Expert Systems**, The MIT Press, Cambridge, Massachusetts.

Galloway, M.M. 1975. Texture analysis using gray level run lengths. **Computer Graphics and Image Processing**, Vol. 4. pp. 172-179.

Gaö, B.C. 1993. An operational method for estimating signal to noise ratios from data acquired with imaging spectrometers. **Remote Sensing of Environment**, Vol. 43. pp. 23-33.

Gauch, H.G., 1982. **Multivariate Analysis in Community Ecology.** Cambridge University Press, London, 298 pp.

Gemmel, F.M.; Goodenough, D.G. 1992. Estimating timber volume from TM data: The importance of scale and accuracy of forest cover data. pp. 297-306, In A.P. Cracknell & R.A. Vaughan (Eds.), **Remote Sensing from Research to Operation**, Proceedings of the 18th Annual Conference of the Remote Sensing Society, September 15-17, 1992, University of Dundee, Dundee, Scotland, Remote Sensing Society, Nottingham, England, 620 pp.

Gholz, H.L. 1982. Environmental limits on above-ground net primary production, leaf area, and biomass in vegetation zones of the Pacific Northwest. **Ecology**, Vol. 63. pp. 469-481.

Gillespie, R.T., Franklin, S.E., Titus, B. & Pike, A. 1992. Detection and mapping of Kalmia on regenerating forest sites using the compact airborne spectrographic imager. pp. 129-132, In J.K. Hornsby, D.J. King and N.A. Prout (Eds.), **15th Canadian Symposium on Remote Sensing: A World of Applications**, June 1-4, 1992, Toronto, Ontario, Ontario Ministry of Natural Resources, Ontario Centre for Remote Sensing, North York, Ontario, 504 pp.

Gimbarzevsky, P. 1978, Land classification as a base for integrated inventories of renewable resources. pp. 169-177, In **Integrated Inventories of Renewable Natural Resources**, Proceedings of a Workshop, January 8-12, 1978, Tucson, Arizona, Forestry Service, U.S. Department of Agriculture Forestry Service, Rocky Mountain Forest Station, Fort Collins, Colorado, General Technical Report, RM-55, 482 pp.

Ginsberg, J.R., 1987. What is conservation biology? **Trends in Ecological Evolution** Vol. 2. pp. 262-264.

Goel, N. 1988. Models of vegetation canopy reflectance and their use in estimation of biophysical parameters from reflectance data, **Remote Sensing Reviews**, Vol. 4. Harwood Academic Publishers, 212 pp.

Goel, N. & Grier, T. 1986a. Estimation of canopy parameters for inhomogeneous vegetation canopies from reflectance data, I. two dimensional row canopy. **International Journal of Remote Sensing**, Vol. 7. pp. 665-681.

Goel, N. & Grier, T. 1986b. Estimation of canopy parameters for inhomogeneous vegetation canopies from reflectance data, II. estimation of leaf area index and percentage ground cover for row canopies. **International Journal of Remote Sensing**, Vol. 7. pp. 1263-1286.

Goel, N. & Grier, T. 1988. Estimation of canopy parameters for inhomogeneous vegetation canopies from reflectance data, III. TRIM: a model for radiative transfer in heterogeneous three-dimensional canopies. **International Journal of Remote Sensing**, Vol. 25. pp. 255-293.

Goetz, A.F.H. & Herring, M. 1989. The high resolution imaging spectrometer (HIRIS) for EOS. **IEEE Transactions on Geoscience and Remote Sensing**, Vol. 27(2). pp. 136-143.

Gong, P. 1994. Reducing boundary effects in a kernal-based classifier. **International Journal of Remote Sensing**, Vol. 15(5). pp. 1131-1139.

Gong, P. & Howarth, P.J. 1992. Frequency-based contextual classification and gray-level vector reduction for land-use identification. **Photogrammetric Engineering and Remote Sensing**, Vol. 58(4). pp. 423-437.

Gong, P., Pu, R. & Miller, J. R. 1992a. Correlating leaf area index of ponderosa pine with hyperspectral CASI data. **Canadian Journal of Remote Sensing**, Vol. 18(4). pp. 275-282

Gong, P., Marceau, D.J. & Howarth, P.J. 1992b. A comparison of spatial feature extraction algorithms for land-use classification with SPOT HRV. **Remote Sensing of Environment**, Vol. 40. pp. 137-151.

Gougeon, F.A., 1995. A crown-following approach to the automatic delineation of individual tree crown in high spatial resolution aerial images. **Canadian Journal of Remote Sensing**, Vol. 21(3). pp. 274-284.

Gower, J.F.R., Borstad, G.A., Anger, C.D. & Edel, H.R. 1992. CCD-based imaging spectrometry for remote sensing: the FLI and CASI programs, **Canadian Journal of Remote Sensing**, Vol. 18(4). pp. 199-208.

Goward, S.N., Haemmrich, K.F. & Waring, R.H. 1994. Visible-near infrared spectral reflectance of landscape components in western Oregon. **Remote Sensing of Environment**, Vol. 47. pp. 190-203.

Granö, J.G., 1929. Reine Geographie: eine methodologische Studie beleuchtet mit Beispielen aus Finnland und Estland. **Acta Geographica**, Vol. 2(2).

Gurney, C.M. & Townshend, J.R.G. 1983. The use of contextual information in the classification of remotely sensed data. **Photogrammetric Engineering and Remote Sensing**, Vol. 49(1). pp. 55-64.

Gu, X.F., Guyot, G. & Verbrugghe, M. 1992. Evaluation of measurement errors in ground surface reflectance for satellite calibration, **International Journal of Remote Sensing**, Vol. 13. pp. 2531-2546.

Guo, L.J. & Haigh, J.D. 1994. A three-dimensional feature space iterative clustering method for multispectral image classification. **International Journal of Remote Sensing**, Vol. 15(3). pp. 633-644.

Guyot, G., Guyon, D. & Riom, J. 1989. Factors affecting the spectral response of forest canopies: a review. **Geocarto International**, Vol. 3. pp. 3-18.

Hall, R.; Morton, R.; Nesby, R. 1989. A comparison of existing models for DBH estimation from large-scale photos. **The Forestry Chronicle**, Vol. 65. pp. 114-120.

Halliday, W.E.D. 1937. **A Forest Classification for Canada**, Forest Service Bulletin 89, Department of Mines and Resources, Ottawa, Ontario, Canada.

Hame, T. 1984. Landsat-aided forest site type mapping. **Photogrammetric Engineering and Remote Sensing**, Vol. 50(8). pp. 1175-1183.

Hansson, L., 1992. Introduction: Applied ecological principles and their implementation in nature conservation, pp. 1-8, In L. Hansson (Ed.), **Ecological Principles of Nature Conservation, Applications in Temperate and Boreal Environments**, Elsevier Applied Science, New York, 425 pp.

Hansson L., & Angelstrom, P., 1991. Landscape ecology as a basis for nature conservation. **Landscape Ecology**, Vol. 5(4), pp. 191-201.

Haralick, R. M. 1979. Statistical and structural approaches to texture. **Proceedings of the IEEE**, Vol. 67(5). pp. 786-804.

Haralick, R.M., 1986. Statistical image texture analysis, In Young, T.Y. & K.S. Fu (Eds.), **Handbook of Pattern Recognition and Image Processing**, Academic Press, New York, pp. 247-279.

Haralick, R.M., Shanmugam, K. & Dinstein, I. 1973. Texture features for image classification. **IEEE Transactions on Systems, Man, and Cybernetics**, Vol. 3(6). pp. 610-621.

Hardisky, M.A., Klemas, V. & Smart, R.M. 1983. The influence of soil salinity, growth form, and leaf moisture on the spectral radiance of Spartina alterniflora canopies. **Photogrammetric Engineering and Remote Sensing**, Vol. 49. pp. 77-83.

Hartshorne, R., 1939. The Nature of Geography: A critical survey of current thought in the light of the past. **Annals of the Association of American Geographers**, Vol. 29(3/4). 482 pp.

Hay, G.J., & K.O. Niemann, 1994. Visualizing 3-D texture: a three dimensional structural approach to model forest texture. **Canadian Journal of Remote Sensing**, Vol. 20(2), pp. 90-101.

Hay, G.J. & Niemann, K.O. 1996. Selecting the most appropriate upscaling algorithm: a multi-scale approach. pp. 435-438, In Proceedings, **26th International Symposium on Remote Sensing of Environment / 18th Canadian Symposium on Remote Sensing**, Information Tools for Sustainable Development, March 25-29, Vancouver, B.C., 632 pp.

Hay, G.J., Goodenough, D.G. & Niemann, K.O. 1996. Spatial thresholds, image-objects, and upscaling: a multi-scale evaluation. **Remote Sensing of Environment**, (in review).

Hecht-Nielsen, R. 1990. **Neurocomputing**. Addison-Wesley Publishing Co., Reading Mass., 433 p.

Hellpach, W. 1935. **Geopsyche**, originally published as Die geopsychischen Erscheinungen in 1917, Leipzig.

Henderson-Sellers, A., Wilson, M.F., & Thomas, G. 1985. The effect of spatial resolution on archives of land cover type. **Climatic Change**, Vol. 7, pp. 391-402.

Herwitz, S.R., Peterson, D.L. & Eastman, J.R. 1989. Thematic Mapper detection of change in the leaf area index of closed canopy pine plantations in Central Massachusetts. **Remote Sensing of Environment**, Vol. 29. pp. 129-140.

Hill, M.O., 1979. **DECORANA, a Fortran program for Detrended Correspondence Analysis and Reciprocal Averaging**, Department of Ecology and Systematics, Cornell University, Ithaca, New York, 52 pp.

Hills, G. A. 1952. **The Classification and Evaluation of Site for Forestry.** Ontario Department of Lands and Forests, Toronto. Research Report No. 24. 41 pp.

Hills, G. A. 1953. The use of site in forest management. **Forestry Chronicle**, Vol. 29. pp. 128-136.

Hills, G.A. 1958. Soil-forest relationships in the site regions of Ontario, **First North American Forest Soils Conference**, Bulletin of the Agricultural Experimental Station, Michigan State University, East Lansing, Michigan. pp. 190-212.

Hills, G. A. 1960. Regional site research. **Forestry Chronicle**, Vol. 36. pp. 401-423.

Hills, G. A. 1961. **The Ecological Basis for Land Use Planning.** Ontario Department of Lands and Forests, Toronto, Ontario. Research Report No. 46.

Hills, G. A. 1976. An integrated iterative holistic approach to ecosystem classification. pp. 73-97, In J. Thie & G. Ironside, (Eds). **Proceedings of the First Meeting, Canada Committee on Ecological (Biophysical) Land Classification**, Ecological Land Classification Series 1, Lands Directorate, Environment Canada, Ottawa, Ontario.

Hills, G. A. & Pierpoint, G. 1960. **Forest Site Evaluation in Ontario.** Ontario Department of Lands and Forests, Toronto, Ontario, Research Report. No. 46.

Hills, G.A., Love, D.V., & Lacate, D.S., 1970. **Developing a Better Environment: Ecological Land Use Planning in Ontario.** Ontario Economics Council, Toronto, Ontario, 182 pp.

Hodgson, M.E. & Jensen, J.R. 1987. Interrelationships between spatial resolution and per-pixel classifiers for extracting information classes, Part II: the natural environment. pp. 130-139, In Proceedings, **1987 ASPRS-ACSM Annual Convention**, March 29-30, 1987, Baltimore, Maryland, American Society of Photogrammetry, Falls Church, Virginia.

Hopkins, P.F., MacLean, A.L. & Lillesand, T.M. 1988. Assessment of Thematic Mapper imagery for forestry applications under lake states conditions. **Photogrammetric Engineering and Remote Sensing**, Vol. 54(1). pp. 61-68.

Horler, D.N.H., Dockray, M. & Barber, J. 1983. The red edge of plant leaf reflectance. **International Journal of Remote Sensing**, Vol. 4(2). pp. 273-288.

Horler, D.N.H. & Ahern, F.J. 1986. Forestry information content of Thematic Mapper data. **International Journal of Remote Sensing**, Vol. 7(3). pp. 405-428.

Hsu, S. 1978. Texture-tone analysis for automated land-use mapping. **Photogrammetric Engineering and Remote Sensing**, Vol. 11. pp. 1393-1404.

Hudson, W. D. 1987. Evaluation of several classification schemes for mapping forest cover types in Michigan. **International Journal of Remote Sensing**, Vol. 8(12). pp. 1785-1796

Huete, A.R. 1986. Separation of soil-plant spectral mixtures by factor analysis. **Remote Sensing of Environment**, Vol. 19. pp. 237-251.

Huete, A.R. 1988. A soil adjusted vegetation index (SAVI). **International Journal of Remote Sensing**, Vol. 9. pp. 295-309.

Huete, A.R., Jackson, R.D. & Post, D.F. 1985. Spectral response of a plant canopy with different soil backgrounds. **Remote Sensing of Environment**, Vol. 17. pp. 37-53.

Huete, A.R. & Tucker, C.J. 1991. Investigation of soil influences in AVHRR red and near infrared vegetation index imagery. **International Journal of Remote Sensing**, Vol. 12. pp. 1223-1242.

Huete A.R., Liu, H.Q., Batchily, K., &Van Leeuwen, W. 1997. A comparison of vegetation indices over a global set of TM images for EOS-MODIS. **Remote Sensing of Environment**, Vol. 59. pp. 440-451.

Hughes, J.S., Evans, D.L., Burns, P.Y. & Hill, J.M. 1986. Identification of two southern pine species in high-resolution aerial MSS data. **Photogrammetric Engineering and Remote Sensing**, Vol. 52(8). pp. 1175-1180.

Huijbregts, C.J. 1975. Regionalized variables and quantitative analysis of spatial data. pp. 38-53, In J.C. Davis & M.J. McCullagh (Eds.), **Display and Analysis of Spatial Data.** John Wiley and Sons, London.

Hunt, E.R., Rock, B.N. & Nobel, P.S. 1987. Measurement of leaf relative water content by infrared reflectance. **Remote Sensing of Environment**, Vol. 22. pp. 429-435.

Hutchinson, C. 1982. Techniques for combining Landsat and ancillary data for digital classification improvement. **Photogrammetric Engineering and Remote Sensing**, Vol. 48(1). pp. 123-130.

Hutchinson, M.F., 1988. Calculation of hydrologically sound digital elevation models, In Proceedings, **Third International Symposium on Spatial Data Handling,** August 17-19, 1988, International Geographic Union, Columbia, Ohio.

Hutchinson, M.F., 1989. A new procedure for gridding elevation and stream line data with automatic removal of pits. **Journal of Hydrology**, Vol. 106, pp. 211-232.

Hutchinson, M.F. & Dowling, T.I., 1991. A continental assessment of hydrological applications of a new grid-based digital elevation model for Australia. **Hydrological Processes**, Vol. 5, pp. 45-58.

Iantosca, E.T., Gray, L.H., Buxton, R.A.H. & Bézy, J.-L. 1992. Characterization of CCD detector arrays for ESA's Earth-orbiting imaging spectrometers. **Canadian Journal of Remote Sensing**, Vol. 18(4). pp. 223-232.

Irons, J.R. & Petersen, G.W. 1981. Texture transforms of remote sensing data. **Remote Sensing of Environment**, Vol. 11. pp. 359-370.

Irons, J.R., Peterson, G.W., Nelson, R.F., Toll, D.L., Williams, D.L., Latty, R.S. & Staufer, M.L. 1985. The effects of spatial resolution on the classification of TM data. **International Journal of Remote Sensing**, Vol. 6(8). pp. 1385-1403.

Irons, J.R., Ranson, K.J., Williams, D., Irish, R. & Huegel, F. 1991. An off-nadir-pointing imaging spectroradiometer for terrestrial ecosystem studies. **IEEE Transactions on Geoscience and Remote Sensing**, Vol. 29(1). pp. 66-74.

Jaggi, S., Quatrochi, D.A. & Lam, N.S.-N. 1993. Implementation and operation of three fractal measurement algorithms for analysis of remote-sensing data. **Computers and Geosciences**, Vol. 19(6). pp. 745-767.

Jensen, J.R. 1983. Biophysical remote sensing. **Annals of the Association of American Geographers**, Vol. 73(1). pp. 111-132.

Jensen, M.E. & Everett, R. 1994. An overview of ecosystem management principles, In M.E. Jensen & P.S. Bourgeron (Eds.) **Ecosystem Management: Principles and Applications, Eastside Forest Ecosystem Health Assessment**, USDA Forest Service, Pacific Northwest Research Station, General Technical Report PNW-GTR-318.

Jensen, J.R. & Hodgson, M.E. 1985. Remote sensing forest biomass: an evaluation using high resolution remote sensor data and Loblolly pine plots. **Professional Geographer**, Vol. 37(1). pp. 46-56.

Jensen, J.R. & Hodgson, M.E. 1987. Interrelationships between spatial resolution and per-pixel classifiers for extracting information classes Part I, pp. 121-129, In Proceedings, **1987 ASPRS-ACSM Annual Convention**, March 29-30, 1987, Baltimore, Maryland, American Society of Photogrammetry, Falls Church, Virginia.

Jensen, J.R. & Toll D.L. 1982. Detecting residential land-use development at the urban fringe. **Photogrammetric Engineering and Remote Sensing**, Vol. 48(4). pp. 629-643.

Jones, R. K., Pierpoint, G., Wickware, G. M., Jeglum, J. K., Arnup, R. W. & Bowles, J. M. 1983. **Field Guide to the Forest Ecosystem Classification for the Clay Belt, Site Region 3E.** Ontario Ministry of Natural Resources, Toronto, Ontario. 123 pp.

Joria, P.E., Ahearn, S.C. & Connor, M. 1991. A comparison of the SPOT and Landsat Thematic Mapper satellite systems for detecting gypsy moth defoliation in Michigan. **Photogrammetric Engineering and Remote Sensing**, Vol. 57(12). pp. 1605-1612.

Julesz, B., 1975. Experiments in the visual perception of texture. **Scientific American**, Vol. 232(4). pp. 34-43.

Julesz, B., 1981. Textons, the elements of texture perception, and their interactions. **Nature**, Vol. 290. pp. 91-97.

Jupp, D. L. B., Strahler, A. H. & Woodcock, C. E. 1989. Autocorrelation and regularization in digital images. II. Simple image models. **IEEE Transactions on Geoscience and Remote Sensing**, Vol. 27(3). pp. 247-257

Jupp, D. L. B., Strahler, A. H. & Woodcock, C. E. 1988. Autocorrelation and regularization in digital images. I. Basic theory. **IEEE Transactions on Geoscience and Remote Sensing**, Vol. 26(4). pp. 463-473

Kalensky, Z.D., Moore, W.C., Campbell, G.A., Wilson, D.A. & Scott, A.J. 1981. **Summary Forest Resource Data from Landsat Images,** Final Report of a Pilot Study for Northern Saskatchewan, Report PI-X-5, Petawawa National Forestry Institute, Canadian Forestry Service, 36 pp.

Kalnins, V. J., Treitz, P. M. & Howarth, P. J. 1994. **Rinker Lake Data Report 1993 - 1994.** Earth-Observations Laboratory, Technical Report ISTS-EOL-TR94-002, Waterloo, Ontario, variously paged.

Karpuk, E.W. 1978. **Ecological Land Classification South-East of Lesser Slave Lake, Alberta, using Airborne and Landsat Remote Sensing.** Unpublished

MSc. Thesis, Department of Geography, McMaster University, Hamilton, Ontario, Canada, 274 pp.

Karteris, M.A. 1990. The utility of digital Thematic Mapper data for natural resources classification. **International Journal of Remote Sensing**, Vol. 11(9). pp. 1589-1598.

Kaufman, Y.J., & Tanré, D. 1992. Atmospherically resistant vegetation index (ARVI) for EOS-MODIS. **IEEE Transactions on Geoscience and Remote Sensing**, Vol. 30. pp. 261-270.

Kershaw, C.D. 1987. Discrimination problems for satellite images. **International Journal of Remote Sensing**, Vol. 8(9). pp. 1377-1383.

Kimes, D.S., Newcomb, W.W., Nelson, R.F. & Schutt, J.B. 1986. Directional reflectance distributions of a hardwood and pine forest canopy. **IEEE Transactions on Geoscience and Remote Sensing**, Vol. 24. pp. 281-293.

King, A.W., 1991. Translating models across scales in the landscape, pp. 479-517, In M.G. Turner & R.H. Gardner (Eds.), **Quantitative Methods in Landscape Ecology, The Analysis and Interpretation of Landscape Heterogeneity**, Ecological Studies Series, Vol 82, Springer-Verlag, New York, 536 pp.

Kleckner, R.L., 1981. What is Classification?, pp. 128-134, In T.B. Brann, L.O. House IV, and H.G. Lund (Eds.), **In-Place Resource Inventories: Principles and Practices**, Proceedings, August 9-14, 1981, University of Maine, Orono, Maine, Society of American Foresters, Bethesda, Maryland.

Klemes, V. 1983. Conceptualization and scale in hydrology. **Journal of Hydrology**, Vol. 65. pp. 1-23.

Klinka, K., Nuszdorfer, F.C. & Skoda, L. 1979. **Biogeoclimatic Units of Central and Southern Vancouver Island.** B.C. Ministry of Forests, Victoria B.C., 120 pp. (+ 1:500,000 scale mapsheet).

Klinka, K., van der Horst, W.D., Nuszdorfer, F.C. & Harding, R.G. 1980. An ecosystematic approach to forest planning. **The Forestry Chronicle**, Vol. 56(3). pp. 97-103.

Kneppeck, I.D. & Ahern, F.J. 1989. A comparison of images from a pushbroom scanner with normal color aerial photographs for detecting scattered recent conifer mortality. **Photogrammetric Engineering and Remote Sensing**, Vol. 55(3). pp. 333-337.

Kogan, F.N. 1990. Remote sensing of weather impacts on vegetation in non-homogeneous areas. **International Journal of Remote Sensing**, Vol. 11(8). pp. 1405-1419.

Krajina, V.J. 1965. Biogeoclimatic zones and classification of British Columbia. **Ecology of Western North America**, Vol. 1. pp. 1-17.

Krajina, V. 1969. Ecology of forest trees in British Columbia. **Ecology of Western North America**, Department of Botany, University of B.C., Vancouver, B.C. Vol 2. pp. 1-144.

Kruse, F.A., Lefkoff, A.B., Boardman, J.W., Heidebrecht, K.B., Shapiro, A.T., Barloon, P.J. & Goetz, A.F.H. 1993. The spectral imaging processing system (SIPS) - Interactive visualization and analysis of imaging spectrometer data. **Remote Sensing of Environment**, Vol. 44. pp. 145-163.

Labovitz, M.L. & Masuoka, E.J. 1984. The influence of autocorrelation on signature extraction - an example from a geobotanical investigation of Cotter Basin, Montana. **International Journal of Remote Sensing**, Vol., 5(2). pp. 315-332.

Lacate, D.S. 1969. **Guidelines for Bio-Physical Land Classification: for Classification of Forest Lands and Associated Wildlands.** A progress report based on Bio-physical Land Classification pilot projects and discussions of the Subcommittee on Bio-physical Land Classification, National Committee on Forest Land, Ministry of Fisheries and Forestry, Ottawa, 59 pp.

Lambin, E.F., & Ehlich, D. 1995. Combining vegetation indices and surface temperature for land-cover mapping at broad spatial scales. **International Journal of Remote Sensing**, Vol. 16(3). pp. 573-579.

Lam, N.S.-N, 1990. Description and measurement of Landsat TM images using fractals. **Photogrammetric Engineering and Remote Sensing**, Vol. 56(2). pp. 187-195.

Lam, N.S.-N. & De Cola, L. 1993. Multifractals in image processing and process imaging. In N.S.-N. Lam & L. De Cola (Eds.), pp. 282-304, In **Fractals in Geography**, Prentice Hall, Enbglewood Cliffs, New Jersey, 308 pp.

Lam, N.S.-N. & Quattracchi, D.A. 1992. On the issue of scale, resolution and fractal analysis in the mapping sciences. **Professional Geographer**, Vol. 44. pp. 88-98.

Lathrop, R. G. J. & Pierce, L. L. 1991. Ground-based canopy transmittance and satellite remotely sensed measurements for estimation of coniferous forest canopy structure. **Remote Sensing of the Environment**, Vol. 36. pp. 179-188

Latty, R.S. & Hoffer, R.M. 1981. Computer-based classification accuracy due to the spatial resolution using per-point and per-field classification techniques. pp. 384-392, In P.G. Burroff and D.B. Morrison (Eds.), Proceedings, **7th Machine Processing of Remotely Sensed Data Symposium**, June 23-26, 1981, Purdue University, West Lafayette, Indiana, Purdue Research Foundation, West Lafayette, Indiana, 728 pp.

Laur, H., LeToan, T., & Lopes, A. 1987. Textural segmentation of SAR images using first Order Statistical Parameters. pp. 1463-1468, In Proceedings, **International Geoscience and Remote Sensing Symposium (IGARSS'87)**, May 18-21, 1987, Ann Arbor, Michigan, Published by IGARSS'87.

Leckie, D.G. 1987. Factors affecting defoliation assessment using airborne multispectral scanner data. **Photogrammetric Engineering and Remote Sensing**, Vol. 53(12). pp. 1665-1674.

Leckie, D.G. & Dombrowski, A. 1984. Enhancement of high resolution MEIS II data for softwood species discrimination. pp. 617-626, In Proceedings, **9th Canadian Symposium on Remote Sensing**, August 14-17, 1984, St. John's, Newfoundland, Canada.

Leckie, D.G. & Ostaff, D.P. 1988. Classification of airborne multispectral scanner data for mapping current defoliation caused by the spruce budworm. **Forest Science**, Vol. 34(2). pp. 259-275.

Leckie, D.G., Teillet, P.M., Ostaff, D.P. & Fedosejevs, G. 1988a. Sensor band selection for detecting current defoliation caused by the spruce budworm. **Remote Sensing of Environment**, Vol. 26. pp. 31-50.

Leckie, D.G., Teillet, P.M., Fedosejevs, G. & Ostaff, D.P. 1988b. Reflectance characteristics of cumulative defoliation of balsam fir. **Canadian Journal of Forest Research**, Vol. 18(8). pp. 1008-1016.

Leckie, D.G., Ostaff, D.P., Teillet, P.M. & Fedosejevs, G. 1989. Spectral characteristics of tree components of balsam fir and spruce damaged by spruce budworm. **Forest Science**, Vol. 35(2). pp. 582-600.

Leckie, D.G., Yuan, X. Ostaff, D.P. Piene, H. & MacLean, D.A. 1992. Analysis of high resolution multispectral MEIS imagery for Spruce Budworm damage assessment on a single tree basis. **Remote Sensing of Environment**, Vol. 40(2). pp. 125-136.

Leckie, D.G., Beaubien, J., Gibson, J.R., O'Neill, N.T., Piekutowski, T., & Joyce, S.P., 1995. Data processing and analysis for MIFUCAM: a trial of MEIS imagery for forest inventory mapping. **Canadian Journal of Remote Sensing**, Vol. 21(3), pp. 337-356.

Lee, T., Richards, J. & Swain, P. 1987. Probabilistic and evidential approaches for multi-source data analysis. **IEEE Transactions on Geoscience and Remote Sensing**, Vol. 25(3). pp. 283-292.

Lee, J.-H. & Philpot, W.D. 1991. Spectral texture pattern matching: a classifier for digital imagery. **IEEE Transactions on Geoscience and Remote Sensing**, Vol. 29(4). pp. 545-554.

Lendaris, G., & Stanley, G. 1970. Diffraction pattern samplings for automatic pattern recognition. **Proceedings IEEE**, Vol. 58, pp. 198-216.

Levac, P. 1991. Integrated Management of Forest Resources, pp. 144-148, In D.G. Brand (Ed.), **National Conference on Canada's Timber Resources**, June 3-5, 1990, Victoria, B.C., Forestry Canada, Petawawa National Forestry Institute, Chalk River, Ontario, Information Report PI-X-101, 174 pp.

Leverington, D.W. & Duguay, C.R. 1996. Evaluation of neural network performance in land cover classification. pp. 83-86, In Proceedings, **26th International Symposium on Remote Sensing of Environment / 18th Canadian Symposium on Remote Sensing**, Information Tools for Sustainable Development, March 25-29, Vancouver, B.C., 632 pp.

Li, X. & Strahler, A. 1985. Geometrical-optical modeling of a conifer forest canopy. **IEEE Transactions on Geoscience and Remote Sensing**, Vol. 23. pp. 705-721.

Li, X. & Strahler, A. 1986. Geometrical-optical bidirectional reflectance modeling of a conifer forest canopy. **IEEE Transactions on Geoscience and Remote Sensing**, Vol. 24. pp. 906-919.

Lillesand, T. M. & Kiefer, R. W. 1987. **Remote Sensing and Image Interpretation.** John Wiley and Sons, Toronto, Ontario. 721 pp.

Liu, H.Q., & Huete, A.R. 1995. A feedback based modification of the NDVI to minimize canopy background and atmospheric noise. **IEEE Transactions on Geoscience and Remote Sensing**, Vol 33. 457-465.

Lulla, K. 1983. The Landsat satellites and selected aspects of physical geography. **Progress in Physical Geography**, Vol. 7(1)1-45.

Mack, A.R., Desjardins, R.L., MacPherson, J.I. & Schuepp, P.H. 1990. Relative photosynthetic activity of agricultural lands from airborne carbon dioxide and satellite data. **International Journal of Remote Sensing**, Vol. 11(2). pp. 237-251.

Mackey, B.G., Sims, R.A., Baldwin, K.A., & Moore, I.D., 1994a. Spatial analysis of boreal forest ecosystems: results from the Rinker Lake case study, In **Second International Conference / Workshop on GIS and Environmental Modelling**, Breckenridge, Colorado, USA, 26-30 September 1993, NCGIA.

Mackey, B.G., McKenney, D.W., Widdifield, C.A., Sims, R.A., Lawrence, K., & Szcyrek, N., 1994b. **A New Digital Elevation Model of Ontario**, Canadian Forest Service, Sault Ste. Marie, Ontario, Northern Forestry Program (NODA/NFP) Technical Report No. TR-6, 26 pp.

Maclean, A.L., Reed, D.D., Mroz, G.D., Lyon, G.W. & Edison, T. 1992. Using GIS to estimate forest resource changes: A case study in northern Michigan. **Journal of Forestry**, Vol. 90(12). pp. 22-25.

Major, D.J., Baret, F. & Guyot, G. 1990. A ratio vegetation index adjusted for soil brightness. **International Journal of Remote Sensing**, Vol. 11(5). pp. 727-740.

Marceau, D. 1989. **A Review of Image Classification Procedures with Special Emphasis on the Grey-Level Coocurrence Matrix Method for Texture Analysis**, Earth Observations Laboratory, Institute for Space and Terrestrial Science, Report No. ISTS-EOL-TR89-007.

Marceau, D.J., Howarth, P.J., Dubois, J.M. & Gratton, D.J. 1990. Evaluation of the grey-level co-occurrence matrix method for land-cover classification using SPOT imagery. **IEEE Transactions on Geoscience and Remote Sensing**, Vol. 28(4). pp. 513-519.

Marceau, D. 1992. **The Problem of Scale and Spatial Aggregation in Remote Sensing: an Empirical Investigation using Forestry Data**, Unpublished PhD Thesis, Department of Geography, University of Waterloo, Waterloo, Ontario, 180 pp.

Marceau, D.J., Howarth, P.J. & Gratton, D.J. 1994a. Remote sensing and the measurement of geographical entities in a forested environment. 1. The scale and spatial aggregation problem. **Remote Sensing of Environment**, Vol. 49. pp. 93-104.

Marceau, D.J., Gratton, D.J., Fournier, R.A. & Fortin, J.-P. 1994b. Remote sensing and the measurement of geographical entities in a forested environment. 2. The optimal spatial resolution. **Remote Sensing of Environment**, Vol. 49. pp. 105-117.

Markham, B.L. & Townshend, J.R.G. 1981. Land cover classification accuracy as a function of sensor spatial resolution. pp. 1075-1090 In Proceedings, **15th International Symposium on Remote Sensing of Environment**, May 11-15, 1981, Ann Arbor, Michigan, Environmental Research Institute of Michigan, Ann Arbor, Michigan, 3 Volumes, 1556 pp.

Martin, L.R.G., Howarth, P.J. & Holder, G.H. 1988. Multispectral classification of land use at the rural-urban fringe using SPOT data. **Canadian Journal of Remote Sensing**, Vol. 14(2). pp. 72-79.

Mason, D.C., 1979. Segmentation of terrain images using textural and spectral characteristics. **Computers and Digital Techniques**, Vol. 2(6). pp. 251-259.

Matheron, G. 1963. Principles of geostatistics. **Economic Geology**, Vol. 58. pp. 1246-1266.

Matsuyama, T., Miura, S.I., & Nagao, M., 1983. Structural analysis of natural textures by Fourier transformation. **Computer Graphics and Image Processing**, Vol. 24, pp. 347-362.

Maus, P., Landrum, V., Johnson, J., Lachowski, H., Platt, B. & Schanta, M. 1992. Utilizing satellite data and GIS to map land cover change. pp. 1-6, In **GIS'92: Working Smarter**, Proceedings of the 6th International Symposium on Geographic Information Systems, February 10-13, 1992, Vancouver, British Columbia, Polaris Learning Associates, Vancouver, B.C., FRDA Report 173, 300 pp.

Mayer, K.E. & Fox, L. 1981. Identification of conifer species grouping from Landsat digital classifications. **Photogrammetric Engineering and Remote Sensing**, Vol. 47(11). pp. 1607-1614.

McCarthy, T.G., R.W. Arnup, J. Nieppola, B.G. Merchant, K.C. Taylor, & Parton, W.J. 1994. **Field Guide to Forest Ecosystems of Northeastern Ontario**, NEST Field Guide FG-001, Northeast Science and Technology Unit, Ontario Ministry of Natural Resources, Timmins, Ontario. variously paged.

McCormick, R.J., 1966. The Canada Land Inventory of ARDA. **Forestry Chronicle**, Vol 42, pp. 45-50.

McCormick, R.J., 1970. **The Canada Land Inventory, Land Capability Classification for Forestry**, Report No. 4, Department of Regional Economic Expansion, Ottawa, Ontario, 72 pp.

McGwire, K., Friedl, M. & Estes, J.E. 1993. Spatial structure, sampling design and scale in remotely-sensed imagery of a California savanna woodland. **International Journal of Remote Sensing**, Vol. 14(11). pp. 2137-2164.

McLean, N. H. & Uhlig, P. W. C. 1987. **Field Methods Training Manual for the Northwest Region FEC Mensuration Unit**, Timber Sales Branch, Ontario Ministry of Natural Resources.

McLeod, S.D. & Running, S.W. 1988. Comparing site quality indices and productivity in ponderosa pine stands in western Montana. **Canadian Journal Forest Research**, Vol. 18. pp. 346-352.

Meades, W. J. & Moores, L. 1989. **Forest Site Classification Manual: A Field Guide to the Damman Forest Types in Newfoundland**, Forestry Canada and the Department of Forestry and Agriculture, FRDA Report No. 003, Government of Newfoundland and Labrador.

Meentemeyer, V., 1989. Geographical perspectives of space, time and scale. **Landscape Ecology**, Vol. 3. pp. 163-173.

Meentemeyer, V. & Box, E. O., 1987. Scale effects in landscape studies. pp. 15-34, In M.G. Turner (Ed.), **Landscape Heterogeneity and Disturbance**, Ecological Studies, Vol. 64, Springer-Verlag, New York, 239 pp.

Meidinger, D. & Pojar, J. (Eds). 1991. **Ecosystems of British Columbia.** British Columbia Ministry of Forests, Crown Publications, Victoria, B.C., 330 pp.

Merchant, B. G., Baldwin, R. D., Taylor, E. P., Chambers, B. A., Gordon, A. M. & Jones, R. K. 1989. **Field Guide to a Productivity Oriented Pine Forest Ecosystem Classification for the Algonquin Region, Site Region 5E, first approximation.** Ontario Ministry of Natural Resources, Toronto, Ontario. 131 pp.

Merchant, J.W., 1984. Using spatial logic in classificaiton of Landsat TM data, **IEEE Pecora IX Symposium**, October 2-4, 1984, Sioux Falls, SD, pp. 378-385.

Miller, J.R., Elvidge, C.D., Rock, B.N. & Freemantle, J.R. 1990a. An airborne perspective on vegetation phenology from the analysis of AVIRIS data sets over the Jasper Ridge Biological Preserve. pp. 565-568, In R. Mills (Ed.), **International Geoscience and Remote Sensing Symposium (IGARSS'90): Remote Sensing for the Nineties**, May 20-24, 1990, University of Maryland, College Park, Maryland, Institute of Electrical and Electronics Engineers, New York, New York, 3 Volumes, 2488 pp.

Miller, J.R., Hare, E.W. & Wu, J. 1990b. Quantitative characterization of the vegetation red edge reflectance 1. An inverted-Gaussian reflectance model. **International Journal of Remote Sensing**, Vol. 11(10). pp. 1755-1773.

Miller, J.R., Wu, J., Boyer, M.G., Belanger, G. & Hare, E.W. 1991. Seasonal patterns in leaf reflectance red edge characteristics. **International Journal of Remote Sensing**, Vol. 12(7). pp. 1509-1523.

Mitchell, O.R., C.R. Myers & W. Boyne, 1977. A max-min measure for image texture analysis. **IEEE Transactions on Computers**, Vol. 26. pp. 408-416.

Mitchell O.R., & S.G. Carlton, 1978. Image segmentation using a local extrema texture measure. **Pattern Recognition**, Vol. 10, pp. 205-210.

Mollard, D.G. & Mollard, J.D. 1981. **Heaven Lake Area (NTS 52H/SW), District of Thunder Bay; Ontario Geological Survey, Northern Ontario Engineering Geology Terrain Study 41**, Ministry of Natural Resources, 26 pp. Accompanied by Map 5051, Scale 1:100 000.

Moore, I.D., Grayson, R.B., & Ladson, A.R., 1991. Digital terrain modelling: a review of hydrological, geomorphological and biological applications. **Hydrological Processes**, Vol., 5, pp. 3-30.

Muchoney D.M. & Haack, B.N. 1994. Change detection for monitoring forest defoliation. **Photogrammetric Engineering and Remote Sensing**, Vol. 60(10), pp. 1243-1251.

Mueller-Dombois, D. & Ellenberg, H. 1974. **Aims and Methods of Vegetation Ecology.** John Wiley and Sons, Toronto, 547 pp.

Musick, H.B. & Pelletier, R.E. 1988. Response to soil moisture of spectral indices derived from bidirectional reflectance in Thematic Mapper Bands. **Remote Sensing of Environment**, Vol. 25. pp. 167-184.

Musick, H.B. & Grover, H.D. 1990. Image textural measures as indices of landscape pattern, pp. 77-103. In M.G. Turner & R.H. Gardner (Eds.), **Quantitative Methods in Landscape Ecology, The Analysis and Interpretation of Landscape Heterogeneity**, Ecological Studies Series, Vol 82, Springer-Verlag, New York, 536 pp.

National Aeronautics and Space Administration (NASA), 1987. **HIRIS High Resolution Imaging Spectrometer: Science Opportunities for the 1990s**, Earth Observing System, Volume IIc, Instrument Panel Report, NASA, 74 pp.

National Forest Strategy Coalition, 1994. **National Forest Strategy, Sustainable Forests: A Canadian Commitment**, Mid-term Evaluation Report, Prepared by the Blue Ribbon Panel for the National Forest Strategy Coalition, variously paged.

National Vegetation Working Group, 1990. **The Canadian Vegetation Classification System**, W.L. Strong, E.J. Oswald & D.J. Downing (Eds.), National Vegetation Working Group, Canada Committee on Ecological Land Classification, Ecological Land Classification Series, No. 25, Environment Canada, Ottawa, Canada, 22 pp.

Nemani, R. & Running, S. 1989. Testing a theoretical climate-soil-leaf area index using a hydrologic equilibrium of forests using satellite data and ecosystem simulation. **Agriculture and Forest Meteorology**, Vol. 44. pp. 245-260.

Nemani, R., Pierce, L., Running, S. & Band, L. 1993. Forest ecosystem processes at the watershed scale: sensitivity to remotely-sensed Leaf Area Index estimates. **International Journal of Remote Sensing**, Vol. 14(13). pp. 2519-2534.

Neville, R.A., Rowlands, N., Marois, R., & Powell, I., 1995. SFSI: Canada's first airborne SWIR imaging spectrometer. **Canadian Journal of Remote Sensing**, Vol. 21, No. 3, pp. 328-336.

Nelson, R.F. 1983. Detecting forest canopy change due to insect activity using Landsat MSS. **Photogrammetric Engineering and Remote Sensing**, Vol. 49(9). pp. 1303-1314.

Nir, D., 1987. Regional geography considered from the systems approach. **Geoforum**, Vol 18(2), pp. 187-202.

Ojedele, B. 1987. Airborne multispectral scanner data for land cover classification. pp. 527-532, In **Advances in Digital Image Processing**, Proceedings of the Thirteenth Annual Conference of the Remote Sensing Society, September 7-11, 1987, Department of Geography, University of Nottingham, Nottingham, England, Remote Sensing Society, Nottingham, England, 675 pp.

Olea, R.A., 1977. **Measuring Spatial Dependence With Semi-Variograms**, Kansas Geological Survey, Campus West, Lawrence, Kansas.

Oliver, M. A. & Webster, R. 1989. A geostatistical basis for spatial weighting in multivariate classification. **Mathematical Geology**, Vol. 21(1). pp. 15-35

Oliver, M., Webster, R. & Gerrard, J. 1989. Geostatistics in physical geography. Part 1: theory. **Transactions of the Institute of British Geography**, Vol. 14. pp. 259-269

O'Neill, R.V., Johnson, A.R., & King, A.W., 1989. A hierarchical framework for the analysis of scale. **Landscape Ecology**, Vol. 3. pp. 193-205.

Openshaw, S., 1978. An empirical study of some zone-design criteria, **Environment and Planning A**, Vol 10, pp. 781-794.

Openshaw, S., 1984. **The Modifiable Areal Unit Problem, Concepts and Techniques in Modern Geography**, Concepts and Techniques in Modern Geography CATMOG Series, Geo Books, Regency House, Norwich, Vol. 38, 40 pp.

Openshaw, S. & Taylor, P.J. 1979. A million or so correlation coefficients: three experiments on the modifiable areal unit problem. pp. 127-144, In N. Wrigley, **Statistical Applications in the Spatial Sciences**, Pion, London, 310 pp.

Osborn, J., 1989. The forest database. pp. 155-169 In R.F. Calvert, B. Payandeh, M.F. Squires & W.D. Baker (Eds.), **Forest Investment: A Critical Look**, Forestry Canada, Sault Ste. Marie, Ontario, Information Report No. 0-P-17, 216 pp.

Otterman, J., Strebel, D. & Ranson, K. 1987. Inferring spectral reflectances of plant elements by simple inversion of bidirectional reflectance measurements. **Remote Sensing of Environment**, Vol. 21. pp. 215-228.

Ovington, J.D. 1962. Quantitative ecology and the woodland ecosystem concept. **Advanced Ecological Research**, Vol. 1. pp. 103-192.

Palmier, C. & Ansseau, C. 1992. Remote sensing of physiological disturbances related to sugar maple dieback in southern Québec: potentials of imaging spectrometry. pp. 133-137, In J.K. Hornsby, D.J. King and N.A. Prout (Eds.), **15th Canadian Symposium on Remote Sensing: A World of Applications**, June 1-4, 1992, Toronto, Ontario, Ontario Ministry of Natural Resources, Ontario Centre for Remote Sensing, North York, Ontario, 504 pp.

Pao, Y-H. 1989. **Additive Pattern Recognition and Neural Networks.** Addison-Wesley Publishing Co., Reading, Mass., 309 p.

Paradine, D.B., 1994a. **Empirical Identification of Forest Ecological Parameters from Airborne and Satellite Imagery of Northwestern Ontario**, Unpublished MES Thesis, Department of Geography, University of Waterloo, Waterloo, Ontario, 156 pp.

Paradine, D. 1994b. Section 4.3 FEC Data Collection. pp. 4-23 to 4-37, In V. J. Kalnins, P. M. Treitz & P. J. Howarth (Eds.), **Rinker Lake Data Report: 1993 - 1994**, Earth-Observations Laboratory, Technical Report ISTS-EOL-TR94-002, Waterloo, Ontario, variously paged.

PCI Inc., 1996. **EASI/PACE Image Analysis System Manual, Version 6.0.** PCI Inc., Toronto, Ontario, Canada, variously paged.

Peddle, D.R. 1993. An empirical comparison of evidential reasoning, linear discriminant analysis and maximum likelihood algorithms for alpine land cover classification. **Canadian Journal of Remote Sensing**, Vol. 19(1). pp. 31-45.

Peddle, D.R. & Franklin, S.E. 1991. Image texture processing and data integration for surface pattern discrimination. **Photogrammetric Engineering and Remote Sensing**, Vol. 57(4). pp. 413-420.

Peterson, D.L., Westman, W.E., Stephenson, N.J., Ambrosia, V.G., Brass, J.A. & Spanner, M.A. 1986. Analysis of forest structure using Thematic Mapper Simulation data. **IEEE Transactions on Geoscience and Remote Sensing**, Vol. 24(1). pp. 113-121.

Peterson, D.L., Spanner, M.A., Running, S.W. & Teuber, K.B. 1987. Relationship of Thematic Mapper simulator data to leaf area index of temperate coniferous forests. **Remote Sensing of Environment**, Vol. 22. pp. 323-341.

Peterson, D.L., Aber, J.D., Matson, P.A., Card, D.H., Swanberg, N., Wessman, C. & Spanner, M. 1988. Remote sensing of forest canopy and leaf biochemical contents. **Remote Sensing of Environment**, Vol. 24. pp. 85-108.

Pettinger, L.R. 1982. **Digital Classification of Landsat Data for Vegetation and Land-Cover Mapping in the Blackfoot River Watershed, Southeastern Idaho**, U.S. Geological Survey, Alexandria, Virginia, 33 pp.

Pierpoint, G. 1986. An orientation to site classification in Ontario, pp. 24-28, In G.M. Wickware & W.C. Stevens (Eds.), **Site Classification in Relation to Forest Management**, August 27-29, 1985, Sault Ste. Marie, Ontario, Canadian Forestry Service, Sault Ste. Marie, Ontario, COJFRC Symposium Proceedings , Report No. O-P-14, 142 pp.

Pierpoint, G. & Uhlig, P. 1985. **Catalogue of Land Resource Surveys in Ontario of Major Value in Forest Management**, Ontario Ministry of Natural Resources, Toronto, Ontario, 50 pp.

Pilon, P.G. & Wiart, R.J. 1990. Operational forest inventory applications using Landsat TM data: the British Columbia experience. **Geocarto International**, Vol. 5(1). pp. 25-30.

Plonski, W. L. 1974. **Normal Yield Tables (Metric) for Major Forest Species of Ontario.** Ontario Ministry of Natural Resources, Toronto, Ontario. 40 pp.

Pojar, J., Klinka, K. & Meidinger, D.V. 1987. Biogeoclimatic ecosystem classification in British Columbia. **Forest Ecology and Management**, Vol. 22. pp. 119-154

Price, M. 1986. The analysis of vegetation change by remote sensing. **Progress in Physical Geography**, Vol. 10(4). pp. 473-491.

Pultz, T.J., & Brown, R.J. 1987. SAR image classification of agricultural targets using first- and second-order statistics. **Canadian Journal of Remote Sensing**, Vol. 13(2). pp. 85-91.

Pye, E. G. 1968. **Geology of the Lac des Iles Area.** Ontario Dept. of Mines, Geological Report No. 64. 47 pp. + 2 maps.

Qi, J., Huete, A.R., Moran, M.S., Chehbouni, A., & Jackson, R.D. 1993. Interpretation of vegetation indices derived from multi-temporal SPOT images, **Remote Sensing of Environment**, Vol. 44, pp. 89-101.

Qi, J., Chehbouni, A., Huete, A.R., & Kerr, Y.H. 1994. Modified Soil Adjusted Vegetation Index (MSAVI), **Remote Sensing of Environment**, Vol. 48. pp. 119-126.

Racey, G.D., Whitfield, T.S. & Sims, R.A. 1989. **Northwestern Ontario Forest Ecosystem Interpretations**, NWOFTDU Technical Report No. 46, Ontario Ministry of Natural Resources, Thunder Bay, Ontario, Canada, 160 pp.

Ramstein, G. & Raffy, M. 1989. Analysis of the structure of radiometric remotely-sensed images. **International Journal of Remote Sensing**, Vol. 10(6). pp. 1049-1073

Ranson, K.J., Daughtry, C.S.T. & Biehl, L.L. 1986. Sun angle, view angle, and background effects on spectral response of simulated balsam fir canopies. **Photogrammetric Engineering and Remote Sensing**, Vol. 52(5). pp. 649-658.

Ranson, K.J., Irons, J.R. & Williams, D.L. 1994. Multispectral bidirectional reflectance of northern forest canopies with the Advanced Solid-State Array Spectroradiometer (ASAS). **Remote Sensing of Environment**, Vol. 47. pp. 276-289.

Rees, W.E. 1977. **The Canada Land Inventory in Perspective**, Lands Directorate, Environment Canada, Ottawa, Ontario, Report No. 12, 40 pp.

Rencz, A.N. & Nemeth, J. 1985. Detection of mountain pine beetle infestation using Landsat and simulated Thematic Mapper data. **Canadian Journal of Remote Sensing**, Vol. 11(1). pp. 50-58.

Richards, J.R. 1993. **Remote Sensing and Digital Image Processing: An Introduction**, Springer-Verlag, New York, 297 pp.

Richards, J.A. & Kelly, D.J. 1984. On the concept of spectral class. **International Journal of Remote Sensing**, Vol. 5(6). pp. 987-991.

Richardson, A.J., & Wiegand, C.L. 1977. Distinguishing vegetation from soil-background information. **Photogrammetric Engineering and Remote Sensing**, Vol. 43. pp. 1541-1542.

Richardson, A.J. & Wiegand, C.L. 1990. Comparison of two models for simulating the soil-vegetation composite reflectance of a developing cotton canopy. **International Journal of Remote Sensing**, Vol. 11(3). pp. 447-459.

Riordan, C.J. 1982. Change detection for resource inventories using digital remote sensing data, pp. 278-283, In T.B. Brann, L.O. House IV, and H.G. Lund (Eds.), **In-Place Resource Inventories: Principles and Practices**, Proceedings, August 9-14, 1981, University of Maine, Orono, Maine, Society of American Foresters, Bethesda, Maryland.

Ripple, W.J., Wang, S., Isaacson, D.L. & Paine, D.P. 1991. A preliminary comparison of Landsat Thematic Mapper and SPOT-1 HRV multispectral data for estimating coniferous forest volume. **International Journal of Remote Sensing**, Vol. 12(9). pp. 1971-1977.

Risser, P.G., Karr, J.R. & Forman, R.T.T. 1984. **Landscape Ecology, Directions and Approaches, Vol. III**, Natural History Survey Special Publications, No. 2.

Roach, D. & Fung, K.B., 1994. Fractal-based textural descriptors for remotely sensed forestry data. **Canadian Journal of Remote Sensing**, Vol. 20(1). pp. 59-70.

Roan S.J. & Aggarwal, J.K., 1987. Multiple resolution imagery and texture analysis. **Pattern Recognition**, Vol. 20(1), pp. 17-31.

Robinove, C.J. 1981. The logic of multispectral classification and mapping of land. **Remote Sensing of Environment**, Vol. 11. pp. 231-244.

Roberts, D.A., Smith, M.O. & Adams, J.B. 1993. Green vegetation, non-photosynthetic vegetation, and soils in AVIRIS data. **Remote Sensing of Environment**, Vol. 44. pp. 255-269.

Rock, B.N., Williams, D.L. & Vogelmann, J.E. 1985. Field and airborne spectral characterization of suspected acid deposition damage in red spruce (Picea rubens) from Vermont. pp. 71-81, In S.K. Mengel and D.B. Morrison (Eds.), **11th International Symposium on Machine Processing of Remotely Sensed Data**, June 25-27, 1985, Purdue University, West Lafayette, Indiana, Purdue Research Foundation, West Lafayette, Indiana, 370 pp.

Rock, B.N., Hoshaki, T. & Miller, J.R. 1988. Comparison of in situ and airborne spectral measurements of the blue shift associated with forest decline. **Remote Sensing of Environment**, Vol. 24. pp. 109-127.

Rock, B.N., Williams, D.L., Moss, D.M., Lauten, G.N. & Kim, M. 1994. High spectral resolution field and laboratory optical reflectance measurements of red spruce and eastern hemlock needles and branches. **Remote Sensing of Environment**, Vol. 47. pp. 176-189.

Rosenfield G.H. & Fitzpatrick-Lins, K. 1986. A coefficient of agreement as a measure of thematic classification accuracy. **Photogrammetric Engineering and Remote Sensing**, Vol. 52(2). pp. 223-227.

Rosenfeld, A., C.Y. Wang, & A.Y. Wu, 1982. Multispectral texture. **IEEE Transactions on Systems, Man and Cybernetics**, Vol. SMC-12, No. 1, pp. 79-83.

Rosenfeld, A., Lee, Y.H. & Thomas, R.B. 1970. Edge and curve detection for texture discrimination. pp. 381-387, In B.C. Lipkin and A. Rosenfeld (Eds.), **Picture Processing and Psychopictorics**, Academic Press, New York, 526 pp.

Rossi, R. E., Mulla, D. J., Journel, A. G. & Franz, E. H. 1992. Geostatistical tools for modeling and interpreting ecological spatial dependence. **Ecological Monographs**, Vol. 62(2). pp. 277-314.

Rotherham, T. 1993. The evolution of forest management philosophy in Canada. **Forestry Chronicle**, Vol. 69(2). pp. 115-116.

Rotunno, O.C., Treitz, P.M., Soulis, E.D., Howarth, P.J. & Kouwen, N. 1996. Texture processing of synthetic aperture radar data using second-order spatial statistics. **Computers and Geosciences**, Vol. 22(1). pp. 27-34.

Rouse, J.W., Haas, R.H., Schell, J.A. & Deering, D.W. 1974. Monitoring vegetation systems in the Great Plains with ERTS. pp. 309-317, In S.C. Freden, E.P. Mercanti and M.A. Becker (Eds.), **Third Earth Resources Technology Satellite-1 Symposium,** December 10-14, 1973, Goddard Space Flight Centre, Washington, D.C., National Aeronautics and Space Administration, Scientific and Technical Information Office, Washington, Dc., 3 Volumes, NASA SP-351.

Rowe, J.S., 1961. The level-of-integration concept and ecology. **Ecology**, Vol. 42, pp. 420-427.

Rowe, J.S. 1972. **Forest Regions of Canada**, Canadian Forestry Service, Department of the Environment, Ottawa, Ontario, Canada, Publication No. 1300, 172 pp.

Rowe, J. S. 1979. Revised working paper on methodology / philosophy of ecological land classification in Canada. pp. 23-30, In **Applications of Ecological (Biophysical) Land Classification in Canada**, Victoria, B.C., Canada Committee on Ecological (Biophysical) Land Classification, Ecological Land Classification Series Number 7.

Rowe, J.S., 1980. The common denominator in land classification in Canada: An ecological approach to mapping. **Forest Chronicle**, Vol. 56. pp. 19-20.

Rowe, J.S., 1984. **Understanding forest landscapes: what you conceive is what you get**, The Leslie L. Schaffer Forestry Lecture Series in Forest Science, October 1994, Vancouver, B.C., 13 pp.

Rowe, J.S., & Sheard, J.W., 1981. Ecological land classification: a survey approach. **Environmental Management**, Vol. 5. pp. 451-464.

Rowe, J.S., Haddock, P.G., Hills, G.A., Krajina, V.J. & Linteau, A. 1961. The ecosystem concept in forestry. pp. 55-59, Appendix H, In V.J. Krajina (Ed.), **1960 Progress**

Report - Ecology of the Forests of the Pacific Northwest, University of British Columbia, Vancouver, B.C., 62 pp. + appendices.

Rubec, C.D.A. 1983. Applications of remote sensing in ecological land surveys in Canada. **Canadian Journal of Remote Sensing**, Vol. 9(1). pp. 19-30.

Running, S.W., Peterson, D.L., Spanner, M.A. & Teuber, K.B. 1986. Remote sensing of coniferous forest leaf area. **Ecology**, Vol. 67. pp. 273-276.

Salwasser, H. 1990. Conserving biological diversity: A perspective on scope and approaches. **Forest Ecology and Management**, Vol. 35. pp. 79-90.

Schowengerdt, R.A. & Wang, H. 1989. A general purpose expert system for image processing. **Photogrammetric Engineering and Remote Sensing**, Vol. 55(9). pp. 1277-1284.

Schreuder, H.T. & Bonner, G.M. 1987. Forest inventories in the United States and Canada. **The Forestry Chronicle**, Vol. 63(12). pp. 431-434.

Sellers, P.J. 1985. Canopy reflectance, photosynthesis and transpiration. **International Journal of Remote Sensing**, Vol. 6(8). pp. 1335-1372.

Sellers, P.J., Berry, J.A., Collatz, G.J., Field, C.B., & Hall, F.G. 1992. Canopy reflectance, photosynthesis, and transpiration. III. A reanalysis using improved leaf models and a new canopy integration scheme. **Remote Sensing of Environment**, Vol. 42, pp. 187-216.

Shanmugan, K.S., F.M. Dickey & J.A. Green, 1979. An optimal frequency domain filter for edge detection in digital pictures. **IEEE Transactions on Pattern Analysis and Machine Intelligence**, Vol. PAMI-1, No. 1, pp. 37-49.

Shen, S.S., Badhwar, G.D. & Carnes, J.G. 1985. Separability of boreal forest species in the Lake Jennette area, Minnesota. **Photogrammetric Engineering and Remote Sensing**, Vol. 51(11). pp. 1775-1783

Shepherd, P.R. 1996. **Personal communication**, August 1996.

Shepherd, P.R. 1994. Section 3.3 Airborne Remote Sensing Data. pp. 3-19 to 3-48, In V. J. Kalnins, P. M. Treitz & P. J. Howarth (Eds.), **Rinker Lake Data Report - 1993 - 1994**, Earth-Observations Laboratory, Technical Report ISTS-EOL-TR94-002, Waterloo, Ontario, variously paged.

Shepherd P.R., Freemantle, J.R., McArdle, S., & Miller, J.R., 1995. A comparison of different operational reflectance generation methods applied to airborne CASI imagery, pp. 268-273, In Proceedings, **17th Canadian Symposium on Remote Sensing: Radar Remote Sensing: A Tool for Real-Time Land Cover Monitoring and GIS Integration**, June 13-15, 1995, Saskatoon, Saskatchewan, 816 pp.

Shilts, W.W., Aylsworth, J.M., Kaszycki, C.A. & Klassen, R.A. 1987. Canadian Shield. pp. 119-162, In W. L. Graf (Ed.), **Geomorphic Systems of North America.** The Geological Society of America, Boulder, Colorado, 643 pp.

Simonett, D.S. & Coiner, J.C. 1971. Susceptibility of environments to low resolution imaging for land-use mapping, pp. 373-394, In Proceedings, **Seventh International Symposium on Remote Sensing of Environment**, Ann Arbor, Michigan, Environmental Research Institute of Michigan, Ann Arbor, Michigan.

Sims, R. 1994. **Personal communication**, July 1994.

Sims, R. A., Towill, W. D., Baldwin, K. A. & Wickware, G. M. 1989. **Field Guide to the Forest Ecosystem Classification for Northwestern Ontario.** Ontario Ministry of Natural Resources, Toronto, Ontario. 191 pp.

Sims, R. A. & Uhlig, P. 1992. The current status of forest site classification in Ontario. **Forestry Chronicle**, Vol. 68(1). pp. 64-77.

Sims, R.A. & Baldwin, K.A. 1991. **Landform Features in Northwestern Ontario**, Canada-Ontario Forest Resources Development Agreement, COFRDA Report 3312, Forestry Canada - Ontario Region, Sault Ste. Marie, Ontario, NWOFTDU Technical Report 60, Ontario Ministry of Natural Resources, Thunder Bay, Ontario, Canada, 63 pp.

Sims, R.A., Kershaw, H.M. & Wickware, G.M. 1990. **The Autecology of Major Tree Species in the North Central Region of Ontario**, Canada-Ontario Forest Resources Development Agreement, COFRDA Report 3302, Forestry Canada - Ontario Region, Sault Ste. Marie, Ontario, and NWOFTDU Technical Report 48, Ontario Ministry of Natural Resources, Thunder Bay, Ontario, Canada, 126 pp.

Sims, R.A., Mackey, B.G., & Baldwin, K.A., 1994. Stand and landscape level applications of a forest ecosystem classification for northwestern Ontario Canada, Annales des Sciences Forestiere; Re Proceedings, **IUFRO 1.02-06 Site Classification and Evaluation Research Group Workshop**, October 19-22, 1993, Clermont-Ferrand, France.

Sims, R.A., & Mackey B.G., 1994. Development of spatially-based ecosystem models for the Rinker Lake Research Area in northwestern Ontario's boreal forest, pp. 665-674, In **GIS'94**, Proceedings of the 8th International Symposium on Geographic Information Systems, Vancouver, British Columbia

Singh, K. D. 1986. Conceptual framework for the selection of appropriate remote sensing techniques. pp. 1-14, In S. Sohlberg & V. E. Sokolov (Eds.), **Practical Application of Remote Sensing in Forestry**, Martinus Nijhoff Publishers, Boston, U.S.A.

Sirois, J. & Ahern, F.J. 1988. An investigation of SPOT HRV data for detecting recent Mountain Pine beetle mortality. **Canadian Journal of Remote Sensing**, Vol. 14(2). pp. 104-108.

Skidmore, A.K. 1989. An expert system classifies Eucalypt forest types using Thematic Mapper data and a digital terrain model. **Photogrammetric Engineering and Remote Sensing**, Vol. 55(10). pp. 1449-1464.

Skidmore, A.K. & Turner, B.J. 1988. Forest mapping accuracies are improved using a supervised nonparametric classifier with SPOT data. **Photogrammetric Engineering and Remote Sensing**, Vol. 54(10). pp. 1415-1421.

Smith, J.A., 1983. Matter-energy interaction in the optical region. pp. 62-113, In R.N. Colwell (Ed.), **Manual of Remote Sensing, Vol. I**, Second Edition, American Society of Photogrammetry and Remote Sensing, Falls Church, Virginia, 1232 pp.

Smith, J.L. 1986. Evaluation of the effects of photo measurement errors on predictions of stand volume from aerial photography. **Photogrammetric Engineering and Remote Sensing**, Vol. 52. pp. 401-410.

Smith, M.O., Austin, S.L., Adams, J.B. & Gillespie, A.R. 1990a. Vegetation in deserts: I. A regional measure of abundance from multispectral images. **Remote Sensing of Environment**, Vol. 31. pp. 1-26.

Smith, M.O., Austin, S.L., Adams, J.B. & Gillespie, A.R. 1990b. Vegetation in deserts: II. Environmental influences on regional abundances. **Remote Sensing of Environment**, Vol. 31. pp. 27-52.

Smith G.M. & Curran, P.J. 1995. The estimation of foliar biochemical content of a slash pine canopy from AVIRIS imagery. **Canadian Journal of Remote Sensing**, Vol. 21(3). pp. 234-244.

Society of American Foresters, 1950. **Forestry terminology**, Society of American Foresters, 75 pp.

Soulé, M.E. (Ed.). 1986. **Conservation Biology, The Science of Scarcity and Diversity**, Sinaur Associates, Sunderland, Massachusetts, 584 pp.

Spanner, M.A., Brass, J.A. & Peterson, D.L. 1984a. Feature selection and the information content of Thematic Mapper Simulator data for forest structural assessment. **IEEE Transactions on Geoscience and Remote Sensing**, Vol. 22(6). pp. 482-489.

Spanner, M.A., Peterson, D.L., Hall, M.H., Wrigley, R.C., Card, D.H. & Running, S.W. 1984b. Atmospheric effects on the remote sensing estimation of forest leaf area index., pp. 1295-1308, **Eighteenth International Symposium on Remote Sensing of Environment**, Paris, France, Environmental Research Institute of Michigan, Ann Arbor, Michigan.

Spanner, M.A., Pierce, L.L., Peterson, D.L. & Running, S.W. 1990a. Remote sensing of temperate coniferous forest leaf area index: the influence of canopy closure, understory vegetation and background reflectance. **International Journal of Remote Sensing**, Vol. 11 pp. 95-111.

Spanner, M.A., Pierce, L.L., Running, S.W. & Peterson, D.L. 1990b. The seasonality of AVHRR data of temperate coniferous forests: relationship with leaf area index. **Remote Sensing of Environment**, Vol. 33. pp. 97-112.

Srinivasan, A. & Richards, J.A. 1990. Knowledge-based techniques for multi-source classification. **International Journal of Remote Sensing**, Vol. 11(3). pp. 505-525.

Stanclik, G.E., 1986. The use of site classification by Abitibi-Price Inc. in the Iroquois Falls forest, In G.M. Wickware & W.C. Steven (Eds.), **Site Classification in Relation to Forest Management**, Canadian Forest Service, Sault Ste. Marie, Ontario, COJFRC Symposium Proceedings No. 0-P-14, 142 pp.

Stanek, W. & Orloci, L. 1987. **Some Silvicultural Ecosystems in the Yukon,** Canadian Forest Service, Victoria, B.C. Information Report BC-X-293, 56 pp.

Stenback, J. M. & Congalton, R. G. 1990. Using Thematic Mapper Imagery to Examine Forest Understory. **Photogrammetric Engineering and Remote Sensing**, Vol. 51(9). pp. 1285-1290.

Stohr, C.J. & West, T.R. 1985. Terrain and look angle effects upon multispectral scanner response. **Photogrammetric Engineering and Remote Sensing**, Vol. 51(2). pp. 229-235.

Stone, K.H. 1972. A geographer's strength: the multiple-scale approach. **The Journal of Geography**, Vol. 71(6). pp. 354-362.

Strahler, A.H. 1980. The use of prior probabilities in maximum likelihood classification of remotely sensed data. **Remote Sensing of Environment**, Vol. 10. pp. 505-525.

Strahler, A., Woodcock C.E. & Logan, T.L. 1980. Forest Stratification for timber inventory using registered digital Landsat and terrain model data in northern California. pp. 413-419, In T.T. Alfoldi (Ed.), **6th Canadian Symposium on Remote Sensing**, May 21-23, 1980, Halifax, Nova Scotia, Canadian Aeronautics and Space Institute, Ottawa, Ontario, 699 pp.

Strahler, A.H., Woodcock, C.E. & Smith, J.A. 1986. On the nature of models in remote sensing. **Remote Sensing of Environment**, Vol. 20. 121-139.

Sukachev, V. 1945. Biogeocoenology and phytocoenology. **C.R. Acad. Science USSR**, Vol. 47. pp. 429-431.

Sun, C. & Wee, W.G. 1983. Neighbouring gray level dependence matrix for texture classification. **Computer Vision, Graphics, and Image Processing**, Vol. 23. pp. 341-352.

Swain, P. H. & Davis, S. M. 1978. **Remote Sensing: the Quantitative Approach.** McGraw Hill, Inc., Toronto, Ontario, 396 pp.

SYSTAT Inc., 1992. **SYSTAT User's Guide - Statistics.** Evanston, Illinois, 724 pp.

Tansley, A.G., 1935. The use and abuse of vegetational concepts and terms. **Ecology**, Vol. 16. pp. 284-307.

Thie, J. 1974. Remote sensing for northern inventories and environmental monitoring. pp. 81-97, In **Canada's Northlands: Proceedings of a Technical Workshop to Develop an Integrated Approach to Base Data Inventories for Canada's Northlands**, April 17-19, 1974, Toronto, Ontario, Environment Canada, Lands Directorate Ottawa, Technical Paper 74-13, 298 pp.

Thomas, I.L. 1980. Spatial post-processing of spectrally classified Landsat data. **Photogrammetric Engineering and Remote Sensing**, Vol. 46. pp. 1201-1206.

Thompson, W.B., 1977. Textural boundary analysis. **IEEE Transactions on Computers**, Vol. 26. pp. 272-276.

Thompson, I.D., & Welsh, D.A., 1993. Integrated resource management in boreal forest ecosystems - impediments and solutions. **Forestry Chronicle**, Vol. 69, No. 1, pp. 32-39.

Tobler, W.R., 1969. Geographical Filters and their inverses. **Geographical Annals**, Vol. 1, pp. 234-253.

Toll, D.L. 1985. Landsat-4 Thematic Mapper scene characteristics of a suburban and rural area. **Photogrammetric Engineering and Remote Sensing**, Vol. 51(9). pp. 1471-1482.

Tom, C.H. & Miller, L.D. 1980. Forest site index mapping and modeling. **Photogrammetric Engineering and Remote Sensing**, Vol. 46(12). pp. 1585-1596.

Tom, C.H. & Miller, L.D. 1984. An automated land-use mapping comparison of the Bayesian maximum likelihood and linear discriminant analysis algorithms. **Photogrammetric Engineering and Remote Sensing**, Vol. 50(2). pp. 193-207.

Ton, J., Sticklen, J. & Jain, A.K. 1991. Knowledge-based segmentation of Landsat images. **IEEE Transactions on Geoscience and Remote Sensing**, Vol. 29(2). pp. 22-231.

Towill, W.D., Barauskas, A. & Johnston, R. 1988. **A Pre-cut Survey Method Incorporating the Northwestern Ontario Forest Ecosystem Classification.** Northwestern Ontario Forestry Technology Development Unit, Ontario Ministry of Natural Resources, Thunder Bay, Ontario, Technical Report No. 2, 25 pp.

Townshend, J.R.G. & Justice, C.O. 1980. Unsupervised classification of MSS Landsat data for mapping spatially complex vegetation. **International Journal of Remote Sensing**, Vol. 1(2). pp. 105-120.

Townshend, J.R.G. 1981. The spatial resolving power of earth resources satellites. **Progress in Physical Geography**, Vol. 5. pp. 32-55.

Townshend, J.R.G. 1983. Effects of spatial resolution on the classification of land cover type, pp. 101-112, In **Ecological Mapping from Ground, Air and Space**, November 25-27, 1981, Monks Wood Experiment Station, United Kingdom, Institute of Terrestrial Ecology, Cambridge, United Kingdom, Natural Environment Research Council, Institute of Terrestrial Ecology Symposium No. 10, 142 pp.

Treitz, P.M., & P.J. Howarth, 1996. **Remote Sensing for Forest Ecosystem Classification: A Review,** Natural Resources Canada, Canadian Forest Service - Sault Ste. Marie, Sault Ste. Marie ON. NODA/NFP Technical Report TR-12, 49 pp.

Treitz, P.M., Rotunno, O.C., Soulis, E.D., & P.J. Howarth, 1996. Textural Processing of Multi-Polarization SAR for Agricultural Crop Classification, pp. 1986-1988, In Proceedings, **International Geoscience and Remote Sensing Symposium (IGARSS'96)**, May 27-31, 1996, Lincoln, Nebraska.

Treitz, P.M., Howarth, P.J., Suffling, R.C. & Smith, P. 1992a. Application of detailed ground information to vegetation mapping with high spatial resolution digital imagery. **Remote Sensing of Environment**, Vol. 42. pp. 65-82.

Treitz, P.M., P.J. Howarth, & P. Gong. 1992b. Application of satellite and GIS technologies for land-cover and land-use mapping at the rural-urban fringe: a case study. **Photogrammetric Engineering and Remote Sensing**, Vol. 58(4). pp. 439-448.

Troll, C., 1971. Landscape ecology (geo-ecology) and bio-ceonology - a terminology study. **Geoforum**, Vol. 8. pp. 43-46.

Tucker, C.J. 1977. Asymptotic nature of grass canopy spectral reflectance. **Applied Optics**, Vol. 16. pp. 1151-1157.

Tucker, C.J. 1979. Red and photographic infrared linear combinations for monitoring vegetation. **Remote Sensing of Environment**, Vol. 8. pp. 127-150.

Tucker, C.J., Holben, B.N., Elgin, J.H. & McMurtry, J. 1981. Remote sensing of total dry matter accumulation in winter wheat. **Remote Sensing of Environment**, Vol. 11. pp. 171-189.

Tucker, C.J., Fung, I.Y., Keeling, C.D. & Gammon, R.H. 1986. Relationship between atmospheric CO_2 variations and a satellite-derived vegetation index. **Nature**, Vol. 319. pp. 195-199.

Tukey, J. W. 1977. **Exploratory Data Analysis.** Addison-Wesley Publishing Company, Don Mills, Ontario. 688 pp.

Turner, M.G., Dale, V.H., & Gardner, R.H., 1989a. Predicting across scales: Theory development and testing. **Landscape Ecology**, Vol. 3(3/4). pp. 245-252.

Turner, M.G., O'Neill, R.V., Gardner, R.H., & Milne, B.T., 1989b. Effects of changing spatial scale on the analysis of landscape pattern. **Landscape Ecology**, Vol. 3(3/4). pp. 153-162.

Uhlig, P.W.C., & Jordan, J.K., 1995. A spatial hierarchical framework for the co-management of ecosystems in Canada and the United Sates for the Upper Great Lakes Region, pp. 59-74, In R.A. Sims, I.G.W. Corns, and K. Klinka (Eds.), **Global to Local: Ecological Land Classification**, August 14-17, 1994, Thunder Bay, Ontario, Kluwer Academic Publishers, London, 610 pp.

Ulaby, F.T., Kouyate, F., Brisco, B. & Williams, T.H.L. 1986. Textural information in SAR images. **IEEE Transactions on Geoscience and Remote Sensing**, Vol. GE-24(2). pp. 235-245.

Urban, D.L., O'Neill, R.V. & Shugart, H.H., 1987. Landscape ecology - a hierarchical perspective can help scientists understand spatial patterns. **BioScience**, Vol 37. pp. 119-127.

Vane, G., Chrien, T.G., Miller, E.A. & Reimer, J.H. 1987. Spectral and radiometric calibration of the Airborne Visible/Infrared Imaging Spectrometer. **SPIE**, Vol. 834. pp. 91-105.

Vane, G., Green, R.O., Chrien, T.G., Enmark, H.T., Hansen, E.G. & Porter, W.M. 1993. The Airborne Visible/Infrared Imaging Spectrometer (AVIRIS). **Remote Sensing of Environment**, Vol. 44. pp. 127-143.

Van Gool, L., Dewaele, P. & Osterlinck, A. 1985. Texture analysis anno 1983. **Computer Vision, Graphics and Image Processing**, Vol. 29. pp. 336-357.

Veronese, V.F. & Mather, P.M. 1992. The incorporation of collateral information to image classification: A GIS/RS interface approach to remote sensing, pp. 590-599. In A.P. Cracknell & R.A. Vaughan (Eds.), **Remote Sensing from Research to Operation**, Proceedings of the 18th Annual Conference of the Remote Sensing Society, September 15-17, 1992, University of Dundee, Dundee, Scotland, Remote Sensing Society, Nottingham, England, 620 pp.

Vickers, A.L., & Modestino, J. W., 1982. A maximum likelihood approach to texture classification. **IEEE Transactions on Pattern Analysis and Machine Intelligence**. Vol. PAMI-4(1). pp.61-68.

Vilnrotter, F.M., R. Nevatia, & K.E. Price, 1986. Structural analysis of natural textures. **IEEE Transactions on Pattern Analysis and Machine Intelligence**, Vol. 8(1). pp. 76-89.

Vogelmann, J.E. & Rock, B.N. 1988. Assessing forest damage in high-elevation coniferous forests in Vermont and New Hampshire using Thematic Mapper. **Remote Sensing of Environment**, Vol. 24. pp. 227-246.

Vogelmann, J.E., Rock, B.N. & Moss, D.M. 1993. Red edge spectral measurements in sugar maple leaves. **International Journal of Remote Sensing**, Vol. 14. pp. 1563-1575.

Walsh, S. A., Sims, R. & Ford, J. 1994. Section 2.1 General Description of the Rinker Lake Research Area. pp. 2-5 to 2-14 In V. J. Kalnins, P. M. Treitz & P. J. Howarth (Eds.), **Rinker Lake Data Report - 1993**, Earth-Observations Laboratory, Technical Report ISTS-EOL-TR94-002, Waterloo, Ontario, variously paged.

Walsh, S.A. & Wickware, G.M. 1991. **Stand and Site Conditions Associated with the Occurrence and Distribution of Black Spruce Advance Growth in North Central Ontario**, Canada-Ontario Forest Resources Development Agreement, COFRDA Report 3309, Forestry Canada - Ontario Region, Sault Ste. Marie, Ontario, and NWOFTDU Technical Report 24, Ontario Ministry of Natural Resources, Thunder Bay, Ontario, Canada, 37 pp.

Walsh, S.J., 1980. Coniferous tree species mapping using Landsat data. **Remote Sensing of Environment**, Vol. 9, pp. 11-26.

Wang, Y. & Civco, D.L. 1996. Land cover classification from multisource data by three artificial neural networks paradigms. pp. 79-82. In Proceedings, **26th International Symposium on Remote Sensing of Environment / 18th Canadian Symposium on Remote Sensing, Information Tools for Sustainable Development**, March 25-29, Vancouver, B.C., 632 pp.

Wang, F. 1990a. Fuzzy supervised classification of remote sensing images. **IEEE Transactions on Geoscience and Remote Sensing**, Vol. 28(2). pp. 194-201.

Wang, F. 1990b. Improving remote sensing image analysis through fuzzy information representation. **Photogrammetric Engineering and Remote Sensing**, Vol. 56(8). pp. 1163-1169.

Wang, F. & Newkirk, R. 1988. A knowledge-based system for highway network extraction. **IEEE Transactions on Geoscience and Remote Sensing**, Vol. 26(5). pp. 525-530.

Wang, L. & He, D.C. 1990. A new statistical approach for texture analysis. **Photogrammetric Engineering and Remote Sensing**, Vol. 56(1). pp. 61-66.

Webster, R. 1985. Quantitative spatial analysis of soil in the field. **Advances in Soil Science**, Vol. 3. pp. 1-70.

Webster, R., Curran, P.J. & Munden, J.W., 1989. Spatial correlation in reflected radiation from the ground and its implications for sampling and mapping by ground-based radiometry. **Remote Sensing of Environment**, Vol. 29. pp. 67-78.

Wessman, C.A., Aber, J.D., Peterson, D.L. & Melillo, J. 1988. Remote Sensing of canopy chemistry and nitrogen cycling intemperate forest ecosystems. **Nature**, Vol. 335. pp. 154-156.

Wessman, C.A., Aber, J.D. & Peterson, D.L. 1989. An evaluation of imaging spectrometry for estimating forest canopy chemistry. **International Journal of Remote Sensing**, Vol. 10(8). pp. 1293-1316.

Weszka, J. C., Dyer, R. & Rosenfeld, A. 1976. A comparative study of texture measures for terrain classification. **IEEE Transactions on Systems, Man and Cybernetics**, Vol. 6. pp. 265-285

Wharton, S.W. 1982. A contextual classification method for recognizing land use patterns in high resolution remotely sensed data. **Pattern Recognition**, Vol. 15(4). pp. 317-324.

White, K. 1991. Progress Reports: Remote Sensing. **Progress in Physical Geography**, Vol. 15(1). pp. 71-76.

White, P.S., 1987. Natural disturbance, path dynamics, and landscape patterns in natural areas. **Natural Areas Journal**, Vol. 7(1). pp. 14-22.

Wilkinson, G.G. & Megier, J. 1990. Evidential reasoning in a pixel classification hierarchy - a potential method for integrating image classifiers and expert system rules based on geographic context. **International Journal of Remote Sensing**, Vol. 11(10). pp. 1963-1968.

Whittaker, R. H., 1957. The kingdoms of the living world. **Ecology**, Vol. 38(3). pp. 536-538.

Wickware, G.M. 1989. **Forest Ecosystem Classification of the Turkey Lakes Watershed, Ontario**, Lands Directorate, Environment Canada, Ottawa, Ontario, Ecological Land Classification Series, No. 18, 33 pp.

Wickware, G.M., 1989. **Photo interpretation of the NW Ontario FEC vegetation and soil types for the Aulneau Peninsula, northwestern Ontario**, Northwestern Ontario Forest Technology Development Unit, Ontario, Ministry of Natural Resources, Thunder Bay, Ontario, Technical Report No. 54, 32 pp.

Wickware, G.M. & Howarth, P.J. 1981. Change detection in the Peace-Athabasca Delta using digital Landsat data. **Remote Sensing of Environment**, Vol. 11. pp. 9-25.

Wickware, G. M. & Rubec, C. D. A. 1989. **Ecoregions of Ontario**, Sustainable Development Branch, Environment Canada, Ottawa, Ontario, Canada. Ecological Land Classification Series No. 26, 37 pp.

Wiegand, C.L., Richardson, A.J., Escobar, D.E. & Gerbermann, A.H. 1991. Vegetation indices in crop assessment. **Remote Sensing of Environment**, Vol. 35. pp. 105-119.

Wiersma, W. & Landgrebe, D. 1979. The analytical approach to the design of spectral measurements in the design of multispectral sensors. pp. 331-341, In I.M. Tendam and D.B. Morrison (Eds.), **5th Machine Processing of Remotely Sensed Data Symposium**, June 27-29, 1979, Purdue University, West Lafayette, Indiana, Institue of Electrical and Electronics Engineers, New York, New York, 468 pp.

Wiken, E.B. 1986. **Ecozones of Canada**, Ecological Land Classification Series, No. 19, Lands Directorate, Environment Canada, Ottawa, Ontario, Canada, 26 pp.

Wiken, E.B., Senyk, J.P. & Oswald, E., 1981. Inventorying land resources through an ecologically based approach. pp. 144-148, In T.B. Brann, L.O. House IV, and H.G. Lund (Eds.), **In-Place Resource Inventories: Principles and Practices**, Proceedings, August 9-14, 1981, University of Maine, Orono, Maine, Society of American Foresters, Bethesda, Maryland.

Wiken, E. B. & Ironside, G. 1977. The development of ecological (biophysical land classification in Canada. **Landscape Planning**, Vol. 4. pp. 273-282

Williams, D.L. & Nelson, R.F. 1986. Use of remotely sensed data for assessing forest stand conditions in the eastern United States. **IEEE Transactions on Geoscience and Remote Sensing**, Vol. 24(1). pp. 130-138.

Woodcock, C.E., 1985. **Understanding Spatial Variation in Remotely Sensed Imagery**, Ph.D. Dissertation, University of California, Santa Barbara, pp. 136 pp.

Woodcock, C.E. & Strahler, A.H. 1985. Relating ground scenes to spatial variation in images. pp. 393-449, In Proceedings, **Third NASA Conference on Mathematical Pattern Recognition and Image Analysis**, June 10-11, 1985, Texas A and M University, Texas, Texas A and M University, College Station, Texas, 535 pp.

Woodcock, C.E. & Strahler, A. H. 1987. The factor of scale in remote sensing. **Remote Sensing of Environment**, Vol. 21. pp. 333-339.

Woodcock, C.E., Strahler, A.H. & Jupp, D.L.B. 1988a. The use of variograms in remote sensing: I. Scene models and simulated images. **Remote Sensing of Environment**, Vol. 25. pp. 323-348.

Woodcock, C.E., Strahler, A.H. & Jupp, D.L.B. 1988b. The use of variograms in remote sensing: II. Real images. **Remote Sensing of Environment**, Vol. 25. pp. 349-379.

Yoder, B.J., & Waring, R.H. 1994. The Normalized Difference Vegetation Index of small Douglas-Fir canopies with varying chlorophyll concentrations. **Remote Sensing of Environment**, Vol. 49 pp. 81-91.

Yuan, X., King, D. & Vlcek, J. 1991. Sugar Maple decline assessment based on spectral and textural analysis of multispectral aerial videography. **Remote Sensing of Environment**, Vol. 37. pp. 47-54.

Zelazny, V.F., Ng, T.T.M., Hayter, M.G., Bowling, C.L., & Bewick, D.A., 1989. **Field Guide to Forest Site Classification in New Brunswick**, Department of Natural Resources and Energy, Fredericton, N.B., unpaginated.

Zoltai, S.C. 1965. **Forest Site Regions 5S and 4S, Northwestern Ontario, Volume I**, Research Report 65, Ontario Department of Lands and Forests, Toronto, Ontario, 121 pp.

Zoltai, S.C. 1974. **Forest Site Regions 5S and 4S, Northwestern Ontario, Volume II**, Research Report No. 95, Forest Research Branch, Ontario Ministry of Natural Resources, Toronto, Ontario, 96 pp.

Zonneveld, I.S., 1989. The land unit - A fundamental concept in landscape ecology, and its applications. **Landscape Ecology**, Vol. 3(2). pp. 67-86.

APPENDIX A

SUSTAINABLE FORESTS: A CANADIAN COMMITMENT

APPENDIX A

SUSTAINABLE FORESTS: A CANADIAN COMMITMENT

The Canadian Council of Forest Ministers (CCFM) is the trustee of the National Forest Strategy - *"Sustainable Forests: A Commitment to Canadians."* The overall goal of CCFM related to sustainable forests is "...to maintain and enhance the long-term health of our forest ecosystems, for the benefit of all living things both nationally and globally, while providing environmental, economic, social and cultural opportunities for the benefit of present and future generations" (CCFM, 1992, p. 7). In 1991, CCFM held a series of public forums, soliciting the Canadian public to express their concerns, hopes and ideas for Canada's forests. Emerging from these consultations was a series of strategic directions and commitments, some of which pertain to the research presented in this thesis. These are as follows:

Strategic Direction 1: Forest Stewardship - The Forest Environment

Commitment - to improve our ability to manage forest ecosystems and to maintain their productive capacity and resilience:

Task 1.1 Governments will complete an ecological classification of forest lands.

The majority of provinces are currently developing ecological classification systems with associated field guides. Although substantial progress is being made in the development of ecological site classification tools, only a small percentage of Canada's forests have been mapped by site classification (CCFM 1992).

Strategic Direction 2: Forest Stewardship - Forest Management Practices

Commitment - to improve our ability to plan for a full range of forest values:

Task 2.1 Public and private forest management agencies will broaden the scope of their inventories to include the additional information needed to manage forests on an ecosystem basis, to provide for a full range of forest values and to forecast the growth and yield of various forest resources.

Planning and implementing new forest inventory systems is a time consuming and challenging undertaking, particularly at the site level. In order to meet this directive, a cost-effective method of collecting ecosystem information is required to effectively map forest ecosystems.

Strategic Direction 3: Public Participation - Expanding the Dialogue

Commitment - to improve public access to easy-to-understand information on forests:

Task 3.4 By 1993, the CCFM will prepare a plan to upgrade the national database on forests to improve information on forest regeneration, and to include data on non-timber values such as wildlife, wilderness and recreation.

Plans are in place to expand on the reporting of regeneration results in the National Forestry Database Program (NFDP) (CCFM, 1992). In addition to regeneration results, non-timber values will be incorporated into this database, once national standards for reporting on such amenities are developed. This commitment incorporates a monitoring component that will provide accurate and timely information on forest resources. This suggests ongoing monitoring and updating activities that will require remote sensing and GIS technologies to maintain such a database.

Strategic Direction 4: Economic Opportunities - A Changing Framework

Commitment - to increase the use of Canadian goods and services in world markets:

Task 4.14 Industry and governments will promote exports based on science and technology applications and services related to natural resources, such as Geographic Information Systems (GISs), biotechnology and remote sensing.

There is a commitment to share Canadian expertise in science and technology related to forest measurement and mapping. This expertise can be exported in the form of applications and services, contributing to the nation's revenue related to the forest industry.

APPENDIX B

LOW-ALTITUDE SEMIVARIOGRAM ANALYSIS

APPENDIX B

LOW-ALTITUDE SEMIVARIOGRAM ANALYSIS

Transect A (#Lags = 20)
Aspen Dominated Hardwood (V5/V8)

Transect	Range (pixels)	Range (m)	Range (m^2)	Sill (10^3)	Cov/Cor (10^3)	IGF (10-9) Type	Comments
a13	4.80	3.36	18.01	126.40	156.83	4.72 Periodic	difficult to fit model (10 pixel cycle)
a23	13.00	9.10	46.78	289.00	232.04	0.82 Classic	slight dip @ 4-5 pixels
a33	10.20	7.14	38.27	395.00	305.72	5.33 Periodic-Classic	smooth curve
a43	10.00	7.00	37.52	390.00	310.01	6.46 Periodic-Classic	very similar to periodic-classic curve in Curran for deciduous
a53	5.00	3.50	18.76	180.00	162.06	9.50 Periodic-Classic	poor fit due to periodicity
a63	6.00	4.20	22.51	440.00	392.41	2.77 Classic	
Mean	8.17	5.72	30.64	303.40	259.85		
Median	8.00	5.60	30.02	339.50	268.88		
Std. Dev.	3.37	2.36	12.66	127.53	92.89		
Minimum	4.80	3.36	18.01	126.40	156.83		
Maximum	13.00	9.10	48.78	440.00	392.41		
a17	5.80	4.06	21.76	13020.00	20832.70	2.55 Periodic-Classic	smooth curve
a27	9.20	6.44	34.52	14600.00	13249.00	2.96 Periodic-Classic	
a37	10.20	7.14	38.27	21000.00	18811.50	1.74 Classic	difficult to identify sill and range
a47	10.80	7.56	40.52	24000.00	18640.00	2.95 Classic	variable sill
a57	7.00	4.90	26.26	10600.00	11828.40	7.09 Multi-frequency	1st sill used in range determination
a67	9.20	6.44	34.52	24200.00	30073.20	1.58 Periodic-Classic	10 pixel cycle
Mean	8.70	6.09	32.64	17903.33	18922.47		
Median	9.20	6.44	34.52	17800.00	18725.75		
Std. Dev.	1.92	1.35	7.21	5907.70	6495.94		
Minimum	5.80	4.06	21.76	10600.00	11828.40		
Maximum	10.80	7.56	40.52	24200.00	30073.20		

Transect B (#Lags = 15)
Lowland Black Spruce (V36/V37/V38)

Transect	Range (pixels)	Range (m)	Range (m^2)	Sill (10^3)	Cov/Cor (10^3)	IGF (10-9) Type	Comments
b13	2.40	1.68	9.00	121.80	132.78	1.75 Classic	a second structure should be used (e.g., exponential)
b23	2.80	1.96	10.51	97.50	113.29	3.49 Classic-Multifrequency	variable sill
b33	2.20	1.54	8.25	120.00	119.69	6.97 Periodic	repeatable pattern @ 7-8 pixels, sill difficult to define
b43	2.80	1.96	10.51	194.00	198.37	1.96 Periodic-Classic	variable sill
b53	2.40	1.68	9.00	105.00	99.41	2.72 Classic	variable sill
Mean	2.52	1.76	9.46	127.66	132.71		
Median	2.40	1.68	9.00	120.00	119.69		
Std. Dev.	0.27	0.19	1.01	38.46	38.62		
Minimum	2.20	1.54	8.25	97.50	99.41		
Maximum	2.80	1.96	10.51	194.00	198.37		
b17	8.60	6.02	32.27	1600.00	1558.73	3.77 Periodic-Classic	requires 2 models to fit 1st/2nd structures
b27	11.40	7.98	42.77	2350.00	2146.34	0.94 Classic	slight dip @ 4-5 pixels
b37	4.00	2.80	15.01	1400.00	1175.26	2.06 Periodic	sill forced due to periodicity
b47	6.00	4.20	22.51	3192.00	3764.57	1.67 Classic	variable sill
b57	5.00	3.50	18.76	1650.00	1578.60	7.03 Periodic-Classic	
Mean	7.00	4.90	26.26	2038.40	2044.90		
Median	6.00	4.20	22.51	1650.00	1578.60		
Std. Dev.	3.00	2.10	11.24	737.99	1021.85		
Minimum	4.00	2.80	15.01	1400.00	1175.26		
Maximum	11.40	7.98	42.77	3192.00	3764.57		

Transect D (#Lags = 20)
Aspen Dominated Hardwood (V5/V8)

Transect	Range (pixels)	Range (m)	Range (m^2)	Sill (10^6)	Cov/Cor (10^6)	IGF (10^{-6})	Type	Comments
d13	13.60	9.52	51.03	240.00	180.62	7.16	Classic-Periodic	strong inflection pt @ 6 pixels (Sill=165000)
d23	5.20	3.64	19.51	150.00	129.10	7.11	Periodic-Classic	cycle = 10 pixels
d33	5.20	3.64	19.51	135.00	176.10	1.49	Classic-Periodic	flat sill 5-12 pixels, then rises to 180000
d43	9.80	6.86	36.77	120.00	94.88	1.39	Classic	good fit
d53	7.20	5.04	27.01	150.00	143.27	0.76	Classic	good fit, variable sill
d63	5.60	3.92	21.01	82.00	62.48	9.54	Classic-Periodic	10 pixels cycle
d73	5.00	3.50	18.76	101.75	108.96	0.96	Classic	good fit, variable sill
Mean	7.37	5.16	27.66	139.82	125.06			
Median	5.60	3.92	21.01	135.00	129.10			
Std. Dev.	3.24	2.27	12.15	50.75	39.38			
Minimum	5.00	3.50	18.76	82.00	62.48			
Maximum	13.60	9.52	51.03	240.00	176.10			
d17	15.20	10.64	57.03	18000.00	12370.40	3.46	Classic-Periodic	strong inflection pt @ 7 pixels
d27	16.00	12.60	67.54	21000.00	14202.70	2.41	Classic	inflection pt @ 6 pixels
d37	7.60	5.46	29.27	10400.00	12023.30	2.32	Classic-Periodic	flat sill 5-12 pixels, then rises
d47	13.20	9.24	49.53	14000.00	9963.51	2.24	Classic	good fit
d57	7.60	5.32	28.52	11800.00	10086.90	4.85	Classic	sill declines
d67	6.20	4.34	23.26	7900.00	7079.03	5.97	Classic-Periodic	period not as strong as visible
d77	6.80	4.76	25.51	9600.00	9404.89	2.75	Classic	sill rises to 11000000 @ 12 pixels
Mean	10.69	7.48	40.09	13242.86	10732.96			
Median	7.80	5.46	29.27	11800.00	10086.90			
Std. Dev.	4.71	3.30	17.68	4749.69	2327.72			
Minimum	6.20	4.34	23.26	7900.00	7079.03			
Maximum	16.00	12.60	67.54	21000.00	14202.70			

Transect E (#Lags = 20)
Lowland Black Spruce (V35/36)

Transect	Range (pixels)	Range (m)	Range (m^2)	Sill (10^6)	Cov/Cor (10^6)	IGF (10^{-6})	Type	Comments
e13	4.40	3.08	16.51	139.50	158.26	2.75	Classic	sharp peak @ 15 pixels
e23	7.00	4.90	26.26	270.00	235.02	1.77	Classic	slow decline in sill > 8 pixels
e33	6.40	4.48	24.01	270.00	226.46	11.00	Classic-Periodic	cycle = 16 pixels
e43	4.40	3.08	16.51	313.50	327.13	1.94	Classic	small 8 pixel cycle
e53	7.20	5.04	27.01	420.00	311.79	4.96	Classic	1st period = 12 pixels
e63	4.20	2.94	15.76	110.00	111.93	2.95	Classic	difficult fit (variable sill with peak at 3 and 8 pixels
e73	3.80	2.66	14.26	145.00	137.40	1.56	Classic	variable sill, particularly at longer lag
e83	8.60	6.02	32.27	290.00	218.39	3.32	Classic-Periodic	cycle = 20 pixels
e93	4.20	2.94	15.76	190.00	173.30	1.33	Classic	variable sill
e103	6.00	4.20	22.51	200.00	168.69	4.91	Classic	variable sill
Mean	5.62	3.93	21.09	234.80	206.84			
Median	5.20	3.64	19.51	235.00	195.85			
Std. Dev.	1.65	1.15	6.17	95.43	71.15			
Minimum	3.80	2.66	14.26	110.00	111.93			
Maximum	8.60	6.02	32.27	420.00	327.13			
e17	5.40	3.78	20.26	3660.00	6058.85	2.63	Classic	sharp peak @ 15 pixels
e27	8.40	4.48	24.01	5300.00	5286.74	4.46	Classic	steady increase > 15 pixels
e37	6.20	4.34	23.26	5900.00	5210.46	13.17	Classic-Periodic	cycle = 16 pixels
e47	6.00	4.20	22.51	6045.00	6420.84	1.88	Classic	variable sill
e57	9.00	6.30	33.77	9700.00	7280.66	2.90	Classic	slow decline > 10 pixels
e67	4.60	3.22	17.26	1965.00	2762.97	3.38	Classic-Multifrequency	steady rise between 8 to 16 pixels
e77	4.80	3.36	18.01	3000.00	2646.02	6.88	Classic-Periodic	large dip @ 16 pixels
e87	8.20	5.74	30.77	7100.00	6290.33	2.81	Classic	
e97	6.00	4.20	22.51	7600.00	5848.26	12.14	Periodic	cycle = 10 pixels
e107	9.80	6.86	36.77	3800.00	3081.32	3.47	Classic-Periodic	18 pixel cycle
Mean	6.64	4.65	24.91	5407.00	5088.46			
Median	6.10	4.27	22.89	5600.00	5616.50			
Std. Dev.	1.77	1.24	6.63	2358.02	1671.93			
Minimum	4.60	3.22	17.26	1965.00	2646.02			
Maximum	9.80	6.86	36.77	9700.00	7280.66			

Transect F (#Lags = 15)
Lowland Black Spruce (V37)

Transect	Range (pixels)	Range (m)	Range (m^2)	Sill (10^3)	Cov/Cor (10^3)	IQF (10-3)	Type	Comments
f13	4.00	2.80	15.01	82.00	71.45	5.27	Classic	variable sill (difficult to fit with single model)
f23	3.80	2.66	14.26	89.00	78.74	9.59	Classic	variable sill (periodic)
f33	5.40	3.78	20.26	114.00	113.05	2.32	Classic	variable sill (sharp rise again at 18 pixels)
f43	2.80	1.96	10.51	180.00	165.48	7.75	Periodic-Classic	variable (periodic) sill
Mean	4.00	2.80	15.01	116.25	107.18			
Median	3.90	2.73	14.63	101.50	95.89			
Std. Dev.	1.07	0.75	4.02	44.66	42.89			
Minimum	2.80	1.96	10.51	82.00	71.45			
Maximum	5.40	3.78	20.26	180.00	165.48			
f17	4.00	2.80	15.01	1200.00	1100.15	7.74	Classic	sill has less variability than viable
f27	4.80	3.36	18.01	1430.00	1379.48	4.29	Classic	sill is less variable but still has periodic tendencies
f37	5.80	4.06	21.76	1804.00	2118.63	4.65	Classic	good classic curve except for rise at 16 pixels
f47	3.80	2.66	14.26	2100.00	1855.86	12.50	Periodic-Classic	very poor fit of classic curve due to variability/periodicity
Mean	4.60	3.22	17.26	1633.50	1613.56			
Median	4.40	3.08	16.51	1617.00	1617.72			
Std. Dev.	0.91	0.64	3.41	398.34	459.07			
Minimum	3.80	2.66	14.26	1200.00	1100.15			
Maximum	5.80	4.06	21.76	2100.00	2118.63			

Transect K (#Lags = 20)
Upland Black Spruce (V33)

Transect	Range (pixels)	Range (m)	Range (m^2)	Sill (10^3)	Cov/Cor (10^3)	IQF (10-3)	Type	Comments
k13	6.20	4.34	23.26	130.00	125.74	2.41	Classic-Multifrequency	2nd peak @ 13 (160000
k23	11.60	8.12	43.52	125.37	123.68	1.24	Classic	inflection pt @ 5.8 (80000)
k33	7.20	5.04	27.01	190.71	210.07	2.55	Classic-Multifrequency	not smooth curve, below the cov/corr level, peaks @ 10 and 20
k43	8.40	5.88	31.52	223.20	230.50	4.03	Multifrequency	smooth curve, peaks @ 8 and 20 (modal to fit 1st peak)
k53	4.80	3.36	18.01	84.37	93.87	1.78	Classic-Multifrequency	not smooth curve, below cov/corr level, similar to k33
k63	5.80	4.06	21.76	153.60	159.57	2.16	Classic	variable sill
k93	3.80	2.66	14.26	176.40	172.18	4.53	Classic-Multifrequency	decline > 4 pixels, variable sill
k103	6.00	4.20	22.51	220.00	215.21	5.97	Multifrequency	2nd peak @ 13 (Sill=2,900,000)
k113	6.00	4.20	22.51	230.00	221.96	2.77	Classic	not a smooth curve
k123	6.40	4.48	24.01	140.00	128.22	3.13	Classic	not a smooth curve, declines > 14 pixels
Mean	6.62	4.63	24.84	167.37	168.10			
Median	6.10	4.27	22.89	165.00	165.88			
Std. Dev.	2.14	1.50	8.03	48.78	49.14			
Minimum	3.80	2.66	14.26	84.37	93.87			
Maximum	11.60	8.12	43.52	230.00	230.50			
k17	13.50	9.45	50.65	3400.00	2479.44	2	Classic	inflection pt @ 6 pixels
k27	14.00	9.80	52.53	3600.00	3384.31	1.18	Classic	inflection pt @ 6 pixels
k37	9.00	6.30	33.77	2985.00	4146.94	0.65	Classic	inflection pt @ 4-5 pixels, variable sill
k47	8.40	5.88	31.52	2400.00	1797.38	6.22	Classic	decline > 8 pixels
k57	6.40	4.48	24.01	1745.00	2243.09	3.31	Classic	decline > 7 pixels, dip @ 19 pixels
k67	6.60	4.62	24.76	2000.00	1926.49	5.33	Classic-Periodic	peak @ 7 and 18 pixels
k97	5.80	4.06	21.76	2500.00	2208.84	15.59	Multifrequency	large peak @ 6 pixels, 2nd peak > 20 pixels
k107	6.00	4.20	22.51	3600.00	3759.98	7.9	Multifrequency	levels off @ 6 pixels, then rises to peak @ 14 pixels
k117	13.00	9.10	48.78	3900.00	3695.62	2.86	Multifrequency	inflection point @ 6 pixels
k127	6.20	4.34	23.26	2200.00	2166.30	5.89	Multifrequency	levels off @ 6-10 pixels, then rises to peak at 14 pixels
Mean	8.89	6.22	33.36	2853.00	2780.74			
Median	7.50	5.25	28.14	2742.50	2361.27			
Std. Dev.	3.35	2.35	12.57	787.34	869.84			
Minimum	5.80	4.06	21.76	1745.00	1797.38			
Maximum	14.00	9.80	52.53	3900.00	4146.94			

Transect M (#Lags = 20)
Lowland Black Spruce (V34/V35/V36)

Transect	Range (pixels)	Range (m)	Range (m^2)	Sill (10^6)	Cov/Cor (10^6)	IQF (10-5)	Type	Comments
m13	4.00	2.80	15.01	225.40	229.67	4.56	Classic-Periodic	Dip @ 7-8 pixels
m23	6.80	4.76	25.51	430.00	322.72	11.06	Classic-Periodic	peaks @ 7 and 19 pixels (poor fit)
m33	5.40	3.78	20.26	410.00	316.30	15.35	Classic-Periodic	poor fit -periodicity
m43	6.00	4.20	22.51	540.00	534.56	3.68	Multifrequency	2nd peak @ 19 (Sill=650000)
Mean	5.55	3.89	20.82	401.35	350.86			
Median	5.70	3.99	21.38	420.00	319.51			
Std. Dev.	1.18	0.83	4.43	130.48	129.56			
Minimum	4.00	2.80	15.01	225.40	229.67			
Maximum	6.80	4.76	25.51	540.00	534.56			
m17	13.60	9.52	51.03	4411.50	5014.21	0.91	Classic	inflection point @ 6-7 pixels, smooth curve
m27	6.00	4.20	22.51	5400.00	4251.52	9.44	Classic-Periodic	peaks @ 6 and 18 pixels
m37	8.40	5.88	31.52	9000.00	8386.08	5.67	Classic	
m47	6.60	4.62	24.76	5491.00	6763.87	16.90	Classic-Multifrequency	2nd peak @ 20 (Sill=1100000)
Mean	8.65	6.06	32.45	6075.63	6103.95			
Median	7.50	5.25	28.14	5446.50	5889.09			
Std. Dev.	3.45	2.42	12.96	2009.94	1848.57			
Minimum	6.00	4.20	22.51	4411.50	4251.52			
Maximum	13.60	9.52	51.03	9000.00	8386.08			

Transect N (#Lags = 20)
Lowland Black Spruce (V35)

Transect	Range (pixels)	Range (m)	Range (m^2)	Sill (10^6)	Cov/Cor (10^6)	IQF (10-5)	Type	Comments
n13	4.50	3.15	16.88	150.00	200.13		Multifrequency	two or more models required
n23	3.40	2.38	12.76	315.00	326.98		Multifrequency	different scales of information
n33	2.80	1.96	10.51	200.00	212.11		Multifrequency	very variable sill
n43	4.00	2.80	15.01	220.00	258.76		Multifrequency	large peak @ 10-12 pixels
Mean	3.68	2.57	13.78	221.25	249.50			
Median	3.70	2.59	13.88	210.00	235.43			
Std. Dev.	0.74	0.52	2.76	69.09	57.52			
Minimum	2.80	1.96	10.51	150.00	200.13			
Maximum	4.50	3.15	16.88	315.00	326.98			
n17	12.20	8.54	45.77	4000.00	3352.29	1.76	Classic-Periodic	levels off and then drops
n27	6.00	4.20	22.51	4500.00	5751.50		Multifrequency	levels off slightly @ 6 pixels and then climbs
n37	11.00	7.70	41.27	6900.00	4188.39		Classic-Periodic	single peak - 7.2x10(-7) (cycle > 20 pixels)
n47	9.20	6.44	34.52	4074.00	4888.22	1.88	Classic-Periodic	smooth curve (continues to increase beyond 20 pixel lag)
Mean	9.60	6.72	36.02	4868.50	4545.10			
Median	10.10	7.07	37.90	4287.00	4536.31			
Std. Dev.	2.70	1.89	10.12	1372.14	1020.32			
Minimum	6.00	4.20	22.51	4000.00	3352.29			
Maximum	12.20	8.54	45.77	6900.00	5751.50			

Transect P (#Lags = 20)
Aspen Complex (V8/V10/V11)

Transect	Range (pixels)	Range (m)	Range (m^2)	Sill (10^3)	Cov/Cor (10^3)	IGF (10-3)	Type	Comments
p23	5.60	3.92	21.01	410.00	379.63	4.64	Classic(Periodic)	periodic sill
p33	9.40	6.58	35.27	405.60	518.89	10.10		could be classed as unbounded, sill @ 9 and 19 pixels
p43	8.60	6.02	32.27	273.28	335.10	0.62	Classic	slightly variable sill
p53	13.40	9.38	50.28	270.00	268.18	0.43	Classic	sill has slight periodicity
p63	6.80	4.76	25.51	205.00	189.89	5.76	Classic	variable sill - declines beyond range
p73	5.00	3.50	18.76	300.00	297.00	5.83	Classic-Multifrequency	second range @ 14 pixels with sill of 350,000
p83	6.00	4.20	22.51	221.20	277.46	5.76	Classic-Multifrequency	first levels off 6 then peaks at 13 (max sill = 310,000)
p93	6.40	4.48	24.01	300.50	249.86	9.24	Classic-Periodic	periodic sill-high variability-difficult to determine range; sill
p103	9.20	6.44	34.52	345.50	392.11	2.72	Classic-Multifrequency	classed as unbounded-second range@18 pixels, sill of 470,000
p113	7.60	5.32	28.52	380.00	278.15	9.98	Classic-Periodic	large 17 pixel cycle
p123	15.00	10.50	56.28	680.00	500.64	0.63	Classic	could be classed as unbounded
Mean	8.45	5.92	31.72	344.64	335.16			
Median	7.60	5.32	28.52	300.50	297.00			
Std. Dev.	3.20	2.24	12.02	130.78	103.61			
Minimum	5.00	3.50	18.76	205.00	189.89			
Maximum	15.00	10.50	56.28	680.00	518.89			
p27	6.00	4.20	22.51	16800.00	23589.30	2.19	Classic	good fit
p37	13.40	9.38	50.28	24000.00	21146.00	1.35	Classic	requires 2 models (range 6/16 pixels)
p47	11.00	7.70	41.27	16875.00	19386.80	1.66	Classic	good fit (sill begins climbing @ 18 pixels)
p57	8.20	5.74	30.77	12600.00	17069.20	5.79	Multifrequency	curve first levels off at 8 pixels, peaks at 14 (sill=1,810,000)
p67	6.60	4.62	24.76	7088.00	8163.49	4.41	Classic-Periodic	sill is variable with second peak
p77	17.00	11.90	63.78	23000.00	15683.00	2.87	Classic	could be classed as unbounded (range 8/16)
p87					12561.10		Unbounded	inflection points @ 6, 12, 18 pixels
p97	7.40	5.18	27.76	19800.00	20961.90	9.57	Multifrequency	peak @ 7 pixels and > 20
p107	11.00	7.70	41.27	10500.00	19783.70	5.61	Classic-Unbounded	could be unbounded (1st sill @ 11 pixels)
p117	7.00	4.90	26.26	24300.00	9057.95	12.00	Classic-Periodic	cycle = 15 pixels (very poor fit)
p127	10.00	7.00	37.52	25800.00	25707.20	4.47	Classic-Unbounded	curve continues rising after initial sill
Mean	9.76	6.83	36.62	18076.30	17554.51			
Median	9.10	6.37	34.14	18337.50	19386.80			
Std. Dev.	3.47	2.43	13.03	6428.23	5699.79			
Minimum	6.00	4.20	22.51	7088.00	8163.49			
Maximum	17.00	11.90	63.78	25800.00	25707.20			

Transect PNW (#Lags = 20)
Aspen Complex (V8/V10/V11)

Transect	Range (pixels)	Range (m)	Range (m^2)	Sill (10^3)	Cov/Cor (10^3)	IGF (10-3)	Type	Comments
pnw13	4.00	2.80	15.01	200.00	186.04	3.49	Classic-Periodic	variable sill (periodic)
pnw23	4.60	3.22	17.26	208.92	261.27	3.39	Classic-Multifrequency	sill shows linear trend upward > 6 pixels
pnw33	6.00	4.20	22.51	340.00	242.16	23.33	Classic-Periodic	cycle=15 pixels (very poor fit)
pnw43	5.40	3.78	20.26	161.04	254.73	2.56	Classic-Periodic	variable sill
pnw53	12.00	8.40	45.02	330.00	243.05	4.05	Classic-Periodic	large peak @ 12 pixels, inflection point @ 6 pixels
pnw63	8.40	5.88	31.52	320.00	310.15	1.76	Classic-Periodic	2nd peak @ 15 pixels
Mean	6.73	4.71	25.26	259.99	249.56			
Median	5.70	3.99	21.39	264.46	248.89			
Std. Dev.	3.00	2.10	11.24	78.62	39.92			
Minimum	4.00	2.80	15.01	161.04	186.04			
Maximum	12.00	8.40	45.02	340.00	310.15			
pnw17	8.20	5.74	30.77	16150.00	16463.40	1.96	Classic	variable sill (2nd peak @ 10 pixels; sill = 18500000)
pnw27	13.60	9.52	51.03	20000.00	15103.60	1.16	Classic	good fit
pnw37	11.20	7.84	42.02	18000.00	17118.50	1.3	Classic	after range, sill continues to rise gradually to 19 pixels
pnw47	7.00	4.90	26.26	12015.00	17532.10	1.67	Classic	sill peaks @ 14 pixels; sill = 1350000
pnw57	7.00	4.90	26.26	7900.00	7348.55	6.8	Classic-Periodic	cycle = 17-18 pixels
pnw67	16.00	11.20	60.03	15500.00	13366.80	0.82	Classic	good fit
Mean	10.50	7.35	39.40	14927.50	14481.99			
Median	9.70	6.79	36.39	15825.00	15793.50			
Std. Dev.	3.75	2.62	14.05	4355.71	3815.17			
Minimum	7.00	4.90	26.26	7900.00	7348.55			
Maximum	16.00	11.20	60.03	20000.00	17532.10			

Transect PSE (#Lags = 20)
Aspen Complex (V9/V10/V11)

Transect	Range (pixels)	Range (m)	Range (m^2)	Sill (10^3)	Cov/Cor (10^6)	IGF (10-9)	Type	Comments
pse13	15.00	10.50	56.28	400.00	300.73	3.76	Classic-Multifrequency	inflection pts @ 5 and 10 pixels
pse23	8.00	5.60	30.02	185.00	178.86	2.21	Classic	2nd peak @ 14 pixels: sill=220000
pse33	7.40	5.18	27.76	360.00	333.55	2.8	Classic-Periodic	cycle=13 pixels
pse43	7.00	4.90	26.26	410.00	500.43	1.73	Classic	variable sill
pse53	5.60	3.92	21.01	216.20	222.52	1.35	Classic	variable sill
pse63	10.40	7.28	39.02	610.00	531.42	1.43	Classic	
Mean	8.90	6.23	33.39	363.53	344.59			
Median	7.70	5.39	28.89	360.00	317.14			
Std. Dev.	3.38	2.36	12.67	153.51	143.95			
Minimum	5.60	3.92	21.01	185.00	178.86			
Maximum	15.00	10.50	56.28	610.00	531.42			
pse17	19.00	13.30	71.29	33300.00	36217.30	0.25	Classic	good fit
pse27	8.40	5.88	31.52		14104.40	4.98	Classic	Gaussian model would give a better fit
pse37	10.20	7.14	38.27	26000.00	25956.50	2.85	Classic	relatively good fit
pse47	12.00	8.40	45.02	20460.00	21114.80	1.21	Classic	relatively good fit
pse57	6.00	4.20	22.51	10500.00	7876.48	2.19	Classic-Periodic	10 pixel cycle
pse67	13.00	9.10	48.78	33000.00	25388.30	3.55	Classic-Periodic	Gaussian model would give a better fit
Mean	11.43	8.00	42.90	24652.00	21776.46			
Median	11.10	7.77	41.65	26000.00	23252.05			
Std. Dev.	4.48	3.13	16.80	9541.31	9915.35			
Minimum	6.00	4.20	22.51	10500.00	7876.48			
Maximum	19.00	13.30	71.29	33300.00	36217.30			

Transect Q (#Lags = 20)
Lowland / Wetland Black Spruce (V37/V38)

Transect	Range (pixels)	Range (m)	Range (m^2)	Sill (10^3)	Cov/Cor (10^6)	IGF (10-9)	Type	Comments
q13	4.40	3.08	16.51	260.60	233.78	3.56	Classic	variable
q33	4.00	2.80	15.01	210.00	208.19	2.05	Classic	simple fit, variable sill
q43	4.60	3.22	17.26	172.78	222.63	2.89	Classic	steady rise between 7-17 pixels
q53	3.40	2.38	12.76	152.78	276.74	0.46	Classic	variable sill
q63	5.60	3.92	21.01	260.40	274.85	1.56	Classic	variable sill
q73	3.60	2.52	13.51	201.60	203.23	2.62	Classic-Periodic	variable sill, valley between 9-16 pixels
q83	3.40	2.38	12.76	285.20	307.86	1.79	Classic	variable sill, possible 11 pixel cycle
q93	2.60	1.82	9.76	232.80	230.98	6.13	Periodic	7 pixel cycle
q103	3.80	2.66	14.26	277.19	270.71	1.62	Classic	variable sill
Mean	3.93	2.75	14.76	228.15	247.66			
Median	3.80	2.66	14.26	232.80	233.78			
Std. Dev.	0.86	0.60	3.23	46.84	36.00			
Minimum	2.60	1.82	9.76	152.78	203.23			
Maximum	5.60	3.92	21.01	285.20	307.86			
q17	9.20	6.44	34.52	12500.00	7856.61	23.57	Periodic	Cycle=17 pixels (Sill Valley=600 000)
q37	5.60	3.92	21.01	5500.00	5309.18	3.52	Classic-Periodic	good fit (periodic sill)
q47	14.60	10.22	54.78	7256.25	7621.97	0.37	Classic	inflection pt @ 4 pixels
q57	6.20	4.34	23.26	6815.00	11458.60	2.12	Classic-Periodic	dip @ 11 pixels
q67	5.00	3.50	18.76	12740.00	12462.00	4.68	Classic-Periodic	periodic sill
q77	8.00	5.60	30.02	5834.00	6880.20	1.10	Classic	good fit
q87	6.20	4.34	23.26	5200.00	4404.43	12.44	Classic-Periodic	large initial period, falls & levels out@13 pixels(sill=360000)
q97	5.00	3.50	18.76	7200.00	7119.01	4.76	Classic-Periodic	variable sill, general decline > 10 pixels
q107	5.60	3.92	21.01	12000.00	10100.00	15.13	Classic-Periodic	sill drops > 5 pixels (sill=600,000) and levels off @ 10 pixels
Mean	7.27	5.09	27.26	8363.92	8135.67			
Median	6.20	4.34	23.26	7200.00	7621.97			
Std. Dev.	3.09	2.16	11.58	3126.71	2701.85			
Minimum	5.00	3.50	18.76	5200.00	4404.43			
Maximum	14.60	10.22	54.78	12740.00	12462.00			

Transect Se (#Lags = 20)
Aspen Mixedwood (V6/V11/V19)

Transect	Range (pixels)	Range (m)	Range (m^2)	Sill (10^6)	Cov/Cor (10^6)	IGF (10^{-6})	Type	Comments
se13	7.60	5.32	28.52	215.00	188.80	1.22	Classic-Multifrequency	periodic within sill
se23	8.00	5.60	30.02	171.00	187.82	6.11	Classic-Periodic	cycle=14 pixels, poor fit of model
se33	6.60	4.62	24.76	175.25	195.56	1.54	Classic-Periodic	cycle=15 pixels
se43	10.20	7.14	38.27	313.12	362.57	0.68	Classic-Multifrequency	sill continues to rise > 14 pixels
se53	5.40	3.78	20.26	205.80	201.52	6.87	Classic	variable sill
Mean	7.56	5.29	28.37	216.03	227.25			
Median	7.60	5.32	28.52	205.80	195.56			
Std. Dev.	1.79	1.25	6.70	57.49	75.85			
Minimum	5.40	3.78	20.26	171.00	187.82			
Maximum	10.20	7.14	38.27	313.12	362.57			
se17	8.20	5.74	30.77	17600.00	19629.60	5.66	Multifrequency	sill continues to rise between 12-22 pixels
se27	8.00	5.60	30.02	9940.00	13279.00	6.42	Classic-Periodic	cycle = 17 pixels
se37	9.20	6.44	34.52	14000.00	13313.60	3.26	Classic-Periodic	Gaussian model would provide better fit
se47	8.20	5.74	30.77	15540.00	20087.10	2.3	Classic-Multifrequency	sill increases > 14 pixels
se57	7.80	5.46	29.27	12160.00	18338.80	3.35	Classic-Multifrequency	sill increases > 12 pixels
Mean	8.28	5.80	31.07	13848.00	16929.64			
Median	8.20	5.74	30.77	14000.00	18338.80			
Std. Dev.	0.54	0.38	2.03	2961.64	3378.18			
Minimum	7.80	5.46	29.27	9940.00	13279.00			
Maximum	9.20	6.44	34.52	17600.00	20087.10			

Transect Sw (#Lags = 20)
Aspen Dominated Hardwood (V6/V8)

Transect	Range (pixels)	Range (m)	Range (m^2)	Sill (10^6)	Cov/Cor (10^6)	IGF (10^{-6})	Type	Comments
sw13	8.20	5.74	30.77	280.00	213.55	12.36	Classic-Periodic	cycle = 17 pixels
sw23	7.20	5.04	27.01	117.30	160.90	2.34	Classic-Multifrequency	variable sill
sw33	6.60	4.62	24.76	119.60	122.76	3.69	Classic-Multifrequency	sill decreases from 7-10 pixels, then stabilizes @ 90000
sw43	4.00	2.80	15.01	85.80	103.80	3.35	Classic	two models required; sill continues to rise from 4-9 pixels
sw53	4.80	3.36	18.01	145.00	124.47	9.38	Classic-Multifrequency	periodic sill; cycle 9-10 pixels
Mean	6.16	4.31	23.11	149.54	145.10			
Median	6.60	4.62	24.76	119.60	124.47			
Std. Dev.	1.73	1.21	6.49	75.89	43.49			
Minimum	4.00	2.80	15.01	85.80	103.80			
Maximum	8.20	5.74	30.77	280.00	213.55			
sw17	9.40	6.58	35.27	20000.00	15393.40	11.40	Classic-Periodic	cycle = 17 pixels
sw27	8.40	5.88	31.52	11100.00	11435.50	4.36	Classic-Periodic	cycle = 18 pixels; poor fit of model
sw37	8.00	5.60	30.02	6232.00	7558.43	2.35	Classic-Multifrequency	2nd peak @ 15 pixels, sill = 755000
sw47	8.40	5.88	31.52	9100.00	8087.20	3.83	Classic-Multifrequency	periodic sill
sw57	5.00	3.50	18.76	8200.00	6824.37	14.02	Classic-Multifrequency	periodic sill, 8-10 pixel cycle; poor fit
Mean	7.84	5.49	29.42	10926.40	9859.78			
Median	8.40	5.88	31.52	9100.00	8087.20			
Std. Dev.	1.67	1.17	6.26	5365.79	3562.16			
Minimum	5.00	3.50	18.76	6232.00	6824.37			
Maximum	9.40	6.58	35.27	20000.00	15393.40			

Transect T (#Lags = 20)
Conifer Mixedwood (V8/V14/V15/V16/V19)

Transect	Range (pixels)	Range (m)	Range (m^2)	Sill (10^3)	Cov/Cor (10^3)	IGF (10^{-3})	Type	Comments
t13	8.00	5.60	30.02	240.00	213.09	7.74	Periodic	poor fit due to large cycle of 18 pixels
t23	5.40	3.78	20.26	175.00	169.64	2.52	Classic-Periodic	peaks @ 5 and 17 pixels
t33	7.20	5.04	27.01	205.94	240.26	1.31	Classic-Multifrequency	sill continues to rise > 11 pixels
t43	5.60	3.92	21.01	230.00	196.24	4.26	Classic-Multifrequency	variable sill
t53	6.00	4.20	22.51	230.00	189.49	4.02	Multifrequency	variable sill
t63	13.80	9.66	51.78	320.00	275.28	2.39	Multifrequency	strong inflection point @ 6 pixels
t73	9.20	6.44	34.52	290.00	196.97	16.69	Periodic	cycle = 18 pixels
t83	6.80	4.76	25.51	190.00	168.09	1.93	Classic	variable sill
t93	7.20	5.04	27.01	294.50	309.42	1.58	Classic	variable sill
t103	5.20	3.64	19.51	225.32	348.28	2.58	Periodic-Classic	peaks @ 5 and 16 pixels
Mean	7.44	5.21	27.91	240.08	231.68			
Median	7.00	4.90	26.26	230.00	206.29			
Std. Dev.	2.56	1.79	9.61	47.34	60.87			
Minimum	5.20	3.64	19.51	175.00	168.09			
Maximum	13.80	9.66	51.78	320.00	348.28			
t17	7.00	4.90	26.26	9790.00	10044.70	2.01	Classic	sill declines > 8 pixels
t27					17158.50		Unbounded	inflection point @ 6 pixels
t37	9.40	6.58	35.27	20160.00	20676.40	2.06	Classic	sill declines gradually > 9 pixels
t47	8.00	5.60	30.02	20580.00	20024.50	5.05	Classic-Periodic	cycle = 16 pixels
t57	7.80	5.46	29.27	20370.00	20618.30	5.10	Classic-Periodic	cycle = 16 pixels
t67	16.40	11.48	61.53	30000.00	29305.40	0.79	Classic	inflection point @ 8 pixels
t77	10.60	7.42	39.77	20500.00	16517.60	4.86	Classic-Periodic	smooth curve
t87	14.00	9.80	52.53	19000.00	15203.80	1.75	Classic	may be unbounded with inflection point @ 8-10 pixels
t97	12.00	8.40	45.02	27000.00	21036.10	3.33	Classic-Periodic	smooth curve
t107	17.00	11.90	63.78	33000.00	25252.70	1.21	Classic-Periodic	inflection point @ 6 pixels
Mean	11.36	7.95	42.61	22266.67	19603.80			
Median	10.60	7.42	39.77	20500.00	20321.40			
Std. Dev.	3.74	2.62	14.04	6871.62	5346.29			
Minimum	7.00	4.90	26.26	9790.00	10044.70			
Maximum	17.00	11.90	63.78	33000.00	29305.40			

Transect Ua (#Lags = 20)
Lowland Black Spruce (V35/V36/V37)

Transect	Range (pixels)	Range (m)	Range (m^2)	Sill (10^3)	Cov/Cor (10^3)	IGF (10^{-3})	Type	Comments
ua13	3.60	2.52	13.51	220.00	215.33	1.52	Classic	variable sill, possible 11 pixel cycle
ua23	4.80	3.36	18.01	230.00	195.23	8.22	Classic-Periodic	periodic sill (10 pixel cycle)
ua33	5.00	3.50	18.76	190.00	182.88	4.96	Classic	variable sill, drops off > 17 pixels
ua43	3.60	2.52	13.51	220.00	193.75	2.47	Classic	variable sill
ua53	2.80	1.96	10.51	210.00	200.76	3.98	Classic-Periodic	large dip @ 12 pixels (potential cycle)
Mean	3.96	2.77	14.86	214.00	197.59			
Median	3.60	2.52	13.51	220.00	195.23			
Std. Dev.	0.92	0.64	3.46	15.17	11.85			
Minimum	2.80	1.96	10.51	190.00	182.88			
Maximum	5.00	3.50	18.76	230.00	215.33			
ua17	6.20	4.34	23.26	4200.00	3602.30	6.75	Classic-Periodic	10 pixel cycle
ua27	5.80	4.06	21.76	3400.00	2711.95	12.27	Classic-Periodic	10 pixel cycle
ua37	7.80	5.46	29.27	3136.00	3185.25	1.74	Classic	relatively good fit
ua47	4.80	3.36	18.01	3300.00	2991.17	8.81	Periodic	13 pixel cycle
ua57	6.00	4.20	22.51	2050.00	1780.32	7.26	Classic-Periodic	sill drops to 150000 @ 12 pixels and levels off
Mean	6.12	4.28	22.96	3217.20	2854.20			
Median	6.00	4.20	22.51	3300.00	2991.17			
Std. Dev.	1.08	0.76	4.06	770.57	682.18			
Minimum	4.80	3.36	18.01	2050.00	1780.32			
Maximum	7.80	5.46	29.27	4200.00	3602.30			

Transect Ub (#Lags = 20)
Lowland Black Spruce (V35/V36/V37)

Transect	Range (pixels)	Range (m)	Range (m^2)	Sill (10^3)	Cov/Cor (10^3)	IGF (10-9) Type	Comments
ub13	3.20	2.24	12.01	82.00	77.20	2.34 Classic	initial sill @ 2 pixels then rises to 6 pixels before levelling off
ub23	5.20	3.64	19.51	240.00	195.23	8.63 Periodic-Classic	cycle=10 pixels, reaches peak (245000) 2 6 pixels
ub33	5.60	3.92	21.01	235.00	202.19	2.48 Classic-Periodic	variable sill
ub43	3.80	2.66	14.26	205.00	173.43	9.54 Periodic-Classic	large cycle = 13 pixels, sub-cycle = 7 pixels
ub53	6.40	4.48	24.01	240.00	238.70	1.09 Classic	relatively good model approximation
Mean	4.84	3.39	18.16	200.40	177.35		
Median	5.20	3.64	19.51	235.00	195.23		
Std. Dev.	1.31	0.92	4.93	67.77	60.72		
Minimum	3.20	2.24	12.01	82.00	77.20		
Maximum	6.40	4.48	24.01	240.00	238.70		
ub17	4.20	2.94	15.76	1400.00	1716.00	2.33 Classic-Periodic	variable sill
ub27	7.80	5.46	29.27	5400.00	4443.00	2.63 Periodic-Classic	cycle = 16 pixels
ub37	6.40	4.48	24.01	5300.00	5100.00	2.72 Classic-Periodic	sill rises slightly > 10 pixels
ub47	4.60	3.22	17.26	3600.00	3289.00	5.87 Classic	variable sill
ub57	5.40	3.78	20.26	4950.00	5621.00	2.42 Classic	
Mean	5.68	3.98	21.31	4130.00	4033.80		
Median	5.40	3.78	20.26	4950.00	4443.00		
Std. Dev.	1.45	1.02	5.45	1687.31	1561.28		
Minimum	4.20	2.94	15.76	1400.00	1716.00		
Maximum	7.80	5.46	29.27	5400.00	5621.00		

Transect X (#Lags = 20)
Cedar Mixedwood (V22)

Transect	Range (pixels)	Range (m)	Range (m^2)	Sill (10^3)	Cov/Cor (10^3)	IGF (10-9) Type	Comments
x13	7.00	4.90	26.26	200.00	180.62	1.82 Classic	variable sill
x23	7.00	4.90	26.26	380.00	331.35	5.43 Multifrequency	requires more than 1 model (range 5-6); poor fit
x33	4.00	2.80	15.01	170.00	153.18	3.74 Classic	variable sill
x43	4.20	2.94	15.76	204.00	239.89	5.77 Classic	classic up to lag 13, then rises and falls
x53	7.40	5.18	27.76	400.00	319.23	1.05 Classic	slight periodicity in sill
x63	6.00	4.20	22.51	420.00	357.40	9.66 Multifrequency	sill could be estimated to be higher
x73	9.00	6.30	33.77	720.00	511.41	12.70 Classic-Periodic	very poor fit of model (period > 20)
x83	6.60	4.62	24.76	430.00	340.44	3.81 Classic-Periodic	variable sill
Mean	6.40	4.48	24.01	365.50	304.19		
Median	6.80	4.76	25.51	390.00	325.29		
Std. Dev.	1.66	1.16	6.23	179.64	113.55		
Minimum	4.00	2.80	15.01	170.00	153.18		
Maximum	9.00	6.30	33.77	720.00	511.41		
x17	7.60	5.32	28.52	6400.00	6386.66	5.38 Classic-Periodic	variable sill (cycle = 16)
x27	9.80	6.86	36.77	10500.00	10547.30	4.06 Classic-Periodic	large dip after sill is reached (cycle = 18)
x37	6.80	4.76	25.51	9000.00	8066.83	4.00 Classic	curve rises after lag 15
x47	6.20	4.34	23.26	4951.00	6746.50	2.93 Classic-Periodic	smooth periodic curve (cycle = 12)
x57	7.60	5.32	28.52	10500.00	8277.18	1.37 Classic-Periodic	smooth periodic curve (cycle = 13)
x67	9.80	6.86	36.77	10100.00	7991.85	2.09 Classic-Periodic	single smooth curve (cycle = 18)
x77	6.00	4.20	22.51	9600.00	11327.10	5.09 Classic-Periodic	periodic sill = 10 pixels
x87	7.60	5.32	28.52	14000.00	10882.00	13.84 Classic-Periodic	requires 2 models to fit (range 6-10); poor fit
Mean	7.68	5.37	28.80	9388.88	8778.18		
Median	7.60	5.32	28.52	9850.00	8172.00		
Std. Dev.	1.45	1.02	5.45	2756.76	1900.20		
Minimum	6.00	4.20	22.51	4951.00	6386.66		
Maximum	9.80	6.86	36.77	14000.00	11327.10		

Transect Y (#Lags = 20)
Aspen Dominated Hardwood (V6/V8)

Transect	Range (pixels)	Range (m)	Range (m^2)	Sill (10^3)	Cov/Cor (10^3)	IGF (10^{-3})	Type	Comments
y13	10.00	7.00	37.52	180.00	146.91	8.84	Classic-Periodic	cycle = 15 pixels
y23	5.60	3.92	21.01	146.52	161.66	5.86	Classic-Periodic	sill increase > 8 pixels
y33	7.00	4.90	26.26	110.00	97.72	3.87	Classic-Multifrequency	not a smooth fit
y43	9.80	6.86	36.77	370.00	352.97	1.93	Classic-Multifrequency	second peak @ 10 pixels
y53	10.00	7.00	37.52	680.00	600.87	1.82	Classic	
y63	16.00	11.20	60.03	250.00	247.58	3.20	Classic	inflection pts @ 4, 8, 15 pixels; very general fit
y73	8.60	6.02	32.27	320.00	244.61	1.13	Classic	relatively good fit
y83	6.80	4.76	25.51	280.00	264.94	2.55	Classic-Multifrequency	poor fit/estimate (variable sill)
y93	6.60	4.62	24.76	260.00	226.56	2.97	Classic	sill levels off at range but continues to rise gradually to lag=15
y103	4.80	3.36	18.01	135.00	110.85	8.24	Classic-Periodic	cycle = 14 pixels
Mean	8.52	5.96	31.97	273.15	245.47			
Median	7.80	5.46	29.27	255.00	235.58			
Std. Dev.	3.22	2.25	12.08	166.09	147.31			
Minimum	4.80	3.36	18.01	110.00	97.72			
Maximum	16.00	11.20	60.03	680.00	600.87			
y17	9.60	6.72	36.02	13500.00	12087.40	4.68	Classic-Periodic	16 pixel cycle
y27	19.40	13.58	72.78	28500.00	18520.80	1.16	Classic	almost unbounded at 20 pixel lag
y37	18.00	12.60	67.54	26000.00	16208.40	1.88	Classic-Periodic	30 pixel cycle?
y47	8.60	6.02	32.27	31000.00	23009.20	18.27	Classic-Periodic	cycle = 15 pixels, Gaussian model range = 7 pixels
y57	8.00	5.60	30.02	30000.00	27403.50	12.28	Classic-Periodic	poor fit due to periodicity
y67	8.60	6.02	32.27	28800.00	29782.50	4.08	Classic-Periodic	low amplitude period; Gaussian model - range = 7.2
y77	8.40	5.88	31.52	20000.00	15535.80	5.43	Classic	low amplitude period
y87	12.20	8.54	45.77	31000.00	25875.00	1.57	Classic	check larger lag for period
y97	14.00	9.80	52.53	30000.00	18830.10	10.56	Classic-Periodic	check larger lag for period
y107	10.00	7.00	37.52	17000.00	12122.20	9.84	Classic-Periodic	
Mean	11.68	8.18	43.82	25580.00	19937.50			
Median	9.80	6.86	36.77	28650.00	18675.50			
Std. Dev.	4.16	2.91	15.60	6380.76	6294.37			
Minimum	8.00	5.60	30.02	13500.00	12087.40			
Maximum	19.40	13.58	72.79	31000.00	29782.50			

APPENDIX C

MEDIUM-ALTITUDE SEMIVARIOGRAM ANALYSIS

APPENDIX C

MEDIUM-ALTITUDE SEMIVARIOGRAM ANALYSIS

Transect A (#Lags = 20)
Aspen Dominated Hardwood (V5/V6/V8/V9)

Transect	Range (pixels)	Range (m)	Range (m^2)	Sill (10^3)	Cov/Cor (10^3)	IGF (10^{-3})	Type	Comments
a13	10.00	13.90	74.50	120.00	83.00	13.30	Periodic-Classic	Poor fit; requires 2 models to fit curve
a23	4.60	6.39	34.27	118.35	118.00	1.98	Classic	Good fit; variable sill
a33	4.60	6.39	34.27	35.40	59.00	0.82	Classic	Cov/Cor much greater than sill
a43	6.40	8.90	47.68	120.00	112.00	5.76	Periodic-Classic	1st cycle 11-12 pixels
a53	6.00	8.34	44.70	114.40	126.00	0.91	Classic	good fit
a63	6.60	9.17	49.17	131.25	144.00	1.12	Classic	beyond 10 pixels sill rises to equal cov/cor
a73	12.20	16.96	90.89	183.00	134.40	1.03	Classic	could be classed as unbounded (inflection pt @ 7 pixels)
Mean	7.20	10.01	53.64	117.49	110.91			
Median	6.40	8.90	47.68	120.00	118.00			
Std. Dev.	2.85	3.96	21.25	43.29	30.00			
Minimum	4.60	6.39	34.27	35.40	59.00			
Maximum	12.20	16.96	90.89	183.00	144.00			
a17	13.00	18.07	96.88	12000.00	10400.00	1.57	Classic	periodic sill (variable); inflection pt @ 5 pixels
a27	7.60	10.56	56.62	9900.00	9900.00	2.62	Classic	good fit; sill drops off > 15 pixels
a37	5.80	9.45	50.66	6000.00	5346.00	4.41	Classic	variable (periodic) sill
a47	8.40	11.68	62.58	8400.00	8690.00	2.66	Classic	smooth curve
a57	6.40	8.90	47.68	7400.00	6930.00	4.60	Classic	variable sill; smooth curve
a67	8.20	11.40	61.09	10300.00	8250.00	3.88	Classic	good fit ; smooth curve
a77	14.00	19.46	104.31	9400.00	6844.00	1.36	Classic	inflection pt @ 7 pixels
Mean	9.20	12.79	68.54	9057.14	8051.43			
Median	8.20	11.40	61.09	9400.00	8250.00			
Std. Dev.	3.04	4.22	22.61	1981.46	1798.84			
Minimum	6.40	8.90	47.68	6000.00	5346.00			
Maximum	14.00	19.46	104.31	12000.00	10400.00			

Transect B (#Lags = 15)
Black Spruce Complex (V36/V37/V38)

Transect	Range (pixels)	Range (m)	Range (m^2)	Sill (10^3)	Cov/Cor (10^3)	IGF (10^{-3})	Type	Comments
b13	3.00	4.17	22.35	42.75	51.38		Unbounded	poss. ranges3 & 11 @ inflection points (two scales of features)
b23	4.00	5.56	29.80	65.00	65.00	2.07	Classic	nugget exists (approx. 10000; variable sill, incr. >12 pixel)
b33	2.40	3.34	17.88	48.51	56.00	2.80	Multi-frequency	initial sill approx. 2 pixels; peak @ 7 pixels; variable sill
b43	2.25	3.13	16.76	65.70	72.50	2.39	Classic	variable sill increases cov/corr
b53	3.75	5.21	27.94	118.00	89.00	1.80	Periodic-Classic	two peaks @ 4 and 11 pixels; poor fit due to periodicity
b63	2.85	3.96	21.23	110.00	106.50	2.31	Classic	variable sill
Mean	3.04	4.23	22.66	75.00	75.06			
Median	2.93	4.07	21.79	65.35	68.75			
Std. Dev.	0.71	0.98	5.27	31.62	19.19			
Minimum	2.25	3.13	16.76	42.75	56.00			
Maximum	4.00	5.56	29.80	118.00	106.50			
b17							Unbounded	inflection point @ 6 pixels
b27	7.00	9.73	52.15	1258.00	1650.00	2.22	Classic-Periodic	curve continues rising > 11 pixels
b37	6.15	8.55	45.82	643.00	690.00	6.92	Classic-Periodic	1st cycle = 11 pixels
b47							Unbounded	inflection point @ 5 pixels
b57	5.40	7.51	40.23	1100.00	810.00	19.20	Classic-Periodic	1st cycle = 14 pixels
b67	7.50	10.43	55.88	1490.00	1580.00	1.15	Classic	poor fit due to periodicity
Mean	6.51	9.05	48.52	1122.75	1182.50			
Median	6.58	9.14	48.99	1179.00	1195.00			
Std. Dev.	0.93	1.29	6.91	357.70	502.62			
Minimum	5.40	7.51	40.23	643.00	690.00			
Maximum	7.50	10.43	55.88	1490.00	1650.00			

Transect F (#Lags = 150)
Black Spruce (V37)

Transect	Range (pixels)	Range (m)	Range (m^2)	Sill (10^3)	Cov/Cor (10^3)	IGF (10^{-3})	Type	Comments
f13	2.40	3.34	17.88	77.00	73.00	3.89	Classic	short range, sill decreases steadily after 3 pixels
f23	2.25	3.13	16.76	58.75	61.50	4.64	Multi-frequency	nugget variance approx. 9000; peak between 4 & 8 pixels
f33	2.10	2.92	15.65	42.20	46.50	1.93	Multi-frequency	very variable, probably should not be modelled
f43	4.50	6.26	33.53	61.40	96.00	2.51	Classic	unbounded-short sill between 4-7 pixels; 2nd sill at 9 pixels
f53	3.30	4.59	24.59	107.00	94.00	1.79	Classic	variable (periodic) sill
f63	3.15	4.38	23.47	91.30	100.00	5.11	Classic	could be classed as unbounded
Mean	2.95	4.10	21.98	72.94	78.50			
Median	2.78	3.86	20.67	69.20	83.50			
Std. Dev.	0.90	1.26	6.73	23.64	21.69			
Minimum	2.10	2.92	15.65	42.20	46.50			
Maximum	4.50	6.26	33.53	107.00	100.00			
f17	4.65	6.46	34.64	752.50	800.00	9.25	Classic-Periodic	1st cycle = 11 pixels; poor fit due to periodicity
f27	7.20	10.01	53.64	950.00	650.00	19.80	Classic-Periodic	1st cycle = 13 pixels; poor fit due to periodicity
f37	10.65	14.80	79.35	1188.00	1710.00	0.46	Classic	Smooth Curve
f47	5.40	7.51	40.23	522.00	580.00	5.99	Classic-Periodic	1st peak = 522000; 2nd peak = 750000 @ 13 pixels
f57	5.10	7.09	38.00	1250.00	1130.00	8.52	Classic-Periodic	1st peak-5 pixels@1250000; 2nd peak-13 pixels@1700000
f67	14.00	19.46	104.31	2200.00	1470.00	3.43	Unbounded	inflection point @ 5 and 13 pixels
Mean	7.83	10.89	58.36	1143.75	1056.67			
Median	6.30	8.76	46.94	1069.00	965.00			
Std. Dev.	3.74	5.20	27.85	586.14	460.77			
Minimum	4.65	6.46	34.64	522.00	580.00			
Maximum	14.00	19.46	104.31	2200.00	1710.00			

Transect K (#Lags = 20)
Black Spruce / Feathermoss - V33

Transect	Range (pixels)	Range (m)	Range (m^2)	Sill (10^3)	Cov/Cor (10^3)	IGF (10^{-3})	Type	Comments
k13	3.40	4.73	25.33	147.00	143.12	3.39	Classic-Periodic	valley @ 7 pixels
k23	3.00	4.17	22.35	150.00	149.22	4.45	Multifrequency	poor fit - steady decline > 3 pixels
k33	5.00	6.95	37.25	195.99	193.79	1.37	Classic	variable sill
k43	3.20	4.45	23.84	160.00	190.60	2.49	Classic	variable sill
k53	3.00	4.17	22.35	115.00	109.90	3.39	Classic	very variable sill
Mean	3.52	4.89	26.23	153.60	157.33			
Median	3.20	4.45	23.84	150.00	149.22			
Std. Dev.	0.84	1.17	6.29	29.09	35.19			
Minimum	3.00	4.17	22.35	115.00	109.90			
Maximum	5.00	6.95	37.25	195.99	193.79			
k17	5.20	7.23	38.74	1080.00	1150.73	15.18	Multi-frequency	levels off @ 5.2 pixels, then rises to 170,000 @ 13 pixels
k27	6.00	8.34	44.70	2170.00	1684.63	18.47	Periodic-Multifrequency	14 pixel cycle
k37	5.40	7.51	40.23	1250.00	1169.48	4.04	Classic	relatively flat sill
k47	5.00	6.95	37.25	1200.00	1123.67	3.56	Classic	relatively good fit
k57	6.40	8.90	47.68	1700.00	1457.57	9.05	Classic-Periodic	initial 12 pixel period (peak = 6 pixels, valley = 12)
Mean	5.60	7.78	41.72	1480.00	1317.22			
Median	5.40	7.51	40.23	1250.00	1169.48			
Std. Dev.	0.58	0.81	4.34	451.61	245.81			
Minimum	5.00	6.95	37.25	1080.00	1123.67			
Maximum	6.40	8.90	47.68	2170.00	1684.63			

Transect N (#Lags = 20)
Black Spruce / Speckled Alder / Sphagnum - V36

Transect	Range (pixels)	Range (m)	Range (m^2)	Sill (10^3)	Cov/Cor (10^3)	IGF (10^{-3})	Type	Comments
n13	4.50	6.26	33.53	295.00	287.00	2.94	Classic-Periodic	2 peaks, sharp decline/rise after sill
n23	4.50	6.26	33.53	272.80	275.00	1.10	Classic	variable sill
n33	5.25	7.30	39.11	270.00	220.00	5.71	Classic-Periodic	large cycle, approx. 12 pixels
Mean	4.75	6.60	35.39	279.27	260.67			
Median	4.50	6.26	33.53	272.80	275.00			
Std. Dev.	0.43	0.60	3.23	13.70	35.73			
Minimum	4.50	6.26	33.53	270.00	220.00			
Maximum	5.25	7.30	39.11	295.00	287.00			
n17	5.70	7.92	42.47	5500.00	4700.00	14.50	Classic-Periodic	peak @ 5-6 pixels (5.6 x 10(6)); cycle = 11 pixels, poor fit
n27	5.25	7.30	39.11	5000.00	4900.00	7.46	Classic-Periodic	peaks @ 5 pixels and > 15 pixels; poor fit due to periodicity
n37	7.00	9.73	52.15	3100.00	2450.00	8.72	Classic-Periodic	large cycle up to 13 pixels
Mean	5.98	8.32	44.58	4533.33	4016.67			
Median	5.70	7.92	42.47	5000.00	4700.00			
Std. Dev.	0.91	1.26	6.77	1266.23	1360.45			
Minimum	5.25	7.30	39.11	3100.00	2450.00			
Maximum	7.00	9.73	52.15	5500.00	4900.00			

Transect P (#Lags = 20)
Trembling Aspen Complex (V8/V10/V11)

Transect	Range (pixels)	Range (m)	Range (m^2)	Sill (10^3)	Cov/Cor (10^3)	IQF (10-9)	Type	Comments
p13	4.00	5.56	29.80	124.20	227.70	2.25	Classic	high cov/cor, sill increases beyond range
p23	8.40	11.68	62.58	330.00	311.50	1.18	Classic	inflection point @ 4 pixels
p33	4.40	6.12	32.78	230.00	220.80	6.58	Classic-Periodic	periodic sill (poor fit)
p43	9.40	13.07	70.03	310.00	276.50	4.16	Classic-Periodic	1st sill = strong inflection point
p53	7.80	10.84	58.11	160.00	140.00	5.79	Classic Periodic	inflection point @ 3-4 pixels; periodic sill (difficult fit)
p63	4.40	6.12	32.78	167.60	226.50	4.96	Classic-Periodic	periodic sill; peaks @ 4,11,18 (7 pixel cycle)
p73	3.60	5.00	26.82	126.40	157.80	3.73	Classic (Multi)	1st sill = 3-4 pixels (large peak at end of curve)
p83	4.40	6.12	32.78	158.40	158.80	2.95	Classic	difficult to identify range
p93	4.40	6.12	32.78	145.00	134.30	4.12	Classic-Periodic	minimum 2 models required, inflection begins @ 3 pixels
Mean	5.64	7.85	42.06	194.62	205.89			
Median	4.40	6.12	32.78	160.00	220.80			
Std. Dev.	2.22	3.09	16.54	77.63	62.51			
Minimum	3.60	5.00	26.82	124.20	134.30			
Maximum	9.40	13.07	70.03	330.00	311.50			
p17	7.00	9.73	52.15	9450.00	26150.00	0.66	Classic-Periodic	very high cov/cor
p27	13.60	18.90	101.33	32500.00	26800.00	2.09	Classic	sill decreases > 14 pixels
p37	5.40	7.51	40.23	10800.00	12100.00	7.20	Multi-frequency	1st sill is 3-4 pixels; 2nd peak at 12 pixels (1.48 x 10(7))
p47	13.40	18.63	99.84	16000.00	12300.00	2.19	Classic	2 models req'd, 1st infl. = 8 pixels; peak @ 14 (1.7 x 10(7))
p57	8.00	11.12	59.60	10000.00	7807.00	20.70	Classic-Periodic	cycle=16 pixels; smooth periodic curve; poor fit (periodicity)
p67	7.00	9.73	52.15	12600.00	14020.00	3.19	Classic-Periodic	cycle = 16 pixels
p77	6.00	8.34	44.70	6880.00	8030.00	2.55	Classic	good fit
p87	8.00	11.12	59.60	5400.00	4812.00	3.52	Classic-Periodic	range questionable; periodic sill; inflection point = 4 pixels
p97	9.00	12.51	67.05	13000.00	11150.00	4.10	Classic	periodic sill
Mean	8.60	11.95	64.07	12958.89	13696.56			
Median	8.00	11.12	59.60	10800.00	12100.00			
Std. Dev.	2.98	4.14	22.20	7992.59	7765.64			
Minimum	5.40	7.51	40.23	5400.00	4812.00			
Maximum	13.60	18.90	101.33	32500.00	26800.00			

Transect Q (#Lags = 20)
Lowland Black Spruce - V37/V38

Transect	Range (pixels)	Range (m)	Range (m^2)	Sill (10^3)	Cov/Cor (10^3)	IQF (10-9)	Type	Comments
q13	3.60	5.00	37.28	190.00	181.17	3.07	Classic	Variable sill
q23	4.20	5.84	43.50	197.60	251.85	2.13	Classic	Variable sill, increases > 13 pixels
q33	4.80	6.67	49.71	131.00	125.77	3.59	Classic	Variable sill, decreases > 13 pixels
q43	5.80	8.06	60.07	189.00	203.59	4.30	Periodic-Classic	Gradual decrease from 7-16 pixels, then increases > 16 pixels
q53	5.20	7.23	53.85	180.00	144.01	8.53	Classic-Periodic	sill peaks @6, 18 pixels
q63	6.20	8.62	64.21	200.00	173.50	1.62	Classic	Variable sill
q73	6.40	8.90	66.28	150.00	135.28	1.94	Classic	Variable sill
Mean	5.17	7.19	53.56	176.80	173.60			
Median	5.20	7.23	53.85	189.00	173.50			
Std. Dev.	1.04	1.45	10.79	26.20	44.16			
Minimum	3.60	5.00	37.28	131.00	125.77			
Maximum	6.40	8.90	66.28	200.00	251.85			
q17	6.60	9.17	68.35	2900.00	2810.39	9.77	Periodic-Classic	2nd period range = 18 pixels, sill = 4 x 10(7)
q27	7.00	9.73	72.49	4782.37	7368.86	6.67	Classic	sill @ 6-10 pixels,then increases to 19 pixels
q37	11.60	16.12	120.13	3600.00	2437.86	14.08	Periodic-Classic	large peak @ 11 pixels (sill = 3.6 X 10(7))
q47	5.40	7.51	55.92	3381.84	5310.45	3.41	Classic-Periodic	relatively good fit
q57	5.20	7.23	53.85	4600.00	3686.40	25.58	Periodic-Classic	large period 0-10 pixels, flatter period 10-20 pixels
q67	6.00	8.34	62.14	4200.00	4019.81	3.52	Classic	Variable sill
q77	8.40	11.68	86.99	5600.00	4803.93	1.61	Classic	Variable sill
Mean	7.17	9.97	74.27	4180.60	4362.54			
Median	6.60	9.17	68.35	4200.00	4019.81			
Std. Dev.	2.23	3.10	23.11	981.15	1679.21			
Minimum	5.20	7.23	53.85	2900.00	2437.86			
Maximum	11.60	16.12	120.13	5600.00	7368.86			

Transect T (#Lags = 20)
Aspen Dominated Hardwood - V5/V8

Transect	Range (pixels)	Range (m)	Range (m^2)	Sill (10^6)	Cov/Cor (10^6)	IGF (10-9)	Type	Comments
t13	10.60	14.73	78.97	160.00	148.44	1.762	Classic	inflection pt @ 4 pixels; max sill @ 12 pixels (1.7 x 10(6))
t23	6.20	8.62	46.19	300.00	234.74	8.7936	Multifrequency	poor fit, max sill @ 8 pixels; inflection pt @ 4 pixels
t33	5.00	6.95	37.25	220.00	216.60	2.8112	Classic	variable sill
t43	4.80	6.67	35.76	232.80	236.54	6.7322	Multifrequency	2nd peak @ approx. 14 pixels, sill approx. 300 000
t53	7.40	10.29	55.13	265.00	194.36	14.271	Periodic-Classic	period = 12 pixels; poor fit of model
t63	6.00	8.34	44.70	139.00	113.66	8.0669	Periodic-Classic	period = 13 pixels
t73	6.00	8.34	44.70	120.00	97.75	3.1843	Classic	inflection pt @ 4 pixels; peak @ 8 pixels; variable sill
t83	6.20	8.62	46.19	184.01	207.44	3.377	Classic	sill rises gradually beyond range to 240 000 @ 19 pixels
t93	4.60	6.39	34.27	218.06	259.67	1.6368	Classic	variable sill
t103	5.00	6.95	37.25	141.00	148.46	0.96791	Classic	variable sill
Mean	6.18	8.59	46.04	197.98	185.76			
Median	6.00	8.34	44.70	201.04	200.90			
Std. Dev.	1.77	2.46	13.21	59.11	55.44			
Minimum	4.60	6.39	34.27	120.00	97.75			
Maximum	10.60	14.73	78.97	300.00	259.67			
t17	12.00	16.68	89.40	14850.00	1493.95	2.8274	Classic	Gaussian model would provide nearly perfect fit with range=10
t27	8.00	11.12	59.60	23500.00	1858.65	11.3	Periodic-Classic	sine-like curve (smooth); period=17 pixels; poor fit
t37	9.60	13.34	71.52	13500.00	1094.70	2.3232	Classic	inflection point @ 6 pixels
t47	5.20	7.23	38.74	11000.00	1504.63	6.8554	Multifrequency	2nd peak @ approx. 12 pixels; sill 1.6 x 10(7)
t57	8.40	11.68	62.58	17500.00	1571.40	4.7576	Periodic-Classic	small period @ 13 pixels; then increases
t67	12.00	16.68	89.40	15000.00	1251.94	12.876	Periodic	13 pixel cycle (poor fit of model); smooth sine curve
t77	19.00	26.41	141.56	16000.00	1433.32	1.1147	Classic	inflection point @ 4 pixels; almost unbounded
t87	9.00	12.51	67.05	13020.00	1316.93	4.5582	Classic	sill rises gradually > range; peaks @ 20 pixels; 1.7 x 10(7)
t97	10.00	13.90	74.50	17000.00	1330.89	3.6719	Classic	sill declines beyond range
t107	7.20	10.01	53.64	12500.00	1199.60	4.6018	Classic	good classic curve fit
Mean	10.04	13.96	74.80	15387.00	1405.60			
Median	9.30	12.93	69.29	14925.00	1382.11			
Std. Dev.	3.77	5.23	28.05	3503.10	217.89			
Minimum	5.20	7.23	38.74	11000.00	1094.70			
Maximum	19.00	26.41	141.56	23500.00	1858.65			

Transect U (#Lags = 20)
Lowland black Spruce - V35/V36/V37

Transect	Range (pixels)	Range (m)	Range (m^2)	Sill (10^6)	Cov/Cor (10^6)	IGF (10-9)	Type	Comments
u13	2.40	3.34	17.88	112.00	137.91	2.49	Classic	variable sill (valley @ 6 pixels)
u23	6.40	8.90	47.68	110.00	86.62	12.12	Classic-Periodic	large period (15 pixels); inflection pt @ 2 pixels; difficult fit
u33	2.40	3.34	17.88	92.00	91.51	2.38	Classic	variable sill, coarse curve
u43	2.60	3.61	19.37	113.40	132.26	3.30	Classic	very variable sill, coarse curve
u53	2.60	3.61	19.37	110.00	97.69	4.11	Classic	very variable sill, coarse curve
Mean	3.28	4.56	24.44	107.48	109.20			
Median	2.60	3.61	19.37	110.00	97.69			
Std. Dev.	1.75	2.43	13.02	8.77	24.04			
Minimum	2.40	3.34	17.88	92.00	86.62			
Maximum	6.40	8.90	47.68	113.40	137.91			
u17	5.00	6.95	37.25	1232.00	2194.19	1.74	Classic	sill increases gradually > 10 pixels
u27	8.00	11.12	59.60	1650.00	1221.68	28.13	Classic-Periodic	smooth curve, period = 15 pixels; peaks @ 8 pixels
u37	12.40	17.24	92.38	809.10	868.60	4.55	Multifrequency	inflection point @ 5 pixels
u47	5.40	7.51	40.23	1500.00	2025.72	4.64	Classic-Periodic	peaks @ 5/15 pixels; valleys 9/19 pixels
u57	7.80	10.84	58.11	1230.00	903.26	1.36	Classic-Periodic	peak @ 8 pixels; declines, sill 12-18 pixels
Mean	7.72	10.73	57.52	1284.22	1442.69			
Median	7.80	10.84	58.11	1232.00	1221.68			
Std. Dev.	2.95	4.10	21.97	320.84	627.31			
Minimum	5.00	6.95	37.25	809.10	868.60			
Maximum	12.40	17.24	92.38	1650.00	2194.19			

Transect X (#Lags = 20)
Cedar Mixedwood - V22

Transect	Range (pixels)	Range (m)	Range (m^2)	Sill (γ^2)	Cov/Cor (γ^0)	IGF (10-9)	Type	Comments
x13	8.80	12.23	65.56	306.00	292.50	0.94	Classic	good fit
x23	3.00	4.17	22.35	145.00	124.25	17.20	Classic-Periodic	cycle=6 pixels (poor fit)
x33	6.00	8.34	44.70	180.00	151.50	3.20	Classic	second sill @ 13 pixels, approx. 210 000
x43	5.60	7.78	41.72	318.00	327.75	1.63	Classic	second sill @ 14 pixels, approx. 360 000
x53	6.40	8.90	47.68	200.00	259.19	1.60	Classic	difficult to identify range, could be 2 sills @ 3, 9 pixels
x63	4.80	6.67	35.76	235.00	220.30	3.60	Classic	sill steady decline > 9 pixels
x73	3.20	4.45	23.84	96.00	142.00	9.53	Multi-frequency	a two-stepped variogram
x83	6.40	8.90	47.68	260.00	199.20	21.30	Periodic	peak @ 6 pixels, decline to 17 pixels
Mean	5.53	7.68	41.16	217.50	214.58			
Median	5.80	8.06	43.21	217.50	209.75			
Std. Dev.	1.88	2.62	14.02	77.25	74.20			
Minimum	3.00	4.17	22.35	96.00	124.25			
Maximum	8.80	12.23	65.56	318.00	327.75			
x17	12.60	17.51	93.88	5800.00	4604.00	2.69	Classic	inflection point @ 5 pixels, large periodic curve
x27	7.60	10.56	56.62	2440.00	2920.00	1.84	Classic-Periodic	second sill levels off, peaks at 16 pixels
x37	13.40	18.63	99.84	10100.00	6115.00	4.85	Classic-Periodic	inflection point @ 6 pixels, large period peaks @ 13 pixels
x47	8.00	11.12	59.60	6960.00	6114.00	6.11	Classic-Periodic	sill declines > 8 < 18 pixels
x57	10.40	14.46	77.48	3500.00	6020.00	0.48	Classic	inflection points @ 4 and 8 pixels
x67	6.20	8.62	46.19	6200.00	5490.00	11.80	Classic-Periodic	poor fit due to periodicity
x77	17.20	23.91	128.15	3300.00	2436.00	1.30	Classic	inflection point @ 5 and 11 pixels
x87	6.00	8.34	44.70	3600.00	3186.00	14.30	Classic-Periodic	poor fit due to periodicity
Mean	10.18	14.14	75.81	5230.00	4610.50			
Median	9.20	12.79	68.54	4700.00	5047.00			
Std. Dev.	3.97	5.52	29.57	2533.50	1553.98			
Minimum	6.00	8.34	44.70	2440.00	2436.00			
Maximum	17.20	23.91	128.15	10100.00	6115.00			

Transect Y (#Lags = 20)
Aspen Dominated Hardwood - V6/V8

Transect	Range (pixels)	Range (m)	Range (m^2)	Sill (γ^2)	Cov/Cor (γ^0)	IGF (10-9)	Type	Comments
y13	4.60	6.39	34.27	190.80	222.29	1.39	Classic	variable sill; rises to cov/cor @ 16 pixels
y23	4.20	5.84	31.29	150.00	138.84	4.27	Classic	very variable sill
y33	4.40	6.12	32.78	157.00	126.34	7.88	Classic	variable sill; decreases to cov/cor beyond range
y43	8.20	11.40	61.09	390.00	329.78	3.98	Periodic-Classic	inflection point @ 7 pixels; peak @ 15 pixels
y53	9.60	13.34	71.52	275.00	207.24	9.72	Periodic-Classic	steady decline beyond range; period = 20?
y63	8.00	11.12	59.60	265.00	240.58	2.05	Classic	relatively flat sill
y73	5.00	6.95	37.25	155.00	148.88	2.30	Classic	valley @ 17 pixels
Mean	6.29	8.74	46.83	226.13	202.01			
Median	5.00	6.95	37.25	190.80	207.24			
Std. Dev.	2.24	3.11	16.66	89.10	71.62			
Minimum	4.20	5.84	31.29	150.00	126.34			
Maximum	9.60	13.34	71.52	390.00	329.78			
y17	5.80	8.06	43.21	8578.00	14027.20	5.73	Multifrequency	2nd sill @ 17 pixels; 1.4 x 10(7)
y27	13.40	18.63	99.84	31000.00	18968.90	9.10	Periodic	period > 20 pixels
y37	7.00	9.73	52.15	6545.00	7692.75	6.84	Multifrequency	extended inflection pt @ 7 pixels; 2nd peak @ 17 pixels
y47	9.00	12.51	67.05	17000.00	13646.60	4.50	Classic-Periodic	sill flat from 9-15 pixels; then rapid decline
y57	10.40	14.46	77.48	14500.00	10501.30	14.30	Periodic-Classic	poor fit - range at peak of period
y67	8.60	11.95	64.07	25500.00	19533.50	12.01	Classic-Periodic	steady decline > range
y77	10.00	13.90	74.50	14100.00	13277.70	3.21	Classic-Periodic	small valley @ 15 pixels
Mean	9.17	12.75	68.33	16746.14	13949.71			
Median	9.00	12.51	67.05	14500.00	13646.60			
Std. Dev.	2.47	3.43	18.38	8781.57	4241.89			
Minimum	5.80	8.06	43.21	6545.00	7692.75			
Maximum	13.40	18.63	99.84	31000.00	19533.50			

APPENDIX D

MENSURATION DATA FOR FEC PLOTS

APPENDIX D

MENSURATION DATA FOR FEC PLOTS

Ecological Parameter Data (for detailed stand information by plot, see Kalnins *et al*., 1994)
Working Group Key (1) conifer pure; (2) 50+ conifer; (3) 50% + deciduous; (4) deciduous pure

Stand	Plot #	Working Group	V-Type	Age (years)	Height (m)	DBH (cm)	Basal Area (m^2/ha)	Density (#/HA)	Spacing Interval	Tree Cover (%)	MMCD	High Shrub (%)	Low Shrub (%)
Stand A	2605	4	V5	60	22.6	27.4	30	800	4.3	65	4.5	90	7
	2606	4	V5	66	20.8	22.6	46	1000	2.9	55	5.0	65	32
	2607	4	V5	53	19.2	25.3	32	500	4.2	65	5.5	40	23
				60	**21**	**25**	**36**	**767**	**4**	**62**	**5**	**65**	**21**
Stand S	2630	3	V8	**65**	**18.5**	**19.9**	**32**	**600**	**3.6**	**41**	**4.0**	**60**	**47**
Stand D	2654	3	8	87	26.1	22.2	30	500	3.8	68	7.5	83	19
	2655	3	6	96	29.0	32.1	22	500	6.3	40	5.5	115	63
				92	**28**	**27**	**26**	**500**	**5**	**54**	**7**	**99**	**41**
Stand Y	2619	3	V8	93	22.0	20.7	40	600	2.8	60	4.8	60	18
	2620	3	V6	89	24.5	21.9	39	600	3.1	60	4.0	47	10
				91	**23**	**21**	**40**	**600**	**3**	**60**	**4**	**54**	**14**
Stand P	2670	2	10	76	18.1	23.4	13	900	4.8	45	4.8	9	58
	2671	2	10	75	17.9	20.7	23	800	4.7	65	4.8	33	45
				75	18	22	18	850	5	55	5	21	52
				77	**22**	**23**	**38**	**663**	**4**	**54**	**5**	**60**	**35**
Stand T	2631	4	V4	83	17.8	19.5	33	1200	2.2	56	5.4	60	4
	2632	3	V6	89	20.8	22.7	29	900	3.7	77	4.5	65	32
				86	**19**	**21**	**31**	**1050**	**3**	**66**	**5**	**63**	**18**
Stand X	2621	1	V22	128	11.9	19.1	18	1300	2.7	26	2.0	8	34
	2641	1	V22	220	12.3	25.3	27	1700	1.9	83	2.5	22	16
				174	**12**	**22**	**23**	**1500**	**2**	**54**	**2**	**15**	**25**
Stand K	2664	4	33	64	11.0	12.1	36	2000	2.0	50	1.5	6	6
	2665	4	33	62	9.6	12.0	38	700	3.0	70	1.0	20	21
				63	**10**	**12**	**37**	**1350**	**3**	**60**	**1**	**13**	**14**
Stand M	2667	4	35	**175**	**19.8**	**16.7**	**17**	**300**	**5.3**	**8**	**1.5**	**11**	**86**
Stand N	2668	4	35	**174**	**14.4**	**16.2**	**18**	**900**	**3.5**	**25**	**2.5**	**30**	**49**
Stand E	2656	1	35	96	15.9	15.3	29	1400	3.1	40	1.8	9	24
	2608	1	V35	93	13.5	12.5	38	3200	2.1	42	1.8	16	8
				95	**15**	**14**	**34**	**2300**	**3**	**41**	**2**	**13**	**16**
Stand U	2611	1	V36	83	13.2	13.4	40	1700	1.9	26	2.5	4	47
	2612	1	V36	87	10.8	11.7	31	2500	1.8	44	2.5	0	30
				85	**12**	**13**	**36**	**2100**	**2**	**35**	**3**	**2**	**39**
Stand F	2601	1	V37	89	13.5	12.2	43	2500	1.5	35	1.8	1	40
	2602	1	V37	88	16.5	11.6	42	3300	1.6	40	1.8	5	9
				89	**15**	**12**	**43**	**2900**	**2**	**38**	**2**	**3**	**25**
Stand B	2650	1	37	88	11.0	12.5	22	1000	2.3	50	2.0	17	22
	2651	1	36	91	13.0	11.9	37	2200	1.9	58	2.0	5	28
				90	**12**	**12**	**30**	**1600**	**2**	**54**	**2**	**11**	**25**
				118	**15**	**14**	**29**	**1683**	**3**	**33**	**2**	**12**	**40**
Stand Q	2622	1	V38	141	9.7	11.7	10	500	4.3	10	1.5	0	40
	2623	1	V37	126	10.9	10.1	18	1300	3.9	9	1.5	0	93
				134	**10**	**11**	**14**	**900**	**4**	**10**	**2**	**0**	**67**

APPENDIX E

GEOMETRIC CORRECTION OF CASI FLIGHT LINES

APPENDIX E

GEOMETRIC CORRECTION OF CASI FLIGHT LINES

Geometric Correction Report for CASI Flight Line 1

GCPREP Ground Control Point Segment Report V5.3 EASI/PACE 10:01 02-Jan-96

fec1.pix [S 9PIC 670P 3043L] 04-May-94

Set 2 Units:UTM 16 U E000 Set 1 Units:PIXEL Number GCPs: 153

Model	Parameters	FX	FY
1	CONS	0.691909E+09	-.129877E+08
2	X	-.233577E+03	0.106808E+02
3	Y	-.242034E+03	0.417519E+01
4	X * Y	0.206353E-04	-.793945E-06
5	X**2	0.365787E-03	-.197144E-04
6	Y**2	0.215657E-04	-.351160E-06
7	X**2 * Y	-.151623E-20	0.321544E-22
8	X * Y**2	-.385016E-22	0.796296E-24
9	X**3	-.368490E-09	0.198814E-10
10	Y**3	-.191211E-23	0.419295E-25
11	X**2 * Y**2	-.275098E-27	0.715061E-29
12	X**3 * Y	-.332412E-26	0.121240E-27
13	X * Y**3	-.134647E-28	0.270927E-30
14	X**4	0.129101E-24	-.223168E-26
15	Y**4	0.169475E-31	0.373143E-32
16	X**3 * Y**2	-.135187E-32	0.460309E-34
17	X**2 * Y**3	-.900199E-34	0.225458E-35
18	X**4 * Y	0.110079E-31	0.202556E-33
19	X * Y**4	-.298567E-35	0.637967E-37
20	X**5	0.144524E-29	-.265483E-31
21	Y**5	-.466503E-37	0.214418E-38

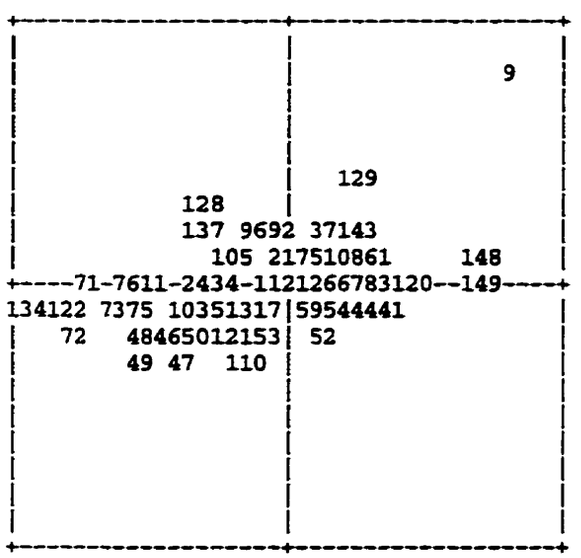
GCP's are ordered from worst to best residuals.

GCP No.	Set 2 GCP's (UTM 16 U E000)		Set 1 GCP's (PIXEL)		Residual (PIXEL)		Distance
9	326590.0,	5449494.0)	256.8,	1670.2)	27.72,	27.47)	39.03
134	327002.5,	5447738.0)	644.5,	1417.5)	-31.70,	-2.66)	31.82
72	326712.5,	5449884.0)	95.2,	1650.2)	-26.67,	-7.25)	27.63
148	332523.1,	5445711.0)	482.2,	362.2)	26.49,	2.06)	26.57
122	319472.5,	5451783.0)	568.5,	2980.5)	-26.21,	-4.01)	26.51
149	332605.6,	5445742.0)	458.2,	350.2)	25.62,	0.48)	25.63
71	326982.0,	5449458.0)	169.8,	1576.8)	-25.26,	0.35)	25.27
73	327320.5,	5449142.0)	215.6,	1490.1)	-20.44,	-3.79)	20.79
49	326129.0,	5449935.0)	152.2,	1746.8)	-18.31,	-9.43)	20.60
74	327259.5,	5449104.0)	232.4,	1496.6)	-20.14,	-3.77)	20.49
76	328481.5,	5448869.0)	154.4,	1281.4)	-20.16,	-1.32)	20.20
48	326007.0,	5450021.0)	145.2,	1774.8)	-17.56,	-8.73)	19.61
75	328507.5,	5448878.0)	151.1,	1277.1)	-18.41,	-2.17)	18.54
129	324777.5,	5449533.0)	446.5,	1952.5)	9.79,	15.04)	17.95
120	321102.5,	5451758.0)	345.2,	2725.2)	17.34,	-0.08)	17.34
10	328135.0,	5448677.0)	244.2,	1319.8)	-16.69,	-1.96)	16.81
11	328073.0,	5448651.0)	258.8,	1328.2)	-16.04,	-1.15)	16.08
46	325930.0,	5449946.0)	175.5,	1781.5)	-13.76,	-7.74)	15.79
47	325967.0,	5449967.0)	167.8,	1775.8)	-12.39,	-9.39)	15.54
121	321323.8,	5451684.0)	330.2,	2681.8)	15.44,	-1.71)	15.53
45	325926.0,	5449894.0)	192.5,	1774.5)	-10.00,	-10.76)	14.69
41	324029.0,	5450581.0)	260.2,	2149.2)	14.45,	-2.44)	14.65
127	322297.5,	5450953.0)	386.5,	2461.5)	13.96,	-0.56)	13.97
25	319949.5,	5453018.0)	170.1,	3021.9)	-13.76,	-1.22)	13.81
8	324803.5,	5450379.0)	219.4,	2005.9)	12.67,	-3.31)	13.10
128	324733.8,	5448931.0)	614.1,	1899.4)	-9.23,	9.26)	13.08
50	325469.0,	5449839.0)	256.8,	1847.2)	-11.16,	-6.67)	13.00
143	328758.8,	5447239.0)	592.5,	1101.5)	10.94,	6.82)	12.89
61	323186.5,	5450889.0)	281.9,	2319.6)	11.71,	5.23)	12.83
42	324223.0,	5450461.0)	265.8,	2106.2)	12.31,	-3.53)	12.81
62	323235.5,	5450906.0)	271.1,	2312.4)	11.59,	4.28)	12.36
4	330363.3,	5447764.0)	234.2,	886.2)	12.01,	2.87)	12.35
83	330235.0,	5447911.0)	214.2,	917.8)	12.16,	1.05)	12.21
103	332945.0,	5446575.0)	143.2,	363.2)	-11.42,	-4.19)	12.16
40	324185.5,	5450646.0)	222.6,	2129.6)	11.83,	-2.78)	12.15
63	323135.0,	5451063.0)	242.2,	2343.8)	10.45,	5.40)	11.76
44	324427.0,	5450597.0)	206.2,	2085.2)	11.04,	-3.97)	11.74
125	320392.5,	5451763.0)	449.5,	2836.5)	11.15,	-1.57)	11.26
137	328192.5,	5447348.0)	620.5,	1202.5)	-8.24,	7.51)	11.15
36	323283.5,	5451183.0)	192.9,	2331.1)	9.26,	5.74)	10.89
39	323901.5,	5450887.0)	194.6,	2200.9)	10.78,	1.24)	10.85
24	319938.5,	5452942.0)	192.9,	3017.4)	-10.73,	-0.51)	10.75

110(	321368.8,	5450616.0)(	611.5,	2568.5)(	-3.51,	-9.99)	10.59
43(	324401.0,	5450729.0)(	175.8,	2102.8)(	10.01,	-2.46)	10.30
3(	324557.5,	5450730.0)(	157.6,	2076.4)(	9.40,	-3.75)	10.13
108(	322253.8,	5450451.0)(	532.2,	2428.2)(	8.77,	5.02)	10.10
66(	322699.0,	5451413.0)(	207.8,	2442.8)(	9.56,	3.04)	10.03
23(	319895.5,	5452763.0)(	244.1,	3006.6)(	-9.75,	-1.67)	9.89
26(	319877.8,	5452870.0)(	220.6,	3019.4)(	-9.75,	-1.45)	9.86
65(	322927.0,	5451277.0)(	212.2,	2395.8)(	8.56,	4.80)	9.82
70(	322859.0,	5451297.0)(	215.8,	2408.2)(	8.61,	4.61)	9.77
53(	324892.5,	5450147.0)(	264.6,	1971.6)(	9.30,	-2.50)	9.63
35(	323345.5,	5451234.0)(	170.4,	2326.9)(	6.58,	6.84)	9.49
147(	332412.5,	5445283.0)(	613.5,	343.5)(	9.04,	2.89)	9.49
99(	332455.5,	5446707.0)(	188.4,	452.6)(	-8.49,	-4.22)	9.48
96(	331187.0,	5447691.0)(	131.2,	753.2)(	-3.84,	8.58)	9.41
12(	327935.0,	5448657.0)(	281.8,	1346.8)(	-7.65,	-5.40)	9.36
135(	327386.3,	5448109.0)(	500.4,	1392.4)(	-9.26,	0.57)	9.28
142(	328921.3,	5447234.0)(	567.5,	1073.5)(	7.47,	5.28)	9.15
21(	319909.0,	5452445.0)(	323.8,	2975.8)(	-8.99,	-1.24)	9.07
133(	325606.3,	5448606.0)(	592.5,	1718.5)(	-8.46,	-2.89)	8.94
67(	322555.0,	5451291.0)(	256.2,	2452.8)(	8.87,	1.07)	8.93
68(	322531.5,	5451353.0)(	243.4,	2462.1)(	8.79,	1.07)	8.86
54(	324949.5,	5450163.0)(	252.1,	1962.1)(	7.54,	-4.27)	8.66
37(	323437.5,	5451261.0)(	152.4,	2314.1)(	5.81,	6.42)	8.66
116(	320458.8,	5451381.0)(	528.8,	2792.8)(	-8.62,	0.29)	8.63
52(	324953.5,	5450027.0)(	284.9,	1947.1)(	5.56,	-6.46)	8.52
136(	326557.5,	5448643.0)(	456.5,	1578.5)(	-5.86,	6.17)	8.50
91(	331321.0,	5447423.0)(	179.2,	708.2)(	-2.18,	8.21)	8.50
92(	331249.0,	5447489.0)(	175.2,	725.8)(	0.23,	8.46)	8.47
138(	328232.5,	5447473.0)(	581.5,	1207.5)(	-3.17,	7.82)	8.43
100(	332331.0,	5446601.0)(	235.8,	462.8)(	-6.88,	-4.85)	8.42
64(	323027.0,	5450925.0)(	288.8,	2346.8)(	7.55,	3.60)	8.36
115(	322762.5,	5450453.0)(	455.5,	2344.5)(	8.10,	1.96)	8.33
69(	322439.0,	5451257.0)(	279.8,	2467.2)(	8.31,	0.13)	8.31
55(	324932.5,	5450122.0)(	261.6,	1958.6)(	4.52,	-6.84)	8.20
90(	329500.5,	5448508.0)(	154.1,	1084.4)(	7.69,	-2.48)	8.08
119(	321242.5,	5451123.0)(	490.5,	2641.5)(	7.24,	-3.52)	8.05
51(	325403.0,	5449951.0)(	240.2,	1869.8)(	-6.42,	-4.78)	8.01
93(	331127.0,	5447373.0)(	220.8,	734.8)(	1.06,	7.92)	7.99
13(	324882.5,	5450545.0)(	164.6,	2008.4)(	7.39,	-2.92)	7.95
106(	321169.0,	5452273.0)(	182.2,	2767.8)(	-4.93,	6.03)	7.79
82(	329179.0,	5448575.0)(	173.8,	1140.8)(	6.80,	-3.77)	7.78
38(	323517.5,	5451279.0)(	137.4,	2302.9)(	4.27,	6.40)	7.69
102(	332893.0,	5446447.0)(	188.2,	360.8)(	-6.43,	-4.01)	7.58
105(	321305.0,	5452399.0)(	133.5,	2756.5)(	-5.25,	4.98)	7.24
144(	331636.3,	5445796.0)(	575.5,	503.5)(	-5.03,	-5.03)	7.11
60(	324731.5,	5450640.0)(	156.9,	2040.4)(	6.06,	-3.71)	7.10
85(	330207.0,	5448255.0)(	130.8,	952.8)(	6.78,	1.71)	6.99
153(	330305.0,	5446895.0)(	459.5,	810.5)(	-2.61,	-6.42)	6.93
81(	329151.0,	5448743.0)(	127.2,	1157.8)(	-3.53,	-5.93)	6.90
34(	322003.5,	5451978.0)(	141.4,	2600.4)(	-6.70,	-1.58)	6.89
151(	331217.5,	5446423.0)(	463.5,	623.5)(	1.94,	-6.40)	6.69
18(	320782.5,	5452654.0)(	152.1,	2863.9)(	2.59,	6.05)	6.58
104(	332925.0,	5446285.0)(	224.8,	343.8)(	-6.21,	-2.01)	6.53
20(	319951.0,	5452503.0)(	304.8,	2974.2)(	-6.12,	-1.44)	6.29
84(	330159.0,	5448133.0)(	164.2,	947.2)(	6.21,	-0.94)	6.28
118(	321287.5,	5451043.0)(	500.5,	2624.5)(	1.07,	-6.07)	6.16
124(	319932.5,	5451758.0)(	513.5,	2906.5)(	-4.91,	-3.54)	6.05
146(	332137.5,	5445448.0)(	599.2,	393.2)(	-2.70,	-5.33)	5.97
113(	321712.5,	5450538.0)(	576.8,	2515.2)(	-5.68,	-1.74)	5.94
150(	331327.5,	5446123.0)(	533.5,	580.5)(	1.26,	-5.71)	5.85
5(	331661.0,	5447207.0)(	191.8,	631.2)(	3.87,	4.34)	5.81
86(	330567.0,	5448049.0)(	133.8,	878.2)(	4.97,	3.00)	5.80
131(	325398.8,	5448849.0)(	549.5,	1775.5)(	-5.72,	-0.95)	5.79
95(	331115.0,	5447731.0)(	133.8,	765.2)(	-1.17,	5.57)	5.69
87(	330737.0,	5447863.0)(	154.2,	836.8)(	2.84,	4.92)	5.68
33(	321945.5,	5451891.0)(	171.1,	2601.4)(	-5.33,	-1.96)	5.68
22(	319973.0,	5452405.0)(	327.2,	2962.2)(	-5.55,	-0.97)	5.64
56(	325245.5,	5450394.0)(	149.1,	1937.4)(	-5.23,	-2.00)	5.60
17(	320757.5,	5452689.0)(	146.6,	2870.1)(	1.83,	5.14)	5.46
98(	331793.0,	5447287.0)(	153.2,	617.2)(	2.89,	4.59)	5.43
88(	330807.0,	5447919.0)(	128.8,	830.8)(	-0.91,	5.34)	5.42
32(	321966.5,	5451829.0)(	184.4,	2591.4)(	-4.52,	-2.99)	5.41
14(	322835.5,	5451571.0)(	147.1,	2435.6)(	4.11,	3.51)	5.40
16(	322941.5,	5451569.0)(	133.6,	2419.6)(	2.69,	4.67)	5.39
132(	325186.3,	5448824.0)(	587.5,	1810.5)(	-4.84,	2.32)	5.37
59(	324790.5,	5450744.0)(	123.6,	2040.1)(	3.78,	-3.74)	5.32
15(	322859.5,	5451557.0)(	147.4,	2430.6)(	3.88,	3.61)	5.30
31(	321970.5,	5451768.0)(	199.6,	2584.6)(	-3.80,	-3.57)	5.21
126(	320162.5,	5452008.0)(	413.5,	2897.5)(	5.17,	0.64)	5.21
94(	331551.0,	5447265.0)(	192.2,	653.2)(	3.42,	3.71)	5.05
109(	322236.3,	5450251.0)(	586.8,	2412.8)(	-0.18,	5.04)	5.04
57(	325231.5,	5450478.0)(	131.1,	1947.4)(	-4.71,	-1.74)	5.02
80(	329077.0,	5448655.0)(	157.8,	1163.2)(	-1.72,	-4.70)	5.00
78(	329031.0,	5448479.0)(	211.8,	1158.8)(	4.82,	-1.25)	4.98
19(	320638.5,	5452659.0)(	170.6,	2885.6)(	2.15,	4.47)	4.96
123(	319827.5,	5451983.0)(	467.5,	2948.5)(	-4.79,	1.20)	4.93
29(	321993.5,	5451596.0)(	241.4,	2564.6)(	-2.27,	-4.30)	4.86
145(	331545.0,	5445965.0)(	548.5,	535.5)(	4.16,	-2.29)	4.75
130(	325378.8,	5449016.0)(	510.5,	1798.5)(	2.66,	3.83)	4.66
89(	330533.0,	5448091.0)(	126.8,	887.2)(	3.57,	2.89)	4.60

```
141(    328448.8,    5448234.0)(   342.8,   1234.8)(    3.84,     2.53)     4.59
  7(    332529.0,    5446373.0)(   269.2,    412.2)(   -1.95,    -4.15)     4.58
 28(    322153.5,    5451736.0)(   184.6,   2552.6)(   -2.91,    -3.47)     4.52
 30(    322034.5,    5451506.0)(   259.4,   2550.1)(   -1.83,    -4.09)     4.48
152(    331442.5,    5446443.0)(   425.5,    594.5)(    4.27,    -1.23)     4.45
107(    321521.0,    5452249.0)(   142.2,   2705.8)(   -3.48,     2.26)     4.15
  6(    332585.0,    5446417.0)(   248.8,    407.8)(   -2.13,    -3.51)     4.10
 79(    329071.0,    5448589.0)(   176.2,   1159.2)(    0.45,    -3.90)     3.93
117(    320762.5,    5451318.0)(   508.5,   2738.5)(    3.92,    -0.28)     3.93
101(    332041.0,    5446743.0)(   246.2,    524.8)(   -3.55,    -1.38)     3.81
  2(    321064.5,    5452080.0)(   247.6,   2763.9)(   -2.16,     3.13)     3.80
 58(    325090.5,    5450510.0)(   146.1,   1972.4)(    2.92,    -2.31)     3.72
111(    321997.5,    5450343.0)(   593.8,   2452.2)(   -2.76,    -1.74)     3.26
 27(    322223.0,    5451675.0)(   192.2,   2536.8)(   -1.37,    -2.72)     3.05
 97(    331879.0,    5447151.0)(   172.8,    589.8)(    1.55,     2.57)     3.00
 77(    328965.0,    5448477.0)(   217.8,   1171.2)(    2.71,     0.80)     2.82
114(    322687.5,    5450273.0)(   513.5,   2339.5)(    2.35,     1.42)     2.75
139(    328401.3,    5448114.0)(   378.2,   1231.8)(    1.03,     2.46)     2.67
  1(    328735.5,    5448385.0)(   265.4,   1201.6)(    0.52,     2.20)     2.26
140(    328491.3,    5448086.0)(   375.2,   1212.2)(    1.72,    -0.11)     1.72
112(    321957.5,    5450403.0)(   584.8,   2466.2)(    0.33,     0.43)     0.54

Residual Plot (PIXEL):                              RMS=(   10.71,     5.44)    12.01
```



Geometric Correction Report for CASI Flight Line 2

GCPREP Ground Control Point Segment Report V5.3 EASI/PACE 12:46 18-Dec-95

rinker.pix [S 13BIC 3500P 3000L] 30-Nov-95

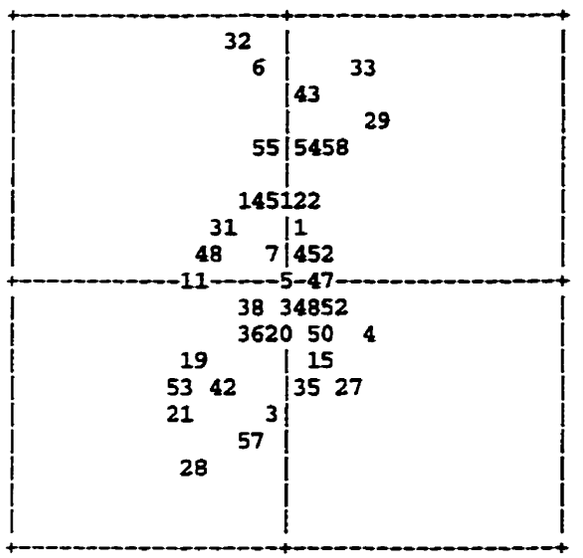
Set 2 Units:UTM 16 U E000 Set 1 Units:PIXEL Number GCPs: 58

Model	Parameters	FX	FY
1	CONS	0.179373E+07	0.221942E+07
2	X	0.777547E+00	-.193668E+02
3	Y	-.298146E+00	0.246329E+00
4	X * Y	-.127747E-05	-.165169E-05
5	X**2	0.140922E-04	0.601746E-04
6	Y**2	-.186695E-20	0.649413E-20
7	X**2 * Y	-.150403E-11	0.721890E-11
8	X * Y**2	0.106457E-25	-.541937E-26
9	X**3	-.587923E-11	-.101837E-09
10	Y**3	-.430848E-27	0.333914E-26
11	X**2 * Y**2	0.548616E-31	-.151130E-31
12	X**3 * Y	0.910114E-30	0.464649E-29
13	X * Y**3	0.270182E-19	-.257983E-19
14	X**4	0.224640E-29	-.929761E-28
15	Y**4	0.565654E-34	0.838351E-33

GCP's are ordered from worst to best residuals.

GCP No.	Set 2 GCP's (UTM 16 U E000)		Set 1 GCP's (PIXEL)		Residual (PIXEL)		Distance
32(	321666.0,	5452150.0)(	405.5,	396.5)(	-2.61,	15.01)	15.24
33(	322226.0,	5451714.0)(	540.4,	443.4)(	5.19,	13.99)	14.92
6(	322226.0,	5452358.0)(	475.5,	263.5)(	-1.99,	12.92)	13.07
28(	325262.0,	5451306.0)(	1045.6,	141.4)(	-4.95,	-11.99)	12.97
43(	328950.0,	5450058.0)(	1748.8,	34.2)(	1.76,	11.74)	11.87
29(	326862.0,	5450834.0)(	1352.1,	89.1)(	5.92,	9.33)	11.05
21(	325418.0,	5451074.0)(	1089.8,	189.8)(	-6.24,	-7.66)	9.88
57(	329962.0,	5448874.0)(	2011.5,	200.5)(	-2.04,	-9.50)	9.71
53(	330414.0,	5448982.0)(	2069.8,	112.8)(	-6.02,	-7.16)	9.35
3(	324630.0,	5450922.0)(	983.9,	330.4)(	-1.13,	-9.07)	9.14
9(	329550.0,	5449430.0)(	1897.4,	105.1)(	-1.02,	-9.03)	9.09
58(	328986.0,	5449326.0)(	1821.5,	224.5)(	3.46,	7.65)	8.39
27(	329510.0,	5448790.0)(	1953.2,	286.2)(	4.04,	-6.87)	7.97
54(	328018.0,	5449434.0)(	1656.5,	321.5)(	1.82,	7.68)	7.89
16(	326754.0,	5450034.0)(	1401.5,	320.5)(	0.94,	7.84)	7.89
42(	319922.0,	5452618.0)(	89.4,	477.1)(	-3.54,	-6.98)	7.82
55(	327214.0,	5449602.0)(	1511.5,	379.5)(	-0.63,	7.69)	7.72
41(	319910.0,	5453222.0)(	37.2,	309.2)(	0.41,	-7.69)	7.70
19(	325926.0,	5451142.0)(	1165.5,	108.5)(	-4.85,	-5.77)	7.53
39(	324346.0,	5450618.0)(	964.8,	453.2)(	-2.65,	-6.25)	6.79
35(	323778.0,	5451394.0)(	809.8,	311.8)(	1.50,	-6.14)	6.32
15(	324242.0,	5451562.0)(	868.8,	206.8)(	2.29,	-5.55)	6.01
37(	323150.0,	5450870.0)(	759.5,	538.5)(	3.23,	-4.97)	5.93
4(	324090.0,	5451786.0)(	827.1,	167.1)(	4.70,	-2.66)	5.40
22(	320926.0,	5453570.0)(	166.8,	88.2)(	1.90,	4.73)	5.10
11(	330010.0,	5447706.0)(	2120.6,	519.6)(	-5.10,	-0.13)	5.10
25(	326204.7,	5449934.0)(	1317.5,	410.5)(	-5.01,	0.18)	5.01
51(	332722.0,	5447802.0)(	2548.2,	120.8)(	-0.09,	4.98)	4.98
50(	331674.0,	5447198.0)(	2438.5,	423.5)(	2.82,	-3.97)	4.87
44(	328886.0,	5449590.0)(	1780.2,	162.8)(	1.68,	4.56)	4.85
14(	321362.0,	5453010.0)(	281.5,	186.5)(	-1.86,	4.40)	4.78
31(	330906.0,	5448150.0)(	2225.1,	281.1)(	-3.23,	3.41)	4.69
48(	330766.0,	5447850.0)(	2228.8,	379.8)(	-4.19,	1.83)	4.57
1(	328291.0,	5449125.0)(	1726.8,	366.6)(	1.15,	4.05)	4.21
26(	328102.0,	5448686.0)(	1735.5,	510.5)(	0.50,	3.78)	3.82
36(	324382.0,	5452050.0)(	843.5,	56.5)(	-1.48,	-3.29)	3.61
20(	330850.0,	5448522.0)(	2186.1,	181.4)(	-0.07,	-3.57)	3.57
24(	328494.0,	5448906.0)(	1779.5,	398.5)(	2.02,	2.89)	3.52
52(	331270.0,	5447434.0)(	2353.5,	419.5)(	3.18,	-0.99)	3.33
40(	320438.0,	5453258.0)(	116.9,	232.4)(	0.63,	-3.22)	3.28
46(	329502.0,	5448462.0)(	1975.8,	380.2)(	-1.54,	-2.90)	3.28
18(	328370.0,	5449554.0)(	1698.5,	232.5)(	-1.33,	-2.88)	3.17
47(	330498.0,	5448090.0)(	2171.8,	349.2)(	2.89,	-0.47)	2.93
2(	328691.0,	5448351.0)(	1860.9,	522.4)(	2.39,	1.69)	2.93
38(	324310.0,	5450346.0)(	984.1,	537.1)(	-1.99,	-1.97)	2.81
7(	326346.0,	5450474.0)(	1295.6,	246.4)(	-0.93,	2.16)	2.36
12(	322570.0,	5451314.0)(	627.5,	495.5)(	2.34,	-0.10)	2.35
34(	323618.0,	5451882.0)(	740.2,	201.2)(	0.90,	-2.16)	2.34
49(	330450.0,	5447738.0)(	2190.8,	450.2)(	-2.00,	-1.14)	2.30
45(	327478.0,	5449902.0)(	1528.8,	257.2)(	1.60,	1.39)	2.11
23(	325734.0,	5450378.0)(	1208.5,	346.5)(	0.25,	-2.03)	2.05
30(	327702.0,	5450514.0)(	1509.4,	61.4)(	1.32,	1.50)	2.00
13(	320642.0,	5452670.0)(	202.5,	373.5)(	1.61,	1.14)	1.97
10(	331398.0,	5448334.0)(	2291.8,	161.2)(	1.59,	1.12)	1.95
8(	327990.0,	5450234.0)(	1580.1,	98.4)(	1.36,	-0.86)	1.61
56(	329098.0,	5448410.0)(	1919.2,	451.2)(	1.46,	0.33)	1.49
17(	322830.0,	5452542.0)(	555.5,	120.5)(	-0.62,	-1.01)	1.19

```
   5(    322770.0,    5451858.0)(   608.1,   318.9)(    0.27,   -0.03)    0.27
Residual Plot (PIXEL):                          RMS=(    3.27,    7.03)    7.76
```



Geometric Correction Report for CASI Flight Line 3

GCPREP Ground Control Point Segment Report V5.3 EASI/PACE 10:02 02-Jan-96

fec3.pix [S 9PIC 586P 2953L] 04-May-94

Set 2 Units:UTM 16 U E000 Set 1 Units:PIXEL Number GCPs: 134

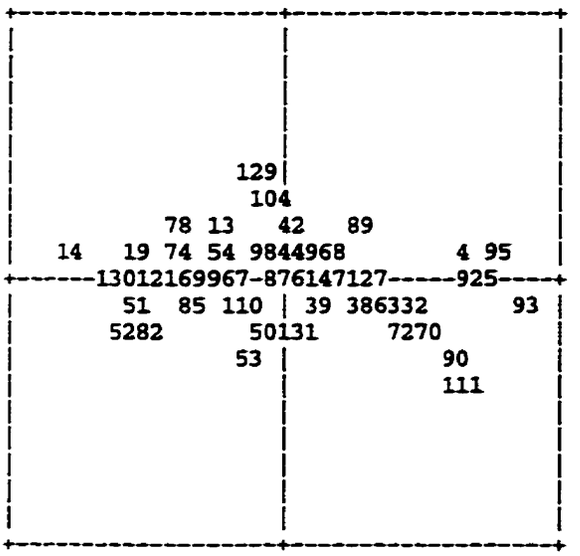
Model	Parameters	FX	FY
1	CONS	0.165962E+08	-.721058E+07
2	X	-.156820E+03	0.469937E+02
3	Y	-.859291E+00	0.112439E+01
4	X * Y	0.168105E-04	-.106464E-04
5	X**2	0.359725E-03	-.477261E-04
6	Y**2	-.160135E-06	0.772057E-07
7	X**2 * Y	-.296041E-10	0.149986E-10
8	X * Y**2	-.460865E-24	0.719130E-25
9	X**3	-.201560E-09	-.354547E-10
10	Y**3	-.795149E-26	-.135634E-26
11	X**2 * Y**2	-.177204E-29	0.576284E-30
12	X**3 * Y	-.635747E-29	0.197246E-28
13	X * Y**3	0.951722E-32	-.362327E-31
14	X**4	0.184828E-26	-.618482E-27
15	Y**4	-.327551E-32	0.647390E-33
16	X**3 * Y**2	-.326987E-36	0.742576E-35
17	X**2 * Y**3	-.110824E-35	0.404325E-36
18	X**4 * Y	0.333663E-33	0.277814E-35
19	X * Y**4	-.408800E-37	0.198620E-38
20	X**5	0.109920E-31	-.428244E-32
21	Y**5	-.202035E-38	0.554986E-39

GCP's are ordered from worst to best residuals.

GCP No.	Set 2 GCP's (UTM 16 U E000)		Set 1 GCP's (PIXEL)		Residual (PIXEL)		Distance
93	330048.5,	5449444.5)	406.9,	1011.4)	26.63,	-3.18)	26.82
111	323115.0,	5453785.0)	83.5,	2481.5)	21.25,	-10.86)	23.87
95	329809.5,	5449191.5)	502.9,	1033.1)	23.52,	1.81)	23.59
14	326729.5,	5450743.5)	390.1,	1657.9)	-22.27,	3.33)	22.52
103	326919.5,	5450721.5)	373.4,	1625.9)	-22.22,	3.02)	22.42
5	329454.5,	5449743.5)	388.4,	1136.6)	21.97,	0.77)	21.98
92	329972.5,	5449210.5)	476.1,	1005.6)	21.18,	-1.10)	21.21
90	330553.0,	5449093.0)	438.8,	894.8)	19.10,	-8.06)	20.73
73	330290.5,	5448902.5)	522.6,	921.6)	18.33,	-7.40)	19.77
4	329550.5,	5449458.5)	454.1,	1099.4)	19.27,	3.50)	19.58
52	320285.8,	5453789.8)	470.9,	2925.9)	-16.47,	-5.12)	17.25
130	327162.5,	5451597.5)	109.5,	1662.5)	-16.93,	0.34)	16.93
70	330115.5,	5448928.5)	533.4,	954.1)	15.92,	-5.37)	16.80
91	330723.0,	5448991.0)	443.8,	860.8)	15.42,	-5.74)	16.46
72	330515.0,	5448825.0)	513.8,	878.8)	13.96,	-7.33)	15.76
19	326830.5,	5450164.5)	542.9,	1590.4)	-15.44,	2.90)	15.71
18	326863.5,	5450233.5)	520.4,	1591.9)	-15.20,	3.44)	15.58
21	326694.5,	5450270.5)	530.1,	1619.9)	-15.45,	1.79)	15.55
83	332372.5,	5447878.5)	532.9,	495.1)	-14.20,	-6.30)	15.53
75	330505.0,	5448849.0)	508.2,	883.2)	14.05,	-6.50)	15.48
51	320349.5,	5453584.5)	515.1,	2898.6)	-15.09,	-3.05)	15.40
32	324429.5,	5452094.5)	349.4,	2130.9)	15.03,	-2.66)	15.26
94	328935.5,	5450045.5)	357.6,	1240.1)	14.38,	-4.89)	15.19
71	329909.5,	5448945.5)	551.1,	991.6)	14.43,	-2.48)	14.64
118	326552.5,	5451592.5)	187.9,	1757.6)	-14.46,	-0.05)	14.47
82	332376.5,	5447854.5)	540.6,	492.4)	-12.85,	-6.37)	14.34
17	326249.5,	5450760.5)	451.4,	1731.4)	-14.31,	0.40)	14.32
100	327558.5,	5450398.5)	394.4,	1497.4)	-13.63,	3.34)	14.03
76	331249.5,	5448229.5)	567.9,	717.6)	-13.93,	1.68)	14.03
12	326385.5,	5450443.5)	521.6,	1682.4)	-13.80,	0.79)	13.82
65	324065.5,	5451506.5)	552.4,	2134.4)	13.53,	-1.85)	13.66
40	322636.5,	5453056.5)	335.6,	2496.1)	13.09,	-2.95)	13.42
77	331405.5,	5448301.5)	530.1,	699.9)	-12.68,	3.35)	13.12
125	331767.5,	5449332.5)	192.5,	728.5)	-12.33,	4.31)	13.06
116	328427.5,	5450982.5)	130.5,	1406.5)	-12.80,	-1.08)	12.85
88	331003.0,	5448987.0)	408.8,	818.2)	12.64,	-2.27)	12.85
63	323394.5,	5451846.5)	549.9,	2268.4)	12.39,	-2.21)	12.59
37	323215.5,	5452652.5)	360.6,	2370.4)	12.32,	-1.93)	12.47
117	328187.5,	5451002.5)	154.5,	1449.5)	-12.04,	1.97)	12.20
115	321438.8,	5454373.8)	141.8,	2808.8)	-11.94,	1.09)	11.99
62	323305.5,	5451870.5)	554.9,	2284.1)	11.73,	-2.35)	11.96
27	326361.5,	5451061.5)	358.4,	1741.4)	-11.90,	1.06)	11.95
66	326245.5,	5450575.5)	504.6,	1714.4)	-11.79,	-0.74)	11.81
26	326368.5,	5451105.5)	346.1,	1743.9)	-11.33,	0.74)	11.35
129	321187.5,	5454772.5)	86.5,	2895.5)	-1.99,	11.17)	11.35
78	331511.5,	5448516.5)	458.9,	702.6)	-10.03,	5.28)	11.34
102	327463.0,	5450669.0)	333.8,	1532.8)	-11.28,	-0.11)	11.28
119	326442.5,	5451737.5)	165.1,	1788.9)	-11.22,	1.04)	11.27
74	331301.5,	5448303.5)	543.9,	717.1)	-10.74,	3.41)	11.26
127	330222.5,	5450247.5)	144.5,	1056.5)	11.08,	1.20)	11.14
81	331151.5,	5448419.5)	528.6,	749.6)	-10.83,	1.56)	10.94

120(	325982.5,	5452297.5)(	70.5,	1911.5)(	-10.79,	1.54)	10.90
16(	326169.5,	5450761.5)(	464.4,	1742.4)(	-10.74,	-1.14)	10.80
34(	323160.5,	5452693.5)(	355.6,	2382.9)(	10.59,	-1.70)	10.73
24(	326108.5,	5450921.5)(	428.9,	1767.1)(	-10.24,	-0.16)	10.24
89(	331455.0,	5448873.0)(	383.2,	741.2)(	9.09,	4.44)	10.12
79(	331528.5,	5448482.5)(	467.4,	695.9)(	-9.18,	4.20)	10.10
121(	325641.2,	5451968.8)(	204.8,	1938.8)(	-8.50,	4.90)	9.81
38(	322910.5,	5452844.5)(	349.1,	2434.4)(	9.27,	-2.75)	9.67
85(	332513.0,	5447975.0)(	492.8,	483.8)(	-9.34,	-2.41)	9.64
113(	322222.5,	5454127.5)(	107.5,	2668.5)(	7.13,	5.66)	9.10
98(	327678.5,	5450423.5)(	378.1,	1479.4)(	-8.79,	2.05)	9.03
35(	324069.5,	5452097.5)(	389.4,	2187.9)(	8.63,	-1.63)	8.78
3(	324126.5,	5451901.5)(	434.1,	2161.9)(	8.60,	-0.95)	8.65
105(	332492.5,	5448732.5)(	278.5,	550.5)(	-8.22,	-2.65)	8.64
101(	327706.5,	5450402.5)(	381.6,	1474.6)(	-7.75,	3.56)	8.53
128(	330377.5,	5449962.5)(	202.5,	1001.5)(	7.37,	-4.18)	8.48
2(	324184.5,	5451924.5)(	420.1,	2154.6)(	8.34,	-1.33)	8.44
31(	324547.5,	5451385.5)(	517.1,	2049.4)(	8.29,	-1.54)	8.43
20(	325094.5,	5451238.5)(	486.6,	1949.9)(	7.74,	-3.22)	8.38
30(	324605.5,	5451397.5)(	506.4,	2041.4)(	8.18,	-1.68)	8.35
99(	327702.5,	5450506.5)(	353.1,	1482.1)(	-8.10,	1.29)	8.21
53(	320373.5,	5454024.5)(	409.4,	2932.4)(	-3.06,	-7.45)	8.06
1(	324181.5,	5451869.5)(	434.9,	2150.9)(	8.01,	-0.54)	8.03
15(	326378.5,	5450360.5)(	550.9,	1676.1)(	-7.95,	0.83)	8.00
13(	327850.5,	5450114.5)(	446.4,	1428.9)(	-5.32,	5.77)	7.85
33(	325142.5,	5451721.5)(	350.1,	1986.4)(	7.25,	-2.84)	7.78
22(	325025.5,	5451208.5)(	502.9,	1958.4)(	7.25,	-2.69)	7.73
11(	327742.5,	5449996.5)(	492.8,	1436.2)(	-4.06,	6.42)	7.59
48(	320592.5,	5453662.5)(	463.6,	2870.4)(	-7.48,	-1.18)	7.58
57(	320648.5,	5453277.5)(	554.6,	2827.4)(	-7.45,	0.97)	7.51
104(	332672.5,	5448887.5)(	219.5,	543.5)(	0.12,	7.45)	7.45
36(	323121.5,	5452654.5)(	367.9,	2386.1)(	7.13,	-0.88)	7.18
54(	320785.5,	5453333.5)(	519.6,	2813.9)(	-6.38,	3.29)	7.18
131(	329055.0,	5450465.0)(	215.8,	1256.2)(	3.51,	-6.06)	7.00
42(	321365.5,	5453194.5)(	474.1,	2714.9)(	1.32,	6.81)	6.94
44(	321369.5,	5453337.5)(	435.6,	2727.6)(	0.73,	6.73)	6.77
50(	320541.5,	5453952.5)(	403.1,	2900.4)(	-0.93,	-6.59)	6.66
69(	328362.5,	5449558.5)(	548.6,	1299.1)(	3.24,	5.44)	6.34
55(	320891.5,	5453394.5)(	489.6,	2804.4)(	-3.97,	4.36)	5.90
47(	320775.5,	5453841.5)(	401.4,	2858.9)(	5.73,	-1.35)	5.88
68(	328889.5,	5449541.5)(	494.4,	1210.6)(	5.53,	2.00)	5.88
134(	329295.0,	5450635.0)(	138.5,	1233.5)(	2.38,	-5.04)	5.57
39(	322988.5,	5452751.5)(	357.9,	2413.1)(	4.33,	-3.36)	5.48
97(	328585.0,	5450033.0)(	393.2,	1300.8)(	5.30,	1.01)	5.40
45(	321497.5,	5453038.5)(	496.4,	2677.6)(	2.77,	4.56)	5.33
49(	320570.5,	5453728.5)(	460.6,	2885.4)(	3.13,	4.16)	5.20
109(	324352.5,	5452752.5)(	166.5,	2200.5)(	-1.88,	-4.85)	5.20
86(	331438.0,	5448802.0)(	399.5,	737.5)(	3.06,	3.91)	4.97
7(	328172.5,	5450347.5)(	354.4,	1393.1)(	4.92,	0.51)	4.95
122(	323477.5,	5453232.5)(	153.5,	2384.5)(	-4.87,	-0.63)	4.92
67(	325983.0,	5450703.0)(	508.8,	1767.2)(	-4.89,	-0.04)	4.89
60(	322954.5,	5452226.5)(	501.9,	2373.4)(	4.87,	0.12)	4.87
133(	322797.5,	5453962.5)(	62.5,	2562.5)(	2.13,	4.36)	4.85
110(	324727.5,	5452767.5)(	112.5,	2144.5)(	-2.56,	-3.87)	4.64
28(	325666.5,	5451077.5)(	447.1,	1848.6)(	-3.95,	-1.33)	4.17
9(	327962.5,	5450311.5)(	381.9,	1426.1)(	-2.32,	3.44)	4.15
23(	325194.5,	5451243.5)(	468.9,	1936.6)(	3.88,	-1.44)	4.14
126(	331447.5,	5449657.5)(	147.5,	804.5)(	-4.01,	-0.06)	4.01
84(	332168.5,	5448325.5)(	444.1,	576.6)(	0.34,	3.79)	3.81
41(	322113.5,	5453113.5)(	384.4,	2588.4)(	1.55,	3.25)	3.60
61(	322455.5,	5452294.5)(	552.4,	2456.9)(	3.48,	0.60)	3.53
46(	320708.5,	5453854.5)(	405.6,	2869.6)(	2.75,	-2.20)	3.52
64(	325755.0,	5450847.0)(	499.2,	1816.8)(	-3.25,	1.18)	3.46
124(	330547.5,	5449592.5)(	282.5,	945.5)(	3.30,	-0.88)	3.41
108(	325116.2,	5452611.2)(	106.8,	2070.2)(	0.12,	-3.38)	3.38
96(	328417.5,	5450094.5)(	393.4,	1333.4)(	2.79,	1.68)	3.26
10(	328212.5,	5450124.5)(	405.4,	1369.9)(	-1.01,	3.08)	3.24
132(	331395.0,	5449945.0)(	76.5,	834.5)(	0.46,	-3.12)	3.15
8(	328048.5,	5450294.5)(	378.4,	1410.4)(	-0.36,	2.77)	2.79
56(	321995.0,	5452663.0)(	520.6,	2562.6)(	2.36,	1.27)	2.68
106(	332952.5,	5449137.5)(	110.5,	512.5)(	-0.87,	2.53)	2.68
107(	332812.5,	5449232.5)(	99.5,	542.5)(	-2.45,	1.01)	2.65
29(	325669.5,	5451254.5)(	400.4,	1864.6)(	-2.49,	-0.73)	2.59
58(	322311.5,	5452462.5)(	527.4,	2493.4)(	2.16,	-0.63)	2.25
80(	332233.5,	5448146.5)(	486.6,	549.1)(	-0.54,	2.13)	2.19
43(	322587.0,	5452657.0)(	436.8,	2470.2)(	1.90,	0.58)	1.98
112(	323027.5,	5453457.5)(	159.5,	2475.5)(	-1.81,	-0.18)	1.82
123(	323897.5,	5453012.5)(	159.5,	2301.5)(	-0.20,	1.74)	1.75
6(	328084.5,	5450348.5)(	360.6,	1407.4)(	1.05,	0.74)	1.29
25(	325418.5,	5451130.5)(	468.4,	1892.4)(	0.89,	-0.81)	1.21
114(	321832.5,	5454157.5)(	151.5,	2726.5)(	1.00,	0.29)	1.04
87(	332525.0,	5448151.0)(	450.2,	498.2)(	0.27,	-0.67)	0.72
59(	322062.5,	5452486.5)(	554.1,	2534.9)(	-0.61,	0.36)	0.70

Residual Plot (PIXEL): RMS=(11.33, 3.94) 11.99


129
104
78 13 42 89
14 19 74 54 9844968 4 95
13012169967-876147127 925
51 85 110 39 386332 93
5282 50131 7270
53
90
111

Geometric Correction Report for CASI Flight Line 4

GCPREP Ground Control Point Segment Report V5.3 EASI/PACE 10:03 02-Jan-96

fec4.pix [S 9PIC 640P 2712L] 10-May-94

Set 2 Units:UTM 16 U E000 Set 1 Units:PIXEL Number GCPs: 80

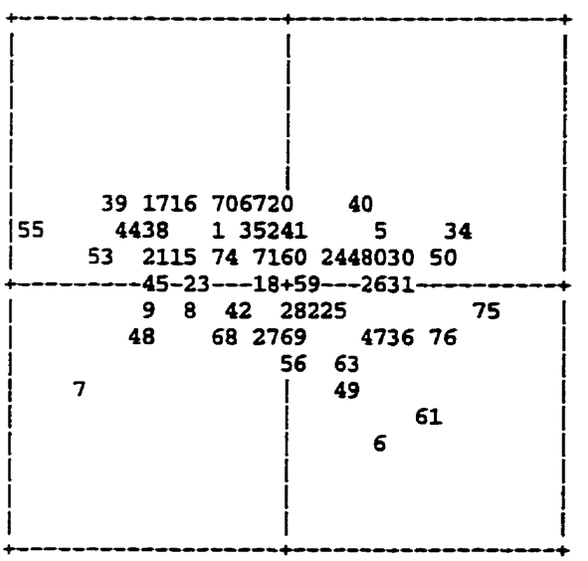
Model	Parameters	FX	FY
1	CONS	0.308224E+07	0.102739E+07
2	X	0.803993E+00	0.184924E+01
3	Y	-.936789E+00	-.338685E+00
4	X * Y	-.585540E-07	0.680365E-06
5	X**2	0.573678E-04	-.173068E-04
6	Y**2	0.617776E-20	0.111135E-19
7	X**2 * Y	-.310733E-23	0.188751E-24
8	X * Y**2	0.189716E-12	0.534765E-13
9	X**3	-.289752E-09	0.661972E-12
10	Y**3	0.700756E-26	0.562266E-26
11	X**2 * Y**2	-.176445E-29	0.120030E-30
12	X**3 * Y	-.488937E-28	0.677517E-29
13	X * Y**3	0.204395E-31	0.371787E-32
14	X**4	0.351603E-15	0.271652E-16
15	Y**4	0.329219E-32	0.160581E-32

GCP's are ordered from worst to best residuals.

GCP	Set 2 GCP's		Set 1 GCP's		Residual		Distance
No.	(UTM 16 U E000)		(PIXEL)		(PIXEL)		
55	329479.0,	5450357.0)	534.8,	962.8)	-17.32,	3.89)	17.75
7	321837.5,	5454917.5)	181.5,	2500.5)	-14.67,	-7.59)	16.52
61	326013.0,	5451933.0)	584.2,	1616.8)	10.21,	-10.31)	14.51
75	320879.0,	5453925.0)	589.2,	2593.8)	14.28,	-1.69)	14.38
53	329795.0,	5449933.0)	612.2,	879.2)	-12.90,	2.73)	13.19
34	320887.5,	5455462.5)	138.5,	2700.5)	12.40,	3.67)	12.93
6	332798.8,	5449238.8)	411.2,	350.2)	6.40,	-11.05)	12.77
39	323017.5,	5453457.5)	484.5,	2223.5)	-11.15,	5.51)	12.44
76	321101.0,	5454039.0)	532.8,	2562.8)	11.45,	-4.44)	12.29
44	321652.5,	5453807.5)	525.2,	2466.2)	-10.62,	3.77)	11.27
50	331779.0,	5449043.0)	606.2,	500.8)	11.15,	1.19)	11.22
9	321847.5,	5454612.5)	273.5,	2484.5)	-10.00,	-1.24)	10.08
48	330361.0,	5449947.0)	534.5,	785.5)	-9.18,	-4.06)	10.04
17	331772.5,	5450762.5)	123.2,	644.2)	-8.21,	5.41)	9.83
36	320308.8,	5454058.8)	595.2,	2692.2)	8.78,	-4.28)	9.77
49	332137.0,	5449569.0)	409.2,	479.2)	4.61,	-8.37)	9.55
38	322031.2,	5453538.8)	567.1,	2386.4)	-8.80,	3.43)	9.44
30	326158.8,	5453081.2)	241.5,	1690.5)	8.80,	2.47)	9.14
45	321822.5,	5454162.5)	407.2,	2459.8)	-9.02,	0.61)	9.04
31	325752.5,	5453417.5)	197.5,	1777.5)	9.00,	0.40)	9.00
73	322213.0,	5453429.0)	580.8,	2349.2)	-8.31,	3.22)	8.91
21	329127.5,	5450312.5)	603.8,	1012.2)	-8.55,	1.74)	8.73
40	324778.8,	5453271.2)	353.8,	1927.8)	5.92,	6.02)	8.44
54	330201.0,	5450229.0)	480.2,	837.2)	-8.29,	0.75)	8.33
58	327121.0,	5451363.0)	598.8,	1408.2)	8.22,	0.41)	8.23
63	325447.0,	5452221.0)	568.8,	1732.2)	4.83,	-6.61)	8.18
16	331512.5,	5450697.5)	177.2,	677.8)	-6.46,	4.91)	8.11
47	327822.5,	5452412.5)	213.2,	1372.2)	7.12,	-3.43)	7.91
5	332511.2,	5448741.2)	583.5,	367.5)	6.52,	3.53)	7.42
62	325693.0,	5452123.0)	565.2,	1686.2)	4.36,	-6.00)	7.42
70	323191.0,	5453007.0)	602.2,	2164.8)	-3.74,	6.15)	7.19
8	322297.5,	5454547.5)	250.5,	2407.5)	-6.93,	-1.58)	7.10
80	331635.0,	5449365.0)	534.5,	548.5)	6.83,	1.10)	6.92
15	331207.5,	5450722.5)	211.2,	722.2)	-6.57,	1.17)	6.67
72	322911.0,	5453193.0)	580.2,	2222.8)	-2.99,	5.92)	6.63
26	325702.5,	5453142.5)	278.8,	1764.2)	6.57,	-0.75)	6.61
77	321149.0,	5454097.0)	505.2,	2559.8)	5.31,	-3.59)	6.41
1	326557.5,	5451592.5)	595.5,	1519.5)	-4.36,	4.66)	6.38
56	328579.0,	5450775.0)	559.8,	1126.2)	0.53,	-6.07)	6.09
51	330823.0,	5449769.0)	523.8,	707.2)	-5.19,	3.13)	6.06
65	325155.0,	5452439.0)	544.2,	1801.2)	5.96,	-0.28)	5.97
35	320562.5,	5454652.5)	396.8,	2695.2)	5.84,	0.30)	5.85
57	327775.0,	5451107.0)	580.8,	1285.8)	5.54,	1.10)	5.65
20	330247.5,	5451052.5)	257.5,	899.5)	0.23,	5.54)	5.54
4	332331.2,	5448953.8)	549.2,	410.2)	5.11,	1.82)	5.42
23	324267.5,	5452717.5)	560.5,	1963.5)	-5.30,	-0.84)	5.37
67	324786.5,	5452457.5)	576.4,	1867.1)	-1.50,	4.98)	5.20
78	321478.0,	5454270.0)	413.5,	2522.3)	-5.08,	0.34)	5.09
68	323801.5,	5452815.5)	588.4,	2043.1)	-3.62,	-3.36)	4.94
74	322445.0,	5453507.0)	538.2,	2316.2)	-4.20,	2.39)	4.84
11	327362.5,	5451852.5)	417.5,	1405.5)	-4.73,	-0.57)	4.76
27	324647.5,	5453962.5)	166.5,	1987.5)	-0.60,	-4.71)	4.75
3	323742.5,	5453837.5)	303.5,	2131.5)	-3.10,	3.53)	4.70
66	325037.0,	5452359.0)	579.8,	1816.2)	4.37,	1.51)	4.62
12	326802.5,	5451442.5)	605.5,	1464.5)	-4.53,	-0.08)	4.53
32	321172.5,	5455412.5)	111.5,	2650.5)	-3.62,	2.55)	4.43
25	325657.5,	5452882.5)	355.2,	1752.2)	4.18,	-0.98)	4.30

46(	329047.5,	5452032.5)(	153.5,	1154.5)(	4.09,	-1.07)	4.22
24(	325047.5,	5452682.5)(	486.5,	1837.5)(	4.06,	1.15)	4.22
69(	323877.0,	5453021.0)(	525.8,	2044.8)(	1.14,	-4.04)	4.20
22(	324722.5,	5452762.5)(	502.5,	1896.5)(	3.52,	2.21)	4.16
52(	330821.0,	5449659.0)(	558.2,	699.8)(	-0.90,	4.03)	4.13
79(	326444.3,	5451861.9)(	542.2,	1550.8)(	3.35,	-2.07)	3.94
64(	325255.0,	5452247.0)(	582.2,	1768.2)(	1.91,	-3.34)	3.85
37(	320411.2,	5454326.2)(	501.5,	2694.5)(	2.12,	-3.18)	3.82
33(	321302.5,	5455367.5)(	114.5,	2627.5)(	-1.81,	3.35)	3.81
13(	328422.5,	5451007.5)(	517.5,	1171.5)(	1.48,	-3.23)	3.55
2(	327072.5,	5452912.5)(	166.5,	1528.5)(	2.40,	-2.61)	3.55
42(	325983.8,	5452278.8)(	477.5,	1655.5)(	-2.92,	-1.56)	3.31
41(	324843.0,	5452910.9)(	443.5,	1888.5)(	1.12,	2.92)	3.13
71(	323237.0,	5453225.0)(	537.2,	2169.2)(	-1.10,	2.88)	3.08
28(	324847.5,	5454057.5)(	117.5,	1964.5)(	0.85,	-2.69)	2.82
14(	328087.5,	5450962.5)(	575.5,	1222.5)(	1.98,	-1.71)	2.62
43(	325936.2,	5452496.2)(	427.5,	1679.5)(	2.33,	-1.06)	2.56
59(	327065.0,	5451577.0)(	540.2,	1433.2)(	2.15,	0.53)	2.22
19(	332437.5,	5450252.5)(	179.1,	496.4)(	-1.49,	-1.53)	2.14
60(	326771.0,	5451609.0)(	568.2,	1483.8)(	0.73,	1.79)	1.94
10(	329352.5,	5451417.5)(	277.5,	1062.5)(	-0.32,	1.76)	1.79
29(	324402.5,	5453867.5)(	223.5,	2023.5)(	0.85,	-1.00)	1.31
18(	331992.5,	5449947.5)(	321.5,	540.5)(	-0.52,	0.48)	0.71

Residual Plot (PIXEL): RMS=(7.38, 4.19) 8.48



Geometric Correction Report for CASI Flight Line 5

GCPREP Ground Control Point Segment Report V5.3 EASI/PACE 10:05 02-Jan-96

fec5.pix [S 9PIC 626P 2970L] 10-May-94

Set 2 Units:UTM 16 U E000 Set 1 Units:PIXEL Number GCPs: 98

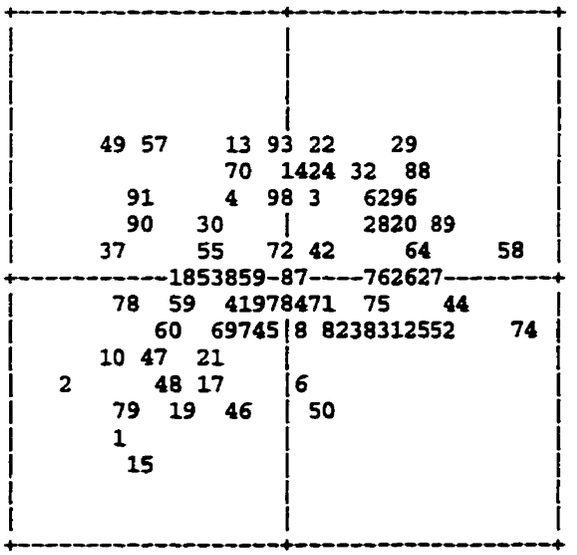
Model	Parameters	FX	FY
1	CONS	0.223880E+09	0.123792E+08
2	X	-.810416E+02	-.354412E+01
3	Y	-.589912E+02	-.332638E+01
4	X * Y	0.103762E-04	0.132961E-05
5	X**2	0.728318E-04	-.122457E-04
6	Y**2	0.521098E-19	0.789119E-21
7	X**2 * Y	-.533103E-22	-.343253E-23
8	X * Y**2	-.345628E-23	-.189634E-24
9	X**3	-.726469E-10	0.129099E-10
10	Y**3	0.620120E-12	0.333490E-13
11	X**2 * Y**2	-.114402E-28	-.869748E-30
12	X**3 * Y	-.109065E-27	-.126789E-28
13	X * Y**3	-.463535E-30	-.237180E-31
14	X**4	0.586516E-26	0.416191E-27
15	Y**4	-.636278E-32	-.591880E-33

GCP's are ordered from worst to best residuals.

GCP No.	Set 2 GCP's (UTM 16 U E000)		Set 1 GCP's (PIXEL)		Residual (PIXEL)		Distance
74	322017.5,	5455622.5)	340.6,	2791.4)	13.36,	-2.74)	13.64
2	323710.5,	5453914.5)	584.6,	2378.6)	-11.57,	-5.75)	12.92
58	332778.5,	5449821.5)	507.9,	581.4)	12.26,	2.00)	12.42
15	323356.5,	5454252.5)	537.4,	2458.9)	-7.09,	-9.89)	12.17
1	323612.5,	5454079.5)	552.1,	2405.1)	-8.71,	-8.34)	12.06
49	330948.5,	5450616.5)	535.9,	948.1)	-9.07,	7.32)	11.65
79	324192.5,	5455372.5)	121.5,	2417.5)	-7.86,	-7.40)	10.80
29	325693.5,	5453418.5)	481.3,	2030.8)	6.49,	7.73)	10.10
57	332585.2,	5449659.2)	565.4,	603.1)	-6.86,	7.10)	9.87
10	321081.5,	5455150.5)	577.4,	2903.6)	-8.58,	-4.38)	9.64
44	329730.5,	5451693.5)	424.6,	1227.4)	9.46,	-1.07)	9.52
88	326347.5,	5454187.5)	188.5,	1987.5)	7.50,	5.86)	9.52
52	331712.5,	5450743.5)	405.9,	826.9)	9.02,	-2.80)	9.44
86	330767.5,	5452092.5)	158.5,	1093.5)	-8.46,	-4.08)	9.39
89	326186.2,	5454658.8)	87.2,	2049.8)	8.82,	2.80)	9.25
37	326781.5,	5452604.5)	553.6,	1781.6)	-8.76,	1.50)	8.88
48	330435.5,	5450940.5)	521.4,	1044.4)	-5.97,	-6.54)	8.85
91	326977.5,	5453742.5)	213.5,	1848.5)	-7.20,	5.07)	8.81
78	323812.5,	5455367.5)	167.5,	2483.5)	-8.43,	-1.84)	8.62
63	324306.2,	5455088.8)	182.2,	2381.2)	-8.23,	-2.14)	8.50
27	324908.5,	5453787.5)	481.6,	2179.6)	8.47,	-0.48)	8.48
19	323671.5,	5454329.5)	475.4,	2417.1)	-5.03,	-6.83)	8.48
90	326767.5,	5453592.5)	279.5,	1867.5)	-7.78,	2.99)	8.33
67	329621.2,	5452731.2)	143.5,	1337.5)	-7.95,	2.35)	8.29
61	321251.2,	5455698.8)	396.8,	2927.8)	-6.96,	4.28)	8.16
65	327212.5,	5453827.5)	161.5,	1815.5)	-7.73,	2.51)	8.12
47	330490.5,	5450909.5)	521.6,	1034.9)	-6.58,	-4.55)	8.00
96	322437.5,	5455292.5)	372.8,	2704.8)	6.44,	4.53)	7.87
50	331905.5,	5450221.5)	517.4,	746.1)	2.41,	-7.36)	7.74
25	325226.5,	5453618.5)	486.6,	2112.1)	7.12,	-2.80)	7.65
54	332187.5,	5449906.5)	556.4,	676.4)	-6.03,	-4.69)	7.64
32	326137.5,	5453093.5)	513.4,	1930.4)	4.79,	5.77)	7.49
64	328077.5,	5453462.5)	164.5,	1645.5)	7.31,	1.63)	7.49
33	326202.5,	5453113.5)	498.1,	1921.9)	3.97,	6.13)	7.30
13	322253.0,	5454635.0)	577.8,	2684.8)	-2.41,	6.85)	7.26
95	322492.5,	5455217.5)	385.2,	2690.8)	4.86,	5.38)	7.25
46	330316.5,	5451448.5)	399.4,	1106.6)	-1.94,	-6.96)	7.23
93	331233.8,	5450841.2)	439.2,	921.8)	-0.10,	7.21)	7.21
31	325336.5,	5453820.5)	414.1,	2110.1)	6.22,	-3.56)	7.17
17	323318.5,	5454634.5)	435.1,	2499.6)	-4.07,	-5.86)	7.13
22	324714.5,	5454014.5)	436.4,	2236.6)	2.39,	6.70)	7.11
43	329363.5,	5451416.5)	551.9,	1265.6)	6.70,	1.81)	6.94
20	324821.2,	5453933.8)	449.4,	2208.6)	6.48,	2.45)	6.93
26	325206.5,	5453587.5)	497.9,	2115.9)	6.85,	0.25)	6.85
62	321251.2,	5455588.8)	440.2,	2919.2)	5.09,	4.42)	6.74
24	324445.5,	5454094.5)	448.6,	2286.1)	2.30,	6.25)	6.66
14	322323.5,	5454699.5)	552.1,	2678.1)	0.48,	6.55)	6.57
5	331402.5,	5450600.5)	488.1,	869.4)	5.75,	2.65)	6.33
60	324182.5,	5454892.5)	252.5,	2384.5)	-5.69,	-2.69)	6.30
51	331567.5,	5450776.5)	415.1,	855.6)	6.29,	-0.03)	6.29
6	327057.5,	5452929.5)	433.1,	1756.4)	0.80,	-6.14)	6.19
39	328145.0,	5452357.0)	452.8,	1536.8)	5.55,	-2.67)	6.16
28	324831.5,	5453812.5)	481.6,	2197.4)	5.48,	2.78)	6.14
23	324574.2,	5453646.2)	559.3,	2228.6)	0.88,	5.81)	5.88
21	323909.5,	5454125.5)	504.4,	2364.4)	-3.48,	-4.67)	5.82
75	321942.5,	5455382.5)	409.8,	2785.2)	5.42,	-1.89)	5.73
70	331629.4,	5451440.6)	218.1,	909.1)	-2.19,	5.28)	5.71

59(	324032.5,	5455117.5)(	210.5,	2428.5)(	-5.46,	-1.14)	5.58
3(	321877.5,	5454922.5)(	547.2,	2766.4)(	1.31,	5.10)	5.26
38(	327420.5,	5452300.5)(	567.1,	1649.1)(	4.56,	-2.45)	5.18
16(	323116.8,	5454611.2)(	475.8,	2532.6)(	3.65,	-3.66)	5.16
76(	321482.5,	5455732.5)(	369.5,	2889.5)(	5.12,	0.60)	5.15
30(	325991.8,	5453638.8)(	369.8,	1995.9)(	-4.07,	2.84)	4.96
94(	322567.5,	5455492.5)(	299.2,	2695.8)(	4.93,	0.46)	4.95
18(	324081.5,	5454042.5)(	504.1,	2334.4)(	-4.94,	-0.16)	4.95
73(	332442.5,	5451347.5)(	135.8,	764.2)(	4.02,	-2.86)	4.94
11(	322655.0,	5454519.0)(	562.8,	2607.8)(	2.50,	4.15)	4.84
4(	331272.5,	5450513.5)(	523.6,	883.9)(	-2.77,	3.87)	4.75
55(	332425.5,	5449885.5)(	527.9,	643.4)(	-3.91,	2.14)	4.46
82(	327202.5,	5453232.5)(	332.5,	1761.5)(	3.11,	-3.01)	4.33
35(	326426.5,	5453417.5)(	375.9,	1907.6)(	-3.11,	2.87)	4.23
83(	327747.5,	5453927.5)(	81.5,	1733.5)(	3.14,	-2.63)	4.10
68(	330204.4,	5452586.9)(	110.5,	1232.5)(	-3.03,	2.48)	3.91
7(	321379.5,	5455293.5)(	501.4,	2867.9)(	-2.33,	-3.10)	3.88
53(	332387.5,	5449944.5)(	516.9,	652.9)(	-3.86,	0.44)	3.88
98(	324467.5,	5454147.5)(	428.5,	2284.5)(	0.07,	3.88)	3.88
69(	331544.4,	5451801.9)(	135.1,	946.6)(	-2.77,	-2.43)	3.69
45(	329863.5,	5451293.5)(	508.1,	1169.4)(	-0.90,	-3.56)	3.68
77(	323407.5,	5455402.5)(	215.5,	2549.5)(	0.03,	-3.63)	3.63
8(	321476.5,	5455214.5)(	514.4,	2845.6)(	0.51,	-3.49)	3.53
92(	325247.5,	5454527.5)(	222.5,	2187.5)(	-3.00,	1.28)	3.26
34(	326681.5,	5453253.5)(	390.9,	1846.9)(	-0.45,	-3.19)	3.22
12(	322893.0,	5454441.0)(	551.8,	2555.8)(	0.49,	-3.11)	3.15
71(	332623.8,	5450923.8)(	218.8,	698.8)(	2.25,	-2.20)	3.15
41(	328531.5,	5451874.5)(	528.6,	1434.6)(	-2.40,	-1.93)	3.08
80(	327657.5,	5452982.5)(	339.5,	1667.5)(	0.88,	-2.93)	3.06
40(	328486.5,	5451853.5)(	541.6,	1439.9)(	-1.72,	-2.17)	2.77
42(	329236.5,	5452113.5)(	369.4,	1344.6)(	2.51,	1.14)	2.76
56(	332332.5,	5450254.5)(	443.4,	686.6)(	2.08,	-1.63)	2.64
66(	329003.1,	5453119.4)(	131.6,	1468.9)(	1.59,	1.90)	2.48
85(	329548.8,	5452541.2)(	207.9,	1330.4)(	-2.47,	0.09)	2.47
36(	326428.5,	5452766.5)(	565.4,	1851.6)(	1.74,	1.01)	2.01
72(	332783.8,	5451313.8)(	93.2,	712.2)(	0.31,	1.86)	1.88
84(	328277.5,	5453592.5)(	99.5,	1621.5)(	0.42,	-1.61)	1.66
9(	320924.5,	5455390.5)(	534.6,	2952.6)(	-1.52,	0.55)	1.62
81(	327937.5,	5453237.5)(	232.5,	1646.5)(	-1.34,	-0.60)	1.47
87(	331973.8,	5451733.8)(	98.4,	875.1)(	1.10,	-0.13)	1.10
97(	324052.5,	5454427.5)(	402.5,	2369.5)(	-0.50,	-0.81)	0.95

Residual Plot (PIXEL): RMS=(5.98, 4.49) 7.48



APPENDIX F

FIELD SAMPLE LOCATIONS

APPENDIX F

FOREST ECOSYSTEM SAMPLE SITE LOCATIONS

Ecosystem Class Description	V-Type(s)	Calibration Sample	Calibration Lat./Long. Coordinates	Calibration UTM Coordinates	Validation Sample	Validation Lat./Long. Coordinates	Validation UTM Coordinates
Aspen Dominated	V5, V6, V7,	2606	N 49° 11' 33.0"	E 325498	2645	N 49° 11' 51.0"	E 322950
Hardwood and	V8, V9, V10	(V5)	W 89° 23' 42.1"	N 5451398	(V5)	W 89° 25' 48.9"	N 5452038
Mixedwood	(V11)	T1	N 49° 10' 38.8"	E 324922	S28	N 49° 10' 52.2"	E 325806
		(V5)	W 89° 24' 08.0"	N 5449742	(V5)	W 89° 23' 24.9"	N 5450129
		2655	N 49° 12' 02.5"	E 320782	2620	N 49° 10' 30.5"	E 326379
		(V6)	W 89° 27' 36.6"	N 5452462	(V6)	W 89° 22' 55.6"	N 5449439
		A37	N 49° 11' 40.2"	E 325450	2648	N 49° 11' 43.0"	E 325906
		(V6)	W 89° 23' 44.8"	N 5451622	(V6)	W 89° 23' 22.5"	N 5451694
		2610	N 49° 10' 55.4"	E 326574	2639	N 49° 10' 49.8"	E 327371
		(V7)	W 89° 22' 47.1"	N 5450202	(V7)	W 89° 22' 07.5"	N 5450005
		A17	N 49° 11' 42.8"	E 325487	PP26	N 49° 11' 15.4"	E 324122
		(V7)	W 89° 23' 43.2"	N 5451702	(V7)	W 89° 24' 49.3"	N 5450898
		A27	N 49° 11' 35.3"	E 325403	2619	N 49° 10' 34.9"	E 326630
		(V8)	W 89° 23' 46.9"	N 5451474	(V8)	W 89° 22' 43.4"	N 5449566
		T25	N 49° 10' 39.4"	E 325435	S10	N 49° 10' 44.7"	E 325582
		(V8)	W 89° 23' 42.6"	N 5449746	(V8)	W 89° 23' 35.6"	N 5449905
		2649	N 49° 11' 39.1"	E 325667	2658	N 49° 11' 28.3"	E 323030
		(V9)	W 89° 23' 34.1"	N 5451582	(V8)	W 89° 25' 43.8"	N 5451333
		2671	N 49° 11' 24.1"	E 323946	2609	N 49° 10' 54.2"	E 326495
		(V10)	W 89° 24' 58.4"	N 5451174	(V10)	W 89° 22' 51.0"	N 5450169
White Spruce /	V14, V15,	G1	N 49° 11' 33.3"	E 322946	095	N 49° 10' 40.7"	E 327035
Balsam Fir	V16, V24,	(V14)	W 89° 25' 48.2"	N 5451490	(V14)	W 89° 22' 23.7"	N 5449734
Conifer	V25	T17	N 49° 10' 31.6"	E 325586	T13	N 49° 10' 40.8"	E 325450
Mixedwood	(V21) (V19)	(V14)	W 89° 23' 34.8"	N 5449498	(V14)	W 89° 22' 22.9"	N 5449446
		2637	N 49° 11' 02.7"	E 323018	038	N 49° 10' 30.9"	E 330022
		(V15)	W 89° 25' 43.2"	N 5450542	(V15)	W 89° 19' 55.6"	N 5449339
		2657	N 49° 11' 32.0"	E 325982	T21	N 49° 10' 36.6"	E 325611
		(V15)	W 89° 25' 46.4"	N 5451449	(V15	W 89° 23' 33.8"	N 5449654
		T22	N 49° 10' 37.4"	E 325571	2659	N 49° 11' 25.8"	E 323126
		(V15)	W 89° 23' 35.8"	N 5449678	(V16)	W 89° 25' 39.0"	N 5451254
		T14	N 49° 10' 29.1"	E 325490	T15A	N 49° 10' 28.7"	E 325530
		(V16)	W 89° 23' 39.4"	N 5449425	(V16)	W 89° 23' 37.4"	N 5449410
		2628	N 49° 12' 11.5"	E 322242	T15B	N 49° 10' 28.1"	E 325562
		(V16)	W 89° 26' 24.9"	N 5452694	(V16)	W 89° 23' 35.8"	N 5449390
		T20	N 49° 10' 35.9"	E 325650	I6	N 49° 12' 17.3"	E 324106
		(V16)	W 89° 23' 31.9"	N 5449630	(V24)	W 89° 24' 53.1"	N 5452814
		032	N 49° 10' 26.9"	E 329935	026	N 49° 10' 17.7"	E 329731
		(V25)	W 89° 19' 59.8"	N 5449218	(V25)	W 89° 20' 09.4"	N 5448938
		037	N 49° 10' 31.2"	E 329998	033	N 49° 10' 26.0"	E 329943
		(V25)	W 89° 19' 56.8"	N 5449350	(V25)	W 89° 19' 59.4"	N 5449190
Upland Black	V20, V31,	034	N 49° 10' 25.8"	E 329979	2629	N 49° 12' 11.1"	E 322346
Spruce / Jack Pine	V32, V33	(V31)	W 89° 19' 57.6"	N 5449181	(V31)	W 89° 26' 19.8"	N 5452677
	(V19)	PP12	N 49° 11' 30.6"	E 324075	PP16B	N 49° 11' 28.9"	E 323870
		(V31)	W 89° 24' 52.3"	N 5451370	(V31)	W 89° 25' 02.4"	N 5451326
		PP16A	N 49° 11' 27.4"	E 323858	2640B	N 49° 10' 37.7"	E 326935
		(V31)	W 89° 25' 02.9"	N 5451278	(V32)	W 89° 22' 28.5"	N 5449645
		S15	N 49° 10' 41.2"	E 325819	2665	N 49° 10' 12.6"	E 329939
		(V31)	W 89° 23' 23.8"	N 5449788	(V33)	W 89° 19' 58.9"	N 5448776
		2640A	N 49° 10' 36.0"	E 326934	K2	N 49° 10' 12.9"	E 329678
		(V32)	W 89° 22' 28.4"	N 5449594	(V33)	W 89° 20' 11.8"	N 5448794
		031	N 49° 10' 17.1"	E 329798	2666	N 49° 10' 23.8"	E 328615
		(V33)	W 89° 20' 06.1"	N 5448919	(V33)	W 89° 21' 04.8"	N 5449162
		2664	N 49° 10' 11.1"	E 329750	A7	N 49° 11' 34.1"	E 325694
		(V33)	W 89° 20' 08.1"	N 5448733	(V33)	W 89° 23' 32.5"	N 5451426
		K8	N 49° 10' 14.5"	E 329890	K7	N 49° 10' 13.5"	E 329983
		(V33)	W 89° 20' 01.4"	N 5448837	(V33)	W 89° 19' 56.8"	N 5448800
		A31	N 49° 11' 35.2"	E 325655	A30	N 49° 11' 36.2"	E 325618
		(V33)	W 89° 23' 34.5"	N 5451462	(V33)	W 89° 23' 36.3"	N 5451494
		S5	N 49° 10' 48.3"	E 325358	R25	N 49° 11' 14.5"	E 325919
		(V33)	W 89° 23' 46.9"	N 5450022	(V33)	W 89° 23' 20.4"	N 5450813

Ecosystem Class Description	V-Type(s)	Calibration Sample	Lat./Long. Coordinates	UTM Coordinates	Validation Sample	Lat./Long. Coordinates	UTM Coordinates
Cedar Mixedwood	V22	2621	N 49° 10' 34.5"	E 326198	2641	N 49° 10' 34.8"	E 326190
			W 89° 23' 04.7"	N 5449570		W 89° 23' 05.1"	N 5449577
		X1	N 49° 10' 46.7"	E 326427	X3	N 49° 10' 44.3"	E 326358
			W 89° 22' 54.0"	N 5449938		W 89° 22' 57.3"	N 5449866
		X2	N 49° 10' 45.6"	E 326394	X4	N 49° 10' 43.4"	E 326328
			W 89° 22' 55.6"	N 5449906		W 89° 22' 58.8"	N 5449842
		X6	N 49° 10' 40.9"	E 326263	X5	N 49° 10' 42.6"	E 326290
			W 89° 23' 01.8"	N 5449766		W 89° 23' 00.6"	N 5449818
		X7	N 49° 10' 39.7"	E 326299	X9	N 49° 10' 37.4"	E 326231
			W 89° 23' 00.0"	N 5449726		W 89° 23' 03.2"	N 5449658
		X8	N 49° 10' 38.6"	E 326262	X10	N 49° 10' 36.2"	E 326199
			W 89° 23' 01.7"	N 5449694		W 89° 23' 04.8"	N 5449622
		X12	N 49° 10' 33.7"	E 326159	X11	N 49° 10' 34.9"	E 326150
			W 89° 23' 06.6"	N 5449545		W 89° 23' 07.1"	N 5449582
		W1	N 49° 12' 13.5"	E 324102	W4	N 49° 12' 12.7"	E 324095
			W 89° 24' 53.1"	N 5452694		W 89° 24' 53.4"	N 5452670
		W2	N 49° 12' 13.5"	E 324131	W5	N 49° 12' 12.7"	E 324122
			W 89° 24' 51.7"	N 5452694		W 89° 24' 52.0"	N 5452670
		W3	N 49° 12' 13.5"	E 324159	W6	N 49° 12' 11.9"	E 324106
			W 89° 24' 50.3"	N 5452694		W 89° 24' 52.8"	N 5452645
Lowland Black Spruce	V23, V34, V35, V36, V37	PP25	N 49° 11' 17.1"	E 324042	2633	N 49° 11' 02.0"	E 326122
		(V34)	W 89° 24' 53.3"	N 5450954	(V34)	W 89° 23' 09.8"	N 5450423
		2656	N 49° 11' 09.1"	E 324118	2608	N 49° 11' 08.4"	E 324270
		(V35)	W 89° 24' 49.1"	N 5450706	(V35)	W 89° 24' 41.6"	N 5450678
		2668	N 49° 10' 26.5"	E 327974	A23	N 49° 11' 41.8"	E 325238
		(V35)	W 89° 21' 36.6"	N 5449266	(V35)	W 89° 23' 55.4"	N 5451678
		A19	N 49° 11' 45.1"	E 325447	2613	N 49° 11' 01.6"	E 326057
		(V35)	W 89° 22' 45.3"	N 5451775	(V36)	W 89° 23' 13.0"	N 5450410
		R29	N 49° 11' 10.9"	E 326038	2651	N 49° 11' 34.7"	E 324618
		(V35)	W 89° 23' 14.4"	N 5450698	(V36)	W 89° 24' 25.7"	N 5451478
		2611	N 49° 11' 00.5"	E 326510	N1	N 49° 10' 27.1"	E 328014
		(V36)	W 89° 22' 50.5"	N 5450361	(V37)	W 89° 21' 34.7"	N 5449282
		2612	N 49° 11' 03.3"	E 326494	U1	N 49° 11' 06.7"	E 326407
		(V36)	W 89° 22' 51.5"	N 5450449	(V36)	W 89° 22' 56.0"	N 5450559
		2601	N 49° 11' 33.7"	E 324374	U2	N 49° 11' 08.3"	E 326493
		(V37)	W 89° 24' 37.7"	N 5451458	(V36)	W 89° 22' 51.8"	N 5450603
		2602	N 49° 11' 32.8"	E 324451	2650	N 49° 11' 37.6"	E 324570
		(V37)	W 89° 24' 33.9"	N 5451426	(V37)	W 89° 24' 28. 2"	N 5451570
		2623	N 49° 09' 54.2"	E 329314	2653	N 49° 12' 01.3"	E 325639
		(V37)	W 89° 20' 28.9"	N 5448226	(V37)	W 89° 23' 36.6"	N 5452269
Wetland Black Spruce	V38	2622	N 49° 09' 49.8"	E 329154	Q2	N 49° 09' 51.5"	E 329223
			W 89° 20' 36.6"	N 5448094		W 89° 20' 33.3"	N 5448145
		Q8	N 49° 09' 55.1"	E 329474	Q6	N 49° 09' 51.1"	E 329182
			W 89° 20' 21.0"	N 5448249		W 89° 20' 35.3"	N 5448134
		Q9	N 49° 09' 56.2"	E 329486	Q7	N 49° 09' 50.4"	E 329210
			W 89° 20' 20.5"	N 5448281		W 89° 20' 33.8"	N 5448113
		Q10	N 49° 09' 56.1"	E 329518	J7	N 49° 12' 55.3"	E 324262
			W 89° 20' 18.9"	N 5448277		W 89° 24' 47.2"	N 5453982
		R31A	N 49° 11' 08.2"	E 326026	J8	N 49° 12' 54.4"	E 324291
			W 89° 23' 14.8"	N 5450617		W 89° 24' 45.7"	N 5453953
		R31B	N 49° 11' 08.3"	E 326063	C6	N 49° 12' 01.3"	E 325542
			W 89° 23' 13.0"	N 5450617		W 89° 23' 41.3"	N 5452273
		2663	N 49° 12' 54.4"	E 324258	2642	N 49° 12' 04.1"	E 323666
			W 89° 24' 47.3"	N 5453954		W 89° 25' 14.2"	N 5452418
		J6	N 49° 12' 55.3"	E 324294	V1	N 49° 12' 03.3"	E 323646
			W 89° 24' 45.6"	N 5453982		W 89° 25' 15.1"	N 5452394
		C1	N 49° 11' 58.1"	E 325403	V2	N 49° 12' 4.2"	E 323694
			W 89° 23' 48.0"	N 5452178		W 89° 25' 12.8"	N 5452422
		2652	N 49° 11' 58.1"	E 325450	V3	N 49° 12' 05.0"	E 323710
			W 89° 23' 45.7"	N 5452178		W 89° 25' 12.0"	N 5452446

APPENDIX G

AVERAGE JEFFRIES-MATUSITA DISTANCE MEASURES

APPENDIX G

AVERAGE JEFFRIES-MATUSITA DISTANCE MEASURES

Number of CASI Features	CASI Features	Average JMD Measures
1	Band 2	0.24387
	Band 3	0.21659
	Band 4	0.16988
	Band 5	0.19361
	Band 6	0.57070
	Band 7	0.59092
2	Bands 2,3	0.41087
	Bands 2,4	0.33565
	Bands 2,5	0.35754
	Bands 2,6	0.86887
	Bands 2,7	0.87660
	Bands 3,4	0.26072
	Bands 3,5	0.32655
	Bands 3,6	0.86175
	Bands 3,7	0.86539
	Bands 4,5	0.32950
	Bands 4,6	0.78104
	Bands 4,7	0.78844
	Bands 5,6	0.78393
	Bands 5,7	0.79267
	Bands 6,7	0.72680
3	Bands 2,3,4	0.47944
	Bands 2,3,5	0.57408
	Bands 2,3,6	0.91553
	Bands 2,3,7	0.92204
	Bands 2,4,5	0.49840
	Bands 2,4,6	0.91572
	Bands 2,4,7	0.92173
	Bands 2,5,6	0.96637
	Bands 2,5,7	0.97448
	Bands 2,6,7	0.98307
	Bands 3,4,5	0.42197
	Bands 3,4,6	0.90470
	Bands 3,4,7	0.90884
	Bands 3,5,6	0.98212
	Bands 3,5,7	0.98721
	Bands 3,6,7	0.97564
	Bands 4,5,6	0.91823
	Bands 4,5,7	0.92588
	Bands 4,6,7	0.90446
	Bands 5,6,7	0.90945

4	Bands 2,3,4,5	0.64254
	Bands 2,3,4,6	0.94550
	Bands 2,3,4,7	0.95159
	Bands 2,3,5,6	1.01555
	Bands 2,3,5,7	1.02087
	Bands 2,4,5,6	1.04262
	Bands 2,4,5,7	1.04808
	Bands 2,4,6,7	1.02477
	Bands 2,5,6,7	1.07057
	Bands 3,4,5,6	1.03396
	Bands 3,4,5,7	1.03813
	Bands 3,5,6,7	1.08055
	Bands 4,5,6,7	1.02403
5	Bands 2,3,4,5,6	1.07545
	Bands 2,3,4,5,7	1.08071
	Bands 2,3,5,6,7	1.11120
	Bands 2,4,5,6,7	1.13588
	Bands 3,4,5,6,7	1.12686
6	Bands 2,3,4,5,6,7	1.16545

APPENDIX H

GENERATION OF CASI SPATIAL FEATURES

APPENDIX H

GENERATION OF CASI SPATIAL FEATURES

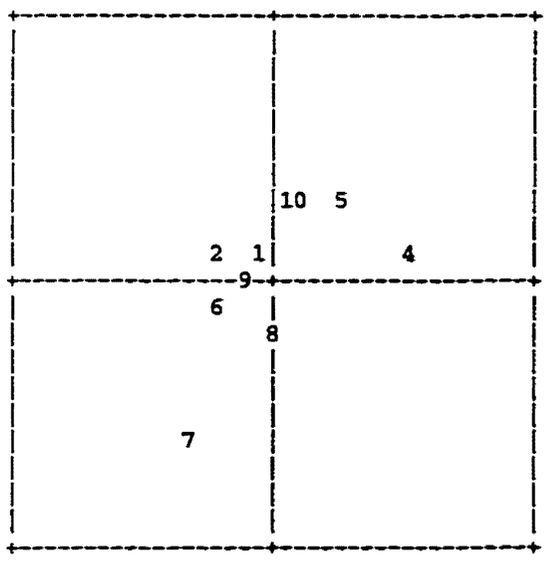
```
FIVE.pix                                    [S    3PIC    2800P    2400L] 22-Aug-96

   2:GCP5m     Type:214 [Ground Control Points ]   Last Update: 13:56 26-Aug-96
     Contents: GCP's for 5m data
     Set 2 Units:UTM    16 U E000 Set 1 Units:PIXEL          Number GCPs:  10

Model Parameters        FX           FY
 1  CONS            -.637879E+05  0.109141E+07
 2  X               0.199992E+00  -.467051E-04
 3        Y         -.170899E-05  -.200035E+00

GCP's are ordered from worst to best residuals.
  GCP        Set 2 GCP's            Set 1 GCP's          Residual      Distance
  No. ---(UTM    16 U E000)----  -----(PIXEL)-----  ---------(PIXEL)----------
    7(    326498.2,   5450390.2)(  1499.4,  1121.4)(   -0.34,   -0.62)    0.70
    4(    324294.2,   5449713.8)(  1059.6,  1257.6)(    0.57,    0.08)    0.58
    5(    327230.2,   5453829.8)(  1646.4,   434.3)(    0.28,    0.31)    0.42
   10(    332561.8,   5445733.8)(  2712.6,  2053.6)(    0.13,    0.33)    0.35
    2(    324558.2,   5451714.2)(  1111.6,   857.4)(   -0.23,    0.14)    0.26
    8(    331721.8,   5450730.8)(  2544.4,  1053.4)(    0.01,   -0.26)    0.26
    6(    328438.2,   5448042.2)(  1887.6,  1591.6)(   -0.20,   -0.08)    0.22
    9(    332382.2,   5448781.8)(  2676.4,  1443.6)(   -0.09,    0.03)    0.10
    3(    319941.8,   5451789.8)(   188.4,   842.4)(   -0.09,    0.02)    0.09
    1(    322302.2,   5454538.2)(   660.6,   292.6)(   -0.04,    0.06)    0.07

Residual Plot (PIXEL):                          RMS=(    0.30,    0.31)    0.44
```



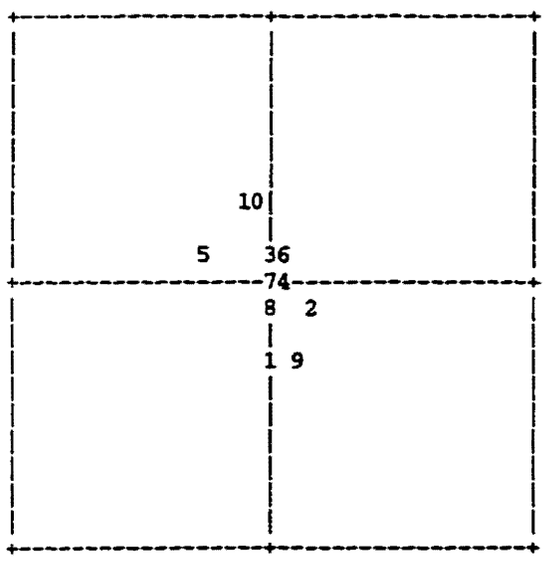
```
SIX.pix                                    [S    3PIC    2333P    2000L] 22-Aug-96

   2:GCP6m     Type:214 [Ground Control Points ]   Last Update: 14:49 26-Aug-96
     Contents: GCPs for 6m CASI Data
     Set 2 Units:UTM    16 U E000 Set 1 Units:PIXEL          Number GCPs:  10

Model Parameters        FX           FY
 1  CONS           -.532206E+05  0.909496E+06
 2  X               0.166666E+00 -.124817E-04
 3         Y       0.996850E-05 -.166696E+00

GCP's are ordered from worst to best residuals.
  GCP        Set 2 GCP's            Set 1 GCP's          Residual      Distance
  No. ---(UTM    16 U E000)----  -----(PIXEL)-----  ---------(PIXEL)----------
   10(    328146.8,   5450317.2)(  1524.6,   947.4)(   -0.06,    0.34)    0.34
    5(    324710.2,   5449613.8)(   951.6,  1064.6)(   -0.31,    0.15)    0.34
    1(    322380.2,   5454572.2)(   563.6,   237.6)(   -0.02,   -0.32)    0.32
    9(    332496.8,   5445699.2)(  2249.7,  1716.6)(    0.11,   -0.29)    0.31
    2(    319148.2,   5451898.2)(    25.1,   683.6)(    0.17,   -0.11)    0.20
    3(    324558.2,   5451714.2)(   926.6,   714.4)(    0.01,    0.17)    0.17
    6(    328386.2,   5448066.2)(  1564.6,  1322.4)(    0.05,    0.11)    0.12
    8(    332639.8,   5448879.8)(  2273.4,  1186.6)(    0.00,   -0.11)    0.11
    4(    327161.8,   5453686.2)(  1360.6,   385.6)(    0.07,    0.05)    0.09
    7(    331555.2,   5450776.2)(  2092.7,   870.6)(   -0.02,    0.02)    0.03


Residual Plot (PIXEL):                      RMS=(    0.14,    0.23)    0.28
```



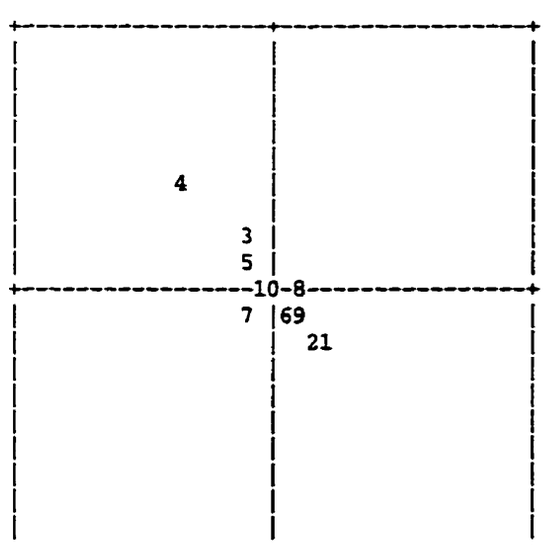
```
SEVEN.pix                                [S    3PIC    2000P    1714L] 22-Aug-96

   2:GCP7m     Type:214 [Ground Control Points ]   Last Update: 15:15 26-Aug-96
     Contents: GCPs for 7m CASI data
     Set 2 Units:UTM    16 U E000 Set 1 Units:PIXEL          Number GCPs:  10

Model Parameters        FX           FY
 1  CONS           -.455734E+05  0.779139E+06
 2  X               0.142857E+00  0.511796E-04
 3         Y       0.374717E-06  -.142807E+00

GCP's are ordered from worst to best residuals.
  GCP        Set 2 GCP's            Set 1 GCP's          Residual     Distance
  No. ---(UTM    16 U E000)----  -----(PIXEL)-----  ---------(PIXEL)----------
    4(    326370.2,   5451105.2)(  1052.7,   699.7)(   -0.38,    0.40)    0.55
    1(    321374.2,   5455433.8)(   339.6,    80.7)(    0.21,   -0.21)    0.29
    3(    324332.2,   5455137.8)(   761.8,   123.6)(   -0.11,    0.25)    0.27
    2(    321800.8,   5451451.2)(   400.4,   649.4)(    0.16,   -0.21)    0.26
    6(    330138.2,   5452811.2)(  1591.4,   455.7)(    0.08,   -0.17)    0.19
    9(    332553.8,   5445733.2)(  1936.6,  1466.7)(    0.14,   -0.08)    0.16
    7(    330361.8,   5449972.2)(  1623.2,   861.2)(   -0.10,   -0.11)    0.14
    5(    325153.8,   5448771.8)(   879.2,  1032.6)(   -0.09,    0.09)    0.13
    8(    332639.8,   5448870.2)(  1948.8,  1018.8)(    0.10,    0.03)    0.10
   10(    330366.8,   5447765.8)(  1624.0,  1176.4)(    0.00,    0.00)    0.00

Residual Plot (PIXEL):                        RMS=(    0.20,    0.23)    0.30
```



APPENDIX I

CLASSIFICATION ACCURACY (DISCRIMINANT FUNCTION) - CONTINGENCY TABLES FOR VALIDATION DATA

APPENDIX I

CLASSIFICATION ACCURACY (DISCRIMINANT FUNCTION) - CONTINGENCY TABLES FOR VALDIATION DATA

Table 1: Landsat Thematic Mapper Bands 2, 3, and 4 (3 Variables)

TABLE OF GROUP (ROWS) BY PREDICT (COLUMNS)
FREQUENCIES

	1.000	2.000	3.000	4.000	5.000	6.000	TOTAL
1.000	114	59	42	10	0	25	250
2.000	44	45	71	75	15	0	250
3.000	23	19	146	16	0	46	250
4.000	29	0	21	72	118	10	250
5.000	0	0	0	93	157	0	250
6.000	34	82	45	12	0	77	250
TOTAL	244	205	325	278	290	158	1500

TABLE OF GROUP (ROWS) BY PREDICT (COLUMNS)
ROW PERCENTS

	1.000	2.000	3.000	4.000	5.000	6.000	TOTAL	N
1.000	45.60	23.60	16.80	4.00	0.00	10.00	100.00	250.00
2.000	17.60	18.00	28.40	30.00	6.00	0.00	100.00	250.00
3.000	9.20	7.60	58.40	6.40	0.00	18.40	100.00	250.00
4.000	11.60	0.00	8.40	28.80	47.20	4.00	100.00	250.00
5.000	0.00	0.00	0.00	37.20	62.80	0.00	100.00	250.00
6.000	13.60	32.80	18.00	4.80	0.00	30.80	100.00	250.00
TOTAL	16.27	13.67	21.67	18.53	19.33	10.53	100.00	
N	244	205	325	278	290	158	1500	

TEST STATISTIC	VALUE	DF	PROB
PEARSON CHI-SQUARE	1428.999	25	0.000
LIKELIHOOD RATIO CHI-SQUARE	1552.849	25	0.000
MCNEMAR SYMMETRY CHI-SQUARE	224.243	15	0.000

COEFFICIENT	VALUE	ASYMPTOTIC STD ERROR
GOODMAN-KRUSKAL GAMMA	0.362	0.026
KENDALL TAU-B	0.312	0.022
STUART TAU-C	0.311	0.022
COHEN KAPPA	0.289	0.015
SPEARMAN RHO	0.368	0.026

Table 2: CASI Bands 3, 5, and 7 (3 Variables)

TABLE OF GROUP (ROWS) BY PREDICT (COLUMNS)
FREQUENCIES

	1.000	2.000	3.000	4.000	5.000	6.000	TOTAL
1.000	196	42	9	1	0	2	250
2.000	37	83	54	27	41	8	250
3.000	3	58	103	43	6	37	250
4.000	11	40	25	35	84	55	250
5.000	0	10	2	30	158	50	250
6.000	0	6	55	6	4	179	250
TOTAL	247	239	248	142	293	331	1500

TABLE OF GROUP (ROWS) BY PREDICT (COLUMNS)
ROW PERCENTS

	1.000	2.000	3.000	4.000	5.000	6.000	TOTAL	N
1.000	78.40	16.80	3.60	0.40	0.00	0.80	100.00	250.00
2.000	14.80	33.20	21.60	10.80	16.40	3.20	100.00	250.00
3.000	1.20	23.20	41.20	17.20	2.40	14.80	100.00	250.00
4.000	4.40	16.00	10.00	14.00	33.60	22.00	100.00	250.00
5.000	0.00	4.00	0.80	12.00	63.20	20.00	100.00	250.00
6.000	0.00	2.40	22.00	2.40	1.60	71.60	100.00	250.00
TOTAL	16.47	15.93	16.53	9.47	19.53	22.07	100.00	
N	247	239	248	142	293	331	1500	

TEST STATISTIC	VALUE	DF	PROB
PEARSON CHI-SQUARE	1830.912	25	0.000
LIKELIHOOD RATIO CHI-SQUARE	1680.062	25	0.000
MCNEMAR SYMMETRY CHI-SQUARE	149.855	15	0.000

COEFFICIENT	VALUE	ASYMPTOTIC STD ERROR
GOODMAN-KRUSKAL GAMMA	0.701	0.016
KENDALL TAU-B	0.612	0.015
STUART TAU-C	0.609	0.015
COHEN KAPPA	0.403	0.015
SPEARMAN RHO	0.717	0.015

Table 3: CASI "Optimal" Spatial Resolutions (Bands 3, 5, and 7) (3 Variables)

TABLE OF GROUP (ROWS) BY PREDICT (COLUMNS)
FREQUENCIES

	1.000	2.000	3.000	4.000	5.000	6.000	TOTAL
1.000	181	50	17	0	0	2	250
2.000	39	81	69	19	37	5	250
3.000	5	37	157	27	1	23	250
4.000	11	47	27	38	90	37	250
5.000	0	10	6	30	159	45	250
6.000	0	7	63	7	2	171	250
TOTAL	236	232	339	121	289	283	1500

TABLE OF GROUP (ROWS) BY PREDICT (COLUMNS)
ROW PERCENTS

	1.000	2.000	3.000	4.000	5.000	6.000	TOTAL	N
1.000	72.40	20.00	6.80	0.00	0.00	0.80	100.00	250.00
2.000	15.60	32.40	27.60	7.60	14.80	2.00	100.00	250.00
3.000	2.00	14.80	62.80	10.80	0.40	9.20	100.00	250.00
4.000	4.40	18.80	10.80	15.20	36.00	14.80	100.00	250.00
5.000	0.00	4.00	2.40	12.00	63.60	18.00	100.00	250.00
6.000	0.00	2.80	25.20	2.80	0.80	68.40	100.00	250.00
TOTAL	15.73	15.47	22.60	8.07	19.27	18.87	100.00	
N	236	232	339	121	289	283	1500	

TEST STATISTIC	VALUE	DF	PROB
PEARSON CHI-SQUARE	1913.452	25	0.000
LIKELIHOOD RATIO CHI-SQUARE	1740.575	25	0.000
MCNEMAR SYMMETRY CHI-SQUARE	170.259	15	0.000

COEFFICIENT	VALUE	ASYMPTOTIC STD ERROR
GOODMAN-KRUSKAL GAMMA	0.710	0.016
KENDALL TAU-B	0.620	0.015
STUART TAU-C	0.615	0.015
COHEN KAPPA	0.430	0.015
SPEARMAN RHO	0.721	0.015

Table 4: CASI 5 metre Spatial Resolution (Bands 3, 5, and 7) (3 Variables)

TABLE OF GROUP (ROWS) BY PREDICT (COLUMNS)
FREQUENCIES

	1.000	2.000	3.000	4.000	5.000	6.000	TOTAL
1.000	195	44	8	1	0	2	250
2.000	41	96	66	19	26	2	250
3.000	0	38	146	43	3	20	250
4.000	8	58	27	35	83	39	250
5.000	0	5	7	32	166	40	250
6.000	0	0	44	4	2	200	250
TOTAL	244	241	298	134	280	303	1500

TABLE OF GROUP (ROWS) BY PREDICT (COLUMNS)
ROW PERCENTS

	1.000	2.000	3.000	4.000	5.000	6.000	TOTAL	N
1.000	78.00	17.60	3.20	0.40	0.00	0.80	100.00	250.00
2.000	16.40	38.40	26.40	7.60	10.40	0.80	100.00	250.00
3.000	0.00	15.20	58.40	17.20	1.20	8.00	100.00	250.00
4.000	3.20	23.20	10.80	14.00	33.20	15.60	100.00	250.00
5.000	0.00	2.00	2.80	12.80	66.40	16.00	100.00	250.00
6.000	0.00	0.00	17.60	1.60	0.80	80.00	100.00	250.00
TOTAL	16.27	16.07	19.87	8.93	18.67	20.20	100.00	
N	244	241	298	134	280	303	1500	

TEST STATISTIC	VALUE	DF	PROB
PEARSON CHI-SQUARE	2263.986	25	0.000
LIKELIHOOD RATIO CHI-SQUARE	2022.006	25	0.000
MCNEMAR SYMMETRY CHI-SQUARE	158.812	15	0.000

COEFFICIENT	VALUE	ASYMPTOTIC STD ERROR
GOODMAN-KRUSKAL GAMMA	0.776	0.013
KENDALL TAU-B	0.686	0.013
STUART TAU-C	0.682	0.013
COHEN KAPPA	0.470	0.015
SPEARMAN RHO	0.785	0.012

Table 5: CASI 6 metre Spatial Resolution (Bands 3, 5, and 7) (3 Variables)

TABLE OF GROUP (ROWS) BY PREDICT (COLUMNS)
FREQUENCIES

	1.000	2.000	3.000	4.000	5.000	6.000	TOTAL
1.000	181	52	15	1	0	1	250
2.000	30	92	70	21	32	5	250
3.000	0	35	159	33	1	22	250
4.000	9	56	30	43	71	41	250
5.000	0	1	4	31	189	25	250
6.000	0	0	48	4	2	196	250
TOTAL	220	236	326	133	295	290	1500

TABLE OF GROUP (ROWS) BY PREDICT (COLUMNS)
ROW PERCENTS

	1.000	2.000	3.000	4.000	5.000	6.000	TOTAL	N
1.000	72.40	20.80	6.00	0.40	0.00	0.40	100.00	250.00
2.000	12.00	36.80	28.00	8.40	12.80	2.00	100.00	250.00
3.000	0.00	14.00	63.60	13.20	0.40	8.80	100.00	250.00
4.000	3.60	22.40	12.00	17.20	28.40	16.40	100.00	250.00
5.000	0.00	0.40	1.60	12.40	75.60	10.00	100.00	250.00
6.000	0.00	0.00	19.20	1.60	0.80	78.40	100.00	250.00
TOTAL	14.67	15.73	21.73	8.87	19.67	19.33	100.00	
N	220	236	326	133	295	290	1500	

TEST STATISTIC	VALUE	DF	PROB
PEARSON CHI-SQUARE	2333.569	25	0.000
LIKELIHOOD RATIO CHI-SQUARE	2052.226	25	0.000
MCNEMAR SYMMETRY CHI-SQUARE	167.300	15	0.000

COEFFICIENT	VALUE	ASYMPTOTIC STD ERROR
GOODMAN-KRUSKAL GAMMA	0.759	0.014
KENDALL TAU-B	0.670	0.014
STUART TAU-C	0.666	0.014
COHEN KAPPA	0.488	0.015
SPEARMAN RHO	0.769	0.013

Table 6: CASI 6 and 7 metre Spatial Resolution (Bands 3, 5, and 7) (3 Variables)

TABLE OF GROUP (ROWS) BY PREDICT (COLUMNS)
FREQUENCIES

	1.000	2.000	3.000	4.000	5.000	6.000	TOTAL
1.000	180	49	18	1	0	2	250
2.000	39	92	64	20	30	5	250
3.000	3	53	143	26	0	25	250
4.000	12	46	36	39	76	41	250
5.000	0	2	5	31	191	21	250
6.000	0	0	53	4	2	191	250
TOTAL	234	242	319	121	299	285	1500

TABLE OF GROUP (ROWS) BY PREDICT (COLUMNS)
ROW PERCENTS

	1.000	2.000	3.000	4.000	5.000	6.000	TOTAL	N
1.000	72.00	19.60	7.20	0.40	0.00	0.80	100.00	250.00
2.000	15.60	36.80	25.60	8.00	12.00	2.00	100.00	250.00
3.000	1.20	21.20	57.20	10.40	0.00	10.00	100.00	250.00
4.000	4.80	18.40	14.40	15.60	30.40	16.40	100.00	250.00
5.000	0.00	0.80	2.00	12.40	76.40	8.40	100.00	250.00
6.000	0.00	0.00	21.20	1.60	0.80	76.40	100.00	250.00
TOTAL	15.60	16.13	21.27	8.07	19.93	19.00	100.00	
N	234	242	319	121	299	285	1500	

TEST STATISTIC	VALUE	DF	PROB
PEARSON CHI-SQUARE	2180.558	25	0.000
LIKELIHOOD RATIO CHI-SQUARE	1946.477	25	0.000
MCNEMAR SYMMETRY CHI-SQUARE	145.642	15	0.000

COEFFICIENT	VALUE	ASYMPTOTIC STD ERROR
GOODMAN-KRUSKAL GAMMA	0.748	0.014
KENDALL TAU-B	0.658	0.014
STUART TAU-C	0.654	0.014
COHEN KAPPA	0.469	0.015
SPEARMAN RHO	0.759	0.013

Table 7: Mean Texture Variables (Bands 3 and 7) (2 Variables)

TABLE OF GROUP (ROWS) BY PREDICT (COLUMNS)
FREQUENCIES

	I.000	2.000	3.000	4.000	5.000	6.000	TOTAL
1.000	177	73	0	0	0	0	250
2.000	41	64	47	22	70	6	250
3.000	0	32	135	12	0	71	250
4.000	3	29	11	74	111	22	250
5.000	0	0	0	57	184	9	250
6.000	0	0	27	0	0	223	250
TOTAL	221	198	220	165	365	331	1500

TABLE OF GROUP (ROWS) BY PREDICT (COLUMNS)
ROW PERCENTS

	1.000	2.000	3.000	4.000	5.000	6.000	TOTAL	N
1.000	70.80	29.20	0.00	0.00	0.00	0.00	100.00	250.00
2.000	16.40	25.60	18.80	8.80	28.00	2.40	100.00	250.00
3.000	0.00	12.80	54.00	4.80	0.00	28.40	100.00	250.00
4.000	1.20	11.60	4.40	29.60	44.40	8.80	100.00	250.00
5.000	0.00	0.00	0.00	22.80	73.60	3.60	100.00	250.00
6.000	0.00	0.00	10.80	0.00	0.00	89.20	100.00	250.00
TOTAL	14.73	13.20	14.67	11.00	24.33	22.07	100.00	
N	221	198	220	165	365	331	1500	

TEST STATISTIC	VALUE	DF	PROB
PEARSON CHI-SQUARE	2502.472	25	0.000
LIKELIHOOD RATIO CHI-SQUARE	2392.345	25	0.000
MCNEMAR SYMMETRY CHI-SQUARE	159.947	15	0.000

COEFFICIENT	VALUE	ASYMPTOTIC STD ERROR
GOODMAN-KRUSKAL GAMMA	0.741	0.015
KENDALL TAU-B	0.658	0.015
STUART TAU-C	0.652	0.015
COHEN KAPPA	0.486	0.015
SPEARMAN RHO	0.754	0.013

Table 8: Mean (CASI3 and CASI7) and Disimilarity (CASI7) Texture Variables (3 Variables)

TABLE OF GROUP (ROWS) BY PREDICT (COLUMNS)
FREQUENCIES

	1.000	2.000	3.000	4.000	5.000	6.000	TOTAL
1.000	177	71	2	0	0	0	250
2.000	33	79	48	45	39	6	250
3.000	0	24	140	13	1	72	250
4.000	0	46	4	91	86	23	250
5.000	0	0	0	23	217	10	250
6.000	0	0	27	0	0	223	250
TOTAL	210	220	221	172	343	334	1500

TABLE OF GROUP (ROWS) BY PREDICT (COLUMNS)
ROW PERCENTS

	1.000	2.000	3.000	4.000	5.000	6.000	TOTAL	N
1.000	70.80	28.40	0.80	0.00	0.00	0.00	100.00	250.00
2.000	13.20	31.60	19.20	18.00	15.60	2.40	100.00	250.00
3.000	0.00	9.60	56.00	5.20	0.40	28.80	100.00	250.00
4.000	0.00	18.40	1.60	36.40	34.40	9.20	100.00	250.00
5.000	0.00	0.00	0.00	9.20	86.80	4.00	100.00	250.00
6.000	0.00	0.00	10.80	0.00	0.00	89.20	100.00	250.00
TOTAL	14.00	14.67	14.73	11.47	22.87	22.27	100.00	
N	210	220	221	172	343	334	1500	

TEST STATISTIC	VALUE	DF	PROB
PEARSON CHI-SQUARE	2784.333	25	0.000
LIKELIHOOD RATIO CHI-SQUARE	2524.263	25	0.000
MCNEMAR SYMMETRY CHI-SQUARE	164.528	15	0.000

COEFFICIENT	VALUE	ASYMPTOTIC STD ERROR
GOODMAN-KRUSKAL GAMMA	0.764	0.014
KENDALL TAU-B	0.684	0.014
STUART TAU-C	0.679	0.014
COHEN KAPPA	0.542	0.015
SPEARMAN RHO	0.776	0.013

Table 9: Mean (CASI3 and CASI7) and Correlation (CASI7) Texture Variables (3 Variables)

TABLE OF GROUP (ROWS) BY PREDICT (COLUMNS)
FREQUENCIES

	1.000	2.000	3.000	4.000	5.000	6.000	TOTAL
1.000	196	44	8	2	0	0	250
2.000	50	48	48	25	69	10	250
3.000	0	4	165	9	1	71	250
4.000	9	16	13	63	129	20	250
5.000	0	0	0	45	201	4	250
6.000	0	0	49	0	0	201	250
TOTAL	255	112	283	144	400	306	1500

TABLE OF GROUP (ROWS) BY PREDICT (COLUMNS)
ROW PERCENTS

	1.000	2.000	3.000	4.000	5.000	6.000	TOTAL	N
1.000	78.40	17.60	3.20	0.80	0.00	0.00	100.00	250.00
2.000	20.00	19.20	19.20	10.00	27.60	4.00	100.00	250.00
3.000	0.00	1.60	66.00	3.60	0.40	28.40	100.00	250.00
4.000	3.60	6.40	5.20	25.20	51.60	8.00	100.00	250.00
5.000	0.00	0.00	0.00	18.00	80.40	1.60	100.00	250.00
6.000	0.00	0.00	19.60	0.00	0.00	80.40	100.00	250.00
TOTAL	17.00	7.47	18.87	9.60	26.67	20.40	100.00	
N	255	112	283	144	400	306	1500	

TEST STATISTIC	VALUE	DF	PROB
PEARSON CHI-SQUARE	2495.781	25	0.000
LIKELIHOOD RATIO CHI-SQUARE	2364.010	25	0.000
MCNEMAR SYMMETRY CHI-SQUARE	201.356	15	0.000

COEFFICIENT	VALUE	ASYMPTOTIC STD ERROR
GOODMAN-KRUSKAL GAMMA	0.704	0.017
KENDALL TAU-B	0.623	0.017
STUART TAU-C	0.614	0.016
COHEN KAPPA	0.499	0.015
SPEARMAN RHO	0.717	0.015

Table 10: Mean (CASI3; CASI7), Dissimilarity (CASI7) and Correlation (CASI7) Texture Variables (4 Features)

TABLE OF GROUP (ROWS) BY PREDICT (COLUMNS)
FREQUENCIES

	1.000	2.000	3.000	4.000	5.000	6.000	TOTAL
1.000	203	38	9	0	0	0	250
2.000	51	46	62	47	42	2	250
3.000	0	4	169	3	4	70	250
4.000	11	17	17	76	109	20	250
5.000	0	0	0	26	220	4	250
6.000	0	0	50	0	0	200	250
TOTAL	265	105	307	152	375	296	1500

TABLE OF GROUP (ROWS) BY PREDICT (COLUMNS)
ROW PERCENTS

	1.000	2.000	3.000	4.000	5.000	6.000	TOTAL	N
1.000	81.20	15.20	3.60	0.00	0.00	0.00	100.00	250.00
2.000	20.40	18.40	24.80	18.80	16.80	0.80	100.00	250.00
3.000	0.00	1.60	67.60	1.20	1.60	28.00	100.00	250.00
4.000	4.40	6.80	6.80	30.40	43.60	8.00	100.00	250.00
5.000	0.00	0.00	0.00	10.40	88.00	1.60	100.00	250.00
6.000	0.00	0.00	20.00	0.00	0.00	80.00	100.00	250.00
TOTAL	17.67	7.00	20.47	10.13	25.00	19.73	100.00	
N	265	105	307	152	375	296	1500	

TEST STATISTIC	VALUE	DF	PROB
PEARSON CHI-SQUARE	2658.796	25	0.000
LIKELIHOOD RATIO CHI-SQUARE	2468.054	25	0.000
MCNEMAR SYMMETRY CHI-SQUARE	223.094	15	0.000

COEFFICIENT	VALUE	ASYMPTOTIC STD ERROR
GOODMAN-KRUSKAL GAMMA	0.736	0.016
KENDALL TAU-B	0.655	0.016
STUART TAU-C	0.646	0.015
COHEN KAPPA	0.531	0.015
SPEARMAN RHO	0.748	0.014

Table 11: Mean (CASI3; CASI7), Dissimilarity (CASI3; CASI7) and Correlation (CASI7) Texture Variables (5 Features)

TABLE OF GROUP (ROWS) BY PREDICT (COLUMNS)
FREQUENCIES

	1.000	2.000	3.000	4.000	5.000	6.000	TOTAL
1.000	202	38	7	3	0	0	250
2.000	50	45	58	47	41	9	250
3.000	0	3	162	5	4	76	250
4.000	11	17	22	79	106	15	250
5.000	0	0	0	26	217	7	250
6.000	0	0	17	0	0	233	250
TOTAL	263	103	266	160	368	340	1500

TABLE OF GROUP (ROWS) BY PREDICT (COLUMNS)
ROW PERCENTS

	1.000	2.000	3.000	4.000	5.000	6.000	TOTAL	N
1.000	80.80	15.20	2.80	1.20	0.00	0.00	100.00	250.00
2.000	20.00	18.00	23.20	18.80	16.40	3.60	100.00	250.00
3.000	0.00	1.20	64.80	2.00	1.60	30.40	100.00	250.00
4.000	4.40	6.80	8.80	31.60	42.40	6.00	100.00	250.00
5.000	0.00	0.00	0.00	10.40	86.80	2.80	100.00	250.00
6.000	0.00	0.00	6.80	0.00	0.00	93.20	100.00	250.00
TOTAL	17.53	6.87	17.73	10.67	24.53	22.67	100.00	
N	263	103	266	160	368	340	1500	

TEST STATISTIC	VALUE	DF	PROB
PEARSON CHI-SQUARE	2784.867	25	0.000
LIKELIHOOD RATIO CHI-SQUARE	2502.518	25	0.000
MCNEMAR SYMMETRY CHI-SQUARE	249.479	15	0.000

COEFFICIENT	VALUE	ASYMPTOTIC STD ERROR
GOODMAN-KRUSKAL GAMMA	0.771	0.014
KENDALL TAU-B	0.690	0.014
STUART TAU-C	0.680	0.014
COHEN KAPPA	0.550	0.015
SPEARMAN RHO	0.778	0.013

Table 12: Mean (CASI3; CASI7), Dissimilarity (CASI3; CASI7) and Correlation (CASI3; CASI7) Texture Variables (Total=6)

TABLE OF GROUP (ROWS) BY PREDICT (COLUMNS)
FREQUENCIES

	1.000	2.000	3.000	4.000	5.000	6.000	TOTAL
1.000	195	43	10	2	0	0	250
2.000	51	46	57	47	42	7	250
3.000	0	3	162	5	0	80	250
4.000	11	16	23	100	83	17	250
5.000	0	0	0	31	211	8	250
6.000	0	0	14	0	0	236	250
TOTAL	257	108	266	185	336	348	1500

TABLE OF GROUP (ROWS) BY PREDICT (COLUMNS)
ROW PERCENTS

	1.000	2.000	3.000	4.000	5.000	6.000	TOTAL	N
1.000	78.00	17.20	4.00	0.80	0.00	0.00	100.00	250.00
2.000	20.40	18.40	22.80	18.80	16.80	2.80	100.00	250.00
3.000	0.00	1.20	64.80	2.00	0.00	32.00	100.00	250.00
4.000	4.40	6.40	9.20	40.00	33.20	6.80	100.00	250.00
5.000	0.00	0.00	0.00	12.40	84.40	3.20	100.00	250.00
6.000	0.00	0.00	5.60	0.00	0.00	94.40	100.00	250.00
TOTAL	17.13	7.20	17.73	12.33	22.40	23.20	100.00	
N	257	108	266	185	336	348	1500	

TEST STATISTIC	VALUE	DF	PROB
PEARSON CHI-SQUARE	2825.320	25	0.000
LIKELIHOOD RATIO CHI-SQUARE	2539.873	25	0.000
MCNEMAR SYMMETRY CHI-SQUARE	236.397	15	0.000

COEFFICIENT	VALUE	ASYMPTOTIC STD ERROR
GOODMAN-KRUSKAL GAMMA	0.773	0.014
KENDALL TAU-B	0.693	0.014
STUART TAU-C	0.685	0.014
COHEN KAPPA	0.560	0.015
SPEARMAN RHO	0.780	0.013

Table 13: Local Relief (Elevation Range) (1 Variable)

TABLE OF GROUP (ROWS) BY PREDICT (COLUMNS)
FREQUENCIES

	1.000	2.000	3.000	4.000	5.000	6.000	TOTAL
1.000	60	21	72	66	31	0	250
2.000	71	54	60	40	0	25	250
3.000	0	0	135	0	44	71	250
4.000	42	16	78	39	0	75	250
5.000	0	0	90	0	81	79	250
6.000	0	0	23	0	36	191	250
TOTAL	173	91	458	145	192	441	1500

TABLE OF GROUP (ROWS) BY PREDICT (COLUMNS)
ROW PERCENTS

	1.000	2.000	3.000	4.000	5.000	6.000	TOTAL	N
1.000	24.00	8.40	28.80	26.40	12.40	0.00	100.00	250.00
2.000	28.40	21.60	24.00	16.00	0.00	10.00	100.00	250.00
3.000	0.00	0.00	54.00	0.00	17.60	28.40	100.00	250.00
4.000	16.80	6.40	31.20	15.60	0.00	30.00	100.00	250.00
5.000	0.00	0.00	36.00	0.00	32.40	31.60	100.00	250.00
6.000	0.00	0.00	9.20	0.00	14.40	76.40	100.00	250.00
TOTAL	11.53	6.07	30.53	9.67	12.80	29.40	100.00	
N	173	91	458	145	192	441	1500	

TEST STATISTIC	VALUE	DF	PROB
PEARSON CHI-SQUARE	1025.990	25	0.000
LIKELIHOOD RATIO CHI-SQUARE	1210.143	25	0.000
MCNEMAR SYMMETRY CHI-SQUARE	440.173	15	0.000

COEFFICIENT	VALUE	ASYMPTOTIC STD ERROR
GOODMAN-KRUSKAL GAMMA	0.504	0.019
KENDALL TAU-B	0.418	0.016
STUART TAU-C	0.404	0.015
COHEN KAPPA	0.248	0.014
SPEARMAN RHO	0.522	0.018

Table 14: Digital Elevation Model (DEM) (1 Variable)

TABLE OF GROUP (ROWS) BY PREDICT (COLUMNS)
FREQUENCIES

	1.000	2.000	3.000	4.000	5.000	6.000	TOTAL
1.000	25	125	50	0	25	25	250
2.000	0	100	25	104	0	21	250
3.000	0	0	175	75	0	0	250
4.000	24	50	26	50	50	50	250
5.000	0	0	50	50	150	0	250
6.000	50	0	0	7	25	168	250
TOTAL	99	275	326	286	250	264	1500

TABLE OF GROUP (ROWS) BY PREDICT (COLUMNS)
ROW PERCENTS

	1.000	2.000	3.000	4.000	5.000	6.000	TOTAL	N
1.000	10.00	50.00	20.00	0.00	10.00	10.00	100.00	250.00
2.000	0.00	40.00	10.00	41.60	0.00	8.40	100.00	250.00
3.000	0.00	0.00	70.00	30.00	0.00	0.00	100.00	250.00
4.000	9.60	20.00	10.40	20.00	20.00	20.00	100.00	250.00
5.000	0.00	0.00	20.00	20.00	60.00	0.00	100.00	250.00
6.000	20.00	0.00	0.00	2.80	10.00	67.20	100.00	250.00
TOTAL	6.60	18.33	21.73	19.07	16.67	17.60	100.00	
N	99	275	326	286	250	264	1500	

TEST STATISTIC	VALUE	DF	PROB
PEARSON CHI-SQUARE	1820.898	25	0.000
LIKELIHOOD RATIO CHI-SQUARE	1848.809	25	0.000
MCNEMAR SYMMETRY CHI-SQUARE	428.479	15	0.000

COEFFICIENT	VALUE	ASYMPTOTIC STD ERROR
GOODMAN-KRUSKAL GAMMA	0.469	0.026
KENDALL TAU-B	0.408	0.023
STUART TAU-C	0.404	0.022
COHEN KAPPA	0.334	0.015
SPEARMAN RHO	0.465	0.026

Table 15: Slope Model (1 Variable)

TABLE OF GROUP (ROWS) BY PREDICT (COLUMNS)
FREQUENCIES

	1.000	2.000	3.000	4.000	5.000	6.000	TOTAL
1.000	75	35	40	30	46	24	250
2.000	100	25	44	40	6	35	250
3.000	0	0	140	0	20	90	250
4.000	50	0	105	5	12	78	250
5.000	0	0	83	0	67	100	250
6.000	0	0	12	0	15	223	250
TOTAL	225	60	424	75	166	550	1500

TABLE OF GROUP (ROWS) BY PREDICT (COLUMNS)
ROW PERCENTS

	1.000	2.000	3.000	4.000	5.000	6.000	TOTAL	N
1.000	30.00	14.00	16.00	12.00	18.40	9.60	100.00	250.00
2.000	40.00	10.00	17.60	16.00	2.40	14.00	100.00	250.00
3.000	0.00	0.00	56.00	0.00	8.00	36.00	100.00	250.00
4.000	20.00	0.00	42.00	2.00	4.80	31.20	100.00	250.00
5.000	0.00	0.00	33.20	0.00	26.80	40.00	100.00	250.00
6.000	0.00	0.00	4.80	0.00	6.00	89.20	100.00	250.00
TOTAL	15.00	4.00	28.27	5.00	11.07	36.67	100.00	
N	225	60	424	75	166	550	1500	

TEST STATISTIC	VALUE	DF	PROB
PEARSON CHI-SQUARE	1047.070	25	0.000
LIKELIHOOD RATIO CHI-SQUARE	1119.594	25	0.000
MCNEMAR SYMMETRY CHI-SQUARE	627.303	15	0.000

COEFFICIENT	VALUE	ASYMPTOTIC STD ERROR
GOODMAN-KRUSKAL GAMMA	0.516	0.020
KENDALL TAU-B	0.422	0.017
STUART TAU-C	0.399	0.016
COHEN KAPPA	0.228	0.013
SPEARMAN RHO	0.516	0.019

Table 16: Aspect Model (1 Variable)

TABLE OF GROUP (ROWS) BY PREDICT (COLUMNS)
FREQUENCIES

	1.000	2.000	3.000	4.000	5.000	6.000	TOTAL
1.000	95	20	5	6	54	70	250
2.000	13	55	91	0	0	91	250
3.000	0	60	80	0	0	110	250
4.000	105	36	46	25	0	38	250
5.000	15	78	25	3	0	129	250
6.000	0	38	59	35	0	118	250
TOTAL	228	287	306	69	54	556	1500

TABLE OF GROUP (ROWS) BY PREDICT (COLUMNS)
ROW PERCENTS

	1.000	2.000	3.000	4.000	5.000	6.000	TOTAL	N
1.000	38.00	8.00	2.00	2.40	21.60	28.00	100.00	250.00
2.000	5.20	22.00	36.40	0.00	0.00	36.40	100.00	250.00
3.000	0.00	24.00	32.00	0.00	0.00	44.00	100.00	250.00
4.000	42.00	14.40	18.40	10.00	0.00	15.20	100.00	250.00
5.000	6.00	31.20	10.00	1.20	0.00	51.60	100.00	250.00
6.000	0.00	15.20	23.60	14.00	0.00	47.20	100.00	250.00
TOTAL	15.20	19.13	20.40	4.60	3.60	37.07	100.00	
N	228	287	306	69	54	556	1500	

TEST STATISTIC	VALUE	DF	PROB
PEARSON CHI-SQUARE	886.711	25	0.000
LIKELIHOOD RATIO CHI-SQUARE	868.167	25	0.000
MCNEMAR SYMMETRY CHI-SQUARE	547.479	15	0.000

COEFFICIENT	VALUE	ASYMPTOTIC STD ERROR
GOODMAN-KRUSKAL GAMMA	0.130	0.025
KENDALL TAU-B	0.105	0.021
STUART TAU-C	0.100	0.020
COHEN KAPPA	0.098	0.013
SPEARMAN RHO	0.133	0.025

Table 17: Local Relief and DEM (2 Variables)

TABLE OF GROUP (ROWS) BY PREDICT (COLUMNS)
FREQUENCIES

	1.000	2.000	3.000	4.000	5.000	6.000	TOTAL
1.000	50	55	95	40	10	0	250
2.000	25	100	60	40	0	25	250
3.000	0	0	175	0	0	75	250
4.000	25	50	50	0	59	66	250
5.000	0	0	72	0	150	28	250
6.000	0	0	50	0	25	175	250
TOTAL	100	205	502	80	244	369	1500

TABLE OF GROUP (ROWS) BY PREDICT (COLUMNS)
ROW PERCENTS

	1.000	2.000	3.000	4.000	5.000	6.000	TOTAL	N
1.000	20.00	22.00	38.00	16.00	4.00	0.00	100.00	250.00
2.000	10.00	40.00	24.00	16.00	0.00	10.00	100.00	250.00
3.000	0.00	0.00	70.00	0.00	0.00	30.00	100.00	250.00
4.000	10.00	20.00	20.00	0.00	23.60	26.40	100.00	250.00
5.000	0.00	0.00	28.80	0.00	60.00	11.20	100.00	250.00
6.000	0.00	0.00	20.00	0.00	10.00	70.00	100.00	250.00
TOTAL	6.67	13.67	33.47	5.33	16.27	24.60	100.00	
N	100	205	502	80	244	369	1500	

TEST STATISTIC	VALUE	DF	PROB
PEARSON CHI-SQUARE	1397.919	25	0.000
LIKELIHOOD RATIO CHI-SQUARE	1448.472	25	0.000
MCNEMAR SYMMETRY CHI-SQUARE	457.992	15	0.000

COEFFICIENT	VALUE	ASYMPTOTIC STD ERROR
GOODMAN-KRUSKAL GAMMA	0.529	0.019
KENDALL TAU-B	0.442	0.016
STUART TAU-C	0.427	0.016
COHEN KAPPA	0.320	0.014
SPEARMAN RHO	0.545	0.018

Table 18: Local Relief, DEM and Slope (3 Variables)

TABLE OF GROUP (ROWS) BY PREDICT (COLUMNS)
FREQUENCIES

	1.000	2.000	3.000	4.000	5.000	6.000	TOTAL
1.000	70	55	75	31	19	0	250
2.000	0	100	46	79	0	25	250
3.000	0	0	175	0	0	75	250
4.000	53	42	50	0	39	66	250
5.000	0	0	72	0	150	28	250
6.000	0	0	50	0	25	175	250
TOTAL	123	197	468	110	233	369	1500

TABLE OF GROUP (ROWS) BY PREDICT (COLUMNS)
ROW PERCENTS

	1.000	2.000	3.000	4.000	5.000	6.000	TOTAL	N
1.000	28.00	22.00	30.00	12.40	7.60	0.00	100.00	250.00
2.000	0.00	40.00	18.40	31.60	0.00	10.00	100.00	250.00
3.000	0.00	0.00	70.00	0.00	0.00	30.00	100.00	250.00
4.000	21.20	16.80	20.00	0.00	15.60	26.40	100.00	250.00
5.000	0.00	0.00	28.80	0.00	60.00	11.20	100.00	250.00
6.000	0.00	0.00	20.00	0.00	10.00	70.00	100.00	250.00
TOTAL	8.20	13.13	31.20	7.33	15.53	24.60	100.00	
N	123	197	468	110	233	369	1500	

TEST STATISTIC	VALUE	DF	PROB
PEARSON CHI-SQUARE	1668.875	25	0.000
LIKELIHOOD RATIO CHI-SQUARE	1636.639	25	0.000
MCNEMAR SYMMETRY CHI-SQUARE	469.246	15	0.000

COEFFICIENT	VALUE	ASYMPTOTIC STD ERROR
GOODMAN-KRUSKAL GAMMA	0.492	0.020
KENDALL TAU-B	0.417	0.017
STUART TAU-C	0.406	0.017
COHEN KAPPA	0.336	0.015
SPEARMAN RHO	0.516	0.019

Table 19: Local Relief, DEM, Slope and Aspect (4 Variables)

TABLE OF GROUP (ROWS) BY PREDICT (COLUMNS)
FREQUENCIES

	1.000	2.000	3.000	4.000	5.000	6.000	TOTAL
1.000	91	44	40	56	19	0	250
2.000	0	100	77	49	8	16	250
3.000	0	0	160	0	0	90	250
4.000	33	42	15	39	86	35	250
5.000	0	0	72	0	96	82	250
6.000	0	0	62	0	28	160	250
TOTAL	124	186	426	144	237	383	1500

TABLE OF GROUP (ROWS) BY PREDICT (COLUMNS)
ROW PERCENTS

	1.000	2.000	3.000	4.000	5.000	6.000	TOTAL	N
1.000	36.40	17.60	16.00	22.40	7.60	0.00	100.00	250.00
2.000	0.00	40.00	30.80	19.60	3.20	6.40	100.00	250.00
3.000	0.00	0.00	64.00	0.00	0.00	36.00	100.00	250.00
4.000	13.20	16.80	6.00	15.60	34.40	14.00	100.00	250.00
5.000	0.00	0.00	28.80	0.00	38.40	32.80	100.00	250.00
6.000	0.00	0.00	24.80	0.00	11.20	64.00	100.00	250.00
TOTAL	8.27	12.40	28.40	9.60	15.80	25.53	100.00	
N	124	186	426	144	237	383	1500	

TEST STATISTIC	VALUE	DF	PROB
PEARSON CHI-SQUARE	1393.975	25	0.000
LIKELIHOOD RATIO CHI-SQUARE	1501.420	25	0.000
MCNEMAR SYMMETRY CHI-SQUARE	450.149	15	0.000

COEFFICIENT	VALUE	ASYMPTOTIC STD ERROR
GOODMAN-KRUSKAL GAMMA	0.517	0.020
KENDALL TAU-B	0.438	0.017
STUART TAU-C	0.428	0.017
COHEN KAPPA	0.317	0.015
SPEARMAN RHO	0.535	0.019

Table 20: Spatial and Textural Variables (6 Variables)

TABLE OF GROUP (ROWS) BY PREDICT (COLUMNS)
FREQUENCIES

	1.000	2.000	3.000	4.000	5.000	6.000	TOTAL
1.000	176	71	1	2	0	0	250
2.000	32	112	55	31	18	2	250
3.000	0	23	191	11	0	25	250
4.000	0	66	25	54	99	6	250
5.000	0	1	6	27	213	3	250
6.000	0	0	53	0	0	197	250
TOTAL	208	273	331	125	330	233	1500

TABLE OF GROUP (ROWS) BY PREDICT (COLUMNS)
ROW PERCENTS

	1.000	2.000	3.000	4.000	5.000	6.000	TOTAL	N
1.000	70.40	28.40	0.40	0.80	0.00	0.00	100.00	250.00
2.000	12.80	44.80	22.00	12.40	7.20	0.80	100.00	250.00
3.000	0.00	9.20	76.40	4.40	0.00	10.00	100.00	250.00
4.000	0.00	26.40	10.00	21.60	39.60	2.40	100.00	250.00
5.000	0.00	0.40	2.40	10.80	85.20	1.20	100.00	250.00
6.000	0.00	0.00	21.20	0.00	0.00	78.80	100.00	250.00
TOTAL	13.87	18.20	22.07	8.33	22.00	15.53	100.00	
N	208	273	331	125	330	233	1500	

TEST STATISTIC	VALUE	DF	PROB
PEARSON CHI-SQUARE	2948.784	25	0.000
LIKELIHOOD RATIO CHI-SQUARE	2576.633	25	0.000
MCNEMAR SYMMETRY CHI-SQUARE	132.373	15	0.000

COEFFICIENT	VALUE	ASYMPTOTIC STD ERROR
GOODMAN-KRUSKAL GAMMA	0.798	0.013
KENDALL TAU-B	0.715	0.013
STUART TAU-C	0.709	0.014
COHEN KAPPA	0.554	0.015
SPEARMAN RHO	0.805	0.012

Table 21: Spatial and Terrain Variables (6 Variables)

TABLE OF GROUP (ROWS) BY PREDICT (COLUMNS)
FREQUENCIES

	1.000	2.000	3.000	4.000	5.000	6.000	TOTAL
1.000	194	21	33	1	0	1	250
2.000	13	108	67	56	5	1	250
3.000	0	12	197	9	8	24	250
4.000	15	45	43	35	72	40	250
5.000	0	0	9	1	204	36	250
6.000	0	0	46	0	4	200	250
TOTAL	222	186	395	102	293	302	1500

TABLE OF GROUP (ROWS) BY PREDICT (COLUMNS)
ROW PERCENTS

	1.000	2.000	3.000	4.000	5.000	6.000	TOTAL	N
1.000	77.60	8.40	13.20	0.40	0.00	0.40	100.00	250.00
2.000	5.20	43.20	26.80	22.40	2.00	0.40	100.00	250.00
3.000	0.00	4.80	78.80	3.60	3.20	9.60	100.00	250.00
4.000	6.00	18.00	17.20	14.00	28.80	16.00	100.00	250.00
5.000	0.00	0.00	3.60	0.40	81.60	14.40	100.00	250.00
6.000	0.00	0.00	18.40	0.00	1.60	80.00	100.00	250.00
TOTAL	14.80	12.40	26.33	6.80	19.53	20.13	100.00	
N	222	186	395	102	293	302	1500	

TEST STATISTIC	VALUE	DF	PROB
PEARSON CHI-SQUARE	2809.626	25	0.000
LIKELIHOOD RATIO CHI-SQUARE	2322.704	25	0.000
MCNEMAR SYMMETRY CHI-SQUARE	257.480	15	0.000

COEFFICIENT	VALUE	ASYMPTOTIC STD ERROR
GOODMAN-KRUSKAL GAMMA	0.775	0.014
KENDALL TAU-B	0.689	0.014
STUART TAU-C	0.679	0.014
COHEN KAPPA	0.550	0.015
SPEARMAN RHO	0.784	0.012

Table 22: Spatial, Texture and Terrain Variables (9 Variables)

TABLE OF GROUP (ROWS) BY PREDICT (COLUMNS)
FREQUENCIES

	1.000	2.000	3.000	4.000	5.000	6.000	TOTAL
1.000	193	48	7	2	0	0	250
2.000	22	116	56	55	0	1	250
3.000	0	6	213	7	0	24	250
4.000	0	56	38	59	87	10	250
5.000	0	0	8	6	233	3	250
6.000	0	0	50	0	0	200	250
TOTAL	215	226	372	129	320	238	1500

TABLE OF GROUP (ROWS) BY PREDICT (COLUMNS)
ROW PERCENTS

	1.000	2.000	3.000	4.000	5.000	6.000	TOTAL	N
1.000	77.20	19.20	2.80	0.80	0.00	0.00	100.00	250.00
2.000	8.80	46.40	22.40	22.00	0.00	0.40	100.00	250.00
3.000	0.00	2.40	85.20	2.80	0.00	9.60	100.00	250.00
4.000	0.00	22.40	15.20	23.60	34.80	4.00	100.00	250.00
5.000	0.00	0.00	3.20	2.40	93.20	1.20	100.00	250.00
6.000	0.00	0.00	20.00	0.00	0.00	80.00	100.00	250.00
TOTAL	14.33	15.07	24.80	8.60	21.33	15.87	100.00	
N	215	226	372	129	320	238	1500	

TEST STATISTIC	VALUE	DF	PROB
PEARSON CHI-SQUARE	3395.687	25	0.000
LIKELIHOOD RATIO CHI-SQUARE	2854.184	25	0.000
MCNEMAR SYMMETRY CHI-SQUARE	182.028	15	0.000

COEFFICIENT	VALUE	ASYMPTOTIC STD ERROR
GOODMAN-KRUSKAL GAMMA	0.814	0.013
KENDALL TAU-B	0.737	0.013
STUART TAU-C	0.730	0.013
COHEN KAPPA	0.611	0.014
SPEARMAN RHO	0.822	0.011

APPENDIX J

MAXIMUM LIKELIHOOD CLASSIFICATION ACCURACY - CONTINGENCY TABLES FOR VALIDATION DATA

APPENDIX J

MAXIMUM LIKELIHOOD CLASSIFICATION ACCURACY - CONTINGENCY TABLES FOR VALIDATION DATA

Table 1: CASI 4 metre Spatial Resolution (Bands 3, 5, and 7) (3 Variables)

TABLE OF GROUP (ROWS) BY PREDICT (COLUMNS)
FREQUENCIES

	1.000	2.000	3.000	4.000	5.000	6.000	UC	TOTAL
1.000	154	46	20	4	0	0	26	250
2.000	52	65	65	31	28	3	6	250
3.000	13	31	112	49	11	28	6	250
4.000	17	27	25	37	106	34	4	250
5.000	0	11	5	16	192	24	2	250
6.000	0	2	42	3	15	184	4	250
TOTAL	236	182	269	140	352	273	48	1500

Table 2: CASI 6 metre Spatial Resolution (Bands 3, 5, and 7) (3 Variables)

TABLE OF GROUP (ROWS) BY PREDICT (COLUMNS)
FREQUENCIES

	1.000	2.000	3.000	4.000	5.000	6.000	UC	TOTAL
1.000	134	59	22	1	0	0	34	250
2.000	37	90	67	29	23	0	4	250
3.000	0	25	169	34	2	20	0	250
4.000	9	43	32	48	81	30	7	250
5.000	0	1	3	20	199	27	0	250
6.000	0	0	40	2	7	184	17	250
TOTAL	180	218	333	134	312	261	62	1500

Table 3: Mean (CASI3 and CASI7) and Dissimilarity (CASI7) Texture Variables (3 Variables)

TABLE OF GROUP (ROWS) BY PREDICT (COLUMNS)
FREQUENCIES

	1.000	2.000	3.000	4.000	5.000	6.000	UC	TOTAL
1.000	135	58	5	2	0	0	50	250
2.000	44	91	38	36	12	12	17	250
3.000	0	6	151	8	1	82	2	250
4.000	3	34	20	83	96	8	6	250
5.000	0	0	0	51	187	12	0	250
6.000	0	0	47	0	0	203	4	250
TOTAL	182	189	261	180	296	317	75	1500

Table 4: Local Relief, DEM and Slope (3 Variables)

TABLE OF GROUP (ROWS) BY PREDICT (COLUMNS)
FREQUENCIES

	1.000	2.000	3.000	4.000	5.000	6.000	UC	TOTAL
1.000	83	25	5	83	54	0	0	250
2.000	21	129	40	19	16	25	0	250
3.000	0	0	194	0	0	56	0	250
4.000	88	3	16	5	100	34	4	250
5.000	0	0	78	0	124	48	0	250
6.000	0	0	9	0	5	236	0	250
TOTAL	192	157	342	107	299	399	4	1500

Table 5: Spatial and Textural Variables (6 Variables)

TABLE OF FREQUENCIES	GROUP (ROWS) BY PREDICT (COLUMNS)							
	1.000	2.000	3.000	4.000	5.000	6.000	UC	TOTAL
1.000	125	53	6	3	0	0	63	250
2.000	43	110	30	24	7	0	36	250
3.000	0	25	189	8	0	16	12	250
4.000	5	60	15	82	44	22	22	250
5.000	0	6	1	59	168	15	1	250
6.000	0	1	35	0	0	189	25	250
TOTAL	173	255	276	176	219	242	159	1500

Table 6: Spatial and Terrain Variables (6 Variables)

TABLE OF FREQUENCIES	GROUP (ROWS) BY PREDICT (COLUMNS)							
	1.000	2.000	3.000	4.000	5.000	6.000	UC	TOTAL
1.000	152	30	1	3	0	0	64	250
2.000	14	144	15	29	4	0	44	250
3.000	9	8	190	17	0	11	15	250
4.000	14	1	19	33	83	1	99	250
5.000	1	0	0	34	171	42	2	250
6.000	2	0	4	11	1	190	42	250
TOTAL	192	183	229	127	259	244	266	1500

Table 7: Spatial, Texture and Terrain Variables (6 Variables)

TABLE OF FREQUENCIES	GROUP (ROWS) BY PREDICT (COLUMNS)							
	1.000	2.000	3.000	4.000	5.000	6.000	UC	TOTAL
1.000	166	22	0	0	0	0	62	250
2.000	9	148	13	35	0	0	45	250
3.000	0	12	182	2	1	14	39	250
4.000	11	6	9	60	49	15	100	250
5.000	0	0	0	71	142	29	8	250
6.000	0	3	0	0	0	181	66	250
TOTAL	186	191	204	168	192	239	320	1500

APPENDIX K

NEURAL NETWORK CLASSIFICATION ACCURACY - CONTINGENCY TABLES FOR VALIDATION DATA

APPENDIX K

NEURAL NETWORK CLASSIFICATION ACCURACY - CONTINGENCY TABLES FOR VALIDATION DATA

Table 1: CASI 4 metre Spatial Resolution (Bands 3, 5, and 7) (3 Variables)

TABLE OF FREQUENCIES GROUP (ROWS) BY PREDICT (COLUMNS)

	1.000	2.000	3.000	4.000	5.000	6.000	UC	TOTAL
1.000	215	3	32	0	0	0	0	250
2.000	53	86	98	5	5	3	0	250
3.000	15	35	151	20	0	29	0	250
4.000	13	76	50	48	30	33	0	250
5.000	0	86	9	103	35	17	0	250
6.000	0	3	59	21	2	165	0	250
TOTAL	296	289	399	197	72	247	0	1500

Table 2: CASI 6 metre Spatial Resolution (Bands 3, 5, and 7) (3 Variables)

TABLE OF FREQUENCIES GROUP (ROWS) BY PREDICT (COLUMNS)

	1.000	2.000	3.000	4.000	5.000	6.000	UC	TOTAL
1.000	208	4	37	1	0	0	0	250
2.000	51	94	98	1	3	3	0	250
3.000	4	26	199	8	0	13	0	250
4.000	16	78	61	46	36	13	0	250
5.000	0	57	5	82	100	6	0	250
6.000	0	0	61	11	11	167	0	250
TOTAL	279	259	461	149	150	202	0	1500

Table 3: Mean (CASI3 and CASI7) and Dissimilarity (CASI7) Texture Variables (3 Variables)

TABLE OF FREQUENCIES GROUP (ROWS) BY PREDICT (COLUMNS)

	1.000	2.000	3.000	4.000	5.000	6.000	UC	TOTAL
1.000	238	0	12	0	0	0	0	250
2.000	87	24	73	22	41	3	0	250
3.000	0	0	166	63	0	21	0	250
4.000	20	48	26	116	25	15	0	250
5.000	0	42	0	120	88	0	0	250
6.000	0	0	34	36	0	180	0	250
TOTAL	345	114	311	357	154	219	0	1500

Table 4: Local Relief, DEM and Slope (3 Variables)

TABLE OF FREQUENCIES GROUP (ROWS) BY PREDICT (COLUMNS)

	1.000	2.000	3.000	4.000	5.000	6.000	UC	TOTAL
1.000	175	5	50	20	0	0	0	250
2.000	121	10	75	19	0	25	0	250
3.000	0	0	229	0	0	21	0	250
4.000	128	22	75	0	25	0	0	250
5.000	0	0	100	0	150	0	0	250
6.000	0	0	85	0	165	0	0	250
TOTAL	424	37	614	39	340	46	0	1500

Table 5: Spatial and Textural Variables (6 Variables)

TABLE OF FREQUENCIES	GROUP (ROWS) BY PREDICT (COLUMNS)							
	1.000	2.000	3.000	4.000	5.000	6.000	UC	TOTAL
1.000	243	0	7	0	0	0	0	250
2.000	105	71	43	20	11	0	0	250
3.000	26	7	142	72	0	3	0	250
4.000	26	48	37	106	22	11	0	250
5.000	0	26	0	114	110	0	0	250
6.000	0	0	85	23	0	142	0	250
TOTAL	400	152	314	335	143	156	0	1500

Table 6: Spatial and Terrain Variables (6 Variables)

TABLE OF FREQUENCIES	GROUP (ROWS) BY PREDICT (COLUMNS)							
	1.000	2.000	3.000	4.000	5.000	6.000	UC	TOTAL
1.000	221	5	1	23	0	0	0	250
2.000	125	61	6	14	40	4	0	250
3.000	27	2	141	1	51	26	2	250
4.000	89	12	8	56	85	0	0	250
5.000	0	14	2	2	231	0	1	250
6.000	0	0	50	0	44	156	0	250
TOTAL	462	94	208	96	451	186	3	1500

Table 7: Spatial, Texture and Terrain Variables (6 Variables)

TABLE OF FREQUENCIES	GROUP (ROWS) BY PREDICT (COLUMNS)							
	1.000	2.000	3.000	4.000	5.000	6.000	UC	TOTAL
1.000	247	0	3	0	0	0	0	250
2.000	132	62	16	20	6	3	11	250
3.000	19	0	156	22	1	52	0	250
4.000	47	49	12	50	79	8	5	250
5.000	0	56	0	38	156	0	0	250
6.000	0	0	51	24	2	173	0	250
TOTAL	445	167	238	154	244	236	16	1500